National Research Council Canada

Conseil national de recherches Canada

NRC · CNRC

Canadian Journal of Fisheries and Aquatic Sciences

Journal canadien des sciences halieutiques et aquatiques

http://cjfas.nrc.ca

http://jcsha.cnrc.ca

ISSN 0706-652X / CJFSDX 59(2) 197–403 (2002)

The *Canadian Journal of Fisheries and Aquatic Sciences*, previously published as *Contributions to Canadian Biology* 1901–1925, *Contributions to Canadian Biology and Fisheries* 1926–1934, *Journal of the Biological Board of Canada* 1934–1937, and *Journal of the Fisheries Research Board of Canada* 1938–1979, is issued monthly to form annual volumes of 12 numbers plus supplements.

Editorial policy: The Journal publishes original research articles, perspectives (syntheses, critiques, re-evaluations), discussions (comment and reply), and rapid communications. Manuscripts may concern cells, organisms, populations, communities, ecosystems, or processes that affect aquatic systems. They may cover a range of disciplines including biology and ecology of marine and freshwater organisms, limnology, oceanography, physiology, toxicology, genetics, economics, disease, and management. Preference will be given to manuscripts that emphasize understanding of observed phenomena and interpretation of experimental results. The Journal encourages papers that lead from clearly stated purpose or rationale and from testable hypotheses, concepts, or questions to identifiable conclusions or syntheses. Such papers may amplify, modify, question, or redirect accumulated knowledge embodied in contemporary perceptions of a particular state of aquatic sciences. The Journal discourages papers that are essentially descriptive, except in emerging disciplines; have only site-specific or local applications (a certain year, place, taxon, chemical compound, etc.); only confirm previously established principles; or apply standard techniques without breaking new methodological ground.

Manuscripts for publication should be submitted to the Editors, *Canadian Journal of Fisheries and Aquatic Sciences*, Department of Zoology, University of Guelph, Guelph, ON N1G 2W1, Canada (519-824-4120 ext. 2646; fax: 519-767-9798; e-mail: cjfas@uoguelph.ca).

Submissions in either English or French are acceptable. The information must be original, that is, not copyrighted, published, or submitted elsewhere except in abstract form or unless by written consent of the Editor. NRC accepts no responsibility for statements or opinions expressed by a contributor. Acceptance of an advertisement, announcement, or other material does not imply endorsement by either the Journal's Editors or NRC. The use of proprietary names does not imply endorsement of the product or company.

Correspondence concerning accepted manuscripts and corrected proofs should be sent to NRC Research Press, National Research Council of Canada, Ottawa, ON K1A 0R6, Canada (fax: 613-952-7656; e-mail: research.press@nrc.ca).

Instructions to Authors are published once a year in the first issue of each volume. Copies are available from NRC Research Press or at http://cjfas.nrc.ca. The **Publication Policy** of NRC Research Press is available at http://cjfas.nrc.ca.

The National Research Council of Canada accepts no responsibility for statements or opinions expressed by a contributor. Acceptance of an advertisement, announcement, or other material does not imply endorsement by either the Journal's Editors or NRC.

Microfilm: Issues from 1934 through the current volume can be purchased on 16- or 35-mm microfilm. Photocopies of individual articles or issues can be purchased from University Microfilms International, 330 North Zeeb Road, Ann Arbor, MI 48106, U.S.A.

U.S. periodical postage paid at Champlain, N.Y., and at additional mailing offices. Attention U.S. POSTMASTER: Send address changes to **Canadian Journal of Fisheries and Aquatic Sciences**, c/o USACAN Media Distribution Center, P.O. Box 2888, Plattsburg, NY 12901, U.S.A.

Publié sans interruption depuis 1901, le *Journal canadien des sciences halieutiques et aquatiques* a paru sous plusieurs titres : *Contributions to Canadian Biology* 1901–1925, *Contributions to Canadian Biology and Fisheries* 1926–1934, *Journal of the Biological Board of Canada* 1934–1937, et *Journal of the Fisheries Research Board of Canada* 1938–1979. Le Journal paraît tous les mois, formant ainsi un volume de 12 numéros, et offre en plus jusqu'à deux suppléments par année.

Politique éditoriale : On publie, dans le Journal, des articles rendant compte de recherche originale, des perspectives (synthèses, critiques et réévaluations), des discussions (commentaires et réponses) et des communications rapides. Les documents peuvent porter sur les cellules, organismes, populations, communautés, écosystèmes ou processus qui affectent les systèmes aquatiques. Ils peuvent relever de divers domaines y compris la biologie et l'écologie des organismes marins et d'eau douce, la limnologie, l'océanographie, la physiologie, la toxicologie, la génétique, l'économie, la pathologie et la gestion. On accorde la préséance aux articles qui contribuent à la compréhension de phénomènes observés et à l'interprétation de résultats expérimentaux. On invite les auteurs à soumettre des articles ayant des objectifs précis ou relevant d'hypothèses, de concepts ou de questions vérifiables et se terminant par de solides conclusions ou d'utiles synthèses. Ces articles enrichissent, changent, mettent en question ou réorientent les connaissances acquises sur divers aspects des sciences aquatiques. On décourage toutefois la soumission d'articles simplement descriptifs (à moins qu'il ne s'agisse de nouvelles disciplines), d'application très limitée (applicables à une seule année, une seule région ou un seul taxon, portant sur un unique composé chimique, etc.); d'articles qui ne font que reprendre les principes énoncés dans des articles précédents; et d'articles rendant compte de l'application de normes sans gain de méthodologie.

Les auteurs voudront adresser leurs **manuscrits** aux directeurs scientifiques, *Journal canadien des sciences halieutiques et aquatiques*, Department of Zoology, University of Guelph, Guelph, ON N1G 2W1, Canada (519-824-4120 poste 2646; télécopieur : 519-767-9798; courriel : cjfas@uoguelph.ca).

Les contributions peuvent être en anglais ou en français. Elles doivent être originales, c.-à.-d. qu'elles ne doivent pas avoir fait l'objet d'un copyright, avoir été publiées ou soumises ailleurs, sauf sous forme abrégée ou avec le consentement du rédacteur. Le CNRC ne se tient en aucune façon responsable des opinions exprimées par un collaborateur ou des déclarations qui pourrait faire ce dernier. La publication d'annonces publicitaires, d'avis et autres n'implique pas l'endossement de leur contenu par les directeurs du Journal ou du CNRC. L'utilisation des noms de marques de commerce ne signifie aucunement une sanction du produit en question ou de la compagnie qui le fabrique.

La correspondance ayant trait aux manuscrits acceptés et les **épreuves corrigés** doivent être envoyées aux Presses scientifiques du CNRC, Conseil national de recherches du Canada, Ottawa, ON K1A 0R6, Canada (télécopieur : 613-952-7656; courriel : presses.scientifiques@cnrc.ca).

Les Recommandations aux auteurs sont publiées une fois par année dans le premier numéro de chaque volume. Des copies sont disponibles auprès du Bureau de la rédaction aux Presses scientifiques du CNRC ou au http://jcsha.cnrc.ca. **La Politique de publication** est disponible auprès des Presses scientifiques du CNRC ou au http://jcsha.cnrc.ca.

Le Conseil national de recherches du Canada ne se tient en aucune façon responsable des opinions exprimées par un collaborateur ou des déclarations que pourrait faire ce dernier. La publication d'annonces publicitaires, d'avis et autres n'implique pas l'endossement de leur contenu par les directeurs de la Revue ou du CNRC.

Microfilms : On peut acheter sur microfilms de 16 ou 35 mm tous les numéros depuis 1934. Des photocopies d'articles ou de numéros individuels sont aussi en vente auprès de University Microfilms International, 330 North Zeeb Road, Ann Arbor, MI 48106, É.-U.

This Journal is indexed or abstracted in / Cette revue est signalée ou résumée dans

ABSEARCH, Aquatic Sciences and Fisheries Abstracts, Biological Abstracts, Biological & Agricultural Index, CAB Abstracts, Chemical Abstracts, Current Contents, Elsevier BIOBASE, Environmental Abstracts, Environmental Periodicals Bibliography, GEOBASE, GeoRef, Internationale Bibliographie der Zeitschriftenliteratur, Life Sciences Collection, Meteorological and Geoastrophysical Abstracts, Oceanic Abstracts, PASCAL Database, and Science Citation Index.

Volume 59, Number 2, February 2002

Canadian Journal of Fisheries and Aquatic Sciences

Published by the National Research Council of Canada

Volume 59, numéro 2, février 2002

Journal canadien des sciences halieutiques et aquatiques

Publié par le Conseil national de recherches du Canada

Editors / directeurs scientifiques John C. Roff and Moira M. Ferguson

Assistant to the Editors / adjointe aux directeurs scientifiques **Holly Foster**

Associate Editors / directeurs scientifiques associés

M.T. Arts, *Environment Canada, Burlington*
D. Boisclair, *Université de Montréal*
U. Borgmann, *Environment Canada, Burlington*
S.E. Campana, *DFO/MPO, Dartmouth*
R. Carignan, *Université de Montréal*
D.G. Dixon, *University of Waterloo*
A.E. Dizon, *National Marine Fisheries Service, La Jolla, Calif.*
J.J. Dodson, *Université Laval*
J.A. Downing, *Iowa State University*
K.T. Frank, *DFO/MPO, Dartmouth*
D.F. Houlihan, *University of Aberdeen, Aberdeen, Scotland*
F.A. Huntingford, *University of Glasgow*
J.A. Hutchings, *Dalhousie University*
G.S. Jamieson, *DFO/MPO, Nanaimo*
B. Jonsson, *Norwegian Institute for Nature Research, Oslo, Norway*
D.M. Mason, *NOAA-Great Lakes Environmental Research Laboratory, Ann Arbor, Mich.*
A. Mazumder, *University of Victoria*
D.L. Parrish, *Vermont Cooperative Fish and Wildlife Research Unit (USGS/BRD), University of Vermont*
P. Pepin, *DFO/MPO, St. John's*
T.M. Powell, *University of California, Berkeley, Calif.*
E.E. Prepas, *University of Alberta*
T.J. Quinn II, *University of Alaska–Fairbanks, Juneau, Alaska*
T.P. Quinn, *University of Washington*
R.D. Robarts, *Environment Canada, Saskatoon*
B. Sainte-Marie, *DFO/MPO, Mont-Joli*
D.W. Schindler, *University of Alberta*
S.J. Smith, *DFO/MPO, Dartmouth*
W.G. Sprules, *University of Toronto*
R.J. Thompson, *Memorial University of Newfoundland*
C.J. Walters, *University of British Columbia*
R.D. Ward, *CSIRO Marine Research, Australia*
C.M. Wood, *McMaster University*
B. de Young, *Memorial University of Newfoundland*

NRC Research Press / Presses scientifiques du CNRC

Editor-in-chief / directeur général **Bruce P. Dancik**

Assistant Editor-in-chief / directeur général adjoint **Iain E.P. Taylor**

Journals Program / Programme des revues

(Fax / télécopieur : 613-952-7656; e-mail / courriel : research.press@nrc.ca; URL: http://researchpress.nrc.ca)

Director / directrice **Aldyth Holmes**

Business Manager / gestionnaire des affaires **Paul McClymont**

Managing Editor / rédactrice administrative **Cecily M. Pearson (613-993-9099)**

Publication Officers / agentes de publication **Jennifer McColl and Lee Murphy**

Advertising / annonces publicitaires **Judy Heyman (613-993-0151)**

Reprints / tirés à part **Roxanne Landriault (613-990-2254)**

Subscriptions / abonnements **Helen Goulet (613-993-9084)**

© National Research Council of Canada 2002. World rights reserved. No part of this publication may be reproduced, stored, or transmitted in any form or by any means, without the written permission of the publisher, except as stated below.

The National Research Council of Canada grants **permission*** to individuals to make single copies of articles for personal use. Any person may reproduce short excerpts from articles in the journal for any purpose that respects the moral rights of authors, provided that the source is fully acknowledged. As a courtesy, the consent of authors of such material should be obtained directly from the author.

Authorization to reproduce items for other than personal use, as stated above, is granted by the National Research Council of Canada provided that the copyright fee of $7.00 per copy is paid directly to CANCOPY, One Yonge Street, Suite 1900, Toronto, ON M5E 1E5, Canada.

*The above permission does not extend to other kinds of copying, such as copying for general distribution, for advertising, or promotional purposes, for creating new collective works, or for resale. For such copying, arrangements must be made with the publisher, National Research Council of Canada, Ottawa, ON K1A 0R6, Canada.

© Conseil national de recherches du Canada 2002. Tous droits réservés. Il est interdit de reproduire, de sauvegarder ou de transmettre quelque partie de la présente publication dans quelque format ou de quelque façon sans le consentement écrit de l'éditeur, à l'exception des conditions suivantes.

Le Conseil national de recherches du Canada accorde aux particuliers le droit de faire des copies individuelles pour leur usage personnel. Toute personne peut reproduire de courts extraits des articles de la Revue pour autant que les droits moraux de l'auteur soient respectés et que la mention de provenance soit clairement indiquée. Il est de convenance de demander le consentement de l'auteur avant de faire mention de son travail.

On obtiendra l'autorisation de reproduire des articles à d'autres fins que l'usage personnel (tel qu'on l'a décrit ci-dessus) auprès du Conseil national de recherches du Canada pour autant que des redevances de droits d'auteurs de 7,00 $/copie soient versées au CANCOPY, 1, rue Yonge, bureau 1900, Toronto, ON M5E 1E5, Canada.

*La permission ci-dessus ne s'applique pas à la reproduction à grande échelle, telle que la reproduction aux fins de distribution générale, publicitaire ou promotionnelle, de compilation de nouveaux ouvrages collectifs ou de revente. Dans de tels cas, il faudra ratifier une entente particulière avec l'éditeur, le Conseil national de recherches du Canada, Ottawa, ON K1A 0R6, Canada.

Subscription information

The *Canadian Journal of Fisheries and Aquatic Sciences* (ISSN 0706-652X) is published monthly by the National Research Council of Canada. 2002 annual subscription rates (second class postage) for Canada are $732CAN institutional and $227CAN personal, for US & foreign $732US institutional and $227US personal. For air mail add $175US to foreign rate. Canadian customers please include 7% GST (business no. 12149 1807 RT 0275). Subscriptions are entered for the calendar year. Remittances should be made payable to the Receiver General for Canada credit NRC. Price for regular single issues: institutional, $95.00; personal, $30.00. Supplements will be priced separately. Special rates apply to members of Canadian scientific and engineering societies if they subscribe through their respective societies.

There are no refunds on cancelled subscriptions once delivery has begun. Claims for missing issues should be made within four months (N. America) or six months (outside N. America) following the date of publication. The publisher expects to supply missing issues only when losses have occurred in transit and when the reserve stock will permit. For change of address and subscription enquiries: Subscription Office, NRC Research Press, National Research Council of Canada, Ottawa, ON K1A 0R6, Canada; tel.: 613-993-9084; fax: 613-952-7656; e-mail: research.press@nrc.ca.

Microform backfiles are available from UMI, P.O. Box 1346, Ann Arbor, MI 48106-1346, U.S.A., and Micromedia Ltd., 20 Victoria St., Toronto, ON M5C 2N8, Canada.

All issues of the *Canadian Journal of Fisheries and Aquatic Sciences* since 1996 are available on the Web. Pricing information can be found at http://cjfas.nrc.ca.

Renseignements sur l'abonnement

Journal canadien des sciences halieutiques et aquatiques (ISSN 0706-652X) est une publication mensuelle du Conseil national de recherches du Canada. Le prix de l'abonnement annuel au Canada (courrier de deuxième classe) est de 732 $CAN pour les organismes et de 227 $CAN pour les particuliers. À l'étranger (y compris les É.-U.), le prix de l'abonnement est de 732 $US pour les organismes et de 227 $US pour les particuliers. L'expédition par avion exige des frais de 175 $US en sus du prix d'abonnement à l'étranger. Les clients du Canada doivent ajouter la TPS de 7% (numéro d'entreprise 12149 1807 RT 0275). Les abonnements sont pour l'année civile. Tout paiement doit être adressé au Receveur général du Canada, crédit du CNRC. Le prix par numéro est de 95 $ pour les organismes et de 30 $ pour les particuliers. Le prix des hors-série varie. Les membres des sociétés canadiennes de sciences et de génie bénéficient de taux préférentiels en s'abonnant via leurs sociétés respectives.

Aucun remboursement ne sera accordé ni aucune annulation acceptée une fois que les livraisons auront commencé. Les réclamations de numéros manquants devront être soumises dans les quatre mois (Amérique du Nord) ou dans les six mois (à l'extérieur de l'Amérique du Nord) suivant la date de publication. L'éditeur ne fournira de numéros manquants que si le document a été perdu pendant l'expédition et que si le stock le permet. Adressez tout changement d'adresse ou toute question quant à l'abonnement au : Bureau des abonnements, Presses scientifiques du CNRC, Conseil national de recherches Canada, Ottawa, ON K1A 0R6, Canada; téléphone : 613-993-9084; télécopieur : 613-952-7656; courriel : presses.scientifiques@nrc.ca.

On peut obtenir les fichiers rétrospectifs sur **microforme** auprès de UMI, P.O. Box 1346, Ann Arbor, MI 48106-1346, É.-U., et auprès de Micromedia Ltée, 20 rue Victoria, Toronto, ON M5C 2N8, Canada.

À partir de 1996, tous les numéros de *Journal canadien des sciences halieutiques et aquatiques* sont accessibles sur le Web. On trouvera des renseignements sur les tarifs à http://jcsha.cnrc.ca.

Channel head dynamics: capelin (*Mallotus villosus*) aggregation in the tidally driven upwelling system of the Saguenay – St. Lawrence Marine Park's whale feeding ground

Yvan Simard, Diane Lavoie, and François J. Saucier

Abstract: Capelin (*Mallotus villosus*) tridimensional distribution at the head of the Laurentian Channel in the St. Lawrence estuary was investigated using 38- and 120-kHz acoustic surveys in the summers of 1994, 1995, 1997, and 1998. The results are interpreted with the help of a high-resolution tridimensional tidal circulation model. Total biomasses were small (93–4583 t) and showed rapid fluctuations, whereas mesoscale distribution was more constant. Capelin tended to occupy the very end of the channel head, especially the slopes and shallows surrounding the basins. This pattern did not coincide with the krill distribution, but the two total biomass series were significantly correlated. Capelin tidal dynamics is characterized by herding of capelin against the channel head slopes by the starting flooding currents, followed by an upwelling over the sills and shallows during maximum flood currents, and a return to the channel by the surface outflow during ebb. Each side of the channel head has a distinct capelin retention tidal cycle involving passive advection, swimming, and the two-layer estuarine circulation. This capelin distribution and tidal dynamics closely match the local fin whale (*Balaenoptera physalus*) and minke whale (*Balaenoptera acutorostrata*) distributions observed from the whale-watching fleet and typical tidal feeding strategies at the channel head.

Résumé : La répartition tridimensionnelle du capelan (*Mallotus villosus*) à la tête du Chenal Laurentien dans l'estuaire du Saint-Laurent a été examinée à l'aide de missions acoustiques (38 et 120 kHz) aux étés 1994, 1995, 1997 et 1998. Les résultats sont interprétés à l'aide d'un modèle tridimensionnel à haute résolution des courants de marée. La biomasse totale était faible (93–4583 t) et fluctuait rapidement, alors que la répartition à méso-échelle était plus constante. Le capelan tendait à occuper la toute fin de la tête du chenal, spécialement les talus et les hauts-fonds entourant les bassins. Cette répartition ne coïncidait pas avec celle du krill, mais les deux séries de biomasse étaient significativement corrélées. La dynamique du capelan pendant un cycle de marée est caractérisée par un rassemblement contre les talus à la tête du chenal par les courants au début du flot, suivie par un saut au-dessus des hauts-fonds pendant le maximum du flot et d'un retour au chenal par les courants de surface sortant pendant le jusant. Chaque côté de la tête du chenal est caractérisé par une boucle distincte de rétention du capelan sur un cycle de marée, chacune faisant intervenir l'advection passive, la nage et la circulation estuarienne en deux couches. Cette répartition du capelan et sa dynamique en fonction du cycle de marée sont étroitement appariées avec la répartition locale des rorquals communs (*Balaenoptera physalus*) et des rorquals nains (*Balaenoptera acutorostrata*) observée par la flottille des bateaux d'observation ainsi qu'avec leurs stratégies typiques d'alimentation en relation avec le cycle de marée.

Introduction

Ocean upwelling systems are environments where biological production and transfer through the food web is strongly enhanced compared to surrounding areas (Hagen and da Silva 1995). Likewise, topographic features such as shelves, sea-mounts, banks, canyons, and sills affect circulation in various ways that control oceanographic processes, enhancing the regional production and generating spatial structures that are fundamental for energy transfer to higher trophic levels (e.g., Genin et al. 1994; Mackas et al. 1997; Wiebe et al. 2001). Such special oceanographic areas are most generally sites where fish aggregate and intensive fishing occurs. The head of the Laurentian Channel (LC) in the St. Lawrence estuary (Fig. 1) is such an area where intense upwelling is maintained by the interaction of the tidal circulation with shallow topographic features obstructing the upstream flow during flood (Saucier and Chassé 2000 and references therein). Complex local hydrodynamics spins out a simple pelagic trophic pathway involving zooplankton,

Received 24 July 2001. Accepted 12 December 2001. Published on the NRC Research Press Web site at http://cjfas.nrc.ca on 7 February 2002.
J16460

Y. Simard,[1] D. Lavoie, and F.J. Saucier. Department of Fisheries and Oceans, Maurice Lamontagne Institute, P.O. Box 1000, 850 Route de la Mer, Mont-Joli, QC G5H 3Z4, Canada.

[1]Corresponding author (e-mail: simardy@dfo-mpo.gc.ca).

 DOI: 10.1139/F01-210 © 2002 NRC Canada

Fig. 1. Map of the study area showing the systematic sampling grid with primary (single letters) and secondary (double letters) acoustic transects. The polygon (broken line) delimits the 1319-km^2 study area used for biomass estimation. Sa, Sb, and Sc indicate sills a, b, and c, respectively. (*a*) Transects in delimited subareas were subject to repeated surveys on a semidiurnal tidal cycle on 10 August 1995, 23 May 1998, and 12 August 1997. (*b*) The two capelin (*Mallotus villosus*) retention cells N and S are identified.

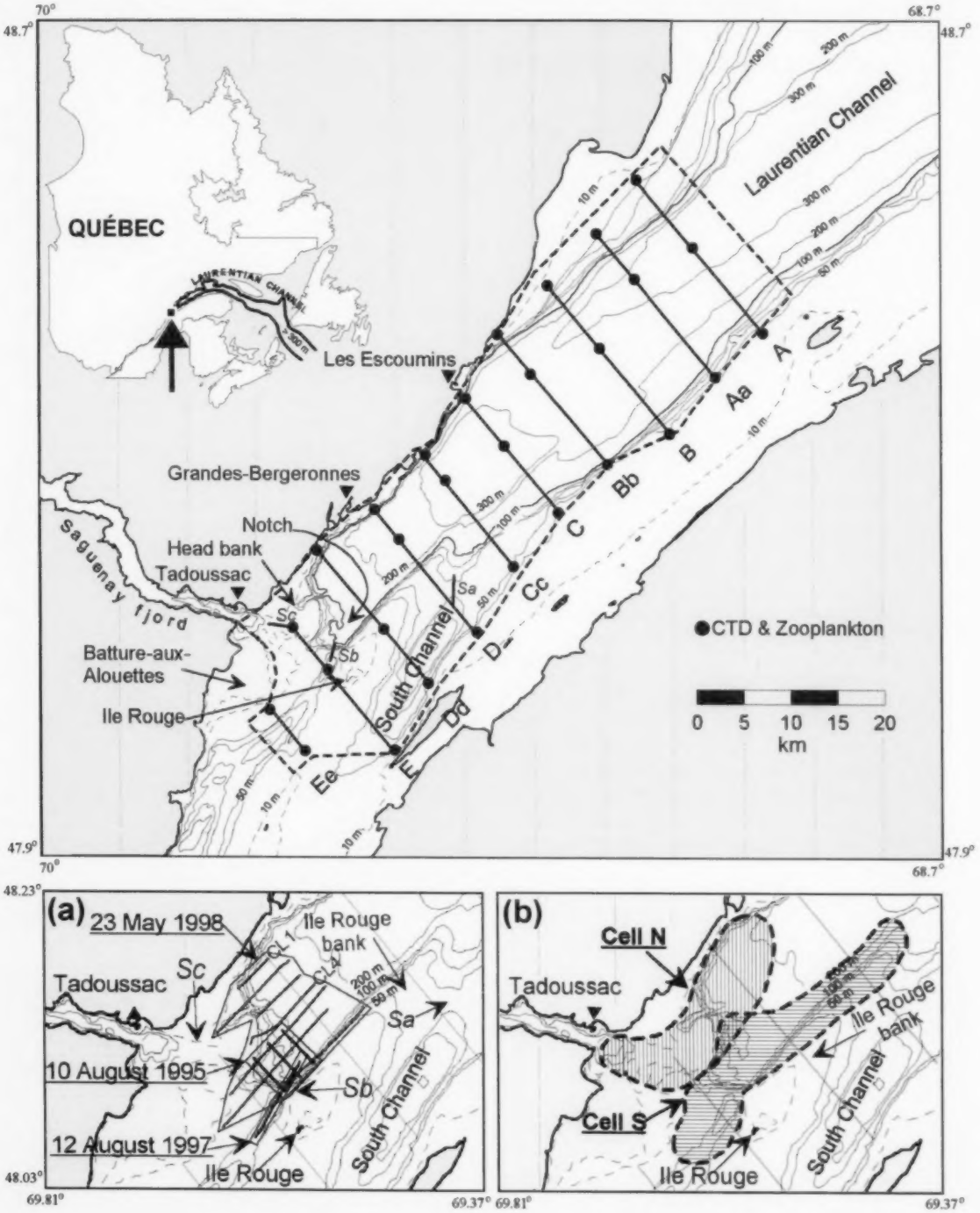

© 2002 NRC Canada

capelin (*Mallotus villosus*), and whales. The region is the site of a rich and persistent zooplankton aggregation (Simard and Lavoie 1999) resulting from the pumping of krill by the strong estuarine two-layer circulation (Saucier and Chassé 2000 and references therein), and its concentration–aggregation by the intense tidally driven upwelling and other hydrodynamic processes that are closely linked to the local topographic features (Lavoie et al. 2000). The shallows at the head of the LC are known aggregation areas for juvenile capelin, where they often form dense shoals and concentration peaks along fronts in the upper water column (Bailey et al. 1977; Ménard 1998; Marchand et al. 1999).

Local aggregations of both krill and capelin attract several species of baleen and toothed whales, which for centuries have gathered in this region during summer (Lavigueur et al. 1993; Turgeon 1994; Michaud et al. 1997). This traditional whale feeding ground has become over the last decade one of the most important whale-watching sites in the world, attracting more than 300 000 ecotourists annually (Anonymous 2000). The baleen whales most frequently observed by the whale-watching fleet at the head of the LC in the vicinity of Tadoussac, the main starting port, are fin whales (*Balaenoptera physalus*) and minke whales (*Balaenoptera acutorostrata*) (Michaud et al. 1997). The ecotourism industry targets the large species, especially fin whales. The observations of fin whales at the LC head are concentrated in a 1- to 4 km-wide band around the LC slope, upstream of transect D (Fig. 1) (Michaud et al. 1997). Higher concentrations in 1994 to 1996 summers were found at the LC head northern corner, a small basin nicknamed the Notch on the lee side of sill b, and the end of Ile Rouge bank, including south channel mouth (Fig. 1). The tracking of 25 tagged fin whales has shown that the whales are closely aligned along the 100-m depth contour at maximum flood, where their feeding dives are U-shaped and deeper than 50 m (Michaud and Giard 1998). This slope concentration is then gradually reduced, up to a widespread dispersion of whales over the channel head at low water. Though minke whales were also present in this LC slope band, they were more frequently observed over the shallows, on the boats' sailing path to and from Tadoussac (Michaud et al. 1997). If zooplankton abundance and their aggregation mechanism are now better known, this is not the case for the more mobile juvenile capelin, whose biomass, distribution, short-term variability, and links with the local hydrodynamic regime and whale feeding remain elusive. The present paper is a contribution to address these questions from a hydroacoustic and oceanographic data set acquired in the region since 1994. The observed capelin distribution is interpreted using the tidal current structure from the high-resolution three-dimensional circulation model of the St. Lawrence estuary (Saucier and Chassé 2000).

Material and methods

Sampling

Capelin biomass was measured by echointegration at 120 kHz. The main sampling was done in the summers of 1994 and 1995 on a regular grid of 10 transects crossing the head of the LC over a study area of 1319 km^2 (Fig. 1). The grid was visited eight times over four surveys. The surveys were in daytime only to facilitate the separation of fish echoes from krill echoes. A complete visit of the grid took two days under optimal conditions, and at times a few secondary transects were omitted because of time constraints (Table 1; Fig. 1). A grid of stations (Fig. 1) was sampled during each survey to acquire CTD (conductivity, temperature, depth) profiles (Lavoie et al. 1996) and zooplankton samples over the entire water column. Besides this main survey design, finer sampling was used to get denser spatial and temporal data around the LC head shallows where the fish were concentrated. This sampling included, among others: repeated surveys on 10 August 1995 of a small grid over a semidiurnal tidal cycle in the Notch, where the upstream flow converges during floods; a 12-h time series of a longitudinal transect over sill b on 12 August 1997; and two surveys of the LC head at flooding and ebbing tides on 23 May 1998 (Fig. 1*a*). Overall, more than 500 h of acoustic data were recorded. During 1994 survey 3 and in 1997, an ADCP (acoustic Doppler current profiler) (150 kHz or 600 kHz, RD Instruments, San Diego, Calif.) was used to record the currents along the ship tracks.

The acoustic echointegration system was composed of a Biosonics 102 echosounder, equipped with two dual-beam transducers operating at 120 kHz (3.3° and 10°) and 38 kHz (10° and 25°), except for the second visit of survey 3, where only the 120 kHz was used. In 1998, the 38-kHz data were collected from a Simrad EK500 7° split-beam system. Ping repetition rate was 1 s^{-1} and pulse duration was 0.5 ms. The echosounders were linked to computers, via a Biosonics ESP A/D interface and ESP-EI echointegration software (Biosonics, Inc., Seattle, Wash.) in 1994 and 1995 and through CH1 software (Simard et al. 1998) in 1997–1998, which simultaneously recorded positions from GPS (global positioning system) or DGPS (differential GPS) receivers. At the beginning of each survey, the ambient noise level at the survey speed was recorded for each frequency, with the transducers in passive mode (i.e., not transmitting). ESP-EI and CH1 used an echo intensity threshold profile slightly higher than the noise level profile for data acquisition. The systems were regularly calibrated using the standard sphere method for each frequency (Foote et al. 1987), and the calibrations were consistent throughout the series.

For 1994–1995, echointegration (MacLennan and Simmonds 1992) along transects from the narrow beam of the transducers was done with ESP-EI on 5-m-thick vertical strata over most of the water column, and 1-m-thick strata over the bottom 30 m. Horizontally, echointegration was done every 10 s or 20 s depending on the visit; corresponding distances are given in Table 1. For 1997 and 1998 data, the analysis was done with CH2 software (Simard et al. 2000) on the high-resolution HAC standard data format (Simard et al. 1997), with 1-m bins vertically and 10 s horizontally.

Fish were sampled with small-mesh midwater trawls by the CCGS *Calanus II* (20 m, FRV trawler). In 1994 and 1995, a Marinovich trawl was used. In 1998, the trawl was a Nordsea small midwater trawl. Both trawl codends had a 5–6 mm mesh liner. They were equipped with a Scanmar CGM4-SRU-01 acoustic trawl monitoring system (Scanmar AS, Åsgårdstrand, Norway). The number of hauls (n = 39) was limited because of the difficulty of trawling in presence of strong shearing currents and complex topography, but it

© 2002 NRC Canada

Table 1. Survey attributes for each visit of the main sampling grid in 1994–1995 and the echo classification used over the transects.

	Survey 1, Visit No.		Survey 2, Visit No.		Survey 3, Visit No.		Survey 4, Visit No.	
	1	2	1	2	1	2	1	2
Dates	28–29 June 1994	2–3 July 1994	26–27 July 1994	31 July – 1 Aug. 1994	24–25 Aug. 1994	28–29 Aug. 1994	7–8 Aug. 1995	17–18 Aug. 1995
Days from last spring tide	4–5	8–9	2–3	7–8	2–3	6–7	10–11	5–6
Transect No.	7	7	8	10	7	7	9	10
Speed (kn)	~6	~6	~8	~8	~6	~6	~8	~8
Echointegration unit (m)	~30	~30	~80	~80	~60	~30	~80	~80
B_z No.	2904	2673	1520	1931	1536	3160	1757	2050
Classification: krill or fish								
Depth <35 m	C1	C1	C1	C1	C1	Fish	C1	C1
Depth >35 m	C3	C2	C1	C1	C1	C3	C4	C2

Note: C1: 120–38 kHz s_v ratio on transects A–Dd, fish on transects E and Ee; C2: krill on transects A–Dd, fish on transects E and Ee; C3, krill on transects A–D and 35–105 m on transect Dd, fish on transects E and Ee and >105 m on transect Dd; C4, krill on transects A–D and >105 m on transect Dd, fish on transects E and Ee and 35–105 m on transect Dd.

was sufficient to get the species and length compositions of fish responsible for the dominant sound backscattering. The catch was weighted and subsamples were used to measure the fish length, weight, and other biological characteristics, either immediately at sea or later in the laboratory.

Data analysis

The acoustic data were handled as in Simard and Lavoie (1999). Cleaned volume backscattering coefficients (s_v) were corrected for the absorption (François and Garrison 1982) and sound speed profiles associated to the vertical structure of the water column (Lavoie et al. 1996). Krill echoes were sorted out using the s_v ratio at the two frequencies, and with high-resolution echograms in some cases (see Table 1, and Simard and Lavoie 1999). Since 2-year-old (and 1-year old, on occasions) capelin strongly dominated the catch associated to the fish echo traces (Marchand et al. 1999; Y. Simard, unpublished data 1998), the remaining s_v at 120 kHz was used for the present capelin biomass estimates. Local capelin target strength (TS) as function of fish length and acoustic frequency was obtained from backscattering models and in situ single target tracking (Y. Simard, J.K. Horne, D. Lavoie, and I. McQuinn, unpublished data). This TS vs. length function gave a s_v-to-biomass conversion factor ($\overline{TS}_w$) of –31.5 dB·kg^{-1} when combined with the consistent length–frequency distribution observed in this region in summer from the trawl samples and the average length vs. weight relationship ($w_g = 9.4986 \cdot 10^{-7} \cdot TL_{mm}^{3.2628}$, where TL is the fresh total length; see Lambert and Bernier 1989). TS analysis showed that this average conversion factor is a few dBs smaller at 120 kHz compared with 38 kHz, the difference being length dependent. This conversion factor was used throughout this study to transform the backscattering energy in capelin biomass.

The biomass·m^{-3} ($B = s_v/10^{\overline{TS}_w/10}$) was integrated over the water column to get the total biomass·m^{-2} (B_z) for the echointegration units along transects. Total biomass estimates over the study area ($\hat{B}T_v$) and maps were computed for each visit (v) of the survey grid using the following geostatistical methods (Chiles and Delfiner 1999). Ordinary point kriging over a 1 km mesh grid, made of 1319 nodes (Figs. 1 and 2), was used for the total biomass estimations. Since capelin local distribution was slightly related to bathymetric contours, cokriging (Marcotte 1991) with the bottom depth as an auxiliary variable was used to compute the maps. The experimental variograms (γ) computed for each visit ignored a few outliers. In modelling the variograms, the nugget term was augmented by the equivalent reduction of variance this procedure accounted for, as suggested by Rivoirard et al. (2000). The kriging elliptic neighbourhood (axes 4 × 16 km) was oriented along the main axis of the estuary. The search was done by iteration on four quadrants to get a maximum of eight observations belonging to at least two quadrants. The total biomass estimates over the study area for each visit ($\hat{B}T_v$) were obtained by expanding the mean of the kriged local estimates at the n nodes of the grid ($\hat{B}_{z_v}$) to the surface (A) of the etimation polygon (1319 km^2)

$$(1) \qquad \hat{B}T_v = \frac{1}{n}\sum_{1}^{n} \hat{B}_{z_v} \cdot A$$

where n represents the number of local estimates.

The estimation variance is obtained from the geostatistical equation

$$(2) \qquad \sigma^2_{\hat{B}_{z_v}} = 2\overline{\gamma}(x_{va}, S) - \overline{\gamma}(S, S) - \overline{\gamma}(x_{va}, x_{vb})$$

where $\overline{\gamma}$ is the average value of the variogram, x_{va} stands for an iteration over all observations, x_{vb} stands for an iteration over all pairs of the observations, and S is the estimation polygon.

The estimation standard deviation and the 95% confidence limits of the mean are expanded to the estimation polygon by multiplying by its area to get the error statistics of the total estimates $\sigma_{\hat{B}T_v}$ and $CI95\%_{\hat{B}T_v}$.

Three-dimensional circulation model

The three-dimensional circulation model used to interpret the capelin distribution is described in Saucier and Chassé (2000). It reproduces the circulation and density changes associated with tidal propagation and river runoff in the upper and lower Estuary (about 380 km in distance), including the Saguenay Fjord, with a 400-m horizontal resolution and 20 layers in the vertical. The model has been validated through comparisons with various current measurements and is at the origin of the St. Lawrence tidal current atlas (Canadian Hy-

© 2002 NRC Canada

Fig. 2. Maps of the vertically integrated capelin biomass in the systematic survey area during the eight visits in 1994 and 1995. Kriging grid mesh: 1 km × 1 km. The fortnightly tidal phase (number of days after spring (S) or neap (N) tide) is indicated for each visit.

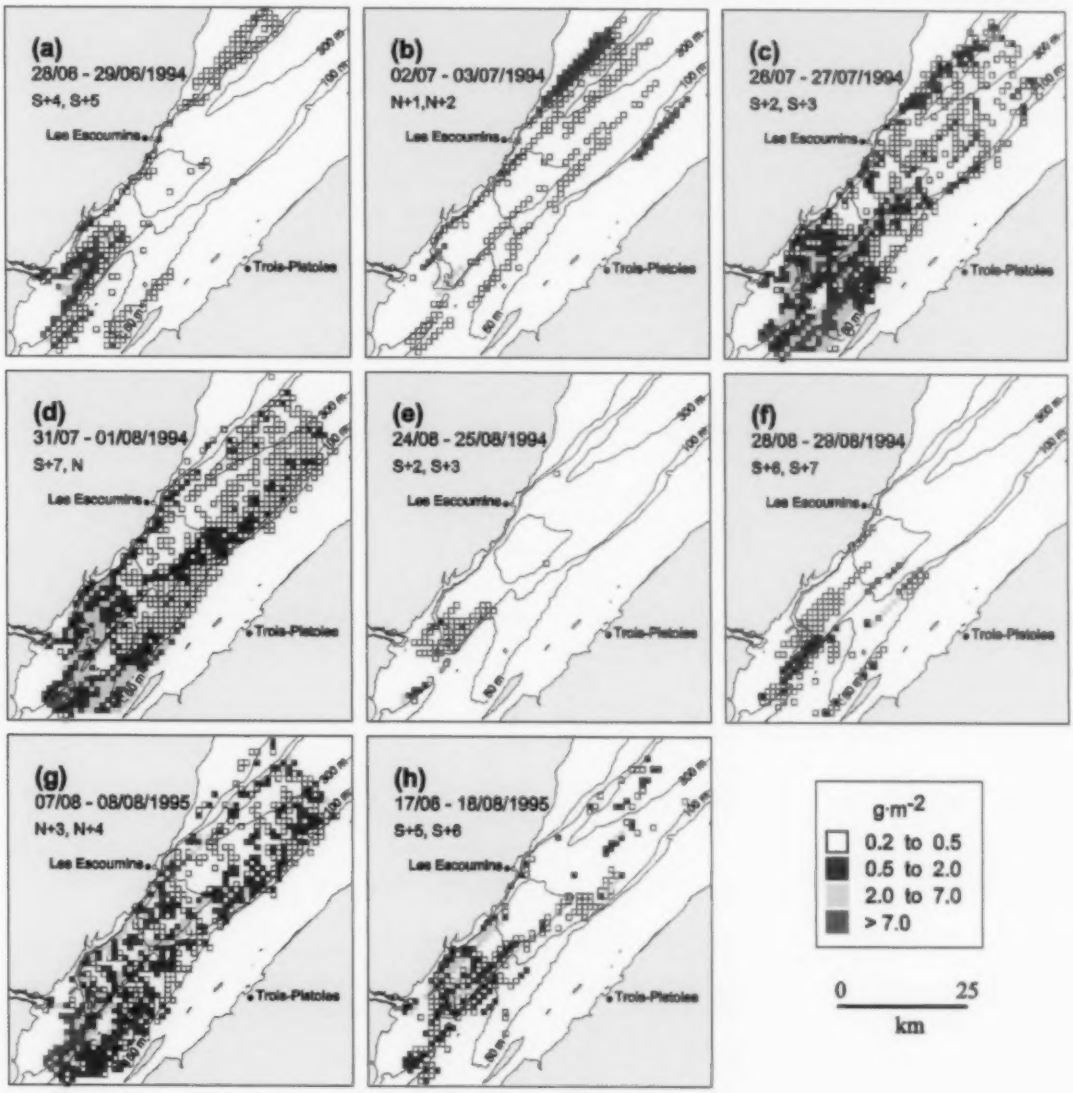

drographic Service 1997; Saucier et al. 1999). Hourly currents for a typical semidiurnal cycle (M_2) of mean tidal range were used for the present paper.

Results

Capelin total biomass estimates in the study area in 1994–1995 varied widely, up to a factor of almost 50 from a maximum of 4.583 kt in late July 1994 to a minimum of 0.093 kt one month later (Table 2). Their ranking was significantly positively correlated (Kendall's $\tau = 0.643$, $p < 0.05$) with the corresponding simultaneous total krill biomass estimates from Simard and Lavoie (1999). The coefficients of variation ($\sigma_{\hat{B}T_v}/\hat{B}T_v$) were large, ranging from 22% to 95% over the eight estimates. The spatial distribution was less variable, with the major part of the biomass found in the upstream third of the study area on seven of the eight visits (Fig. 2). Densities always increased around the ~50-m depth margin of the basins throughout the study area. Densest aggregations were most generally found over the shallows (<50-m depth) around the LC heading shoals, both during the systematic surveys and the additional sampling. The plateau northeast of Les Escoumins is another notable area where significant concentrations were found at the beginning of the summer (Figs. 2*a*–2*c*). In the downstream part of the study area, capelin were present in low density in the upper 20 m of the water column, above the thermocline, more

© 2002 NRC Canada

Table 2. Estimates of total biomass ($\hat{BT}_v$) in the study area for the eight visits of the main sampling grid in 1994 and 1995.

	Survey 1, Visit No.		Survey 2, Visit No.		Survey 3, Visit No.		Survey 4, Visit No.	
	1	2	1	2	1	2	1	2
Dates	28–29 June 1994	2–3 July 1994	26–27 July 1994	July 31 – 1 Aug. 1994	24–25 Aug. 1994	28–29 Aug. 1994	7–8 Aug. 1995	17–18 Aug. 1995
Total biomass								
$\hat{BT}_v$ (t)	260	240	4583	1047	93	210	2108	370
$\sigma_{\hat{BT}_v}$ (t)	58	28	2312	263	88	67	838	158
$CI95\%_{\hat{BT}_v}$ (t)	[146,374]	[184,295]	[53,9114]	[531,1562]	[0,265]	[80,341]	[465,3752]	[60,680]

Fig. 3. Sketches of the general capelin (*Mallotus villosus*) distribution and currents over the semidiurnal tidal cycle (see text). White arrows indicate upper water column currents, and the yellow arrows are for the deeper layer currents. White lines on bottom project transects Dd and L1–L3. The red aggregates nonexhaustively locate capelin observed on a number of echograms. Inset (b1) of a 120-kHz S_v binned echogram of capelin and krill upwelled over the end of Ile Rouge bank from 3 h after LW to HW on 15 August 1995, along a track sampled by a tagged fin whale (*Balaenoptera physalus*).

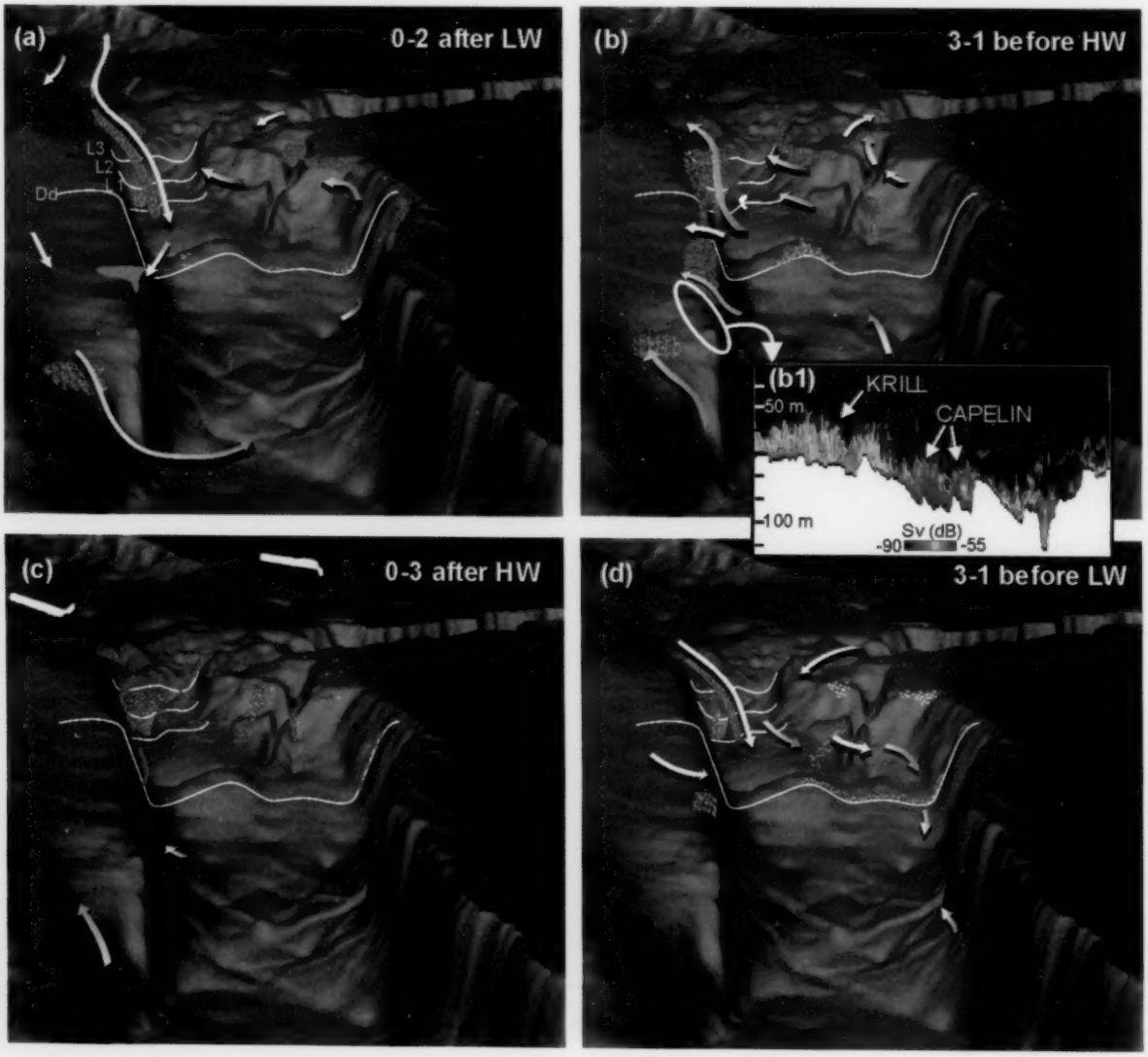

© 2002 NRC Canada

Fig. 4. Vertical current structures at transect Dd and maps of vertically integrated currents in the area for layers where the capelin (*Mallotus villosus*) aggregations are found over a semidiurnal tidal cycle. Transects Dd and L1–L3 of Fig. 6 are superimposed on the maps. The rectangle on the vertical cross-sections indicates the area corresponding to the echograms of Fig. 6. Current speeds in $m \cdot s^{-1}$.

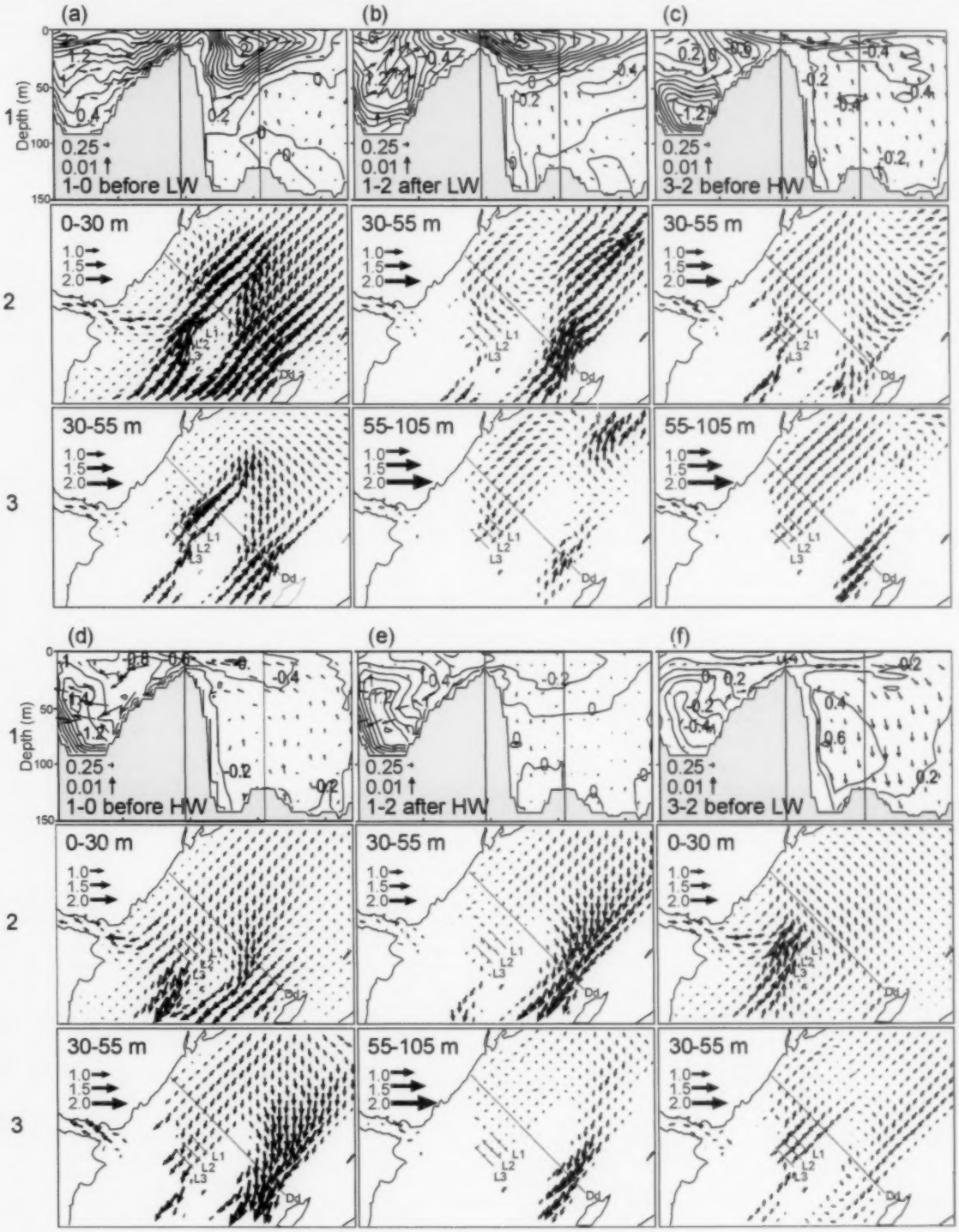

© 2002 NRC Canada

frequently during the rich periods, and often with peak concentrations at the frontal interfaces between the different surface water masses (see Marchand et al. 1999).

The analysis of the acoustic data with the modelled M_2 tidal currents led to the following conceptual model for capelin distribution and movement dynamics at the LC head, upstream of the junction with the south channel (Figs. 1 and 3). We distinguish two main distribution cells: cell N on the LC northern side, and cell S on the LC southern side, which includes the Notch and the northwestern flank of Ile Rouge bank (Fig. 1*b*). The semidiurnal tidal cycle in these two cells proceeds as follows. At the end of ebb to the beginning of flood, 1 h before to 2 h after low water (LW), the downwelling of an intermediate density water mass into the LC from the south channel (see Lavoie et al. 2000) initiates an upstream current in the subsurface layers of the northern part of the LC head, which steers towards the south at the head bank (Figs. 3*a*, 4*a*, 4*b*). Currents along the north shore are then very weak in the upper water column (~0–30 m). Most cell-N capelin are then abutting the upper 75 m of the LC northern slope, with higher concentrations in the head northern corner and into sill-c depression towards the Saguenay entrance where the flow is advecting capelin (e.g., Figs. 3*a* and 5*a*). During the same period, cell-S capelin are subject to the strong surface outflow, which developed above the Notch a few hours earlier (Figs. 4*a*, 4*b*1, 4*f*), resulting in a different dynamics for cell-S capelin. Capelin found on the upstream shallows and in the surface layer concentrate in the convergence zone of the front formed at the southern edge of the jet, and are entrained downwards by the front vertical circulation cell (Figs. 4*a*1, 6*a*). During current reversal, around 1 to 2 h after LW, capelin move down along the slope of Ile Rouge bank (Figs. 6*b*2–3). The current vectors rotate clockwise and the flow begins to accelerate towards the Notch and Ile Rouge bank (transition between Figs. 4*b* and 4*c*). Capelin are advected by the flow and aggregate in a dense shoal along the slopes of Ile Rouge bank and sill b (Figs. 3*b*, 6*b*, 7*b*). In cell N, the capelin carried by the surface outflow from the shallows to the LC and the slope capelin are found in a layer capping the upward-forced zooplankton scattering layer (SL) (e.g., Fig. 5*c*). They are starting to be advected and herded towards the slope and the sills by the deeper currents. The capelin bottom shoal in the Notch may be stretched vertically by the vertical currents (Figs. 3*b*, 4*c*–4*d*, 6*c*). Tidal upwelling peaks during the 2 h preceding high water (HW) and moves the aggregating capelin on the slopes over sills c and b (e.g., Fig. 7*c*) and Ile Rouge bank, mainly in its deepest part near the south channel mouth (Figs. 3*b*, 3*b*1). Capelin are then often concentrated in a thin layer blanketing the slopes (e.g., Fig. 7*c*). From HW to 2 h after (Fig. 3*c*), more capelin are found upstream of the sills (e.g., Fig. 7*d*) and over the banks in both cells N and S, sometime in dense shoals (Figs. 2*c*, 2*d*, 2*g*), and those found in the Notch are concentrated in the lower part of the water column (Figs. 6*d* and 7*d*). Currents are still slowly upstream in the upper layer (Fig. 4*e*1) and the upwelled water mass still blocks the upper estuary outflow and frontal activity is still intense at the interface (e.g., Fig. 7*d*). Capelin aggregations are frequently observed near the fronts, notably at the Saguenay entrance (Marchand et al. 1999). Current reversal in the surface layer, upstream of transect Dd, starts 2–3 h after HW, and around 1 h later in the south channel (transition between Figs. 4*e* and 4*f*). The capelin found on the shallows are brought back over the LC channel in the surface layer (Fig. 5*b*), first in cell N by the outflow of the Saguenay, which partly merges with the forming surface jet above the Notch (Fig. 4*f*2). Cell-N capelin found over the head bank may then sometime merge with cell S. The northern side of this outflow is forced back towards the north shore, forming a loop that converges towards Grandes-Bergeronnes. A strong downwelling is observed in this region (Saucier and Chassé 2000). Capelin would eventually be entrained downward and then aggregated along the slope by the upstream currents generated by the density gyre (Fig 3*a*). This circulation pattern contributes to the retention of capelin in cell N. Capelin found on the shallows south of the Batture-aux-Alouettes will be brought back in over the LC by the strong surface jet (cell S; see beginning of this section). Downwelling of the upwelled waters also occurs and flushes the zooplankton SLs and deep capelin downstream (Figs. 3*d*, 4*f*, 6*e*1, 7*a*, and 5*d*). An internal undular jump developed at sill b (Fig. 7*a*) possibly concentrates surface capelin and other particles. Not shown on echograms, capelin is also often found in low density spread over the LC floor, mainly on the northern side (Fig. 3*d*).

Discussion

Total biomass and distribution patterns

Capelin total biomass in the study area was generally low, averaging 1.1 ± 1.6 kt (0.84 ± 1.18 t·km^{-2}). This represents only 2.0% ± 2.0% (range 0.3–6.0%) of the krill biomass over the same period (Simard and Lavoie 1999), which is the other whale's prey. The capelin capacity to feed a large number of whales in this area is thus limited compared with that of krill. Capelin concentrations higher than 2 t·km^{-2} were always observed around the LC head slope in summer, making this part of the study area more attractive for capelin-seeking predators. However, rich capelin concentrations were scarcer than rich krill concentrations, the richest 1% of the capelin densities per km^2 exceeding the mean krill density in only one out of the eight visits. The whale's interest for capelin may therefore not only rely upon areal density, but also on other foraging factors such as the prey density·m^{-3} and (or) the probability of capture.

The redistribution of capelin through the semidiurnal tidal circulation could produce some aliasing in biomass estimates, including biases owing to temporary concentration peaks and double counting. For instance, the third visit progressed upstream with the flood, and its biomass estimate might be inflated as a result of that. Future surveys of this area should benefit from denser and faster sampling, from more than one platform, to minimize the risk of advection-induced biases and to reduce the variance. Despite the errors in each estimate, the large variations in total capelin biomass and relative distribution were often significant. The loss and gain of capelin across the boundaries of the estimation polygon, either because of migrations or transport by currents, are the most probable cause for the total biomass fluctuations. Note that the surveys excluded near shore and shallow areas where the ship could not transit, which may be responsible for the exclusion of some fish schools.

© 2002 NRC Canada

Fig. 5. High-resolution 120-kHz S_v echograms of capelin (*Mallotus villosus*) (red) and krill (blue–green–orange) distributions on (*a* and *b*) transects CL1 and (*c* and *d*) CL4 at the head of the Laurentian channel during the flooding and ebbing tides on 23 May 1998 indicated on Fig. 1*a*. Arrows indicate relative current speeds and directions from the circulation model. Open circles indicate current directed through the sheet, crosses are entering. Time is EDT.

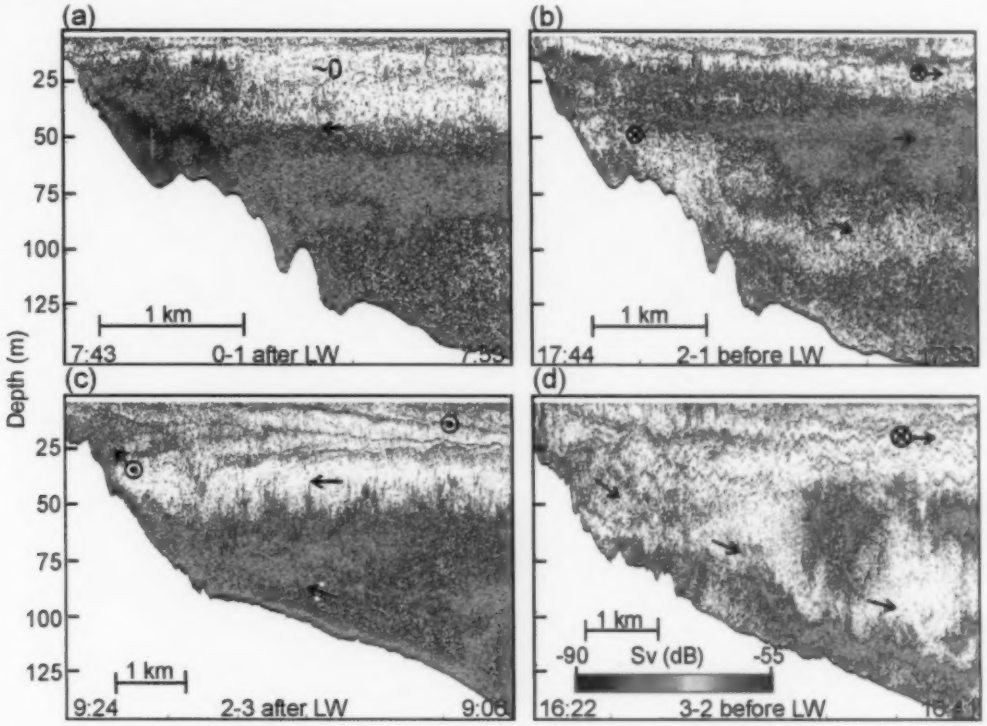

Bailey et al. (1977) suggested that the juvenile capelin found near the LC head migrate with the adults from the downstream source in Gulf of St. Lawrence (Jacquaz et al. 1977; Gagné and Sinclair 1990) in November. The rapid appearances and disappearances of most capelin between surveys showed that its residence time in the area is very short, of the order of weeks to months and perhaps shorter. Important redistributions over the Estuary and Gulf system may be more frequent than once per year. A juvenile capelin swimming at 1–2 body lengths (BL)·s^{-1} can cross the distance separating the LC head and the Gulf (~200 km) within about one to two weeks, taking into account the prevailing mean currents (Misund et al. 1993; Hafsteinsson and Misund 1995). The high correlation between the total biomass series for krill and capelin suggests that advection plays similar roles in determining their mesoscale distribution and abundance (see Lavoie et al. 2000), though at smaller scales, predator–prey coupling may also be important. Like krill, capelin probably exit the study area through the southern side of the LC, downstream of the retention cell S and the mouth of the south channel. A third capelin retention cell involving the strong two-layer tidal circulation may exist in the south channel, though it is not yet fully documented.

Upstream retention and M_2 tidal dynamics

The upstream retention of capelin at the LC head appears to be tightly linked to the tidal upwelling–downwelling dynamics and the capelin's own ability to redistribute in the vertical. The large variability in total biomass estimates over the area also suggests other changes at subtidal frequencies. Early during tidal flood the zooplankton SL is advected upstream and gradually lifted up along the LC slopes. It is then surrounded by the capelin from above and along its advancing margin, most likely for feeding (Ménard 1998). Cell-N capelin can then extend 3–4 km over the LC away from the head bank, a possible but difficult swimming distance in a couple of hours at 2–4 BL·s^{-1}. The surface outflow from the Saguenay entrance at the end of ebb can help bringing back the previously upwelled capelin over the shallows and extend their distribution away from the slope. This horizontal displacement could be associated with a dive to the top of the zooplankton SL to close the vertical loop of the retention cell. At the beginning of the upwelling, the capelin feeding isolumes are likely deepening because of the displacement of the surface waters by less opaque deeper waters (see Marchand et al. 1999). This should enhance the visibility of zooplankters by capelin at the top of the zooplankton SL (Kaartvedt et al. 1996 and references therein). Ménard's (1998) observations from a few trawl samples, showing that capelin stomach contents at the LC head were higher and fresher during flood and HW in daytime, give more credit to a flooding active feeding strategy. More intensive and complete sampling is required to test this hypothesis. Such tidal feeding should begin sooner in cell N than cell S according

© 2002 NRC Canada

Fig. 6. Semidiurnal time series of 120-kHz S_v binned echograms at transects L1–L3 shown on Figs. 1*a*, 3, and 4 on 10 August 1995. Time is EDT.

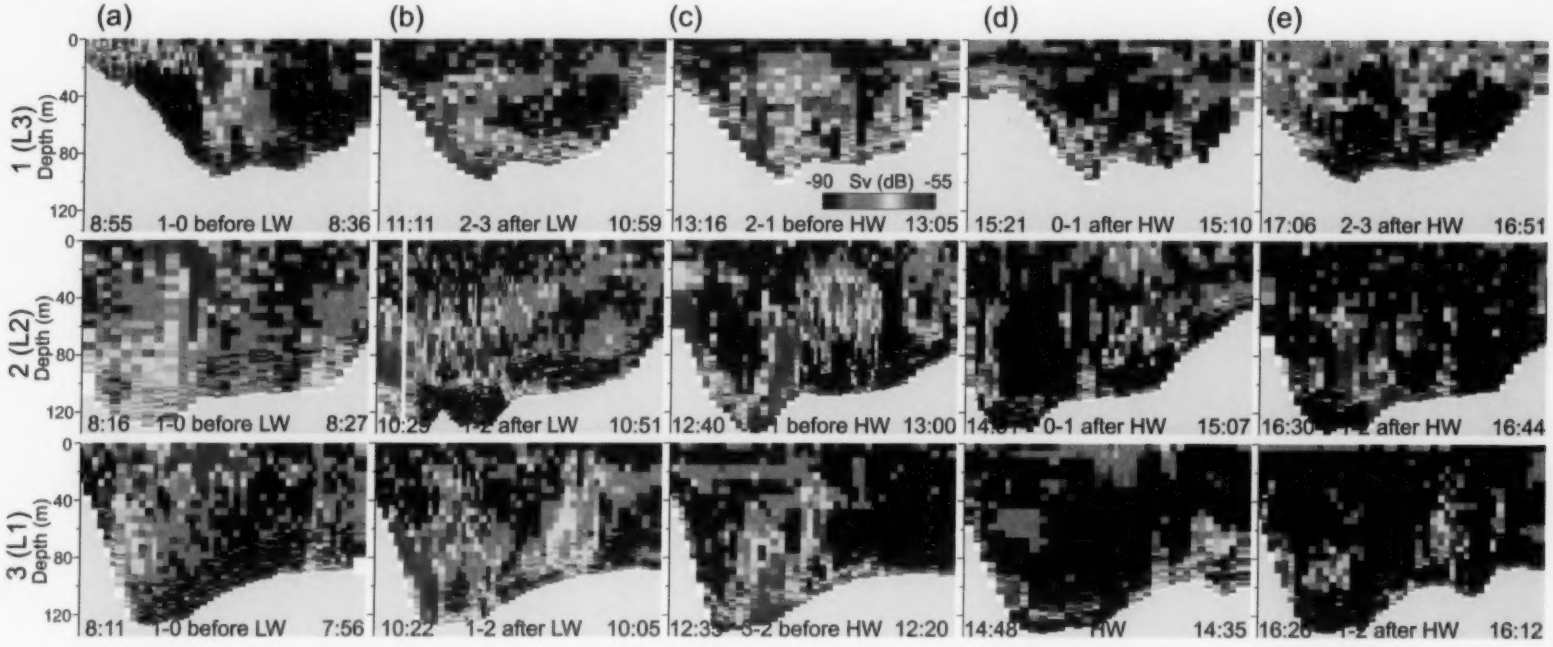

© 2002 NRC Canada

Fig. 7. High-resolution 120-kHz S_v echograms of capelin (*Mallotus villosus*) (most of echoes except the thin green and blue layers) showing (*a*) the downwelling during ebb and (*b–d*) upwelling over sill b during flood on a longitudinal transects over the Notch and sill b on 12 August 1997. Arrows indicate relative current speeds and directions from simultaneous ADCP measurements and the circulation model. Time is EDT.

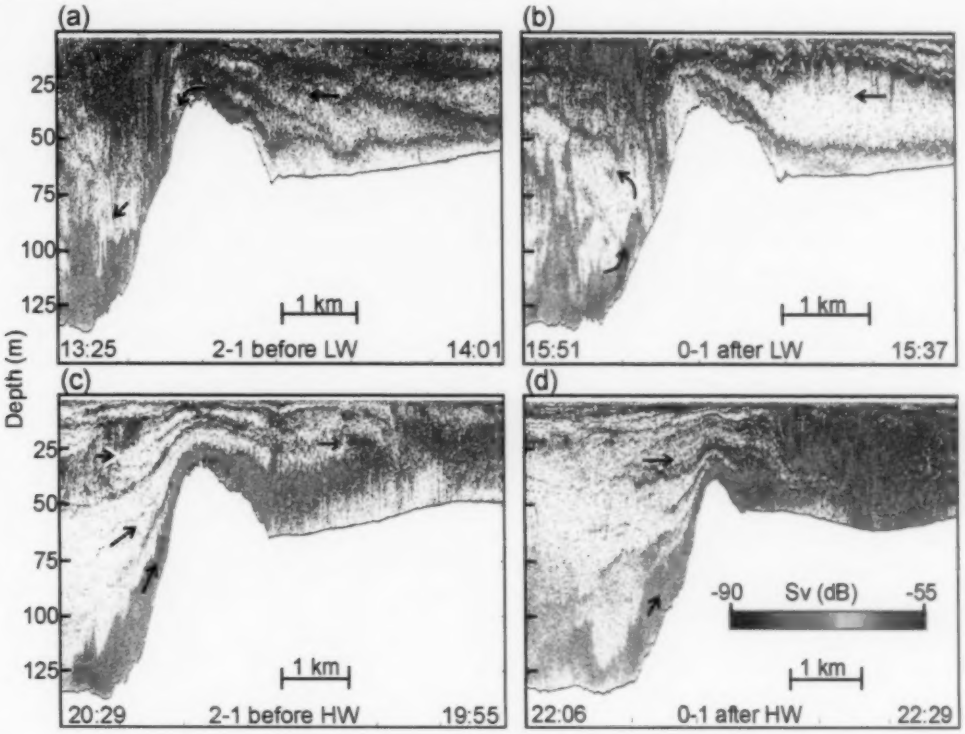

to the spatial progression of the tidal upwelling (Canadian Hydrographic Service 1997). Although capelin were generally found outside the CIL (cold intermediate layer, <2°C) temperature range (e.g., Marchand et al. 1999), they can be found closer to the coldest CIL temperature depths during this likely feeding period. Considering the horizontal distributions, though cell N appears to be closed by a return flow towards the north coast, losses of capelin towards the richer cell S are probable and likely significant at mid-term. The southward-directed flooding slope current at the head bank, the converging currents towards the Notch during flood, and the Saguenay transverse surface current during ebb all favour such exports. These capelin losses in cell N may in part be compensated by imports from downstream along the LC northern slope.

Capelin upwelling over the shallow areas during flood is also intense in cell S, but the set-up is distinct from cell N. In the Notch, 1–2 h after LW, capelin are found in the lower part of the water column close to the bottom, but were still in the downstream flowing surface jet 1 h earlier. Capelin appear to dive and (or) be entrained by the intense downwelling (propagating internal bore, see Saucier and Chassé 2000; Lavoie et al. 2000) to the deep layers along Ile Rouge bank just after LW. An active or passive vertical behaviour is essential to maintain their upstream position. Shortly after LW, vertical currents along the southern side of the surface jet where the capelin are concentrated reverse from >5 $cm \cdot s^{-1}$ downward to upward (see also Fig. 7 in Saucier and Chassé 2000), and the horizontal currents reverse in the deeper layers. Such a change in vertical forcing may be perceptible by capelin. The herding of capelin in the Notch by the converging strong flooding currents at depth can recruit within a radius of ~3–4 km (20 $cm \cdot s^{-1} \times 5$ h). The upstream part of this aggregated capelin at depth in the Notch, which is transported over sill b in a strong benthic boundary flow (about 1 $m \cdot s^{-1}$ during spring tides, F.J. Saucier, unpublished data) along the slope for ~2 h at maximum flood, is the source of the capelin brought back into the LC during ebb by the surface jet. This upwelled capelin can be transported upstream in the deeper layer by as much as ~5 km (0.75 $m \cdot s^{-1} \times 2$ h). The distance travelled by capelin advected in this ebb current during about 4 h at 0.5–1 $m \cdot s^{-1}$ is 7–14 km. While the first-upwelled capelin in a tidal cycle would still be in the Notch recruitment radius after this journey, the last-upwelled capelin leading the surface jet could be advected as far downstream as the end of Ile Rouge bank and the mouth of the south channel. Capelin excluded from the recycling in the Notch become involved in the upwelling over Ile Rouge bank and into the mouth of the south channel, where they could reside for some time before being recycled again in cell S or flushed further downstream. All these capelin come in contact with the upwelling zooplankton SL during flood and their food supply is not reduced. The capelin remaining at depth in the Notch are also in a rich food environment,

© 2002 NRC Canada

but the light conditions may not be favourable for predation. Feeding mechanisms other than visual predation may then be acting.

The other capelin found sporadically on the LC floor at depths <200 m, notably on transect Dd, could be involved in a larger-scale recirculation that is partly entrained by the cyclonic density gyre resulting from the discharge of tidally mixed waters from the south channel (see Lavoie et al. 2000). It could also result from diel vertical migrations of a subset of the capelin, possibly the adults (Gjosaeter 1998), or from a dive and (or) downwelling along the slopes. At these bottom depths, capelin are in the same ambient temperatures as those found in the upper water column, the CIL minimum temperature oscillating around 75 m (Lavoie et al. 1996). Another source of variability in the spatial distribution of capelin seems to be the presence of krill at the head of LC, upstream of transect Dd (see Lavoie et al. 2000). More capelin is found there when more krill is present (r^2 = 0.59). Whether this is related to common advective processes or to predator–prey relationships is unknown.

Significance for whales

The general distribution of fin whale observations by the whale-watching fleet and their concentration along the slope at the LC head closely match the capelin distribution. The LC head corner, the Notch, and the end of Ile Rouge bank and south channel mouth are the areas where the observations are concentrated (Mingelbier and Michaud 1996; Michaud et al. 1997). What else do the present results bring to the understanding of whale feeding dynamics on capelin? First, the typical tidal aggregation behaviour of fin whales at the LC head slopes observed some years in daytime (Michaud 1991; Mingelbier and Michaud 1996; Michaud and Giard 1998) likely depends on capelin availability to whales. We have shown that the availability would be imprinted by M_2 tidal fluctuations because a large part of the capelin is herded towards the slopes by the flooding currents before being transported over the shallows in the 2–3 h preceding HW. Then, basin and slope feeders such as fin whales loose parts of their resources to the benefit of minkes, well-known shallow-water and tidal-front specialized feeders (Gaskin 1982; Lynas and Sylvestre 1988; Piatt et al. 1989). In particular, whale feeding success at the mouth of the Saguenay should be higher in the 3 h preceding HW. The ability to capture capelin at the LC head should be enhanced during flood, as a result of this herding effect of the flooding and upwelling currents against the slopes and into the Notch, notably in the capelin-rich benthic boundary flow. The herding may be needed to reach the whale foraging threshold concentration (Piatt and Metven 1992) and enhance the school encounter probability by whales. The direction of motion of capelin is also predictable from the currents, an information that may be used by the whales to increase their capture rate (Parrish 1992). Capelin are also pushed towards the bottom boundary of the slope, which further limits their freedom of movement and eases their capture. Having to cope with fast-changing environmental conditions (pressure, temperature, light, food, currents, bottom proximity) and physiological adaptations (swimbladder volume, metabolic temperature, swimming effort, feeding), their escape capacity could be reduced. Yet, whales are gregarious during their feeding in this area around HW (Michaud 1991; Mingelbier and Michaud 1996). It is not yet clear how the limited extent of the capelin concentrations controls this behaviour as opposed to a synergetic feeding strategy among the whales. After the flood, there should be a time interval of few hours during ebb when fin whales' feeding success on capelin at the LC head is significantly reduced because of the disappearance of the slope aggregation mechanism. During the ebb the fin whales slope aggregation is relaxed and a downstream movement is observed (Mingelbier et al. 1995; Michaud and Giard 1998). Capelin that come back to the LC during ebb are doing so mostly through the surface layer. A break in whale feeding dive pattern time series should therefore mark the flood–ebb change at the LC head, as Giard and Michaud's (1997) data suggest. The frequency of shallow daytime dives for feeding on capelin should increase during ebb or dives could be temporarily interrupted, though deep dives directed towards bottom capelin could still be successful. Michaud and Giard (1998) observed a decrease in daytime dive depths starting 2 h after HW, with minimum values at LW ± 2 h. Night-time whale diving activity was also reduced and limited to the surface layer, a likely response to the vertical migration of capelin (Bailey et al. 1977) and their zooplankton preys, including the krill SL (Simard et al. 1985, 1986). Since capelin and krill (see Lavoie et al. 2000) concentrations are temporally and spatially structured in three dimensions over a wide range of scales in the study area, the whale dive depth patterns should reflect this. The tracks of tagged fin whales from Michaud and Giard (1997) clearly indicate convoluted spatial and temporal effects on the dive patterns. Consequently, the dive patterns should be carefully analysed for their space–time variability in the correct interpretation of the whale's response to anthropic or natural factors. For instance, the large fluctuations in capelin total abundance in the study area should affect this whale's tidal feeding dynamics at the LC head. The size of the LC head capelin "stock" unit is relatively small. Its carrying capacity for predators is therefore limited, especially given its inherent large variability. The interest of the LC head as a whale feeding ground also relies on another important resource, being the rich krill aggregation (Simard and Lavoie 1999) on which capelin feed and with which their total biomass covaries in the study area.

Acknowledgments

We thank the crews of the research and fishing vessels and the numerous persons who have participated in data collection and processing. We are indebted to D. Marcotte for geostatistical programs and helpful suggestions and also to Y. Gratton. Comments on the manuscript from J. Piatt and an anonymous reviewer were appreciated. This research was funded by the Department of Fisheries and Oceans and the St. Lawrence Vision 2000 program, project IML 113-94-9.

References

Anonymous. 2000. Etude socio-économique d'un secteur retenu pour l'identification d'une zone de protection marine pilote: Estuaire du Saint-Laurent. Tecsult Environment Inc. Rapport final à Pêche et

© 2002 NRC Canada

Océans Canada, Région Laurentienne. Tecsult Environnement Inc., 4700 Boul. Wilfrid-Hamel, Québec, QC G1P 2J9.

Bailey, R.F.J., Able K.W., and Leggett, W.C. 1977. Seasonal and vertical distribution and growth of juvenile and adult capelin (*Mallotus villosus*) in the St. Lawrence estuary and western Gulf of St. Lawrence. J. Fish. Res. Board Can. **34**: 2030–2040.

Canadian Hydrographic Service. 1997. Atlas of tidal currents: St. Lawrence Estuary, from Cap de Bon-Désir to Trois-Rivières. Department of Fisheries and Oceans, Canadian Hydrographic Service, Ottawa.

Chiles, J.-P., and Delfiner, P. 1999. Geostatistics, modeling spatial uncertainty. John Wiley & Sons, New York.

Foote, K.G., Knudsen, H.P., Vestnes, G., MacLennan, D.N., and Simmonds, E.J. 1987. Calibration of acoustic instruments for fish density estimation: a practical guide. ICES Coop. Res. Rep. No. 144.

François, R.E., and Garrison, G.R. 1982. Sound absorption based on ocean measurements: Part II: boric acid contribution and equation for total absorption. J. Acoust. Soc. Am. **72**: 1879–1890.

Gagné, J.A., and Sinclair, M. 1990. Marine fisheries resources and oceanography of the St. Lawrence estuary. *In* Oceanography of a large-scale estuarine system: the St. Lawrence. *Edited by* M.I. El-Sabh and N. Silverberg. Coastal and Estuarine Studies No. 39. Springer-Verlag, New York. pp. 358–377.

Gaskin, D.E. 1982. The ecology of whales and dolphins. Heinemann, London.

Genin, A., Greene, C., Haury, L., Wiebe, P., Gal, G., Kaartvedt, S., Meir, E., and Fey, C. 1994. Zooplankton patch dynamics: daily gap formation over abrupt topography. Deep-Sea Res. **41**: 941–951.

Giard, J., and Michaud, R. 1997. L'observation des rorquals sous surveillance par télémétrie VHF. Nat. Can. (Que.), **121**(2): 25–29.

Gjosaeter, H. 1998. The population biology and exploitation of capelin (*Mallotus villosus*) in the Barents Sea. Sarsia, **83**: 453–496.

Hafsteinsson, M.T., and Misund, O.A. 1995. Recording the migration behavior of fish schools by multi-beam sonar during conventional acoustic surveys. ICES J. Mar. Sci. **52**: 915–924.

Hagen, E., and da Silva, A.J. 1995. Dynamics of upwelling in the ICES area. ICES Coop. Res. Rep. No. 206.

Jacquaz, B., Able, K.W., and Leggett, W.C. 1977. Seasonal distribution, abundance, and growth of larval capelin (*Mallotus villosus*) in the St. Lawrence Estuary and northwestern Gulf of St. Lawrence. J. Fish. Res. Board Can. **34**: 2015–2029.

Kaartvedt, S., Melle, W., Knutsen, T., and Skjoldal, H.R. 1996. Vertical distribution of fish and krill beneath water of varying optical properties. Mar. Ecol. Prog. Ser. **136**: 51–58.

Lambert, J.D., and Bernier, B. 1989. Observations on 4RST capelin in the Gulf of St. Lawrence. (A retrospective, 1984–1987.) CAFSAC Res. Doc. 89/8.

Lavigueur, L., Hammil, M.O., and Asselin, S. 1993. Distribution et biologie des phoques et autres mammifères marins dans la région du parc marin du Saguenay. Rapp. Manuscrit Can. Sci. Halieut. Aquat. No. 2220.

Lavoie, D., Simard, Y., Benoit, J., Larouche, P., and Thibeault, B. 1996. Distribution des masses d'eau à la tête du Chenal Laurentien dans l'Estuaire du Saint-Laurent aux étés 1994 et 1995. Rapp. Tech. Can. Hydrogr. Sci. Océan. No. 176.

Lavoie, D., Simard, Y., and Saucier, F.J. 2000. Aggregation and dispersion of krill at channel heads and shelf edges: the dynamics in the Saguenay – St. Lawrence Marine Park. Can. J. Fish. Aquat. Sci. **57**: 1853–1869.

Lynas, E.M., and Sylvestre, J.P. 1988. Feeding techniques and foraging strategies of minke whales (*Balaenoptera acutorostrata*) in the St. Lawrence river Estuary. Aquat. Mamm. **14**: 21–32.

Mackas, D.L., Kieser, R., Saunders, M., Yelland, D.R., Brown, R.M., and Moore, D.F. 1997. Aggregation of euphausiids and Pacific hake (*Merluccius productus*) along the outer continental shelf off Vancouver Island. Can. J. Fish. Aquat. Sci. **54**: 2080–2096.

MacLennan, D.N., and Simmonds, E.J. 1992. Fisheries acoustics. Chapman and Hall, London.

Marchand, C., Simard, Y., and Gratton, Y. 1999. Concentration of capelin in tidal upwelling fronts at the head of the Laurentian channel in the St. Lawrence estuary. Can. J. Fish. Aquat. Sci. **56**: 1832–1848.

Marcotte, D. 1991. Cokriging with Matlab. Comput. Geosci. **17**: 1265–1280. (Corrigendum, Comput. Geosci. **19**: 871.)

Ménard, N. 1998. Répartition spatiale et structure des bancs de poissons pélagiques dans une aire d'alimentation des cétacés de l'estuaire du Saint-Laurent. M.Sc. thesis, Univ. Laval, Ste-Foy, Québec, Canada.

Michaud, R. 1991. Variations saisonnières de l'abondance des rorquals communs dans l'estuaire maritime du Saint-Laurent. Rapport final à Pêche et Océans Canada, Région du Québec. GREMM, 108 de la Cale Sèche, Tadoussac, QC G0T 2A0.

Michaud, R., and Giard, J. 1997. Les rorquals communs et les activités d'observation en mer des cétacés dans l'estuaire maritime du Saint-Laurent en 1994–1996. 1: Étude de l'utilisation du territoire et évaluation de l'exposition aux activités d'observation en mer à l'aide de la télémétrie VHF. Final report to Parks Canada, Canadian Heritage Department, Ottawa. GREMM, 108 de la Cale Sèche, Tadoussac, QC G0T 2A0.

Michaud, R., and Giard, J. 1998. Les rorquals communs et les activités d'observation en mer des cétacés dans l'estuaire maritime du Saint-Laurent en 1994–1996. 2: Évaluation de l'impact des activités d'observation en mer sur le comportement des rorquals communs. Final report to Parks Canada, Canadian Heritage Department, Ottawa. GREMM, 108 de la Cale Sèche, Tadoussac, QC G0T 2A0.

Michaud, R., Bédard, C., Mingelbier, M., and Gilbert, M.C. 1997. Les activités d'observation en mer des cétacés dans l'estuaire maritime du Saint-Laurent 1985–1996: une étude de la répartition spatiale des activités et des facteurs favorisant la concentration des bateaux sur les sites d'observation. Final report to Parks Canada, Canadian Heritage Department, Ottawa. GREMM, 108 de la Cale Sèche, Tadoussac, QC G0T 2A0.

Mingelbier, M., and Michaud, M. 1996. Étude des activités d'observation en mer des cétacés de l'estuaire maritime du Saint-Laurent: compte rendu de l'échantillonnage de 1995 et synthèse des données prélevées de 1984 à 1995. Final report to Parks Canada, Canadian Heritage Department, Ottawa. GREMM, 108 de la Cale Sèche, Tadoussac, QC G0T 2A0.

Mingelbier, M., Giard, J., and Michaud, R. 1995. Les rorquals communs et les activités d'observation dans l'estuaire maritime du Saint-Laurent: étude du comportement à l'aide de la télémétrie VHF; 1995: prenière saison d'échantillonnage. Report to Parks Canada, Canadian Heritage Department. Ottawa. GREMM, 108 de la Cale Sèche, Tadoussac, QC G0T 2A0.

Misund, O.A., Aglen, A., Johanessen, S.O., Skagen, D., and Totland, B. 1993. Assessing the reliability of fish density estimates by monitoring the swimming behaviour of fish schools during acoustic surveys. ICES Mar. Sci. Symp. **196**: 202–206.

Parrish, J.K. 1992. Do predators "shape" fish schools: interactions between predators and their schooling prey. Neth. J. Zool. **42**: 358–370.

Piatt, J.F., and Metven, D.A. 1992. Threshold foraging behavior of baleen whales. Mar. Ecol. Prog. Ser. **84**: 205–210.

Piatt, J.F., Methven, D.A., and Burger, A.E. 1989. Baleen whales and their prey in a coastal environment. Can. J. Zool. **67**: 1523–1530.

© 2002 NRC Canada

Rivoirard, J., Simmonds, J., Foote, K.G., Fernandes, P., and Bez, N. 2000. Geostatistics for estimating fish abundance. Blackwell Science, Oxford.

Saucier, F.J., and Chassé, J. 2000. Tidal circulation and buoyancy effects in the St. Lawrence estuary. Atmos. Ocean. **38**: 505–556.

Saucier, F.J., Chassé, J., Couture, M., Dorais, R., D'Astous, A., Lefaivre, D., and Gosselin, A. 1999. The making of a surface current atlas of the St. Lawrence Estuary, Canada. *In* Proceedings of the Fourth International Conference on Computer Modelling of Seas and Coastal Regions. *Edited by* C.A. Brebbia and P. Anagnostopoulos. Wessex Institute of Technology Press, Boston. pp. 87–97.

Simard, Y., and Lavoie, D. 1999. The rich krill aggregation of the Saguenay – St. Lawrence Marine Park: hydroacoustic and geostatistical biomass estimates, structure, variability and significance for whales. Can. J. Fish. Aquat. Sci. **56**: 1182–1197.

Simard, Y., Lacroix G., and Legendre, L. 1985. In situ twilight grazing rhythm during diel vertical migrations of a scattering layer of *Calanus finmarchicus*. Limnol. Oceanogr. **30**: 598–606.

Simard, Y., Lacroix G., and Legendre, L. 1986. Diel vertical migrations and nocturnal feeding of a dense coastal krill scattering layer (*Thysanoessa raschi* and *Meganyctiphanes norvegica*) in stratified surface waters. Mar. Biol. **91**: 93–105.

Simard, Y., McQuinn, I., Montminy, M., Lang, C., Miller, D., Stevens, C., Wiggins, D., and Marchalot, C. 1997. Description of the HAC standard format for raw and edited hydroacoustic data, version 1.0. Can. Tech. Rep. Fish. Aquat. Sci. No. 2174.

Simard, Y., McQuinn, I., Montminy, M., Samson, Y., Lang, C., Stevens, C., and Miller, D. 1998. CH1, Canadian hydroacoustic data analysis tool 1, user's manual (version 2.0). Can. Tech. Rep. Fish. Aquat. Sci. No. 2256.

Simard, Y., McQuinn, I., Montminy, M., Lang, C., Stevens, C., Goulet, F., Lapierre, J.-P., Beaulieu, J.-L., Landry, J., Samson, Y., and Gagné, M. 2000. CH2, Canadian hydroacoustic data analysis tool 2 user's manual (version 2.0). Can. Tech. Rep. Fish. Aquat. Sci. No. 2332.

Turgeon, L. 1994. Les migrations des baleines franches boréales dans l'estuaire du Saint-Laurent. L'Euskarien, **16**(2): 44–47.

Wiebe, P.H., Beardsley, R.C., Bucklin, A.C., and Mountain, D.G. (*Editors*). 2001. Coupled biological and physical studies of plankton populations: Georges Bank and related North Atlantic regions. Deep-Sea Res. **48**, Nos. 1–3.

© 2002 NRC Canada

Stock–environment recruitment models for Norwegian spring spawning herring (*Clupea harengus*)

Øyvind Fiksen and Aril Slotte

Abstract: Different stock–environment recruitment models for Norwegian spring spawning herring (*Clupea harengus*) are fitted to a time series of spawning stock, recruitment, and temperature data extending back to 1907. In addition to the traditional temperature index from the Barents Sea (the average annual temperature in the Kola transect), we also developed a new index based on the temperature in the larval drift trajectories during early larval life. The models show highly significant effects of both spawning stock and temperature. The inclusion of the temperature term in the stock–recruitment models removes the autocorrelation from the residuals and improves their explanatory ability by 6–9%. We explore the interdependence between recruitment success and subsequent spawning stock biomass and conclude that this is not likely to generate the stock–recruitment relationship. Our analysis suggests that the collapse of the Norwegian spring spawning herring stock in the period 1950–1970 was not caused by reduced recruitment, but by the drop in spawning stock biomass induced by the increased fisheries in this period.

Résumé : Divers modèles de stock–recrutement reliés à l'environnement appliqués à des harengs norvégiens à reproduction printanière (*Clupea harengus*) sont ajustés ici à des séries temporelles de données remontant à 1907 sur les stocks des géniteurs, le recrutement et la température. En plus du coefficient traditionnel de température dans la mer de Barents (la température annuelle moyenne sur le transect de Kola), nous avons créé un nouvel indice basé sur la température le long des trajectoires de dérive des larves au cours du début de leur vie. L'insertion du terme de température dans les modèles de stock–recrutement enlève l'autocorrélation des rédiduels et améliore le potentiel explicatif des modèles de 6–9 %. Un examen de l'interdépendance entre le succès du recrutement et la biomasse subséquente du stock des géniteurs nous amène à conclure que ce n'est vraisemblablement pas ce qui génère la relation stock-recrutement. Notre analyse laisse croire que l'effondrement du stock norvégien de harengs à reproduction printanière dans la période 1950–1970 n'est pas dû à une réduction du recrutement, mais à une diminution de la masse du stock des géniteurs à cause de l'accroissement des activités de pêche à cette époque.

[Traduit par la Rédaction]

Introduction

Relating environmental variability and spawning stock biomass (SSB) to fluctuations in recruitment (*R*) is an intensive area of research and discussion in fisheries science (e.g., Myers and Barrowman 1996; Gilbert 1997; Myers 1997). Establishing stock–recruitment models is difficult for several reasons. First, the biomass of spawners has turned out to be a weak indicator of egg production in some populations (Marshall et al. 1999). Second, there is often a lack of data at extreme population levels and long, high-quality time series of stock abundance and recruitment success are only rarely available. Third, the inherent variability of recruitment from other sources such as predation, competition, and the physical environment often hide the signal from the spawning stock size (Walters and Korman 1999). Finally, stock–recruitment analysis is difficult because of the lack of independence between the spawning stock and recruitment. Since all recruits eventually become part of the spawning stock, a spurious SSB–*R* relationship may be generated if there is periodicity in recruitment success (Sparholt 1996; Myers and Barrowman 1996).

Recently, Toresen and Østvedt (2000) compiled an extensive time series on the abundance and age structure of Norwegian spring spawning herring (NSS herring, *Clupea harengus*) back to 1907. During the period 1950–1970 the SSB of NSS herring was decimated from about 16 million to only a few thousand tonnes (Fig. 1). This dramatic event has been related to a very high fishing pressure, particularly on the juvenile stages (Dragesund et al. 1980), and to climatic changes (Cushing and Dickson 1976; Toresen and Østvedt 2000). The climatic changes can be tracked by two comparably long time series of sea temperature at the spawning grounds along the Norwegian coast (Aure and Østensen 1993) and at the nursery grounds in the Barents Sea (Bochkov 1982).

It is these historic data on fluctuations in temperature, SSB, and recruitment of NSS herring that form the basis of the present paper. Our main objective is to differentiate

Received 9 March 2001. Accepted 18 December 2001. Published on the NRC Research Press Web site at http://cjfas.nrc.ca on 13 February 2002.
J16251

Ø. Fiksen.[1] Department of Fisheries and Marine Biology, University of Bergen, P.O. Box 7800, N-5020 Bergen, Norway.
A. Slotte. Institute of Marine Research, P.O. Box 1870 Nordnes, N-5817 Bergen, Norway.

[1]Corresponding author (e-mail: oyvind.fiksen@ifm.uib.no).

 DOI: 10.1139/F02-002 © 2002 NRC Canada

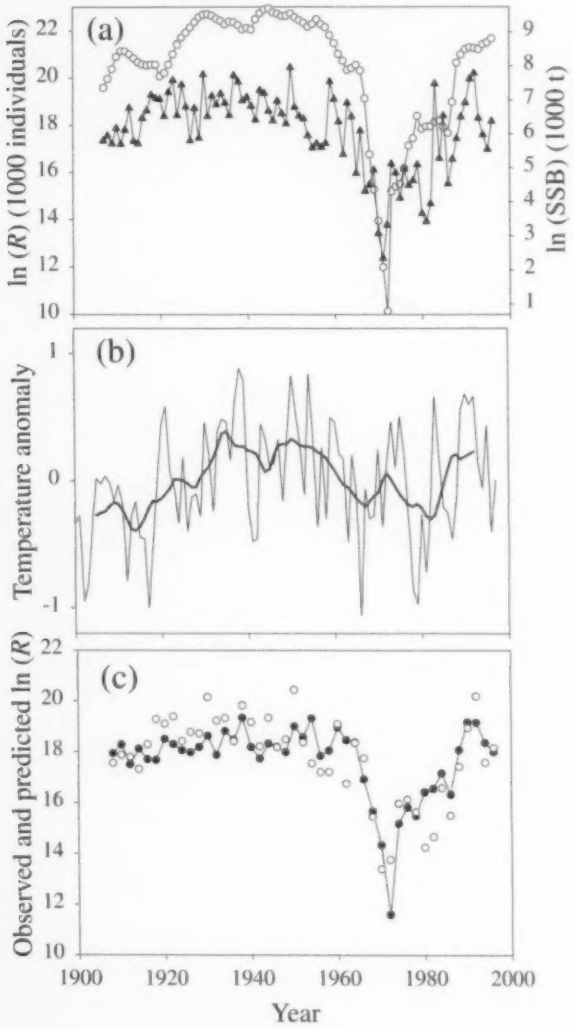

Fig 1. (*a*) The data on spawning stock biomass (ln SSB, in t × 10^3, ○) and recruitment (0-group, ln(individuals × 10^{-3}), ▲). (*b*) The annual mean temperature in the Kola transect (thin line) and its 10-year running mean (thick line). (*c*) Predicted (●) and observed (○) values from fitting a Ricker model with temperature using every second year to estimate the parameters and the remaining years to test the predictions.

between the respective influences of SSB and climate in the recruitment process of NSS herring, in particular with regard to the collapse and recovery of the stock. We search for the appropriate stock–recruitment model, including the effect of sea temperature, and explore the susceptibility of the model to the interdependence of SSB and recruitment success.

Materials and methods

The stock and temperature data

Toresen and Østvedt (2000) describe the stock structure of NSS herring back to 1907 using virtual population analysis (VPA) and we applied these data for this study (Fig. 1). In NSS herring, the VPA seems to produce estimates of recruitment that agree reasonably well with both larval indices as well as acoustic and abundance estimates of the 0-group from the Barents Sea and Norwegian fjords (ICES 2000). The larval index is most variable compared to the VPA estimate, whereas the two 0-group indices correlate quite well.

We have analyzed two different indices of the sea temperature that are likely to affect larval herring. The first of these is the annual mean temperature in the 0- to 200-m Kola transect at 33°00′E in the Barents Sea (Fig. 1), which has proven to be a reasonably good statistic of the climatic fluctuations in the area (Ottersen et al. 2000). A record back to the year 1900 of regular measurements in this section is available (Bochkov 1982; Toresen and Østvedt 2000). However, the Barents Sea temperatures may deviate from the ambient temperatures experienced by the larvae drifting in the Norwegian Coastal Current. Thus, we have included sea temperatures that have been measured at several fixed locations along the Norwegian coast since 1936 (Aure and Østensen 1993). These measures have high resolution (up to several per week) and correspond well with the drift route of the herring larvae (Slotte and Fiksen 2000). NSS herring spawn along the Norwegian coast from the southern tip of Norway to Lofoten, northern Norway (Slotte 1999). After hatching, the larvae drift northwards in the Norwegian Coastal Current. Some of the larvae end up in coastal waters and fjords, but the majority end up in the Barents Sea (Holst and Slotte 1998), where they stay until 2–3 years of age before joining the adult population in the Norwegian Sea (Dragesund et al. 1980).

Based on the data from the coastal stations, we have developed an index that should correspond closely to the temperature experienced by the larvae (Fiksen and Slotte 2000). We interpolated the data in time and space, such that for each day, a temperature is accessible for each 25th kilometre along the Norwegian coast from south to north. We assumed that the temperature at a depth of 10 m is the most relevant to herring larvae. The interpolation was linear between each measured point, and done for Julian day 91–140 (i.e., starting 1 April) for all 65 years from 1936 to 2000. In addition, we assumed a normal distribution of egg deposition along the coast and a major northward shift after 1950 (Dragesund et al. 1980). By assuming the larvae drift with the average current speed (12.5 km·day^{-1}), we obtained a measure of the integrated temperature that fish larvae were exposed to during their first seven weeks. In some years the coastal temperature data were scarce or missing. When the missing data were at Lista or Ingøy (at the southern and northern boundaries), these data were extrapolated from the nearest station using the long-term monthly average difference (from Aure and Østensen 1993) between the two locations. This was necessary for 1936–1941 and 1954–1957 at Lista (the most southern station), and for 1945–1968 and 1977–1978 at Ingøy (the most northern station, at the entrance to the Barents Sea). If data from the other intermediate stations were missing, data were interpolated between adjacent stations to the north and south, balanced by the distance between them. This was done for the station Bud (western Norway) during 1936–1946, 1955–1971, and 1994–1995, and for Eggum (Lofoten, northern Norway) in 1972.

© 2002 NRC Canada

A comparison of the two temperature indices reveals that they are positively correlated ($r = 0.67$, $p < 0.0001$, $N = 61$), but variable enough to warrant separate examinations for their abilities to predict recruitment success.

Data analysis

The models used for the analysis were the Ricker model

$$(1) \qquad R = \mathrm{SSB}\exp(a - b\mathrm{SSB} + cT + w)$$

and the Beverton–Holt model

$$(2) \qquad R = \left(\frac{a\mathrm{SSB}}{b + \mathrm{SSB}}\right)\exp(cT + w)$$

where w is the unexplained variance (residuals), a, b, and c are parameters, T is the temperature index (as deviations from the mean), R is recruitment (numbers at age 0 from the VPA), and SSB is in $t \times 10^3$. General discussions of these methods can be found in Hilborn and Walters (1992), among others. The stock–recruitment models were fitted with and without the environmental terms.

The residuals w were checked for autocorrelation $r(k)$ at lag k (in years) using the formulation suggested by Hilborn and Walters (1992, p. 281)

$$(3) \qquad r(k) = \left[\frac{\Omega - 1}{\Omega - 1 - k}\right]\frac{\sum_{y=1}^{\Omega-k}\hat{w}_y\hat{w}_{y+k}}{\sum_{y=1}^{\Omega}\hat{w}_y^2}$$

Here, $\hat{w}$ is the residual from any particular year, y, and Ω is the total number of years included. In addition, the Durbin–Watson statistic (D–W) was calculated to check for significant first order serial correlation, and all residuals were tested for normality.

Results

We fitted the models with no term for temperature (Table 1). Clearly, both models explain the data quite well (56% for the Ricker and 57% for the Beverton–Holt model). However, D–W revealed a significant first-order serial correlation for both models ($r(1) = 0.29$, $r(2) = 0.16$, $r(3) = 0.0$), suggesting that there is an additional factor influencing the recruitment success. The residuals from the Ricker model were checked for additional effects from sea temperature on recruitment success (Fig. 2). These plots indicate that both the average Barents Sea temperature and the coastal sea temperature explain some (13% versus 15%, respectively) of the residual variance. If the Barents Sea time series is limited to the years 1936–1996 (as the coastal index), then they become very similar (15%).

The logged recruitment index ($\ln R$) is correlated with the Barents Sea temperature ($r = 0.36$, $p < 0.01$; or $r = 0.47$, $p < 0.01$ for the period 1936–1996), the coastal temperature index ($r = 0.52$, $p < 0.01$), and SSB ($r = 0.57$, $p < 0.01$). Including the sea temperature in the stock–recruitment model increased the r^2 values by 6–9% and revealed highly significant environmental terms (Table 1). Both indices of sea temperature improved the models equally well for the period 1936–1996, whereas recruitment success seems to have been less associated with the Barents Sea temperature index during 1907–1936. More importantly, including sea temperature in the stock–recruitment model removed the serial correlation in the residuals (Table 1). This is explained by the effect temperature has on the recruitment success and the strong correlation between temperature in adjacent years y and $y + 1$. The first-order autocorrelation coefficients are 0.44 for the Barents Sea temperature and 0.37 for our coastal temperature index, whereas no autocorrelation is evident at higher lags.

To facilitate transparency and repeatability, we use the temperature from the Kola transect for our remaining analyses. The original stock–recruitment data, the corresponding data corrected for the temperature effect, and the values predicted by the model including both stock and environment are presented (Fig. 3). Clearly, correcting for temperature tends to draw the points closer to the fitted line, particularly for high SSB and recruitment success (the upper right corner of Fig. 3).

The long time series allows us to split the data in two groups, so that one group can be used for estimating parameters and the other group for testing the predictions. We removed every second year and fitted an environmental stock–recruitment curve to the remaining data. This model explains the independent data quite well and suggests that the model is a robust representation of the recruitment process in NSS herring (Fig. 1*c*). Reversing the model gave similar results.

The model can also be applied to study the cause of the collapse of the stock in the late 1960s. The smoothed temperature fluctuations (Fig. 1*b*) indicate that the climate switched from a warm to a colder period as the herring stock was reduced (Toresen and Østvedt 2000). If this climatic change contributed to the stock collapse by reducing recruitment, this should be evident as a systematic negative deviation from the long-term stock–recruitment relationship in the period when the stock was reduced. Similarly, for the recovery period, a positive deviation from the stock–recruitment curve would be expected. However, no such trends in the residuals are evident (Fig. 4), either for the model with or the model without the temperature term. In addition, the drop in recruitment and SSB in the 1960s is not lagged, thus there is no sign that the climate affected the collapse, at least not through recruitment.

Discussion

Our analysis shows that there is a strong relationship between SSB and recruitment in NSS herring. The inclusion of sea temperature in the stock–recruitment model increased the explanatory ability and removed the autocorrelation from the residual variability. The model is based on a time series that is probably among the most extensive in the history of fisheries science, and appears to be a robust representation of the recruitment dynamics in this stock. The NSS herring underwent a dramatic reduction in spawning stock size, from about 16 million tonnes at its peak level in 1945 to 2000 tonnes at the lowest in 1972 (Toresen and Østvedt 2000). This event revealed a clear effect of spawning stock size on recruitment, an effect that probably would not be clear if the stock had remained at historic levels. Zheng (1996) found significant relationships between spawning biomass and year

© 2002 NRC Canada

Table 1. The stock–recruitment models with and without a term for sea temperature (from 1907 or 1936 to 1996).

Model	Temperature index	a	b	c	$R^2_{adj.}$	N	D–W
Beverton–Holt	None	1.88×10^8	5139	0	0.57	89	1.43
		$p = 0.0009$	$p = 0.034$				(1.68)
	Barents Sea	2.71×10^6	3129	1.015	0.63	89	1.71
	(1907–1996)	$p = 0.36$	$p = 0.0195$	$p = 0.0002$			(1.70)
	Barents Sea	6.3×10^6	2280	1.30	0.66	60	2.0
	(1936–1996)	$p = 0.47$	$p = 0.037$	$p = 0.0002$			(1.65)
	Coastal	1.11×10^8	2189	1.050	0.66	60	1.94
	(1936–1996)	$p = 0.0002$	$p = 0.038$	$p = 0.0002$			(1.65)
Ricker	None	10.36	8.95×10^{-5}	0	0.56	89	1.43
		$p < 0.0001$	$p = 0.0004$				(1.68)
	Barents Sea	10.52	-1.2×10^{-4}	1.030	0.62	89	1.71
	(1907–1996)	$p < 0.0001$	$p < 0.0001$	$p = 0.0002$			(1.70)
	Barents Sea	565	-1.26×10^{-4}	1.22	0.65	60	1.89
	(1936–1996)	$p < 0.0001$	$p < 0.0001$	$p = 0.0005$			(1.65)
	Coastal	10.50	-1.2×10^{-4}	0.960	0.64	60	1.80
	(1936–1996)	$p < 0.0001$	$p < 0.0001$	$p = 0.0006$			(1.65)

Note: The Ricker model was fitted using $\ln(R) = a - b\text{SSB} + \ln(\text{SSB}) + cT$, and the Beverton–Holt model with $\ln(R) = \ln(a\text{SSB}/(b + \text{SSB})) + cT$ (Hilborn and Walters 1992). D–W, Durbin–Watson statistic with the corresponding significance threshold (at $p = 0.05$) in parentheses (Hamilton 1992); N, number of years available for each analysis; $R^2_{adj.}$, R^2 adjusted.

class strength in only about half of 19 different herring stocks. It appears as if a very large reduction in spawning biomass is required to expose the downside of the stock–recruitment curve in herring. We think the extreme fluctuations in spawning biomass of NSS herring have generated a quite reliable stock–recruitment model.

The study by Fossum (1996) indicated that the match between first feeding of the larvae and the abundance of prey affected the survival of the early herring larvae, in particular, the 1993 year class experienced a favourable prey situation. Some of the remaining unexplained variance in our model may be due to variations in prey availability, but the available data on prey abundance and overlap with first feeding larvae is too scarce to be included in the stock–recruitment models.

The NSS herring matures at age 3–5 (Toresen and Østvedt 2000), so the variability of recruitment also depends on the conditions for the juveniles in the Barents Sea. Among the factors influencing the juvenile survival are the predation pressure from cod, temperature, and the prey availability in the adolescent period (Hamre and Hatlebakk 1998). Still, there is a reasonably good correlation between the abundance of 0-group and the age-3 group in the VPA data ($r = 0.49$, $p < 0.01$), and a full treatment of the survival to age 3 is beyond the scope of this paper.

The models revealed significant terms for density dependence in the recruitment success. The mechanism behind this is not clear, but could be related to a limiting number of suitable spawning areas. Although the Norwegian coast is long, NSS herring deposit their eggs quite patchily, and at specific depths, bottom substrata, and current conditions (Runnstrøm 1941). Sometimes thick layers of eggs (up to 1 m thick) have been observed (Runnstrøm 1941), and several authors have pointed out that this will increase the mortality of the eggs (Runnstrøm 1941; Hourston and Rosental 1981; Zheng 1996). It is therefore not unlikely that a large spawning stock size and a massive egg deposition could cause increased egg mortality rates at the preferred spawning grounds.

Several authors (Ottersen and Sundby 1995; Ottersen and Loeng 2000; Toresen and Østvedt 2000) have noted the importance of sea temperature and climate for the recruitment of fish in the Barents Sea. Ottersen and Loeng (2000) found that the abundance of 0-group individuals of cod (*Gadus morhua*), haddock (*Melanogrammus aeglefinus*), and herring were positively correlated with their length. They also found that the average 0-group individual was longer in warm years compared with cold years. This suggests that the improved recruitment success with temperature is related to enhanced growth during the early stages. The positive effect on growth from increased temperature given sufficient food is well known from models and rearing experiments of herring larvae (Fiksen and Folkvord 1999).

It has been a general consensus that the intense herring fisheries following the invention of the power block in the early 1960s induced the collapse of the stock (Dragesund et al. 1980). However, the long-term drop in temperature that coincided with the stock decline has raised some questions on how severe the decline of the stock would have been if the climate were favourable during this period (Toresen and Østvedt 2000). The present results suggest that the climate (temperature) in fact played a minor role in the collapse. We found no trend in the residuals from the stock–recruitment model, and conclude that there was no recruitment-driven reduction in the stock biomass for NSS herring. This interpretation is also supported from the simultaneous drop in the SSB and the recruitment, i.e., there is no temporal lag in the reduction of the SSB with recruitment.

Potential effects from the dependence of SSB on recruitment success

To what extent is the predicted stock–recruitment relationship of NSS herring a result of the dependence of SSB on preceding recruitment success? According to Myers and Barrowman (1996), the erroneous explanatory effect of SSB on recruitment is given by r^{2m}, where r is autocorrelation in the time series of recruitment and m is age at maturity. For

© 2002 NRC Canada

Fig. 2. The unexplained variances from the Ricker model without temperature in Table 1 versus (*a*) the average annual temperature in the Kola transect and (*b*) our temperature index. The fitted lines are given by (*a*) $w = -3.66 + 0.93T$ ($r^2 = 0.13$, $p < 0.001$, $n = 89$) for the Kola index and (*b*) $w = -4.6 + 0.86T$ ($r^2 = 0.15$, $p = 0.0012$, $n = 60$) for the coastal temperature index.

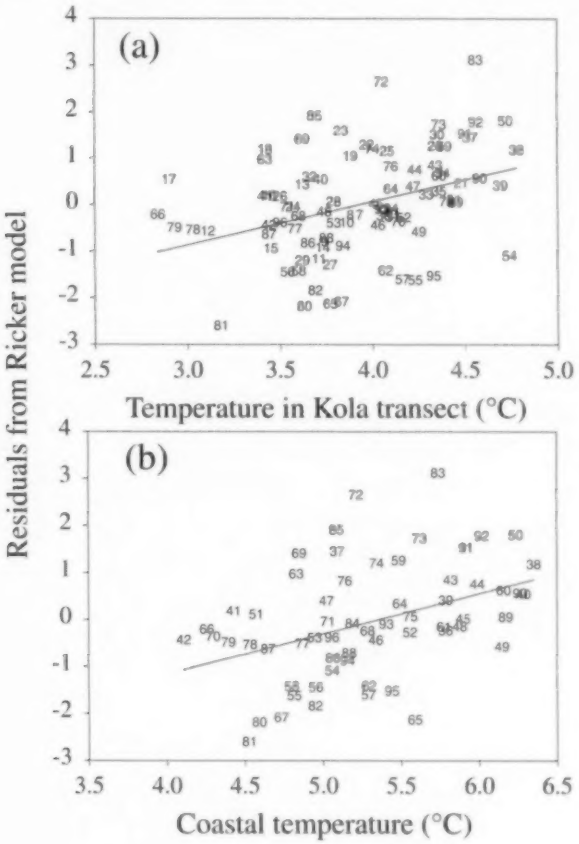

Fig. 3. This figure shows the observed values of ln SSB (spawning stock biomass) versus ln(*R*) (○), the recruitment at each SSB after correcting for the effect of temperature ($\ln R - cT$, where c is from Table 1) in the Barents Sea (●), the predicted recruitment from the Ricker model including the temperature (+), and the fitted Ricker model with no environmental term (line).

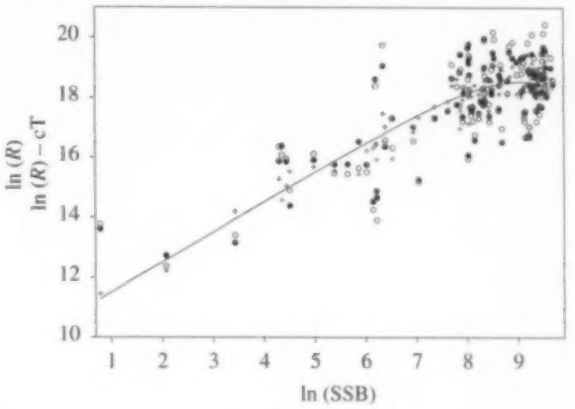

Fig. 4. The residuals of the Ricker model with (●) and without (△) the Barents Sea temperature term for the period of the collapse and recovery of the stock. The spawning stock biomass (SSB) reached its minimum in 1971, and there are no systematic trends in the residuals that can explain the collapse or the recovery.

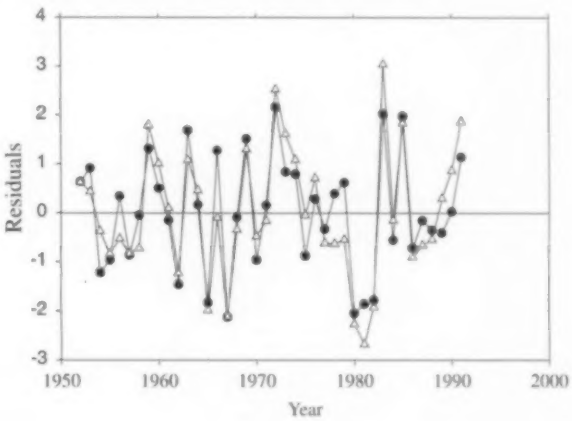

NSS herring, we estimated the first-order autocorrelation in recruitment (before correcting for the influence of temperature) to 0.272, and since age at maturity is four years, the "false" explanatory element from SSB should be negligible. However, there are examples where this effect causes difficulties, such as in Baltic cod where a spurious SSB–*R* relationship is evident (Sparholt 1996). The problem is detected from strong autocorrelation in the residuals of the fitted curve, but since there is no significant autocorrelation in our data (after correction for temperature), we do not expect this "chicken or egg" effect to be strong in NSS herring.

To illustrate how recruitment-driven fluctuations in SSB might generate a stock–recruitment curve in NSS herring, we have performed some simulations with a simple age-structured population model. Let $N_{a,y}$ be the number of individuals of age a in year y, and

$$N_{a,y} = N_{a-1,y-1}\exp(-\mu), \quad \mathrm{SSB}_y = \sum_{a=m}^{15} N_{a,y}, \quad R_y = N_{0,y}$$

where m is the age at maturation (4 years), μ is the annual mortality rate (0.3), and the maximum age is 15. Note that recruitment in year y varies independently of SSB, and that we assume SSB to be proportional to mature population abundance $N_{a>m}$ (i.e., no growth after maturity). We then feed this model with the recruitment time series of NSS herring back to 1907, and obtain a corresponding time series of SSB (Fig. 5*a*) and a (spurious) stock–recruitment relationship (Fig. 5*b*). Fitting Beverton–Holt or Ricker curves to the modelled SSB–*R* data in Fig. 5*b* did not yield significant values for the parameters a or b, whereas the linear regression $\ln(R) = a + b\ln(\mathrm{SSB})$ (i.e., the Cushing model) gave b significantly different from zero ($r^2 = 0.22$, $p < 0.0001$). These regressions all reveal strongly autocorrelated residuals (D–W = 0.85), and the statistical analysis is therefore invali-

© 2002 NRC Canada

Fig. 5. Predicted spawning stock biomass (SSB) from a simple age-structured model where R is independent of SSB. (*a*) The observed time series of R_y (recruitment in year y) in NSS herring (○) and the modelled SSB_y (■). (*b*) The combinations of (SSB_y, R_y) emerging from the simulations.

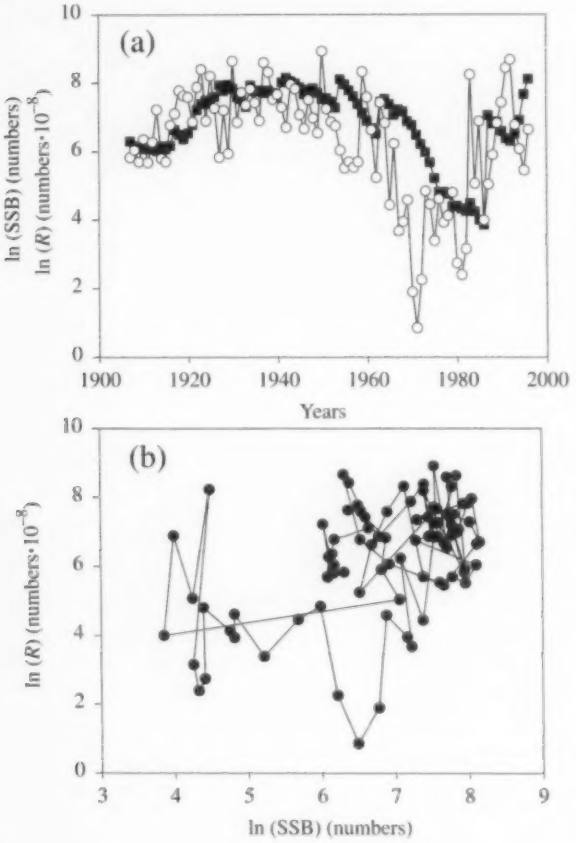

dated. We consider it quite unlikely that recruitment-driven variations in SSB could generate our stock–recruitment relationship without significant autocorrelation in the residuals. If we double the mortality rate ($\mu = 0.6$) from 1965 to 1973 to mimic the high fishing pressure during this period, the artificial Cushing SSB–R relationship improves ($r^2 = 0.42$, D–W = 1.15), but is still far from the critical Durbin–Watson value of 1.68 ($N = 89$, $p = 0.05$; Hamilton 1992). In addition, we performed a number of similar simulations with stochastic (lognormally distributed deviates) and autocorrelated time series of recruitment, and found it quite impossible to generate significant stock–recruitment relationships even with autocorrelation coefficients >0.9 ($m = 4$ years). This is in agreement with the equation from Myers and Barrowman (1996), but a more thorough treatment of the issue is warranted.

Acknowledgements

We thank Reidar Toresen for kindly providing us with his NSS herring data, and B.R. MacKenzie, G. Ottersen, A. Folkvord, and the referees R.A. Myers and D.J. Gilbert for valuable comments. Øyvind Fiksen was supported by a post-doctoral scholarship from the Norwegian Research Council. Aril Slotte was supported by the EU-project DST2.

References

Aure, J., and Østensen, Ø. 1993. Hydrographic normals and long-term variations in Norwegian coastal waters. Fisken Havet, **6**.

Bochkov, Y.A. 1982. Water temperature in the 0–200 m layer in the Kola-Meridian in the Barents Sea, 1900–1981. Sbornik Naucnykh Trudov PINRO, Murmansk, **46**: 113–122. [In Russian.]

Cushing, D.H., and Dickson, R.R. 1976. The biological response in the sea to climatic changes. Adv. Mar. Biol. **14**: 1–122.

Dragesund, O., Hamre, J., and Ulltang, Ø. 1980. Biology and population dynamics of the Norwegian spring-spawning herring. Rapp. P.-V. Reun. Cons. Int. Explor. Mer, **177**: 43–71.

Fiksen, Ø., and Folkvord, A. 1999. Modelling growth and ingestion processes in herring *Clupea harengus* larvae. Mar. Ecol. Prog. Ser. **184**: 273–289.

Fiksen, Ø., and Slotte, A. 2000. Recruitment variability in Norwegian spring-spawning herring (*Clupea harengus* L.): the effect of temperature in larval drift trajectories. ICES CM 2000/N:08.

Fossum, P. 1996. A study of first feeding herring (*Clupea harengus* L.) larvae during the period 1985–1993. ICES J. Mar. Sci. **53**: 51–59

Gilbert, D.J. 1997. Towards a new recruitment paradigm for fish stocks. Can. J. Fish. Aquat. Sci. **54**: 969–977.

Hamilton, L.H. 1992. Regression with graphics. A second course in applied statistics. Duxbury Press, Pacific Grove, Calif., U.S.A.

Hamre, J., and Hatlebakk, E. 1998. System model (Systmod) for the Norwegian Sea and the Barents Sea. *In* Models for multispecies management. *Edited by* T. Rødseth. Physica-Verlag, Heidelberg.

Hilborn, R., and Walters, C.J. 1992. Quantitative fisheries stock assessment: choice, dynamics and uncertainty. Chapman and Hall, New York.

Holst, J.C., and Slotte, A. 1998. Effects of juvenile nursery on geographic spawning distribution in Norwegian spring spawning herring (*Clupea harengus* L.). ICES. J. Mar. Sci. **55**: 987–996.

Hourston, A.S., and Rosental, H. 1981. Data summaries for viable hatch from Pacific eggs deposited at different intensities on a variety of substrates. Can. Data Rep. Fish. Aquat. Sci. No. 267.

International Council for the Exploration of the Sea (ICES). 2000. Report of the northern pelagic and blue whiting fisheries working group. ICES CM 2000/AFCM:16. (http://www.ices.dk/reports/acfm/2000/wgnpbw/report.pdf)

Marshall, T.C., Yaragina, N.A., Lambert, Y., and Kjesbu, O.S. 1999. Total lipid energy as a proxy for total egg production by fish stocks. Nature (London), **402**: 288–290.

Myers, R.A. 1997. Comment and reanalysis: paradigms for recruitment studies. Can. J. Fish. Aquat. Sci. **54**: 978–981.

Myers, R.A., and Barrowman, N.J. 1996. Is fish recruitment related to spawner abundance? Fish. Bull. **94**: 707–724.

Ottersen, G., and Loeng, H. 2000. Covariability in early growth and year-class strength of Barents Sea cod, haddock, and herring: the environmental link. ICES J. Mar. Sci. **57**: 339–348.

Ottersen, G., and Sundby, S. 1995. Effects of temperature, wind and spawning stock biomass on recruitment of Arcto-Norwegian cod. Fish. Oceanogr. **4**: 278–292.

Ottersen, G., Ådlandsvik, B., and Loeng, H. 2000. Predicting the temperature of the Barents Sea. Fish. Oceanogr. **9**: 121–135.

© 2002 NRC Canada

Runnstrøm, S. 1941. Quantitative investigations on herring spawning and its yearly fluctuations at the west coast of Norway. Fiskeridir. Dir. Skr. Ser. Havunders. **6**(8): 5–71.

Slotte, A. 1999. Effects of fish length and condition on spawning migration in Norwegian spring spawning herring (*Clupea harengus* L.). Sarsia, **84**: 111–127.

Slotte, A., and Fiksen, Ø. 2000. State-dependent spawning migration in Norwegian spring-spawning herring. J. Fish Biol. **56**: 138–162.

Sparholt, H. 1996. Causal correlation between recruitment and spawning stock size of central Baltic cod? ICES J. Mar. Sci. **53**: 771–779.

Toresen, R., and Østvedt, O.J. 2000. Variation in abundance of Norwegian spring spawning herring (*Clupea harengus*, Clupeidae) throughout the 20th century and the influence of climatic fluctuations. Fish Fish. Ser. **1**: 231–256.

Walters, C., and Korman, J. 1999. Linking recruitment to trophic factors: revisiting the Beverton–Holt recruitment model from a life history and multispecies perspective. Rev. Fish Biol. Fish. **9**: 187–202.

Zheng, J. 1996. Herring stock–recruitment relationships and recruitment patterns in the North Atlantic and Northeast Pacific oceans. Fish. Res. **26**: 257–277.

© 2002 NRC Canada

Transferability of habitat suitability criteria of juvenile Atlantic salmon (*Salmo salar*)

Aki Mäki-Petäys, Ari Huusko, Jaakko Erkinaro, and Timo Muotka

Abstract: We constructed generalized habitat criteria for juvenile Atlantic salmon (*Salmo salar*) based on four river-specific suitability indices for depth, water velocity, and substrate to assess whether habitat criteria for juvenile Atlantic salmon are transferable across rivers. We first tested whether salmon are more likely to occupy higher-quality habitats than generally available in a stream reach based on these composite criteria. We then repeated the same procedure using the river-specific criteria of this study and the generalized habitat suitability criteria of Heggenes. As expected, the river-specific criteria were generally the most effective ones in predicting fish habitat use. However, both of the two generalized criteria also transferred fairly well to the test sites. Viewed across salmon size-classes (<9 cm and >9 cm), the river-specific criteria passed the test in ten of eleven cases (91%), and the two generalized criteria passed in nine (82%) of eleven. Thus, it appears that with respect to summertime habitat criteria for juvenile Atlantic salmon, criteria transference is conceivable at least on a regional scale, and perhaps even on a more "universal" scale.

Résumé : Nous avons élaboré des critères généraux pour évaluer l'habitat de jeunes saumons de l'Atlantique (*Salmo salar*) d'après quatre indices de qualité spécifiques à des cours d'eau particuliers et basés sur la profondeur de l'eau, la vitesse du courant et le substrat dans le but de déterminer si ces critères pouvaient s'appliquer à d'autres rivières. Nous avons d'abord vérifié si les saumons étaient plus susceptibles de se retrouver dans les habitats de qualité supérieure définis par ces critères composites que dans les habitats généralement disponibles dans la section de rivière. Nous avons répété l'opération à l'aide de des indices spécifiques à une rivière et des critères généraux de qualité de l'habitat de Heggenes. Tel que prévu, les indices spécifiques étaient les plus efficaces pour prédire l'utilisation de l'habitat par les poissons. Cependant, les deux séries de critères généraux convenaient assez bien aux sites expérimentaux. Appliqués aux classes de taille de saumons (<9 cm et >9 cm), les critères spécifiques aux rivières se sont avérés adéquats dans dix (91 %) des onze cas et les deux séries de critères généraux dans neuf (82 %) cas. Il apparaît donc que l'on puisse transférer d'un cours d'eau à l'autre les critères de qualité de l'habitat des jeunes saumons de l'Atlantique en été, au moins dans une même région et peut-être même à une échelle plus « universelle ».

[Traduit par la Rédaction]

Introduction

Habitat selection is an important component of animal distribution, linking together behavioural ecology and population ecology (Kramer et al. 1997). For stream fishes, habitat selection is often related to trade-offs among swimming costs, prey capture success, and risk from predators or adverse environmental conditions (Hughes and Dill 1990; Heggenes et al. 1993). The relative importance of various habitat factors influencing fish distribution and abundance depends upon the scale at which they are examined. Viewed across stream reaches, some species or size- classes may be pool or riffle dwellers (Angermeier and Karr 1983), whereas at the within-reach scale, depth, water velocity, substrate, and cover are commonly considered as the main variables affecting the distribution of fishes (e.g., Heggenes 1990). Suitability criteria for these instream variables at different life stages of fish are used as biological components in habitat hydraulic models (e.g., physical habitat simulation, PHABSIM; Bovee 1982) to estimate the quantity of habitat suitable for fish at different flows.

Early attempts to model fish habitats in streams assumed that habitat requirements of fish are "universal" (Morantz et al. 1987). This assumption implies that fish prefer similar habitat conditions regardless of habitat availability, which would make site-specific habitat studies unnecessary. This notion has been invalidated, however, in many studies emphasizing the influence of habitat availability on habitat use

Received 24 April 2001. Accepted 7 December 2001. Published on the NRC Research Press Web site at http://cjfas.nrc.ca on 15 February 2002.
J16320

A. Mäki-Petäys[1] **and J. Erkinaro.** Finnish Game and Fisheries Research Institute, Oulu Game and Fisheries Research, FIN-90570 Oulu, Finland.
A. Huusko. Finnish Game and Fisheries Research Institute, Kainuu Fisheries Research and Aquaculture, FIN-88300 Paltamo, Finland.
T. Muotka. Department of Biological and Environmental Science, University of Jyväskylä, P.O. Box 35, 40351 Jyväskylä, Finland.

[1]Corresponding author (e-mail: aki.maki-petays@rktl.fi).

 DOI: 10.1139/F01-209 © 2002 NRC Canada

by fish (e.g., Heggenes 1990). In addition, habitat use may be affected by other factors, such as food availability, competition, predation (e.g., Orth 1987), water temperature (Mäki-Petäys et al. 1997), time of day (Heggenes et al. 1993), and discharge (Pert and Erman 1994). Therefore, many authors have cautioned against generalizations based on single "snapshot" studies and have recommended the use of site-specific habitat criteria whenever possible (e.g., Moyle and Baltz 1985; Greenberg et al. 1996). Nevertheless, fisheries managers are often required to make prompt decisions regarding stream habitat enhancement and protection, and it is not logistically and economically feasible to develop habitat criteria for all environmental conditions that may influence fish habitat. Therefore, it is a common practice to apply habitat criteria to streams other than those for which they were developed (Armour and Taylor 1991). Notwithstanding the increasing need for habitat hydraulic models in stream management, only a few tests of the transferability of habitat criteria have been performed (but see Thomas and Bovee 1993; Groshens and Orth 1994; Freeman et al. 1997). Such tests are needed, however, because these criteria constitute a major component of habitat hydraulic models and should therefore reliably reflect the habitat requirements of a target species. One approach for conducting such tests is to assess whether fish habitats predicted by the criteria constitute a subset of higher-quality habitats than generally available in a stream.

In the present study, we examined whether habitat criteria developed for juvenile Atlantic salmon (*Salmo salar*) are transferable across rivers. Heggenes (1990) suggested that studies on habitat use by salmon would be most rewarding when conducted in streams with widely differing habitat availability. We examined the summer habitat use by juvenile salmon in four geographically distinct Finnish rivers supporting genetically separate populations of Atlantic salmon (Nilsson et al. 2001). These rivers form a continuum from a naturally reproducing salmon population to a population maintained through regular stocking, and their fish assemblages show variation from a salmon-dominated assemblage to a diverse fish community. For each of these rivers, we developed suitability curves for two size-classes of salmon using three habitat variables: depth, water velocity, and substrate. We also constructed composite suitability curves based on the four river-specific curves to avoid biases caused by snapshot studies in one place and time. Finally, we assessed the transferability of these generalized curves in two ways. First, we compared the curves developed in this study with the generalized habitat curves for juvenile Atlantic salmon constructed by Heggenes (1990). Then, we tested whether juvenile salmon are more likely to occupy higher-quality habitats than generally available in the study section based on (*i*) river-specific criteria, (*ii*) generalized criteria of this study, and (*iii*) generalized criteria of Heggenes (1990).

Materials and methods

Study areas

This study was performed in four Finnish rivers: Tenojoki, Simojoki, Pyhäjoki, and Koitajoki (Fig. 1). The largest and northernmost of these is River Tenojoki (70°N, 28°E, mean flow 160 $m^3 \cdot s^{-1}$), which flows through subarctic terrain and drains into the Arctic Ocean. It has extremely clear water with low concentrations of nutrients (Table 1). The rivers Simojoki (66°N, 25°E, mean flow 38 $m^3 \cdot s^{-1}$) and Pyhäjoki (64°N, 25°E, mean flow 29 $m^3 \cdot s^{-1}$) discharge into the Bothnian Bay, Baltic Sea. River Koitajoki (63°N, 30°E, mean flow 2 $m^3 \cdot s^{-1}$) is a second-order inland river discharging into River Pielisjoki. Koitajoki has a fixed regulated flow because of the diversion of the main flow from the original route for power production. These three rivers run through boreal coniferous forests and agricultural landscapes and are characterized by brown waters and higher nutrient concentrations (Table 1).

Given the size of the river, an annual catch of 100–200 tonnes (t) of salmon, and high juvenile salmon densities, River Tenojoki supports probably the largest wild Atlantic salmon population in the world (Niemelä et al. 1999). The occurrence of other fish species in the shallow fluvial habitats of this river is negligible (Table 1).

In River Simojoki, wild Baltic salmon stocks decreased dramatically during the latter half of the 20th century, but recent efforts to enhance the remaining stocks have been successful: densities of wild juvenile salmon in River Simojoki increased substantially in the late 1990s, approaching those in River Tenojoki. A salmon stock rebuilding programme in River Pyhäjoki started in the late 1990s, and the first signs of wild salmon reproduction have been detected recently. However, a great majority of juvenile salmon in River Pyhäjoki is still of hatchery origin. Fishes other than salmon constitute a considerable proportion of the fish assemblage in the two Baltic rivers Simojoki and Pyhäjoki (Table 1).

The land-locked salmon stock of River Koitajoki declined in the early 1960s when hydropower development shut off the migration route for spawners, thus preventing natural reproduction. Nowadays the salmon population is maintained through regular stocking of salmon parr. Fish species other than salmon constitute a considerable proportion of the fish species assemblage in River Koitajoki. High density of brown trout (*Salmo trutta*) is the main difference compared with other study rivers (Table 1).

Field protocols

Habitat use by juvenile salmon was studied in July–September 1994 (Tenojoki), 1997 (Pyhäjoki), and 1999 (Koitajoki and Simojoki). Water temperature exceeded 10°C in all study rivers during these months, which facilitates among-river comparison of fish habitat use because an autumnal shift in habitat use and behaviour of salmonids is reported to occur at water temperatures below +10°C (e.g., Cunjak 1988; Heggenes et al. 1993).

According to Heggenes (1990), no method for locating fish (surface observation, diving, electrofishing) works well in all habitat conditions. Therefore, we chose to use both underwater observation and electrofishing in this study. Underwater observation was the most appropriate method in River Tenojoki, where water visibility is good and the study sites are rather deep (see Table 1). Because of lower water visibility (<3 m) and shallower stream habitats, electrofishing was used in other rivers. Obviously, these differences in field methods may cause some apparent differences in fish habitat

© 2002 NRC Canada

Fig.1. Location of the study areas and study reaches (●) in rivers Koitajoki (63°N, 30°E), Pyhäjoki (64°N, 25°E), Simojoki (66°N, 25°E), and Tenojoki (70°N, 28°E) in Finland.

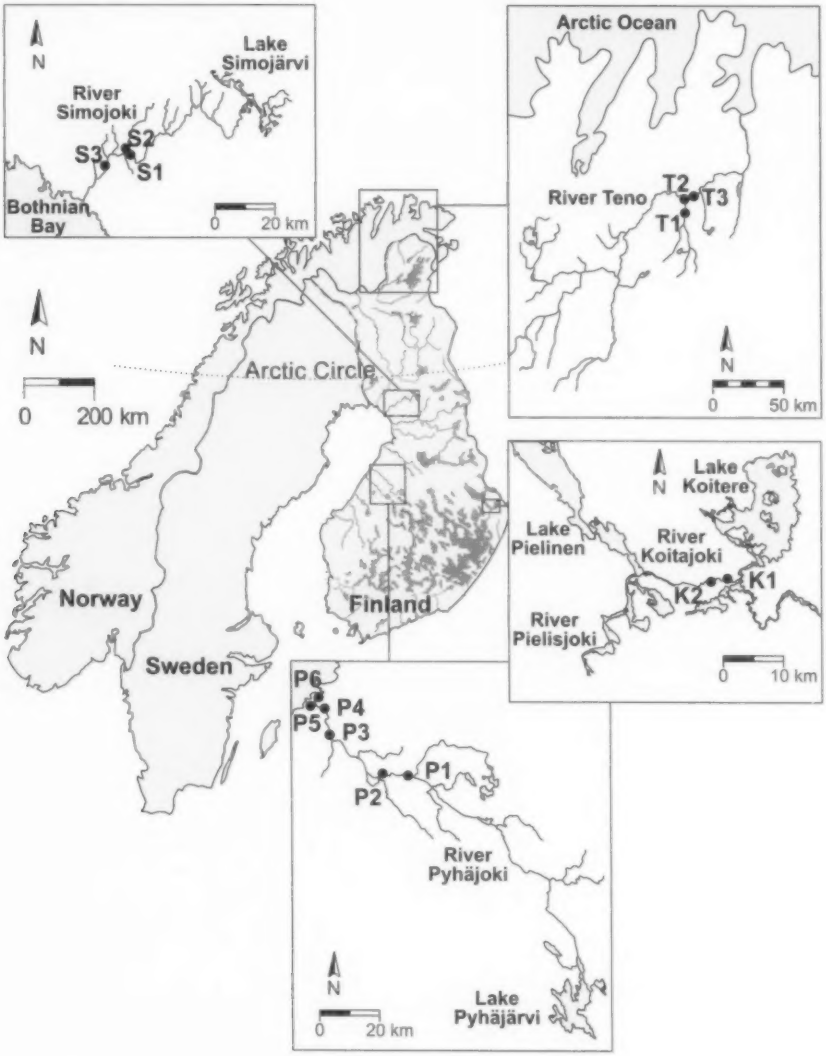

use between River Tenojoki and the other rivers, because underwater observation misses fish in shallow (<20 cm) water and electrofishing misses fish in deep waters (Heggenes 1990).

Underwater observations were made with a mask and snorkel using methods described by Heggenes (1991). A diver moved systematically upstream in a zigzag fashion to randomize any bias associated with nearshore or offshore observations. Once an undisturbed fish was located, fish length was estimated and assigned to one of two size-classes, <9 cm or >9 cm. These size-classes correspond roughly to age-0 and age-1 fish, respectively, except for River Tenojoki, where juvenile salmon grow more slowly (see Erkinaro and Niemelä 1995) and, therefore, fish smaller than 9 cm included many age-1 fish.

A point electrofishing procedure was used to reduce the potential fright bias caused by electrofishing (e.g., Moyle and Baltz 1985; Heggenes 1991). The anode was submersed at equidistant points (0.5 m) along transects spaced 1 m apart along the stream section to be sampled. Backpack electroshocker with low voltage (350 V) and a 10-cm-diameter anode was used to reduce the positive galvanotaksis induced by DC electroshockers (Copp 1989). Fish position was ascribed to the point of first sighting of a fish. Salmon captured were measured to the nearest millimetre.

Depth of water column, mean water velocity, and substratum particle size were recorded for each fish position. Mean water velocities were measured at 0.6 × depth with a Schiltknecht MiniAir2 flow meter (Schiltknecht Messtechnik AG, Gossau, Switzerland) fitted with a 20-mm propeller. Dominant substrate was determined visually in 0.8 × 0.8 m quadrats directly below the fish. Substrate particle size was classified

© 2002 NRC Canada

Table 1. Main characteristics of the study rivers.

	River Koitajoki	River Pyhäjoki	River Simojoki	River Tenojoki
General				
Location	63°N, 30°E	64°N, 25°E	66°N, 25°E	70°N, 28°E
Catchment area (km^2)	6795	3711	3160	16 386
Annual mean flow ($m^3 \cdot s^{-1}$)[a]	2[a]	29	38	160
Water quality[b]				
pH	6.5–7.0	6.5–7.0	6.5–7.0	6.8–7.9
Alkalinity ($meq \cdot L^{-1}$)	0.08–0.1	0.1–0.3	0.1–0.3	0.2–0.4
Conductivity ($mS \cdot m^{-1}$)	2.1–3.0	4.0–22.0	2.1–6.5	3.2–8.0
Total P ($mg \cdot L^{-1}$)	10–15	40–50	17–22	3–11
Colour ($mg\ Pt \cdot L^{-1}$)	80–120	140–200	90–140	15–20
Fish density[c] **(individuals/100 m^2)**				
Atlantic salmon (*Salmo salar*)	26–86	2–47	42–117	26–160
Brown trout (*Salmo trutta*)	61–156	0–3	0	0
Sculpins (*Cottus* sp.)	27–100	5–83	14–42	0–2
Grayling (*Thymallus thymallus*)	0	0–3	2–15	0
Minnow (*Phoxinus phoxinus*)	0	0–8	2–45	0
Burbot (*Lota lota*)	28–100	0–2	1–2	0
Stone loach (*Noemacheilus barbatulus*)	31–71	27–113	16–34	0

[a]Based on at least 20 years of daily flow measurements.
[b]Regulated fixed flow, during short periods (<1 month annually) discharge exceeds up to 100 $m^3 \cdot s^{-1}$.
[c]Range among study sites.

according to a modified Wentworth scale, using categories from sand to bedrock in Heggenes' (1991) classification (<5, <32 mm; 5, 32.1–64 mm; 6, 64.1–128 mm; 7, 128.1–256 mm; 8, 256.1–512 mm; 9, 512.1–1024 mm; 10, bedrock). To quantify habitat availability at each study site, the same variables were measured at 1.0-m intervals (0.5 m in River Tenojoki) along 5–30 equidistant transects perpendicular to the flow. Because of variable fish density, the area sampled varied between 100 m^2 and 2500 m^2, resulting in 1056, 648, 1313, and 711 measurement points in rivers Koitajoki, Pyhäjoki, Simojoki, and Tenojoki, respectively (see Table 2).

Data analysis

Habitat selection of fish is based on concurrent evaluation of several interacting habitat characteristics (Shirvell and Dungey 1983; Heggenes 1991). Multivariate analyses are successful in addressing such problems, because they summarize multivariate information into a few ecologically interpretable gradients (e.g., Grossman and Freeman 1987; Mäki-Petäys et al. 1997). Accordingly, we used principal component analysis (PCA) to examine among-river differences in habitats available for and used by juvenile salmon. Data from systematic sampling points, as well as those used by fish, in each study river were pooled for this analysis. Among-river differences in PCA scores of habitats available and used by fish along the first PCA axis were evaluated by one-way analysis of variance (ANOVA), followed by Tukey's test for pairwise comparisons.

We developed river-specific habitat suitability criteria (hereafter HC1) by constructing suitability curves for each variable using the method described by Baltz (1990). Habitat suitabilities were defined as (proportional use)/(proportional availability) and they were standardized to range from 0.0 (unsuitable) to 1.0 (optimal). A smoothed suitability curve was fitted to the data using the distance weighted least squares (DWLS) smoothing option in SYSTAT (SYSTAT 1992). We then constructed "general" suitability curves for each habitat variable (hereafter HC2) by using the arithmetic means of the river-specific suitability indices for each increment. This should mitigate any bias caused by snapshot studies at one place and time and should give a more general view of the habitat requirements of juvenile salmon (Heggenes et al. 1996).

We then estimated the transferability of the HC2 curves in two ways. First, we compared our HC2 curves with the generalized habitat suitability curves for juvenile Atlantic salmon constructed by Heggenes (1990) (hereafter HC3). For this purpose, the HC3 curves were also standardized to range from 0.0 to 1.0.

Secondly, based on the HC2 criteria, we examined whether juvenile salmon are more likely to occupy high-quality habitats than habitats classified as suboptimal. For this purpose, we used a method based on Thomas and Bovee (1993), with some modifications. We first converted habitat variables for each sampling point to a range of 0.0 to 1.0, using the HC2 curves for depth, water velocity, and dominant substrate. We then calculated the geometric mean of the suitability index of the three variables to form a single composite index for each sample point. The use of joint-suitability indices has been criticized (e.g., Heggenes et al. 1996), because they assume that fish select each habitat variable independently of other variables. However, Vadas and Orth (2001) have recently shown that such aggregation of suitability indices for individual habitat variables can reliably be used to predict fish density in streams. Habitats with a combined suitability value ≥ 0.75 were defined as optimal, whereas habitats with an index value between 0.50 and 0.75 were defined as suitable, and those less than 0.50 were defined as unsuitable for juvenile salmon of each size-class. Thomas and Bovee (1993) showed that with less than 55 occupied cells, the incidence of type I, and especially of type II, errors increases

© 2002 NRC Canada

Table 2. Habitats available for and used by two size-classes (<9 cm and >9 cm) of juvenile salmon in the study rivers.

River		Water temperature (°C)	Depth (cm)	Mean water velocity ($cm \cdot s^{-1}$)	Dominant substrate (class)	*N*
Koitajoki	Availability	14–20	27 ± 17.2	28 ± 27.5	7.9 ± 1.2	1056
	<9 cm		29 ± 10.5	33 ± 26.8	7.8 ± 0.9	137
	>9 cm		33 ± 13.5	40 ± 29.4	8.0 ± 0.9	169
Pyhäjoki	Availability	13–17	31 ± 13.3	30 ± 16.2	7.5 ± 1.2	648
	<9 cm		33 ± 7.6	32 ± 16.1	7.3 ± 1.2	83
	>9 cm		34 ± 10.1	28 ± 14.5	7.7 ± 1.2	124
Simojoki	Availability	12–16	37 ± 20.4	39 ± 31.0	7.4 ± 2.1	1313
	<9 cm		37 ± 15.1	40 ± 27.9	6.7 ± 2.0	229
	>9 cm		38 ± 15.2	35 ± 28.5	7.9 ± 1.6	135
Tenojoki	Availability	11–15	47 ± 21.8	33 ± 18.2	6.7 ± 1.1	711
	<9 cm		52 ± 19.2	32 ± 11.8	6.6 ± 0.7	79
	>9 cm		56 ± 17.4	34 ± 15.7	7.1 ± 1.1	59

Note: Means ± standard deviations are shown for depth, mean water velocity, and dominant substrate size. *N* = number of measurements. Substrate is classified according to the Wentworth scale (modified from Heggenes 1991): 1, 0.07–2 mm; 2, 2.1–8 mm; 3, 8.1–16 mm; 4, 16.1–32 mm; 5, 32.1–64 mm; 6, 64.1–128 mm; 7, 128.1–256 mm; 8, 256.1–512 mm; 9, 512.1–1024 mm; 10, bedrock.

dramatically. Because such a large sample size of occupied habitats was obtained only rarely in our study, we relaxed this assumption somewhat and accepted data with more than 30 observations for habitat occupied by fish, provided that the number of measurements for habitat availability was sufficiently large (>200; see Thomas and Bovee 1993). Accordingly, transferability tests were performed in five study sites for salmon <9 cm (one site in rivers Pyhäjoki, Tenojoki, and Koitajoki each, two in River Simojoki) and in six sites for salmon >9 cm (three sites in River Simojoki, two in Koitajoki, one in Pyhäjoki). A two-tailed χ^2 test was used to test for nonrandom habitat selection by fish. The same procedure was repeated using the HC1 and HC3 curves to compare the transferability of the HC2 curves with both more site-specific (HC1) and more general (HC3) habitat criteria.

Results

PCA on habitat use and availability

PCA on habitat availability and use (data pooled across study rivers) extracted one component with eigenvalue > 1.0 (42.0% of variance explained; Fig. 2). This component represented a gradient from shallow, low-velocity habitats with coarse substrates to deep, swift currents with finer substrates. ANOVA indicated significant river-specific differences in habitat use by juvenile salmon, but this mainly reflected a parallel change in habitat availability (see also Table 2). All pairwise differences in habitat availability between the study rivers were significant (Tukey's test, $p < 0.05$; see Fig. 2*a*). The deepest habitats were found in River Tenojoki, and the shallowest ones were found in River Koitajoki (Table 2). Habitat use by small salmon (<9 cm) largely paralleled variation in availability, with all pairwise differences being significant except that between rivers Koitajoki and Pyhäjoki (Tukey's test, $p > 0.05$). For larger salmon (>9 cm), only habitats used in River Tenojoki differed significantly (deeper water) from those used in other rivers.

Fig. 2. Principal component analysis (PCA) on among-river differences in habitat availability and use by juvenile Atlantic salmon. Mean PCA scores, with 95% confidence intervals, along the first component are presented for (*a*) habitat availability and use by (*b*) salmon <9 cm and (*c*) salmon >9 cm. Rivers (■, Koitajoki; ◆, Pyhäjoki; ●, Simojoki; ▲, Tenojoki) sharing a letter do not differ significantly (ANOVA followed by Tukey's pairwise comparisons). Loadings for the original variables along the first PCA axis are also given.

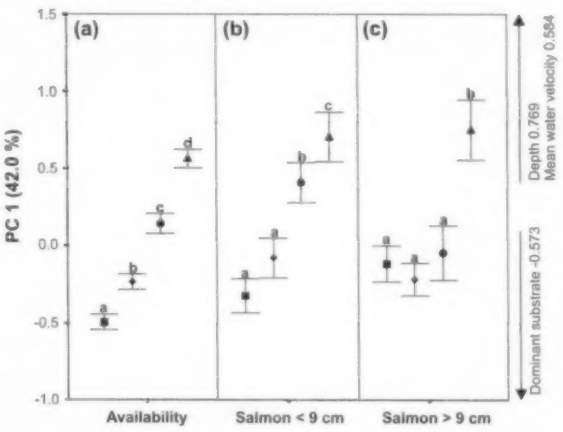

Habitat suitability criteria of juvenile Atlantic salmon

Wide tolerance of various habitat conditions by juvenile salmon was well indicated by their habitat suitability curves (Figs. 3*a* and 3*b*). In particular, both size-classes seemed rather indifferent with respect to mean water velocity, because optimum velocities varied from 20 to 80 $cm \cdot s^{-1}$. River Tenojoki excluded, the among-river variation in optimum depths varied from 15 to 60 cm and from 25 to 65 cm for small and large juvenile salmon, respectively. In Tenojoki, optimal habitats were at about 20 cm deeper stream areas (Fig. 3). Cobble-to-boulder substrates were used selectively by both size-classes in all four rivers, though smaller salmon preferred slightly finer substrates. The apparent avoidance of

© 2002 NRC Canada

Fig. 3. Suitability curves for depth, mean water velocity, and dominant substrate for juvenile Atlantic salmon (*a*) <9 cm and (*b*) >9 cm in the study rivers (—, Koitajoki; — —, Pyhäjoki; – –, Simojoki; ....., Tenojoki).

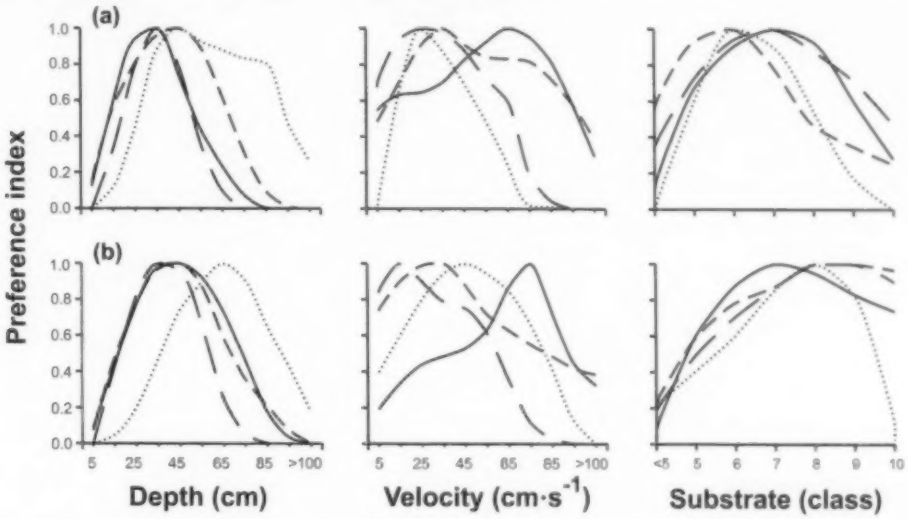

Fig. 4. Generalized, across-river habitat suitability criteria of this study (HC2, solid line) and generalized criteria modified from Heggenes (1990; HC3, dotted line) for depth, mean water velocity, and dominant substrate for juvenile Atlantic salmon (*a*) <9 cm and (*b*) >9 cm. HC3 curves are standardized to range from 0 to 1. Arrows indicate the lower and upper limits of the optimal suitabilities (index values > 0.75) for the HC2 criteria, based on the four river-specific (HC1) criteria (means ± standard error). Note that Heggenes' size-class separation (<7 cm for age-0, >7 cm for parr) differs slightly from that used in this study.

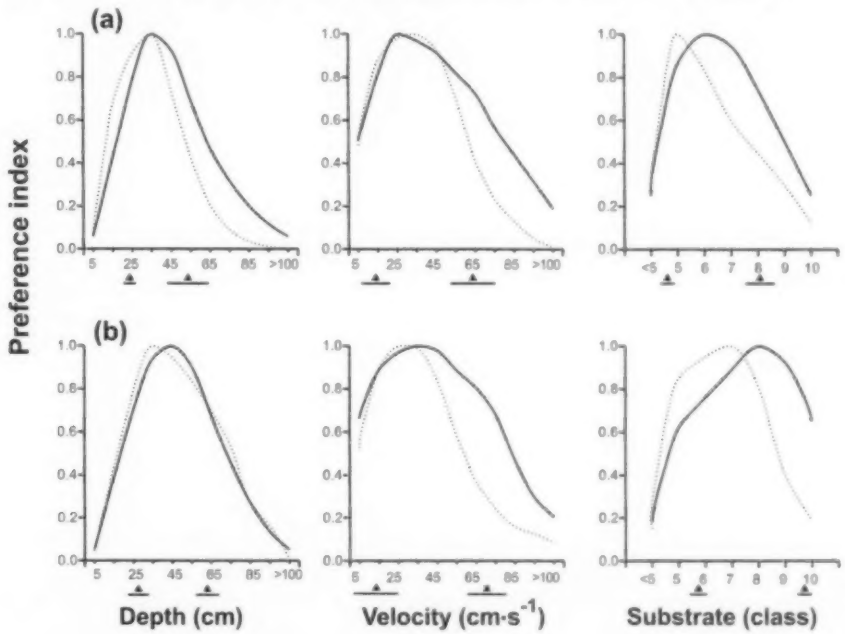

large-boulder areas in River Tenojoki was mainly caused by the of lack such substrates in this river.

Transferability of habitat criteria

Despite their different origins, both generalized habitat criteria (HC2 vs. HC3) indicated surprisingly similar habitat suitabilities by both size-classes of juvenile salmon (Figs. 4*a* and 4*b*). However, the HC2 curves indicated tolerance of up to 20 cm·s^{-1} swifter currents than the HC3 curves. According to HC2, the ranges of optimum velocities were 15–60 cm·s^{-1} and 15–70 cm·s^{-1} for small and large juvenile salmon, respectively. Depth and substrate curves showed

© 2002 NRC Canada

Fig. 5. The quality of habitat available for (open bars) and used (shaded bars) by salmon <9 cm in five study reaches (see Fig. 1 for location of the sites) based on river-specific habitat suitability criteria (HC1), generalized criteria of the present study (HC2), and generalized suitability criteria of Heggenes (1990; HC3). Asterisks indicate results from a two-sided χ^2 transferability tests: ***, $p < 0.001$; **, $p < 0.01$; *, $p < 0.05$; (*), $p < 0.10$; ns, nonsignificant.

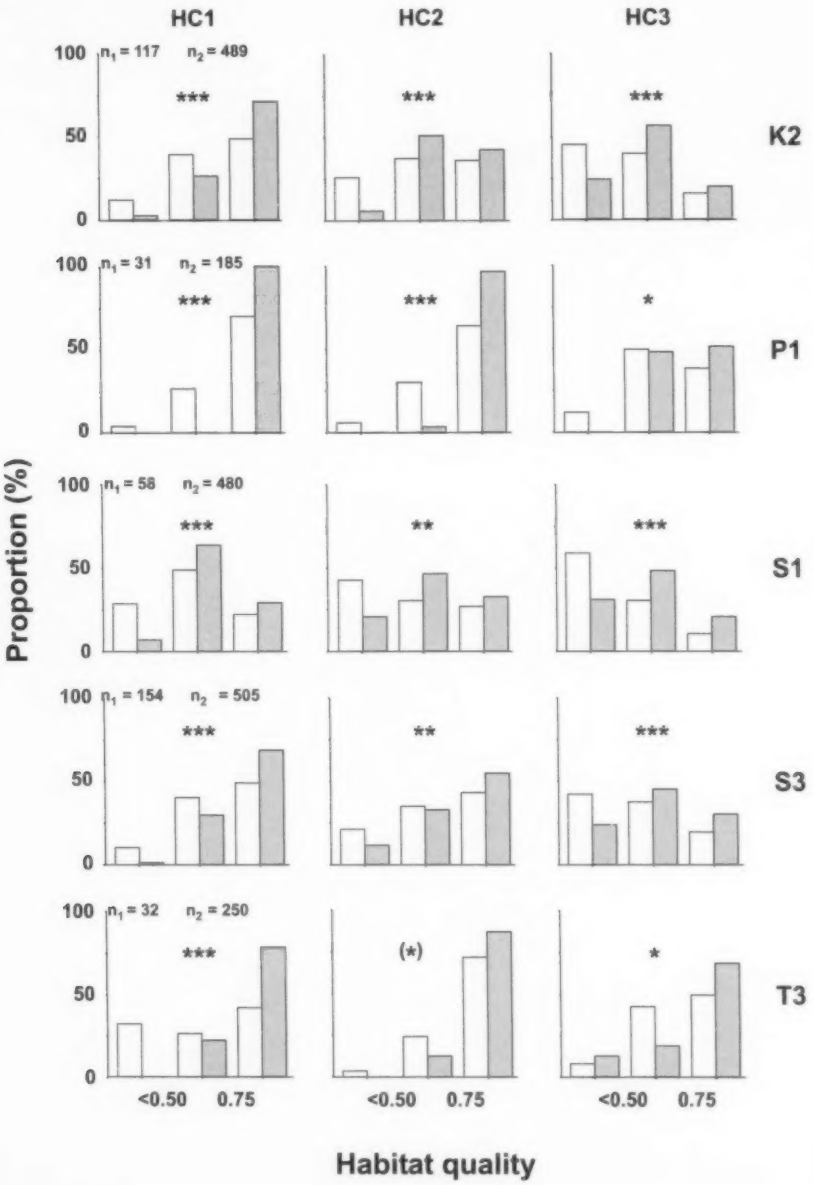

similar size-related changes in habitat suitability. The range of optimum depth for HC2 curves was 25–55 cm and 25–60 cm for smaller and larger salmon, respectively. The most distinct difference between the two types of criteria was that the HC2 substrate curves were more biased towards large particles, indicating preference for these particle sizes by juvenile salmon. Using HC2 curves, the optimal substrate size varied from large pebbles to boulders for salmon <9 cm and from cobbles to large boulders for salmon >9 cm.

For smaller salmon, both HC1 and HC3 criteria transferred well to all five test sites, and HC2 criteria transferred well to four of the five test sites (Fig. 5). For larger salmon, HC1 and HC2 criteria had successful transference to five test sites, and HC3 criteria had successful transference to four of the six test sites (Fig. 6). The river-specific criteria (HC1) were, however, overall the most effective ones in pre-

© 2002 NRC Canada

Fig. 6. The quality of habitat available for (open bars) and used (shaded bars) by salmon >9 cm in six study reaches (see Fig. 1 for location of the sites) based on river-specific habitat suitability criteria (HC1), generalized criteria of the present study (HC2), and generalized criteria of Heggenes (1990; HC3). For other details, see Fig. 5.

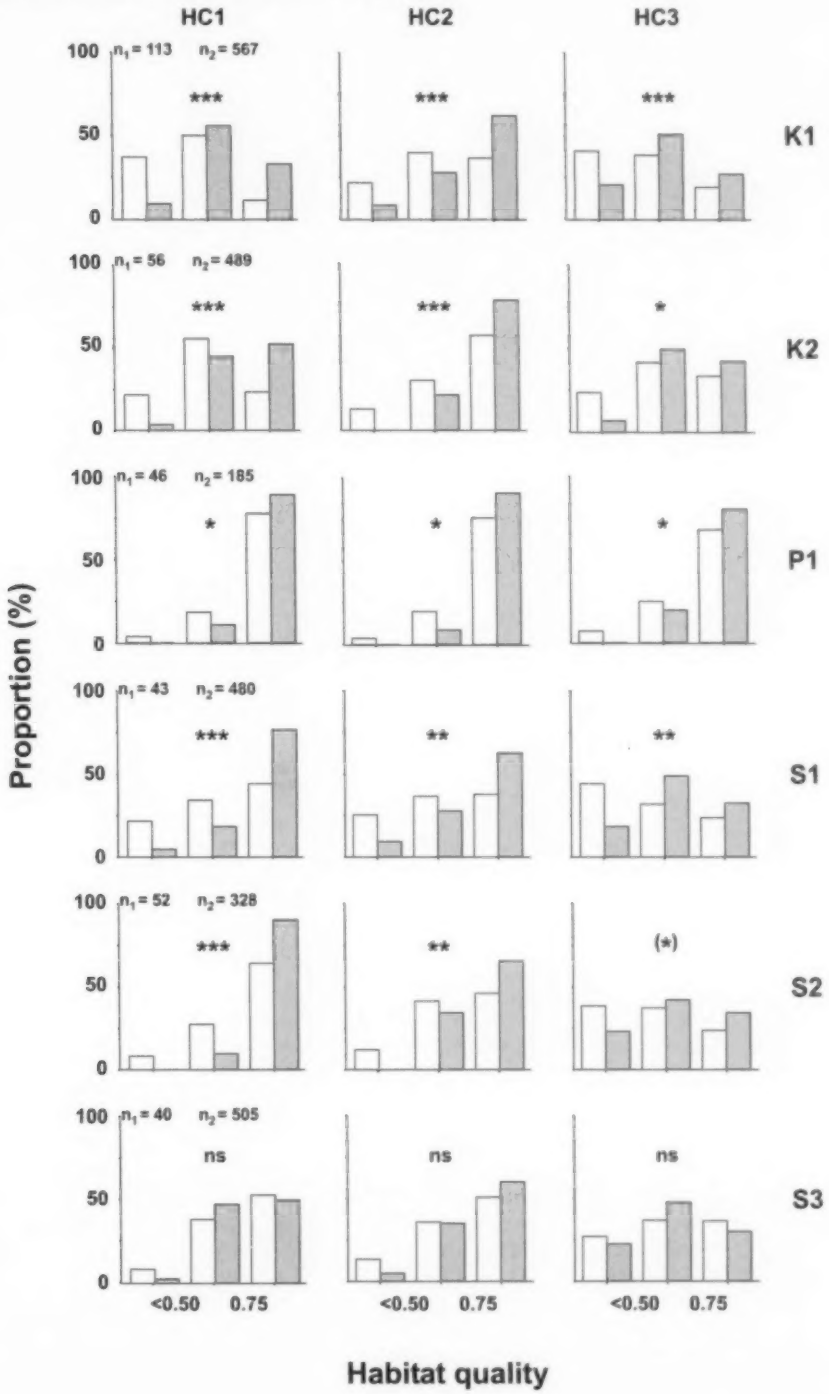

© 2002 NRC Canada

dicting fish habitat use. For one site (S3 for larger salmon), all transferability tests failed; this site had a low (but not the lowest) sample size for habitats occupied by fish (n = 40; see Fig. 6).

Discussion

Rivers of this study are geographically distinct, representing a gradient of contrasting habitat availability for juvenile salmon. River Tenojoki is a near-pristine river and is one of the northernmost salmon rivers in the world. By contrast, the other study rivers, located 500–900 km southward from River Tenojoki, are variously affected by human activities (forestry, agriculture, power production). Furthermore, the rivers harbour widely differing fish assemblages, with potentially large variation in the importance of biotic interactions on fish habitat selection. Despite such wide heterogeneity among the rivers, our results on habitat use by different-sized juvenile Atlantic salmon were rather consistent and well in accordance with previous findings (see Heggenes 1990; Heggenes et al. 1996, 1999). Habitat selection by juvenile salmon was clearly size-structured, larger fish preferring deeper, faster-flowing water with coarser substrates. Our results also demonstrated that river-specific differences in habitat use and suitability by salmon mainly reflect a concurrent change in habitat availability among the rivers (see also Heggenes 1991).

Thomas and Bovee (1993) argued that the most significant source of error in habitat hydraulic modeling is the selection of habitat criteria applied. Many authors have suggested that because so many factors influencing fish habitat use vary locally, habitat criteria should be developed in situ instead of using universal criteria or transferring criteria among streams (e.g., Moyle and Baltz 1985; Heggenes 1990). This, however, is an unattainable goal, and the often uncritical acceptance of criteria developed in another stream will likely remain a prevailing option in many, if not most, modeling applications. The generalized criteria for juvenile Atlantic salmon developed in this study (HC2 curves) converged to the generalized suitability criteria of Heggenes (1990) (HC3 curves), suggesting that summertime habitat requirements of juvenile Atlantic salmon are relatively invariable. However, a mere visual inspection of suitability curves gives little basis for arguments about criteria transferability. Transferability tests developed by Thomas and Bovee (1993) represent a step forward, although they were criticized by Williams et al. (1999) as being generally weak and of limited biological value. Obviously, a more comprehensive test would link habitat criteria with hydraulic models to predict fish distributions in a test riffle at various discharges (e.g., Guay et al. 2000), but this was not the goal of our study. Instead, we wanted to test directly the transferability of habitat criteria, which themselves constitute a major component of habitat hydraulic models. We thus concur with Freeman et al. (1999) in that transferability tests do provide biologically valuable information with obvious importance to stream managers, albeit inefficient to some degree. This is because they assess whether fish habitats predicted by these criteria constitute a subset of higher-quality habitats than generally available in a stream, and by doing so, they test whether the input variables (depth, velocity, substrate) are able to capture the key elements of habitats required by a target species. Such information on the predictability of fish habitat requirements is of considerable practical value in stream fisheries management, regardless of its role in modeling applications (e.g., Mäki-Petäys et al. 1999).

In this study, both the river-specific (HC1) and the generalized (HC2 and HC3) habitat criteria transferred fairly well to test sites. Viewed across salmon size-classes, the HC1 criteria passed the test in ten of eleven cases (91%), and the HC2 and HC3 criteria passed in nine of eleven cases (82%). Thus, with respect to summertime habitat criteria for juvenile Atlantic salmon, it appears that criteria transference is conceivable, at least on a regional scale (see Greenberg et al. 1996), and perhaps even on a more universal scale. It could even be argued that considering the spatially and temporally dynamic nature of habitat selection by fish, the use of generalized criteria might be advisable in most modeling contexts. This is because site-specific criteria are commonly based on snapshot studies covering only a fragment of the range of habitats suitable for salmon (e.g., Heggenes et al. 1996). Furthermore, although site-specific criteria are bound to provide the best fit to site-specific data on fish habitat use, the rationale behind this approach is somewhat circular: data used to develop suitability criteria are also used to predict suitability.

The generally good transferability of habitat criteria in our study is in accordance with the suggestion by Freeman et al. (1997) that criteria for riffle-dwelling fishes provide more transferable measures of habitat quality than those for species mostly found in deeper habitats. Juvenile salmon mostly occupy riffle habitats with swift currents, and deep pools are less typical for their residence (e.g., Heggenes et al. 1999; but see Bremset and Berg 1997). The good transferability of the criteria indicates that they reflect rather well the habitat conditions that best support the survival and growth of salmon parr in the test sites (see Freeman et al. 1997). Transference would probably have been even better if habitat conditions in the test sites had been more diverse. Examination of the overall quality of the test sites based on these criteria showed that most habitats available in these sites represented nearly optimal habitat conditions for both size-classes of salmon.

It is important to realize, however, that fish abundance may be limited by habitat suitable for a previous life stage as in the population under study (Fausch et al. 1988; Mäki-Petäys et al. 1999). In boreal streams, lack of suitable overwintering areas and sedimentation of salmon spawning grounds by humic substances are obvious candidates for factors that operate beyond the seasonal and (or) life stage constraints of traditional fish habitat studies (Mäki-Petäys et al. 1999; Laine and Heikkinen 2000; Solazzi et al. 2000). Therefore, to increase the applicability of habitat modeling in stream fisheries management, future studies on habitat use by juvenile salmonids should identify and test the generality of the key factors underlying the most limiting "bottleneck" stages during the life cycle of a fish.

Acknowledgments

We thank Olli van der Meer, Petri Kreivi, Alpo Huhmarniemi, Ari Kauttu, Igor Schurov, and Slava Maslov for conducting the

© 2002 NRC Canada

fieldwork for this study. Eero Niemelä is acknowledged for logistical help during the fieldwork in River Tenojoki. We warmly acknowledge the critical review by Leo Kuikka on an earlier version of the manuscript.

References

Angermeier, P.L., and Karr, J.R. 1983. Fish communities along environmental gradients in system of tropical streams. Environ. Biol. Fishes, **9**: 117–135.

Armour, C.L., and Taylor, J.G. 1991. Evaluation of the Instream Flow Incremental Methodology by U.S. Fish and Wildlife Service Users. Fisheries, **16**: 36–43.

Baltz, D.M. 1990. Autecology. *In* Methods for fish biology. *Edited by* C.B. Schreck and P.B. Moyle. American Fisheries Society, Bethesda, Md. pp. 585–607.

Bovee, K.D. 1982. A guide to stream habitat analysis using the Instream Flow Incremental Methodology. Instream flow information paper No. 12. FWS/OBS-82/26, U.S. Fish and Wildlife Service, Washington, D.C.

Bremset, G., and Berg, O.K. 1997. Density, size-at-age, and distribution of young Atlantic salmon (*Salmo salar*) and brown trout (*Salmo trutta*) in deep river pools. Can. J. Fish. Aquat. Sci. **54**: 2827–2836.

Copp, G.H. 1989. Electrofishing for larvae and 0+ juveniles: equipment modifications for increased efficiency with short fishes. Aquacult. Fish. Manag. **20**: 177–186.

Cunjak, R.A. 1988. Behaviour and microhabitat of young Atlantic salmon (*Salmo salar*) during winter. Can. J. Fish. Aquat. Sci. **45**: 2156–2160.

Erkinaro, J., and Niemelä, E. 1995. Growth differences between the Atlantic salmon parr, *Salmo salar*, of nursery brooks and natal rivers in the River Teno watercourse in northern Finland. Environ. Biol. Fishes, **42**: 277–287.

Fausch, K.D., Hawkes, C.L., and Parsons, M.G. 1988. Models that predict standing crop of stream fish from habitat variables: 1950–1985. U.S. Forest Service General Technical Report PNW-213.

Freeman, M.C., Bowen, Z.H., and Crance, J.H. 1997. Transferability of habitat suitability criteria in warmwater streams. N. Am. J. Fish. Manag. **17**: 20–31.

Freeman, M.C., Bowen, Z.H., and Bovee, K.D. 1999. Transferability of habitat suitability criteria: response to comment. N. Am. J. Fish. Manag. **19**: 626–628.

Greenberg, L., Svendsen, P., and Harby, A. 1996. Availability of microhabitats and their use by brown trout (*Salmo trutta*) and grayling (*Thymallus thymallus*) in the River Vojmån, Sweden. Regul. Rivers Res. Manag. **12**: 287–303.

Groshens, T.P., and Orth, D.J. 1994. Transferability of habitat suitability criteria for smallmouth bass, *Micropterus dolomieu*. Rivers, **4**: 194–212.

Grossman, G.D., and Freeman, M.C. 1987. Microhabitat use in a stream fish assemblage. J. Zool. (London), **212**: 151–176.

Guay, J.C., Boisclair, D., Rioux, D., Leclerc, M., Lapointe, M., and Legendre, P. 2000. Development and validation of numerical habitat models for juveniles of Atlantic salmon (*Salmo salar*). Can. J. Fish. Aquat. Sci. **57**: 2065–2075.

Heggenes, J. 1990. Habitat utilization and preferences in juvenile Atlantic salmon (*Salmo salar*) in streams. Regul. Rivers Res. Manag. **5**: 341–354.

Heggenes, J. 1991. Comparisons of habitat availability and habitat use by an allopatric cohort of juvenile Atlantic salmon (*Salmo salar*) under conditions of low competition in a Norwegian stream. Holarct. Ecol. **14**: 51–62.

Heggenes, J., Krog, O.M.W., Lindås, O.R., Dokk, J.G., and Bremnes, T. 1993. Homeostatic behavioural responses in a changing environment: brown trout (*Salmo trutta*) become nocturnal during winter. J. Anim. Ecol. **62**: 295–308.

Heggenes, J., Saltveit, S.J., Vaskinn, K.A., and Lingås, O. 1996. Predicting fish habitat use to changes in water flow: modelling critical minimum flows for Atlantic salmon, *Salmo salar*, and brown trout, *S. trutta*. Regul. Rivers Res. Manag. **12**: 331–344.

Heggenes, J., Bagliniere, J.L., and Cunjak R.A. 1999. Spatial niche variability for young Atlantic salmon (*Salmo salar*) and brown trout (*S. trutta*) in heterogeneous streams. Ecol. Freshw. Fish, **8**: 1–21.

Hughes, N.F., and Dill, L.M. 1990. Position choice of drift-feeding salmonids: model and test for Arctic grayling (*Thymallus arcticus*) in subarctic mountain streams, interior Alaska. Can. J. Fish. Aquat. Sci. **47**: 2039–2048.

Kramer, D.L., Rangeley, R.W., and Chapman, L.J. 1997. Habitat selection: patterns of spatial distribution from behavioural decisions. *In* Behavioural ecology of teleost fishes. *Edited by* J-G.J. Godin. Oxford University Press, Oxford. pp. 37–80.

Laine, A., and Heikkinen, K. 2000. Peat mining increasing fine-grained organic matter on the riffle beds of boreal streams. Arch. Hydrobiol. **148**: 9–24.

Morantz, D.L., Sweeney, R.K., Shirvell, C.S., and Longard, D.A. 1987. Selection of microhabitat in summer by juvenile Atlantic salmon (*Salmo salar*). Can. J. Fish. Aquat. Sci. **44**: 120–129.

Moyle, P.B., and Baltz, D.M. 1985. Microhabitat use by an assemblage of California stream fishes: developing criteria for instream flow determinations. Trans. Am. Fish. Soc. **114**: 695–704.

Mäki-Petäys, A., Muotka, T., Huusko, A., Tikkanen, P., and Kreivi, P. 1997. Seasonal changes in habitat use and preferences by juvenile brown trout, *Salmo trutta*, in a northern boreal river. Can. J. Fish. Aquat. Sci. **54**: 520–530.

Mäki-Petäys, A., Muotka, T., and Huusko, A. 1999. Densities of juvenile brown trout (*Salmo trutta*) in two subarctic rivers: assessing the predictive capability of habitat preference indices. Can. J. Fish. Aquat. Sci. **56**: 1420–1427.

Niemelä, E., Julkunen, M., and Erkinaro, J. 1999. Revealing trends in densities of juvenile Atlantic salmon by clusterizing long-term monitored sampling sites in a large subarctic river. Fish. Manag. Ecol. **6**: 207–220.

Nilsson, J., Gross, R., Asplund, T., Dove, O., Jansson, H., Kelloniemi, J., Kohlmann, K., Löytynoja, A., Nielsen, E.E., Paaver, T., Primmer, C.R., Titov, S., Vasemägi, A., Veselov, A., Öst, T., and Lumme, J. 2001. Matrilinear phylogeography of Atlantic salmon (*Salmo salar* L.) in Europe and postglacial colonisation of the Baltic Sea area. Mol. Ecol. **10**: 89–102.

Orth, D.J. 1987. Ecological consideration in the development and application of instream flow-habitat models. Regul. Rivers Res. Manag. **1**: 171–181.

Pert, E.J., and Erman, D.C. 1994. Habitat use by adult rainbow trout under moderate artificial fluctuations in flow. Trans. Am. Fish. Soc. **123**: 913–923.

Shirvell, C.S., and Dungey, R.G. 1983. Microhabitats chosen by brown trout for feeding and spawning in rivers. Trans. Am. Fish. Soc. **112**: 355–367.

Solazzi, M.F., Nickelson, T.E., Johnson, S.L., and Rodgers, J.D. 2000. Effects of increasing winter habitat rearing habitat on abundance of salmonids in two coastal Oregon streams. Can. J. Fish. Aquat. Sci. **57**: 906–914.

SYSTAT 1992. SYSTAT for Windows: graphics. Version 5. Systat Inc., Evanston, Ill.

Thomas, J.A., and Bovee, K.D. 1993. Application and testing of a procedure to evaluate transferability of habitat suitability criteria. Reg. Rivers Res. Manag. **8**: 285–294.

© 2002 NRC Canada

Vadas, R.L., Jr., and Orth, D.J. 2001. Formulation of habitat suitability models for stream fish guilds: do the standard method work? Trans. Am. Fish. Soc. **130**: 217–235.

Williams, J.G., Speed, T.P., and Forrest, W.F. 1999. Comment: transferability of habitat suitability criteria. N. Am. J. Fish. Manag. **19**: 623–625.

© 2002 NRC Canada

Shifting gears: enzymatic evidence for the energetic advantage of switching diet in wild-living fish

Graham D. Sherwood, Ivano Pazzia, Andrew Moeser, Alice Hontela, and Joseph B. Rasmussen

Abstract: Large variations in the activity and scaling patterns of enzymes involved in anaerobic metabolism exist and appear to be related to species differences in the locomotory habits of fish. Here, we show how the scaling of muscle lactate dehydrogenase (LDH) activity is highly variable in fish, not only among species, but also among populations of yellow perch (*Perca flavescens*) and lake trout (*Salvelinus namaycush*) exhibiting large differences in the scaling of fish activity costs. These differences in LDH scaling properties were significantly related to differences in diet ontogeny. Scaling coefficients and adjusted R^2 values of LDH versus body size relationships were both threefold higher in fish that do not make important diet shifts among planktivory, benthivory, and piscivory than in those that do. We argue that fish activity and related glycolytic potential are reset to lower values whenever fish are able to switch diet to larger prey while growing; we implicate the burst component of foraging (mostly attacks) as being responsible for changes in activity costs. Our results suggest that anaerobic power requirements in fish are highly plastic and adapted to local and recent food web conditions. We discuss these findings in relation to optimal foraging theory and the energetic basis of prey-size selection.

Résumé : Il existe de grandes variations dans les patterns d'activité et d'échelonnage des enzymes impliquées dans le métabolisme anaérobique qui semblent être reliées à des différences spécifiques d'habitudes locomotrices chez les poissons. Nous démontrons ici que l'échelonnage de l'activité de la lactate déshydrogénase (LDH) du muscle est très variable chez les poissons, non seulement d'une espèce à l'autre, mais aussi d'une population à l'autre chez la perchaude (*Perca flavescens*) et le touladi (*Salvelinus namaycush*), lorsque les populations possèdent d'importantes différences dans l'échelonnage des coûts de leurs activités. Ces variations dans l'échelonnage de la LDH sont reliées de façon significative à des différences dans l'ontogénie de l'alimentation. Les coefficients d'échelonnage ainsi que les valeurs ajustées de R^2 des relations de la LDH à la taille du corps sont trois fois plus élevés chez des poissons qui ne font pas de changements majeurs dans leur alimentation que chez ceux qui se nourrissent successivement au cours de leur développement de plancton, de benthos et de poissons. Nous pensons que l'activité du poisson et le potentiel glycolytique correspondant s'ajustent à des valeurs plus basses à chaque fois que le poisson peut, au cours de sa croissance, changer son alimentation pour des proies plus grandes; la composante « emballement » de la quête de nourriture (surtout des attaques) est sans doute responsable des changements dans le coût des activités. Nos résultats laissent croire que les besoins de puissance anaérobique sont très variables chez les poissons et que ces besoins s'adaptent aux conditions locales et récentes du réseau alimentaire. Ces résultats sont examinés en relation avec la théorie de la quête optimale de nourriture et de la base énergétique de la sélection des proies en fonction de leur taille.

[Traduit par la Rédaction]

Introduction

Big fish tend to eat big prey. This is a general phenomenon as well known to those who fish as it is to those who study fish. Indeed, the positive trend for larger mean- and maximum-sized prey with increasing body size across numerous predatory fish species, both freshwater (Mittelbach and Persson 1998) and marine (Scharf et al. 2000), is consistent with one of the most basic relationships in animal ecology (e.g., Peters 1983, for the positive correlation between predator and prey

Received 13 July 2001. Accepted 22 November 2001. Published on the NRC Research Press Web site at http://cjfas.nrc.ca on 15 February 2002.
J16446

G.D. Sherwood,[1,2] I. Pazzia, A. Moeser, and J.B. Rasmussen. Department of Biology, McGill University, 1205 Ave. Dr. Penfield, Montreal, QC H3A 1B1, Canada.
A. Hontela. Département Sciences Biologiques, TOXEN Research Centre, Université du Quebéc à Montréal, C.P. 8888, Succ. Centre-ville, Montréal, QC H3C 3P8, Canada.

[1]Corresponding author (e-mail: grahamsherwood@hotmail.com).
[2]Present address: Fisheries Conservation, Fisheries and Marine Institute of Memorial University of Newfoundland, P.O. Box 4920, St. John's, NF A1C 5R3, Canada.

 DOI: 10.1139/F02-001 © 2002 NRC Canada

size in animals). How this occurs is logical; only larger fish are able to overcome constraints, such as gape-size limitation, and effectively handle large prey (Townsend and Winfield 1985). Why big fish select bigger prey and what this means for fish energetics, on the other hand, may only be partially understood. The switch to larger prey as fish grow most likely serves to maintain profitability (e.g., continued growth), which, in turn, should entail maximization of gains and minimization of costs (Townsend and Winfield 1985). The cost function may be further broken down into pre- and post-capture investments. A great deal of information exists with regards to prey size related changes in handling costs, a postcapture variable (Mittelbach and Persson 1998). What is perhaps most lacking from our current understanding of the energetic basis of prey-size selection in actively foraging fish is a clear grasp of the costs incurred before capture (Mittelbach and Persson 1998).

A theoretical basis, as well as empirical support, for how fish energy budgets may be affected by prey-size choice is available. Foraging costs, in terms of the time spent actively searching and the number of feeding attempts (attacks) that would lead to satiation, should go up as prey become small in relation to the size of the predator (Kerr 1971; Kerr and Ryder 1977). Pazzia (2001) showed that fish activity costs increase much faster with body size in lake trout (*Salvelinus namaycush*) that do not make the normal ontogenetic diet shift from small benthic invertebrates to larger prey fish, and thus become stunted, than in those that make diet shifts and grow large. This agrees with earlier findings that diet shifts to piscivory are usually associated with increases in growth rate (e.g., Jones et al. 1994), as well as with the knowledge that to achieve maximum growth in artificially fed fish, food pellet size must increase proportionally with increasing fish size (Wankowski and Thorpe 1979). Taken as a whole, existing theory and observation are convincing with respect to the importance of prey size and diet shifts on fish activity and growth. Methods that would allow for the evaluation of fish activity before and after natural diet shifts would certainly contribute to these findings.

Metabolic enzymes represent a potentially useful approach for quantifying fish activity levels on a short-term and individual basis and, thus, for evaluating the energetic basis of prey-size selection in predatory fish. The maximal activity (V_{max}) of certain glycolytic (anaerobic) enzymes, including that of lactate dehydrogenase (LDH), in the axial musculature of fish has been suggested to be related to foraging behaviour and associated fish activity costs (Sullivan and Somero 1980; Childress and Somero 1990). Glycolytic potential, which LDH and a series of other glycolytic enzymes reflect, may facilitate burst swimming performance, which may be important in sustaining long bouts of spontaneous activity while feeding. Furthermore, the activity of enzymes such as LDH may provide a snapshot of recent (days–weeks) energetic requirements; its activity in fish has been shown to respond to altered energetic demands within at least, but not earlier than, 7 days (Nathanailides 1996; Schulte et al. 2000). Sherwood et al. (2002) applied this information to inferring elevated fish activity costs in stunted yellow perch (*Perca flavescens*) from metal-contaminated lakes where prey choice was low and diet shifts were limited. Interestingly, in the case where diet shifts were possible (for reference populations), LDH activities were observed to decrease sharply at well-defined diet shifts from planktivory to benthivory and from benthivory to piscivory. The results of this study fit well with theory regarding the importance of prey size on fish energetics (Kerr 1971; Kerr and Ryder 1977; i.e., shifting "K-lines") in yellow perch and suggested that LDH would provide a promising biomarker of fish activity applicable to further testing for the influence of diet and habitat shifts on fish energetics in a wide range of species and situations.

In this paper, we explore the relationship between diet shifts and LDH activity and how these both relate to body size and fish energetics (growth and fish activity) in numerous species of fish with different patterns of diet ontogeny. We present a synthesis of three separate field studies examining five different freshwater fish species and complement these findings with an analysis of previously published LDH size-scaling data for numerous marine fish species (Childress and Somero 1990). The overall expectation is that ontogenetic diet shifts towards larger prey types should lead to lower LDH activity corresponding to lower fish activity costs.

Materials and methods

Study sites and study species

Data was collected from three separate regions including a total of five different fish species from eight populations in eastern Canada (Fig. 1). Data for yellow perch came mostly from five lakes in the Eastern Townships of Quebec (sampled in June 1998) and from Lake Hertel, a Quebec lake in close proximity to the first five lakes (sampled in August 2000). Northern pike (*Esox lucius*), pumpkinseed sunfish (*Lepomis gibbosus*), and rock bass (*Ambloplites rupestris*) were also sampled from Lake Hertel in August 2000. Lake trout were sampled from two Algonquin Park, Ontario, lakes in May 2000. Limnological data for Eastern Townships lakes and Lake Hertel is found in Boisclair and Rasmussen (1996).

Fish from the various lakes were collected using a range of capture techniques (seine, gillnet, and rod-and-reel). Fish were sampled from the entire body size range representative of each species and population. All fish were sacrificed in the field within a few hours subsequent to capture, weighed to the nearest gram, and measured to the nearest millimetre (total length). A small sample (1–2 g) of white muscle tissue anterior to the caudal peduncle was excised for enzyme analysis (see Somero and Childress 1980) and placed in liquid nitrogen before freezing (–20°C) of whole carcasses.

Diet and stable carbon isotope analysis

For Lake Hertel fish, diet was determined from stomach contents immediately after fish capture. Individual prey items were identified to order and measured to the nearest millimetre (total length). For Algonquin Park lake trout and Eastern Townships yellow perch, diet items were identified from thawed stomachs in the laboratory. Carbon isotope (^{13}C) analysis was performed on dried lake trout muscle tissue (dorsal, directly posterior to the head) and representative prey items from lake trout stomachs packed in 4 mm × 6 mm tin capsules. ^{13}C, which is a naturally occurring heavy isotope of carbon, is useful for inferring feeding habits of

© 2002 NRC Canada

Fig. 1. Map showing the location of study sites in eastern Ontario and southern Quebec (shaded area in inset map of eastern Canada). Abbreviations in parentheses refer to species sampled for that lake: yellow perch (yp), sunfish (sf), rock bass (rb), northern pike (np), and lake trout (lt).

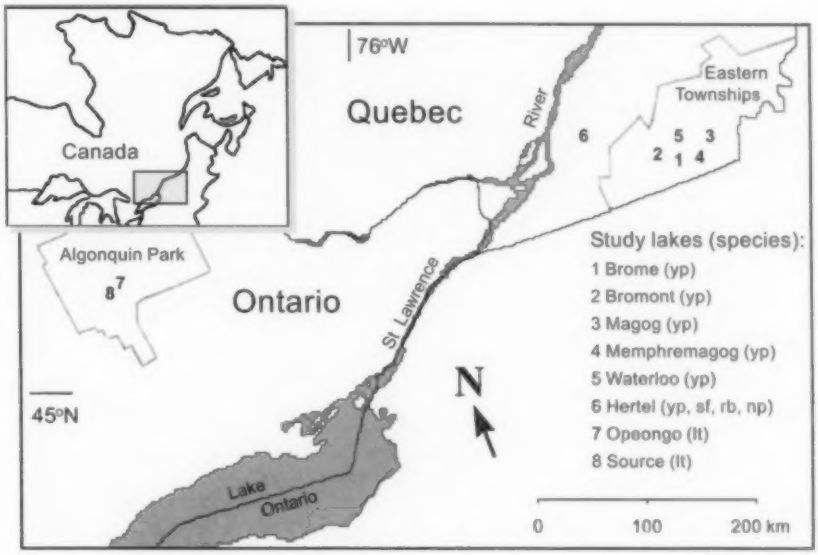

fish because prey from different habitats of lakes (i.e., benthic vs. pelagic) typically have distinct ^{13}C signatures ($^{13}C/^{12}C$) and consumers acquire ^{13}C signatures similar to that of their prey (Vander Zanden and Rasmussen 1999). Stable nitrogen isotope ratios ($^{15}N/^{14}N$), which are also useful in inferring diet shifts (Vander Zanden and Rasmussen 1999), were measured in lake trout but did not provide any additional information beyond that obtained from ^{13}C analysis and are therefore not presented here. Stable carbon signatures were expressed in delta (δ) notation, defined as the parts per thousand (‰) deviation from a standard material (Pee Dee belemnite limestone): $\delta^{13}C = ([R_{sample}/R_{standard}] - 1) \times 1000$; $R = {}^{13}C/{}^{12}C$).

Lactate dehydrogenase assay

LDH assays were performed on frozen white muscle tissue according to kit specifications (LDH-Optimized, Sigma Diagnostics®, St. Louis, Mo.) following a modification of a sample preparation protocol described in Somero and Childress (1980). Before homogenization (using a rough glass and Teflon apparatus) in buffer solution (50 volumes; 0.07 M, pH 7.0 KPO_4 buffer + 1 mM EDTA + 0.2% v/v Triton X-100), muscle samples were crushed to a fine powder in liquid nitrogen to allow for a more complete homogenisation. Fifteen microlitres of sample preparation, versus the 100 µL prescribed by Sigma Diagnostics®, were sufficient to initiate and sustain the LDH reaction for a duration of 1 min for the entire range of LDH activities encountered. LDH activities, measured at 20°C and expressed as arbitrary absorbance units (at 340 nm), were normalized to protein concentration to account for variations in homogenized tissue content from one sample preparation to another as well as variations among individuals. Protein analysis was carried out on sample preparations according to BioRad® (Bio-Rad Laboratories, Hercules, Calif.) specifications. The average coefficient of variation for all LDH assays run in duplicate was less than 5%. We found less than a 1% difference between LDH activities measured on tissue samples stored in liquid nitrogen immediately following field sampling and those resampled from the same fish carcasses stored in the freezer (–20°C).

Data handling and statistical analysis

Four different line-fitting techniques were used to describe the relationship between log(LDH activity) and log(body size). The four line fitting techniques were (*i*) linear regression, (*ii*) locally weighted regression smoothing (lowess), (*iii*) analysis of covariance (ANCOVA), and (*iv*) polynomial regression. Linear regression was performed in all cases and was sufficient where no diet shifts were evident from the diet data, or in cases where incomplete LDH activity versus body size data meant that important shifts might have been missed. When diet shifts were suspected, lowess curve-fitting, which results in superior fits to linear regression by producing locally weighted regression smoothing through an iterative weighted least-squares method (SPSS for Windows 1994) was used. When diet shifts were well characterized by gut content analysis, it was possible to use ANCOVA with log(LDH activity) as the dependent variable, log(body size) as the covariate, and diet stage as a class variable with three categories (planktivory, benthivory, piscivory) coded in two dummy variables (*c* and *d*, see Table 1 caption). In cases where ANCOVA was used (where diet data was sufficient), sample size was restricted to those fish that had stomach contents. We assessed the statistical significance of the increase in "fit" from linear to ANCOVA models by comparing with an *F* test. To facilitate visualization of diet shift patterns, our graphical representation of ANCOVA results

© 2002 NRC Canada

Table 1. Summary of results for lactate dehydrogenase allometry.

Lake	Species	Diet shift	Regression type	Equation parameter*							
				a	*b*	*c*	*d*	R^2_{adj}	*F*	*p*	*n*
Brome	Perch	Yes†	Linear	2.54	–0.07	NA	NA	0.38	11.9	<0.01	19
			Lowess	NA	NA	NA	NA	0.44	15.0	0.001	19
			ANCOVA	Insufficient diet data							
Bromont	Perch	Yes†	Linear	2.57	–0.04	NA	NA	0.01	1.1	0.30	31
			Lowess	NA	NA	NA	NA	0.09	3.8	0.06	31
			ANCOVA	Insufficient diet data							
Magog	Perch	Yes†	Linear	2.48	0.06	NA	NA	0.29	5.9	<0.05	13
			Lowess	NA	NA	NA	NA	NA	NA	NA	NA
			ANCOVA	Insufficient diet data							
Memph	Perch	Yes	Linear	2.51	0.08	NA	NA	0.21	10.9	<0.01	38
			Lowess	NA	NA	NA	NA	0.49	36.5	<0.0001	38
			ANCOVA	2.37	0.29	0.18	0.30	0.34	4.6	<0.05	22
Waterloo	Perch	Yes	Linear	2.68	–0.15	NA	NA	0.14	5.9	<0.05	31
			Lowess	NA	NA	NA	NA	0.32	15.2	<0.001	31
			ANCOVA	2.33	0.23^{ns}	0.29	NA	0.41	6.6	<0.01	17
Hertel	Perch	Yes	Linear	2.37	0.05	NA	NA	0.05	3.2	0.08	47
			Lowess	NA	NA	NA	NA	0.33	23.7	<0.0001	47
			ANCOVA	2.33	0.21	0.12	0.29	0.27	5.0	<0.01	33
Hertel	Sunfish	Yes	Linear	2.00	0.27	NA	NA	0.61	70.0	<0.0001	36
			Lowess	NA	NA	NA	NA	0.51	37.4	<0.0001	36
			ANCOVA	2.05	0.40	0.26	NA	0.75	38.6	<0.0001	26
Hertel	Pike	No	Linear	1.67	0.30	NA	NA	0.77	60.4	<0.0001	19
			Lowess	NA	NA	NA	NA	NA	NA	NA	NA
			ANCOVA	NA	NA	NA	NA	NA	NA	NA	NA
Hertel	Rock bass	No	Linear	1.76	0.27	NA	NA	0.69	32.6	<0.0001	16
			Lowess	NA	NA	NA	NA	NA	NA	NA	NA
			ANCOVA	NA	NA	NA	NA	NA	NA	NA	NA
Opeongo	Lake trout	Yes	Linear	2.81	–0.04	NA	NA	0.00	0.5	0.51	27
			Lowess	NA	NA	NA	NA	0.25	9.9	<0.01	27
			Polynomial	See Note				0.08	3.1	0.09	27
Source	Lake trout	No	Linear	2.27	0.21	NA	NA	0.46	23.1	<0.0001	28
			Lowess	NA	NA	NA	NA	0.55	34.5	<0.0001	28
			Polynomial	See Note				0.61	41.8	<0.0001	28

Note: Memph, Memphremagog; NA, not applicable. Polynomial equations are $\log(LDH) = -0.13\log W^2 + 0.66\log W + 1.92$ for Lake Opeongo lake trout and $\log(LDH) = -0.44\log W^2 + 2.08\log W + 0.34$ for Source Lake lake trout.

*$\text{Log}(LDH) = a + b\log W$ (or $LDH = a \cdot W^b$) for linear regression, and $\log(LDH) = a + b\log W - c - d$ for ANCOVA, where c and d are dummy variables for diet shifts from planktivory to benthivory and from benthivory to piscivory, respectively; all model terms were significant (to at least $p < 0.05$) unless otherwise specified (ns).

†Insufficient diet data for curve fitting purposes does not preclude the knowledge that diet shifts do indeed occur in these populations (G. Sherwood, personal observation).

includes connecting lines between the top and bottom of regression segments for successive and sometimes overlapping diet stages. Finally, when diet shifts were known to occur (by a combination of gut content and stable isotope analyses) but had a high degree of overlap (i.e., diet shifts were not discrete), second-order polynomial regressions were used. Whenever possible and appropriate, multiple line fitting techniques were performed for comparison.

Supplementary data

Published fish activity data for the five Eastern Townships perch populations, as well as for Lake Hertel perch, were available on an age-class basis from Boisclair and Rasmussen (1996). This data was in the form of activity multipliers (A), which is simply a multiplication factor of standard metabolic rate (SMR) in bioenergetics models of the form

$$(1) \qquad G = C - \text{SMR}\cdot A - \text{SDA} - F - U$$

where G is growth rate (both somatic and gonadal), C is consumption rate, SDA is specific dynamic action, F is egestion, and U is excretion (Kitchell et al. 1977). Fish activity data was also available for the two lake trout populations (Pazzia 2001). These independent estimates of fish activity, from both sources, were regressed against body size to obtain allometric scaling coefficients (b from $A = aW^b$; where a is the intercept, and W is body size in grams), which were then compared to scaling coefficients for the LDH activity versus body size relationships over the same body size range for the appropriate species and (or) population.

We supplemented our LDH scaling data with data for 23 marine species from Childress and Somero (1990). The data were divided here into two groups based on diet shift potential (Table 2). Non-diet shifters were those species that are generally considered to be planktivorous (pelagic) for the duration of their lives, whereas diet shifters were species of fish that are generally recognized to shift feeding mode at

© 2002 NRC Canada

Table 2. Published lactate dehydrogenase (LDH) scaling coefficients (b_{LDH}), maximum size (W_{max}), and diet shift behaviour of 23 marine species.

Non-diet-shifting species	b_{LDH}	W_{max} (g)	Diet-shifting species	b_{LDH}	W_{max} (g)
Ceratoscopelus warmingii	0.47	6.6	*Microstomus pacificus*	–0.43	4837
Vinciguerria nimbaria	0.68	1.4	*Gillichthys mirabilis*	0.08	21.6
Vinciguerria lucetia	0.66	1.3	*Halichoeres bivittatus*	–0.01	39
Poromitra crassiceps	0.3	47	*Nezumia bairdii*	0.36	58
Engraulis mordax	0.21	24.5	*Paralabrax clathratus*	0.42	381
Lampanyctus regalis	0.57	54.2	*Paralabrax nebulifer*	0.3	791
Lampanyctus ritteri	0.61	9.1	*Atherinops affinis*	0.22	44.3
Bajacalifornia burragei	0.29	57	*Sebastolobus altivelis*	0.19	250
Parvilux ingens	0.61	85	*Sebastolobus alascanus*	0.25	200
Bathylagus antarcticus	0.23	45	*Coryphaenoides armatus*	0.66	800
Electrona antarctica	0.95	12			
Gymnoscopelus braueri	0.76	20			
Gymnoscopelus opisthopterus	1.02	40			
Mean	0.57	31.0	Mean	0.20*	742.2
Standard error	0.07	7.2	Standard error	0.09	464.4

Note: LDH scaling data from Childress and Somero (1990); diet and size data from Froese and Pauly (2001).
*Means significantly different among groups (*t* test, $p < 0.01$).

some point in their development from planktivory to benthivory (demersal), piscivory, or both. It is acknowledged that this grouping scheme may not be entirely accurate; we had no way of controlling for possible site-specific variations in this classification. However, the groupings were used in any case for general exploratory purposes. The means of the reported LDH scaling coefficients (b from LDH = aW^b, where a is the intercept and W is body size in grams) were compared among these groups by Student's t test.

Results

Eastern Townships yellow perch populations

Muscle lactate dehydrogenase activity and diet were determined for individual yellow perch from various Eastern Townships populations and were plotted as a function of body size (Fig. 2). Lines fitted by lowess and (or) ANCOVA described the relationship between log(LDH activity) and log(body size) better than linear regression (i.e., they had higher adjusted R^2 values, Table 1); the most considerable improvements in adjusted R^2 values were for lakes Memphremagog and Waterloo ($F_{2,18} = 3.6$, $p < 0.05$, and $F_{1,14} = 8.3$, $p < 0.01$, respectively, for the difference between linear and ANCOVA models). For Lake Memphremagog perch (Fig. 2*c*), both the lowess line fit and ANCOVA showed substantial and significant decreases in LDH activity (ANCOVA, $p < 0.05$ for both shifts) at about 15 g and another starting around 60 g. The overall pattern could be described as "saw-toothed" allometry with individual "saw-teeth" corresponding to changes in feeding habit from planktivory (mostly cladocerans of 250–500 µm) to benthivory (various insect larvae and pupae as well as crustaceans 5–20 mm in length) and from benthivory to piscivory (various unidentified minnows and young-of-the-year yellow perch 20–70 mm in total length). A significant drop in LDH activity was also evident for Lake Waterloo (Fig. 2*b*) at about 15 g, again, corresponding to a shift from planktivory to benthivory (various insect larvae and pupae and crustaceans 5–10 mm in length) (ANCOVA, $p < 0.05$). Linear regression results show a large variation in scaling coefficients among populations ($b_{LDH} = 0.08$ to –0.15; Fig. 2*a*). Although specific diet data is lacking, the negative slope for Lake Bromont is likely to reflect a diet shift from zooplankton to benthic invertebrates similar to that for Lake Waterloo. Both lakes are very similar in limnological and food web characteristics (Boisclair and Rasmussen 1996).

Lake Hertel yellow perch, sunfish, rock bass, and northern pike

Muscle lactate dehydrogenase activity and diet were determined for four species of fish from Lake Hertel and were plotted as a function of body size (Fig. 3). For yellow perch, a significantly better relationship between log(body size) and log(LDH activity) was obtained by considering two distinct and well-defined diet shifts from planktivory (mostly cladocerans of 250–500 µm) to benthivory (aquatic insects and crustaceans 10–25 mm in body length) to piscivory (sunfish, golden shiners, *Notemigonus crysoleucas*, and young-of-the-year yellow perch, 20–60 mm in total length) (i.e., by performing an ANCOVA; $F_{2,29} = 6.3$, $p < 0.01$, for the increase in fit from linear to ANCOVA models; see Table 1 for summary of line fit results). For sunfish, a significantly better fit ($F_{1,23} = 15.1$, $p < 0.001$, for the difference between linear and ANCOVA models) was obtained by considering a single diet shift from planktivory (cladocerans of 250–500 µm) to benthivory (in this case, snails 2–10 mm in shell length). For rock bass and pike, linear regression was sufficient to describe the relationship between log(LDH activity) and log(body size). In these species, no diet shifts were present for the range of body sizes sampled; rock bass fed only on benthic invertebrates (odonates and crayfish 5–30 mm in length) and pike fed only on small fish (sunfish, golden shiners, and young-of-the-year yellow perch, 40–75 mm in total length). Overall, the best linear fit between log(LDH activity) and log(body size) was obtained in the species for which the least amount of diet shifting took place (rock bass and pike).

© 2002 NRC Canada

Fig. 2. Log muscle lactate dehydrogenase (LDH) activity (expressed in arbitrary absorbance units per milligram protein) versus body size for Eastern Townships yellow perch. (*a*) Linear regression results for all five populations. Abbreviations in parentheses are first two letters of lake name, except for Lake Bromont (bt). (*b*) Lowess (broken) and ANCOVA (solid) line fits for Lake Waterloo. (*c*) Lowess (broken) and ANCOVA (solid) line fits for Lake Memphremagog. Individual diet, determined from stomach contents, is indicated by symbols: shaded triangles are for zooplankton, shaded squares are for benthic invertebrates, solid diamonds are for fish, and open circles are for empty stomachs (unknown diet). Statistics for all line fits are included in Table 1.

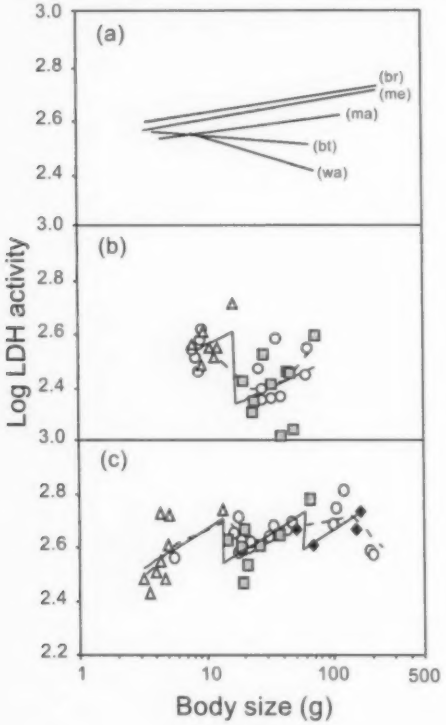

Algonquin Park lake trout

Muscle lactate dehydrogenase activities, $\delta^{13}C$ values, and diet were determined individually and plotted against body size for two populations of lake trout (Fig. 4). The overall pattern for log(LDH activity) versus log(body size) in lake trout was qualitatively different than it was for Lake Hertel fish and Eastern Townships perch. As opposed to positive allometry punctuated by discrete downshifts in LDH activity, there was a gradual downward inflection in LDH activity that was best described by fitting a second-order polynomial to the data (Table 1). These curves also agreed very well with lowess curve fits. This was most true for Lake Opeongo where this downward inflection in LDH activity corresponded to a downward shift in $\delta^{13}C$ values. Gut contents revealed that this shift in $\delta^{13}C$ values was likely the result of a move from feeding on invertebrates and small littoral forage fish (minnows and yellow perch) to feeding on larger pelagic forage fish (cisco, *Coregonus artedii*, and lake whitefish, *Coregonus clupeaformis*). For Source Lake, no diet shifts were evident from gut content analysis (100% chironomids at the time of sampling). For the most part, $\delta^{13}C$ values mirrored this result and suggested that these fish were feeding in the profundal zone on chironomids (which have very negative $\delta^{13}C$ signatures) up until the largest body sizes where a shift to inshore invertebrates or prey fish (which would have more positive $\delta^{13}C$ values) may have taken place as evidenced by significantly higher $\delta^{13}C$ in the four largest individuals (Student's t test, $p < 0.0001$). In the case of Source Lake, LDH activity followed positive allometry for most of the body size range; a slight downward shift in LDH activity in the largest individuals driving the superior polynomial fit corresponded to higher (shifted) $\delta^{13}C$ values. Overall, LDH activity was much less variable, as a function of body size, in Source Lake where limited diet shifting was likely to have occurred compared with Lake Opeongo where more complete diet and habitat shifts took place. This is consistent with the overall finding that adjusted R^2 values for the linear relationship between log(LDH activity) and log(body size) for all species and (or) populations examined were significantly higher (~threefold; Student's t test, $p < 0.05$, $n = 11$) when no diet shifts took place (mean = 0.64 ± 0.16) than when they did (mean = 0.21 ± 0.21). There was no effect of sex or stage of maturity on LDH scaling for lake trout.

LDH scaling versus fish activity scaling

Independent estimates of fish activity (A, see eq. 1) were available from other sources for certain species and (or) populations examined here (Table 3). There was a significant positive relationship between the size scaling of these estimates (b_A) and scaling of LDH activity (b_{LDH}) over the same body size ranges ($R^2 = 0.71$, $p < 0.01$, $n = 8$; $b_A = 1.26b_{LDH} + 0.13$). That is, if the overall slope for LDH versus body size was low in a given population, the slope for activity versus body size was also likely to be low.

LDH scaling versus diet ontogeny

Fish from the present study, as well as those from previous studies (Childress and Somero 1990), were grouped into non-diet shifters, those species that remain planktivorous for their entire lives or in cases where incomplete sampling covered only one diet stage, and into diet shifters, those species that shift diet from planktivory to benthivory, piscivory, or both at some point in their lives (Tables 1 and 2). There was a significant difference in LDH scaling between these two groups ($t = 3.76$, $p < 0.001$, df = 37) such that the scaling coefficient for LDH activity (b_{LDH}) was threefold higher in non-shifters ($b_{LDH} = 0.47 \pm 0.26$) than it was in diet shifters ($b_{LDH} = 0.16 \pm 0.25$). Once diet shifts were taken into account through the use of ANCOVA, there was no difference in LDH scaling among diet groups ($t = 0.92$, df = 22).

Discussion

Glycolytic enzyme scaling and diet ontogeny

It has previously been recognized that the activity of glycolytic (anaerobic) enzymes (including LDH) in fish muscle does not follow the same metabolic size-scaling paradigm that governs activities of aerobic enzymes (Sullivan and Somero 1980; Childress and Somero 1990). As opposed to

© 2002 NRC Canada

Fig. 3. Log muscle lactate dehydrogenase (LDH) activity (expressed in arbitrary absorbance units per milligram protein) versus body size for four species of fish from Lake Hertel. (*a*) Combined best-fit lines for all four species. (*b*) Combined linear regression for all four species. Abbreviations in parentheses (*a*, *b*) refer to species names: yellow perch (yp), pumpkinseed sunfish (sf), rock bass (rb), northern pike (np). (*c*) Lowess (broken) and ANCOVA (solid) line fits for yellow perch. (*d*) Linear regression for northern pike. (*e*) Lowess (broken) and ANCOVA (solid) line fits for sunfish. (*f*) Linear regression for rock bass. Individual diet, determined from stomach contents, is indicated by symbols (*c*–*f*): shaded triangles are for zooplankton, shaded squares are for benthic invertebrates, solid diamonds are for fish, and open circles are for empty stomachs (unknown diet). Statistics for all line fits are included in Table 1.

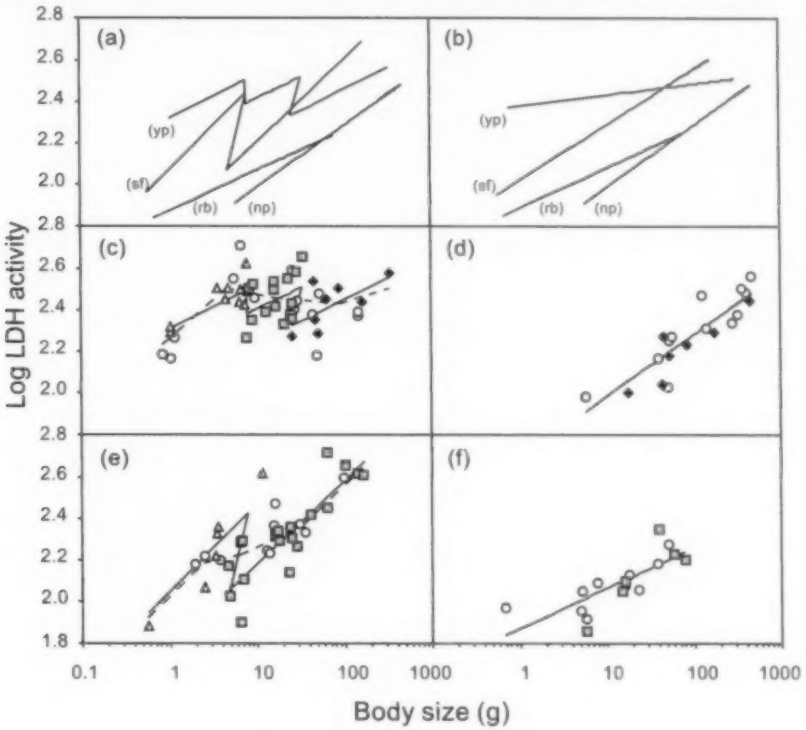

negative allometry confined to a narrow range of scaling coefficients (typical values for aerobic enzymes centre around –0.25), glycolytic enzymes possess highly variable and mostly positive size dependence. The fact that glycolytic enzymes usually scale positively to body size has been suggested to be related to increasing anaerobic power requirements in larger fish that may experience higher drag forces when generating short bursts (Sullivan and Somero 1980). The fact that glycolytic scaling coefficients are highly variable has led to the suggestion that there is strong selection for large differences in anaerobic power requirements related to differences in locomotory habits and feeding types among species (Childress and Somero 1990).

Results of the present study provide further evidence for highly variable scaling of anaerobic metabolism in fish and offer some new insights as to the underlying environmental causes of this variation (within and among species), as well as provide an alternative explanation for predominantly positive size-scaling of anaerobic power requirements. A considerable and consistent effect of diet ontogeny on the scaling properties of muscle lactate dehydrogenase activity was found in a wide range of fish species both within and among species. Tightness of fit (adjusted R^2 values) and slopes (scaling coefficients) for LDH activity versus body size relationships were both greater (threefold) in fish that do not make diet shifts than in those that do. The implication is that the normal tendency for LDH activity, in the absence of appreciable diet shifts and regardless of species, is to increase quite rapidly and invariably with body size. Negative and variable LDH allometries are thus likely to be artefacts of resetting power requirements and glycolytic potential around diet and (or) habitat shifts. Once the effect of diet shifts was taken into account through ANCOVA, the slope for LDH activity versus body size became much less variable (the coefficient of variation decreased from 150% to 36%) and the mean increased threefold to 0.32, which is not significantly different from the average slope obtained for populations in which diet shifting does not occur. These findings suggest that overall glycolytic scaling patterns are not a fixed and selected-for species property. In contrast, they are more likely to be a consequence of variable food web structure and related feeding opportunities, the successful exploitation of which can vary as much within a species (Pazzia 2001) as it can among species.

The observation that LDH activity can be reset to lower values following diet shifts in actively foraging fish calls into question previous interpretations for positive allometry of anaerobic enzymes. In particular, it is difficult to imagine

© 2002 NRC Canada

Fig. 4. (Top panels) Log muscle lactate dehydrogenase (LDH) activity (expressed in arbitrary absorbance units per milligram protein) versus body size for two populations of lake trout from Algonquin Park. Statistics for polynomial and lowess curve fits (seen here) and linear regressions are included in Table 1. (Middle panels) $\delta^{13}C$ versus body size for (*a*) Lake (L.) Opeongo (polynomial regression $R^2 = 0.20$, $p < 0.01$, $n = 51$) and (*b*) Source Lake (polynomial regression $R^2 = 0.43$, $p < 0.001$, $n = 27$). Dotted lines show average $\delta^{13}C$ values for representative profundal (mostly chironomids), littoral (various insects and littoral forage fish), and pelagic (cisco) prey items for each lake (asterisks indicate data from Vander Zanden 1999). (Bottom panels) Diet expressed as range of body sizes observed while feeding on profundal (mostly chironomids), littoral (various insects and small prey fish including young-of-the-year yellow perch and minnows), and pelagic (cisco) prey sources.

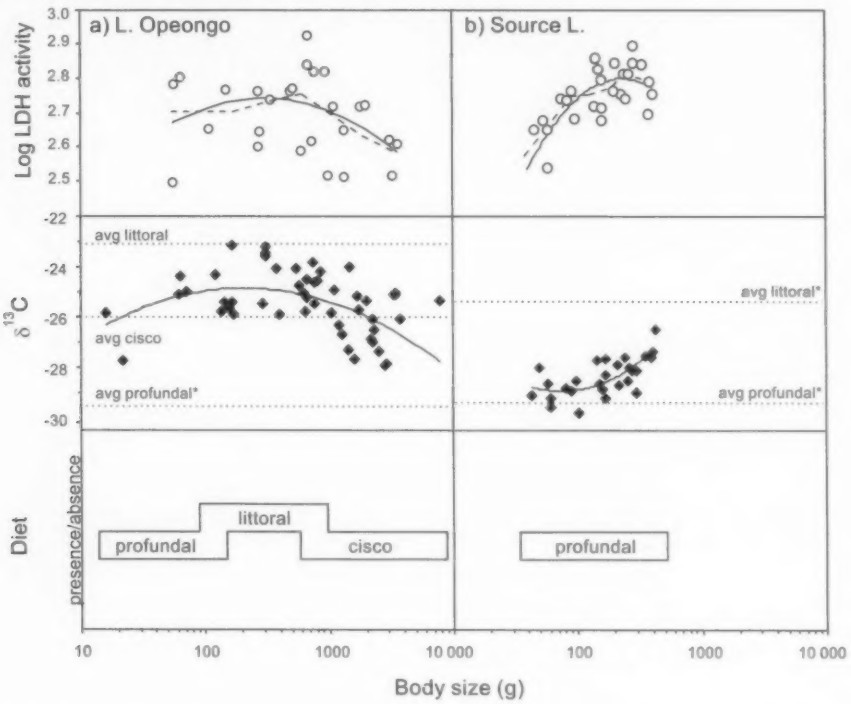

Table 3. Scaling results for fish activity (b_A) and lactate dehydrogenase activity (b_{LDH}) over the same body size range.

Lake	Species	Size range (g)	b_{LDH}	b_A*	Source†
Brome	Yellow perch	1–24.4	0.17	0.43 (2)	1
Bromont	Yellow perch	1–26.5	–0.04	0 (3)	1
Hertel	Yellow perch	1–10.1	0.26	0.41 (4)	1
Magog	Yellow perch	1–31.8	0.09	0.32 (3)	1
Memphremagog	Yellow perch	1–26.4	0.08	0.21 (4)	1
Waterloo	Yellow perch	1–23.0	0.01	0 (4)	1
Opeongo	Lake trout	55–3655	–0.04	0.21 (11)	2
Source	Lake trout	40–382	0.22	0.38 (8)	2

*Regressions for yellow perch include origin; it was assumed that a 1-g fish should have negligible activity costs (i.e., $A = 1$); slope was set at 0 when less than 0 (A values of less than 1 are artefacts of the method used to estimate activity); value in parentheses is sample size for each regression.

†Source for fish activity values: 1, Boisclair and Rasmussen (1996); 2, Pazzia (2001).

why burst swimming requirements, in terms of the power required to generate single bursts, should go down suddenly and significantly in fish that make diet shifts, particularly from benthivory to piscivory. If LDH scaling mirrored power scaling, as suggested by Sullivan and Somero (1980), where power increases with burst speed and body size (Webb 1977), then only decreases in burst speed would account for decreases in power requirements (and hence lower LDH activity) following such a diet shift. It is unlikely that piscivores require lower burst speeds than benthivores. Decreases in burst swimming speed may still be implicated in cases where diet or habitat shifts entail major changes in locomotory habits towards highly sedentary behaviours (e.g., Seibenaller 1984), or if fish suddenly overcome gape limita-

© 2002 NRC Canada

tion of their predators (i.e., enter a size refuge) and need to rely less on escape potential. On the other hand, it is quite reasonable to expect that burst swimming requirements, in terms of number of bursts or duration of burst swimming, should decline quite sharply as prey size suddenly becomes much larger. As an example, to achieve satiation (~5% body weight per day), a 100-g benthivorous perch would need to consume (i.e., actively seek out and attack) about 500 benthic invertebrates (~10 mg each) per day. In addition, time spent actively feeding is time spent interacting with other fish (conspecifics, competitors, as well as predators), which may have important energetic consequences (e.g., Boisclair and Leggett 1989). The same 100-g perch, actively feeding on other fish (~2.5 g each), would only need to make about two attacks per day to satisfy its feeding requirements, thereby spending much less time actively foraging and interacting. Thus, whenever possible (i.e., when prey availability and predator morphology allow), feeding on larger prey should entail considerably less effort in terms of time spent actively foraging and attacking prey. This, in turn, should lead to lower energetic needs, with respect to minimizing time spent bursting, and lower increases in glycolytic potential. Conversely, feeding on constant prey size should lead to rapid increases in activity costs (number of bursts) with body size and highly positive scaling of glycolytic potential. To our knowledge, the influence of prey size and time spent bursting (or number of bursts) on muscle glycolytic potential has never been tested. The predator–prey size ratio dependent and bioenergetic explanation (after Kerr 1971, for the influence of prey size on fish growth) for positive scaling of anaerobic power in fish put forth here, unlike previous explanations based on hydrodynamic theory (Sullivan and Somero 1980), is consistent with the observation that glycolytic potential often scales weakly or negatively to body size (Childress and Somero 1990), even when fish seem to maintain high burst swimming potential (Garenc et al. 1999).

Other examples of ontogenetic shifts in LDH activity

We know of only two other studies where sawtooth-like allometry of LDH activity was discussed in detail. Seibenaller (1984) found that muscle LDH activity dropped sharply in wild-caught *Sebastolobus altivelis* juveniles following a shift from active, pelagic to sedentary, demersal feeding, an ontogenetic vertical migration which involved changes in hydrostatic pressures of 130 atmospheres or more. Adaptation in the expression of different isozyme forms of LDH, with possible differences in substrate-conversion efficiencies (Somero and Seibenaller 1979), to differences in pressure were not involved in this downshift in LDH activity. Instead, it was argued that differences in metabolic requirements arising, in part, from changes in locomotory costs were responsible for changes in enzyme activity levels. More recently, Garenc et al. (1999) reported on a pattern of LDH scaling strikingly similar to what we show here. They noted that LDH activity in the muscle of threespine sticklebacks (*Gasterosteus aculeatus*) reared under controlled laboratory conditions followed positive allometry in juveniles and that this relationship broke down in adults which had significantly lower LDH activities than juveniles. They explained that this may have been due to an increased mobilization of energy reserves in the muscle towards reproductive costs in adults. Although admittedly speculative, our findings suggest that this pattern could also have arisen inadvertently as the result of a facilitated diet shift from fine-ground powdered food (Tetra Marin staple food) to larger *Artemia* and bloodworms. Such a change in diet would be functionally similar to a shift from feeding on zooplankton to benthic invertebrates and may in fact be expected to elicit a decrease in burst swimming requirements in terms of number of feeding bursts. Consideration of burst speed, which continued for the most part to follow positive allometry in adults (Garenc et al. 1999), would not have necessarily captured changes in swim performance in this sense. Future experiments could be designed to specifically test for the possible influence of induced diet shifts towards larger food particles on spontaneous fish activity (measured as rate or number of bursts) and muscle glycolytic potential.

Implications for optimal foraging

The results of the present study provide evidence for the importance of a component of foraging in fish which may be underappreciated in optimality models, that is, the cost of pursuit, attack, and capture. That glycolytic enzymes are involved in supplying quick, burst energy to spontaneous movements in fish (Childress and Somero 1990), that fish body mass is typically made up of >50% white (anaerobic) muscle (Somero and Childress 1980), and that the activity of glycolytic enzymes corresponds very well to independent estimates of total fish activity costs (Sherwood et al. 2002) and diet ontogeny all suggest that spontaneous (anaerobic) activity in fish is not a trivial component of foraging costs. Routine swimming involving spontaneous movements, such as would be required for attacking prey, has been found to be the most costly form of activity in free-swimming fish (Krohn and Boisclair 1994). Optimality models already incorporate activity expenditures associated with obtaining prey, focusing mainly on the amount of time spent searching for and handling prey (Townsend and Winfield 1985), both aerobic forms of activity. Here, we simply add to existing models by suggesting that consideration of how energy is expended during a given bout of foraging (e.g., mostly searching, an aerobic process, versus mostly attacking, an anaerobic process) can be just as important. Explicitly assigning high and variable energy costs to the attack component of foraging, perhaps with the aid of LDH measurements, may result in more finely tuned model predictions of optimal prey size for fish in nature. For example, our results suggest that activity costs should be higher when fish spend most of their time attacking small prey than when they spend most of their time searching for large prey. In this case, prey abundance may become less important in compensating for small prey size (e.g., Kerr 1971). The finding that fish growth usually accelerates after diet shifts to larger prey (Jones et al. 1994), which should be less abundant (Rasmussen 1993) and harder to find (Kerr 1971), would be consistent with this expectation.

Thus, in terms of foraging, highly costly spontaneous activity and high glycolytic potential should be most useful in attacking prey and perhaps less involved in searching for and handling prey, which may implicate aerobic processes. How-

© 2002 NRC Canada

ever, attacking prey may or may not involve burst speeds. For instance, it may be hard to imagine that sunfish "attack" sedentary snails in the same way that pike are likely to attack their fish prey and that attacks are involved in the observed pattern of positive LDH allometry for sunfish. It is possible that fish actually do attack sedentary prey in the same manner that they attack moving prey. The appearance of individual prey items, even sedentary ones, in the presence of potential competitors may be a fleeting phenomenon and require quick reactions and high burst capabilities for successful captures. An alternative explanation is that the time spent searching for and handling prey, which should increase as predator size – prey size ratios increase in the same way that number of attacks should increase, may expose fish to competitive interactions (both exploitative and nonexploitative) and predators that may require high levels of burst swimming performance. All of these possibilities, which are functionally similar, would not be distinguishable from the point of view of enzyme activities. Future studies may be undertaken to explore further the influence of prey type (sedentary versus mobile), competition (both inter- and intra-specific), and predation on fish activity and LDH scaling patterns in fish.

Finally, it should be stated that the saw-toothed model may not always appear as such. For instance, lake trout seem to follow more gradual shifts in diet and associated LDH activity. This probably has more to do with timing than any real modifications on the saw-toothed model itself. In addition to making ontogenetic diet shifts, lake trout are forced to undergo annual habitat shifts from inshore to offshore communities as a result of their intolerance to warm temperatures. Lake trout for the present study were captured in May around the time that they would have been making the characteristic move from inshore, littoral feeding into deeper, colder waters (Pazzia 2001). LDH activities measured at the time of capture should have depended on the length of the time interval that trout were actually feeding offshore (i.e., on large forage fish, such as cisco, which should be less costly) and whether or not they were large enough to make this shift following thermal exclusion from inshore resources. Not moving to colder water may also affect LDH activity directly (e.g., Nathanailides 1996); this would not have affected our results for yellow perch, sunfish, rock bass, and pike as these are all warm-water fish and, at the time of capture, were all foraging in surface waters (1–2 m, 15–20°C) regardless of diet. Those trout not poised to shift to cisco may have continued to make costly forays into warmer waters, either inshore or surface, to exploit smaller forage fish. These considerations should have the effect of increasing the variance in LDH activity around this habitat shift thereby leading to the highly variable and gradual shift patterns that we observe. Regardless of the shape of the relationship, diet and habitat shifts still had the overall effect of lowering LDH activity and fish activity in lake trout.

Implication for bioenergetics models

Our study complements previous findings (Childress and Somero 1990) that the activity of anaerobic enzymes scales mostly positively, but extremely variably, with body size.

Fig. 5. Relationship between body size and consumption rate (C) for yellow perch. Open circles are data from Boisclair and Rasmussen (1996); $C = 0.03 \cdot W^{1.04}$ ($R^2 = 0.63$, $p < 0.0001$). solid circles are data from Sherwood et al. (2000); $C = 0.02 \cdot W^{1.00}$ ($R^2 = 0.75$, $p < 0.0001$). In both cases, C scales isometrically to body size (slopes are not significantly different than 1). Data were not combined because they represent different sampling time intervals and different methodologies; open circles are estimates during summer based on gut clearance models; solid circles are annual estimates made with a radiocesium mass-balance method.

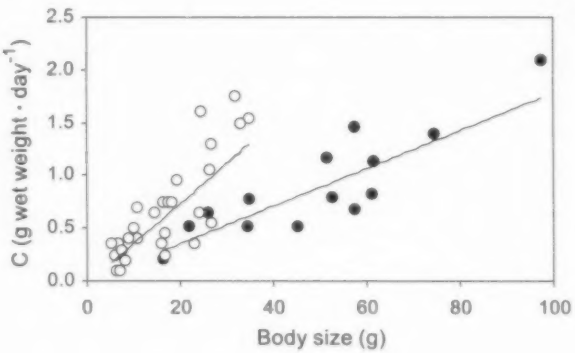

This, as well as the finding that LDH scaling has been found to be strongly related to the scaling of fish activity costs, has important implications for bioenergetic modelling in fish. For example, when consumption rates scale isometrically with body size (Fig. 5), the energy available for growth and activity would increase with body size (Fig. 6). This is because standard metabolic costs tend to decrease with body size, and remaining costs (SDA, F, and U, see eq. 1) are considered to be fixed proportions of consumption rate (Kitchell et al. 1977). The implication of highly variable LDH activity scaling is that when LDH activity, and hence fish activity, increase sharply with body size, the scope for growth should become severely limited and fish should stunt (Fig. 6). Or, when activity costs, plus all other bioenergetic costs (not including growth), equal 100% of the energy budget set by feeding rate, growth efficiency should become zero and growth should cease, thus constituting an energetic bottleneck. In this instance, energy available for reproduction should also be quite limited. In cases where LDH and fish activity do not scale sharply with body size (argued here to occur when fish frequently shift diet), other factors may become more important in limiting growth. This may involve decreasing consumption rates; in an extensive meta-analysis of feeding rates covering numerous fish species with a large range in body sizes, consumption rates were found to scale with an exponent of about –0.2 (Trudel et al. 2000). The important point to note is that generic fish activity multipliers derived from forced swimming trials performed in the laboratory, which are known to greatly underestimate the cost of spontaneous (free) swimming (Krohn and Boisclair 1994), when applied to bioenergetics models (Kitchell et al. 1977), would not allow one to distinguish when fish activity costs are limiting to growth in field

© 2002 NRC Canada

Fig. 6. Typical size scaling of various metabolic costs for two different populations of yellow perch as a proportion of the total energy budget (C, see also eq. 1). SMR is standard metabolic rate; Losses are the sum of all losses resulting from excretion, egestion, and specific dynamic action; and G is growth (both somatic and gonadal). All else being equal, the two panels illustrate fish activity scaling for (*a*) Lake Memphremagog perch (b_{LDH} = 0.08) and (*b*) Lake Hertel perch (b_{LDH} = 0.27; for first diet stage), which were known to stunt at quite small sizes as planktivores (Heath and Roff 1987). The dotted line represents a hypothetical diet shift that would allow stunted perch to grow out of a bottleneck. These two lakes were chosen here for comparison because they have similar specific consumption rates (about 4% body weight per day, Boisclair and Rasmussen 1996) but vastly different LDH activity scaling coefficients. The scaling coefficient for C was set at zero (i.e., C was assumed to be isometric, based on data presented in Fig. 5). The P value (Kitchell et al. 1977) was set so as to result in consumption rates approximating those observed for lakes Hertel and Memphremagog perch. Fish activity (A) was given by $A = W^{b_A}$ (values for b_A are from Table 3). All other model parameters were set as default values given by Kitchell et al. (1977).

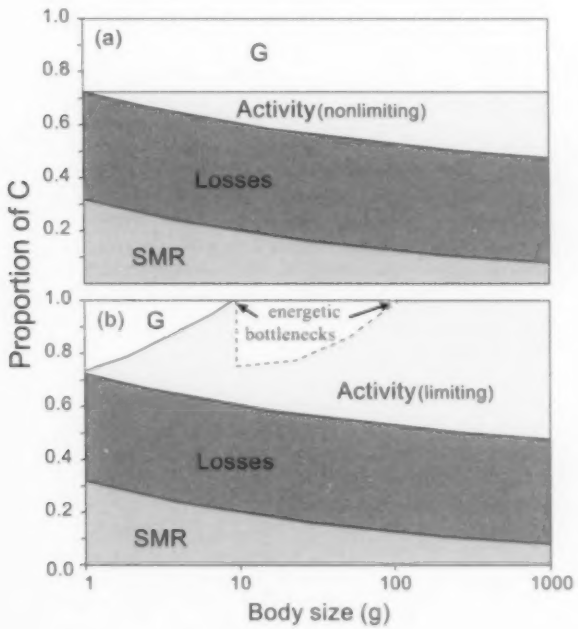

settings. Finally, the idea that fish activity, as inferred from LDH scaling, can be limiting to growth has some empirical support. We found a significant negative relationship between maximum fish size and field-derived LDH scaling across numerous populations and species of fish (Fig. 7; R^2 = 0.37, $p < 0.0001$; relationship without largest extreme value, *Microstomus pacificus*, was significant, R^2 = 0.28, $p < 0.001$).

The above modelling and empirical results for the relationship between LDH activity and fish growth in nature may provide some ecological context for some recent laboratory findings. Positive correlations have been found between various muscle enzyme activities (including LDH) and growth and condition in captive-held Atlantic cod (*Gadus morhua*) (Pelletier et al. 1994; Couture et al. 1998). In these cases, growth was controlled by varying levels of feeding. It was suggested that this information could be useful in estimating growth rates of wild cod (Couture et al. 1998). We caution against this approach, which is likely to lead to overestimation of cod growth rates in nature. Under controlled laboratory conditions, higher growth rates can be achieved by higher feeding rates, which would entail higher fish activity (and therefore higher enzyme activities). However, it would appear that feeding rates in nature are not the only important factor in determining fish growth (Tucker and Rasmussen 1999; Sherwood et al. 2000; Trudel et al. 2001). Perhaps more important, maximum fish growth in nature should coincide with minimal activity costs (Fig. 6). Therefore, as opposed to the above laboratory findings where activity costs would have been artificially manipulated (i.e., kept relatively low) by varying feeding levels on a constant, preferred prey source, we conclude that the highest growth and size in wild-living fish should be accompanied by minimal increases in LDH activities.

Fig. 7. Relationship between LDH scaling coefficient (b_{LDH}) and maximum size (W_{max}) for 23 species of marine fishes (solid circles; Table 2). Open circles are data for freshwater fish presented here (Table 1). Open squares are data for yellow perch from Sherwood et al. (2002).

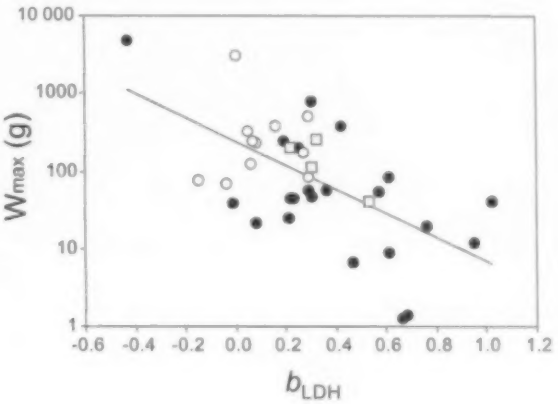

On a final note, our results suggest that any changes in food web structure, either natural or human induced, that limit feeding opportunities may lead to what we call energetic bottlenecks resulting from an inability to shift diet and reset activity costs and, ultimately, stunting in fish. Energetic bottlenecks have been implicated in the stunting of yellow perch living in pollutant-impacted food webs (Sherwood et al. 2002), should be involved in stunting the growth of lake trout living in invasion-impacted food webs (Vander Zanden et al. 1999; Pazzia 2001), and may play an important role in producing variable growth in North Atlantic cod (Krohn et al. 1997) living in fluctuating ocean food webs (Rose et al. 2000). The application of LDH measurements, and perhaps other enzymes involved in anaerobic fish activity, should provide a powerful tool in future ecological studies for as-

© 2002 NRC Canada

sessing the consequence of variable food webs on the bioenergetic performance of wild-living fish.

Acknowledgements

We thank D. Boisclair, M. Trudel, and G. Morinville for helpful comments on earlier drafts of this manuscript. A. Shapiro, C. Raudseppe-Hearne, V. Bussières, R. Pilon, C. Canning, E. Coleman, J. D'Entremont, M. Fillion, M. Filion, C. Gauthier, A. Iles, I. Lesard, É. Laliberté, C. Polzot, E. Shessler, V. Trudeau, and J. Veillette provided valuable field and laboratory assistance. We also thank the staff at the Harknesss Laboratory of Fisheries Research, especially M. Ridgway, G. Ridout, D. Brown, and T. Middel. Research was supported by the Canadian Network of Toxicology Centres (CNTC, Reproductive and Endocrine Toxicology Program), the Metals In The Environment Research Network (MITE-RN, Project C3—Impacts), Natural Science and Engineering Research Council of Canada grants to J.B.R., and a Graduate Fellowship to G.D.S. from the Vineberg Family.

References

Boisclair, D., and Leggett, W.C. 1989. Among-population variability of fish growth. III. Influence of fish community. Can. J. Fish. Aquat. Sci. **46**: 1539–1550.

Boisclair, D., and Rasmussen, J.B. 1996. Empirical analysis of the influence of environmental variables associated with lake eutrophication on perch growth, consumption, and activity rates. Ann. Zool. Fenn. **33**: 507–515.

Childress, J.J., and Somero, G.N. 1990. Metabolic scaling: a new perspective based on scaling of glycolytic enzyme activities. Am. Zool. **30**: 161–173.

Couture, P., Dutil, J.-D., and Guderley, H. 1998. Biochemical correlates of growth and condition in juvenile Atlantic cod (*Gadus morhua*) from Newfoundland. Can. J. Fish. Aquat. Sci. **55**: 1591–1598.

Froese, R., and Pauly, D. (*Editors*). 2001. FishBase. World Wide Web electronic publication (www.fishbase.org).

Garenc, C., Couture, P., Laflamme, M.-A., and Guderley, H. 1999. Metabolic correlates of burst swimming capacity of juvenile and adult threespine stickleback (*Gasterosteus aculeatus*). J. Comp. Physiol. B, **169**: 113–122.

Heath, D., and Roff, D.A. 1987. Test of genetic differentiation in growth of stunted and nonstunted populations of yellow perch and pumpkinseed. Trans. Am. Fish. Soc. **116**: 98–102.

Jones, M.S., Goettl, J.P., Jr., and Flickinger, S.A. 1994. Changes in walleye food habits and growth following a rainbow smelt introduction. North Am. J. Fish. Manag. **14**: 409–414.

Kerr, S.R. 1971. Prediction of fish growth efficiency in nature. J. Fish. Res. Board Can. **28**: 815–819.

Kerr, S.R., and Ryder, R.A. 1977. Niche theory and percid community structure. J. Fish. Res. Board Can. **34**: 1952–1958.

Kitchell, J.F., Stewart, D.J., and Weininger, D. 1977. Applications of a bioenergetics model to yellow perch (*Perca flavescens*) and walleye (*Stizostedion vitreum vitreum*). J. Fish. Res. Board Can. **34**: 1922–1935.

Krohn, M.M., and Boisclair, D. 1994. Use of a stereo-video system to estimate the energy expenditure of free-swimming fish. Can. J. Fish. Aquat. Sci. **51**: 1119–1127.

Krohn, M., Reidy, S., and Kerr, S. 1997. Bioenergetic analysis of the effects of temperature and prey availability on growth and condition of northern cod (*Gadus morhua*). Can. J. Fish. Aquat. Sci. **54**(Suppl. 1): 113–121.

Mittelbach, G.G., and Persson, L. 1998. The ontogeny of piscivory and its ecological consequences. Can. J. Fish. Aquat. Sci. **55**: 1454–1465.

Nathanailides, C. 1996. Metabolic specialization of muscle during development in cold-water and warm-water fish species exposed to different thermal conditions. Can. J. Fish. Aquat. Sci. **53**: 2147–2155.

Pazzia, I. 2001. Influence of food web structure on the growth and bioenergetics of lake trout. MSc. thesis, McGill University, Montreal, Canada.

Pelletier, D., Dutil, J.-D., and Guderley, H. 1994. Relation between growth rate and metabolic organization of white muscle, liver and digestive tract in cod, *Gadus morhua*. J. Comp. Physiol. B, **164**: 179–190.

Peters, R.H. 1983. The ecological implications of body size. Cambridge University Press, New York.

Rasmussen, J.B. 1993. Patterns in the size structure of littoral zone macroinvertebrate communities. Can. J. Fish. Aquat. Sci. **50**: 2192–2207.

Rose, G.A., deYoung, B., Kulka, D.W., Goddard, S.V., and Fletcher, G.L. 2000. Distribution shifts and overfishing the northern cod (*Gadus morhua*): a view from the ocean. Can. J. Fish. Aquat. Sci. **57**: 644–663.

Scharf, F.S., Juanes, F., and Roundtree, R.A. 2000. Predator size – prey size relationships of marine fish predators: interspecific variation and effects of ontogeny and body size on trophic-niche breadth. Mar. Ecol. Prog. Ser. **208**: 229–248.

Schulte, P.M., Glemet, H.C., Fiebig, A.A., and Powers, D.A. 2000. Adaptive variation in lactate dehydrogenase-B gene expression: role of a stress-responsive regulatory element. Proc. Natl. Acad. Sci. U.S.A. **97**: 6597–6602.

Seibenaller, J.F. 1984. Analysis of the biochemical consequences of ontogenetic vertical migration in a deep-living teleost fish. Physiol. Zool. **57**: 589–608.

Sherwood, G.D., Rasmussen, J.B., Rowan, D.J., Brodeur, J., and Hontela, A. 2000. Bioenergetic costs of heavy metal exposure in yellow perch (*Perca flavescens*): in situ estimates with a radiotracer (^{137}Cs) technique. Can. J. Fish. Aquat. Sci. **57**: 441–450.

Sherwood, G.D., Kovecses, J., Hontela, A., and Rasmussen, J.B. 2002. Simplified food webs lead to energetic bottlenecks in polluted lakes. Can. J. Fish. Aquat. Sci. **59**: 1–5.

Somero, G.N., and Childress, J.J. 1980. A violation of the metabolic-size scaling paradigm: activities of glycolytic enzymes in muscle increase in larger-size fish. Physiol. Zool. **53**: 322–337.

Somero, G.N., and Seibenaller, J.F. 1979. Inefficient lactate dehydrogenases of deep-sea fishes. Nature (London), **282**: 100–102.

Sullivan, K.M., and Somero, G.N. 1980. Enzyme activities of fish skeletal muscle and brain as influenced by depth of occurrence and habits of feeding and locomotion. Mar. Biol. **60**: 91–99.

Townsend, C.R., and Winfield, I.J. 1985. The application of optimal foraging theory to feeding behaviour in fish. *In* Fish energetics: new perspectives. *Edited by* P. Tytler and P. Calow. Croom Helm Ltd., London. pp. 67–97.

Trudel, M., Tremblay, M., Schetagne, R., and Rasmussen, J.B. 2000. Estimating food consumption rates of fish using a mercury mass-balance model. Can. J. Fish. Aquat. Sci. **57**: 414–428.

Trudel, M., Tremblay, A., Schetagne, R., and Rasmussen, J.B. 2001. Why are dwarf fish so small? An energetic analysis of dwarfism in lake whitefish (*Coregonus clupeaformis*). Can. J. Fish. Aquat. Sci. **58**: 394–405.

Tucker, S., and Rasmussen, J.B. 1999. Using ^{137}Cs to measure and compare bioenergetic budgets of juvenile Altantic salmon (*Salmo salar*) and brook trout (*Salvelinus fontinalis*) in the field. Can. J. Fish. Aquat. Sci. **56**: 875–887.

© 2002 NRC Canada

Vander Zanden, M.J. 1999. Trophic position in aquatic food webs. PhD. thesis, McGill University, Montreal, Canada.

Vander Zanden, M.J., and Rasmussen, J.B. 1999. Primary consumer $\delta^{15}N$ and $\delta^{13}C$ and the trophic position of primary consumers. Ecology, **80**: 1395–1404.

Vander Zanden, M.J., Casselman, J.M., and Rasmussen, J.B. 1999. Stable isotope evidence for the food web consequences of species invasions in lakes. Nature (London), **401**: 464–467.

Wankowski, J.W.J., and Thorpe, J.E. 1979. The role of food particle size in the growth of juvenile Atlantic salmon (*Salmo salar* L.). J. Fish Biol. **14**: 351–370.

Webb, P.W. 1977. Effects of size on performance and energetics of fish. *In* Scale effects in animal locomotion. *Edited by* T.J. Pedley. Academic Press, New York. pp. 315–322.

© 2002 NRC Canada

Incorporating Allee effects in fish stock–recruitment models and applications for determining reference points

D.G. Chen, J.R. Irvine, and A.J. Cass

Abstract: A new type of stock–recruitment model is examined that incorporates Allee effects, which may occur when fish populations are small. The model is a natural extension of traditional models, which only incorporate the negative effects of increasing density on fecundity and (or) survival. Because the new model is intrinsically nonlinear and because of convergence problems at local optima, we use a maximum likelihood approach with a global genetic search algorithm to estimate model parameters. Parameter uncertainty is obtained from the inverse of the Fisher information matrix. Based on this new model, an extinction probability curve is developed using the parameter defining the Allee effects. This curve can readily be used to calculate the theoretical probability of extinction for a single brood line in one generation for any particular spawner number or biomass. Alternatively, because managers may wish to assign reference points corresponding to particular extinction probabilities, spawner numbers can be determined for these reference points. Two Pacific salmon populations, North Thompson coho (*Oncorhynchus kisutch*) and Chilko sockeye (*O. nerka*), are used to demonstrate the approach. It is found that the Allee effect parameter is statistically significant for the Thompson coho, but not for Chilko sockeye.

Résumé : Nous examinons un nouveau modèle de stock–recrutement qui incorpore les effets Allee qui peuvent se manifester lorsque les densités de populations de poissons sont faibles. Le modèle est une extension naturelle des modèles courants qui ne tiennent compte des effets négatifs sur la fécondité et (ou) la survie que dans le cas de densités croissantes. Cependant, puisque le nouveau modèle est essentiellement non linéaire et qu'il y a des problèmes de convergence aux optimums locaux, nous adoptons, pour estimer les paramètres du modèle, une approche basée sur la vraisemblance maximale et utilisons un algorithme de recherche génétique global. L'incertitude des paramètres a été obtenue à partir de l'inverse de la matrice d'information de Fisher. Le nouveau modèle permet d'établir une courbe de probabilité d'extinction à l'aide du paramètre qui décrit les effets Allee. La courbe peut servir à calculer facilement la probabilité théorique d'extinction pour une seule lignée dans une génération, pour toute densité ou biomasse de reproducteurs. D'autre part, parce que les gestionnaires peuvent vouloir déterminer des points de référence correspondant aux diverses probabilités d'extinction, il est possible de déterminer des densités de reproducteurs pour ces points de référence. Deux populations de saumons du Pacifique, les saumons coho (*Oncorhynchus kisutch*) de la North Thompson et les saumons rouges (*O. nerka*) de la Chilko, servent à illustrer le fonctionnement de la méthode. Le paramètre décrivant l'effet Allee est significatif chez les Saumons coho de la Thompson, mais pas pour les Saumons rouges de la Chilko.

[Traduit par la Rédaction]

Introduction

The analysis of fish stock–recruitment (*S–R*) is often the first step to evaluate and implement fishery policies designed to optimize spawner numbers and exploitation rates. The analysis typically begins with the assumption of a functional relationship, denoted by $F(\cdot)$, between spawners and recruits:

$$(1) \qquad R_t = S_t F(S_t, \theta)$$

where S_t is the spawners at year t, $t = 1$ to n, and R_t is the corresponding recruits for the spawners at that brood year t calculated as total escapements and catches. θ is a vector of parameters associated with this relationship and may be associated with a fishery management policy.

The two most commonly used functional forms based on biologically and statistically sound grounds are the Beverton–Holt model (Beverton and Holt 1957) and the Ricker model (Ricker 1975):

$$(2) \qquad R_t = \frac{\alpha S_t}{1 + \beta S_t} \qquad \text{(Beverton–Holt model)}$$

$$(3) \qquad R_t = S_t e^{\alpha - \beta S_t} \qquad \text{(Ricker model)}$$

Received 16 May 2001. Accepted 21 November 2001. Published on the NRC Research Press Web site at http://cjfas.nrc.ca on 22 February 2002.
J16351

D.G. Chen.[1] International Pacific Halibut Commission, University of Washington, P.O. Box 95009, Seattle, WA 98195, U.S.A.
J.R. Irvine and A.J. Cass. Fisheries and Oceans Canada, Pacific Biological Station, 3190 Hammond Bay Road, Nanaimo, BC V9R 5K6, Canada.

[1]Corresponding author (e-mail: din@iphc.washington.edu).

 DOI: 10.1139/F02-005 © 2002 NRC Canada

where a and b are the parameters to describe productivity of the population at low density and capacity limited by density dependence, respectively. As a unified *S–R* model, Deriso (1980) introduced an additional shape parameter γ and proposed the following model:

$$(4) \qquad R_t = \alpha S_t(1 - \gamma\beta S_t)^{1/\gamma} \quad \text{(Deriso model)}$$

where γ is a shape parameter to modify the *S–R* relationship. It can be seen that the Beverton–Holt model (2) and Ricker model (3) are in fact special cases of the Deriso model (4) when $\gamma = -1$ and $\gamma \to 0$, respectively.

These models allow for compensatory mortality. At high population densities, resources will become limiting and recruits per spawner will decrease. However, the models ignore depensatory population dynamics, which may occur when the population is small. This is known as the Allee effect (Allee et al. 1949) when population growth declines as population density declines. A variety of processes can result in depensation at low abundance. Inbreeding may occur, spawning fish may not find mates, higher mortality may result from predator saturation or fishing, and poor conditioning of the spawning environment and low efficiency of food location may result (Asmussen 1979; Emlen 1984; Hilborn and Walters 1992). When abundances are low, depensation (if it exists) will accelerate population declines and increase their probability of extinction (McElhany et al. 2000). With depensatory effects, stock rebuilding could be delayed or prevented (Walters and Kitchell 2001).

Whether depensation is a significant factor for fish populations is not clear. Myers et al. (1995) found that three of 26 fish stocks had lower than expected recruits per spawner at low densities than would be expected using a Beverton–Holt model. Liermann and Hilborn (1997) examined the same data and found that the most likely values for the stock–recruit relationship were usually close to or within the range of no depensation. However, because there was a significant amount of uncertainty about whether depensation existed, Liermann and Hilborn (1997) concluded that analyses of stock–recruitment data should incorporate spawner–recruit curves that allow for the possibility of depensation.

Several approaches have been used to incorporate possible depensatory effects in the analysis of stock–recruit data. Hilborn and Walters (1992) and Routledge and Irvine (1999) show how to modify the *S–R* curve to incorporate a depensatory parameter. Hilborn and Walters (1992) recommended replacing αS with αS^m where the power parameter m is greater than 1.0. Routledge and Irvine (1999) introduced a cutoff value c to allow for the effects of possible depensation at low abundance and modified their formulas when $S \le c$. Myers et al. (1995), in a meta-analysis of 129 fish stocks, found little statistical evidence for widespread depensation. Liermann and Hilborn (1997) used a Bayesian hierarchical model to calculate the prior distribution for the depensatory parameter. They concluded that the broad tails of distributions for various taxa extend into the depensatory range and suggested that the possibility of depensation should be considered in the population dynamics of fishes.

In the discussion of compensatory population dynamics within a stock complex, Frank and Brickman (2000) were the first to introduce a *S–R* model that incorporated Allee effects by permitting a non-zero intercept representing recruitment failure. They concluded from simulation experiments that aggregated populations could obscure detection of Allee effects. Incorporating depensation, the *S–R* model in eq. 1 becomes

$$(5) \qquad R_t = (S_t - S_{\text{offset}})F(S_t - S_{\text{offset}}, \theta)$$

where S_{offset} is the parameter associated with the Allee effects and is the offset from the origin representing zero recruitment (Frank and Brickman 2000). Hereafter model 5 (eq. 5) will be called Allee *S–R* model. For the *S–R* models 2–4, the corresponding Allee *S–R* models would be

$$(6) \qquad R_t = \frac{\alpha(S_t - S_{\text{offset}})}{1 + \beta(S_t - S_{\text{offset}})}$$

$$(7) \qquad R_t = (S_t - S_{\text{offset}})e^{\alpha - \beta(S_t - S_{\text{offset}})}$$

$$(8) \qquad R_t = \alpha(S_t - S_{\text{offset}})[1 - \gamma\beta(S_t - S_{\text{offset}})]^{1/\gamma}$$

In this paper, we apply a maximum likelihood estimation (MLE) approach to estimate *S–R* parameters using a global search algorithm. We discuss the properties of the parameter S_{offset} associated with Allee effects in the new model, apply it and develop an operational extinction probability curve for a single brood line in one generation, and use this approach to quantify reference points in the domain of risk analysis. The methodology is applied using *S–R* data from North Thompson coho salmon (*Oncorhynchus kisutch*) and Chilko River sockeye salmon (*O. nerka*).

Parameter estimation and global genetic search algorithm

For the purpose of illustration, we shall use model 7, hereafter referred to as the Allee–Ricker model, to illustrate the development of the new model, the estimation of parameters, and also the development of an extinction probability curve and reference points. The same procedures can be readily applied for models 6 and 8, or any extensions of these.

Parameter estimation

To be compatible with the traditional assumptions for the *S–R* analyses, we assume that recruitment is log-normally distributed. Therefore, model 7 is

$$(9) \qquad \ln(R_t) = \ln(S_t - S_{\text{offset}}) + \alpha - \beta(S_t - S_{\text{offset}}) + \varepsilon_t$$

where $\varepsilon_t \sim N(0, \sigma^2)$. The commonly used linear regression estimation approach cannot be used because the new model (eq. 9) is nonlinear for the parameters (S_{offset}, α, β). We therefore utilize theories of nonlinear regression (e.g., Draper and Smith 1981) and MLE (e.g., Kalbfleisch 1985) to estimate model parameters and associated statistical inferences for the parameters and model.

The log-likelihood function for model 9 is defined as

$$(10) \qquad \ln L(S_{\text{offset}}, \alpha, \beta | \text{data}) \propto -\frac{n}{2}\ln(\sigma^2) - \frac{\sum_{i=1}^{n}[\ln(R_t) - \ln(S_t - S_{\text{offset}}) - \alpha + \beta(S_t - S_{\text{offset}})]^2}{2\sigma^2}$$

© 2002 NRC Canada

Conventionally, twice the negative log likelihood is used as the "inference function" in the MLE, which is $l(S_{offset}, \alpha, \beta) = -2\ln[L(S_{offset}, \alpha, \beta|data)]$. According to the theory of MLE, $l(S_{offset}, \alpha, \beta)$ is asymptotically chi-square distributed by the degrees of freedom $n - 3$, i.e., $l(S_{offset}, \alpha, \beta) \sim \chi^2_{n-3}$. Estimates of the parameters $\hat{\Theta} = (\hat{S}_{offset}, \hat{\alpha}, \hat{\beta})$ are obtained by minimizing $l(S_{offset}, \alpha, \beta)$. The uncertainty in $\hat{\Theta} = (\hat{S}_{offset}, \hat{\alpha}, \hat{\beta})$ is assessed from the estimated covariance matrix $\mathrm{Cov}(\hat{S}_{offset}, \hat{\alpha}, \hat{\beta}) = I(\hat{S}_{offset}, \hat{\alpha}, \hat{\beta})^{-1}$, where $I(\hat{S}_{offset}, \hat{\alpha}, \hat{\beta})$ is the Fisher information matrix defined as

$$(11)\quad I(\hat{S}_{offset}, \hat{\alpha}, \hat{\beta}) = -\frac{1}{2} E \begin{pmatrix} \frac{\partial^2 l}{\partial S_{offset}^2}, & \frac{\partial^2 l}{\partial S_{offset}\partial \alpha}, & \frac{\partial^2 l}{\partial S_{offset}\partial \beta} \\ \frac{\partial^2 l}{\partial \alpha \partial S_{offset}}, & \frac{\partial^2 l}{\partial \alpha^2}, & \frac{\partial^2 l}{\partial \alpha \partial \beta} \\ \frac{\partial^2 l}{\partial \beta \partial S_{offset}}, & \frac{\partial^2 l}{\partial \beta \partial \alpha}, & \frac{\partial^2 l}{\partial \beta^2} \end{pmatrix}_{(\hat{S}_{offset}, \hat{\alpha}, \hat{\beta})}$$

The estimated standard error for each parameter can be obtained from the corresponding elements from eq. 11. According to theory of MLE, the parameter estimates $\hat{a}$, $\hat{b}$, and $\hat{S}_{offset}$ in eqs. 9 and 10 are asymptotically normally distributed (Mood et al. 1974, p. 359) as

$$(12)\quad \hat{a} \sim N(a, \sigma_a^2),\ \hat{b} \sim N(b, \sigma_b^2),\ \text{and}\ \hat{S}_{offset} \sim N(S_{offset}, \sigma^2_{S_{offset}})$$

Special attention is paid to the parameter $\hat{S}_{offset}$ because this parameter represents the number of spawners that will theoretically produce zero recruitment. As abundance decreases, there is an increasing probability of extinction. By definition, if the spawning biomass were below $\hat{S}_{offset}$, this brood line would have a high probability of going extinct. Therefore, for a specific population with maximum life span K years, if the spawning biomass were below $\hat{S}_{offset}$ for K years, this population would have a high probability of extinction.

We wish to evaluate whether including the Allee parameter $\hat{S}_{offset}$ improves the model fit from model 7 relative to the traditional Ricker model 3. Because models 3 and 7 are nested, the likelihood ratio test can be used to test whether the inclusion of $\hat{S}_{offset}$ significantly improves the model fit:

$$(13)\quad l(\alpha, \beta) - l(S_{offset}, \alpha, \beta) \sim \chi^2_1$$

where $l(\alpha, \beta)$ and $l(S_{offset}, \alpha, \beta)$ are twice the negative log-likelihood function from models 3 and 7, respectively.

Global genetic search algorithm

The parameter estimates can be obtained from eq. 10 by any of various search algorithms, including gradient and hill-climbing search methods. These search algorithms are known as local search algorithms where the initial starting points are essential. We found that there is more than one local optima for the minimization of eq. 10, depending on the choice of starting points. The global genetic search algorithm (GA) was used to avoid convergence on local optima, often problematic when using classical hill-climbing techniques that require initial starting values. Genetic algorithms designed to find global optima originated from studies of the mechanics of natural selection and genetics with natural populations evolving according to the principles of "survival of the fittest" (Holland 1975). The highly fit individuals are given high opportunities to "reproduce", by "crossing-over" with others in the population. GA differs from conventional search techniques in that it considers many points in the search space simultaneously and therefore has a reduced chance of converging to some local optimum. Since Holland (1975) introduced and investigated this algorithm, the approach has been used in many areas, such as in curve fitting, mathematical optimization, and training neural network models. Recent descriptions of the approach with applications to fisheries are found in Saila (1996) and Chen et al. (2000).

To use the GA in this paper, we specify a large but reasonable range for each parameter in $\theta = (S_{offset}, \alpha, \beta)$ and randomly generate an initial population with 100 starting points. Based on the fundamental "genetic" operators as reproduction, crossover, and mutation, 10% of the best solutions among the 100 are reproduced. By analogy with a biological genetic system where mutations are rare, a higher probability is given to the crossover process than to the mutation process. Therefore, we chose an 80% probability for crossover processes and a 5% probability for mutation processes; convergence was achieved at these levels. This provides a "crossover" mechanism for the search to mix and match desirable qualities through a random process with the occasional "mutation" of a value at a particular search position.

Definition of an extinction probability curve for a single brood line

Spawner numbers or biomass is the most readily available and also the most commonly used quantity in fisheries research and management. Clearly we would like to manage stocks above the parameter S_{offset} with known probability. The extinction probability function of the stock for a single brood line in one generation can be defined as $\Pr(\text{Stock Extinction}) = \Pr(S \le S_{offset})$. Because S_{offset} can be estimated from the MLE (eq. 10) with the distribution in eq. 11, the operational definition of the extinction probability (denoted by OPr(EP)) is

$$(14)\quad \mathrm{OPr(EP)} = \Pr(S \le \hat{S}_{offset}) = \Pr(\hat{S}_{offset} > S) = 1 - \Phi\left(\frac{\hat{S}_{offset} - S}{\sigma_{S_{offset}}}\right)$$

for any level of spawner numbers or biomass S. In eq. 14, $\Phi(\cdot)$ is the cumulative density function for the standard normal distribution. Because $\sigma_{S_{offset}}$ in eq. 14 is generally unknown, then the MLE estimate from eq. 11 can be used to give an estimate of OPr(EP):

$$(15)\quad \widehat{\mathrm{OPr(EP)}} = \Pr(\hat{S}_{offset} > S) = 1 - T\left(\frac{\hat{S}_{offset} - S}{\hat{\sigma}_{S_{offset}}}\right)$$

where $T(\cdot)$ is the cumulative density function for the t distribution with degrees of freedom $n - 3$.

The operational definition of extinction probability (eq. 15) can be used to calculate the probability of extinction

© 2002 NRC Canada

Table 1. Summary of parameter estimates for North Thompson coho and Chilko sockeye salmon and under Ricker *S–R* (stock–recruitment) models and the new Allee–Ricker models.

Stock	Model	α	β	S_{offset}	*l*
North Thompson coho	Ricker	1.281 (0.346)	1.22×10^{-5} (8.39×10^{-6})	NA	–4.818
	Allee–Ricker	1.808 (0.458)	2.13×10^{-5} (9.75×10^{-6})	5 211 (1 680)	–6.518
Chilko sockeye	Ricker	2.155 (0.253)	1.61×10^{-6} (4.95×10^{-7})	NA	–36.715
	Allee–Ricker	2.179 (0.232)	1.65×10^{-6} (5.03×10^{-7})	1 585 (11 065)	–36.740

Note: The column "*l*" is the value for the twice the negative log-likelihood function. Values in parentheses represent the estimated standard error. NA, not applicable.

Fig. 1. Stock–recruitment relationships for North Thompson coho salmon. The solid curve is the Ricker model (eq. 3) fit, the broken line is the Allee–Ricker model (eq. 9) fit, and the straight line is the replacement line. Value "5.211" is the estimated S_{offset} (= 5.211 × 1000).

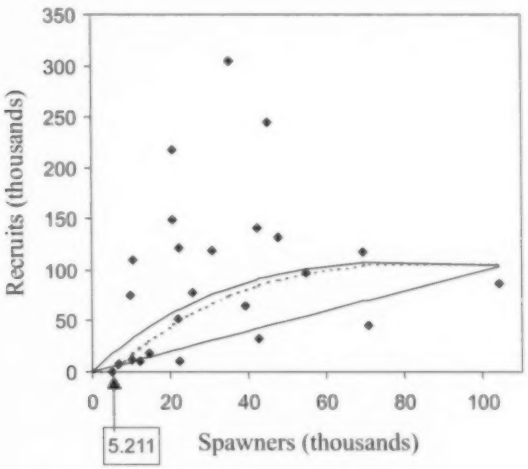

Fig. 2. The performance of the genetic search algorithm using the North Thompson coho data. From top to bottom, the lines represent the worst, median, and best values from the 100 points in every generation.

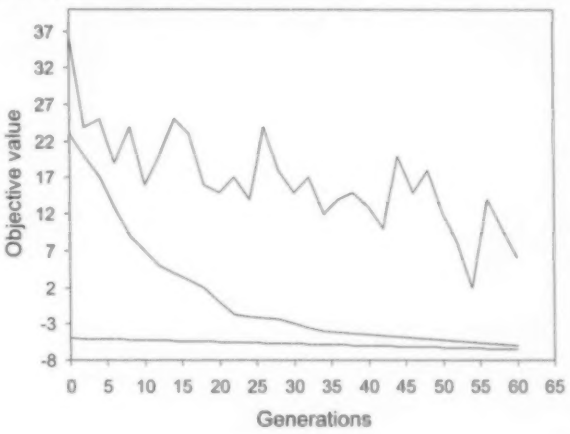

for one brood line for any given spawner number or biomass S_t. It can also be used to obtain reference points for a given extinction probability that is based on an acceptable level of extinction risk.

Data applications

North Thompson coho

Identification of reference points and extinction probabilities at low spawner numbers are needed for coho salmon from the Thompson River watershed in central British Columbia. Numbers of coho salmon returning to the Thompson River have declined significantly in recent years and these fish have been the focus of much attention (Bradford and Irvine 2000). Precise estimates of spawner numbers are available for North Thompson coho commencing in 1975, and annual recruitment (catch plus spawners) was estimated using a time series of fishery exploitation rates (Irvine et al. 2001):

$$(16) \qquad R_t = S_t/(1 - \text{expl}_t)R_t$$

where all spawners were assumed to be 3 years old, and expl_t is the fishery exploitation rate (catch/(catch + spawners)) in year *t*.

We first fit the Ricker model (eq. 3) to *S–R* data for North Thompson coho by a simple regression approach and then fit the same *S–R* data with the Allee–Ricker *S–R* model (eq. 9) by the MLE with the GA approach (Fig. 1). The GA search algorithm with 100 sets of initial points in the search space is illustrated in Fig. 2. It can be seen from Fig. 2 that convergence is achieved after ~60 generations (generation is a term used in GA, which is equivalent to "iterations" in most other search algorithms). Parameter estimates and resulting values for the twice-negative likelihood function are summarized in Table 1. The Allee–Ricker model (eq. 9) gave the lower value (–6.518 for Allee–Ricker model and –4.818 for Ricker model) for the negative log-likelihood function, indicating that the Allee–Ricker model fit the data better than the Ricker *S–R* model. This indicates that the inclusion of the parameter S_{offset} improved the model fit. We conclude that the Allee–Ricker model (eq. 9) should be used to analyze the *S–R* relationship.

For the new model, the estimate of S_{offset} is 5211 coho salmon (Fig. 1) with a standard error of 1680. Therefore, the distribution for $\chi^2_{0.80,1} = 1.642$ can be constructed using eq. 12 (Fig. 3) with the 95% confidence interval, which is (1736, 8686). Because this 95% confidence interval does not cover 0, S_{offset} is statistically significant and therefore the inclusion of S_{offset} significantly improves the model fit.

With the new Allee–Ricker model (eq. 9), the operational extinction probability function from eq. 15 can be constructed. For this stock, the extinction probability as a func-

© 2002 NRC Canada

Table 2. Relationship between calculated extinction probabilities for given spawner numbers (the second and third columns) and the calculated spawner abundance for given extinction probabilities based on eq. 15 (the fourth and fifth columns).

	Spawner abundance	Extinction probability	Extinction probability	Spawner abundance
North Thompson coho	S_{offset}	0.501	0.1	7 438
	Hist. min.	0.191	0.3	6 106
	2 000	0.968	0.5	5 222
	5 000	0.551	0.7	4 316
	10 000	0.005	0.9	2 984
Chilko sockeye	S_{offset}	0.898	0.1	19 200
	Hist. min.	0.139	0.3	12 270
	10 000	0.401	0.5	8 084
	20 000	0.086	0.7	4 680
	30 000	0.009	0.9	1 550

Note: S_{offset} is estimated from the new Allee–Ricker model; Hist. min., the historical minimum of the observed spawner numbers.

Fig. 3. The distribution of $\hat{S}_{offset}$ for North Thompson coho. The vertical line is the estimated $\hat{S}_{offset}$ = 5.211 and the horizontal line with arrows at both ends is the 95% confidence interval.

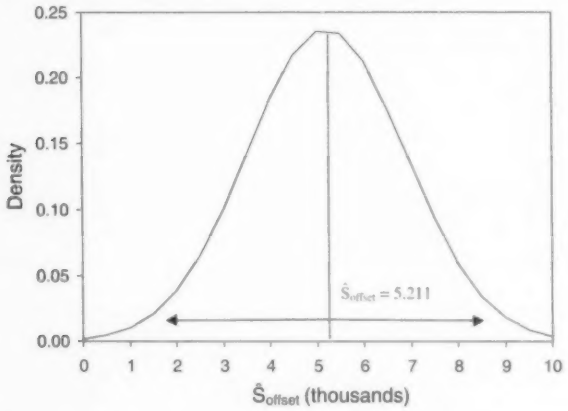

Fig. 4. Probability of extinction of one brood line as a function of North Thompson coho spawner numbers. From left to right, the two vertical lines are the extinction probabilities corresponding to the estimated S_{offset} and the historical minimum spawner number, respectively. The horizontal line depicts the calculated spawner numbers corresponding to the 80% extinction probability.

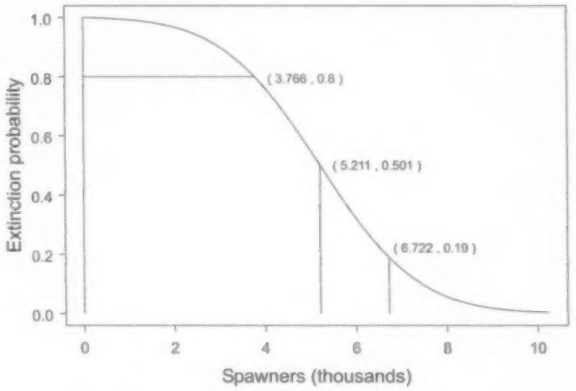

tion of spawner numbers is produced using S_{offset} = 5211 and $\hat{S}_{offset}$ = 1680 (Fig. 4). From this figure, we provide several extinction probabilities calculated from different levels of spawner number, such as, at S_{offset}, the observed historical minimum spawning biomass, 2000, 5000, and 10 000 coho (Table 2). Also, with any extinction probability suggested by managers, the corresponding spawner numbers can be calculated from this function as a management reference point (Fig. 4). In Table 2, we list several reference points for the probabilities of extinction at 0.1, 0.3, 0.5, 0.7, and 0.9.

Patterns in the residuals were examined after the Ricker model (eq. 3) was fit to the data. No apparent relationship was seen between the size of the population and the residuals, but there was evidence of nonstationarity. A sequence of strong positive residuals in the early 1980s preceded a declining trend, with negative residuals occurring in most recent years. In this instance, trends in the residuals do not negate the value of calculating S_{offset} because recent low productivities (α) result in a positive bias in estimates of S_{offset}. We consider that a small positive bias when computing a reference point is acceptable because it is risk averse. The patterns in the residuals may provide an explanation as to why the Allee-Ricker model fit the data better than the traditional Ricker *S–R* model (Table 1). The first-order autocorrelation was significant when the Ricker *S–R* model was applied (Lag 1, autocorrelation coefficient ρ = 0.42) but was not when the Allee-Ricker model was fit to the data (Fig. 5).

Chilko sockeye

Spawner and recruit data for Chilko Lake sockeye are available for brood years 1948 to 1995 (Fig. 6). Chilko Lake is one of the largest producers of sockeye within the Fraser River watershed with an average of 340 000 spawners and 1.4 million recruits per year. This stock has rebuilt since the 1980s and the numbers of spawners has increased to nearly 700 000 per year since 1989. The *S–R* relationship suggests the stock is now near the maximum capacity of Chilko Lake. Chilko Lake was fertilized intermittently in 4 years beginning in 1987 and ending in 1992. Bradford et al. (2000) present evidence for increased sockeye freshwater productivity as a result of fertilization. The *S–R* data used in our analysis exclude the 4 years of fertilization to avoid potential problems of parameter bias.

We first fit the Ricker model (eq. 3) by a simple regression approach and then fit the Allee Ricker *S–R* model

© 2002 NRC Canada

Fig. 5. Autocorrelation function (ACF) for the residuals applying (*a*) the standard Ricker model and (*b*) the Allee–Ricker model to North Thompson coho data. The first-order (i.e., Lag 1) autocorrelation with the standard Ricker model was just significant as it was barely outside the 95% confidence band (dotted lines).

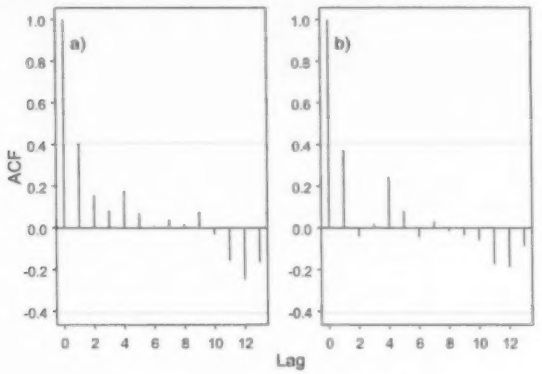

Fig. 6. Stock–recruitment relationships for Chilko River sockeye salmon. Solid curve is the Ricker model (eq. 3) fit, and the broken line is the Allee–Ricker model (eq. 9) fit. Because of the large data range and scale for the spawner abundance, both lines are so close that it is difficult to distinguish them. The straight line is the replacement line. Because the estimated value for S_{offset} (1585 = 1.585 × 1000) is so close to the origin, a plot showing details close to the origin is embedded in the plot. For this embedded plot, the solid line is the Ricker model (eq. 3) fit and the broken line is the fit from the Allee–Ricker model (eq. 9). Value "1.585" is the estimated S_{offset} rescaled by 1000. The only dot in the figure is the last observed *S–R* (stock–recruitment) data point with 17.308 (×1000) spawners and 204.386 (×1000) recruits.

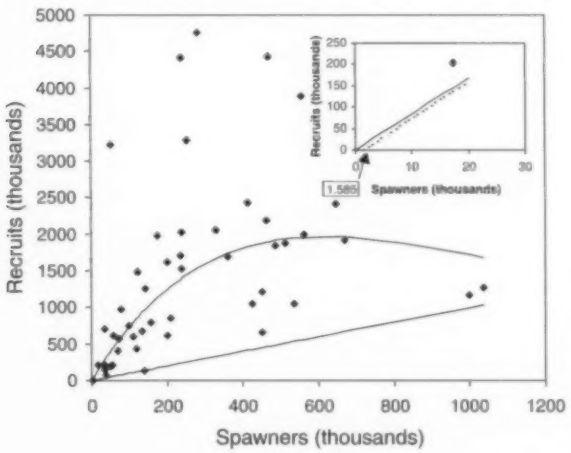

(eq. 9) by the MLE with the GA for the same data. The parameter estimates and the resulting value for the twice-negative likelihood function are summarized in Table 1. The estimate of S_{offset} is 1585 fish with standard error of 11 065. Because S_{offset} is close to the origin of the *S–R* relationship, an inset is provided (Fig. 6) to illustrate S_{offset} relative to the

Fig. 7. The distribution of $\hat{S}_{offset}$ for Chilko sockeye salmon. The vertical line is the estimated $\hat{S}_{offset}$ (= 1.585 × 1000), and the horizontal line with arrows at both ends is the 95% confidence interval.

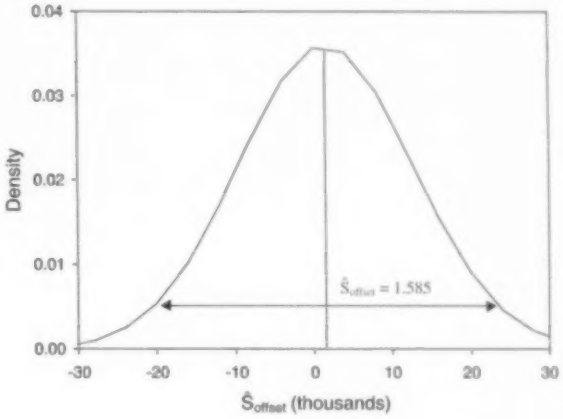

Fig. 8. Extinction probability as function of the Chilko sockeye spawner numbers rescaled so that the extinction probability is zero for the spawner abundance to be zero. From left to right, the two vertical lines are the extinction probabilities corresponding to the estimated S_{offset} and the historical minimum observed spawner numbers, respectively. The horizontal line depicts the calculated spawner numbers corresponding to the 50% extinction probability.

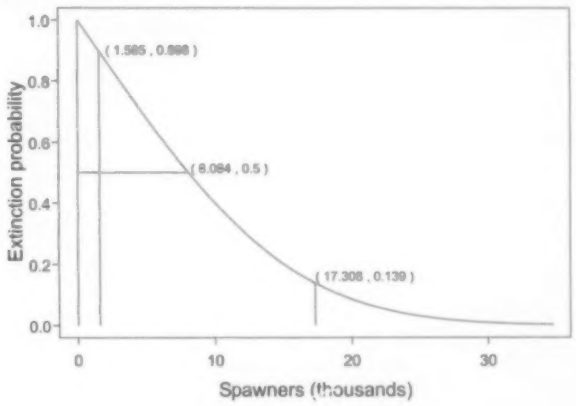

Ricker *S–R* curve. Observed spawning escapements ranged from 17 300 to 1 038 000 fish. The 95% confidence interval of the probability distribution of S_{offset} (12) includes 0 (Fig. 7). Therefore the inclusion of S_{offset} does not significantly improve the model fit.

Even though S_{offset} is not statistically significant different from zero, the estimated distribution can still be used for the calculation of extinction probabilities because eq. 15 is only dependent on the estimated parameter and its associated variance. The extinction probability for Chilko sockeye can be calculated for a given spawner abundance (Fig. 8), and depending on the level of risk tolerance, a management reference point in terms of spawner abundance can be calcu-

© 2002 NRC Canada

lated from this function. In Table 2, we list several reference points for given probabilities.

Discussion

In this paper we make several contributions to the field of conservation biology and in particular the evaluation of extinction risk. First, we demonstrate a new way that traditional *S–R* models can be extended to incorporate potential Allee effects. Methods to estimate parameters and associated statistical inferences are developed including the use of GA. Second, with the extended Allee–Ricker model, we develop an operational formula for the extinction probability function. This formula can be used to calculate the extinction probability for any given spawner abundance and also allows managers the opportunity to define reference points according to particular extinction probabilities.

The precautionary approach is increasingly being applied in fisheries management to comply with international agreements for sustainable resource use (e.g., Richards and Maguire 1999). This approach is intended to ensure that conservation takes precedence over other objectives (NMFS 1999). Reference points provide the primary mechanism by which the precautionary approach can be applied (Richards and Maguire 1999). In our paper, we define the probability distribution associated with S_{offset} and propose this as a suitable reference point that can be used by managers to minimize the possibility of population extinction.

Managers applying the precautionary approach would like a low probability of populations going extinct. One way to do this is to "buffer" reference points by incorporating uncertainty. Sources of uncertainty and statistical pitfalls that can bias stock–recruitment model parameters are discussed in Hilborn and Walters (1992). These include lack of contrast in the spawning escapement variable, measurement errors in escapement and recruitment, temporal autocorrelation in the *S–R* series, and nonstationarity of *S–R* relationships. Apart from the lack of contrast in the escapement time series, various statistical remedies can deal with *S–R* biases. To minimize the likelihood of a population falling below the S_{offset}, the limit should be set higher than the point estimate. For instance, one might wish to select a reference point corresponding to the 10% extinction probability rather than the 50% value. Uncertainty in S_{offset} as a result of *S–R* bias should be carefully examined on a case-specific basis as with any of the classical *S–R* models. If there is a temporal pattern in productivity, one could model productivity as a function of time. Reference points may need to be raised during periods of low productivity. In addition, S_{offset} could be used in a Bayesian decision analysis to evaluate the consequence of alternative management objectives on extinction risk.

The two salmon examples considered here demonstrate the potential effect of data variability at low spawner densities on estimates of S_{offset}. It would be instructive to apply this approach to other species. For North Thompson coho, S_{offset} is statistically significant from zero despite the variability in the data at low spawner densities. Because S_{offset} for Chilko sockeye is not significant, it is unclear if depensatory mortality at low spawner density is negligible or if depensatory mortality is masked by high survival variability and (or) data measurement error. As previously concluded by Liermann and Hilborn (1997), one should not ignore the possibility of an Allee effect because uncertainty in parameter distributions may mask the presence of depensation at low abundance.

The extended model (eq. 5) can also be used to incorporate environmental information and fishery interventions, such as $R_t = (S_t - S_{\text{offset}})F(S_t - S_{\text{offset}}, \mathbf{X}_t, \theta)$, where $\mathbf{X}_t$ is a vector of environmental and fishery intervention variables. This model can be combined with the semiparametric approach discussed in Chen and Irvine (2001) to analyze the compensatory and depensatory effects embedded in the *S–R* relationship with environmental and fishery interventions.

As an extension and further research for the definition of the extinction probability function given by eqs. 14 and 15, we are exploring the possibility of defining the probability of stock extinction as $\Pr(\text{Stock Extinction}) = \Pr(S_t \le S_{\text{offset}}, \forall t = 1,\ldots,K)$, where K is the maximum life span (years) for the specific stock (K would be 4 and 6 for our coho and sockeye examples respectively) and $\forall$ is a logic notation denoting "for all" t. Because S_{offset} is the critical value for the stock below which recruitment would be zero, if the spawner abundance for this stock is below this critical value for K years, the stock would be extinct.

We feel that the new Allee–Ricker model is a useful extension for the traditional *S–R* model to be used for fishery *S–R* analysis, and we believe that the operational definition of the extinction probability function developed in this paper is a useful tool for fishery management.

Acknowledgements

We thank Gayle Brown and Alan Sinclair for helpful comments on the manuscript and approach. We also appreciate constructive comments from two anonymous reviewers, the Associate Editor, and the Editors.

References

Allee, W.C., Emerson, A.E., Park, O., Park, T., and Schmidt, K.P. 1949. Principles of animal ecology. Saunders, Philadelphia.

Asmussen, M.A. 1979. Density-dependent selection. II. The Allee effect. Am. Nat. **114**: 796–809.

Beverton, R.J.H., and Holt, S.J. 1957. On the dynamics of exploited fish population. Fish. Invest. Ser. II, Mar. Fish. G.B. Minist. Agric. Fish. Food, **19**.

Bradford, M.J., and Irvine, J.R. 2000. Land use, fishing, climate change and the decline of Thompson River, British Columbia, coho salmon. Can. J. Fish. Aquat. Sci. **57**: 13–16.

Bradford, M.J., Pyper, B.J., and Shortreed, K.S. 2000. Biological responses of sockeye salmon to the fertilization of Chilko Lake, a large lake in the interior of British Columbia. N. Am. J. Fish. Manag. **20**: 661–671.

Chen, D.G., and Irvine, J.R. 2001. A semiparametric model to examine stock–recruitment relationships incorporating environmental data. Can. J. Fish. Aquat. Sci. **58**: 1178–1186.

Chen, D.G., Hargreaves, N.B., Ware, D.M., and Liu, Y. 2000. A fuzzy logic model with genetic algorithm for analyzing fish stock–recruitment relationships. Can. J. Fish. Aquat. Sci. **57**: 1878–1887.

Deriso, R.B. 1980. Harvesting strategies and parameter estimation for an age-structured model. Can. J. Fish. Aquat. Sci. **37**: 268–282.

© 2002 NRC Canada

Draper, N.R., and Smith, H. 1981. Applied regression analysis. 2nd ed. John Wiley & Sons, Inc., New York.

Emlen, J.M. 1984. Population biology, the coevolution of population dynamics and behavior. Macmillan, New York.

Frank, K.T., and Brickman, D. 2000. Allee effects and compensatory population dynamics within a stock complex. Can. J. Fish. Aquat. Sci. **57**: 513–517.

Hilborn, R., and Walters, C.J. 1992. Quantitative fisheries stock assessment and management: choice, dynamics, and uncertainty. Chapman and Hall Inc., New York.

Holland, J. 1975. Adaptation in natural and artificial systems. University of Michigan Press, Ann Arbor, Mich.

Irvine, J.R., Parken, C.K., Chen, D.G., Candy, J., Ming, T., Supernault, J., Shaw, W., and Bailey, R.E. 2001. 2001 assessment of stock status for coho salmon from the interior Fraser River. Canadian Stock Assessment Secretariat Research Document 2001/083. *Available from* CSAS, 200 Kent St., ON K1A 0E6, Canada, or at http://www.dfo-mpo.gc.ca/csas/.

Kalbfleisch, J.G. 1985. Probability and statistical inference. Vol. 2. Statistical inference. 2nd ed. Springer-Verlag, New York.

Liermann, M., and Hilborn, R. 1997. Depensation in fish stocks: a hierarchical Bayesian meta-analysis. Can. J. Fish. Aquat. Sci. **44**: 1976–1984.

McElhany, P., Ruckelshaus, M.H., Ford, M.J., Wainwright, T.C., and Bjorkstedt, E.P. 2000. Viable salmonid populations and the recovery of evolutionarily significant units. U.S. Department of Commerce, NOAA (National Oceanic and Atmospheric Administration), Washington, D.C., Tech. Memo. NMFS-NWFSC-42.

Mood, A.M, Graybill, F.A., and Boes, D.C. 1974. Introduction to the theory of statistics. McGraw-Hill, Inc., New York.

Myers, R.A., Barrowman, N.J., Hutchings, J.A., and Rosenberg, A.A. 1995. Population dynamics of exploited fish stocks at low population levels. Science (Washington, D.C.), **269**: 1106–1108.

National Marine Fisheries Service (NMFS). 1999. Our living oceans. Report on the status of U.S. living marine resources, 1999. U.S. Department of Commerce, NOAA (National Oceanic and Atmospheric Administration), Washington, D.C., Tech. Memo. NMFS-F/SPO-41.

Richards, L.J., and Maguire, J.J. 1999. Recent international agreements and the precautionary approach: new directions for fisheries management science. Can. J. Fish. Aquat. Sci. **55**: 1545–1552.

Ricker, W.E. 1975. Computation and interpretation of biological statistics of fish populations. Bull. Fish. Res. Board Can. Bull. 191.

Routledge, R.D., and Irvine, J.R. 1999. Chance fluctuations and the survival of small salmon stocks. Can. J. Fish. Aquat. Sci. **56**: 1512–1519.

Saila, S.B. 1996. Guide to some computerised artificial intelligence methods. *In* Computers in fisheries research. *Edited by* B.A. Megrey and E. Moksness. Chapman and Hall, London. pp. 8–40.

Walters, C., and Kitchell, J.F. 2001. Cultivation/depensation effects on juvenile survival and recruitment: implications for the theory of fishing. Can. J. Fish. Aquat. Sci. **58**: 39–50.

© 2002 NRC Canada

PERSPECTIVE

A stage-explicit expression of the von Bertalanffy growth model for understanding age at first reproduction of Great Lakes fishes

Ji X. He and Donald J. Stewart

Abstract: An initial annual growth rate of body length and its regular decrease with increasing age has general linkages with age at first reproduction (t_R). We clarify their combinations and develop predictive functions. We use a complete Ford–Walford plot with yearling size (L_1) on the *y* axis and show a slope transition between the relative yearling growth rate (ρ_y) and the Ford–Walford slope (ρ). The three stage-specific variables define a complete body-length trajectory over ages, including all von Bertalanffy growth parameters and the Ford–Walford intercept (L_{int}). The difference between asymptotic length (L_{inf}) and yearling length is growth potential after the first annulus. Yearling growth is a transition period, so growth potential can be adjusted as ρL_{inf} or $L_{inf} - L_{int}$. Changes in the three life-stage variables have contrasting effects on growth potential and von Bertalanffy growth parameters, so they have contrasting relations with t_R. For most invertebrate-eating fishes in the Laurentian Great Lakes, dominant changes in growth trajectories were reflected in ρ, so t_R was predicted by the von Bertalanffy growth coefficient, *K*. For walleye (*Stizostedion vitreum*) populations around the Great Lakes, dominant changes in growth trajectories were from yearling size or yearling growth, so t_R was predicted using L_{int}. Our results have clear implications for understanding fish population dynamics.

Résumé : Le taux initial de croissance annuelle en taille et sa décroissance graduelle avec l'âge sont en relation générale avec l'âge à la première reproduction (t_R). Nous mettons en lumière les différentes combinaisons de ces liens et développons des fonctions prédictives. Nous utilisons un graphique complet de Ford–Walford avec la taille des poissons de 1 an (L_1) en ordonnée et démontrons l'existence d'une transition de pente entre le taux relatif de croissance des poissons de 1 an (ρ_y) et la pente de Ford–Walford (ρ). Les trois variables spécifiques au stade définissent la trajectoire complète de la taille au cours de la vie, y compris les paramètres de croissance de Bertalanffy et le point de croisement de Ford–Walford (L_{int}). La différence entre la longueur asymptotique (L_{inf}) et la longueur des poissons de 1 an représente le potentiel de croissance après le premier anneau de croissance. Comme la croissance des poissons de 1 an représente une période de transition, le potentiel de croissance peut donc être ajusté en fonction de (ρL_{inf}) ou de ($L_{inf} - L_{int}$). Les variations des trois variables du cycle biologique ont des effets différents sur le potentiel de croissance et les paramètres de von Bertalanffy, et, par conséquent, sur t_R. Chez la plupart des poissons des Grands-Lacs qui se nourrissent d'invertébrés, les changements principaux dans les trajectoires de croissance se reflètent dans les pentes de Ford–Walford et ainsi t_R peut être prédit à partir de *K*. Chez les populations de dorés (*Stizostedion vitreum*) de la région des Grands-Lacs, les changements importants dans les trajectoires de croissance sont reliés à la taille ou à la croissance des poissons de 1 an et t_R peut alors être prédit d'après L_{int}. Nos résultats sont importants pour la compréhension de la dynamique des populations de poissons.

[Traduit par la Rédaction]

Received 10 September 2001. Accepted 24 January 2002. Published on the NRC Research Press Web site at http://cjfas.nrc.ca on 22 February 2002.
J16522

J.X. He[1,2] and D.J. Stewart. State University of New York, College of Environmental Science and Forestry, 103 Illick Hall, 1 Forestry Drive, Syracuse, NY 13210, U.S.A.

[1]Corresponding author (e-mail: jhe@zoo.utoronto.ca).
[2]Present address: Department of Zoology, 25 Harbord Street, University of Toronto, Toronto, ON M5S 3G5, Canada.

 DOI: 10.1139/F02-008 © 2002 NRC Canada

Introduction

Relations between body growth and age at first reproduction need to be further clarified, and the goal is to find quantitative predictive relations. Rapid growth in young ages can lead to early age at first reproduction (e.g., Alm 1959), whereas a slow decrease in annual growth with increasing age may lead to late age at first reproduction (e.g., Martin 1970; Matuszek et al. 1990). Recent studies have addressed combinations of the above two different relations (Hutchings 1993; Jonsson and Jonsson 1993; Fox 1994), but reaction norms summarized by Stearns (1992) did not sufficiently address those complexities (see also Berrigan and Charnov 1994).

There have been many studies that relate age or size at first reproduction to von Bertalanffy growth parameters (Beverton 1992; Charnov 1993; Jensen 1996). Those empirical relations are general patterns, and very often, their emphasis is not accuracy of predictions. A promising approach to understanding age or size at first reproduction is to include more independent variables like mortality (e.g., Roff 1984), but in broad practical applications, body growth is often the only reliable information. In a previous study for 85 marine and freshwater fish species with 235 observations, most of the variance in size and age at first reproduction was explained by body growth alone (He and Stewart 2001). A similar perspective was presented by Shuter et al. (1998). It is still a challenge to build on general patterns and demonstrate accurate prediction of changes in age or size at first reproduction.

We propose that the theoretical basis for practical prediction may have to involve consideration for stage-specific effects of body growth. Along that line, typical life-stage compositions of normal growth trajectories must be demonstrated, although those trajectories have been commonly described as continuous processes. In this paper, we have two sets of objectives. (*i*) To develop a stage-explicit expression of the commonly used von Bertalanffy growth model (VBGM, von Bertalanffy 1938) and to clarify the concept of growth potential that has been used implicitly to study age and size at first reproduction; (*ii*) to apply the stage-explicit model to analyze fishes in the Laurentian Great Lakes, and thereby, to develop accurate predictive relations between body growth and age at first reproduction.

State-explicit expression of VBGM and the concept of growth potential

The commonly used expression of the von Bertalanffy growth model emphasizes continuity of a growth process. With that emphasis alone, there have been difficulties for studying relations between body growth and age at first reproduction.

$$(1) \qquad dL/dt = K(L_{inf} - L)$$

$$(2) \qquad L_t = L_{inf}\,[1 - \exp(-K(t - t_0))]$$

Here, L is body length at a given age (t), K is the von Bertalanffy growth coefficient, and L_{inf} is asymptotic body length. There are three well-known ambiguous concepts in the model expression: (*i*) the maximum growth rate ($E = KL_{inf}$) is hypothetical because it corresponds to zero body length; (*ii*) the coefficient K accounts for both rapid growth and rapid decreases in annual growth; (*iii*) the age with zero body length (t_0) is defined mathematically, and nonzero values for t_0 have not been explained biologically. Assuming t_0 is always negative, a body length at age 0 could be body length at birth or at hatching (Pauly 1981; Charnov 1993). With complete data from age 1 to much older, however, there is no reason to exclude t_0 values that are positive and less than 1.

We can express the same growth process as a combination of stage-specific components:

$$(3) \qquad L_2 = L_1 + \rho_y L_1$$

$$(4) \qquad L_{t+1} - L_t = \rho(L_t - L_{t-1}) \qquad t \geq 2,\ 0 < \rho < 1$$

$$\text{or } L_t = L_{int} + \rho L_{t-1} \qquad t \geq 2,\ 0 < \rho < 1$$

where L_1 is body length at age 1, ρ_y is the relative growth rate of a yearling, ρ is the Ford–Walford slope, and L_{int} is the Ford–Walford intercept (Ford 1933; Walford 1946; Ricker 1975).

Combining eqs. 3 and 4, we have an elementary geometrical progression:

$$(5) \qquad L_t = L_1 + \rho_y L_1 \Sigma \rho^i \qquad i = 0, 1, 2, \ldots, t-1$$

$$\text{or } L_t = L_1 + \rho_y L_1 (1 - \rho^{t-1})/(1 - \rho)$$

With eqs. 3–5, the following biological details are clear. (*i*) When $t = 1$, the whole model is reduced to yearling size, indicating that L_1 is an input variable and is not influenced by the relations that control the subsequent growth process. (*ii*) When $t = 2$, eq. 5 is identical to eq. 3, indicating that the geometric growth of a yearling represents a special transition period. (*iii*) After age 2, annual growth of body length decreases regularly, and ρ is the proportion of annual growth that can be maintained at every age interval (eq. 4).

A critical point of eqs. 1–5 is about biological meanings of L_{int} and the parameter t_0. Those biological meanings were not clear because they have not been defined using measurable variables (see Ford 1933; Walford 1946; Ricker 1975). To clarify conceptual ambiguities, we use a complete Ford–Walford plot that has yearling size on the y axis (Fig. 1*a*). The line from $(0, L_1)$ to (L_1, L_2) has a slope of ρ_y that represents the relative growth rate of a yearling (eq. 3). ρ is for the line starting from (L_1, L_2), and the slope is no longer a growth rate (eq. 4). Quantitatively, ρ_y and ρ often represent a slope transition. L_{int} may differ from yearling size (L_1) simply because of the slope transition (Fig. 1*a*)

$$(6) \qquad L_{int} = L_1(1 + \rho_y - \rho)$$

Correspondingly, the slope transition also leads to a nonzero parameter, t_0, in eq. 2

$$(7) \qquad t_0 = 1 - \ln[\rho_y/(1 + \rho_y - \rho)]/\ln(\rho)$$

If $\rho_y < \rho$, then $L_{int} < L_1$, and t_0 is negative. If $\rho_y > \rho$, then $L_{int} > L_1$ and t_0 is positive. In the latter case with a complete data set including yearling size, t_0 should always be less than 1 because yearling size cannot be zero or negative. In a special case where the two slopes of ρ_y and ρ are quantitatively the same, $t_0 = 0$ and $L_{int} = L_1$.

© 2002 NRC Canada

Fig. 1. A new and complete interpretation of the von Bertalanffy growth model and its implication for predicting age at first reproduction (t_R). Details about data for (*b–d*) are in subsequent sections of the text. (*a*) The complete Ford–Walford plot for a hypothetical body-growth trajectory with von Bertalanffy growth parameters L_{inf} = 90 cm, K = 0.16, and t_0 = –2 (eq. 2). The difference between asymptotic length (L_{inf}) and yearling size (L_1) is growth potential (GP) because L_1 is an input variable on the *y* axis. The slope (ρ_y) is the relative growth rate of yearlings (eq. 3), and the Ford–Walford slope (ρ) after age 2 is not a growth rate (eq. 4). Because yearling growth represented by ρ_y is a transition period, growth potential can be adjusted as ρL_{inf} or $L_{inf} - L_{int}$, where L_{int} is the Ford–Walford intercept (eq. 6). The three stage-specific variables (L_1, ρ_y, ρ) are actually elements that define the growth trajectory (eqs. 5–9). (*b*) Applying eq. 5 to fit growth data, estimated L_1 as a growth parameter is not statistically different from observed yearling size (L_1). (*c*) The parameter t_0 represents the direction and magnitude of slope transition between ρ_y and ρ; the exact relation is eq. 7. (*d*) Two major different tracks for the relation between t_R and the growth coefficient (K). One is for eight walleye populations, and the other is for 23 populations of invertebrate-eating fishes. Those two sets of distinguishable cases may differ in relative dominance of the three major life stages (*a*); details are analyzed in Results.

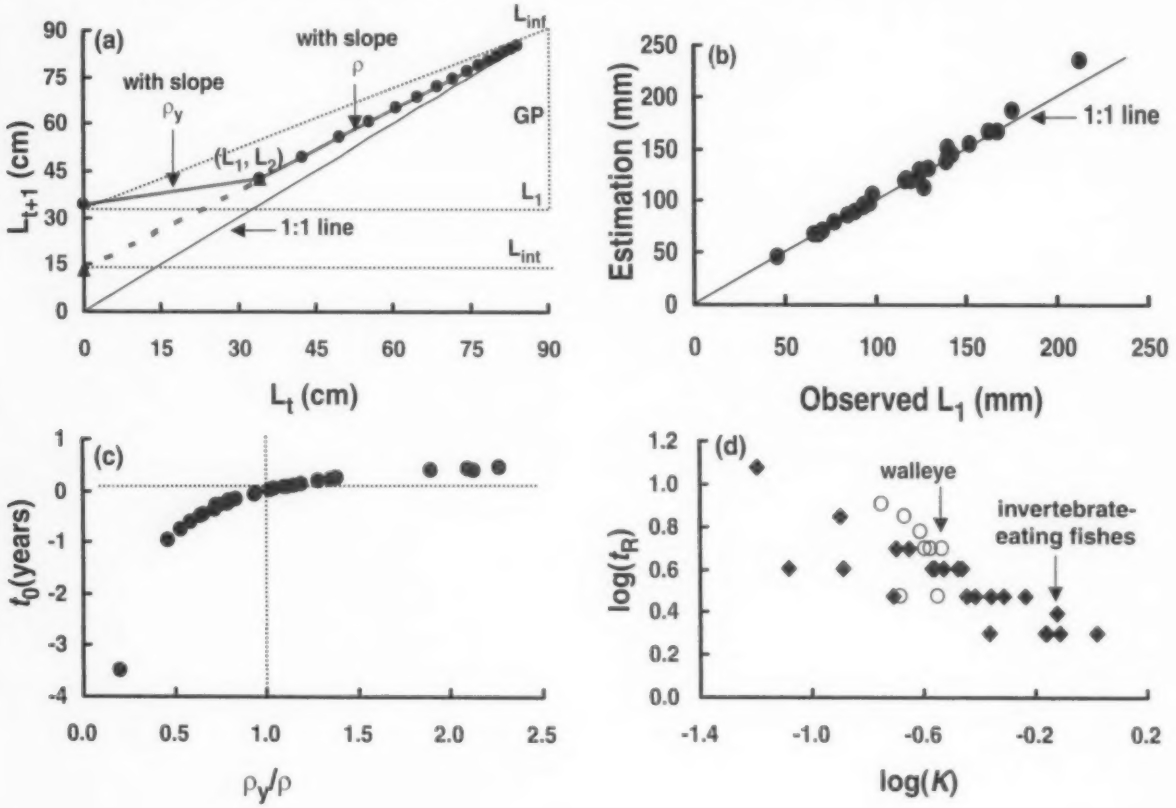

Mathematically, eq. 5 is the simplest form of two general expressions of the von Bertalanffy growth model (Knight 1969; Schnute and Fournier 1980). Other parameters of eqs. 1–2 can be defined also by stage-specific variables in eq. 5

$$K = -\ln(\rho) \quad (8)$$

$$L_{inf} = L_1(1 + \rho_y - \rho)/(1 - \rho) \quad (9)$$

Derivations of eqs. 6–9 are not represented here because they can be obtained by using L_1, ρ_y, and ρ with equations in Knight (1969) and Schnute and Fournier (1980). It is not arbitrary to use the three stage-specific variables (L_1, ρ_y, ρ) because they are elements of a complete growth trajectory and they cannot be further decomposed. They allow us to recognize that the complete Ford–Walford plot (Fig. 1*a*) is an exact expression of the von Bertalanffy growth model (eqs. 1–5). To use the von Bertalanffy growth model, we do not rely on hypothetical concepts such as nonzero body length at age 0 or maximum growth rate with a body length of zero.

With the above stage-explicit expression of the von Bertalanffy growth model, we can specify the concept of growth potential. Rearranging eq. 9, we have

$$(\rho_y L_1)/(1 - \rho) = L_{inf} - L_1 \quad (10)$$

On the left side, the numerator ($\rho_y L_1$) is the maximum annual growth after the first year of a life, and the denominator ($1 - \rho$) is the proportional decay in annual growth after age 2. On the right side, L_1 is an input variable (eq. 5), and L_{inf} is

© 2002 NRC Canada

asymptotic body length. Both sides express growth potential after age 1, and the concept is consistent with eqs. 3–5.

There are two possible ways by which the growth potential may increase or decrease. In the first, with a given set of values for L_1 and ρ_y, the growth potential can be increased by increasing ρ and L_{inf} (Fig. 1*a*). In the second, with a given L_{inf}, the growth potential can be decreased by increasing yearling size (L_1). For the latter case, there may be a negative relation between ($\rho_y L_1$) and ρ, but we must notice that ($\rho_y L_1$) represents a transition period with two components (eqs. 3 and 5; Fig. 1*a*). One component is L_1 and the other component is ρ_y. Increases in ρ_y with a given L_1 may increase the growth potential by increasing asymptotic size, or it may influence ρ without having any impact on the growth potential (eq. 10). The concept of growth potential may need to be adjusted because of the two possibilities of ρ_y effects.

There are a number of ways to adjust the concept of growth potential. From eqs. 6 and 9, we have the commonly used relation between the Ford–Walford intercept and asymptotic size

$$(11) \quad L_{int}/(1-\rho) = L_1(1+\rho_y-\rho)/(1-\rho) = L_{inf}$$

Equation 11 suggests that improvement of body growth at each of the three life stages, represented by L_1, ρ_y, and ρ, can always increase L_{inf}. Such a suggestion is consistent with the model expression of eqs. 1–2, where L_{inf} is regarded as the lifetime growth potential staring from zero body length. Alternatively, we consider that each stage may occupy different environments, and growth in each stage is often controlled by different relations (eqs. 3–5). Rearranging eq. 11, we have

$$(12) \quad (\rho L_{inf}) = (L_{inf} - L_{int})$$

In comparison with eq. 10, L_1 is replaced by L_{int}. The emphasis here is that $\rho_y L_1$ and L_1 jointly represent an early life stage (Fig. 1*a*), whereas ρL_{inf} or $L_{inf} - L_{int}$ are an alternative index of growth potential for subsequent juvenile–adult growth. With a given L_{inf}, an increase in either L_1 or ρ_y can decrease the adjusted growth potential by increasing the intercept (L_{int}, eq. 6; Fig. 1*a*).

It may be worthwhile to mention a qualitative difference between body-length and body-mass growths, because eq. 12 treats adult growth and a major part of juvenile growth as a single stage. Annual growth of somatic body mass increases with age before the first reproduction, and it decreases with increasing age after first reproduction (e.g., Jensen 1985). An emphasis on that stagnation of body-mass growth, however, may not allow us to explore the effects of multiple life stages that significantly influence age at first reproduction long before that age is reached. At the age of first reproduction, an acceleration of decreases in body-length growth has also been suggested (Stamps et al. 1998), but many empirical syntheses have not shown such an acceleration (e.g., Iles 1974; Ricker 1975; Moreau 1987). If age at first reproduction is larger than 2, the annual proportional decrease ($1 - \rho$) in body-length growth is typically the same for both premature and postmature periods. If there is an acceleration of decreases in annual body-length growth corresponding to first reproduction, the commonly used von Bertalanffy growth model would always overestimate body length for mature age classes whenever age at first reproduction is larger than 2.

Growth potential and age at first reproduction

A change in growth potential (eq. 12) should be a basis for predicting changes in age at first reproduction. Such a basis can be justified using functional linkages between body length and age at first reproduction. There is a general pattern as follows (He and Stewart 2001):

$$(13) \quad L_R/(KL_{inf}) = a + bt_R$$

where L_R and t_R are body length and age at first reproduction, a and b are regression parameters, and b is always positive. An alternative expression of the left side is $[1 - \exp(-K(t_R - t_0))]/K$. The two expressions include either L_R or t_R with a given set of growth parameters. Those growth parameters define a functional linkage between L_R and t_R for a given growth trajectory, so we can call the left side an index for growth–reproduction linkage (I_{G-R}). On the right side of eq. 13, the structure with regression parameters is representative of many growth trajectories, so it is not a linear simplification of the left-side structure. There are two interrelated ideas here. (*i*) When the two sides of eq. 13 are equal as demonstrated by empirical data, there must be a fundamental linkage between body length and age at first reproduction regardless of substantial changes in body-growth trajectories. (*ii*) Such a linkage indicates a potential relation between growth potential and age at first reproduction. Because $K = -\ln(\rho)$ (eq. 8), the negative relation between KL_{inf} and t_R suggests that t_R should be positively related to growth potential (ρL_{inf}, eq. 12).

In practical applications, a statistical difficulty may stem from different life stages having contrasting effects on growth potential. When dominant changes are from L_{inf} and ρ, slow decreases in annual growth after age 2 are related to increases in growth potential (eqs. 10 and 12). When dominant changes are from L_1 and ρ_y, large sizes at a given age (particularly a young age) are associated with decreases in growth potential (eq. 12). It is almost impossible to separate those contrasting stage-specific effects.

To overcome the above difficulty, we need case-specific analyses. If dominant changes in body growth are represented by the positive relation between ρ and L_{inf}, or the negative relation between K and L_{inf}, the only dominant predictive variable in eq. 13 will be K. If dominant changes in body growth are represented by L_1 and ρ_y, there will be no significant relation between ρ and L_{inf}, or between K and L_{inf}, but there is always a negative relation between ρ and L_{int} (eq. 6). Comparing the above two typical cases, parameter values for the right side of eq. 13 should be notably different. If we can separate typical cases according to statistical features for life-stage combinations, it may become possible to find an accurate predictive relation between t_R and ρ, or between t_R and L_{int}. The two potential predictive relations are not necessarily interchangeable, although L_{int} and ρ are related to each other for a given growth trajectory (eq. 11). Among various growth trajectories, changes in L_{int} and ρ may have different relative dominances because body-growth trajectories can be influenced mostly

© 2002 NRC Canada

by one or two of the three major life stages, represented by L_1, ρ_y, and ρ.

When we use ρ or L_{int} as an independent variable for predicting changes in age at first reproduction, such a predictive parameter integrates dominant and subordinate factors of growth potential; meanwhile, they also allow for an emphasis on the dominant factor (see eq. 12). If dominant changes are from L_{inf}, the slope ρ will emphasize its positive relation with L_{inf}, while it also integrates potential impacts from the intercept (L_{int}). To demonstrate the point, we can rearrange eqs. 13 and 9, and have

$$(14) \quad \rho = 1 - (L_{int}/L_{inf})$$

$$(15) \quad \rho = [L_{int} - L_1(1 + \rho_y)]/(L_{inf} - L_1)$$

If dominant changes are from L_1 and ρ_y, L_{int} should be used to emphasize changes in those two dominant variables, whereas L_{int} will also integrate subordinate impacts of asymptotic size on ρ (eqs. 6 and 14).

Empirical data, life-history variables, and growth parameters

Our data cover major fish species in the Laurentian Great Lakes, including alewife (*Alosa pseudoharengus*), rainbow smelt (*Osmerus mordax*), lake whitefish (*Coregonus clupeaformis*), round whitefish (*Prosopium cylindraceum*), pygmy whitefish (*Prosopium coulteri*), lake herring (*Coregonus artedii*), kiyi (*Coregonus kiyi*), bloater (*Coregonus hoyi*), gizzard shad (*Dorosoma cepedianum*), yellow perch (*Perca flavescens*), white perch (*Morone americana*), and walleye (*Stizostedion vitreum*).

Most of those species are primarily invertebrate-eating fishes. For those species, we restrict data to populations within the Laurentian Great Lakes because combinations of stage-explicit growth may have different quantitative features in other ecosystems. Walleye is a piscivore, and on a yearly scale, its primary diet typically switches from invertebrates to fish during yearling growth. We included walleye populations from other lakes where prey fishes are major food resources to the predator. Lake trout (*Salvelinus namaycush*) is also a very important species in the Great Lakes, but we have provided analysis elsewhere (He and Stewart 2001). Here, it is sufficient to mention that the relation between body growth and age at first reproduction is similar between walleye and lake trout around the Great Lakes. Sculpins also form an important group of benthic fishes in the Laurentian Great Lakes, but published data are not sufficient for a synthetical analysis in the present context.

Data on size at age and age at first reproduction were collected from published studies on size at age and on age at first reproduction (Appendix A). Information for growth and age at first reproduction was for the same fish population (i.e., from the same area and period). Most of the species have been analyzed independently several times based on hundreds or thousands of samples. Because size at age was from back calculation with large samples, biases were minimized. We only analyzed data for females, although our general methods are applicable to both males and females (He and Stewart 2001). When sex was not identifiable in a young age, growth of males and females was normally the same as was detailed in those empirical studies.

Size at age is the total body length corresponding to an annulus and age 1 is always treated as the age at the first annulus. Age at first reproduction is the number of annuli at first reproduction. If an age-2+ fish has reached sexual maturity and has spawned in the spring or early summer of its third year of life, its age at first reproduction is age 2. If an age-2+ fish has reached sexual maturity but has spawned in the fall or winter of its third year of life, its age at first reproduction is age 3. Such a definition of age at first reproduction reflects the completion of growth seasons and allows for comparisons between spring spawners and fall spawners. We used mean age at first reproduction, or the first age when 50% or more of females attain sexual maturity.

Growth parameters with eqs. 5 and 2 were estimated using nonlinear regression for each fish population (SAS NLIN procedure, SAS Institute Inc. 1999). For three populations of walleye, von Bertalanffy growth parameters are from the original study by Craig et al. (1995).

Results of data analyses

Stage-specific variables and von Bertalanffy growth parameters

Stage-specific variables with eq. 5 and all conventional von Bertalanffy growth parameters with eq. 2 are summarized in Table 1. Except for three walleye populations mentioned in the above section, those variables and parameters were estimated separately with different equations, but estimates for each population are exactly interchangeable using eqs. 6–9. There is no significant difference between estimated and observed yearling sizes (Fig. 1*b*). A plot of estimated parameter t_0 versus the ratio of ρ_y to ρ provides a clear demonstration of the functional relation of eq. 7 (Fig. 1*c*). With limited space, we cannot present all of the statistical details for 28 populations. The essential information represented in Table 1 and Appendix A, however, should be sufficient for residual analysis and for evaluating statistical quality. Our conclusion is that eqs. 5 and 2 properly and even accurately provided the same expression for each body-growth trajectory.

Differences between walleye and invertebrate-eating fishes

For both walleye and invertebrate-eating fishes studied here, L_{int} has a positive correlation with body size at age 2 (L_2) and a negative correlation with ρ (Table 2). Those correlations are consistent with eq. 6. A plot of $\log_{10}(t_R)$ versus $\log_{10}(K)$, however, indicates potential differences between populations of walleye and invertebrate-eating fishes. With a similar range of t_R, there is a much wider range of K values for invertebrate-eating fishes than for walleye (Fig. 1*d*).

For those walleye populations, L_{inf} has positive correlations with both L_2 and L_{int}, but no relation with ρ (Table 2). In such a case, the negative correlation between ρ and L_{int} can be explained as follows. When L_{int}, L_2, and L_{inf} increase, proportional increases in L_{int} and L_2 must be larger than proportional increases in L_{inf}, so ρ can decrease with increasing L_{int} (Fig. 1*a*). The first two years of body growth apparently have the dominant effect that leads to changes in ρ. Varia-

© 2002 NRC Canada

Table 1. Conventional von Bertalanffy growth parameters (L_{inf}, K, t_0) using eq. 2, stage-specific growth parameters (L_1, ρ_y, ρ, L_{int}) using eqs. 5–6, and age at first reproduction (t_R) for 31 fish populations.

Reference	Species	L_{inf}	K	t_0	L_1	ρ_y	ρ	L_{int}	t_R
Van Osten and Hile 1949	Lake whitefish	609	0.345	–0.058	186	0.662	0.708	178	4.0
Van Osten 1939	Lake whitefish	732	0.224	0.258	112	1.111	0.800	147	5.0
Mraz 1964*a*	Lake whitefish	654	0.332	0.114	167	0.827	0.718	185	4.0
Dryer 1963	Lake whitefish	771	0.126	–0.470	130	0.582	0.882	91	7.0
Edsall 1960	Lake whitefish	609	0.063	–3.485	151	0.187	0.939	37	12.0
Bailey 1963	Round whitefish	460	0.201	–0.481	118	0.525	0.818	84	5.0
Mraz 1964*b*	Round whitefish	561	0.268	0.091	121	0.853	0.765	132	4.0
Armstrong et al. 1977	Round whitefish	518	0.382	0.189	138	0.874	0.682	165	3.0
Eschmeyer and Bailey 1954	Pygmy whitefish	151	0.275	–0.289	45	0.565	0.760	36	4.0
Dryer and Beil 1964	Lake herring	391	0.298	–0.216	119	0.591	0.743	101	4.0
Dryer and Beil 1968	Bloater	329	0.196	–0.956	105	0.381	0.822	59	3.0
Deason and Hile 1947	Kiyi	285	0.434	–0.285	122	0.472	0.648	100	2.0
Brown 1972	Alewife	196	0.581	–0.187	98	0.444	0.559	87	3.0
Bronte et al. 1991	Alewife	191	1.053	0.402	89	0.742	0.349	124	2.0
O'Gorman et al. 1997	Alewife	170	0.752	0.013	89	0.480	0.471	90	2.5
Norden 1967	Alewife	183	0.692	–0.039	94	0.474	0.501	91	2.0
Bailey 1964	Rainbow smelt	270	0.488	0.412	67	1.162	0.614	104	3.0
Bodola 1965	Gizzard shad	395	0.775	0.428	142	0.968	0.461	213	2.0
Jobes 1952	Yellow perch	300	0.439	0.134	95	0.768	0.645	107	3.0
El-Zarka 1959	Yellow perch	622	0.083	–0.372	67	0.660	0.920	50	4.0
Hile and Jobes 1942	Yellow perch	472	0.130	–0.243	70	0.696	0.878	57	4.0
Wells 1983	Yellow perch	355	0.358	0.228	86	0.946	0.699	107	3.0
Schaeffer and Margraf 1986	White perch	261	0.682	0.474	79	1.146	0.506	129	2.0
Wolfert 1969, 1977	Walleye	834	0.207	–0.594	234	0.478	0.813	156	3.0
Hile 1954	Walleye	721	0.284	0.082	166	0.830	0.753	178	3.0
Priegel 1969	Walleye	616	0.245	–0.174	154	0.652	0.782	134	6.0
Eschmeyer 1950	Walleye	571	0.266	0.037	129	0.801	0.767	133	5.0
Smith and Pycha 1961	Walleye	543	0.178	–0.744	145	0.448	0.837	88	8.0
Craig et al. 1995	Walleye	622	0.253	–0.193	162	0.634	0.776	139	5.0
Craig et al. 1995	Walleye	544	0.292	–0.682	211	0.399	0.747	138	5.0
Craig et al. 1995	Walleye	466	0.215	–0.632	138	0.460	0.807	90	7.0

Note: Corresponding growth data are in Appendix A. Relations between the two sets of growth parameters are eqs. 7–9. See parameter definitions and estimation methods in text.

tions in t_0 are mostly due to variations in ρ_y (Table 2), although ρ is another component for determining t_0 values (eq. 7).

For those invertebrate-eating fishes, asymptotic size (L_{inf}) has positive correlations with both L_2 and ρ, but no relation with L_{int} (Table 2). In such a case, when L_2 and L_{inf} increase, proportional increases in L_{inf} must be larger than proportional increases in L_2, so ρ can increase with L_{inf} (Fig. 1*a*). Apparently, dominant changes in ρ are related to changes in asymptotic size. Meanwhile, because there is no relation between L_{inf} and L_{int}, and because the negative correlation between L_{int} and ρ is always there, a small L_1, or ρ_y, and a large L_{inf} can both contribute to a large ρ or small K (or vice versa, Fig. 1*a*). It is not surprising that variations in t_0 are due to variations in both ρ_y and ρ (Table 2).

Predicting age at first reproduction using growth parameters

For all invertebrate-eating fishes studied here, we can use K to predict t_R. With 11 species and 23 populations, R^2 is 0.72. Four data points are far outside the confidence limits and are apparent outliers (Fig. 2*a*). Excluding those outliers, we increase R^2 to 0.95 (Fig. 2*b*). The two data points with the largest t_R values are also outside the confidence limits in Fig. 2*a*, but that is because of effects from the four outliers mentioned above. Excluding the two data points with the largest t_R and including the four outliers distorted the regression, R^2 was only 0.59. Excluding all of those six points yielded regression parameters that were not statistically different from those in Fig. 2*b*.

The above results embody two contrasting relations. Because of the negative relation between K and L_{inf} (Table 2), a relatively small K, large ρ, and late t_R are largely due to slow decreases in annual growth after age 2. Because there is no relation between L_{inf} and L_{int} (Table 2), some small K, large ρ, and late t_R are due to very poor yearling growth associated with sufficiently large L_{inf}. The contrasting effects of different life stages can be found in both inter- and intra-specific comparisons (Table 1).

Two of the four outliers are the only two deep-water species in our analyses, bloater and kiyi. The fact that those two coregonines stand apart as outliers may be an indication that they are somehow special, rather than an invalidation of the general relation. Both species often have complex cycling of

© 2002 NRC Canada

Table 2. Correlation coefficients and their p values (below, underlined) among von Bertalanffy growth parameters (eq. 2) and stage-specific variables (eq. 5).

	L_{int}	L_1	ρ_y	L_2	ρ	L_{inf}	K	t_0
Eight populations of walleye								
L_{int}	1.0000	0.4964	0.5563	0.8423	–0.6469	0.7765	0.6457	0.6031
		0.2109	0.1521	0.0087	0.0830	0.0234	0.0838	0.1135
L_1		1.0000	–0.4289	0.8794	–0.0961	0.6390	0.0995	–0.3733
			0.2890	0.0040	0.8210	0.0881	0.8147	0.3624
ρ_y			1.0000	0.0476	–0.4975	0.2617	0.4923	0.9836
				0.9109	0.2097	0.5312	0.2153	<0.0001
L_2				1.0000	–0.3429	0.8596	0.3440	0.0987
					0.4056	0.0062	0.4041	0.8162
ρ					1.0000	–0.0309	–0.9999	–0.5888
						0.9421	<0.0001	0.1246
L_{inf}						1.0000	0.0291	0.2590
							0.9456	0.5357
K							1.0000	0.5822
								0.1300
t_0								1.0000
Twenty-three populations of invertebrate-eating fishes								
L_{int}	1.0000	0.5907	0.5999	0.8635	–0.4411	0.2372	0.4005	0.5582
		0.0030	0.0025	<0.0001	0.0351	0.2759	0.0582	0.0056
L_1		1.0000	–0.1353	0.8884	0.1239	0.5770	–0.1387	–0.2368
			0.5382	<0.0001	0.5733	0.0039	0.5280	0.2766
ρ_y			1.0000	0.3172	–0.2682	0.1113	0.2318	0.7088
				0.1402	0.2159	0.6130	0.2871	0.0002
L_2				1.0000	–0.0236	0.5902	–0.0089	0.1514
					0.9149	0.0030	0.9679	0.4905
ρ					1.0000	0.6856	–0.9902	–0.5643
						0.0003	<0.0001	0.0050
L_{inf}						1.0000	–0.6651	–0.2516
							0.0005	0.2468
K							1.0000	0.5138
								0.0122
t_0								1.0000

Note: Included also are the Ford–Walford intercept (L_{int}) and body length at age 2 (L_2). L_{int} is a combination of three stage-specific variables (eq. 6) and L_2 is a combination of two stage-specific variables (eq. 3).

life-history features, including shifts of sex ratio to about 90% females (Deason and Hile 1947; Brown 1970). The bloater observation plotted represents average growth and age at first reproduction across 10 years (Fig. 2*a*), but cohort-specific observations may be particularly important for studying this species. When more data are available for these and other deep-water fishes, it may be also appropriate to treat them separately with a distinct predictive relation.

The other two outliers are yellow perch populations that mature at age 4. Yellow perch is a typical warm-water species. Other warm-water fishes studied here include white perch and gizzard shad (Appendix A). When t_R is less than 4, values for those warm-water fishes including yellow perch overlap with cool-water invertebrate-eating fishes in our regressions (Figs. 2*a*–2*b*). If we separate warm-water populations as a subgroup including those yellow perch that matured at age four, the relation between K and t_R is linear rather than a power function, and R^2 with six populations is 0.98 (Fig. 2*c*). More data are needed to clarify whether yellow perch alone are distinct or if they might belong to another functional category with other species.

For the eight populations of walleye, age at first reproduction (t_R) can be predicted using L_{int}, and R^2 for the predictive relation is 0.90 (Fig. 2*d*). Two data points are just outside of the confidence limits. They may be related to differences in natural mortality, but more data are needed to test the idea. Statistically, we could exclude those two data points as outliers, but prediction residuals for those data points are still less than 1.

Applications of the index for growth–reproduction linkage

The index for growth–reproduction linkage (eq. 13) is applicable to both invertebrate-eating populations and walleye populations. For invertebrate-eating fishes (Fig. 3*a*), the plot of I_{G-R} versus t_R can be modeled as $I_{G-R} = 0.88t_R - 1.04$, with R^2 of 0.99. For populations of walleye (Fig. 3*b*), the plot of I_{G-R} versus t_R can be modeled as $I_{G-R} = 0.41\ t_R + 0.87$, and R^2 is 0.91. The difference between these two b values for eq. 13 is 0.46 and is statistically significant (df = 23, $p < 0.0001$). Correspondingly, the intercept for invertebrate-eating fishes is negative, whereas the intercept for walleye is positive. In our previous study on lake trout (He and Stewart

© 2002 NRC Canada

Fig. 2. Predicting age at first reproduction (t_R) using the von Bertalanffy growth coefficient (K) or the Ford–Walford intercept (L_{int}). Data are in Table 1 and Appendix A. (*a*) The relation between $\ln(t_R)$ and $\ln(K)$ for 11 species of invertebrate-eating fishes with 23 populations. Four data points are outliers because they are far outside of confidence intervals. See more details in text. (*b*) The relations between t_R and K for 19 populations of invertebrate-eating fishes. Outliers identified in (*a*) are not included. (*c*) The relation between t_R and K for a potential subgroup with six populations of warm-water invertebrate-eating fishes, including yellow perch, white perch, and gizzard shad. (*d*) The relation between t_R and L_{int} for eight populations of walleye.

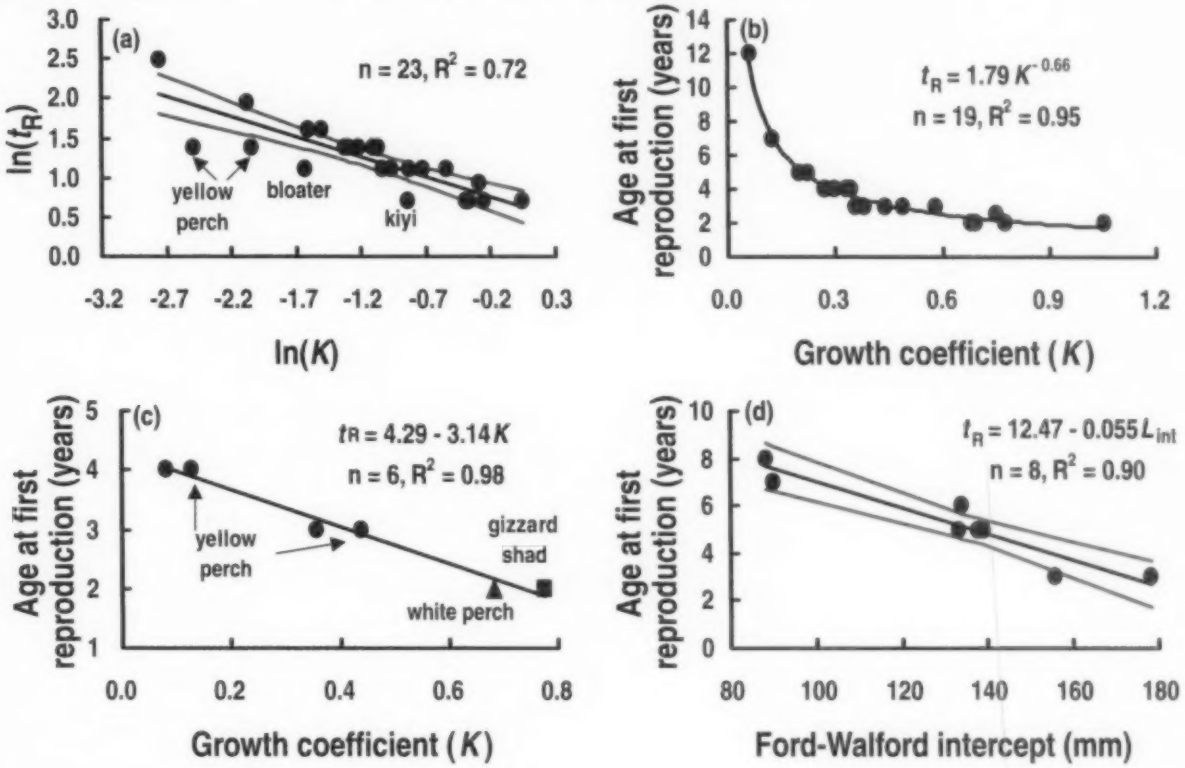

2001), the regression line was $I_{G-R} = 0.42\ t_R + 1.01$, which is very similar to that for walleye populations studied here.

Discussion: body-growth comparisons and their life-history implications

As commonly interpreted, a phase of fast growth often means relatively large size at a given age. Alm (1959) indicated that he used such a notion because he had no better choice. We need to be aware of the vagueness of the commonly used notion of fast growth, slow growth, or no difference in growth. When age is larger than 1, body size at a given age may not be a clear indicator of growth rates or growth condition because it includes effects of previous life stages. Particularly, young-of-the-year growth, yearling growth, and the remaining juvenile–adult growth often have different intrinsic features and are related to different environments (e.g., Balon 1975). To compare body growth, we often need to compare body-growth trajectories with one or another growth model. Using the conventional expression of the von Bertalanffy growth model, however, we often have difficulties drawing clear biological implications, although statistical comparisons can be rigorous. Biological meanings of the model structure and parameters have to be fully clarified.

The biological basis of the von Bertalanffy growth model has been studied mostly from an energetic perspective (von Bertalanffy 1938; Pauly 1981). Along this line, the model can always be criticized for its assumptions, such as scaling body mass to body length cubed, scaling anabolism to two-thirds the power of the body mass, and considering catabolism as a constant proportion of body mass. It is important to understand the energetic basis of a body-growth trajectory (e.g., He and Stewart 1998), but the above sufficient energetic assumptions for the VBGM are all unrealistic and are not necessary. The model has been independently developed by emphasizing proper description of body-growth trajectories (Brody 1927; Ford 1933; Walford 1946). In this paper, we completed the idea of Ford (1933) and Walford (1946), and used three measurable stage-specific variables (L_1, ρ_y, ρ) to express the commonly used von Bertalanffy growth model (eqs. 3–5). Changes in each of these three variables may have different relative dominances, and each of them can lead to a major change in size at ages (eq. 5). Other possible sets of parameters cannot represent distinguishable life stages, so growth comparisons may be improved by focusing on the three major stage-specific variables or elements.

© 2002 NRC Canada

Fig. 3. General linkages between body growth and age at first reproduction. The index of the *y* axis (I_{G-R}) is defined by the left side of eq. 13 and related explanatory text. It represents an intrapopulation linkage or the linkage between body length and age at first reproduction with a given growth trajectory. A complete plot represents interpopulation linkage. With substantial changes in values of growth parameters, the interpopulation linkage between body length and age at first reproduction is representative of many growth trajectories. Data are in Table 1. Outliers identified in Fig. 2*a* are not included. (*a*) Populations of invertebrate-eating fishes. (*b*) Populations of walleye. The differences between populations of invertebrate-eating fishes and walleye are statistically significant (see text).

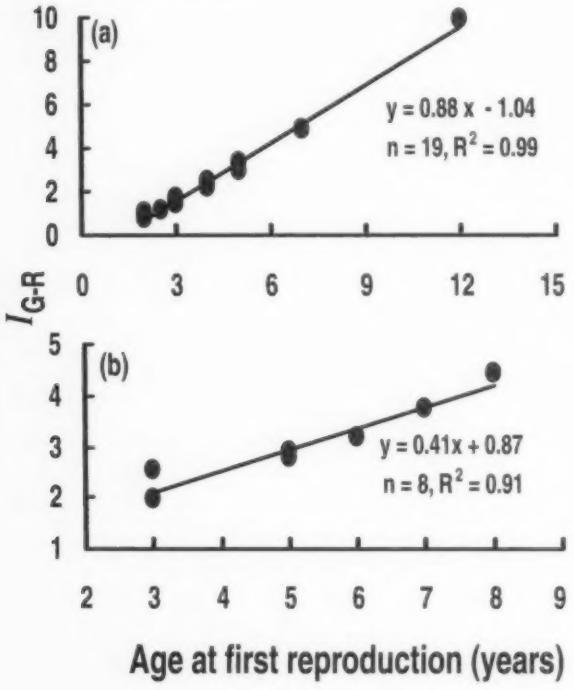

As with this paper, the conventional expression of the von Bertalanffy growth model (eqs. 1–2) will be used continuously on its own right, but biological meanings of von Bertalanffy growth parameters can be better understood from an alternative perspective. It is confusing to use the coefficient K to denote fast growth or slow growth because there are contrasting stage-specific effects on that coefficient. With similar asymptotic size, a relatively smaller Ford–Walford slope (ρ) or larger K (eq. 8) is due to a relatively larger L_1 or ρ_y that leads to relatively larger sizes at young ages (eq. 5). With similar sets of L_1 and ρ_y, however, a relatively smaller ρ or larger K is associated with a relatively smaller asymptotic size, which indicates poor growth condition and rapid decreases in growth rates during the final growth stanza. Precisely, K should be formally named as a coefficient for decay of annual growth rate (Pauly 1981). With a given asymptotic size, a rapid decrease in growth rate must be positively related to a rapid growth in young age, so we have $E/K = L_{inf}$ (see eq. 1 and documentation of its parameters), but a relatively large K always indicates a rapid decrease in annual growth rate.

It is also confusing to use K to discuss the trade-off between growth rate and life span. The positive relation between K and mortality has been well documented (Pauly 1980; Charnov 1993; Jensen 1996), but it should not be explained only in a hypothetical way. The dimension of K is t^{-1}, but it is not a growth rate in the sense of per capita increment per time or increment per time (eq. 1). When a relatively large K is associated with relatively higher mortality, underlying mechanisms may include at least the following contrasting effects from different life stages. A small ρ or large K often indicates poor growth conditions in the final growth stanza, and poor growth condition is often associated with high mortality. When best-growing individuals are selectively removed by predation or fishing, survivors will have a relatively smaller asymptotic size with a relatively larger K. When a small ρ or large K is resulting from a relatively larger yearling size (L_1) or a high relative growth rate of a yearling (ρ_y), there may be subsequent high mortality because of stresses related to early age at first reproduction.

In this paper, we have emphasized that age at first reproduction is predictable using K or L_{int}. A rapid decrease in annual growth after age two may lead to a small ρ or large K and is associated with early age at first reproduction. The result is consistent with the idea that high mortality favors early age at first reproduction (Roff 1984), because unfavorable growth condition and high mortality often happen in concert. For the same reason, when slow growth in the first two years of life leads to small size at subsequent ages and a late age at first reproduction, it is also consistent with the idea that high mortality in early life favors delayed age at first reproduction (Stearns 1992).

We hope that more comparative studies will be conducted and published with a focus on cohort life histories and individual variations. It is fortunate that there have been many well-documented studies in the Great Lakes. Most of those studies are landmarks of fish biology in this region. Early techniques for identifying fish ages may have involved some bias, especially in analyzing very old fishes, but it is hard to imagine that various independent studies reported here can lead to arbitrary relations between growth parameters and age at first reproduction. Future studies may explore other typical cases with the same species or other species similar to those studied here. We believe that they will also confirm the general results in this paper, because our empirical analysis is built on a solid theoretical basis.

When body length shows a normal growth pattern, the von Bertalanffy growth model is typically one of the best models (Ricker 1979; Chen et al. 1992). General linkages between age at first reproduction and growth trajectories are also theoretically sound (Stearns 1992) and empirically well known (Beverton 1992; Shuter et al. 1998; He and Stewart 2001). Additional complexities are related to various combinations of different effects from major life stages (Hutchings 1993; Jonsson and Jonsson 1993; Fox 1994). The three major life stages (represented by L_1, ρ_y, and ρ) have contrasting effects on growth potential, K and L_{int}. They also have contrasting relations to t_R. Implementation of accurate predictive functions calls for consideration of factors that may influence body growth during various life stages in different ways.

© 2002 NRC Canada

Those factors include types of ecosystems, trophic positions, environmental conditions, and spatial heterogeneity. With consideration for all of those complexities, our approach can be tested at various levels, including individual, population, and interspecific comparisons. Such an approach may represent a new perspective for studying fish population dynamics and changes in relative dominance of fish species (e.g., Shuter et al. 1998).

In the Great Lakes, changes in the fish communities have been well documented (e.g., Smith 1968; Christie 1974). More attention is needed to consider that the two upper levels of food webs in the Great Lakes have been operating with relatively short life spans. For *Coregonus*, *Prosopium*, and other native invertebrate-eating fishes, age at first reproduction has a range from 2 to 12. First reproduction at age 4–7 is very common. Predation pressure on those native fishes is normally on immature age classes (Smith 1968). Exotic species such as alewife and rainbow smelt are now among the dominant secondary consumers in all of the lakes. They mostly reach their first reproduction at age 2–3 with relatively smaller sizes. For those exotics and small native species, predation pressure is on both immature and mature age classes. There have been similar changes in life histories of piscivorus fishes. Introduced Pacific salmons reach their first reproduction at age 2–4, much younger than the native lake trout, although similar to burbot (*Lota lota*). All of those changes in age at first reproduction, or successes of fishes with notably different life histories, are associated with their body-growth trajectories. Together, they also have substantial impacts on food-web dynamics and related ecosystem stability. The results of our study have the following implications. For piscivorus fishes, early life growth often has a dominant effect on life history. For hatchery-supported populations with artificially large yearlings, however, potential reductions in asymptotic size may have long-term effects on restoration of naturally reproducing and self-sustaining populations. For secondary consumers, growth potential after age 1 or age 2 is the dominant factor influencing life histories. Rebuilding populations of native fishes that attain relatively larger sizes and spawn at later ages might improve food-web and ecosystem stability.

For harvested fish populations and their prey, the following potential mechanisms deserve further studies and clarifications. When best-growing and large-sized individuals are selectively removed, overall effects of harvests or predation may include three major outcomes. One is a selection for enhanced body growth in the first 2 years of a life, which allows for early age at first reproduction. Such an outcome is likely not sustainable in many natural ecosystems because it requires a very stable ecosystem with high productivity. The second outcome is a selection for survivors with poor growth after age 2, which is also associated with early age at first reproduction. Such an outcome leads to undesirable dominance of small-sized species or populations. It also leads to unstable food webs because both premature and mature fish may be vulnerable to predation. The third outcome is a potential increase in asymptotic size and age at first reproduction due to reductions in intra- and inter-specific competition among fishes of age 2 and older. The last potential outcome is dangerous because delayed reproduction during periods of overexploitation might lead to sudden collapse of fish populations. The above three outcomes are likely to confound each other. Using a stage-explicit perspective to analyze cohort life histories may be an important contribution to improving our understanding of complex fish population dynamics.

Acknowledgments

We thank Bob O'Gorman for comments on an early draft. This paper is a result of research funded by the National Oceanic and Atmospheric Administration (NOAA) award NA86RG0056 to the Research Foundation of State University of New York for New York Sea Grant. The U.S. Government is authorized to produce and distribute reprints for government purposes notwithstanding any copyright notation that may appear hereon. The views expressed herein are those of the authors and do not necessarily reflect the views of NOAA or any of its subagencies.

References

Alm, G. 1959. Connection between maturity, size, and age in fishes. Rep. Inst. Freshwater Res. Drottningholm, **40**: 4–145.

Armstrong, J.W., Liston, C.R., Tack, P.I., and Anderson, R.C. 1977. Age, growth, maturity, and seasonal food habits of round whitefish, *Prosopium cylindraceum*, in Lake Michigan near Ludington, Michigan. Trans. Am. Fish. Soc. **106**: 151–155.

Bailey, M.M. 1963. Age, growth, and maturity of round whitefish of the Apostle Islands and Isle Royale regions, Lake Superior. Fish. Bull. **63**: 63–75.

Bailey, M.M. 1964. Age, growth, maturity, and sex composition of the American smelt, *Osmerus mordax* (Mitchill), of western Lake Superior. Trans. Am. Fish. Soc. **93**: 382–395.

Balon, E.K. 1975. Terminology of intervals in fish development. J. Fish. Res. Board Can. **32**: 1663–1670.

Berrigan, D., and Charnov, E.L. 1994. Reaction norms for age and size at maturity in response to temperature: A puzzle for life historians. Oikos, **70**: 474–478.

Beverton, R.J.H. 1992. Patterns of reproductive strategy parameters in some marine teleost fishes. J. Fish Biol. **42**(Suppl. B): 137–160.

Bodola, A. 1965. Life history of the gizzard shad, *Dorosoma cepedianum* (Le Sueur), in western Lake Erie. Fish. Bull. **65**: 391–425.

Brody, S. 1927. Growth rates. Res. Bull. Mo. Agric. Exp. Stn. **97**.

Bronte, C.R., Selgeby, J.H., and Curtis, G.L. 1991. Distribution, abundance, and biology of the alewife in U.S. waters of Lake Superior. J. Gt. Lakes Res. **17**: 304–313.

Brown, E.H. 1970. Extreme female predominance in the bloater (*Coregonus hoyi*) of Lake Michigan in the 1960's. *In* Biology of coregonid fishes. *Edited by* C.C. Lindsey and C.S. Woods. University of Manitoba Press, Winnipeg, Canada. pp. 501–504.

Brown, E.H. 1972. Population biology of alewives, *Alosa pseudoharengus*, in Lake Michigan, 1949–70. J. Fish. Res. Board Can. **29**: 477–500.

Charnov, E. 1993. Life history invariants. Oxford University Press, New York.

Chen, Y., Jackson, D.A., and Harvey, H.H. 1992. A comparison of von Bertalanffy and polynomial functions in modelling fish growth data. Can. J. Fish. Aquat. Sci. **49**: 1228–1235.

Christie, W.J. 1974. Changes in the fish species composition of the Great Lakes. J. Fish. Res. Board Can. **31**: 827–854.

Craig, J.F., Babaluk, J.A., Stevenson, S.G., and Williams, P.C. 1995. Variation in growth and reproduction of walleye (*Stizostedion vitreum*) in three Manitoba lakes. Can. J. Zool. **73**: 367–372.

© 2002 NRC Canada

Deason, H.J., and Hile, R. 1947. Age and growth of the kiyi, *Leucichthys kiyi* Koelz, in Lake Michigan. Trans. Am. Fish. Soc. **74**: 88–142.

Dryer, W.R. 1963. Age and growth of the whitefish in Lake Superior. Fish. Bull. **63**: 77–95.

Dryer, W.R., and Beil, S. 1964. Life history of lake herring in Lake Superior. Fish. Bull. **63**: 493–529.

Dryer, W.R., and Beil, S. 1968. Growth changes of the bloater (*Coregonus hoyi*) of the Apostle Islands region of Lake Superior. Trans. Am. Fish. Soc. **97**: 146–158.

Edsall, T.A. 1960. Age and growth of the whitefish, *Coregonus clupeaformis*, of Munising Bay, Lake Superior. Trans. Am. Fish. Soc. **89**: 323–332.

El-Zarka, S.E. 1959. Fluctuations in the population of yellow perch, *Perca flavescens* (Mitchill), in Saginaw Bay, Lake Huron. Fish. Bull. **59**: 365–415.

Eschmeyer, P.H. 1950. The life history of the walleye, *Stizostedion vitreum vitreum* (Mitchill), in Michigan. Michigan Dept. Conserv., Inst. Fish. Res. Bull. No. 3.

Eschmeyer, P.H., and Bailey, R.M. 1954. The pygmy whitefish, *Coregonus coulteri*, in Lake Superior. Trans. Am. Fish. Soc. **84**: 161–199.

Ford, E. 1933. An account of the herring investigations conducted at Plymouth during the years from 1924–1933. J. Mar. Biol. Assoc. U.K. **19**: 305–384.

Fox, M.G. 1994. Growth, density, and interspecific influences on pumpkinseed sunfish life histories. Ecology, **75**: 1157–1171.

He, J., and Stewart, D.J. 1998. Ontogeny of energetic relationships and potential effects of tissue turnover: a comparative modeling study on lake trout. Can. J. Fish. Aquat. Sci. **55**: 2518–2532.

He, J.X., and Stewart, D.J. 2001. Age and size at first reproduction of fishes: predictive models based only on growth trajectories. Ecology, **82**: 784–791.

Hile, R. 1954. Fluctuations in growth and year-class strength of the walleye in Saginaw Bay. Fish. Bull. **56**: 7–59.

Hile, R., and Jobes, F.W. 1942. Age and growth of the yellow perch, *Perca flavescens* (Mitchill), in the Wisconsin waters of Green Bay and northern Lake Michigan. Pap. Mich. Acad. Sci. Arts Lett. **27**: 241–266.

Hutchings, J.A. 1993. Adaptive life histories effected by age-specific survival and growth rate. Ecology, **74**: 673–684.

Iles, T.D. 1974. The tactics and strategy of growth in fishes. *In* Sea fisheries research. *Edited by* F.R. Harden Jones. ELEK Science, London. pp. 331–345.

Jensen, A.L. 1985. Relations among net reproductive rate and life history parameters for lake whitefish (*Coregonus clupeaformis*). Can. J. Fish. Aquat. Sci. **42**: 164–168.

Jensen, A.L. 1996. Beverton and Holt life history invariants result from optimal trade-off of reproduction and survival. Can. J. Fish. Aquat. Sci. **53**: 820–822.

Jobes, F.W. 1952. Age, growth, and production of yellow perch in Lake Erie. Fish. Bull. **52**: 205–266.

Jonsson, B., and Jonsson, N. 1993. Partial migration: niche shift versus sexual maturation in fishes. Rev. Fish Biol. Fish. **3**: 348–365.

Knight, W. 1969. A formulation of the von Bertalanffy growth curve when the growth rate is roughly constant. J. Fish. Res. Board Can. **26**: 3069–3072.

Martin, N.V. 1970. Long-term effects of diet on the biology of the lake trout and the fishery in Lake Opeongo, Ontario. J. Fish. Res. Board Can. **27**: 125–146.

Matuszek, J.E., Shuter, B.J., and Casselman, J.M. 1990. Changes in lake trout growth and abundance after introduction of cisco into Lake Opeongo, Ontario. Trans. Am. Fish. Soc. **119**: 718–729.

Moreau, J. 1987. Mathematical and biological expression of growth in fishes: recent trends and further developments. *In* The age and growth of fish. *Edited by* R.C. Summerfelt and G.E. Hall. Iowa State University Press, Ames. pp. 81–113.

Mraz, D. 1964*a*. Age, growth, sex ratio, and maturity of the whitefish in central Green Bay and adjacent waters of Lake Michigan. Fish. Bull. **63**: 619–634.

Mraz, D. 1964*b*. Age and growth of the round whitefish in Lake Michigan. Trans. Am. Fish. Soc. **93**: 46–52.

Norden, C.R. 1967. Age, growth and fecundity of the alewife, *Alosa pseudoharengus* (Wilson), in Lake Michigan. Trans. Am. Fish. Soc. **96**: 387–393.

O'Gorman, R., Johannsson, O.E., and Schneider, C.P. 1997. Age and growth of alewives in the changing pelagia of Lake Ontario, 1978–1992. Trans. Am. Fish. Soc. **126**: 112–126.

Pauly, D. 1980. On the interrelationships between natural mortality, growth parameters, and mean environmental temperature in 175 fish stocks. J. Cons. Int. Explor. Mer, **39**: 175–192.

Pauly, D. 1981. The relationships between gill surface area and growth performance in fish: a generalization of von Bertalanffy's theory of growth. Meeresforschung, **28**: 251–282.

Priegel, G.R. 1969. Age and growth of the walleye in Lake Winnebago. Trans. Wis. Acad. Sci. Arts Lett. **57**: 121–133.

Ricker, W.E. 1975. Computation and interpretation of biological statistics of fish populations. Fish. Res. Board Can. Bull. **191**.

Ricker, W.E. 1979. Growth rate and models. *In* Fish physiology. Vol. 8. *Edited by* W.S. Hoar, D.J. Randall, and J.R. Brett. Academic Press, New York. pp. 677–743.

Roff, D.A. 1984. The evolution of life history parameters in teleosts. Can. J. Fish. Aquat. Sci. **41**: 989–1000.

SAS Institute Inc. 1999. SAS/STAT user's guide, release 7.00 ed. SAS Institute Inc., Cary, N.C.

Schaeffer, J.S., and Margraf, F.J. 1986. Population characteristics of the invading white perch (*Morone americana*) in western Lake Erie. J. Gt. Lakes Res. **12**: 127–131.

Schnute, J., and Fournier, D. 1980. A new approach to length–frequency analysis: growth structure. Can. J. Fish. Aquat. Sci. **37**: 1337–1351.

Shuter, B.J., Jones, M.L., Korver, R.M., and Lester, N.P. 1998. A general, life history based model for regional management of fish stocks: the inland lake trout (*Salvelinus namaycush*) fisheries of Ontario. Can. J. Fish. Aquat. Sci. **55**: 2161–2177.

Smith, L.L., and Pycha, R.L. 1961. Factors related to commercial production of the walleye in Red Lakes, Minnesota. Trans. Am. Fish. Soc. **90**: 190–217.

Smith, S.H. 1968. Species succession and fishery exploitation in the Great Lakes. J. Fish. Res. Board Can. **25**: 667–693.

Stamps, J.A., Mangel, M., and Phillips, J.A. 1998. A new look at relationships between size at maturity and asymptotic size. Am. Nat. **152**: 470–479.

Stearns, S.C. 1992. The evolution of life histories. Oxford University Press, Oxford, U.K.

Van Oosten, J. 1939. The age, growth, sexual maturity, and sex ratio of the common whitefish, *Coregonus clupeaformis* (Mitchill), of Lake Huron. Pap. Mich. Acad. Sci. Arts Lett. **24**(Pt. 2): 195–221.

Van Oosten, J., and Hile, R. 1949. Age and growth of the lake whitefish, *Coregonus clupeaformis* (Mitchill), in Lake Erie. Trans. Am. Fish. Soc. **77**: 178–249.

von Bertalanffy, L. 1938. A quantitative theory of organic growth (inquiries on growth laws. II). Hum. Biol. **10**: 181–213.

Walford, L.A. 1946. A new graphic method of describing the growth of animals. Biol. Bull. **90**: 141–147.

Wells, L. 1983. Population biology of yellow perch in southern Lake Michigan, 1971–79. Tech. Pap. U.S. Fish Wildl. Serv. **109**.

© 2002 NRC Canada

Wolfert, D.R. 1969. Maturity and fecundity of walleyes from the eastern and western basins of Lake Erie. J. Fish. Res. Board Can. **26**: 1877–1888.

Wolfert, D.R. 1977. Age and growth of the walleye in Lake Erie, 1963–1968. Trans. Am. Fish. Soc. **106**: 569–577.

Appendix A.

The von Bertalanffy growth model for each of the following populations was estimated by this study (Table 1).

Table A1. Length at age data for 28 fish populations.

		Body length at ages (mm)											
Reference	Species	1	2	3	4	5	6	7	8	9	10	11	12
Van Osten and Hile 1949	Lake whitefish	175	323	409	460	498	526	544	561	579	589	602	615
Van Osten 1939	Lake whitefish	127	226	312	409	488	544	582	607	630	643	658	676
Mraz 1964*a*	Lake whitefish	168	300	406	480	523	559	582	607	625			
Dryer 1963	Lake whitefish	130	203	277	338	381	424	465	508	544	561		
Edsall 1960	Lake whitefish	140	183	213	239	257	274	292	307	328	345	366	391
Bailey 1963	Round whitefish	117	183	231	274	307	333	356	376	394			
Mraz 1964*b*	Round whitefish	117	229	312	361	399	447	472	498				
Armstrong et al. 1977	Round whitefish	139	255	346	396	436	460	481					
Eschmeyer and Bailey 1954	Pygmy whitefish	46	69	88	107	117	123	130					
Dryer and Beil 1964	Lake herring	119	188	239	282	307	333	343					
Dryer and Beil 1968	Bloater	99	150	183	208	226	239	254	269	285	297		
Deason and Hile 1947	Kiyi	124	173	218	241	259	267	272	274				
Brown 1972	Alewife	97	144	165	177	185	194						
Bronte et al. 1991	Alewife	89	156	176	189	188							
O'Gorman et al. 1997	Alewife	89	131	153	161	164	169						
Norden 1967	Alewife	94	140	159	173								
Bailey 1964	Rainbow smelt	66	150	193	221	239	257						
Bodola 1965	Gizzard shad	140	285	335	366	390							
Jobes 1952	Yellow perch	94	170	216	241	264	279						
El-Zarka 1959	Yellow perch	69	109	150	191	224	259	282					
Hile and Jobes 1942	Yellow perch	71	117	163	203	229	264	287					
Wells 1983	Yellow perch	85	167	227	261	288	310	326					
Schaeffer and Margraf 1986	White perch	78	171	210	239								
Wolfert 1969, 1977	Walleye	213	371	454	513	563	607	649	683	722	760		
Hile 1954	Walleye	163	305	414	480	541	582	617	645	668			
Priegel 1969	Walleye	152	257	338	394	439	480	511	536				
Eschmeyer 1950	Walleye	125	239	315	368	414	455	480	503	518	533		
Smith and Pycha 1961	Walleye	142	211	267	310	345	379	401	424	452			

Note: All body lengths are total body length.

© 2002 NRC Canada

Influence of eastern hemlock (*Tsuga canadensis*) forests on aquatic invertebrate assemblages in headwater streams

Craig D. Snyder, John A. Young, David P. Lemarié, and David R. Smith

Abstract: We conducted a comparative study in the Delaware Water Gap National Recreation Area to determine the potential long-term impacts of hemlock forest decline on stream benthic macroinvertebrate assemblages. Hemlock forests throughout eastern North America have been declining because of the hemlock woolly adelgid, an exotic insect pest. We found aquatic invertebrate community structure to be strongly correlated with forest composition. Streams draining hemlock forests supported significantly more total taxa than streams draining mixed hardwood forests, and over 8% of the taxa were strongly associated with hemlock. In addition, invertebrate taxa were more evenly distributed (i.e., higher Simpson's evenness values) in hemlock-drained streams. In contrast, the number of rare species and total densities were significantly lower in streams draining hemlock, suggesting that diversity differences observed between forest types were not related to stochastic factors associated with sampling and that streams draining mixed hardwood forests may be more productive. Analysis of stream habitat data indicated that streams draining hemlock forests had more stable thermal and hydrologic regimes. Our findings suggest that hemlock decline may result in long-term changes in headwater ecosystems leading to reductions in both within-stream (i.e., alpha) and park-wide (i.e., gamma) benthic community diversity.

Résumé : Une étude comparative dans le Delaware Water Gap National Recreation Area nous a permis de déterminer l'impact potentiel à long terme du déclin des forêts de pruches sur les communautés de macroinvertébrés des cours d'eau. Le déclin des forêts de pruches dans tout l'est de l'Amérique du Nord est causé par le puceron lanigère de la pruche, un ravageur exotique. La structure des communautés d'invertébrés aquatiques est fortement reliée à la composition de la forêt. Les cours d'eau qui coulent dans des forêts de pruches contiennent significativement plus de taxons que ceux qui sont dans des forêts de bois durs mixtes et plus de 8 % des taxons sont fortement associés à la pruche. De plus, les taxons d'invertébrés sont répartis de façon plus régulière (i.e. des valeurs plus élevées de l'indice d'équitabilité de Simpson) dans les cours d'eau des forêts de pruches. En revanche, les nombres d'espèces rares et les densités totales sont significativement plus bas dans les cours d'eau des forêts de pruches, ce qui laisse croire que les différences de diversité observées entre les divers types forestiers ne sont pas reliées à des facteurs stochastiques dus à l'échantillonnage, mais que les cours d'eau qui irriguent les forêts de bois durs mixtes sont probablement plus productives. Une analyse des données sur l'habitat révèle que les régimes thermiques et hydrologiques des cours d'eau des forêts de pruches sont plus stables. Nos résultats laissent entrevoir que le déclin des pruches amènera probablement des changements à long terme dans les écosystèmes d'amont des bassins hydrographiques qui réduiront la diversité des communautés benthiques, tant à l'échelle des cours d'eau individuels (i.e. la diversité alpha) qu'à celle de l'ensemble du parc (i.e. la diversité gamma).

[Traduit par la Rédaction]

Introduction

Eastern hemlock (*Tsuga canadensis*) forests have declined substantially in the last two decades (McClure 1991). Widespread hemlock defoliation and mortality have largely been attributed to the hemlock woolly adelgid (*Adelges tsugae*), an exotic insect that is native to the Far East. Hemlock woolly adelgid is rapidly spreading throughout the eastern U.S., and once infected, hemlock stands may suffer complete mortality within 5 years (McClure 1991). Recent studies suggest that hemlock regeneration following infestation is largely absent, and no infested tree or stand has been found to exhibit any sign of recovery (Orwig and Foster 1999). A similar lack of regeneration occurred during the mid-Holocene period when hemlock forests throughout North American went through a period of rapid, pathogen-induced decline (Fuller 1998). During that bottleneck, it took about 2000 years for hemlock to recover from the decline.

The ecological impact of losing this important climax forest species is poorly understood but has the potential for significant disturbance to biotic communities by changing the energy availability, microclimate, and distribution and abundance of habitat. Recent paleoecological studies suggest that

Received 14 February 2001. Accepted 18 December 2001. Published on the NRC Research Press Web site at http://cjfas.nrc.ca on 28 February 2002.
J16216

C.D. Snyder,[1] J.A. Young, D.P. Lemarié, and D.R. Smith. United States Geological Survey, Biological Resources Division, Leetown Science Center, 1700 Leetown Road, Kearneysville, WV 25430, U.S.A.

[1]Corresponding author (e-mail: craig_snyder@usgs.gov).

 DOI: 10.1139/F02-003 © 2002 NRC Canada

the mid-Holocene hemlock decline had long-term consequences on the species composition of forest plant (Fuller 1998) and lake plankton (Boucherle et al. 1985) communities. The importance of hemlock to some terrestrial assemblages is well documented. For example, hemlock has been shown to be important winter habitat for white-tailed deer (*Odocoileus virginianus*) (e.g., Reay et al. 1990) and porcupines (*Erethizon dorsatum*) (Griesemer et al. 1998) and nesting habitat for woodland hawks (Speiser and Bosakowski 1987; Bosakowski et al. 1992). Moreover, the distribution of numerous song birds and small mammal species have been linked to hemlock (Mitchell 1999; Yamasake et al. 1999). In contrast, the influence of hemlock on aquatic assemblages has received little attention, and relatively few studies have evaluated the long-term consequences of changing forest composition on stream communities (but see Molles 1982; Stout et al. 1992).

Aquatic macroinvertebrates are primary consumers of terrestrial leaf litter, and their distribution and production have been shown to correlate with components of the surrounding forests (Ross 1963; Wallace et al. 1999). In turn, aquatic invertebrates represent a significant food source for fish, and their feeding activity modifies the form and rate with which leaf material is processed and exported (Cuffney et al. 1990). Therefore, changes in macroinvertebrate community structure associated with forest disturbances may cascade to other aquatic assemblages and affect important stream processes. Furthermore, because emerging insects represent a significant energy source for birds, spiders, and other terrestrial fauna (Jackson and Fisher 1986), aquatic macroinvertebrate responses may feed back to the terrestrial system as well.

There have been numerous reports of significant changes in headwater stream habitat and aquatic invertebrate community structure associated with forest disturbances. However, most of these studies have been designed to evaluate the responses of stream ecosystems to the relatively short-term changes that take place between the death or removal of existing riparian forests and the maturation of new overstory canopies. Of particular importance during this period is the shift in the stream energy base associated with large changes in the amount and timing of leaf litter and large woody debris entering the stream and altered light, temperature, and hydrologic regimes (Likens et al. 1970). Such changes have been shown to have significant effects on available habitat (Naiman et al. 1988), nutrient dynamics (Webster et al. 1992), channel morphology (Gregory 1992), and ultimately the trophic structure and productivity of aquatic invertebrate assemblages (Wallace and Gurtz 1986). There is no reason to believe that similar short-term changes would not accompany the decline of hemlock forests in Delaware Water Gap National Recreation Area (DEWA). However, considerably less is known about the long-term consequences to headwater stream ecosystems of pest-induced changes in forest composition.

The objective of this study was to compare benthic macroinvertebrate community structure and stream habitat in streams draining hemlock and mixed hardwood forests in DEWA. We limited the study to headwater catchments so that forest-specific effects could be isolated from other confounding factors that are present in larger watersheds. Results should yield information useful in predicting the long-term consequences of hemlock decline on aquatic invertebrate assemblages. Because hemlock regeneration following hemlock woolly adelgid induced mortality is poor and overstory recruitment is largely limited to mixed hardwood species in affected stands (Fuller 1998; Orwig and Foster 1998), we believe that our predictions reflect realistic assumptions regarding long-term changes in forest composition.

Materials and methods

Study area

Delaware Water Gap National Recreation Area (DEWA) is located in northeastern Pennsylvania and western New Jersey (Fig. 1). The Park encompasses 27 742 ha of forested hills, ravines, and bottom lands straddling the Delaware River. A total of 21 885 ha of DEWA are forested: 18 575 ha are deciduous forest, 1295 ha are evergreen forest, and 2015 ha are mixed evergreen–deciduous forest (Myers and Irish 1981). The dominant hardwood species are red oak (*Quercus rubra*), followed by sugar maple (*Acer saccharum*), chestnut oak (*Quercus prinus*), red maple (*Acer rubrum*), and sweet birch (*Betula lenta*). Dominant evergreens are white pine (*Pinus strobus*), eastern hemlock (*Tsuga canadensis*), and red cedar (*Juniperus virginiana*).

Hemlock stands in DEWA are patchily distributed, occurring largely on relatively cool, moist sites. Though stands containing significant amounts of hemlock comprise only about 5% of the forested landscape in DEWA (1130 ha), where they occur, hemlock often dominates, comprising as much as 77% of the basal area in stands (Sullivan et al. 1998). Recent evidence suggests that before Euro-American settlement, hemlock represented a greater component of many northeastern U.S. forests than it does today and that present-day hemlock stands are often restricted to permanent woodlots with reduced disturbance histories (Foster et al. 1998; McLachlan et al. 2000). In DEWA, many hardwood stands, especially in ravine terrains, are younger on average than hemlock stands and contain a large number of cut, decayed hemlock stumps, suggesting that hemlock was likely once more abundant in DEWA as well (Sullivan et al. 1998).

Hemlock woolly adelgid (HWA) infestations were first detected in DEWA in 1989, and a subsequent survey conducted in 1995 indicated that over half of the Park's hemlock stands were infested (Evans 1995). Nevertheless, at the time of this study, HWA-induced mortality was limited to a few small stands, mostly in the southeastern portion of the Park. Since this study was conducted, impacts from HWA have increased dramatically (R. Evans, Delaware Water Gap National Recreation Area, Charles Pierce House, HC 38, Milford, PA 18337, personal communication).

The topographic setting of DEWA is varied, with terraced benches and ravines to the west, significant river bottom habitats surrounding the Delaware River, and steeply sloping ridge landforms to the east. The minimum elevation is approximately 84 m and maximum elevation is about 490 m. Nearly 60 km of the Delaware River flows through the Park. Additionally, the Park has 87 km of 1st-order streams, 32 km of 2nd-order streams, and 60 km of 3rd-order or higher streams, many of which originate outside the Park.

© 2002 NRC Canada

Fig. 1. Delaware Water Gap National Recreation Area (DEWA) depicting location of the Park (inset) and the study sites. Sites containing temperature loggers are also shown. Site numbers are a hierarchical coding system. First two digits refer to sub-basin number (sub-basins are numbered sequentially from north to south), the third digit refers to the terrain type (1 = bench; 2 = ravine; 3 = midslope), the fourth digit represents stream order (one or two); the fifth digit represents forest type (0 = hardwood; 1 = hemlock); and the sixth digit represents the replicate number (1, 2, or 3).

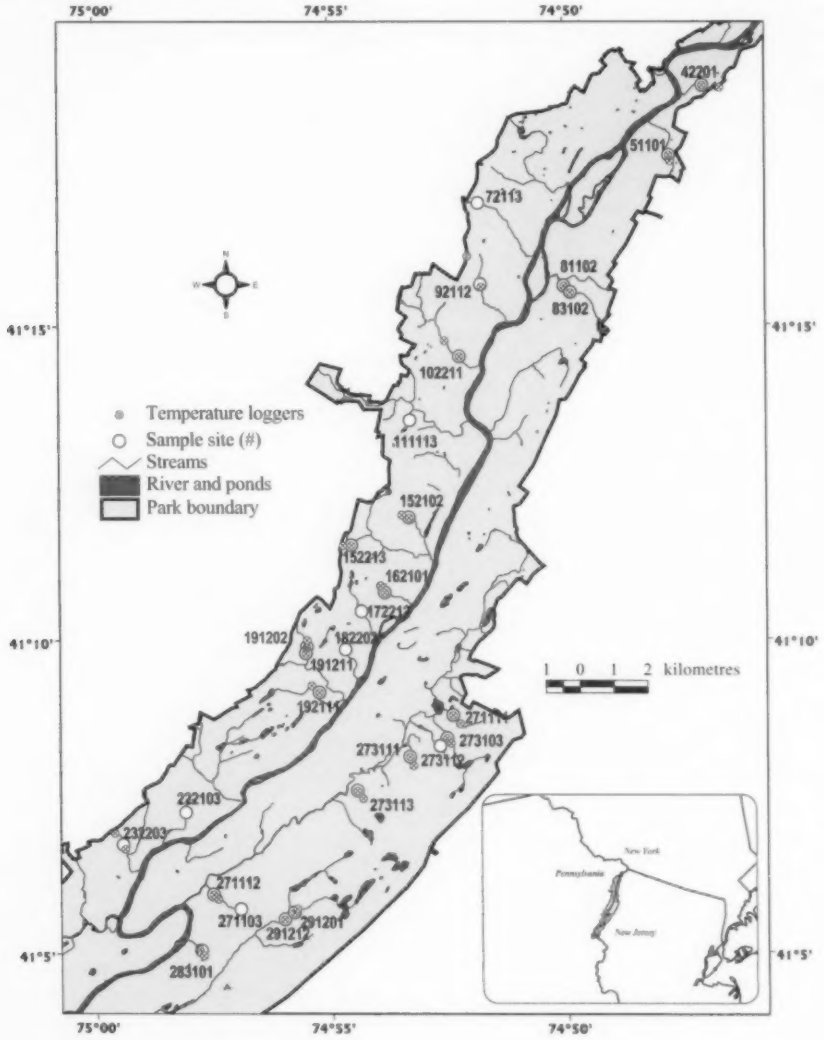

Landscape analysis and sampling design

Our approach was to focus the study on smaller, headwater catchments because larger streams drained areas containing both hemlock and mixed hardwood forest making forest-specific comparison intractable. In addition, most of these larger watersheds were impacted by humans (e.g., impoundments, agriculture, quarries), which could confound our assessment of the influence of hemlock. Even after limiting the study to headwater catchments, other possible confounding factors remained; we controlled for landscape variability (i.e., terrain and stream size) through the sampling design, and we excluded others (i.e., minimum catchment area, beaver activity) through site selection. Because the primary objective was to detect a forest-type effect, we chose to study the endpoints represented by streams draining forest that were either dominated by hemlock or dominated by mixed hardwood. In this way, we maximized the opportunity to detect a forest-type effect if one existed.

We used geographic information systems (GIS) to characterize the landscape in DEWA and to provide the basis for the terrain-based, paired-site sampling design used in this study. Our goal was to sample across the range of landscape variability in the Park and control for the effects of terrain and stream size before comparing aquatic invertebrate community measures between forest types. Landscape analysis consisted of five steps: (*i*) classifying a digital vegetation map (Myers and Irish 1981) into two forest types (hemlock and mixed hardwood), (*ii*) characterizing the diversity of ter-

© 2002 NRC Canada

rain where hemlock occurs, (*iii*) assessing stream order and length by forest stand, (*iv*) defining landscape treatments based on forest type, terrain type, and stream order, and (*v*) pairing hemlock-dominated streams with similarly structured mixed hardwood dominated streams within each treatment (see Young et al. (2002) for a complete description).

We classified forest stands where hemlock represented the primary, secondary, or tertiary component of the stand as "hemlock" and classified stands with little or no hemlock as "hardwood". Later ground surveys indicated that hemlock represented between 25 and 77% (median = 60%) of the total basal area of forests within watersheds above sample sites in selected hemlock stands and between 0 and 32% (median = 2%) within watersheds in selected hardwood stands (Sullivan et al. 1998).

We characterized terrain for each forest stand by deriving measures of elevation, slope, aspect, terrain shape, and solar radiance from a digital elevation model (Young et al. 2002). Subsequently, we used Euclidean distance based *k*-means clustering in SYSTAT (Wilkinson 1998) to classify hemlock stands into three types: bench, ravine, and midslope terrains (Young et al. 2002). Low mean slopes (i.e., topographically flat) distinguished bench sites from the other two terrains. Low terrain shape scores (i.e., watershed gorge-like or concave in cross section) distinguished ravines; and steep slopes, convex terrain shape, and relatively low solar radiance values distinguished midslope sites.

We quantified the length and order (Strahler 1964) of streams flowing through each forest stand using digital stream data (Young et al. 2002). A total of 56 hemlock and 333 hardwood stands contained 1st- and 2nd-order streams. There were hemlock stands in both bench and ravine terrains that contained 1st- and (or) 2nd-order streams. Stands in midslope terrains contained only 1st-order streams. We combined the three terrain types and two stream orders to form sampling strata (hereafter termed "stream types"). We designated the five stream types as follows: 1st-order bench, 2nd-order bench, 1st-order ravine, 2nd-order ravine, and 1st-order midslope.

Before selecting sample sites within each stream type, we imposed two additional constraints on site selection to maximize the probability of detecting a forest-type effect if one existed. First, we only considered hemlock or hardwood forest stands that were greater than a total area of 5 ha within a selected watershed. Second, we required that selected stands contain a minimum of 100 m of 1st-order or 200 m of 2nd-order stream length. We imposed these additional constraints because forest-type effects on aquatic assemblages would most likely be detectable in catchments where long reaches of stream drain a single dominant forest type. One additional hardwood stand was eliminated because there was substantial beaver activity within the watershed. As a result, 29 hemlock stands and 134 hardwood stands comprised our target population.

From the target population, we randomly selected three hemlock stands from each stream type, and then paired each one with a corresponding hardwood site that drained the same stream order and was most similar in terms of the five terrain variables (Young et al. 2002). Upon field inspection, one site-pair in the 2nd-order bench strata was dropped because of clear differences in discharge, leaving a total of 14 site-pairs. Young et al. (2002) found the terrain-based, paired-site study design effectively represented the diversity of environments where hemlock occurred in DEWA and significantly improved statistical inference and power over a simple random sampling design.

Macroinvertebrate sampling and processing

Invertebrate sampling was conducted during the first two weeks of April 1997. Originally, sampling was planned for mid-March. This period was selected to coincide with peak benthic diversity, before the onset of adult emergence for most aquatic insect species and when stream habitat is used most heavily by later instars (Plafkin et al. 1989). However, high stream flows prevented March sampling. Nevertheless, past studies of emergence patterns of aquatic insects inhabiting small, cold-water streams in the region suggest that peak emergence periods for most species occur after the early-April sampling period (Singh et al. 1984; Duffield and Nelson 1990; Masteller 1993). Thus, although emergence of some individuals may have occurred before sampling, it is likely that a significant fraction of individuals of most taxa were represented in the benthos. Furthermore, streams of each hemlock–hardwood site-pair were sampled either on the same day or only one day apart to control for temporal differences in community structure. Sample reaches were defined by a distance of 80 m for 1st-order streams and 160 m for 2nd-order streams. These distances represented approximately 40 mean stream widths and encompassed a minimum of three riffle–pool sequences.

Two approaches were used for invertebrate sampling. First, a combination of systematic and random sampling was used to obtain unbiased estimates of actual and relative abundances. A total of 20 equally spaced transects perpendicular to stream flow were established (i.e., 4 m apart for the 80-m 1st-order reaches and 8 m apart for the 160-m 2nd-order reaches). A single invertebrate sample was collected at a random location along each transect for a total of 20 samples per stream. Sampling consisted of 30-s kicks with a standard D-frame kick net (250 μm mesh) over an area of 0.09 m^2 at each selected site. All 20 samples were combined into a single composite sample and preserved with 80% isopropyl alcohol in the field. Composite samples allowed us to sample more streams and a larger proportion of each stream for a given amount of effort. Because we were interested in comparing biological structure among stream types, as opposed to reaches within a single stream, composite sampling was justified.

Second, a qualitative, microhabitat-based approach was used to maximize the probability of collecting individuals of all species by sampling in all available microhabitats independent of their rarity. The classification approach that we used to define available microhabitats was based on water depth, velocity, and predominant substrate, variables known to be important determinants of aquatic invertebrate distributions (Minshall 1984; Newbury 1984). A rapid approach was used to distinguish microhabitats, relying on visually distinguishable differences in velocity (fast vs. slow water, turbulent vs. nonturbulent) and substrate (pea-sized vs. golf-ball-sized, etc), and easily measured differences in depth (>30 cm vs. <30 cm) (Table 1). Two investigators (one on each bank) searched the entire stream reach for the presence

© 2002 NRC Canada

of each of the 50 possible microhabitat types (Table 1). Individual microhabitats had to be a minimum of 1 m^2 to sample. Attempts were made to collect a minimum of two samples from each available microhabitat type. Qualitative samples were also collected with a D-frame kick net and were composited and preserved as described above for random samples.

In the laboratory, each composite sample (one random and one qualitative sample per site) was split into 16 subsamples by volume. The splitter consisted of a 2.5-gallon bucket centered over a large Plexiglas wedge. The bucket was mounted on a pivot so that it could be tipped evenly and sample contents could be dispersed over the wedge and collected in two large plastic receptacles. This procedure was repeated with each fraction until there were a total of 16 subsamples of approximately equal volume.

For each composite sample, invertebrates were picked, identified, and enumerated from four randomly selected subsamples (i.e., 25% of each composite sample). The 25% was chosen based on the results of an analysis that we conducted to determine the minimum number of subsamples required to accurately represent taxa richness and total abundance in the entire composite sample. Specifically, we determined taxa richness and total abundance for all 16 subsamples from two of the 56 composite samples. Subsequently, by computer, we randomly drew a bootstrap subsample (Manly 1991) from the total (N = 16) and calculated richness and abundance based on the bootstrap subsample. This process was repeated 1000 times for each subsample size (1, 2, 4, and 8). Results of this bootstrapping procedure indicated that taxa richness and total abundance estimated from four subsamples were within 10% of the true value of the entire sample 90% of the time.

Stream habitat sampling

In-stream habitat measurements were taken within the same stream reaches used to collect macroinvertebrates. Water chemistry measurements were taken at each site during spring high-flow conditions proximate to invertebrate sampling in well-mixed areas of high flow. Dissolved oxygen, pH, and specific conductance were measured using a Hydrolab Reporter multiprobe meter (Hydrolab Corp., Austin, Tex.), and turbidity was measured with a LaMotte turbidity meter (model 2008; LaMotte Co., Chestertown, Md.). Nutrients, including total nitrates, total nitrites, reactive phosphates, and ammonia, were measured using a direct-reading spectrophotometer (model DR/2000; HACH Co., Loveland, Colo.). Stream discharge was measured in the spring, during a prolonged period of high stream flows in an area of relatively laminar flow using a digital flowmeter (FloMate model 2000; Marsh-McBirney Inc., Frederick, Md.). Water temperature was measured hourly between 01 April 1997 and 31 March 1998 at 10 of the 28 sites (i.e., two replicate site-pairs for each of the five different stream types; Fig. 1) using Optic StowAway™ temperature loggers (Onset Computer Corp., Pocasset, Mass.). Loggers were placed near the bottom of the sample reaches where invertebrates were collected.

Stream channel measurements included (*i*) microhabitat diversity, (*ii*) large woody debris (LWD), and (*iii*) the extent to which each stream dried during the summer. Microhabitat (classified as in Table 1) was determined at each of the 20 random locations where invertebrate samples were taken. Large woody debris was censused during summer base flow (08 July – 16 July). For each stream reach, all logs and sticks entirely or partially within the bankfull stream channel were classified according to size, based on length and diameter (Dolloff et al. 1993). Measurements were made on the entire log or stick even if only a portion occurred within the stream channel because we were interested in forest-type effects on LWD loading as well as available habitat for invertebrates. The proportion of a stream that dried during the summer was visually estimated to the nearest 10%. Each stream was subsequently classified into one of four categories based on the amount of the bankfull stream channel bottom that remained wetted: wet = completely wet; mostly wet = >50% of channel bottom wetted; mostly dry = <50% of channel bottom wetted; and dry = completely dry.

Statistical analyses

Two primary data matrices from the invertebrate samples were used for analyses. For analyses based on species abundances (e.g., density and relative abundance comparisons), we created a site × species abundance matrix using the random samples only. For analyses based on occurrence or richness of species, we created a presence–absence matrix using data from both the random and qualitative samples.

We compared four measures of invertebrate assemblage structure between streams draining hemlock and hardwood forests: (*i*) taxa richness, (*ii*) Simpson's evenness index (Brower and Zar 1984), (*iv*) total density, and (*v*) number of rare taxa (defined as taxa that occurred at fewer than four sites). Making use of the terrain-based, paired-site design (Young et al. 2002), we tested the null hypothesis that mean differences in each community structure metric between site-pairs were equal to zero. For each metric, we calculated the difference between individual hemlock–hardwood site-pairs by subtracting the value measured in the hardwood site from that in the corresponding hemlock site. We used analysis of variance (ANOVA) to determine if mean differences between forest types varied among stream types. This is analogous to testing the effect of the interaction between forest type and stream type on each response variable. In the absence of an interaction, we used a paired t test to test the main effect of forest type on assemblage structure. Differences approximated a normal distribution so no transformations were required before analysis. We used Systat (Wilkinson 1998) software to conduct ANOVA and paired t tests.

We also compared the taxonomic and trophic composition of aquatic invertebrate assemblages between forest types. For taxonomic composition, we conducted an odds ratio test (Agresti 1990) to determine the association between the presence of each taxon and forest type. The odds of taxon presence is the probability of presence divided by the probability of absence. There are two relevant odds: one specific to hemlock stands and the other specific to hardwood stands. The ratio of these odds is the odds ratio. The natural log of the odds ratio tends to make the statistic normally distributed and more easily interpretable. We computed odds ratios and p values using LogXact (Mehta and Patel 1996).

For trophic composition, we used multiresponse permutation procedure (MRPP) to analyze forest-type effect on the

© 2002 NRC Canada

Table 1. Microhabitat classification matrix used to stratify qualitative invertebrate sampling.

	Slow-water habitats				Fast-water habitats					
	Depth <30 cm		Depth >30 cm		Riffles–rapids		Runs		Waterfalls	
Substrate	HEM	HRD	HEM	HRD	HEM	HRD	HEM	HRD	HEM	HRD
Logs (>30 cm diameter)	0.0	0.0	0.4	0.0	0.0	0.0	0.0	0.0	0.0	0.0
Sticks (<30 cm diameter)	1.8	1.1	0.0	0.0	1.1	1.1	0.4	0.7	0.0	0.0
Leaf packs	1.8	3.2	0.0	0.0	0.0	1.4	0.4	1.8	0.0	0.0
Needle packs	< 0.1	0.0	0.0	0.0	0.4	0.0	0.4	0.0	0.0	0.0
Moss	0.4	0.7	0.0	0.0	5.0	3.2	1.4	1.4	0.0	1.8
Silt–detritus (not mineral) (<6.4 mm)	2.5	1.4	0.0	0.0	0.0	0.0	0.0	0.0	0.0	0.0
Sand (mineral, <pea sized) (<6.4 mm)	1.1	0.7	0.0	0.0	0.0	0.0	0.0	0.0	0.0	0.0
Gravel (mineral, pea – golf ball sized) (6.4–50 mm)	7.9	10.0	1.1	0.0	2.9	3.2	4.3	3.9	0.0	0.4
Cobble (mineral, golf ball – head sized) (50–200 mm)	12.5	8.9	0.4	0.0	20.0	18.9	8.9	14.3	0.0	0.0
Boulder–bedrock (mineral, >head sized) (>200 mm)	5.0	3.9	3.6	1.8	10.0	10.4	4.3	5.7	2.1	0.0

Note: Fast-water habitats were either turbulent (i.e., riffles, rapids, and waterfalls) or nonturbulent (runs). Slow-water habitats (i.e., pools) were either deep (i.e., >30 cm) or shallow. Depth was determined with a pole marked at 30 cm and velocity and turbulence were distinguished by visual inspection. Predominant substrate was classified into one of ten categories that were easily distinguished by eye. A total of 50 microhabitats were possible based on combinations of depth or water velocity and substrate. Percent of available habitat represented by each microhabitat type is shown for each forest type (HEM, hemlock; HRD, hardwood).

proportion of individuals in four trophic groups: shredder–detritivores, collector–detritivores, grazer–algivores, and predators (Merritt and Cummins 1996). MRPP is a nonparametric procedure designed to test for differences in multivariate responses among groups and has the advantage of not requiring multivariate normality and homogeneity of variance that are seldom met with ecological community data (Zimmerman et al. 1985). Initially, we tested whether forest-type effect was homogeneous among stream types. If the effect was homogeneous, we tested whether trophic composition varied between paired hemlock and hardwood stands. We computed MRPP test statistics and p values using BLOSSOM software (Cade and Richards 2000). We also compared paired differences in the proportion of individuals in each trophic group separately using ANOVA and paired t tests as we did for assemblage structure responses.

We evaluated the effect of forest type on stream habitat using the same methods as those used to compare aquatic invertebrate assemblage structure responses. We compared temperature patterns (means, maxima, and minima) of streams in hemlock and hardwood forest types graphically using the hourly temperature data collected with temperature loggers. Finally, we used logistic regression to determine the relationship between the probability of a stream drying and forest type. For all the tests of statistical significance described above, we used an alpha value of $P = 0.10$.

Results

Interaction between stream and forest types

The effect of forest type did not depend on stream type for most biological and stream-habitat responses. Forest-type effect on density, number of rare species, and trophic composition were homogeneous among stream types (density, $F_{[4,9]} = 0.62$, $p = 0.66$; rare species, $F_{[4,9]} = 2.24$, $p = 0.15$; trophic composition, $\delta = 2.15$, $p = 0.15$). Likewise, forest-type effect did not vary among stream types for any of the eight water chemistry variables ($p > 0.27$ for all variables) or in the frequency of LWD in any of the seven size classes or for the total ($p > 0.36$ for all size classes).

In contrast, forest-type effect on taxa richness and Simpson's evenness index did depend on stream type (taxa richness, $F_{[4,9]} = 3.27$, $p = 0.07$; Simpson's evenness, $F_{[4,9]} = 3.32$, $p = 0.06$). Differences between hemlock–hardwood site-pairs in microhabitat diversity also varied among stream types ($F_{[4,9]} = 4.73$, $p = 0.02$), and graphical examination of temperature data suggested that differences in thermal patterns between hemlock and hardwood sites were not independent of stream type. Plots of mean differences by stream type suggested that for response variables where forest-type effect depended on stream type, 1st-order midslope sites showed a different pattern than the other four stream types. In some cases (Simpson's evenness index and temperature patterns), midslope sites showed a pattern opposite that shown by the other stream types, and in others, midslope sites showed no difference or a much smaller mean forest-type difference than the other stream types (taxa richness and microhabitat diversity). We retested the effect of stream type on forest-type differences with midslope sites excluded and found that differences between hemlock–hardwood site-pairs no longer depended on stream type when midslope sites were excluded ($p > 0.20$ for all variables).

In addition, midslope sites represented only a small component of the Park landscape (only five of the 142 hemlock stands in the Park that contained 1st- or 2nd-order streams were classified as midslope). Because all biological and stream-habitat responses were homogeneous among all but midslope stream types and because midslope stream types were rare in the Park, we removed midslope sites from the

© 2002 NRC Canada

analysis and pooled the data from the remaining four stream types. Thus, for the rest of the paper, we discuss results from other than midslope sites.

Aquatic invertebrate community structure

A total of 151 taxa were positively identified from benthic samples; 43 taxa were identified to species, 94 to genus, 13 to family, and 1 to order. The number of taxa collected at any one site ranged between 21 and 66. A total of 64 taxa were considered rare (i.e., occurred at fewer than four sites), and the number of rare taxa ranged between 0 and 10. A total of 53 868 individuals were collected, and density ranged between 116 and 4698 individuals·m^{-2}.

Analysis of data pooled across stream types excluding 1st-order midslope sites indicated that all four invertebrate community structure measures were highly variable, even within a forest type (Fig. 2*a*). Despite the large variances observed within forest types, mean differences between hemlock–hardwood site-pairs were significantly different from zero for all four response variables (Fig. 2*b*). Streams draining hemlock supported on average about 1.5 times more total taxa (mean difference = 14 taxa) and had nearly 9% higher Simpson evenness indices than streams draining hardwood forests. In contrast, streams draining hardwood forests were over 2.7 times more dense (mean difference = 838 individuals·m^{-2}) and supported more rare taxa (mean difference = 2 taxa) than streams draining hemlock.

Results of odds ratio tests for each taxon indicated that forest-specific differences in taxa richness were associated with specific taxa and were not simply a random subset of the community. Eleven taxa (7.3% of total) showed strong associations with hemlock (odds ratio test, $p < 0.10$), whereas no taxa were strongly associated with hardwood forests (Table 2). An additional 17 taxa showed weaker associations with hemlock (odds ratio test, $p < 0.30$), whereas only five taxa showed weak associations with hardwood forests (Table 2). Of the 28 taxa that showed either strong or weak associations with hemlock, three were found to occur exclusively in hemlock-dominated watersheds, whereas no taxa were found to occur in streams only draining hardwood forests.

Trophic composition (i.e., the proportion of individuals in each of the four trophic groups) also differed between streams draining hemlock and hardwood forests ($\delta = 2.18$, $p = 0.009$). Predators comprised a significantly larger fraction and grazer–algivores comprised a significantly smaller fraction of the invertebrate assemblage in hemlock-drained streams (Fig. 3). The proportion of individuals as shredders and collectors did not differ between forest types.

Stream habitat

Water chemistry was highly variable among DEWA streams, with several variables exceeding an order of magnitude in range (Table 3). However, mean differences between hemlock–hardwood site-pairs were not significantly different from zero for any of the eight water chemistry variables measured (Table 3). Similarly, forest type did not affect spring discharge, microhabitat diversity, or the frequency of large wood debris (Table 3).

Median daily stream temperatures at hemlock sites tended to be cooler in the summer, warmer in the winter, and less variable throughout the year (Fig. 4). In addition, summer daily maxima were lower and winter daily minima were higher in hemlock-drained streams. For example, summer daily maxima in streams draining hardwood forests exceeded 20°C 18% of the time compared with less than 3% in streams draining hemlock, and winter minimum daily temperatures dropped below freezing 8% of the time in hardwood sites compared with only 0.2% in hemlock sites (Fig. 5).

We used flow data from the USGS (U.S. Geological Survey) gaging station on the Bushkill River to characterize long-term rainfall patterns in the Park. We found stream flows to be normal (i.e., close to the long-term average) during the spring of 1997, when invertebrate sampling was conducted. However, the summer of 1997 was very dry with stream flows during the months of July and August falling well below what would be considered normal for that time of year. Specifically, over the 90-year period between 1908

Fig. 2. Comparison of four community structure metrics between streams draining hemlock and mixed hardwood forests. (*a*) Comparison of the range of values (limits of boxes) and medians (white lines) for each metric between streams draining hemlock (solid bars) and hardwood (shaded bars) forests. (*b*) Depiction of the average difference (±90% confidence limits, CL) between hemlock–hardwood site-pairs. Positive values indicate higher means for hemlock. Comparisons exclude 1st-order midslope sites, which exhibited distinctly different patterns than the other stream types (see text).

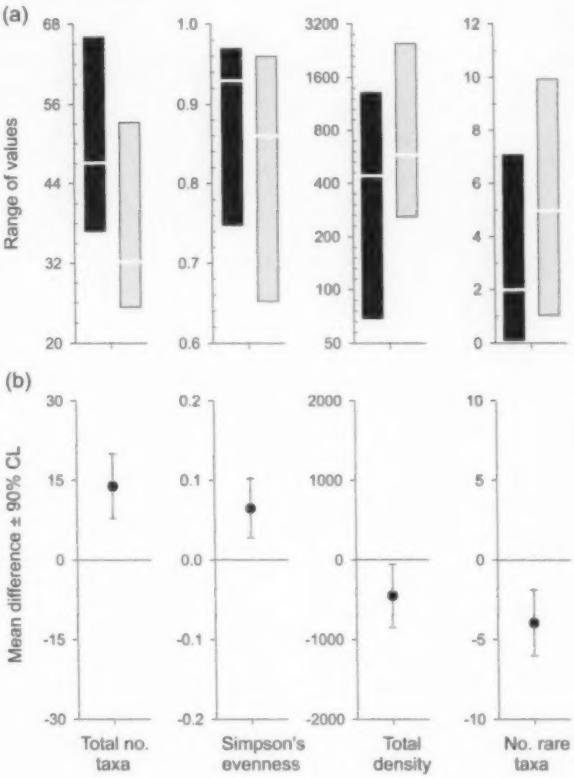

© 2002 NRC Canada

Table 2. Identity of taxa with forest type preferences.

Strong hemlock associates	Weak hemlock associates	Weak hardwood associates
Baetis amplus	*Ephemerella* sp.	*Allocapnia* sp.
Leptophlebiidae	*Eurylophella* sp.	*Prostoia similis*
Lanthus parvulus	*Leuctra* sp.	*Chaetocladius* sp.
Perlidae	*Isoperla* sp.	*Diplocladius* sp.
*Hydropsyche ventura**	*Diplectrona modesta*	*Tipula* sp.
Bezzia sp.	*Lepidostoma* sp.	
Brillia sp.	Limnephilidae	
Psilometrichemus sp.	*Polycentropus* sp.*	
Rheocricotopus sp.	*Rhyacophila minora*	
Hexatoma sp.	*Promoresia* sp.	
Pseudolimnophila sp.	*Ectopria nervosa*	
	Natarsia sp.*	
	Polypedilum sp.	
	Stempellinella sp.	
	Symbiocladius sp.	
	Molophilus sp.	
	Psidium sp.	

Note: Strong preference defined as p values of less than 0.1 in odds ratio test (see Methods). Weak preferences defined as p values less than 0.30. The asterisks (*) indicate taxa found only in streams draining hemlock. There were no strong hardwood associates.

and 1997, only 5.5% of the average flows in July and 6.6% of the average flows in August were as low or lower than those observed in 1997. The result of the dry summer in 1997 was that a substantial portion of our study streams dried completely. We observed forest-specific differences in the extent to which streams dried. In the summer of 1997, 9 of 14 (64%) streams draining hardwood forests became dry or mostly dry, whereas 2 of 14 (14%) streams draining hemlock dried partially. None of the streams draining hemlock dried completely compared with 4 of 14 (29%) streams draining hardwood. Weather patterns during the summer of 1999 were even more severe, with the month of July being one of the driest on record. At our request, DEWA personnel revisited our study sites in July of 1999 and determined which sites remained wet (i.e., contained some water and positive flow). They found 6 of 14 (43%) streams draining hardwood dried completely compared with only 1 of 14 (7%) streams draining hemlock (R. Evans, Delaware Water Gap National Recreation Area, Charles Pierce House, HC 38, Milford, PA 18337, personal communication).

The probability of a stream becoming dry or mostly dry during the summer of 1997 was related to two variables measured: forest type and spring high flows. The likelihood that a stream would dry was higher when the previous spring flows were low (Fig. 6). However, streams draining hemlock were much less likely to dry over a wide range of high-flow discharges. The critical spring flow (i.e., spring discharge where the likelihood of becoming dry exceeds the likelihood of remaining wet) was an order of magnitude lower for streams draining hemlock forests (Fig. 6).

Discussion

After accounting for differences in terrain and stream order, we found that aquatic invertebrate community structure was significantly different between streams draining hemlock and those draining mixed hardwood forests. Streams draining hemlock forests supported more total taxa than those draining hardwood forests, and over 7% of the taxa showed strong associations with hemlock, including three taxa found exclusively in hemlock streams. These patterns suggest that both within-site and park-wide diversity of aquatic invertebrates were enhanced by hemlock or by factors correlated with hemlock. In addition, invertebrate taxa were distributed more evenly (i.e., higher Simpson's evenness values) in hemlock-drained streams, indicating that higher richness values were not associated with the chance occurrence of taxa represented by relatively few individuals. In contrast, the number of rare taxa and total densities were lower in streams draining hemlock, suggesting that diversity differences were not related to stochastic factors associated with sampling (e.g., richness related to number of individuals collected or chance occurrence of rare species) and that streams draining hardwood forests may have been more productive.

Few studies have investigated the influence of hemlock forests on aquatic communities. In a study comparing leaf decomposition rates, Maloney and Lamberti (1995) found that hemlock needles decayed slower and supported fewer macroinvertebrates than the leaves of four other riparian plant species in a northern Michigan stream and suggested that hemlock may contain secondary compounds that inhibit decomposition. Comparative and experimental studies with other confer species (mainly *Pinus*) suggest that conifer needles are relatively poor food sources and are generally avoided by leaf-shredding insects (Webster and Benfield 1986). However, Bowen et al. (1995) found that hemlock logs and branches supported relatively high densities of chironomids and other invertebrates in the littoral zone of two lakes in eastern Canada; but based on species composition (i.e., low proportion of shredders and high proportion of filter feeders and collectors), they hypothesized that colonizing invertebrates were using wood debris mainly as a substrate rather than as a food source. Boucherle et al. (1985) studied

© 2002 NRC Canada

Fig. 3. Comparison of the proportion of individuals in each of four trophic groups. (*a*) Comparison of the range of values (limits of boxes) and medians (white lines) for each metric between streams draining hemlock (solid bars) and hardwood (shaded bars) forests. (*b*) Depiction of the average difference (±90% confidence limits, CL) between hemlock–hardwood site-pairs. Positive values indicate higher means for hemlock. Comparisons exclude 1st-order midslope sites, which exhibited distinctly different patterns than the other stream types (see text).

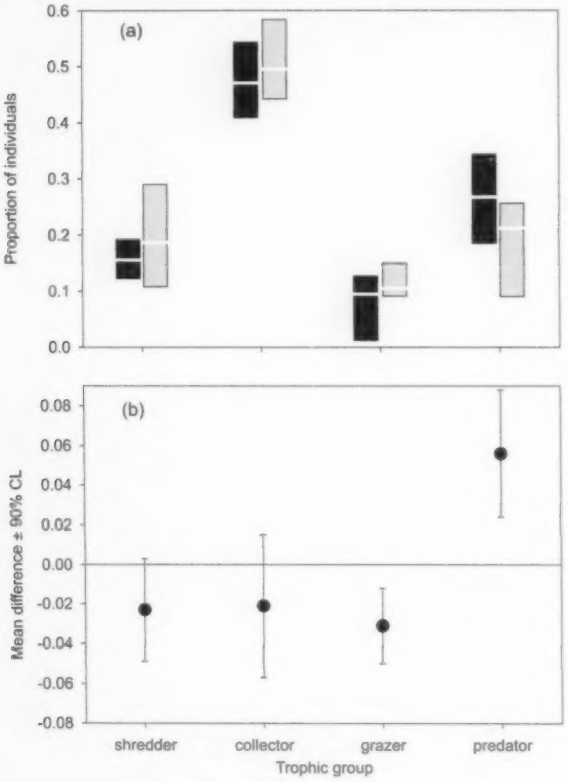

the limnologic consequences of the widespread hemlock decline that occurred during the mid-Holocene period (about 4800 years ago) in three southern Ontario lakes and found that lake trophic status and the species composition of plankton assemblages were altered by historic declines in hemlock forests. Our data suggest that similarly large changes may occur to aquatic invertebrate assemblages in headwater stream ecosystems should hemlock decline continue.

We observed differences in stream habitat that could explain differences in benthic macroinvertebrate diversity observed between forest types. Diel and seasonal thermal regimes were more moderate in hemlock-drained streams, and streams draining hardwood forests were more prone to drought disturbance than those draining hemlock. Higher frequency of subzero temperatures observed in hardwood-drained streams could promote the formation of anchor ice, which has been found to be a major factor regulating benthic assemblages by reducing taxa richness and limiting reproductive habitat (Miller and Stout 1989; Sahade et al. 1998). Moreover, more stable thermal regimes may help minimize exposure of benthic communities to temperatures outside the optimum range for many component species. Although benthic macroinvertebrate diversity has been found to be positively related to thermal heterogeneity at the basin-wide or river-system scale (reviewed in Ward and Stanford 1982), there is evidence that benthic assemblages in headwater streams are more diverse in cooler, more thermally static streams. For example, Kamler (1965) characterized headwater mountain streams in Poland based on thermal patterns and found that streams with more variable thermal regimes supported fewer total taxa than streams with more static thermal regimes and attributed this pattern to the fact that the diversity of two important orders, Ephemeroptera and especially Plecoptera, are comprised of predominantly cold stenothermal species.

Greater stability of summer base flows in hemlock-drained streams may have contributed to forest-type differences in benthic diversity. Fewer streams draining hemlock forests dried up during two separate drought years, and the probability of drying was lower for streams draining hemlock. Moreover, these associations were independent of stream size, which was accounted for in the stratification and pairing procedures of the study design, or high-flow (spring) discharges, which were accounted for post hoc with regression analysis.

There is little doubt that stable base flows would afford, at least, short-term benefits to stream invertebrate communities. Because most aquatic insect species require at least 1 year to complete their life cycle (Wallace 1996), stream drying would likely kill or displace a large fraction of the benthic community leading to lower densities and diversity. Moreover, even if streams do not dry completely, partial drying would likely reduce available habitat to a series of small pools with little or no flow between them. Remaining refuges would likely be more vulnerable to density-dependent sources of mortality such as competition and predation (Power et al. 1988) and at greater risk to environmental extremes such as high water temperature and low dissolved oxygen levels (Lake and Boulton 1990).

In the longer term, disturbances such as droughts and floods could have either beneficial or detrimental effects on diversity depending on their timing, frequency, and severity. The role of disturbance in structuring natural communities has received considerable attention (e.g., Connell 1978; Huston 1979; Sousa 1984), and although there is general agreement that disturbance plays a significant, possibly overriding, role in structuring stream communities, no consensus has been reached regarding the specific mechanism (Resh et al. 1988; Death and Winterbourn 1995). Nevertheless, it is clear that disturbances may cause lasting reductions in the diversity of stream communities if they are severe enough to significantly depress exposed populations and widespread and frequent enough to limit recolonization from unaffected areas (Yount and Niemi 1990).

Hemlock and mixed hardwood forests also differ in their effect on autochthonous and allochthonous sources of energy, and these differences may explain observed differences in total invertebrate density and trophic composition observed between forest types. Streams draining hardwood forests receive more sunlight on an annual basis than those draining hemlock forests because of reduced shading associ-

© 2002 NRC Canada

Table 3. Comparison of water chemistry and physical habitat variables between hemlock (Hem) and mixed hardwood (Hrd) site-pairs in DEWA streams.

Variable	Range of values		Mean difference, Hem – Hrd	*p* value
	Hemlock	Hardwood		
Water chemistry				
Dissolved oxygen ($mg \cdot L^{-1}$)	11.4–13.5	10.3–13.8	0.5	0.29.
Specific conductance ($ms \cdot cm^{-1}$)	15–151	20–193	–33	0.18
pH (–log H^+ ions)[a]	5.70–7.52	5.74–7.98	8.38E-8	0.60
Turbidity (Nephelometric units)	0.10–6.74	0.10–12.50	–1.28	0.33
Ammonia ($mg \cdot L^{-1}$)	0.01–0.31	0.01–0.24	–0.01	0.88
Total nitrates ($mg \cdot L^{-1}$)	0.0–1.2	0.0–1.4	–0.1	0.79
Total nitrites ($mg \cdot L^{-1}$)	0.000–0.002	0.000–0.004	–0.001	0.12
Orthophosphates ($mg \cdot L^{-1}$)	0.00–0.28	0.00–0.28	–0.00	0.36
Physical habitat				
Spring discharge ($m^3 \cdot s^{-1}$)	8.4–985.6	1.4–1070.5	0.3	0.67
Microhabitat diversity [b]	6–14	6–12	0	0.31
LWD ($No. \cdot 100\ m^{-1}$)[c]				+>
LWD: total	35–160	37–154	9	0.94
LWD: size class 1	15–71	8–86	9	0.53
LWD: size class 2	5–69	4–36	5	0.59
LWD: size class 3	0–3	0–6	0	0.36
LWD: size class 4	0–6	0–8	–2	0.18
LWD: size class 5	1–12	1–20	–1	0.79
LWD: size class 6	0–7	0–2	0	0.39
LWD: root wads	2–38	4–55	–2	0.44

Note: The range of values in each forest type, mean difference between site-pairs, and *p* values of *t* tests that test the null hypothesis that the average difference between hemlock–hardwood site-pairs is equal to zero are reported. Values observed in hardwood sites were subtracted from values in hemlock sites, so positive mean differences indicate that hemlock was higher. Midslope site-pairs were excluded from all analyses, so degrees of freedom were 10 for all tests.

[a]Range of pH values are reported but the *t* test was conducted using $[H^+]$ instead of pH and the mean difference between site-pairs reported in the table is $[H^+]$.

[b]Microhabitat diversity refers to the number of microhabitat types as described in Table 1.

[c]LWD refers to large woody debris (i.e., sticks and logs) found within the stream channel and differences in the frequency of LWD between hemlock–hardwood site-pairs were tested for the total (all LWD sizes classes summed) and for six separate size classes and root wads. Size classes were defined by combinations of diameter (cm) and length (m) as follows: size class 1, D = 5–10 cm, L = 1–5 m; size class 2, D = 10–50 cm, L = 1–5 m; size class 3, D = >50 cm, L = 1–5 m; size class 4, D = 5–10 cm, L = >5 m; size class 5, D = 10–50 cm, L = >5 m; size class 6, D = >50 cm, L = >5 m. Root wads refer to tree roots on stream banks capable of providing cover for fish.

ated with seasonal leaf-off periods, and even during leaf-on periods, hemlock forests filter out more sunlight than mixed hardwood forests (Hadley 2000). Because light appears to be the primary factor limiting primary production in these forested headwater stream environments (Hill and Knight 1988; Wellnitz et al. 1996), increases in incident light would stimulate more algal production, potentially increasing the total energy inputs and broadening the food base for stream invertebrates (Minshall 1978; Lamberti and Steinman 1997). Our observation that grazing algivores represented a larger fraction of the benthic community in hardwood-drained streams suggests an assemblage response to higher primary production. Smock and MacGregor (1988) showed that similar changes in trophic composition may have occurred following changes in forest composition resulting from the chestnut blight of the early 1900s.

Although there is some evidence that hemlock and other conifers contribute more allochthonous inputs annually than mixed hardwood forests (Anderson and Sedell 1979; Molles 1982), much of that energy is not available as food for aquatic macroinvertebrates (Webster and Benfield 1986), and so hemlock forests may provide less usable allochthonous energy than mixed hardwood forests. Thus, in addition to more autochthonous-derived energy, greater contributions of high-quality leaf litter may also contribute to the higher total abundances of benthic invertebrates that we observed in hardwood-drained streams.

Taken together, the results of the present study indicate that headwater streams drained by hemlock and mixed hardwood forests support substantially different benthic communities. Further, our results suggest that forest-type differences in light and temperature regimes, stability of summer base flows, and quality of allochthonous inputs are proximate causes of observed differences in benthic assemblage structure and composition. Based on these associations, we predict that pest-induced declines in hemlock will have long-term consequences for aquatic invertebrate assemblages including a reduction in both alpha (i.e., within-stream) and gamma (i.e., park-wide) aquatic invertebrate diversity, and possibly local increases in primary and secondary production.

It is also possible that more moderate thermal regimes and stable base flows were responsible for, rather than a consequence of, the occurrence of hemlock. Although we attempted to account for the effects of landscape determinants in the sampling design, there may have been variables that were not correlated with those that we used to stratify our sampling that were important determinants of both hemlock occurrence and aquatic invertebrate assemblage structure. In

© 2002 NRC Canada

Fig. 4. Mean differences in (*a*) median daily temperature and (*b*) mean diel temperature range between hemlock–hardwood site-pairs. Data were pooled across stream types except for midslope site-pairs, which were not included because they showed a substantially different pattern (see text). Data from the hardwood site of each site-pair was subtracted from its corresponding hemlock site, so values greater than zero indicate that hemlock was (*a*) warmer and (*b*) more variable. Each data point represents the mean difference between six pairs of temperature loggers for a day.

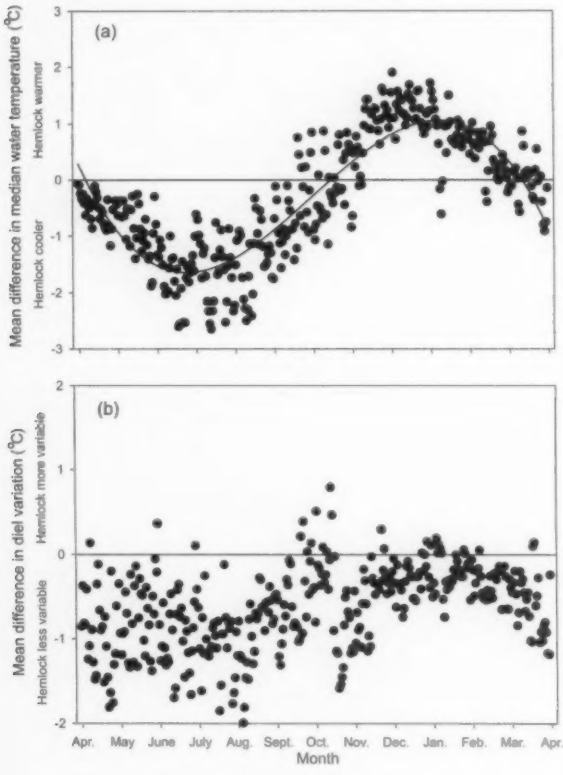

Fig. 5. Comparison of the distributions of (*a*) summer (July–September) maximum temperatures and (*b*) winter (October–February) minimum temperatures between streams draining hemlock and mixed hardwood forests. Solid lines depict hemlock data and broken lines depict hardwood data. Vertical lines represent arbitrary thresholds at 20°C and 0°C for comparisons. Data from temperature loggers placed at midslope sites were excluded because they showed different patterns than other stream types (see text).

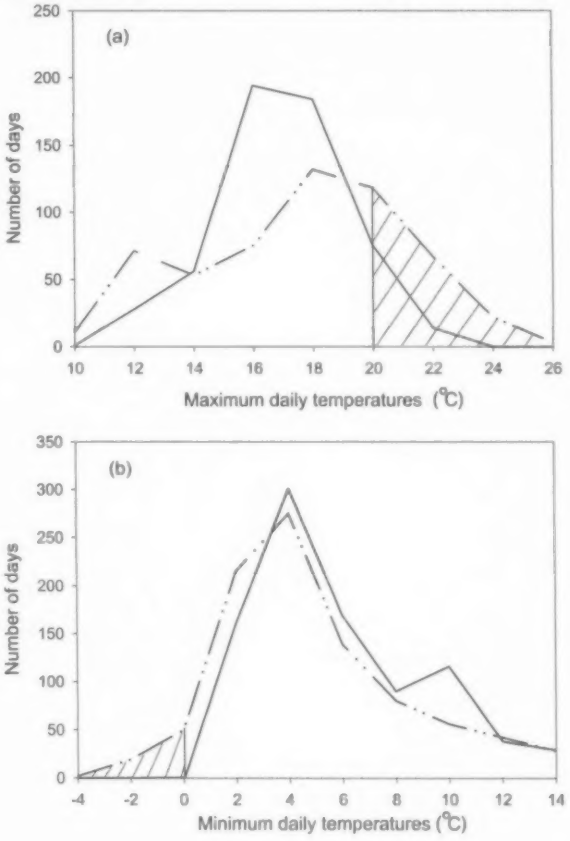

particular, forest-type differences in the proportion of stream flow made up by groundwater could also explain the data. Streams with greater groundwater contributions often have attenuated thermal regimes and are less likely to dry up during droughts (Gordon et al. 1992). In turn, such systems may provide the cool, moist conditions conducive to hemlock growth as well as support more invertebrate species. In this case, hemlock woolly adelgid induced hemlock decline may have little effect on stream communities in the long term.

However, there is evidence to support the argument that hemlock is at least partially responsible for observed patterns in stream habitat and benthic community structure. For example, it has been shown that the deep shade provided by the dense canopy of hemlock stands produces a cooler, damper microclimate in the forest understory relative to other conifer and deciduous forests (Rogers 1978; Hadley 2000). Such conditions could potentially buffer summer stream temperature increases and reduce evaporation rates. In addition, Blair et al. (1994) showed that soils in hemlock forests have a greater moisture-holding capacity than those in mixed hardwood forests, which could result in a more gradual and stable runoff of surface water and more consistent recharge of groundwater aquifers during summer droughts. Finally, many of the mixed hardwood stands in this study were probably once dominated by hemlock that was cleared earlier in the century and replaced by mixed hardwood (Sullivan et al. 1998). This was especially evident in the hardwood ravines where old hemlock stumps and logs were ubiquitous. One would expect that these hardwood stands that were formerly hemlock would have similar groundwater inputs. Therefore, if groundwater sources play a role, then hemlock forests probably influence groundwater contributions in some way.

Thus, there appears to be a strong likelihood that replacement of hemlock stands in DEWA with mature mixed hard-

© 2002 NRC Canada

Fig. 6. Probability of streams becoming dry or mostly dry as a function of discharge of the previous spring and forest type. Actual data represented by symbols were computed by putting spring discharges into four bins or ranges (centered around 3, 17, 90, and 472 $L \cdot s^{-1}$) and plotting the proportion of sites of each forest type that became dry or mostly dry in each discharge range. We used logistic regression to derive predicted probabilities from the data (represented by lines). Solid line depicts hemlock and broken line depicts hardwood sites.

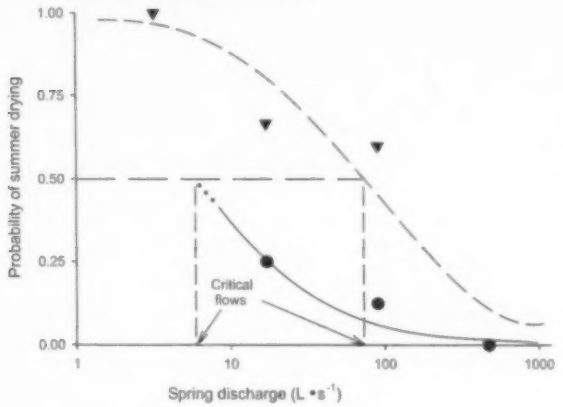

wood stands will have long-term impacts on aquatic communities similar in magnitude to those that have been noted for terrestrial assemblages. Moreover, if hemlock is indeed the ultimate cause of observed patterns in stream habitat and benthic community structure, then predicted changes in the habitat and biological structure of these headwater ecosystems may have a significant influence on other aquatic assemblages throughout the drainage basin. For example, warmer summer temperatures may decrease the abundance and limit the distribution of brook trout (*Salvelinus fontinalis*), an important game species in the Park (Evans 1995). Brook trout spawning is restricted to water of ≤15°C, and adults rarely occur in streams where summer temperatures exceed 20°C (Jenkins and Burkhead 1993). Also, reductions in thermal and hydrologic stability in tributaries could affect the survival and productivity of Delaware River mainstem fishes, such as trout and shad, that may be limited by the relative severity of summer, base-flow conditions. Stable discharges of cooler water from hemlock-dominated sub-basins may provide refugia during these summer extremes.

Acknowledgments

We thank R. Evans, E. Johnson, A. Ambler, K. High, and J. Schreiner of the Delaware Water Gap National Recreation Area for providing digital maps and logistical support for fieldwork. Comments provided by E. Pendleton, E. Benfield, R. Evans, D. Morton, and Z. Johnson were valuable in improving the manuscript. Funding for the research was obtained through the National Park Service's Natural Resources Preservation Program (NRPP).

References

Agresti, A. 1990. Categorical data analysis. John Wiley and Sons, New York.

Anderson, N.H., and Sedell, J.R. 1979. Detritus processing by macroinvertebrates in stream ecosystems. Annu. Rev. Entomol. **24**: 351–377.

Blair, J.M., Parmelee, R.W., and Wyman, R.L. 1994. A comparison of the forest floor invertebrate communities of four forest types in the northeastern U.S. Pedobiologia, **38**: 146–160.

Bosakowski, T., Smith, D.G., and Speiser, R. 1992. Nest sites and habitat selected by Cooper's hawks, *Accipiter cooperii*, in northern New Jersey and southeastern New York. Can. Field-Nat. **106**: 474–479.

Boucherle, M.M., Smol, J.T., Oliver, T.C., Brown, S.R., and McNeely, R. 1985. Limnologic consequences of the decline in hemlock 4800 years ago in three southern Ontario lakes. Paleolimnology, **143**: 217–225.

Bowen, K.L., Kaushik, N.K., Gordon, A.M., Mallory, E., Ridgeway, M., Bachmann, R.W., Jones, J.R., Peters, R.H., and Soballe, D.M. 1995. Invertebrate colonization of coarse woody debris in the littoral zone of two oligotrophic lakes. Lake Reservoir Manag. **11**: 119–120.

Brower, J.E., and Zar, J.H. 1984. Field and laboratory methods for general ecology. 2nd ed. William C. Brown Publishers, Dubuque, Iowa.

Cade, B.S., and Richards, J.D. 2000. User manual for BLOSSOM statistical software. Midcontinent Ecological Research Center, United States Geological Survey, 4512 McMurray Avenue, Fort Collins, CO 80525-3400, U.S.A.

Connell, J.H. 1978. Diversity in tropical rain forests and coral reefs. Science (Washington, D.C.), **199**: 1302–1310.

Cuffney, T.F., Wallace, J.B., and Lugthart, G.J. 1990. Experimental evidence quantifying the role of benthic invertebrates in organic matter dynamics of headwater streams. Freshwater Biol. **23**: 281–299.

Death, R.G., and Winterbourn, M.J. 1995. Diversity patterns in stream benthic invertebrate communities: the influence of habitat stability. Ecology, **76**: 1446–1460.

Dolloff, C.A., Hankin, D.G., and Reeves, G.H. 1993. Basinwide estimation of habitat and fish populations in streams. U.S. Department of Agriculture, Forest Service, Southeastern Forest Experimental Station, Ashville, NC 28804. General Technical Report SE-83.

Duffield, R.M., and Nelson, C.H. 1990. Seasonal emergence patterns and diversity of Plecoptera on Big Hunting Creek, Maryland, with a checklist of the stoneflies of Maryland. Proc. Entomol. Soc. Wash. **92**: 120–126.

Evans, R.A. 1995. Hemlock ravines at Delaware Water Gap National Recreation Area: highly valued, distinctive and threatened ecosystems. *In* Delaware Water Gap National Recreation Area 30th Anniversary symposium. Available from Richard Evans, National Park Service, Delaware Water Gap National Recreation Area, 294 Old Milford Rd., Milford, PA 18337.

Foster, D.R., Motzkin, G., and Slater, B. 1998. Land-use history as long-term broad-scale disturbance: regional forest dynamics in central New England. Ecosystems, **1**: 96–119.

Fuller, J.L. 1998. Ecological impact of the mid-Holocene hemlock decline in southern Ontario, Canada. Ecology, **79**: 2237–2351.

Gordon, N.D., McMahon, T.A., and Finlayson, B.L. 1992. Stream hydrology: an introduction for ecologists. John Wiley and Sons Ltd, West Sussex, England.

Gregory, K.J. 1992. Vegetation and river channel process interactions. *In* River conservation and management. *Edited by* P.J.

© 2002 NRC Canada

Boon, P. Calow, and G.E. Petts. John Wiley and Sons Limited, West Sussex, England. pp. 255–269.

Griesemer, S.J., Fuller, T.K., and Degraaf, R.M. 1998. Habitat use by porcupines (*Erethizon dorsatum*) in central Massachusetts: effects of topography and forest composition. Am. Midl. Nat. **140**: 271–279.

Hadley, J.L. 2000. Understory microclimate and photosynthestic response of saplings in an old-growth eastern hemlock (*Tsuga canadensis* L.) forest. Ecoscience, **7**: 66–72.

Hill, W.R., and Knight, A.W. 1988. Nutrient and light limitation of algae in two northern California streams. J. Phycol. **24**: 125–132.

Huston, M. 1979. A general hypothesis of species diversity. Am. Nat. **113**: 81–101.

Jackson, J.K., and Fisher, S.G. 1986. Secondary production, emergence, and export of aquatic insects of a Sonoran Desert stream. Ecology, **67**: 629–638.

Jenkins, R.E., and Burkhead, N.M. 1993. Freshwater fishes of Virginia. American Fisheries Society, Bethesda, Maryland.

Kamler, E. 1965. Thermal conditions in mountain waters and their influence on the distribution of Plecoptera and Ephemeroptera larvae. Ekol. Pol. Ser. A, **13**: 377–414.

Lake, P.S., and Boulton, A.J. 1990. Ecology of two intermittent streams in Victoria, Australia. I. Multivariate analyses of physicochemical features. Freshwater Biol. **24**: 123–141.

Lamberti, G.A., and Steinman, A.D. 1997. A comparison of primary production in stream ecosystems. *In* Stream organic matter budgets. *Edited by* J.R. Webster and J.L. Meyer. J. North Am. Benthol. Soc. **16**: 3–16.

Likens, G.E., Bormann, F.H., Johnson, N.M., Fisher, D.W., and Pierce, R.S. 1970. The effects of forest cutting and herbicide treatment on nutrient budgets in the Hubbard Brook watershed-ecosystem. Ecol. Monogr. **40**: 23–47.

Maloney, D.C., and Lamberti, G.A. 1995. Rapid decomposition of summer-input leaves in a northern Michigan stream. Am. Midl. Nat. **133**: 184–195.

Manly, F.J. 1991. Randomization and Monte Carlo methods in biology. Chapman and Hall Publishers, New York.

Masteller, E.C. 1993. Comparison of tropical and temperate emergence phenology of aquatic insects from Puerto Rico and Pennsylvania. J. Kans. Entomol. Soc. **66**:192–199.

McClure, M.S. 1991. Density-dependent feedback and population cycles in *Adelges tsugae* (Homoptera: Adelgidae) on *Tsuga canadensis*. Environ. Entomol. **20**: 258–264.

McLachlan, J.S., Foster, D.R., and Menalled, F. 2000. Anthropogenic ties to late-successional structure and composition in four New England hemlock stands. Ecology, **81**: 717–733.

Mehta, C., and Patel, N. 1996. LogXact for Windows. User manual. Cytel Software Corporation, Cambridge, Mass., U.S.A.

Merritt, R.W., and Cummins, K.W. 1996. An introduction to the aquatic insects of North America. Kendall/Hunt Publishing Company, Dubuque, Iowa.

Miller, M.C., and Stout, J.R. 1989. Variability of macroinvertebrate community composition in an Arctic and Subarctic stream. Hydrobiologia, **172**: 111–127.

Minshall, G.W. 1978. Autotrophy in stream ecosystems. BioScience, **28**: 767–771.

Minshall, G.W. 1984. Aquatic insect–substratum relationships. *In* The ecology of aquatic insects. *Edited by* V.H. Resh and D.M. Rosenberg. Praeger Publishers, New York. pp. 358–400.

Mitchell, J.M. 1999. Habitat relationships of five northern bird species breeding in hemlock ravines in Ohio, U.S.A. Nat. Areas J. **19**: 3–11.

Molles, M.C. 1982. Trichopteran communities of streams associated with aspen and conifer forests: long-term structural change. Ecology, **63**: 1–6.

Myers, W.L., and Irish, R.R. 1981. Vegetation survey of Delaware Water Gap National Recreation Area. Final Report, U.S. Department of the Interior, National Park Service, Mid-Atlantic Region. Available from Richard Evans, National Park Service, Delaware Water Gap National Recreation Area, 294 Old Milford Rd., Milford, PA 18337.

Naiman, R.J., Décamps, H., Pastor, J., and Johnston, C.A. 1988. The potential importance of boundaries to fluvial ecosystems. J. North. Am. Benthol. Soc. **7**: 289–306.

Newbury, R.W. 1984. Hydrologic determinants of aquatic insect habitats. *In* The ecology of aquatic insects. *Edited by* V.H. Resh and D.M. Rosenberg. Praeger Publishers, New York. pp. 323–357.

Orwig, D.A., and Foster, D.R. 1998. Forest response to the introduced hemlock woolly adelgid in southern New England, U.S.A. J. Torrey Bot. Soc. **125**: 60–73.

Orwig, D.A., and Foster, D.R. 1999. Stand, landscape, and ecosystem analyses of hemlock woolly adelgid outbreaks in southern New England: an overview. *In* Proceedings: Symposium on Sustainable Management of Hemlock Ecosystems in Eastern North America. *Edited by* D.A. McManus, D.S. Shields, and D.R. Souto. U.S. Department of Agriculture, Forest Service, Newton Square, Pa. pp. 123–125.

Plafkin, J.L., Barbour, M.T., Porter, K.D., Gross, S.K., and Hughes, R.M. 1989. Rapid bioassessment protocols for use in streams and rivers: benthic macroinvertebrates and fish. United States Environmental Protection Agency, Washington, DC 20460. EPA/444/4-89-001.

Power, M.E., Stout, R.J., Cushing, C.E., Harper, P.P., Hauer, F.R., Matthews, W.J., Moyle, P.B., Statzner, B., and Wais De Badgen, I.R. 1988. Biotic and abiotic controls in river and stream communities. J. North Am. Benthol. Soc. **7**: 456–479.

Reay, R.S., Blodgett, D.W., Burns, B.S., Weber, S.J., and Frey, T. 1990. Management guide for deer wintering areas in Vermont. Department of Forests, Parks and Recreation and Department of Fish and Wildlife, Montpelier, Vermont.

Resh, V.H., Brown, A.V., Covich, A.P., Gurtz, M.E., Li, H.W., Minshall, G.W., Reice, S.R., Sheldon, A.L., Wallace, J.B., and Wissmar, R.C. 1988. The role of disturbance in stream ecology. J. North Am. Benthol. Soc. **7**: 433–455.

Rogers, R.S. 1978. Forests dominated by hemlock (*Tsuga canadensis*): distribution as related to site and postsettlement history. Can. J. Bot. **56**: 843–854.

Ross, H.H. 1963. Stream communities and terrestrial biomes. Arch. Hydrobiol. **59**: 235–242.

Sahade, R., Tatian, M., Kowalke, J., Kuehne, S., and Esnal, G.B. 1998. Benthic faunal associations on soft substrates at Potter Cove, King George Island, Antarctica. Polar Biol. **19**: 85–91.

Singh, M.P., Smith, S.M., and Harrison, A.D. 1984. Emergence of some caddisflies (Trichoptera) from a wooded stream in southern Ontario. Hydrobiologia, **112**: 223–232.

Smock, L.A., and MacGregor, C.M. 1988. Impact of the American chestnut blight on aquatic shredding macroinvertebrates. J. North Am. Benthol. Soc. **7**: 212–221.

Sousa, W.P. 1984. The role of disturbance in natural communities. Annu. Rev. Ecol. Syst. **15**: 353–392.

Speiser, R., and Bosakowski, T. 1987. Nest site selection by northern goshawks in northern New Jersey and southeastern New York. Condor, **89**: 387–394.

Stout, B.M., III, Benfield, E.F., and Webster, J.R. 1992. Effects of forest disturbance on shredder production in southern Appalachian headwater streams. Freshwater Biol. **29**: 59–69.

Strahler, A.N. 1964. Quantitative geomorphology of drainage bas-

© 2002 NRC Canada

ins and channel networks. *In* Handbook of applied hydrology. *Edited by* Ven te Cow. McGraw-Hill, New York. pp. 16–33.

Sullivan, K., Black, B., Mahan, C., Abrams, M., Kim, K.C., and Yahner, R. 1998. Overstory tree composition of hemlock and hardwood stands in Delaware Water Gap National Recreation Area. Center for Biodiversity Research, Environmental Resources Research Institute, Pennsylvania State University, University Park, PA 16802, U.S.A.

Wallace, J.B. 1996. Habitat, life history, and behavioral adaptations of aquatic insects. *In* Aquatic insects of North America. *Edited by* R.W. Merritt and K.W. Cummins. Kendall/Hunt Publishing, Dubuque, Iowa. pp. 41–73.

Wallace, J.B., and Gurtz, M.E. 1986. Response of *Baetis* mayflies (Ephemeroptera) to catchment logging. Am. Midl. Nat. **115**: 25–41.

Wallace, J.B., Eggert, S.L., Meyer, J.L., and Webster, J.R. 1999. Effects of resource limitation on a detrital-based ecosystem. Ecol. Monogr. **69**: 409–442.

Ward, J.V., and Stanford, J.A. 1982. Thermal responses in the evolutionary ecology of aquatic insects. Annu. Rev. Entomol. **27**: 97–117.

Webster, J.R., and Benfield, E.F. 1986. Vascular plant breakdown in freshwater ecosystems. Annu. Rev. Ecol. Syst. **17**: 567–594.

Webster, J.R., Golladay, S.W., Benfield, E.F., Meyer, J.L., Swank, W.T., and Wallace, J.B. 1992. Catchment disturbance and stream response: an overview of stream research at Coweeta Hydrologic laboratory. *In* River conservation and management. *Edited by* P.J. Boon, P. Calow, and G.E. Petts. John Wiley and Sons Limited, West Sussex, England. pp. 231–253.

Wellnitz, T.A., Radar, R.B., and Ward, J.V. 1996. Importance of light and nutrients in structuring an algal community in a Rocky Mountain stream. J. Freshwater Ecol. **11**: 399–413.

Wilkinson, L. 1998. SYSTAT 8.0 Statistics (user manual). SPSS, Inc., Chicago, Illinois.

Yamasake, M., DeGraaf, R.M., and Lanier, J.W. 1999. Birds, smaller mammals, and forest carnivores. *In* Proceedings: Symposium on Sustainable Management of Hemlock Ecosystems in Eastern North America. *Edited by* D.A. McManus, D.S. Shields, and D.R. Souto. U.S. Department of Agriculture, Forest Service, Newton Square, Pa. pp. 135–143.

Young, J.A., Smith, D.R., Snyder, C.D., and Lemarié, D.P. 2002. A terrain-based paired-site sampling design to assess biodiversity losses from eastern hemlock decline. Environ. Monit. Assess. In press.

Yount, J.D., and Niemi, G.J. 1990. Recovery of lotic communities and ecosystems from disturbance—a narrative review of case studies. Environ. Manag. **14**: 547–569.

Zimmerman, G.M., Goetz, H., and Mielke, P.W., Jr. 1985. Use of an improved statistical method for group comparisons to study effects of prairie fire. Ecology, **66**: 606–611.

© 2002 NRC Canada

Tributary-specific variation in timing of return of adult Atlantic salmon (*Salmo salar*) to fresh water has a genetic component

David C. Stewart, Gordon W. Smith, and Alan F. Youngson

Abstract: Variation in the timing of return of adult Atlantic salmon (*Salmo salar*) to rivers contributes diversity to salmon fisheries and is therefore an important effect on their economic value. In this paper, we test two sequential null hypotheses: (*i*) that run timing does not vary among populations from different tributaries and (*ii*) that differences in time of return between populations from different tributaries are not evident following transfer to a common location. Adult fish originating from two tributaries of the River Tay, the Almond and Tummel, were caught in local fisheries on different dates. For both tributaries, run timing in two-sea-winter (2SW) fish was earlier than for one-sea-winter (1SW) fish. Within both sea-age classes, recaptures of Tummel fish preceded those from the Almond. After the progeny of Almond and Tummel fish were transferred to a third tributary of the River Tay, the Braan, differences in run timing between the tributary groups were identified for both sea-age classes. The differences were highly consistent with those present in fish that had reared in their native tributaries, indicating a strong heritable component for the run timing trait. Tributary-specific differences in run timing have important implications for the management of seasonally complex fisheries.

Résumé : Les variations dans le calendrier de retour des saumons de l'Atlantique (*Salmo salar*) à la rivière apportent de la diversité dans les pêches de saumons et affectent de façon importante leur valeur économique. Nous éprouvons ici, l'une après l'autre, deux hypothèses nulles: (*i*) le calendrier des retours ne varie pas d'une population à une autre dans les différents tributaires et (*ii*) les variations du moment du retour chez les populations des différents tributaires disparaissent après un transfert dans une localité commune. Des poissons adultes provenant de deux tributaires de la Tay, l'Almond et la Tummel, ont été capturés à des dates différentes dans une même pêche commerciale locale. Dans les deux tributaires, la montaison était plus hâtive chez les poissons ayant passé deux hivers en mer (2SW) que chez ceux qui n'en avaient passé qu'un seul (1SW). Dans chacune de ces classes, la capture des poissons de la Tummel précédait celle de ceux de l'Almond. Après que la progéniture de poissons de l'Almond et de la Tummel eut été transférée dans un troisième tributaire de la Tay, la Braan, des différences dans le moment de la montaison ont continué d'être observées dans les deux classes. Ces différences sont très semblables à celles qui prévalent chez les poissons élevés dans leur habitat naturel, ce qui indique qu'il y a une composante héréditaire importante dans le caractère qui régit la montaison. L'existence de calendriers de montaison différents selon les tributaires a des conséquences importantes sur la gestion de pêches à structure saisonnière complexe.

[Traduit par la Rédaction]

Introduction

The homing of salmonids (Stabell 1984) results in spawning taking place close to the locations that the same fish inhabited as juveniles. Homing is potentially precise and is reportedly within several kilometres for a substantial proportion of spawners in the cases of both Atlantic salmon (*Salmo salar*) (Youngson et al. 1994) and sockeye salmon (*Oncorhynchus nerka*) (Quinn et al. 1999). For Atlantic salmon, dispersal of fry after hatching is local in extent (Gustafson-Greenwood and Moring 1990; Crisp 1995; Raddum and Fjellheim 1995), and as parr, many Atlantic salmon hold fixed territories over long periods of time (Juanes et al. 2000). Juvenile fish imprint to these locations and home to them as adults (Dittman and Quinn 1994). This spatial, behavioural structuring restricts rates of genetic exchange among locations, and consequently, genetic population structuring in Atlantic salmon can be demonstrated down to subcatchment scales (Garant et al. 2000).

Typically, genetic population structuring is demonstrated on the basis of allele frequency differences in assumed adaptively neutral loci. However, the reproductive isolation of populations exploiting disparate environmental locations is expected also to foster the development of adaptive genetic differentiation. For example, environmental temperature is a strong determinant of growth and development and probably, therefore, of fitness. Local temperature regimes often vary grossly and predictably at subcatchment scales, particularly for rivers that cover a large altitudinal range. Explicitly genetic evidence indicates that for Atlantic salmon, allele frequency variation at the *MEP-2** locus is sensitive to envi-

Received 10 July 2001. Accepted 24 January 2002. Published on the NRC Research Press Web site at http://cjfas.nrc.ca on 28 February 2002.
J16437

D.C. Stewart,[1] G.W. Smith, and A.F. Youngson. FRS Freshwater Laboratory, Pitlochry, Perthshire, U.K.

[1]Corresponding author (e-mail: d.c.stewart@marlab.ac.uk).

 DOI: 10.1139/F02-011 © 2002 NRC Canada

ronmental temperature regimes (Verspoor and Jordan 1989). Populations, including those within single catchments, are differentiated with respect to *MEP-2** variation, showing patterns that indicate a response to temperature through natural selection (Verspoor et al. 1991).

These findings alone argue for the adoption of management policies targeted at the genetic population level. This approach underpins current management of the Pacific salmonids (see, e.g., NRC 1996) but is not yet a major feature of Atlantic salmon management. The case for altering management policy to accommodate population-based concepts will be greatly strengthened by the demonstration of a genetic basis for economically relevant phenotypic traits that vary spatially. In this context, run timing (defined as the time of return of adults to rivers from the sea) is a candidate for investigation. Run timing varies within river catchments and has been shown to correlate with the spatial distribution of salmon at spawning time in the Northwest Miramichi catchment in New Brunswick (Saunders 1967) and in a number of Scottish rivers (Laughton and Smith 1992; Walker and Walker 1992; Webb and Campbell 2000). These relationships have important implications for fisheries management because they link temporal aspects of exploitation with the spatial distribution of adults within catchments at spawning time.

Hansen and Jonsson (1991) demonstrated that run timing is a heritable trait in Atlantic salmon that varies between rivers. However, they were unable to demonstrate within-catchment variation, and to address this point, the present study examines run timing data derived from a series of mark–recapture experiments carried out in the River Tay in Scotland. We first describe the run timing characteristics of wild adult salmon previously tagged as juveniles in either of two tributaries within the Tay catchment. Secondly, we test whether the progeny of spawners obtained from the same tributaries show differences in run timing after transfer to a third, intermediate tributary not accessible to spawning salmon.

Materials and methods

This study was conducted on three tributaries of the River Tay: rivers Almond, Tummel, and Braan (Fig. 1). The Almond joins the Tay in its lower reaches, a short distance above the upper tidal limit. The sampled section of the Tummel is located in the upper reaches of the catchment about 75 km from the sea. The confluence of the Braan with the Tay is in an intermediate position about 40 km from the sea, and a waterfall near its junction with the main river forms a total barrier to the upstream passage of adult salmon.

Salmon smolts that had originated from natural spawning were trapped and Carlin-tagged at sites on the lower reaches of the rivers Almond and Tummel (Fig. 1) from 1968 to 1973 (Table 1). Each year, traps were operated to coincide with the main smolt run, which was generally from early March to late May. Individual smolt age was determined in a 20% sample of captured migrants by scale reading. Although smolts were aged from 1 to 5 years, at both sites most migrants (95% on the Almond and 99% on the Tummel) were either 2 or 3 years old.

In September 1988, brood stock was trapped in the Tummel from the later part of the annual run. In the Almond, brood stock at the point of spawning was electrofished below a partial obstruction in early November in 1989 and 1992 (Table 2). For both tributaries, females were crossed with each of two males drawn randomly from the sampled adults. Ova were incubated at a central facility within the Tay catchment. Fry, parr, or smolts were stocked out in the lower 10 km of the Braan catchment, above the waterfall. Parr and smolts were tank-reared and microtagged before transfer; stocked fry were microtagged later as large juveniles, after capture by electrofishing or capture in a temporary smolt trap (Table 3). Stocked fish emigrated as smolts mainly at age 2. The smolt ages of recaptured adults were determined by tag year and confirmed when necessary by scale reading. When all recaptures (excluding those fish stocked near smolting) were considered, 88 of 90 fish sourced from the Almond and 27 of 28 Tummel fish were age 2 at smolt emigration; the others were age 3.

The date of capture of tagged adults in estuary and coastal net fisheries was treated as a measure of their run timing. Reports of tagged adult fish were compiled from commercial nets operating in the Northeast England drift-net fishery, in eastern Scottish coastal waters, and in the estuary of the River Tay. For both the Tummel and Almond groups, most reports each year were from the Tay and all captures were made within 300 km of the estuary. Date of capture was recorded as standard week. In the earlier part of this study, the Tay fishery operated over the whole of the legal netting season (i.e., weeks 5–6 to 33–34). In later years, the fishery operated only between weeks 9 and 33, and effort was relatively low before May (i.e., about week 17). These changes in fishing effort are expected to have resulted in relatively greater truncation of the leading edge of recapture patterns for later years. The Tay fishery ceased operation after 1996 and therefore did not exploit two-sea-winter (2SW) fish derived from stocking the Braan with fry originating from the Almond brood stock of 1992.

Sample sizes of recaptured adults were relatively low and derived from populations in which variances were unknown. Consideration of the distributions also suggested that many were nonnormal (Fig. 2). For these reasons, nonparametric methods are used throughout the analysis of run timing data.

Results

Run timing of native Almond and Tummel fish

Effect of location of capture on run timing

Data obtained from coastal nets and estuary nets were compared to test whether capture location was a perceived effect on run timing. Data were split by sea-age class, tributary of origin, and year of capture. Of the 14 data sets generated, only two showed significant differences (Mann–Whitney U test: Almond, 1SW, 1968, $P = 0.045$; Almond, 1SW, 1972, $P = 0.048$). Combining the data across years indicated no significant differences between the fisheries (Mann–Whitney U test: Almond, 1SW, $P = 0.920$; Almond, 2SW, $P = 0.786$; Tummel, 1SW, $P = 0.910$; Tummel, 2SW, $P = 0.094$). On the basis of these comparisons, data obtained

© 2002 NRC Canada

Fig. 1. Map of the River Tay catchment showing the tributaries mentioned in the text. The locations of smolt trapping and brood stock capture sites are indicated, as is the main site of recapture of adults returning to the river.

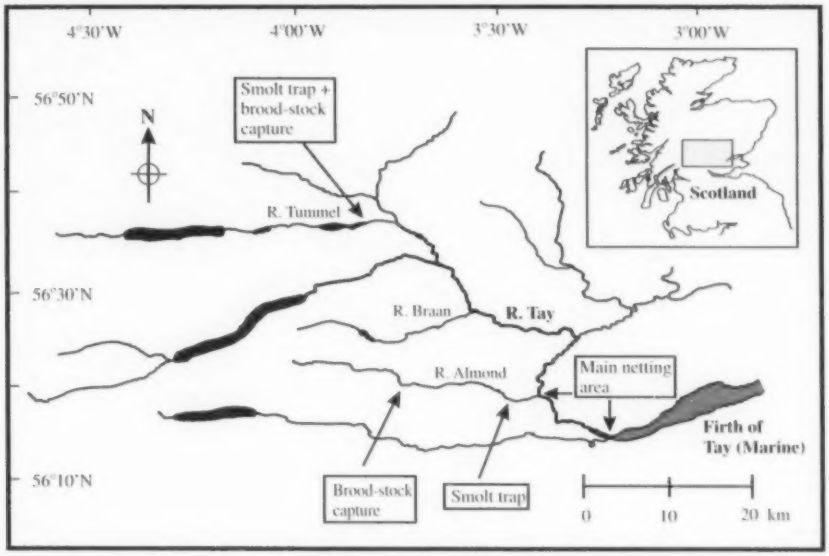

Table 1. Number of native smolts tagged leaving the rivers Almond and Tummel (1968 to 1973) and numbers of returning adults reported caught in local fisheries.

	Smolts tagged		Adults captured	
Source	Year	Number	1SW	2SW
Almond	1968	2779	12	4
	1969	2000	59	2
	1970	6779	161	21
	1971	2768	124	9
	1972	1967	82	3
	1973	2609	78	9
Tummel	1968	2017	0	1
	1969	2350	3	4
	1970	3464	13	12
	1971	1494	6	20
	1972	2656	12	18
	1973	1908	3	13

Note: 1SW and 2SW, one- and two-sea-winters, respectively.

from the coastal and estuary nets were combined for further analysis.

Variation in run timing with year

The distribution of capture dates varied significantly among years for 1SW salmon from the Almond (Kruskal–Wallis test: Almond, 1SW, $N = 516$, $H = 31.664$, $P < 0.001$). Because a year effect on capture date was indicated, further analysis was based on data sets paired by year when possible.

Comparison of run timing between tributaries

For each year, median capture week was used to characterize the run timing of each sea-age class for both Almond and Tummel fish. Comparisons were made between tributaries and sea-age classes by pairing data according to year of capture. For both Almond and Tummel fish, return times differed between 1SW and 2SW salmon (Wilcoxon paired-sample test: Almond, $N = 5$, $Z = 2.032$, $P = 0.042$; Tummel, $N = 5$, $Z = 2.032$, $P = 0.042$). For both tributaries, 2SW fish returned earlier than 1SW fish (Fig. 2*a*). For both sea-age classes, capture dates differed significantly between tributaries (Wilcoxon paired-sample test: 1SW, $N = 5$, $Z = 2.041$, $P = 0.041$; 2SW, $N = 5$, $Z = 2.032$, $P = 0.042$). For both sea-age classes, Tummel fish returned earlier than Almond fish (Fig. 2*a*).

Table 2. Numbers and sea-age of Almond and Tummel brood fish obtained to generate progeny for transfer to the Braan.

		Females		Males	
Source	Year	1SW	2SW	1SW	2SW
Tummel	1988	0	10	8	2
Almond	1989	59	6	30	1
	1992	20	0	15	0

Note: 1SW and 2SW, one- and two-sea-winters, respectively.

Run timing of Almond and Tummel fish transferred to the Braan

The effect of stocking practice

Because some of the potential comparisons did not yield 2SW returns (Table 3), analysis was restricted to the 1SW class. Median date of return was not significantly associated with stage at tagging (Mann–Whitney *U* test: $N = 78$, $U = 392$, $P = 0.460$), with stage of stocking (Kruskal–Wallis one-way analysis of variance: $N = 105$, $H = 1.512$, $P = 0.470$) or with brood stock year (Mann–Whitney *U* test: $N = 112$, $U = 229.0$, $P = 0.091$). On this basis, return dates for Almond fish were combined across all stocking stages and tagging treatments for the purposes of further analysis.

© 2002 NRC Canada

Table 3. Stocking and tagging of fish transferred to the Braan from the Almond and Tummel and the return of tagged adults to local fisheries.

Brood stock source	Stage stocked	Stage tagged (age in years)	Number tagged	Number of adults captured	
				1SW	2SW
Tummel, 1988	Fry	Parr (1)	2153	15	9
	Parr	Parr (1)	2180	2	2
Almond, 1989	Fry	Parr (1)	4270	64	5
	Fry	Smolt (2)	253	14	0
	Smolt	Smolt (1)	8500	14	2
	Smolt	Smolt (2)	3140	13	1
Almond, 1992	Fry	Parr (1)	1448	7	—

Note: 1SW and 2SW, one- and two-sea-winters, respectively.

Fig. 2. Box-and-whisker plots showing the recapture times of one-sea-winter (1SW) and 2SW Tummel (hatched box) and Almond (open box) fish: (*a*) native fish; (*b*) transferred fish. In each case, the box indicates median recapture time with 25% and 75% percentile range. The whiskers indicate the minimum and maximum of each range.

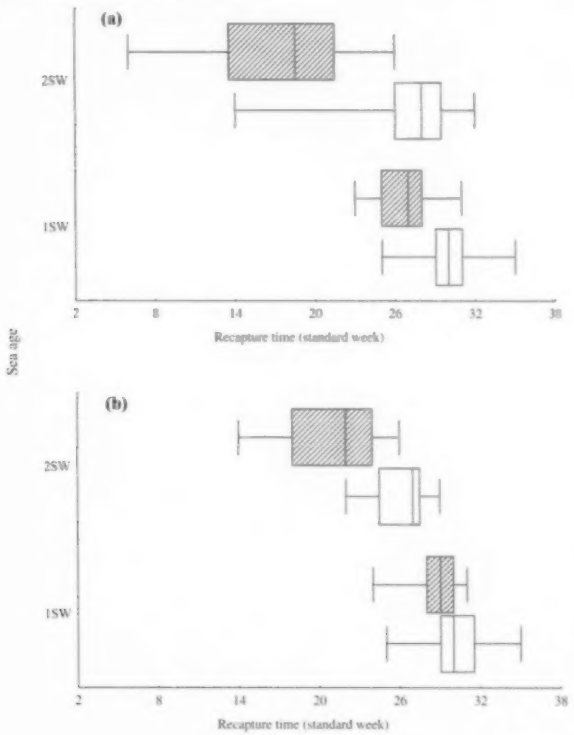

The effect of tributary of origin

For each sea-age class, the capture dates of Tummel fish were significantly different from those of Almond fish (Mann–Whitney *U* test: 1SW, $N = 129$, $U = 1332$, $P = 0.007$; 2SW, $N = 19$, $U = 77.5$, $P = 0.005$). As in the case of native fish, run timing was earlier for Tummel fish of both sea-age classes (Fig. 2*b*).

Comparison of run timing in native and transferred fish

In the case of Almond fish, run timings for both sea-age classes were not significantly different between native and transferred fish (Mann–Whitney *U* test: 1SW, $N = 628$, $U = 28086$, $P = 0.636$; 2SW, $N = 56$, $U = 120.5$, $P = 0.091$). In the case of Tummel fish, the ranges of weeks in which native and transferred fish were captured were similar (see Fig. 2) (1SW native, weeks 23–31, vs 1SW transferred, weeks 24–31; 2SW native, weeks 6–26, vs 2SW transferred, weeks 14–26). However, median return date differed significantly for both the 1SW and 2SW sea-age classes (Mann–Whitney *U* test: 1SW, $N = 54$, $U = 446.5$, $P = 0.013$; 2SW, $N = 79$, $U = 523.5$, $P = 0.034$).

Discussion

Run timing differed between native fish that had reared in the Almond tributary, closest to the sea, or in the Tummel, which is more distant from the sea. Within both sea-age groups, native Tummel fish passed through the fisheries earlier than native Almond fish. For both tributaries, the 2SW group preceded the 1SW group. The differences in run timing between tributary groups might be attributed to the effects of differences in juvenile stream rearing environment (e.g., temperature effects associated with altitude) on adult migratory timing. However, to sustain this case, it would be additionally necessary to hypothesize that younger sea-age constrains the timing of the migration of 1SW relative to 2SW fish such that the first 1SW fish reach the fisheries later than many of the 2SW fish. On this basis, the resulting scenario would envisage run timing within sea-age classes being determined by rearing environment, and spawning location being determined by river-entry date. Early-running 2SW fish would dominate spawning locations in upper catchment areas, and the spawning distribution of 1SW fish would be biased towards the lower reaches.

However, radio-tracking studies in Scottish rivers show that river-entry date is not a limiting factor in the distance subsequently traveled, because early-running fish within the 1SW group penetrated rivers further than 2SW fish entering at about the same time (Laughton and Smith 1992). Furthermore, studies of Atlantic salmon in a Scottish stream showed that homing was a substantial factor in the distribution of both 1SW and 2SW spawners at a subcatchment scale (Youngson et al. 1994). Accordingly, we tested the hy-

© 2002 NRC Canada

pothesis that run timing differences between tributaries are genetically determined. To do this, we compared the behaviour of the progeny of adults sampled from the Almond and Tummel after their transfer to a third, common location. For both sea-age classes, differences in adult run timing were demonstrated between the transferred groups. The differences were highly consistent with the behaviour of fish that reared in their native tributaries. Consequently, we conclude that the run timing variation observed within sea-age classes does have a genetic component.

An environmental effect on run timing may be indicated by interannual variation in one of four possible comparisons within sea-age classes. However, such effects are likely to be attributable, at least in part, to seasonal variations in the effort applied by the fisheries from which the data were generated. Fishing effort is not sufficiently documented to support the analysis but is known to have varied within and among years. This was particularly the case for the earlier months of the fishing season, when adverse seasonal conditions sometimes limited effort. In later years, early-season effort was further restricted owing to both economic and conservation considerations. However, any likely effects of variation in seasonal fishing effort are conservative for the general case we argue, because curtailment of the leading edge of the distribution of early-running fish will have tended to favour acceptance of the null hypothesis regarding the behaviour of transferred fish. More generally, our analysis shows that not only were differences in run timing between the populations maintained after transfer, but also relative run timings, and especially the ranges of weeks over which return took place, were consistent with the run timings of native fish. These observations suggest that the heritable component to run timing variation is substantial.

For the cases of transferred Tummel fish of both the 1SW and 2SW classes, median return timings were slightly delayed relative to timings for native fish, again suggesting an environmental effect. For the 2SW class in particular, this finding may be an artifact attributable to interannual variation in commercial fishing effort, as noted above. On the other hand, a similar effect was evident among the 1SW fish that tended to be captured in the main part of the commercial fishing season, when interannual variation in fishing effort was less likely. In this case, two further possibilities can be identified. First, the brood stock sampled from the Tummel to generate progeny for transfer may not have been entirely representative of the population. Secondly, run timing may have been determined in part by an effect of the rearing environment.

In the case of the oncorhynchids, high heritabilities are indicated for the timing of the adult return migration of both pink (*Oncorhynchus gorbuscha*) (Smoker et al. 1998) and chinook (*O. tshawytscha*) (Quinn et al. 2000) salmon. In the present study, formal heritability estimates cannot be derived, but the extent of the persistence of characteristic run timing differences in both transferred groups, and for both sea-age classes, also indicates high values. Smoker et al.'s (1998) study of pink salmon stresses within-site variation. In the present study, the differences are observed between, rather than within, sites or populations and cannot be plausibly accounted for by selection resulting from direct competition among spawners. It is possible that differences in run timing among tributaries reflect differing selective pressures acting on populations at the subcatchment level. Quinn et al. (2000) speculate that such mechanisms have acted on populations of chinook salmon in New Zealand rivers. Chinook are nonnative to New Zealand, and two populations that have developed from a single-source introduction from California about 100 years ago now show slight heritable differences in run timing. Presumably this is a result of the redistribution of within-group genetic variation derived from the original introduced fish. Quinn et al. (2000) hypothesize that temporal aspects of the spawning environment have effects on fitness and that these effects extend to include run timing, because spawning time and run timing are functionally linked.

This argument cannot be easily extended to cover the findings of the present study because of the time scales involved in river migration. In Scottish rivers, the peak spawning period for salmon extends from November to early December. The migration distance through freshwater to each of the tributaries examined in the present study is relatively short (<100 km). Natural passage is partially obstructed by two generating dams equipped with fish ladders only for those fish returning to the Tummel. The upper dam is less than 15 km short of the main spawning areas in the Tummel. Passage of 2SW fish through the upper dam typically starts in June and peaks in July. Passage of 1SW fish starts in June and typically peaks in August, still 2 or 3 months ahead of spawning time (D.C. Stewart, unpublished data). More generally, observed rates and capacity for upstream movement (Laughton and Smith 1992) suggest that salmon are potentially capable of completing river migration to spawning areas in rivers like the Almond or Tummel in days or weeks.

Yet, in spite of the absence of any obvious difficulty in getting access to their final locations, some 2SW fish originating from the Tummel allocated as long as 11 months, and some 1SW Almond fish allocated 5 months, for the journey through the river to spawn. Corresponding median values were about 6 and 4 months, respectively. Given that both Almond and Tummel fish allocate such long periods of time to make relatively short and undemanding journeys, any selection on run timing cannot be easily attributed to the geographical location of the tributaries themselves. More complex speculations are, of course, possible. However, if sea-age at maturity is also subject to selection, as is likely (Gjerde 1984), difficulties arise in reconciling any hypothesis regarding selection on run timing within sea-age classes with the continued viability within populations of both 1SW and 2SW maturity options. In particular, we find it impossible to construct a single-stage hypothesis regarding selection that will accommodate the observation that the differences in run timing between 2SW fish of the Tummel and Almond populations are approximately matched by those shown, within the Tummel population, by 1SW and 2SW fish.

The findings of our study are consistent with the principles established for Atlantic salmon by Hansen and Jonsson (1991) but extend the concept of heritable, interpopulation differences in run timing to a within-catchment scale. Irrespective of the mechanisms involved, run timing variation has important implications for the regulation of exploitation in relation to spawning escapement, especially in extended

© 2002 NRC Canada

and seasonally complex fisheries like those of Scotland (Shearer 1992). In particular, differential exploitation of seasonal groups is expected to generate spatial variation in the recruitment of spawners at subcatchment scales. Equally, spatial variation in juvenile production within catchments is expected to have an effect on the seasonal strength of the fisheries. It is therefore of great importance that consideration of subcatchment scales is incorporated into management theory and practice. These concepts are established for management in Pacific North America (e.g., NRC 1996), but their likely importance is not reflected in present approaches to the management of Atlantic salmon. Regulating exploitation or managing freshwater production only at catchment scales risks damage to subcatchment populations that contribute to the diversity of the resource and vary in their intrinsic susceptibility to capture in seasonally biased fisheries.

Acknowledgements

We wish to acknowledge the Tay District Salmon Fisheries Board for supporting this work and the efforts of netsmen in reporting tagged fish. We are also indebted to colleagues at the FRS Freshwater Laboratory for their help, in particular Gordon Struthers who supervised the tagging experiments. Bill Jordan of the Institute of Zoology, London, and two anonymous referees provided valued comments on versions of the document.

References

Crisp, D.T. 1995. Dispersal and growth rate of 0-group salmon (*Salmo salar* L.) from pointstocking together with some information from scatter-stocking. Ecol. Freshwater Fish, **4**: 1–8.

Dittman, A.H., and Quinn, T.P. 1994. Homing in Pacific salmon: mechanisms and ecological basis. J. Exp. Biol. **199**: 83–91.

Garant, D., Dodson, J.J., and Bernatchez, L. 2000. Ecological determinants and temporal stability of within-river population structure in Atlantic salmon (*Salmo salar* L.). Mol. Ecol. **9**: 615–628.

Gjerde, B. 1984. Response to individual selection for age at sexual maturity in Atlantic salmon. Aquaculture, **38**: 229–240.

Gustafson-Greenwood, K.I., and Moring, J.R. 1990. Territory size and distribution of newly emerged Atlantic salmon (*Salmo salar*). Hydrobiologia, **206**: 125–131.

Hansen, L.P., and Jonsson, B. 1991. Evidence of a genetic component in the seasonal return pattern of Atlantic salmon, *Salmo salar* L. J. Fish Biol. **38**: 251–258.

Juanes, J., Letcher, B.H., and Gries, G. 2000. Ecology of stream fish: insights gained from an individual-based approach to juvenile Atlantic salmon. Ecol. Freshwater Fish, **9**: 65–73.

Laughton, R., and Smith, G.W. 1992. The relationship between date of river entry and the estimated spawning positions of adult Atlantic salmon (*Salmo salar*) in two major Scottish east coast rivers. *In* Wildlife telemetry: remote monitoring and tracking of animals. *Edited by* I.E. Priede and S.M. Swift. Ellis Horwood Ltd, Chichester. pp. 423–433.

NRC (National Research Council). 1996. Upstream: salmon and society in the Pacific Northwest. National Academy Press, Washington, D.C.

Quinn, T.P., Volk, E.C., and Hendry, A.P. 1999. Natural otolith microstructure patterns reveal precise homing to natal incubation sites by sockeye salmon (*Oncorhynchus nerka*). Can. J. Zool. **77**: 766–775.

Quinn, T.P., Unwin, M.J., and Kinnison, M.T. 2000. Evolution of temporal isolation in the wild: genetic divergence in timing of migration and breeding by introduced chinook salmon populations. Evolution, **54**: 1372–1385.

Raddum, G.G., and Fjellheim, A. 1995. Artificial deposition of eggs of Atlantic salmon (*Salmo salar* L.) in a regulated Norwegian river: hatching, dispersal and growth of fry. Regul. Rivers, **10**: 169–180.

Saunders, R.L. 1967. Seasonal pattern of return of Atlantic salmon in the Northwest Miramichi River, New Brunswick. J. Fish. Res. Board Can. **24**: 21–32.

Shearer, W.M. 1992. The Atlantic salmon: natural history, exploitation and future management. Fishing News Books, Oxford.

Smoker, W.W., Gharret, A.J., and Steckoll, M.S. 1998. Genetic variation of return date in a population of pink salmon: a consequence of fluctuating environment and dispersive selection? Alaska Fish. Res. Bull. **5**: 46–54.

Stabell, O. 1984. Homing and olfaction in salmonids: a critical review with special reference to the Atlantic salmon. Biol. Rev. **59**: 333–388.

Verspoor, E., and Jordan, W.C. 1989. Genetic variation at the Me-2 locus in the Atlantic salmon within and between rivers: evidence for its selective maintenance. J. Fish Biol. **35**(Suppl. A): 205–213.

Verspoor, E., Fraser, N.H.C., and Youngson, A.F. 1991. Protein polymorphisms in the Atlantic salmon within a Scottish river: evidence for selection and estimates of gene flow between tributaries. Aquaculture, **98**: 217–230.

Walker, A.F., and Walker, A.M. 1992. The Little Gruinard Atlantic salmon (*Salmo salar* L) catch and release tracking study. *In* Wildlife telemetry: remote monitoring and tracking of animals. *Edited by* I.E. Priede and S.M. Swift. Ellis Horwood Ltd., Chicester. pp. 434–440.

Webb, J.H., and Campbell, R.N.B. 2000. Patterns of run timing in adult Atlantic salmon returning to Scottish rivers—some new perspectives and management implications. *In* Managing wild Atlantic salmon—new challenges—new techniques. *Edited by* F.G. Whoriskey, Jr., and K.F. Whelan. Atlantic Salmon Federation, St. Andrews, New Brunswick. pp. 100–138.

Youngson, A.F., Jordan, W.C., and Hay, D.W. 1994. Homing of adult Atlantic salmon (*Salmo salar* L.) to a tributary stream in a major river catchment. Aquaculture, **121**: 259–26.

© 2002 NRC Canada

Determination of relative survival of two stocked walleye populations and resident natural-origin fish by microsatellite DNA parentage assignment

William H. Eldridge, Marc D. Bacigalupi, Ira R. Adelman, Loren M. Miller, and Anne R. Kapuscinski

Abstract: Walleye (*Stizostedion vitreum*) from two northern Minnesota spawning stations (Pike River, Hudson Bay drainage, and Little Cutfoot Sioux Lake, Mississippi River drainage) simultaneously stocked as fry into five southern Minnesota lakes had different survival rates. One year after stocking, Pike River walleye were more abundant than their original proportion of 46.5% of the stocked fish, but by the end of their second summer, neither population had a clear survival advantage. In the three lakes where walleye were consistently sampled, natural-origin walleye that descended from previous stockings significantly increased in percent of all sampled walleye over the study ($P = 0.001$). The unmarked and untagged stocked fish ($N = 566$) were assigned to their source population by comparing their genotypes at nine microsatellite DNA loci to the known genotypes of the parent pairs crossed in a hatchery (parentage assignment). Fish not assigned to a parent pair were considered to be the product of natural reproduction ($N = 177$) by previously stocked fish. Simulations indicated that natural-origin walleye were sufficiently excluded from assignment to stocked fish parent pairs so as not to bias the comparison. Parentage assignment is a powerful population discrimination tool if genotypes are known for all parent pairs from all but one putative source.

Résumé : Des dorés (*Stizostedion vitreum*) provenant de deux stations de fraye du nord du Minnesota (la Pike dans le bassin versant de la baie de Hudson et le lac Little Cutfoot Sioux dans le bassin du Mississippi) et ayant servi à aveliner cinq lacs du sud du Minnesota ont eu des taux de survie différents. Un an après l'alevinage, les dorés provenant de la Pike représentaient plus que leur proportion d'origine de 46,5 % des poissons introduits; cependant, à la fin du second été, ni l'une ni l'autre des populations ne présentait de survie clairement supérieure. Dans les trois lacs où les dorés ont été échantillonné régulièrement, les dorés d'origine naturelle issus des alevinages antérieurs représentaient un pourcentage significativement de plus en plus élevé ($P = 0,001$) des dorés totaux au cours de l'étude. Les poissons sans marque ni étiquette ($N = 566$) ont été assignés à leur population d'origine par comparaison de leur génotype à neuf locus microsatellites de l'ADN à des génotypes connus des couples de parents croisés en pisciculture (assignation de filiation). Les poissons non assignés à un couple parental ($N = 177$) étaient considérés être le fruit de la reproduction naturelle de poissons alevinés antérieurement. Des simulations ont confirmé que suffisamment de dorés d'origine naturelle avaient été exclus de l'assignation à des couples parentaux de pisciculture pour ne pas fausser la comparaison. L'assignation de filiation est un outil puissant pour la reconnaissance des populations si on connaît les génotypes de tous les couples parentaux de toutes sauf une des sources possibles.

[Traduit par la Rédaction]

Introduction

Stocking fish originating from populations with superior performance is an effective fishery enhancement tool (Hudy and Berry 1983; Hume and Tsumura 1992; Younk and Strand 1992). The superior population in a given environment may grow faster, survive better, or reproduce more successfully, making it a more cost-effective stocking choice than fish from other sources. Although walleye (*Stizostedion vitreum*) have been stocked for over 120 years and are the subject of numerous stocking evaluations (Laarman 1978; Li et al. 1996*a*, 1996*b*), Terre et al. (1995) reported the only comparison of different walleye source populations in the field. A northern walleye population from Iowa grew faster than a southern population from Arkansas when simultaneously stocked as fingerlings into a central Texas reservoir.

Adaptation to their native environment may be important to the survival of different walleye populations. Fox (1993)

Received 2 October 2001. Accepted 16 January 2002. Published on the NRC Research Press Web site at http://cjfas.nrc.ca on 28 February 2002.
J16557

W.H. Eldridge,[1] M.D. Bacigalupi,[2] I.R. Adelman,[3] L.M. Miller, and A.R. Kapuscinski. Department of Fisheries, Wildlife, and Conservation Biology, University of Minnesota, 1980 Folwell Avenue, St. Paul, MN 55108, U.S.A.

[1]Present address: Northwest Indian Fisheries Commission, 6730 Martin Way East, Olympia, WA 98516, U.S.A.
[2]Present address: Minnesota Department of Natural Resources, 9925 Valley View Road, Eden Prairie, MN 55354, U.S.A.
[3]Corresponding author (e-mail: ira@fw.umn.edu).

 DOI: 10.1139/F02-007 © 2002 NRC Canada

compared zygote survival of two populations from geographically proximate streams. In both streams, the native population hatched in significantly higher numbers than the nonnative population. Jennings et al. (1996) showed that two walleye populations had a heritable preference for their native spawning environment (river versus lake beach) when given native and nonnative "options". Thus, survival of distinct walleye populations may differ when stocked into a nonnative environment.

For many years, the Minnesota Department of Natural Resources (MNDNR) has provided a walleye fishery in southern Minnesota lakes through maintenance stocking (Laarman 1978); natural reproduction in these lakes has been too infrequent to sustain a fishery. Fry and fingerlings from many broodstock sources statewide, but mostly from Pike River (PR), Hudson Bay drainage basin, or Little Cutfoot Sioux Lake (CS), Mississippi River drainage basin, have been stocked into southern Minnesota lakes. The genetic relationship between these two populations is unclear. On the one hand, the two populations clustered more closely to each other than to other populations in their own drainage basin in three studies involving allozyme analyses (McInerny et al. 1991; Fulton et al. 1992; Hudson et al. 1996). On the other hand, Pike River fish showed greater similarity to populations in their originating drainage (Hudson Bay) than to populations in the Mississippi Basin in analyses of mitochondrial DNA variation (Billington et al. 1992; Hudson et al. 1996). Differences between the two populations in survival of eggs to hatching have been observed repeatedly in MNDNR hatcheries. Over the last 10 years, the mean survival to the eyed-embryo stage, which closely relates with survival to hatching (Johnson 1961), was 62% for the CS population and 75% for the PR population (C. Kavanaugh, MNDNR, Grand Rapids, MN 55744, personal communication). The observed differences in hatchery survival led to the hypothesis that differential survival may occur in later life-history stages.

To verify this hypothesis, we conducted this study to determine if offspring of walleye from PR and CS exhibited different survival rates after being simultaneously stocked as fry into the same lakes and if the proportion of stocked to naturally reproduced walleye, if any were present, changed over time. We chose to use microsatellite DNA loci for parentage assignment to assign the stocked fish to their source population and distinguish stocked fish from natural-origin fish.

Parentage assignment matches the genotype of an individual with the mother–father pair that can generate its specific combination of alleles (Estoup et al. 1998). When suitable numbers of variable loci are used, an offspring can be uniquely assigned to its correct parents among many possible parent pairs (see Letcher and King (1999) for simulations of the number of loci needed to uniquely assign offspring). An offspring that does not assign to any pair indicates that its parents are unknown. In our stocking comparison study, unknown parents would be naturally reproducing descendents of previous stockings.

Methods

Study lakes and source populations

The five study lakes were located in southwest Minnesota, U.S.A. (Fig. 1). Isolated lakes were selected to eliminate immigration or emigration of walleye during the course of the study. The lakes were typical of most lakes in this region and had similar physical and chemical features and resident fish communities. Surface area ranged from 104 to 496 ha, and all were less than 5 m maximum depth (100% littoral surface area). The lakes were eutrophic to hypereutrophic with mud, sand, or silt basins. Walleye are not native to the lakes in the region but have been stocked for at least 50 years to provide put–grow–take walleye fisheries. Sporadic natural reproduction of previously stocked walleye does occur in these lakes. Stocked walleye have historically come from MNDNR spawning stations throughout the state, including the two sources used in this study.

We compared walleye from the MNDNR's Pike River (PR) and Little Cutfoot Sioux Lake (CS) spawning stations, approximately 900 km north of the study lakes and approximately 150 km from each other (Fig. 1). PR is in the Hudson Bay drainage and CS is in the Mississippi River drainage. The two populations have been physically separated since the Pleistocene ice age ended 10 000 years ago (Ojakangas and Matsch 1982). As is typical for the MNDNR walleye stocking program, gametes were collected from wild adults, brought to a hatchery to incubate, and stocked after hatching. Gametes collected at PR were from wild-run walleye on their spawning migration from Lake Vermillion into Pike River, and gametes collected at CS were from wild-run walleye on their spawning migration from Lake Winnibigoshish into Little Cutfoot Sioux Lake. The respective spawning stations are the most productive sources of gametes in the MNDNR walleye stocking program.

Hatchery and field methods

On 17 April 1998, 95 pairs of walleye from CS and 89 pairs of walleye from PR were mated, one male with one female, using each fish only once. After a minimum time of 4 min, with at least 2 min of continuous rinsing, fertilized eggs were combined and sealed in oxygenated 80-L plastic bags. Because eggs must be fertilized within 2 min of contact with water and sperm are active and viable for less than 1 min (Malison and Held 1996), it is highly unlikely that fertilization between unintended parental pairs could have occurred when the eggs were combined in the plastic bags. The bags were floated in 190-L tank trucks for immediate transport to the MNDNR hatching facility in St. Paul, where embryos from both source populations were reared under identical conditions. The peak of egg hatching for both populations coincided approximately 21 days after spawning. Estimated egg survival to fry emergence was 64% for CS offspring and 89% for PR offspring. Fin clips and scales were taken from the parent pairs, dried in envelopes, and stored at room temperature for future genetic analysis.

Unfed PR and CS fry were simultaneously stocked into the five study lakes over 2 days at an intended 1:1 ratio and an intended total density of 2477 fry per littoral hectare, the most common walleye stocking density used by MNDNR in this region. Number of fry per gram was estimated by MNDNR's usual procedure with a Von Bayer trough (Piper et al. 1982). The fry were weighed (live weight) and poured into 20-L plastic containers that were half filled with water, inflated with oxygen, and floated in tank trucks for transport

© 2002 NRC Canada

Fig. 1. Location of walleye spawning stations and study lakes: 1, Pike River spawning station; 2, Cutfoot Sioux spawning station; A, Shoakatan Lake; B, School Grove Lake; C, Allie Lake; D, Long Lake; E, Lura Lake. Interior lines delineate major drainage basins within Minnesota: North, Hudson Bay Basin; South, Mississippi River Basin; East, Lake Superior Basin. Insert shows location of Minnesota on map of the U.S.A.

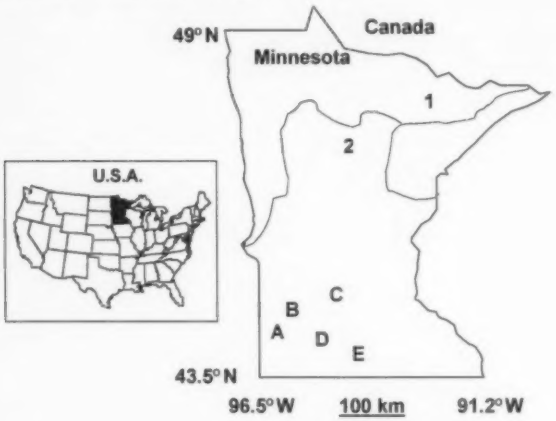

to the study lakes (2–4 h transport time). Fry were acclimated to lake water temperature and released slowly from a boat drifting in open water areas. Because of the potential inaccuracy of this procedure for establishing a 1:1 ratio of the two source populations, a sample of fry from each group was later weighed (dry weight) and the distribution ratio was corrected. Instead of the intended ratio of 50% PR and 50% CS fish, the corrected ratio of fry stocked into each lake was 46.5% PR and 53.5% CS.

At five distinct time periods, beginning within 1 week after stocking and continuing until the following fall, young walleye were sampled from the five lakes using plankton nets (first spring), beach seines (first summer), and trap nets and electrofishing (first fall, second spring, and second fall). These methods were selected because they each target a variety of habitats favored by young walleye during the early life stages. Whole walleye <70 mm were preserved in 70% ethanol at room temperature. Fin clips from walleye >70 mm and both fin clips and scales from walleye >200 mm were sampled in a nonlethal manner. Tissue samples were dried in envelopes and stored at room temperature. Scales were used to verify that large fish were from the 1998 year-class.

Parentage assignment

If inheritance is understood for a species, an offspring can be assigned to its parents by determining a parent pair capable of producing its genotype at multiple variable loci. We selected nine microsatellite loci to assign stocked fish to their hatchery parent pair, six walleye microsatellite loci developed by Borer et al. (1998) plus three additional microsatellite loci developed for walleye following the protocol of Borer et al. (1998). (Microsatellite analysis is described below.) We used the computer program PROBMAX (Danzmann 1997) to identify the parent pair that could generate a sampled fish's genotype through simple Mendelian inheritance. Assignments using PROBMAX are based on loci with genotypes known for the mother, father, and offspring and do not consider loci for which the genotype is known for only one parent. We systematically examined the known parent's genotype not considered in the PROBMAX analysis to confirm or negate assignments made by PROBMAX. When parental genotypes were missing for a locus, a minimum of seven matching loci was necessary before we assigned a fish. Allele scoring was repeated twice for each gel, and discrepancies were examined. Loci that were not definitively scored upon further examination were redone or removed. Parentage was excluded if at least one allele across all examined loci prevented assignment. Mutation was invoked when parentage was excluded because of a single mismatch in which the allele differed by only two base pairs. Individuals for which mutation, by this criterion, prevented assignment were removed from further analysis. Other forms of putative mutation were not considered.

Sampled walleye were placed into one of three categories: stocked PR walleye, stocked CS walleye, or natural-origin walleye (the product of natural reproduction in the study lake). χ^2 tests were used to test the null hypothesis of no difference between the expected proportion of PR fish (46.5%) and CS fish (53.5%) and the actual proportion in each sample. Logistic regression was used to determine if the proportion of stocked walleye (PR + CS) to natural-origin walleye changed between adjacent sampling periods and over the entire study. All statistical analyses were computed using the software MacAnova 4.10 (http://stat.umn.edu/~gary/macanova/macanova.home.html 1999).

Simulations

It was apparent that resident fish successfully reproduced in the study lakes because some sampled offspring did not assign to any of our CS or PR parent pairs. Fish that did not assign to any parents were removed from comparisons of stocked fish and thus did not affect our study. However, it is possible that natural-origin offspring were incorrectly assigned to a parent pair and biased our results. To assess the possibility of incorrectly assigning natural-origin fish to PR or CS parents, we performed simulations to determine the power of our loci to correctly exclude parentage.

We simulated genotypes of 1000 offspring (10 offspring from each of 100 simulated, one by one parent pairs) for PR and CS from the estimated allele frequencies and assuming Hardy–Weinberg equilibrium, statistical independence between loci, and no mutation or error in allele transmission. PROBMAX (Danzmann 1997) was used to test for parentage of the 1000 CS and 1000 PR offspring by all of the real 89 PR parent pairs and 95 CS parent pairs, respectively. The rate of incorrect assignment was the percentage of simulated offspring for whom parentage by all the real parent pairs in the particular population could not be excluded. Nine, eight, and seven microsatellite loci were tested consecutively by removing genotype information in descending order of probability of exclusion.

Microsatellite analysis

The nine microsatellite loci selected for parentage assignment and an additional four microsatellite loci developed for walleye following the protocol of Borer et al. (1998) were

© 2002 NRC Canada

analyzed. Primers for loci Svi6 and Svi26 (Borer et al. 1998) were redesigned using sequences of the flanking regions (Genbank Accession Numbers G36962 and G36965, respectively). DNA was extracted from both fin clips and scales using a 250 μL 5% Chelex solution (Sigma, St. Louis, Mo.) following the protocol of Miller and Kapuscinski (1996) and stored at –20°C. We used tissue samples less than 5 mm^2 as the DNA source because larger samples resulted in weak or no polymerase chain reaction (PCR) amplification. Microsatellite amplification via PCR was performed in either a 96-well plate (Thermoquick PCR plate type 2, Greiner Bio-One, Longwood, Fla.) or a 0.5-mL tube (USA Scientific Inc., Ocala, Fla.). The 15 μL PCR solution contained 0.33 μM forward and 0.33 μM reverse primer, 0.25 mM of each dNTP (Life Technologies (Gibco BRL) Inc., Rockville, Md.), 10 mM Tris–HCl (pH 9.0, 25°C), 50 mM KCl, 0.1% Triton X-100, 1.5 mM Mg^{2+}, 6 μL of Chelex extraction as the DNA template (the concentration of DNA was not predetermined), 0.2 units Taq polymerase (Promega Corp., Madison, Wis.), and water. A negative control reaction containing no DNA was included to detect possible sample contamination of our PCR mixtures.

Amplification was carried out in a thermocycler (Omn-E, Thermo Hybaid, Franklin, Mass.) using the following protocol: 5 min initial denaturation at 95°C, 10 cycles of 1 min denaturation at 94°C, 1 min annealing at 50°C and 1 min elongation at 72°C, 29 cycles with the same conditions except for a reduction of the annealing temperature to 89°C (to preserve the activity of the Taq polymerase enzyme) and a final elongation of 10 min at 72°C.

Products from PCR amplifications were visualized in two ways. Products were first visualized on a 14 cm × 16 cm nondenaturing 8% acrylamide gel (19:1 acrylamide: bisacrylamide) stained with ethidium bromide to confirm amplification of products and for rough estimation of product size. Allele size was determined accurately by end-labeling one primer of each pair was with a fluorescent dye (Fam, Hex, Tet) and electrophoresing products on an ABI Prism 377 DNA Sequencer (PerkinElmer Inc., Wellesley, Mass.). Genotypes were determined using Genescan and Genotyper software (PerkinElmer).

Population genetic statistics for the nine loci selected for parentage assignment were calculated using the parents (190 CS and 178 PR) of the stocked offspring. Heterozygosity and probability of exclusion (E1) were calculated using the computer program Cervus (Marshall et al. 1998). Probability of exclusion is the average exclusion probability for one parent in the absence of genetic information for both parents. Cervus employs the formulas of Nei (1987, eq. 7.8) to calculate expected heterozygosity and a formula from appendix 2 of Marshall et al. (1998) to calculate E1. Exact tests for Hardy–Weinberg equilibrium and tests for population linkage disequilibrium in the two hatchery parent populations were performed using the program Genepop (Markov chain method, default conditions; Raymond and Rousset 1995). Number of alleles per locus and allele size range were determined for all parent pairs and sampled fish for the nine loci selected for parentage assignment and in two individuals from CS for the additional four loci developed for walleye. Seventy offspring of a single informative cross were used to test for physical linkage using the computer program LINKMFX (developed by Roy G. Danzmann, University of Guelph, Ont., Canada).

Results

Survival comparison

The relative survival of PR to CS fish varied over 1.5 years poststocking (Fig. 2*a*). The two samples taken within 1 month of stocking indicated no difference in survival for the two populations. In the two samples from summer 1998, the percentage of CS fish among the stocked fish was significantly higher than expected, based on the original distribution of 46.5% PR and 53.5% CS fish. However, by fall 1998 (169–175 days poststocking) in all five lakes, the percentage of PR fish among the stocked fish was higher than expected. Differences from the expected percentages were significant in three of the five lakes (Table 1). In spring 1999 (348–378 days poststocking), PR fish continued to contribute a larger portion of the stocked age-1 year-class than expected in all five lakes. Differences were significant in three of these lakes, although not the same three as in the previous fall.

The fall 1999 sampling period, 511–540 days poststocking, yielded few definitive results. There were no significant differences from the expected ratio of PR to CS in the three lakes from which walleye were captured. Although the difference was no longer statistically significant, PR walleye in Shoakotan Lake were 16% more abundant than expected in the fall 1999 sample. But in the remaining two lakes, the percentage of PR fish was slightly below the expected percentage. However, sample sizes of assigned fish were relatively small, particularly from School Grove Lake with only 11 stocked fish sampled. No comparison could be made in Lura or Allie lakes, because despite intensive sampling, we failed to capture any 1998 year-class walleye.

Considering the three lakes where we obtained young walleye at the fall 1999 sampling period, the percentage of natural-origin walleye significantly increased with time over the study period from <1% to 55% ($P = 0.001$) (Fig. 2*b*). Over the winter, the percentage of natural-origin walleye in the three lakes decreased slightly 23% to 20% but then increased again in the second growing season to 55%.

Parentage assignment

From five study lakes, 758 walleye were genotyped and 566 of them were assigned to CS or PR hatchery parents. Complete genotypes (i.e., all 9 loci, or 18 alleles) were available for 42% of the assigned fish. In cases where genotypes were missing, 37% of assignments were made on the basis of 16–17 alleles and 20% were made on the basis of 14–15 alleles. Three fish assigned to more than one set of PR parents. These fish were included in further analysis. One hundred and seventy-seven walleye did not assign to any hatchery parents, leading to the inference that these fish were naturally reproduced in the system and therefore were removed from further analysis. Of these natural-origin fish, 70.4% mismatched with all parent pairs at two or more loci. Eight fish were removed from further analysis because of presumed mutation at one allele that prevented assignment to hatchery parents. Seven fish were removed from further

© 2002 NRC Canada

Fig. 2. Percentage of (*a*) Pike River walleye among the stocked walleye and (*b*) natural-origin walleye among all 1998 year-class walleye within each of five lakes and five sampling periods. Fry were stocked at an initial ratio of 46.5% Pike River (indicated by the horizontal dashed line in (*a*) and 53.5% Cutfoot Sioux. Square, Allie Lake; ellipse, Long Lake; diamond, School Grove Lake; inverted triangle, Lura Lake; triangle, Shoakatan Lake.

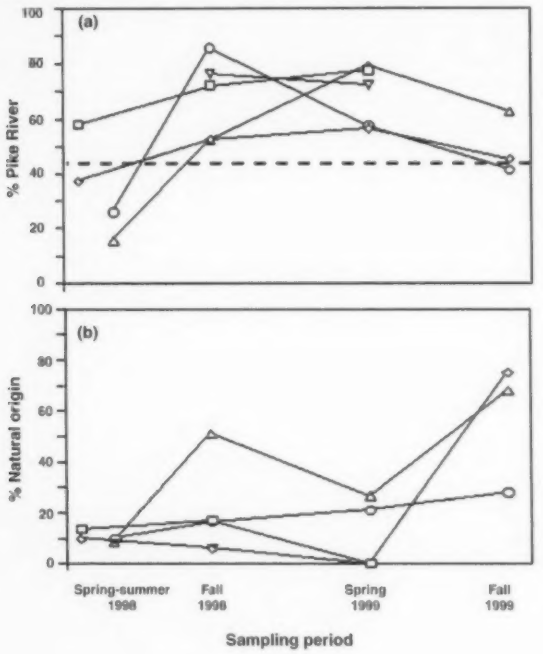

analysis because of assignment to hatchery parents in both populations.

Power of parentage tests

Simulated offspring were correctly excluded from assignments to our actual PR and CS parent pairs frequently (>95%) when parentage tests used data on eight or nine loci, except for 89% exclusion of simulated PR offspring to PR parents with eight loci (Fig. 3). With seven loci, rates of correct exclusion were similar for all offspring versus parent comparisons (74.8–79.9%) except that simulated PR offspring were correctly excluded from CS parents more frequently (88.4%). The relatively small samples of young walleye from each lake (82 or less) and the large number of alleles used to assign individuals in our study (16–18 alleles, 8 or 9 loci) indicate that few of the sampled offspring that assigned to CS or PR parents were likely natural-origin offspring.

Microsatellite loci description

We evaluated 13 microsatellite loci and selected nine for parentage assignment (Table 2). The 13 loci were autosomal, diploid, and inherited in a Mendelian fashion (Eldridge 2000). Examination of 70 progeny of a single cross revealed putative evidence for physical linkage between loci Svi20 and Svi26 (recombination percentage = 0.1 ± 0.036, LOD score = 11.2) (Eldridge 2000).

The nine microsatellite loci chosen for parentage assignment had 4–15 alleles and heterozygosities of 0.41–0.83 in the CS and PR parents (Table 3). No significant deviations from Hardy–Weinberg expectations were found for the 18 probability tests for the CS and PR parents ($P > 0.05$). The P value for population linkage disequilibrium of the potentially linked loci Svi20 and Svi26 was low in the CS population ($P < 0.02$), but it was not significant after a Bonferroni correction for multiple testing (Rice 1989). No other tests for population linkage disequilibrium were significant.

Discussion

We observed a suggestive, but not conclusive, survival advantage for walleye from one source over another when simultaneously stocked into natural lake environments. The first summer after stocking survival for stocked CS offspring was higher than for PR offspring. By the fall, however, survival for stocked PR offspring was higher than for the CS offspring. Over the first winter, PR fish continued to survive in higher numbers than CS fish when the results of the five lakes were combined; however, their survival exhibited a downward trend in two of five lakes. We could not document a continued survival advantage for PR fish by fall 1999. The two lakes in which PR fish were favored slightly, but nonsignificantly, in spring 1999 had reversed to favor CS slightly, but again nonsignificantly. One lake that significantly favored PR fish in spring still showed a relatively large (16%) advantage by fall, but this was not significant, possibly because of the small number of stocked fish recovered in the sample. Unfortunately, we could not capture any walleye in Allie and Lura lakes, two of the lakes where there were significantly larger numbers of PR fish than expected in both fall 1998 and spring 1999. Whether the advantage of PR fish in Long, School Grove, and Shoakotan lakes was lost with time or insufficient capture of stocked fish changed the outcome is unclear. Managers of put–grow–take fisheries would prefer to stock fish with higher survival to the fishery, but because the fish in this study had not yet recruited by fall 1999, we were unable to determine if one population would be more successful at contributing to the fishery than the other.

The cause of the early survival advantage of the stocked CS fish followed by the subsequent reversal to favor PR fish after the first summer is uncertain. PR fry at the time of stocking were about 8.8% larger than CS fish (dry weight); however, this size advantage did not result in better early survival of PR fish. The phenotypes of quantitative traits, such as survival-related and growth-related traits at early life stages, are controlled by a combination of genetic factors, environmental factors, and in some cases, genetic by environment interactions (Falconer 1989). This study, however, was not designed to test for the relative contribution of genetic versus environmental components to performance traits of the stocked walleye in the two source populations. Whatever combination of genetic and environmental factors was responsible for higher mean survival of PR fish to the eyed-embryo stage compared with CS fish, as observed in Minnesota DNR hatcheries over the last 10 years (C. Kavanaugh, MNDNR, Grand Rapids, MN 55744, personal communication), may have carried over into the larger size of PR fish at

© 2002 NRC Canada

Table 1. Number of walleye juveniles sampled from five lakes during five sampling periods assigned to two stocked populations and to the natural-origin population.

Population origin	Allie Lake	Long Lake	School Grove Lake	Lura Lake	Shoakatan Lake	Combined
Spring 1998 (16–18 days poststocking)						
Pike River	11	0	10	0	0	21
Cutfoot Sioux	8	0	17	0	0	25
Natural	1	0	0	0	0	1
Summer 1998 (47–69 days poststocking)						
Pike River	0	7*	0	0	5*	12*
Cutfoot Sioux	0	20*	0	0	27*	47*
Natural	0	5	0	0	5	10
Fall 1998 (169–175 days poststocking)						
Pike River	49*	30*	32	35*	12	158*
Cutfoot Sioux	19*	5*	29	11*	11	75*
Natural	14	7	4	3	24	52
Spring 1999 (348–378 days poststocking)						
Pike River	24*	19	9	28*	26*	106*
Cutfoot Sioux	7*	14	7	11*	7*	46*
Natural	0	9	0	0	12	21
Fall 1999 (511–540 days poststocking)						
Pike River	0	17	5	0	15	37
Cutfoot Sioux	0	24	6	0	9	39
Natural	0	16	26	0	51	93

Note: Asterisks denote a significant difference between the two stocked populations (χ^2, $P < 0.05$).

Fig. 3. Percent of 1000 simulated Little Cutfoot Sioux Lake (CS) and 1000 simulated Pike River (PR) offspring excluded from parentage by any of 95 parent pairs spawned at CS spawning station and 89 parent pairs spawned at PR spawning station using 9, 8, and 7 microsatellite loci, removed in descending order of probability of exclusion. The nine loci, in order of probability of exclusion, were Svi26, Svi6, Svi33, Svi16, Svi4, Svi2, Svi20, Svi18, and Svi17. Solid triangle, PR parents and PR offspring; open triangle, CS parents and PR offspring; solid circle, PR parents and CS offspring; open circle, CS parents and CS offspring.

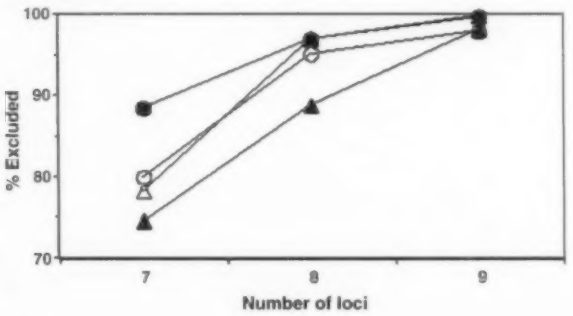

stocking. It is unclear why this larger size advantage of the PR fish at stocking did not provide an early survival advantage. Moodie et al. (1989) observed in tank culture that walleye fry from a population with smaller eggs survived to 13 days posthatch as well as walleye fry from a population with bigger eggs. Recently, Mauk and Brown (2001) found no performance differences in tank culture systems among three walleye populations with historically different egg hatching rates.

An assumption central to this study was that all groups of walleye were equally vulnerable to the sampling gear. If sampling gear was biased with regard to the stocked CS and PR offspring, then the collections would not be random and inferences about relative survival would be erroneous. Such a bias could arise if the two stocked groups favored different habitats within a lake because of genetically based preferences. Jennings et al. (1996) observed putative genetically based preferences for spawning habitat in the offspring of river- and beach-spawning walleye when stocked into the same nonnative lake system with river- and beach-spawning habitat. However, it is unlikely the stocked CS and PR offspring demonstrated differences in genetic-based habitat preference, given the similarity of the juvenile habitat of the CS and PR populations (C. Kavanaugh, MNDNR, Grand Rapids, MN 55744, personal communication). In addition, we mediated against the possibility of sampling bias by electrofishing and setting trap nets over a variety of habitats and locations within each lake.

Natural-origin walleye in the 1998 year-class demonstrated an overall increasing trend in relative abundance in our samples, indicating that local adaptation may be making the naturally spawned fish better suited for survival in southwest Minnesota lakes than the northern-origin stocked populations. Local adaptation appears to be highly important to walleye (Fox 1993), as it is for other fish species (Taylor 1991; Philipp and Claussen 1995). However, we cannot determine whether the natural-origin populations achieved their survival advantage through adaptive response to selection in the stocked lake environments or through historical stocking of walleye from a source that was better adapted at the outset to survival in southwest Minnesota lakes than either of the two source populations compared in this study. Regardless of the reasons why, periodic natural reproduction may contribute a larger percentage of walleye in lakes that are managed as put–grow–take fisheries than has been rec-

© 2002 NRC Canada

Table 2. Microsatellite loci cloned from walleye (*Stizostedion vitreum*), core sequence, primer sequence, number of alleles, and allele size ranges.

Locus	Core sequence	Primers (5′–3′)	Number of alleles	Allele size range (bp)	GenBank accession number
Svi2	$(AC)_{18}$	CAA-CCA-GAC-CCA-ATC-CCT-TG GGG-CCG-AGT-ATA-TCA-GTT-AAC	9	192–208	
Svi3	$(AC)_{18}$	CTG-AGT-GTG-CCA-ATA-CAA-GTC GCC-AGA-ACA-ATC-TAC-CGA-GG	NA	133–163	
Svi4	$(AC)_{16}$	See Borer et al. (1998)	8	102–118	G36961
Svi5	$(AC)_{18}$	CTT-AAT-TCC-CCC-AGC-AAC TGT-GTG-CAT-CAT-TAT-CAC-TG	NA	178–191	
Svi6	$(AC)_{19}$	AGT-CGA-CAT-ATT-ATG-TAG-AGT-GC GAT-CAA-CTG-TGG-AGG-ATG-AGC	18	136–173	G36962
Svi7	$(AC)_{14}$	GAA-ACC-TTA-CAA-AAG-CCT-GG TTA-TCT-GCA-CTT-CTA-CAG-GC	NA	163–173	
Svi14	$(AC)_5n_3(AC)_{31}$	TGT-GTG-GCC-CTT-GGT-CAG-G ATC-TGA-GGA-GTA-TTA-CCG-G	NA	184–200	
Svi16	$(AC)_5n_4(AC)_{30}$	TCA-GCC-TCT-GAA-AAC-ACT-GC CTG-TTT-CAC-AAA-TTG-GCA-CC	18	212–266	
Svi17	$(AC)_{13}$	See Borer et al. (1998)	8	101–115	G36963
Svi18	$(AC)_{11}$	See Borer et al. (1998)	5	118–126	G36964
Svi20	$(AC)_{20}$	CAA-GTG-CGC-AAT-GGT-GCA-TTA-C GAA-TGA-AGA-AAT-GCA-CCC-ATG-C	18	144–193	
Svi26	$(AC)_{13}n_2(AC)_{19}$	CGA-ACT-ACT-TAT-CTT-CTG-GC GTA-AGT-GTG-AAT-CAG-CCA-GAC	16	156–189	G36965
Svi33	$(AC)_3n_8(AC)_{14}$	See Borer et al. (1998)	7	90–104	G36967

Note: Observations based on >900 individuals from northern and southern Minnesota, except Svi3, Svi5, Svi7, and Svi14 were analyzed for two individuals sampled at MNDNR Little Cutfoot Sioux Lake spawning station in northern Minnesota. The first primer in each pair was fluorescently labeled. Primers for Svi6 and Svi26 were redesigned from Borer et al. (1998). Svi3, Svi5, Svi7, and Svi14 were not used in the parentage analyses. The number of alleles at these four loci is not available (NA) because of the small sample. bp, basepairs.

Table 3. Measures of genetic diversity in adult walleye sampled at Little Cutfoot Sioux Lake spawning station (CS) and Pike River spawning station (PR).

	Number of individuals scored		Observed number of alleles		Expected heterozygosity		E1	
Locus	CS	PR	CS	PR	CS	PR	CS	PR
Svi26	152	129	10	13	0.80	0.83	0.45	0.50
Svi6	180	166	13	13	0.77	0.78	0.42	0.41
Svi33	190	177	6	7	0.72	0.73	0.30	0.31
Svi16	179	166	13	13	0.67	0.64	0.28	0.27
Svi4	160	173	6	6	0.72	0.65	0.30	0.23
Svi2	184	178	7	7	0.67	0.66	0.27	0.25
Svi20	189	174	15	15	0.67	0.52	0.29	0.17
Svi18	190	176	5	4	0.67	0.65	0.23	0.22
Svi17	183	167	6	7	0.41	0.41	0.09	0.09
Average total			9.00	9.44	0.68	0.65	0.96	0.95

ognized by managers. To the extent that stocked walleye may compete with the natural walleye (Li et al. 1996*b*), managers might wait to decide on stocking until after completion of a late summer assessment of natural reproduction. Then, if warranted by the absence of natural fish, they could stock fingerlings in the fall.

Parentage assignment might lead to some incorrect assignments. Seven walleye (approximately 1.3% of the stocked walleye sampled) were removed from the analysis because they assigned to parent pairs in both populations, presumably the correct and an incorrect parent pair. Removal of these few individuals is not expected to bias the survival comparison. Additionally, three stocked walleye assigned to multiple parents in the PR population. Our goal in using parentage assignment was to assign individuals to source; therefore, we tolerated assignments to multiple parent pairs in the same population.

We could not determine the number of natural-origin fish that may have incorrectly assigned to a CS or PR parent pair, although we expect that it did not bias the survival

© 2002 NRC Canada

comparison. Many natural-origin fish could easily be excluded by the presence of an allele not found in our parent pairs. This happened most frequently with natural-origin fish in Shoakatan Lake. Alternatively, simulations suggested that few natural-origin fish would incorrectly assign when eight or nine loci were compared, and they were unlikely to assign more to a parent pair from one population than from the other. With seven loci, the potential for incorrect assignments increased, and simulated CS offspring were biased more to one parent population than to the other. This suggests that natural-origin offspring with allele frequency distributions at these loci similar to the CS population may bias the survival comparison. However, as only 20% of the stocked fish assigned to a real parent pair based on seven loci, we expect that few naturally produced offspring incorrectly assigned to parent pairs, and if some were, they were unlikely to bias our CS versus PR comparisons. In addition, we consider our simulations to represent worst-case scenarios in two respects. First, our simulated offspring were generated from populations with the same allele frequencies as those of the parents of our actual stocked fish. The actual parents of natural-origin fish in our study lakes descend from other source populations or, at worst, from earlier generations of CS or PR fish. Therefore, on average, natural-origin fish in our study lakes would be less likely to assign to our CS or PR parents than the simulated natural offspring generated for our analysis. Second, when attempting to assign simulated natural offspring to a real parent pair based on eight or seven loci, we eliminated the most informative markers first. For most of our actual assignments based on fewer than nine loci, the one or two most informative loci were often included in the assignment.

Although genotyping error cannot be disregarded, we expect that it did not prevent assignment of many stocked offspring to their parents (thus categorizing them as natural-origin fish) or lead to biases in our stocked offspring comparisons. To limit genotyping error, gels were scored multiple times, and inconsistent allele scores were redone or excluded. Negative controls without DNA never indicated any contamination of our PCR reactions. Individuals included on multiple gels produced repeatable genotypes. Of those offspring that did not assign to parents, over two-thirds were inconsistent with any possible parent pair at two or more loci, indicating that occasional genotyping errors at single loci were not the cause of many nonassignments. We also found no evidence for gel-wide errors. In many instances, individuals from the same sample groups were included in different gels and the percentage of nonassigning fish was similar from both gels. Although occasional genotyping errors may have increased the numbers of fish considered to be of natural origin, they should not have affected one stocked group more than the other and thus should not have biased our stocked fish comparisons.

Genetic assignment techniques other than parentage assignment would have been inappropriate for this study. Mixed stock analysis (Utter and Ryman 1993) and the assignment calculator (Waser and Strobeck 1997) rely on allele frequency differences between populations to partition a sample into its source components. These two techniques show high error rates when trying to distinguish fish from source populations that have similar allelic frequency distributions. In addition, they cannot separate stocked fish from wild fish if the two populations are genetically related, as can occur in systems with supplemental stocking and was the case in this study. Frequency-based genetic assignment techniques require allele frequency baselines for all source populations to make accurate assignments (see Cornuet et al. (1999) for exceptions). Estimating an accurate baseline for the wild population may be impossible because of small sample size or, in a system with indiscriminant stocking (as in this study), dynamic allele frequencies between generations resulting from fluctuating contributions from parents of multiple sources. Parentage assignment offers a feasible alternative when more than two populations need to be distinguished and allele frequency differences cannot separate the populations. Parentage assignment is limited, however, in that genotypes of all parent pairs from all but one putative source population are required for accurate assignment.

Acknowledgements

We thank William Ardren for genetics assistance, Dennis Cook and Christopher Bingham for statistical consulting, and two anonymous reviewers for suggestions on the manuscript. Minnesota Department of Natural Resources personnel from the Spicer, Hutchinson, Windom, Waterville, Ely, Grand Rapids, and East Metro areas assisted in designing this study as well as in spawning, rearing, and collecting walleyes. Funding was provided by the state of Minnesota through the Legislative Commission on Minnesota Resources, by Wildlife Forever, Minnesota General Agricultural Research funds (projects MIN 41-034 and MIN 41-078), and the Minnesota Sea Grant College Program supported by the NOAA Office of Sea Grant, United States Department of Commerce, under grant No. NOAA-NA-86-RG-0033. The U.S. Government is authorized to reproduce and distribute reprints for government purposes, not withstanding any copyright notation that may appear hereon. This paper is journal reprint No. JR 482 of the Minnesota Sea Grant College Program.

References

Billington, N., Barrette, R.J., and Hebert, P.D.N. 1992. Management implications of mitrochondrial DNA variation in walleye stocks. N. Am. J. Fish. Manag. **12**: 276–284.

Borer, S.O., Miller, L.M., and Kapuscinski, A.R. 1998. Microsatellite markers in walleye *Stizostedion vitreum*. Mol. Ecol. **8**: 336–338.

Cornuet, J.M., Piry, S., Luikart, G., Estoup, A., and Solignac, M. 1999. New methods employing multilocus genotypes to select or exclude populations as origins of individuals. Genetics, **153**: 1989–2000.

Danzmann, R.G. 1997. PROBMAX: a computer program for assigning unknown parentage in pedigree analysis from known genotypic pools of parents and progeny. J. Hered. **88**: 333.

Eldridge, W.H. 2000. Walleye (*Stizostedion vitreum*) population identification using parentage assignment. M.S. thesis, University of Minnesota, St. Paul, Minn.

Estoup, A., Gharbi, K., SanCristobal, M., Chevalet, C., Haffray, P., and Guyomard, R. 1998. Parentage assignment using microsatellites in turbot (*Scophthalmus maximus*) and rainbow trout (*Oncorhynchus mykiss*) hatchery populations. Can. J. Fish. Aquat. Sci. **55**: 715–725.

© 2002 NRC Canada

Falconer, D.S. 1989. Introduction to quantitative genetics. 3rd ed. Longman, New York.

Fox, M.G. 1993. Comparison of zygote survival of native and non-native walleye stocks in two Georgian Bay rivers. Environ. Biol. Fishes, **38**: 379–383.

Fulton, J.E., Otis, J.S., and Guise, K.S. 1992. Discrimination of walleye, *Stizostedion vitreum vitreum* (Mitchill), stocks by isozyme analysis with cellulose acetate. Anim. Genet. **23**: 221–230.

Hudson, J.M., Fields, R.D., and Philipp, D.P. 1996. Population genetic survey of walleye (*Stizostedion vitreum*) using protein electrophoresis and mitochondrial DNA RFLP analysis. *In* Genetic analyses of fish species in the Upper Midwest. Illinois Natural History Survey, Champaign, Ill. pp. 172–190.

Hudy, M., and Berry, C.R., Jr. 1983. Performance of three strains of rainbow trout in a Utah reservoir. N. Am. J. Fish. Manag. **3**: 136–141.

Hume, J.M., and Tsumura, K. 1992. Field evaluations of two rainbow trout strains introduced into three British Columbia lakes. N. Am. J. Fish. Manag. **3**: 136–141.

Jennings, M.J., Claussen, J.E., and Philipp, D.P. 1996. Evidence for heritable preferences for spawning habitat between two walleye populations. Trans. Am. Fish. Soc. **125**: 978–982.

Johnson, F.H. 1961. Walleye egg survival during incubation on several types of bottom in Lake Winnibigoshish, Minnesota, and connecting waters. Trans. Am. Fish. Soc. **90**: 312–322.

Laarman, P.W. 1978. Case histories of stocking walleyes in inland lakes, impoundments, and the Great Lakes—100 years with walleyes. Am. Fish. Soc. Spec. Publ. **11**: 254–260.

Letcher, B.H., and King, T.L. 1999. Targeted stock identification using multilocus genotype 'familyprinting'. Fish. Res. **43**: 99–111.

Li, J., Cohen, Y., Schupp, D.H., and Adelman, I.R. 1996*a*. Effects of walleye stocking on population abundance and fish size. N. Am. J. Fish. Manag. **16**: 830–849.

Li, J., Cohen, Y., Schupp, D.H., and Adelman, I.R. 1996*b*. Effects of walleye stocking on year-class strength. N. Am. J. Fish. Manag. **16**: 840–850.

Malison, J.A., and Held, J.A. 1996. Reproductive biology and spawning. *In* Walleye culture manual. *Edited by* R.C. Summerfelt. North Central Regional Aquaculture Center Publications Office, Iowa State University, Ames, Iowa. NCRAC Culture Series 101. pp. 11–18.

Marshall, T.C., Slate, J., Kruuk, L., and Pemberton, J.M. 1998. Statistical confidence for likelihood-based paternity inference in natural populations. Mol. Ecol. **7**: 639–655.

Mauk, R.J., and Brown, M.L. 2001. Performance of walleye progeny from Missouri River tributaties in South Dakota. N. Am. J. Aquacult. **63**: 167–170.

McInerny, M., Glazer, R., Zarling, G., Fulton, J., Otis, J., and Guise, K. 1991. Genetic description of walleye stocks in Minnesota. Minnesota Department of Natural Resources, St. Paul, Min. Investigational Report 411

Miller, L.M., and Kapuscinski, A.R. 1996. Microsatellite markers reveal new levels of genetic variation in northern pike. Trans. Am. Fish. Soc. **125**: 971–977.

Moodie, G.E.E., Loadman, N.L., Wiegand, M.D., and Mathias, J.A. 1989. Influence of egg characteristics on survival, growth, and feeding in larval walleye (*Stizostedion vitreum*). Can. J. Fish. Aquat. Sci. **46**: 516–521.

Nei, M. 1987. Molecular evolutionary genetics. Columbia University Press, New York.

Ojakangas, R.W., and Matsch, C.L. 1982. Minnesota's geology. University of Minnesota Press, Minneapolis.

Philipp, D.P., and Claussen, J.E. 1995. Fitness and performance differences between two stocks of largemouth bass from different river drainages within Illinois. Am. Fish. Soc. Symp. **15**: 236–243.

Piper, R.G., McElwain, I.B., Orme, L.E., McCraren, J.P., Fowler, L.G., and Leonard, J.R. 1982. Fish hatchery management. U.S. Department of the Interior, Fish and Wildlife Service, Washington, D.C.

Raymond, M., and Rousset, F. 1995. GENEPOP (version 1.2): population genetics software for exact tests and ecumenicism. J. Hered. **86**: 248–249.

Rice, W.R. 1989. Analyzing tables of statistical tests. Evolution, **43**: 223–225.

Taylor, E.B. 1991. A review of local adaptation in Salmonidae, with particular reference to Pacific and Atlantic salmon. Aquaculture, **98**: 185–207.

Terre, D.R., Murphy, B.R., and Provine, W.C. 1995. Growth and spawning characteristics of southern riverine and northern strain walleyes in Texas. Proc. Annu. Conf. Southeast Assoc. Fish Wildl. Agencies, **49**: 118–128.

Utter, F.M., and Ryman, N. 1993. Genetic markers and mixed stock fisheries. Fisheries, **18**(8): 11–21.

Waser, P.M., and Strobeck, C. 1997. Genetic signatures of interpopulation dispersal. Trends Ecol. Evol. **13**(2): 43–42.

Younk, J.A., and Strand, R.F. 1992. Performance evaluation of four muskellunge, *Esox masquinongy*, strains in two Minnesota lakes. Minnesota Department of Natural Resources, St. Paul, Min. Investigational Report 418.

© 2002 NRC Canada

A mixed-species yield model for eastern Bering Sea shelf flatfish fisheries

Paul D. Spencer, Thomas K. Wilderbuer, and Chang Ik Zhang

Abstract: A variety of eastern Bering Sea (EBS) flatfish including yellowfin sole (*Limanda aspera*), rock sole (*Lepidopsetta bilineata*), flathead sole (*Hippoglossoides elassodon*), and Alaska plaice (*Pleuronectes quadrituberculatus*), co-occur in various degrees in EBS trawl fisheries, impeding attempts to obtain single-species management targets. A further complication is the bycatch of Pacific halibut (*Hippoglossus stenolepis*); halibut bycatch limits, rather than single-species catch quotas, have been the primary factor regulating EBS flatfish harvest in recent years. To examine bycatch interactions among the EBS flatfish listed above, an equilibrium mixed-species multifishery model was developed. Equilibrium yield curves, scaled by recent average recruitment, are flat topped or asymptotically increasing, reflecting low fishing selectivity during the first several years of life and low growth relative to natural mortality. A linear programming analysis indicated that relaxation of the halibut bycatch constraint at the optimal solution of catch by fishery would produce approximately 20 times more flatfish yield than a similar relaxation of any flatfish catch quota. A strategy for establishing halibut bycatch limits that considers the foregone revenue in the halibut and flatfish trawl fisheries reveals how the choice of halibut bycatch limit is affected by the management goal for the flatfish complex.

Résumé : Des combinaisons diverses de poissons plats, dont la limande à nageoires jaunes (*Limanda aspera*), la sole du Pacifique (*Lepidopsetta bilineata*), la plie à tête plate (*Hippoglossoides elassodon*) et la plie d'Alaska (*Pleuronectes quadrituberculatus*) se retrouvent dans les récoltes au chalut dans la mer de Béring orientale (EBS), ce qui rend difficile l'établissement d'objectifs de pêche pour chacune de ces espèces. La prise accessoire de flétans du Pacifique (*Hippoglossus stenolepis*) complique la situation encore davantage: en effet, les limites des prises de flétans, plutôt que les quotas des espèces individuelles, ont servi de critère principal de gestion de la pêche aux poissons plats de l'EBS au cours des dernières années. La conception d'un modèle d'équilibre plurispécifique impliquant plusieurs pêches commerciales nous a permis d'examiner les interactions entre la prise accessoire des flétans et les différentes espèces de poissons plats. Les courbes d'équilibre de rendement ajustées au recrutement moyen récent sont aplaties au sommet, ou alors croissent de façon asymptotique, ce qui indique une faible sélectivité de la pêche pendant plusieurs des premières années de la vie et une croissance réduite en regard de la mortalité naturelle. Une analyse de programmation linéaire montre qu'une atténuation des restrictions de la pêche accessoire des flétans au point de résolution optimale des prises par pêche commerciale produirait un rendement de poissons plats 20 fois plus grand que l'atténuation des quotas de pêche de n'importe lequel des poissons plats. Une stratégie pour l'établissement de quotas pour la pêche accessoire de flétans qui prend en considération les revenus perdus dans la pêche au chalut de flétans et de poissons plats montre comment le choix du quota pour la pêche accessoire de flétans est affecté par les objectifs de gestion du complexe de poissons plats.

[Traduit par la Rédaction]

Introduction

Fishery scientists have long recognized that single-species harvest goals are generally unattainable in mixed-species fisheries where several species are harvested simultaneously with the same gear. Pioneering work on this problem of technological interactions was conducted by Beverton and Holt (1957), who used mixed-species yield-per-recruit analysis to derive an optimal level of fishing effort. Further developments have included multifishery mixed-species models (Murawski 1984), incorporation of spawner–recruit relationships and predation mortality (Shepherd 1988; Murawski et al. 1991), and incorporation of fleet dynamics (Laurec et al. 1991). A multifishery mixed-species model is particularly appropriate for eastern Bering Sea (EBS) flatfish, four species of which are assessed with statistical catch-at-age models: yellowfin sole (*Limanda aspera*), rock sole (*Lepidopsetta bilineata*), flathead sole (*Hippoglossoides elassodon*), and Alaska plaice (*Pleuronectes quadrituberculatus*). These species occupy similar habitats on the EBS shelf, are harvested with trawl gear throughout the year, and thus co-occur to varying degrees in the harvest. Management of these flatfish by the National Marine Fisheries Service (NMFS) is conservative in that both retained and discarded

Received 20 July 2001. Accepted 24 January 2002. Published on the NRC Research Press Web site at http://cjfas.nrc.ca on 1 March 2002.
J16456

P.D. Spencer,[1] T.K. Wilderbuer, and C.I. Zhang.[2] Alaska Fisheries Science Center, National Marine Fisheries Service, 7600 Sand Point Way NE, Building 4, Seattle, WA 98115, U.S.A.

[1]Corresponding author (e-mail: paul.spencer@noaa.gov).

[2]Present address: Pukyong National University, Daeyeon-dong, Nam-gu, Pusan 608-737, Republic of Korea.

 DOI: 10.1139/F02-012 © 2002 NRC Canada

Fig. 1. Bering Sea – Aleutian Islands (BSAI) fishery management area in the northeast Pacific. Inset map of North America with study area highlighted.

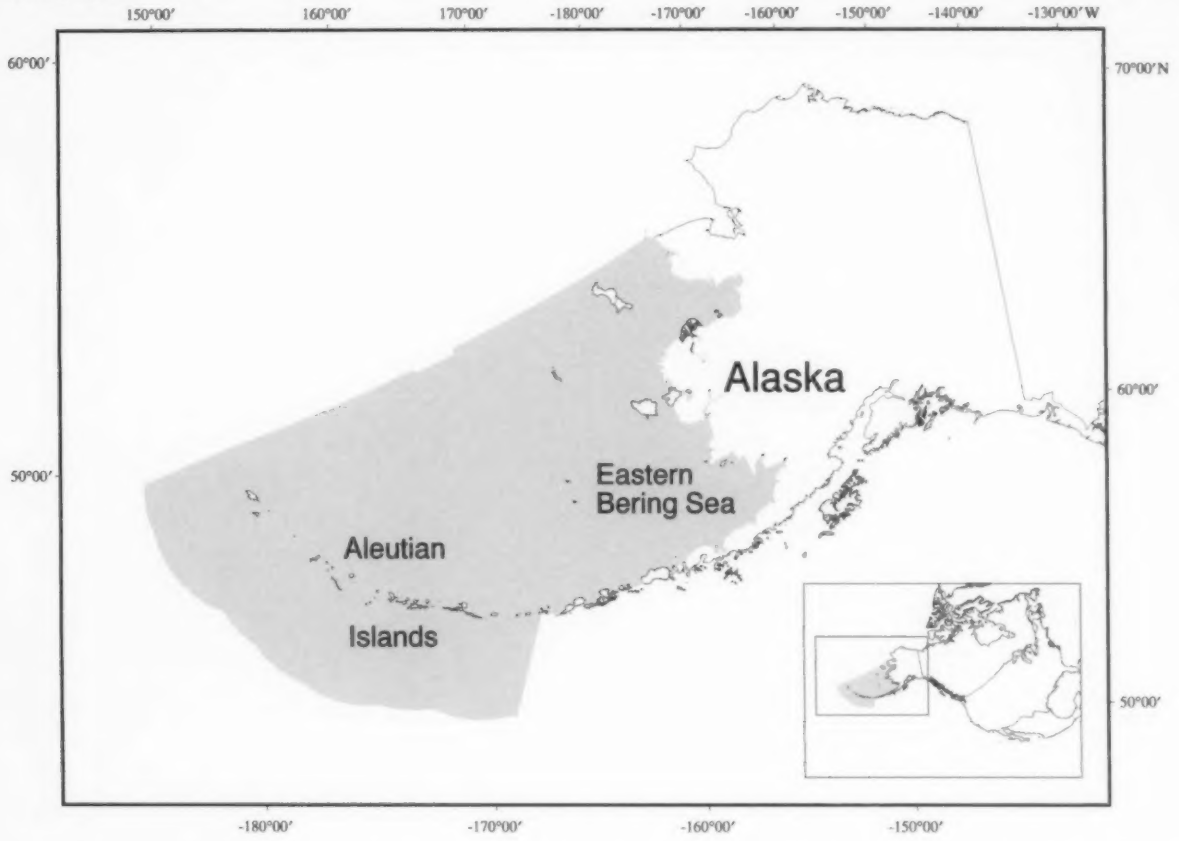

catch are observed and apply towards catch quotas, and specific fisheries are occasionally closed to ensure that any single-species catch quota is not exceeded. (In this paper, "flatfish" refers to the four species listed above, whereas "groundfish" includes additional species managed under Bering Sea – Aleutian Islands (BSAI) groundfish fishery management plan; the BSAI fishery management area is shown in Fig. 1). This strategy essentially results in management focused on protecting the weakest stock in the mixed-species system, although the degree of conservatism is not clear because detailed models describing how fishing effort radiates into species-specific mortality rates in this mixed-species multifishery system have not been developed.

An additional consideration is the bycatch of Pacific halibut (*Hippoglossus stenolepis*), which is managed by the International Pacific Halibut Commission (IPHC). Halibut bycatch in the groundfish fisheries is required to be returned to the water with minimal injury, and thus provide no economic benefit to groundfish fishermen. Because halibut bycatch in the groundfish fisheries limits the quotas for the directed halibut fishery, halibut bycatch limits have been placed upon the groundfish fisheries. In recent years, it has often been the halibut bycatch limits, not the single-species catch quotas, that have limited EBS flatfish fisheries. Thus, there is motivation to develop technology that reduces halibut bycatch, such as halibut excluder devices on trawls and real-time communication of high bycatch areas (Gauvin et al. 1995). However, it is not known how much halibut catchability would have to be reduced to avoid limitation under current halibut bycatch caps, as the catchability of halibut in groundfish trawl fisheries has not been estimated. A further consideration is the effect that halibut bycatch limits have upon the flatfish fisheries, as overly restrictive limits may result in foregone yield. Several authors have recommended the use of economic criteria to identify suitable bycatch levels, in which the marginal revenue for both the halibut fishery and the groundfish fishery with respect to bycatch are considered (Marasco and Terry 1982; Thompson 1993; Terry 1998). To fully address these questions regarding bycatch, detailed models that consider the growth, selectivity, and maturity of the relevant species will need to be developed.

The purpose of this study is to develop a mixed-species multifishery yield-per-recruit model of EBS flatfish with yields scaled by recent recruitment estimates. Estimates of catch and raw effort by fishery are made from observed catch records, and effort is standardized. The nature of the mixed-species multifishery system is revealed by the esti-

© 2002 NRC Canada

mated distribution of catch by species and fishery, which are used to derive species and fishery-specific catchability coefficients. Three analyses regarding the influence of the halibut bycatch limit are conducted. (*i*) An evaluation of the extent to which halibut catchability would have to be reduced from current levels to avoid limitation from the bycatch constraint, (*ii*) a linear programming analysis to identify an optimal catch distribution among fisheries, and (*iii*) an evaluation of a suitable halibut bycatch cap for the groundfish fisheries that considers the foregone revenue from the halibut and flatfish fisheries.

Materials and methods

Estimation of catch and standardized effort

The North Pacific Groundfish Observer Program has been collecting information on fishery catch and effort in the Bering Sea since 1973 (French et al. 1982). Currently, all vessels >60 ft (1 ft = 30.48 cm) are required to have observers for some portion of their days at sea. Selection of sampling units arises at three stages. (*i*) The selection of vessel-days, (*ii*) the selection of hauls within each vessel-day, and (*iii*) the subsampling of species catches within each sampled haul. Although the vessel coverage was generally below 20% during the 1970s (French et al. 1982), since 1990 there has been 100% coverage of vessel-days on vessels larger than 124 ft, and 30% coverage (per quarter) on vessels from 60 to 124 ft. The numbers of trawling vessels in the 60- to 124-ft categories and ≥125 ft have been about equal in recent years, although the larger vessels contribute a large majority of the groundfish trawl catch. A statistically rigorous randomized sampling design for selecting hauls within each vessel-day was implemented in 1991. Although several subsamples are often taken from each sampled haul, observers generally do not record information on this sampling stage. Thus, the observer sampling program is considered here as a two-stage sampling design.

Total annual catch of four commercially exploited flatfish species (yellowfin sole, rock sole, flathead sole, and Alaska plaice) of the EBS trawl fishery, and Pacific halibut, from each vessel during 1995–1999 were estimated from a two-stage cluster sampling estimator (Cochran 1977)

$$(1)\qquad C_k = \sum_v \frac{\mathrm{VD}_v}{\mathrm{vd}_v} \sum_{i=1}^{\mathrm{vd}_v} H_i \left(\frac{1}{h_i} \sum_{j=1}^{h_i} \mathrm{cat}_{i,j,k} \right)$$

where $\mathrm{cat}_{i,j,k}$ is the total catch weight (retained plus discarded) of species k on vessel-day i in haul j, h_i is the number of sampled hauls on vessel-day i, H_i is the number of total hauls on vessel-day i, and vd_v and VD_v are the number of sampled vessel-days and total vessel-days fished, respectively, of vessel v. Because of the sampling program requirement of complete coverage of vessel-days for vessels >124 ft, the VD–vd ratio was assumed to be equal to one for these vessels. For vessels from 60 to 124 ft, the extent to which the actual VD–vd ratio differs from that specified in the sampling design (1/0.3) is not known, as the number of unsampled vessel-days is not available. A VD–vd ratio of (1:0.3) was assigned for these vessels, which contribute a relatively small portion of the groundfish trawl fishery catch.

To estimate the catch by fishery (n), $C_{k,n}$, eq. 1 was applied to vessel-days assigned a particular fishery designation, which was based upon the species composition. For example, a vessel-day was designated as one of several flatfish fisheries if the sum of yellowfin sole, rock sole, flathead sole, Alaska plaice, and other flatfish catch exceeded the catch of any other species group. Further, flatfish fisheries vessel-days where more than 70% of the total flatfish catch consisted of yellowfin sole were designated as being in the yellowfin sole fishery, whereas other flatfish fisheries vessel-days were assigned to specific fisheries on the basis of largest flatfish species group present. Nonflatfish fishery designations were based upon the largest species group. Vessel-days in which walleye pollock (*Theragra chalcogramma*) comprised more than 95% of the total catch are considered to come from the pelagic trawl pollock fishery. A total of 14 fishery designations were used, roughly corresponding to those used in NMFS groundfish management.

A general linear model was used to standardize fishing effort by evaluating how total catch per hour of the five flatfish varied as a function of year (1995–1999), quarter, seven vessel-size categories, and two gear types (nonpelagic trawl and pelagic trawl). Raw effort (hours trawled) was estimated for each combination of year, quarter, vessel size, and gear with eq. 1 by replacing catch with hours trawled. The model coefficients were used to standardize raw effort relative to that of 150- to 200-ft vessels using nonpelagic trawls during the first quarter of 1995, and standardized effort was summed across year, quarter, and fishery. Standardized effort was computed by fishery and month by assuming a uniform distribution of effort within a particular quarter.

Estimates for catchability (q), by species and fishery, were obtained from a linear model relating fishery-specific fishing mortality rate ($F_{k,n}$) to fishery-specific standardized effort (E_n), $F_{k,n} = q_{k,n}E_n$. The fishery-specific mortality rates were obtained by assuming that the distribution of fishing mortality across fisheries was equivalent to the distribution of catch across fisheries, or $F_{k,n} = (C_{k,n}/C_k)F_k$. Estimates of catch were obtained from eq. 1 and fully selected fishing mortality rates were obtained from age-structured stock assessments; mean catch proportions and F_k from 1995 to 1999 were used to estimate $F_{k,n}$. Note that the difference in catch of a species between two fisheries is assumed to reflect differences in the fully selected fishing mortality rate, not differences in selectivity. This assumption was checked by comparing fishery size distributions, which were generally similar for a given species.

Model formulation

The total equilibrium yield over the lifespan of the cohort for an individual species is estimated as

$$(2)\qquad Y = \sum_{t=t_r}^{t_{\max}} \sum_{m=1}^{12} \left[\left(1 - e^{-(F_{t,m}+M_{t,m})}\right) \left(\frac{F_{t,m}}{F_{t,m}+M_{t,m}} \right) N_{t,m} W_{t,m} \right]$$

where time is measured in years (t) and months (m), and $M_{t,m}$, $F_{t,m}$, $N_{t,m}$, and $W_{t,m}$ are the natural mortality and fishing mortality rates, population size, and individual weight, respectively, at year t and month m. The monthly fishing mortality rate accrues from several fisheries:

© 2002 NRC Canada

$$(3) \qquad F_{k,t,m} = \sum_{n=1}^{n_{max}} \text{sel}_{t,m,k}[q_{k,n}(PE_{m,n} \times \text{effort})]$$

where effort is the total annual standardized trawling effort, $PE_{m,n}$ is the proportion of total annual effort exerted in month m by fishery n, $q_{k,n}$ is the catchability for the species k by fishery n, and $\text{sel}_{t,m,k}$ is the fishery selectivity that represents an age-dependent portion of F applied to the cohort. For the nonhalibut species, the selectivity terms were obtained from separable catch-at-age population models and represent age-specific modifiers to the fully selected instantaneous fishing mortality rate. Time series of recruitment values from the 1977 to 1996 year classes, obtained from NMFS catch-at-age assessment models, were used to scale the initial recruitment for rock sole, flathead sole, and Alaska plaice relative to that of yellowfin sole, the most abundant species. Age-specific values of weight and selectivity were converted to monthly values by assuming linear intra-annual increases, with the age-specific values corresponding to 1 January values.

Information on halibut selectivity and recruitment in the BSAI area is not readily available, as age-structured models are not currently used because the directed fishery is small and thus limits fishery-dependent information. Instantaneous annual natural mortality rate for halibut was set to 0.15 and the directed fishery selectivity curve was assumed to be equivalent to that estimated for area 3A, the central Gulf of Alaska (IPHC 2000). A selectivity curve for halibut trawl bycatch was estimated, along with the fully selected trawl bycatch fishing mortality rate, with an equilibrium model. This was achieved by constraining the total prerecruit mortality (ages 1–7) to be 0.20 (Clark and Hare 1998) and fitting the proportional catch-at-age to the observed proportional trawl bycatch age distributions; the latter was obtained from data on bycatch length compositions and an age–length key (W. Clark and S. Hare, IPHC, University of Washington, P.O. Box 95009, Seattle, WA 98145, U.S.A., personal communication). The resultant selectivity curve indicates that most trawl bycatch consists of juvenile halibut, whereas the directed halibut fishery has an age of 50% selectivity of approximately 12 years and is prohibited from retaining halibut <81 cm (Fig. 2).

The relative recruitment multiplier for halibut (age 1) was chosen to result in an age-8 halibut abundance that matched recent estimates in area 3A, as the BSAI area and area 3A recruitment are expected to contain approximately equal numbers of 8-year-olds (Clark and Hare 1998). Estimates of average 3A recruitment (age 8) from 1995 to 1997 range from 2.68×10^6 with a constant selectivity at age to 6.02×10^6 with a constant selectivity at length (Sullivan et al. 1999), and the relative recruitment multiplier chosen here produced an age-8 abundance of 4.35×10^6.

The management of halibut in the BSAI management area involves establishing a total quota based on a fixed proportion of the population, and deducting from that quota any legal-sized (>81 cm) halibut bycatch to calculate the directed fishery quota (Clark and Hare 1998). Although the total quota of 20% is used as a guideline, the exploitation rates of age 8+ halibut (roughly corresponding to legal halibut) in the BSAI have appeared to average approximately 5% in recent years (Table 1). Beginning in 1998, BSAI halibut biomass has been estimated by computing the ratio of BSAI longline survey biomass divided by area 3A survey biomass, and multiplying this ratio by the area 3A biomass estimate from an age-structured population model. This procedure results in BSAI estimates approximately equal to those in area 3A; for example, the 1999 and 2000 BSAI estimates were 88% and 112% of the area 3A estimates. BSAI halibut longline surveys were not conducted prior to the late 1990s, and the area 3A estimates from 1995 to 1997 were taken as estimates for the BSAI exploitable biomass. In the yield model, the exploitation rate of age-8+ halibut was constrained to be 5%, and a directed halibut fishing mortality rate was chosen for each level of trawl effort such that this exploitation rate was produced.

Fig. 2. Selectivity curves for the directed halibut fishery (from the Gulf of Alaska; solid line), and estimated for the Bering Sea – Aleutian Islands (BSAI) trawl bycatch of halibut (dotted line).

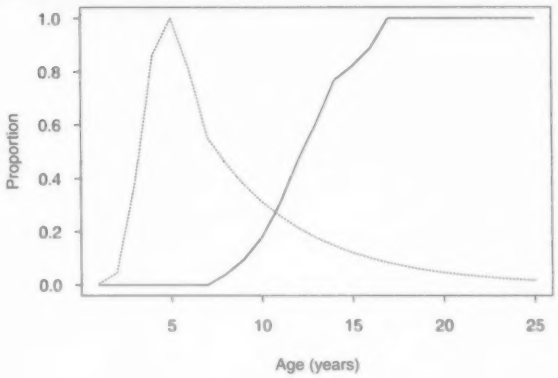

Because a portion of the halibut bycatch may survive upon release, the halibut discard mortality rate was estimated. In the yield calculations, the halibut bycatch yield refers to the bycatch mortality rather than the total amount caught. The expected mortality rate for the halibut caught in trawl gear, derived from tagging studies (Hoag 1975; Clark et al. 1992), ranges from 0.2 to 0.9, depending on the condition. Annual discard mortality rates were estimated for each vessel and an estimate for each fishery was computed as the average of all vessels in a fishery, weighted by each vessel's proportion of the total catch.

Two harvest reference points were used to evaluate benefits from the multispecies complex, each pertaining to a specific management goal. Often, the harvest goal for multispecies complexes is focused on obtaining a target aggregate yield or revenue (Murawski 1984; Pikitch 1987); this goal is represented here by the $f_{0.1}$ reference point, which is the fishing effort at the point where the slope of the tangent of the effort–yield curve is 10% of that at the origin. Alternatively, harvest reference points could be designed to minimize the likelihood of recruitment overfishing, as in the single-species $F_{40\%}$ policies (Clark 1991). An analogous goal in a multispecies situation would be fishing at an effort level, denoted f_{ws}, such that the fishing rate for the weakest stock does not exceed its $F_{40\%}$ rate. These two harvest policies, $f_{0.1}$ and f_{ws}, were used to obtain equilibrium yield under current conditions and under alternative assumptions regarding halibut

© 2002 NRC Canada

Table 1. Directed halibut catch and trawl fishery bycatch caps (t) for the Bering Sea and Aleutian Islands from 1995 to 1999, with estimated exploitation rates.

	Directed fishery						
Year	Quota[a]	Catch[a]	Trawl bycatch cap	Age-8+ trawl bycatch[b]	Total 8+ catch	Exploitable biomass[c]	Exploitation rate
1995	3572	2863	3775	2265	5128	159 026	0.032
1996	3572	3188	3775	2265	5453	157 235	0.035
1997	5429	5288	3775	2265	7553	151 944	0.050
1998	6333	5485	3775	2265	7750	137 079	0.057
1999	7641	7182	3675	2205	9387	84 412	0.111
Average							0.057

[a]From IPHC (2000).
[b]Estimated as 60% of the bycatch (based upon the proportion, by weight, of the bycatch mortality from 1990–1997 that was ≥age 8).
[c]1999 value is from the IPHC (1999), 1998 value is the area 3A value from the IPHC (1998), and 1995–1997 values are the area 3A values from Sullivan et al. (1999).

catchability, effort distribution by fishery, and halibut bycatch constraints.

Sensitivity of multispecies yield to model assumptions regarding halibut bycatch

The two commonly discussed strategies to reduce the catchability of halibut are reducing halibut gear selectivity via gear modifications (i.e., halibut excluder devices) and altering the distribution of fishing effort to avoid areas with high halibut bycatch. The effort levels at which the halibut mortality cap would be reached with various reductions in catchability was derived from eq. 3, where a proportional reduction in q, across all fisheries, can be compensated with a proportional increase in effort to obtain an identical halibut fishing mortality rate. Estimated flatfish yield at the effort levels associated with catchability reductions were obtained from the initial model run and compared to yield and effort levels at the two reference points.

An alternative to changing catchability is to concentrate effort primarily in those fisheries where the ratio of flatfish yield to halibut bycatch is high. Linear programming, an optimization tool designed for problems where the objective function and the system constraints are linear functions of the control variables (Brown et al. 1979; Murawski and Finn 1986; Taha 1987), was used to identify an optimal catch distribution among the fisheries, assuming that the species composition within fisheries is identical to that observed from 1995 to 1999. An advantage of linear programming is that it offers an evaluation of the halibut bycatch constraint relative to other single-species catch constraints, as indicated by the dual, or "shadow", prices. The shadow prices represent the expected increase in the objective function that would result from relaxing each constraint by one unit. Objective functions of either total flatfish catch or total revenue were considered. For example, the objective function of total flatfish catch was computed as

$$\sum_n \sum_k P_{k,n} x_n$$

where x_n is the total annual catch of fishery n (estimated as variables in the linear programming problem), and $P_{k,n}$ is the proportion of the annual fishery n catch consisting of flatfish species k (obtained from the catch estimates in eq. 1). The total catches for the four managed flatfish species were constrained by the equilibrium $F_{40\%}$ yields from the multispecies yield model, whereas halibut bycatch was constrained by the bycatch limit. To ensure that fisheries were not eliminated in the optimal solution, each fishery was constrained to catch at least 60% of the average catch observed from 1995 to 1999; the overall pattern of results are not particularly sensitive to the percentage of recent average catch used as a constraint.

Finally, an economic derivation of the halibut bycatch limit was considered. The existence of halibut bycatch imposes external costs on the halibut fishery from lost revenue (Thompson 1993). If the bycatch cap prematurely closes the groundfish fisheries that produce halibut bycatch, then a cost is imposed here as well. One reasonable choice of a halibut bycatch level would balance these two costs. The cost to the halibut fishery at each level of trawling effort is the reduction of revenue from that obtained if no halibut bycatch occurred. Similarly, the cost to the groundfish fishery is the reduction of total flatfish revenue from that obtained if no bycatch limit existed, and was estimated by subtracting the revenue of retained flatfish obtained at the bycatch limit from the revenue obtained at the $f_{0.1}$ and f_{ws} reference points. The calculation of flatfish revenue loss incorporated species retention rates obtained from the North Pacific Observer Database. Prices were obtained by averaging across the products within each species, weighted by catch, resulting in prices (dollars per kilogram unprocessed weight) of yellowfin sole, rock sole, flathead sole, Alaska plaice, and Pacific halibut of 0.42, 2.09, 0.84, 0.51, and 3.31, respectively (T. Lee, NMFS–AFSC, 7600 Sand Point Way NE, Seattle, WA 98115, U.S.A., personal communication).

Results

The estimated average catch, by species, of each of the four flatfish fisheries from 1995 to 1999 indicates the multispecies nature of the EBS flatfish fisheries (Table 2). For example, rock sole and flathead sole composed 43% and 32% of their target fisheries, respectively, whereas all other flatfish species composed 24% of the rock sole fishery and 27% of the flathead sole fishery. The species compositions of the Alaska plaice and yellowfin sole fisheries are influenced by the requirement that yellowfin sole contributes >70% of the total flatfish catch in the yellowfin sole fishery. Because yellowfin sole and Alaska plaice often co-occur spatially, the Alaska plaice fishery is composed largely of these two spe-

© 2002 NRC Canada

Table 2. Estimated average annual harvest (t) of various species in eastern Bering Sea flatfish fisheries from 1995 to 1999.

	Target fishery				
Species caught	Alaska plaice	Flathead sole	Rock sole	Yellowfin sole	Total
Rock sole	2 100	2 174	37 094	5 586	46 954
Yellowfin sole	11 801	3 985	14 172	101 724	131 682
Flathead sole	1 494	8 753	2 730	2 597	15 574
Alaska plaice	7 344	1 277	2 739	7 400	18 761
Other flatfish	83	35	656	275	1 049
Arrowtooth flounder (*Atheresthes stomias*)	554	1 748	661	845	3 808
Pacific cod	2 252	2 740	11 208	6 917	23 118
Pollock	3 637	3 311	9 579	13 894	30 421
Other fish	2 403	3 278	6 983	8 806	21 471
Total	31 667	27 301	85 822	148 046	292 836

Note: Other flatfish refers to flatfish other than rock sole, yellowfin sole, flathead sole, and Alaska plaice, whereas other fish refers to any species not listed.

cies. Owing to the higher standard for the definition of directed fishing on yellowfin sole, this fishery consists primarily of its target species.

Both catchability (Table 3) and standardized effort (Table 4) affect the harvest of flatfish species, and these two components determine the effect of individual fisheries on halibut bycatch. For example, the yellowfin sole fishery has a relatively low catchability of halibut but high levels of effort (Fig. 3), and is thus a significant source of bycatch mortality. In contrast, flathead sole has a relatively high halibut catchability but lower levels of effort, and rock sole is intermediate in both catchability and effort. The bottom trawl pollock and Pacific cod (*Gadus macrocephalus*) fisheries may be examined for comparison (see Fig. 3). These two fisheries each have substantial amounts of raw effort (also shown in Table 4), but the standardized effort for the pollock fishery is lower because of its ability to avoid flatfish bycatch.

The annual average standardized effort in the BSAI trawl fishery was estimated as 84 061 h (Table 4). Approximately 29% of this effort consisted of the Pacific cod fishery effort, with 24% and 17% in the yellowfin sole and rock sole fisheries, respectively. With the exception of the yellowfin sole fishery, most flatfish fisheries had little effort concentrated in the final quarter of the year. Sixty-one percent of the rock sole fishery effort was concentrated in the first quarter, reflecting the valuable roe fishery on spawning females. The flathead sole and Alaska plaice fisheries had 89% and 80% of their effort concentrated in the second and third quarters, respectively.

The spawning stock biomass (SSB), yield, and instantaneous fishing mortality rate may be shown as a function of total standardized fishing effort across all fisheries (Fig. 4). The yellowfin sole single-species $F_{40\%}$ occurs at a lower level of standardized effort than rock sole, flathead sole, and Alaska plaice $F_{40\%}$ values. This is due to considerable effort in the yellowfin sole fishery and relatively high yellowfin sole catchability in the yellowfin sole and Alaska plaice fisheries. Thus, the yellowfin sole are the weakest stock in the complex, in that they would be the most susceptible to having their fishing rate exceed $F_{40\%}$ under the current conditions. For the flatfish complex, harvesting at the f_{ws} reference point produces an equilibrium yield of 243 kt (units in metric tons), whereas the $f_{0.1}$ reference point produces a yield of 366 kt. The level of standardized effort at which the halibut mortality meets the cap level of 3675 t for the EBS trawl fisheries was 103 000 h (see Fig. 4, which includes yield and SSB levels associated with effort levels ≥103 000 h).

The yield curves do not show clear peaks, but instead are either flat topped or asymptotically increasing (Fig. 4). This condition is related to the generally slow growth of flatfish relative to their natural mortality rates and the low fishing selectivity during the first several years of the cohort. For yellowfin sole and rock sole, the ratio of the von Bertalanffy parameter K to instantaneous natural mortality (M) is approximately unity, whereas this ratio drops to 0.75 and 0.56 for flathead sole and Alaska plaice, respectively. The age at 50% fishery selectivity ranges from approximately 7.5 years in rock sole to 12 years in flathead sole.

Based on current estimates of catchability coefficients and relative recruitment multipliers, substantial reductions in halibut catchability would be necessary to avoid limitation by the current halibut cap of 3675 t (Fig. 5). The f_{ws} reference point is obtained at 122 000 h of standardized effort, an 18% increase from the 103 000 h where the halibut cap is obtained. Thus, the halibut catchability coefficient would need to be multiplied by a factor of 1/1.18, or 0.85, to harvest at the f_{ws} reference point without exceeding the halibut cap. In contrast, the $f_{0.1}$ reference point is obtained at 315 000 h of standardized effort, requiring that the halibut catchability coefficients be multiplied by a factor of 1/3.06, or 0.33, to harvest at this reference point without exceeding the halibut cap.

The linear programming analysis indicated that, with an objective function of maximizing total flatfish catch, the Alaska plaice fishery harvest would be expanded to approximately six times its baseline level observed from 1995 to 1999 (Fig. 6). The substantial increase in the Alaska plaice fishery is explained by the small portion of nonflatfish in this fishery, the low catch rate of halibut, and the low baseline levels of catch. Although the catch in the Alaska plaice and yellowfin sole fisheries are primarily flatfish (72% and 79%, respectively), the high baseline catch level of the yellowfin sole fishery and its high percentage of yellowfin sole (69%) likely preclude this fishery from being substantially expanded without reaching the yellowfin sole harvest limit. In contrast, the optimal catch by fishery under the objective function of maximizing flatfish revenue would in-

© 2002 NRC Canada

Table 3. Catchability coefficients for various flatfish species, by fishery.

Fishery	Species				
	Yellowfin sole	Rock sole	Flathead sole	Alaska plaice	Pacific halibut
Atka mackerel (*Pleurogrammus monopterygius*)	8.08×10^{-11}	8.87×10^{-09}	4.38×10^{-09}	2.20×10^{-11}	2.47×10^{-07}
Alaska plaice	1.68×10^{-06}	2.70×10^{-07}	9.76×10^{-07}	3.64×10^{-06}	4.54×10^{-07}
Pollock (bottom trawl)	2.56×10^{-07}	3.53×10^{-07}	9.66×10^{-07}	1.23×10^{-07}	7.99×10^{-07}
Pacific cod	8.11×10^{-09}	1.34×10^{-07}	1.85×10^{-07}	6.34×10^{-09}	7.18×10^{-07}
Other flatfish	4.79×10^{-08}	1.03×10^{-07}	3.17×10^{-07}	3.62×10^{-08}	1.26×10^{-06}
Rockfish (*Sebastes* spp.)	4.24×10^{-11}	6.41×10^{-09}	1.77×10^{-08}	0.00×10^{00}	5.35×10^{-07}
Flathead sole	4.47×10^{-07}	2.20×10^{-07}	4.50×10^{-06}	4.98×10^{-07}	1.10×10^{-06}
Other fish	6.94×10^{-08}	9.45×10^{-08}	4.17×10^{-07}	3.26×10^{-08}	9.73×10^{-07}
Pollock (pelagic trawl)	3.54×10^{-08}	8.63×10^{-08}	1.39×10^{-06}	5.14×10^{-09}	2.75×10^{-07}
Rock sole	5.34×10^{-07}	1.26×10^{-06}	4.72×10^{-07}	3.59×10^{-07}	8.98×10^{-07}
Sablefish (*Anoplopoma fimbria*)	0.00×10^{00}	0.00×10^{00}	2.28×10^{-07}	0.00×10^{00}	1.55×10^{-06}
Turbot (*Reinhardtius hippoglossoides*)	4.29×10^{-10}	2.75×10^{-09}	2.09×10^{-07}	7.90×10^{-10}	1.16×10^{-06}
Arrowtooth flounder	8.91×10^{-09}	5.06×10^{-08}	6.62×10^{-07}	4.86×10^{-09}	1.52×10^{-06}
Yellowfin sole	2.83×10^{-06}	1.40×10^{-07}	3.32×10^{-07}	7.16×10^{-07}	3.16×10^{-07}

Note: Other flatfish refers to flatfish other than rock sole, yellowfin sole, flathead sole, and Alaska plaice, whereas other fish refers to any species not listed.

Table 4. Estimated average standardized trawl effort and raw effort (in parentheses), measured in hours, from 1995 to 1999, by fishery and quarter, in the eastern Bering Sea and Aleutian Islands.

Fishery	Quarter				
	1	2	3	4	Total
Atka mackerel	2281	2149	462	254	5147
	(1867)	(1190)	(791)	(316)	(4165)
Alaska plaice	567	1473	1623	226	3889
	(536)	(922)	(3037)	(308)	(4803)
Pollock (bottom trawl)	2685	1463	1045	397	5591
	(7772)	(1088)	(8080)	(7053)	(23 992)
Pacific cod	10 560	13 002	108	301	23 970
	(15 157)	(11 188)	(228)	(565)	(27 138)
Other flatfish	20	60	8	4	91
	(21)	(45)	(20)	(7)	(93)
Rockfish	466	441	148	69	1125
	(376)	(250)	(270)	(82)	(978)
Flathead sole	435	2647	1734	125	4941
	(450)	(1791)	(3494)	(187)	(5922)
Other fish	169	414	24	42	649
	(191)	(286)	(100)	(110)	(688)
Pollock (pelagic trawl)	564	5	764	368	1701
	(17 053)	(119)	(29 705)	(10 272)	(57 149)
Rock sole	8966	4141	1464	138	14 710
	(8982)	(2476)	(2516)	(204)	(14 177)
Sablefish	0	5	1	1	7
	0	(3)	(2)	(1)	(6)
Turbot	19	551	98	38	706
	(15)	(467)	(206)	(57)	(745)
Arrowtooth flounder	102	1118	294	122	1636
	(91)	(791)	(589)	(212)	(1682)
Yellowfin sole	1835	8594	5090	4381	19 900
	(1702)	(4881)	(8991)	(5192)	(20 766)
Total	28 669	36 062	12 864	6467	84 061
	(54 212)	(25 497)	(58 029)	(24 567)	(162 305)

Note: Other flatfish refers to flatfish other than rock sole, yellowfin sole, flathead sole, and Alaska plaice, whereas other fish refers to any species not listed.

© 2002 NRC Canada

Fig. 3. Pacific halibut catchability (× 10^6) and standardized fishing effort for selected fisheries in the eastern Bering Sea, 1995–1999.

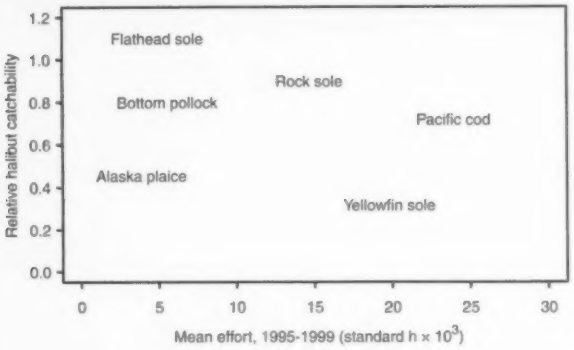

crease the valuable rock sole fishery and slightly increase the yellowfin sole fishery, while decreasing the Alaska plaice fishery.

The shadow prices from the linear programming analysis, under the objective function of maximizing flatfish catch, indicates that the halibut bycatch constraint is considerably more restrictive than any of the flatfish harvest constraints (Table 5). Increasing the halibut bycatch cap by one metric ton at the optimal solution would yield an additional 30 t of flatfish. This high shadow price reflects the increased yield of three species, whereas the shadow prices on each of the nonhalibut catch constraints reflect the increased yield of a single species. At the optimal solution, only yellowfin sole is constrained by its own catch constraint, whereas rock sole, flathead sole, and Alaska plaice are constrained by the halibut cap and thus have shadow prices of zero.

Under the assumed relative recruitment multipliers, a halibut bycatch limit of approximately 3440 t approximately balances the foregone revenue to the halibut fishery and the flatfish fisheries, where the f_{ws} effort level is used to define foregone flatfish revenue (Fig. 7). With no halibut bycatch, the modeled revenue of the halibut fishery was $44.4 M, whereas the revenue at a halibut cap of 3440 t is $26.7 M, resulting in $17.7 M in foregone revenue. Similarly, the flatfish revenue at the f_{ws} reference point was $116.1 M, whereas the revenue at the effort level associated with a cap of 3440 t was $98.7 M. When the $f_{0.1}$ policy is used, a halibut cap of 5749 t balances the foregone revenue. Note that as the bycatch fishing mortality increases, the directed fishery is forced to reduce their exploitation rates to maintain a constant exploitation rate of 5%. At high levels of bycatch mortality rates it is not possible to obtain this exploitation rate, and the directed halibut fishery is eliminated (Fig. 7).

Discussion

The yield curves and recent harvest levels for BSAI flatfish indicate the conservatism in their management, and the two aggregate reference points presented here reflect different views toward the management of species complexes. The management choices for mixed-species fishery systems fall along a continuum with maximization of aggregate yield at one extreme, and full protection with no harvesting at the other (Pikitch 1995). The $f_{0.1}$ reference point follows previous modeling of harvesting species complexes, in which an aggregate output (yield, net revenue, or gross revenue) of the complex is maximized (Murawski 1984; Pikitch 1987; Marchal and Horwood 1996). Except in unusually rare circumstances, this would result in a least one species in the complex being harvested at a rate greater than recommended under single-species management, thus posing problems for U.S. fisheries because of the requirement under the Magnuson–Stevens Fisheries Conservation Act to avoid overfishing. The precautionary approach, as applied to BSAI flatfish, specifies a harvest rate of $F_{40\%}$ as a target to be achieved, whereas $F_{35\%}$ is viewed as an overfishing limit to be avoided. Under these definitions, the $f_{0.1}$ effort level here

Fig. 4. Equilibrium spawning stock biomass (SSB) (*a*), yield (*b*), and fishing mortality (*c*) as a function of standardized fishing effort for four flatfishes in the eastern Bering Sea in 1995–1999. △, single-species $F_{40\%}$ reference points; ▲, aggregate nonhalibut yield associated with f_{ws} reference points; ❑, aggregate nonhalibut yield associated with $f_{0.1}$ reference points. Asterisks represent the observed mean levels of effort, yield, and F from 1995 to 1999. Bold portions of the yield and SSB curves correspond to levels of effort ≥103 000 h, which would exceed the halibut bycatch cap of 3675 t.

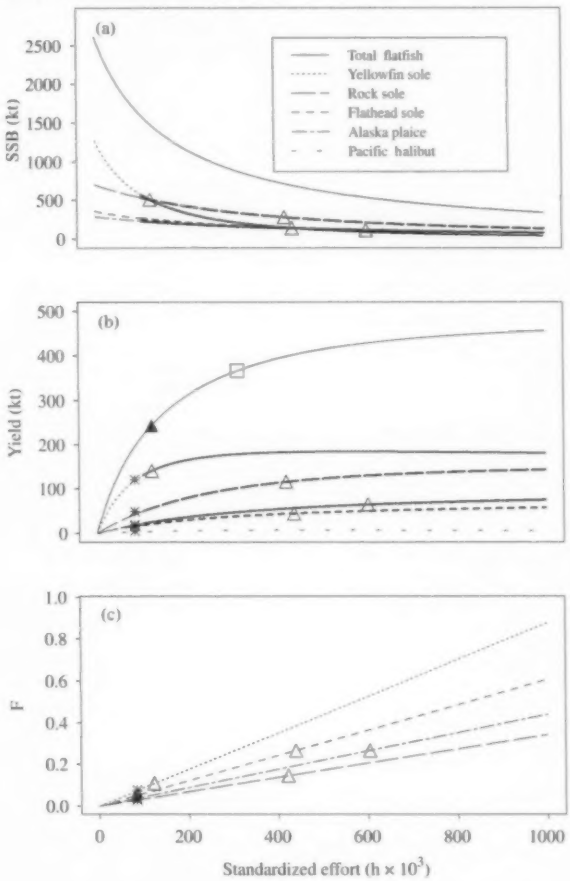

© 2002 NRC Canada

Fig. 5. Yield of flatfish at the Bering Sea – Aleutian Islands (BSAI) trawl halibut bycatch quota of 3675 t with various reductions in halibut catchability.

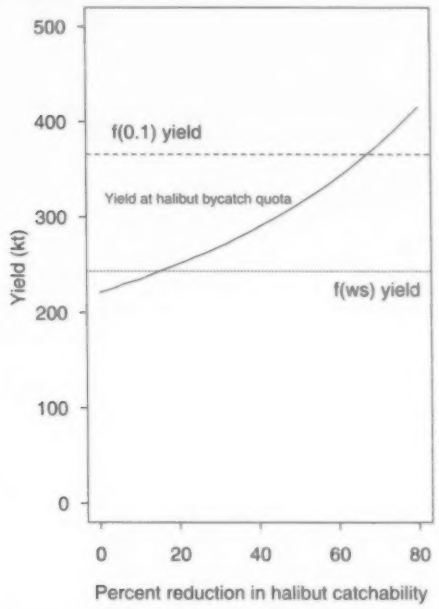

Fig. 6. Distribution of total catch of flatfish by fishery, as determined by linear programming, compared with observed distribution of catch by fishery from 1995 to 1999. The objective function of maximizing total flatfish catch is shown as clear bars, whereas maximization of total revenue is shown as diagonally shaded bars; average flatfish catch by fishery, from 1995 to 1999, is shown by solid bars. A, Atka mackerel; AK, Alaska plaice; B, bottom trawl pollock; C, Pacific cod; F, other flatfish; K, rockfish; L, flathead sole; O, other fish; P, pelagic trawl pollock; R, rock sole; S, sablefish; T, turbot; W, arrowtooth flounder; and Y, yellowfin sole.

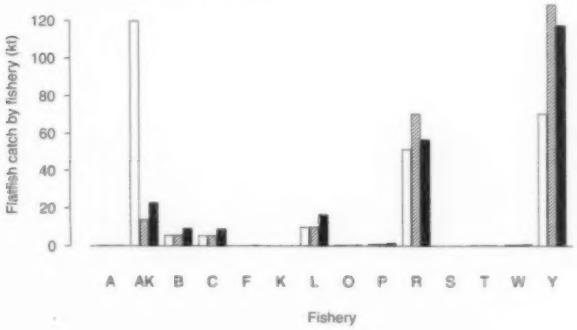

would overfish the yellowfin sole stock, whereas the f_{ws} effort level would not achieve the targets for most flatfish. While it is clear that flatfish discussed here are interrelated and may form a functional management unit, balancing the dual objectives of achieving the optimal yield from the stock complex without overfishing any of the individual stocks is a current point of discussion regarding interpretation of the

Table 5. Shadow prices from the linear programming analysis determining the optimal catch among fisheries, given the single-species harvest constraints, the halibut bycatch constraint, and an objective function of maximizing total catch.

Constraint	Shadow price
Yellowfin sole catch quota	1.57
Rock sole catch quota	0
Flathead sole catch quota	0
Alaska plaice catch quota	0
Pacific halibut bycatch limit	29.61

Fig. 7. Foregone revenue to the flatfish trawl fisheries and the directed halibut fishery. Foregone revenue to the flatfish trawl fisheries (dotted lines) was measured as the positive difference between the flatfish revenue at the halibut cap and the potential revenue available at either the f_{ws} or $f_{0.1}$ reference points. Foregone revenue to the directed halibut fishery (solid line) was measured as difference between the halibut revenue obtained with no bycatch and that obtained at the halibut bycatch cap. High bycatch levels may limit or preclude the halibut directed fishery mortality rate (dashed line) to maintain a constant total exploitation rate of 5%.

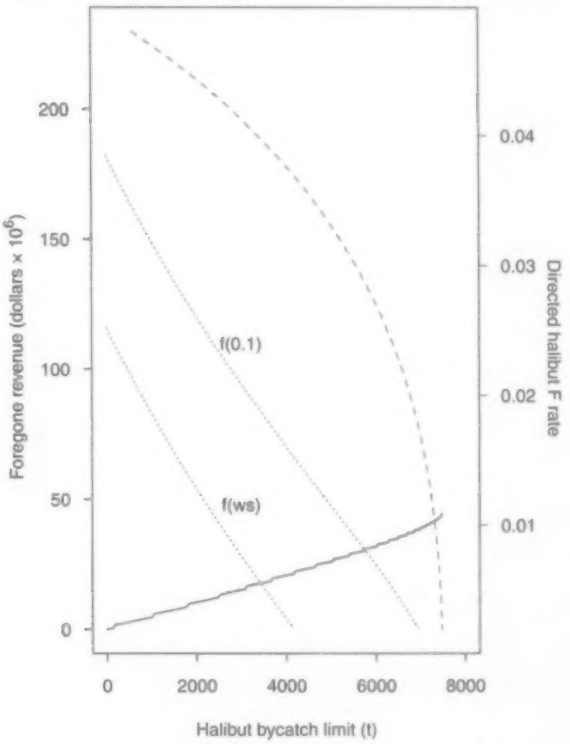

Magnuson–Stevens Fisheries Conservation Act. One potentially effective approach may be to underexploit stocks in cases where we know relatively little about the marine ecosystem and the effects of fishing upon it (Mace 1999).

© 2002 NRC Canada

In contrast to the model presented here, the actual halibut bycatch limit is not implemented as single quantity applied to the sum of BSAI trawl fisheries, but is apportioned among the separate fisheries. The definition of fisheries used here is relatively crude, and is based upon those used by the North Pacific Fishery Management Council to apportion halibut bycatch limits. Recent work on characterizing fishing activities at finer levels of resolution could improve management activities. For example, Pelletier and Ferris (2000) describe fishing tactics based upon multivariate analyses of catch composition, gear, area, and season; other studies have related multivariate analyses of catch composition to easily measured quantities such as season, depth, area, and vessel characteristics (Lewy and Vinther 1994). Regulation of harvest quotas in the BSAI operates primarily by preventing the retention of particular species above specified proportions, and more detailed definitions of fishing strategies will allow more closely focused management on the portions of fishing effort that have the greatest mortality impacts on a particular species.

Fishery management in the North Pacific is perhaps unique in that relatively extensive observer coverage provides reasonable real-time estimates of both retained and discarded catch. This information allows for in-season management that is primarily focused on total catch output (across all fisheries) rather than on effort and gear restrictions by fishery. The linear programming analysis used here is useful in determining the significance of the halibut bycatch constraint, although the logical extension of this analysis—emphasis on particular fisheries—would represent a significant departure from current practices. Indeed, studies on technical interactions often seek an optimal effort level and mesh size, either for a single fishery (Sainsbury 1984; Pikitch 1987) or for multiple fisheries (Murawski 1984; Marchal and Horwood 1996), with respect to some aggregate measure across species. The focus on catch enumeration and limits in the North Pacific has appeared to keep harvest rates fairly conservative, notwithstanding errors in biomass estimates, and the linear programming analysis is intended to illustrate the nature of the multispecies multifishery system and not suggest regulation of effort by fishery. Any benefits from the reallocation of trawl effort from nonflatfish to flatfish fisheries would be tempered unless the fishery-specific halibut caps were also redistributed. Further, this activity would require diverting effort from the relatively lucrative cod and pollock fisheries, as the target species of these fisheries were not considered in this analysis.

The use of foregone revenue in evaluating suitable halibut bycatch limits was motivated more by the distribution of benefits, rather than the total benefits, of the halibut and groundfish fisheries, as this procedure ensures that both sectors remain in existence. Flatfish revenue changes much more rapidly with halibut bycatch than halibut revenue, and a more traditional analysis using marginal revenue curves to maximize joint revenue from both sectors, as suggested by Thompson (1993), would greatly restrict or eliminate the halibut fishery in the BSAI. Extrapolation of revenue at effort levels greatly different than those recently observed is tenuous because the assumption of constant price will not likely hold, and price functions for BSAI flatfish have not been developed. Considering the economic importance of halibut bycatch to both the halibut fishery and the flatfish fisheries, more detailed economic data would help inform management decisions.

The estimates of a suitable halibut bycatch limit with fixed levels of catchability, or of reductions in catchability required to avoid a fixed limit, in this study are clearly influenced by the halibut population size. Thus, focusing on gear restrictions with a fixed bycatch limit may result in no restrictions being necessary with low population sizes, and extensive restrictions required with high population sizes. One approach to mitigate this effect may be to allow market forces to identify a suitable level of bycatch. Halibut have been managed under an individual transferable quota (ITQ) system since 1995, and the price per halibut quota gives an indication of the marginal benefit of halibut. For example, Terry (1998) used ITQ quota price information to estimate the marginal benefit of halibut as $\$2481 \cdot t^{-1}$. Economic theory suggests that establishing a fee for trawlers equal to this marginal benefit would produce an economically efficient level of bycatch (Marasco and Terry 1982; Terry 1998), although this procedure does not explicitly consider the distribution of benefits between the halibut fishery and the flatfish fisheries. Irrespective of the criteria used to establish halibut bycatch limits, it seems reasonable to vary the limits with population size (Salveson at al. 1992). The current limits were derived primarily from non-U.S. fisheries prior to the late 1980s (Thompson 1993) and may not be reflective of current economic and biological conditions. For example, the BSAI trawl bycatch limits have decreased since the early 1990s, whereas our perception of halibut population size has dramatically increased (Sullivan et al. 1999).

An extension to the model would be to compute equilibrium recruitment from a stock–recruitment relationship rather than assume constant recruitment. Simple stock–recruitment models for EBS flatfish generally show overcompensation, such that increases in fishing mortality at high stock sizes reduce stock size and increase recruitment. For this reason, modeled yield curves incorporating the available stock–recruitment relationships generally show the same flat-topped or asymptotically increasing patterns over effort levels of up to five times those of recent averages. However, it is unknown how the apparent stock–recruitment relationships are affected by environmental variability. The pattern of increasing stock size and decreasing recruitment for several flatfish could be influenced by temporal variations in environmental conditions, as indexed by measures like the Arctic oscillation (Hare and Mantua 2000). The influence of environmental variability may be important for EBS flatfish, and is thought to play a major role in driving recruitment variability for Pacific halibut (Clark et al. 1999). Evaluation of recruitment models that consider stock size and environmental variability is a priority for EBS flatfish.

The model presented in this study provides a preliminary description of how the fishing mortalities of several EBS flatfish, including Pacific halibut, are affected by trawling effort, and should be useful in assessing additional strategies for reducing bycatch. For example, although the selectivity ogives for a particular species did not vary by fishery, this could be easily incorporated to consider fishery-specific management measures as more detailed information becomes available. Flatfish harvest levels have typically been

© 2002 NRC Canada

set below their $F_{40\%}$ values in recent years, in recognition that the $F_{40\%}$ levels are typically not attainable with current bycatch limits. The multispecies multifishery model developed here could help inform this quota-setting procedure, although, of course, it is clear that the system is not in equilibrium. In addition to recruitment, species distribution and fishermen behaviour would also be expected to change over time. The underlying biological cause of bycatch is co-distribution of species, and the relationships of species distribution to environmental variables (Murawski and Finn 1988; Gabriel 1992) have not been fully evaluated for EBS flatfish. EBS flatfish usually share a similar habitat and have overlapping distributions in the continental shelf waters, and possible functional interactions may be reflected in diet overlaps and trophic interactions (Zhang et al. 1998). Finally, fishing effort may be redistributed as the matrix of catchability coefficients and (or) species value change (Laurec et al. 1991). Further research in each of these areas will add to our knowledge of the multispecies multifishery system in the eastern Bering Sea.

Acknowledgements

We thank Bill Clark and Steve Hare for providing halibut bycatch data, and Grant Thompson, Joe Terry, Jim Ianelli, Ron Felthoven, Anne Hollowed, Billy Ernst, and Steven Cadrin for their helpful comments on earlier versions of this work.

References

Beverton, R.J.H., and Holt, S.J. 1957. On the dynamics of exploited fish populations. Fish. Invest. (Ser. 2), No 19. U.K. Ministry of Agriculture, Fisheries and Food, London.

Brown, B.E., Brennan, J.A., and Palmer, J.E. 1979. Linear programming simulations of the effects of bycatch on the management of mixed-species fisheries off the northeastern coast of the United States. Fish. Bull. **76**: 851–860.

Clark, W.G. 1991. Groundfish exploitation rates based upon life-history parameters. Can. J. Fish. Aquat. Sci. **48**: 734–750.

Clark, W.G., and Hare, S.R. 1998. Accounting for bycatch in the management of the Pacific halibut fishery. N. Am. J. Fish. Manag. **18**: 809–821.

Clark, W.G., Hoag, S.H., Trumble, R.J., and Williams, G.H. 1992. Re-estimation of survival for trawl-caught halibut released in different condition factors. International Pacific Halibut Commission, Report of Assessment and Research Activities, **92**: 197–206.

Clark, W.G., Hare, S.R., Parma, A.M., Sullivan, P.J., and Trumble, R.J. 1999. Decadal changes in growth and recruitment of Pacific halibut (*Hippoglossus stenolepis*). Can. J. Fish. Aquat. Sci. **56**: 242–252.

Cochran, W.G. 1977. Sampling techniques. 3rd ed. Wiley, New York.

French, R., Nelson, R., Jr., and Wall, J. 1982. Role of the United States Observer Program in management of foreign fisheries in the Northeast Pacific ocean and eastern Bering Sea. N. Am. J. Fish. Manag. **2**: 122–131.

Gabriel, W.L. 1992. Persistence of demersal fish assemblages between Cape Hatteras and Nova Scotia, northwest Atlantic. J. Northw. Atl. Fish. Sci. **14**: 29–46.

Gauvin J.R., Haflinger, K., and Nerini, M. 1995. Implementation of a voluntary bycatch avoidance program in the flatfish fisheries of the eastern Bering Sea. *In* Solving bycatch: considerations for today and tomorrow. Alaska Sea Grant College Program Report No. 96-03. University of Alaska, Fairbanks. pp. 79–86.

Hare, S.M., and Mantua, N.J. 2000. Empirical evidence for North Pacific regime shifts in 1977 and 1989. Prog. Oceanogr. **47**: 103–145.

Hoag, S.H. 1975. Survival of halibut released after capture by trawls. Int. Pac. Halibut Comm. Sci. Rep. No. 57.

International Pacific Halibut Commission (IPHC). 1998. Pacific halibut stock assessment and fishery evaluation. *In* Stock assessment and fishery evaluation report for the groundfish resources of the Bering Sea/Aleutian Islands regions. North Pacific Fishery Management Council, Anchorage, Alaska. pp. 561–592.

International Pacific Halibut Commission (IPHC). 1999. Pacific halibut stock assessment and fishery evaluation. *In* Stock assessment and fishery evaluation report for the groundfish resources of the Bering Sea/Aleutian Islands regions. North Pacific Fishery Management Council, Anchorage, Alaska. pp. 655–692.

International Pacific Halibut Commission (IPHC). 2000. Pacific halibut stock assessment and fishery evaluation. *In* Stock assessment and fishery evaluation report for the groundfish resources of the Bering Sea/Aleutian Islands regions. North Pacific Fishery Management Council, Anchorage, Alaska. pp. 545–582.

Laurec, A., Biseau, A., and Charuau, A. 1991. Modelling technological interactions. ICES Mar. Sci. Symp. **193**: 225–236.

Lewy, P., and Vinther, M. 1994. Identification of Danish North Sea trawl fisheries. ICES J. Mar Sci. **51**: 263–272.

Mace, P.M. 1999. Current status and prognosis for marine capture fisheries. Fisheries, **24**(3): 30.

Marasco, R.J., and Terry, J.M. 1982. Controlling incidental catch: an economic analysis of six management options. Mar. Policy, **6**: 131–139.

Marchal, P., and Horwood, J. 1996. Long-term targets for the Celtic Sea mixed-species multi-métiers fisheries. Aquat. Living Resour. **9**: 81–94.

Murawski, S.A. 1984. Mixed-species yield-per-recruitment analyses accounting for technological interactions. Can. J. Fish. Aquat. Sci. **41**: 897–916.

Murawski, S.A., and Finn, J.T. 1986. Optimal effort allocation among competing mixed-species fisheries, subject to fishing mortality constraints. Can J. Fish. Aquat. Sci. **45**: 1720–1735.

Murawski, S.A., and Finn, J.T. 1988. Biological bases for mixed-species fisheries: species co-distribution in relation to environmental and biotic variables. Can J. Fish. Aquat. Sci. **45**: 1720–1735.

Murawski, S.A., Lange, A.M., and Iodine, J.S. 1991. An analysis of technological interactions among Gulf of Maine mixed-species fisheries. ICES Mar. Sci. Symp. **193**: 237–252.

Pelletier, D., and Ferris, J. 2000. A multivariate approach for defining fishing tactics from commercial catch and effort data. Can. J. Fish. Aquat. Sci. **57**: 51–65.

Pikitch, E.K. 1987. Use of a mixed-species yield-per-recruit model to explore the consequences of various management policies for the Oregon flatfish fishery. Can. J. Fish. Aquat. Sci. **44**(Suppl. 2): 349–359.

Pikitch, E.K. 1995. Objectives for biologically and technically related fisheries. *In* Fisheries science and management: objectives and limitations. *Edited by* W.S. Wooster. Lecture notes on coastal and estuarine studies, Vol. 28. Springer-Verlag, Berlin. pp. 107–136.

Sainsbury, K.J. 1984. Optimal mesh size for tropical multispecies trawl fisheries. J. Cons. Int. Explor. Mer, **41**: 129–139.

Salveson, S., Leaman, B.M., Low, L.-L., and Rice, J.L. 1992. Report of the Halibut Bycatch Work Group. Int. Pac. Halibut Comm. Tech. Rep. No. 25.

Shepherd, J.G. 1988. An exploratory method for the assessment of multispecies fisheries. J. Cons. Int. Explor. Mer, **44**: 189–199.

© 2002 NRC Canada

Sullivan, P.J., Parma, A.M., and Clark, W.G. 1999. The Pacific halibut stock assessment of 1997. Int. Pac. Halibut Comm. Sci. Rep. No. 79.

Taha, H.A. 1987. Operations research: an introduction, 4th ed. MacMillan, New York.

Terry, J.M. 1998. Halibut bycatch in the Alaska groundfish fishery. *In* Managing the nation's bycatch: programs, activities, and recommendations for the National Marine Fisheries Service. National Atmospheric and Oceanic Administration, U.S. Department of Commerce (NOAA–DOC), Washingtion, D.C. pp. 148–151.

Thompson, G. 1993. Compensating for harvest externalities in the management of interjurisdictional fisheries. *In* Proceedings of the international symposium on management strategies for exploited fish populations, 21–24 October 1992, Anchorage, Alaska. *Edited by* G. Kruse, D.M. Eggers, R.J. Marasco, C. Pautzke, and T.J. Quinn, II. Alaska Sea Grant College Program Report No. 93-02, University of Alaska, Fairbanks. pp. 723–744

Zhang, C.I., Wilderbuer, T.K., and Walters,G.E. 1998. Biological characteristics and fishery assessment of Alaska plaice, *Pleuronectes quadrituberculatus*, in the eastern Bering Sea. Mar. Fish. Rev. **60**(4): 16–27.

© 2002 NRC Canada

The effect of visual isolation on territory size and population density of juvenile rainbow trout (*Oncorhynchus mykiss*)

I. Imre, J.W.A. Grant, and E.R. Keeley

Abstract: Visibility is thought to affect the territory size of visually oriented animals but there have been few experimental tests of the hypothesis. We re-examined the relationship between visibility and territory size in juvenile salmonids to test the hypothesis that increasing habitat heterogeneity results in a reduction in territory size and consequently in higher population densities. Equal densities of young-of-the-year rainbow trout (*Oncorhynchus mykiss*) were stocked in two experimental treatments with low visibility and a control treatment with high visibility. Visibility was decreased by placing large stones or plywood dividers onto the substrate of experimental stream channels. As predicted, the size of individual territories decreased with decreasing visibility of the habitat. However, the treatments did not differ significantly in population density or growth rate of the fish. While this study confirms the inverse relationship between habitat visibility and territory size, the decrease in territory size did not produce an increase in population density of juvenile salmonids.

Résumé : La visibilité affecte, croit-on, la taille du territoire chez les animaux qui s'orientent par la vue, bien qu'il y ait peu de vérifications expérimentales de cette hypothèse. Nous avons examiné de nouveau la relation qui existe entre la visibilité et la taille du territoire chez des jeunes salmonidés dans le but d'éprouver l'hypothèse selon laquelle une hétérogénéité accrue de l'habitat réduit la taille du territoire et, par conséquent, permet des densités de population plus élevées. Nous avons établi des densités égales de jeunes truites arc-en-ciel (*Oncorhynchus mykiss*) de l'année dans deux sites expérimentaux à visibilité réduite et un site témoin à visibilité élevée. De grosses pierres ou des panneaux de contre-plaqué placés sur le substrat des ruisseaux artificiels ont servi à diminuer la visibilité. Tel que prédit, la taille des territoires individuels diminue lorsque la visibilité dans l'habitat est réduite. Cependant, il n'en résulte pas de différences dans la densité de population, ni dans le taux de croissance des poissons. Bien que notre étude confirme l'existence d'une relation inverse entre la visibilité dans l'habitat et la taille du territoire, la réduction de la taille du territoire n'entraîne pas d'augmentation de la densité de population chez les jeunes salmonidés.

[Traduit par la Rédaction]

Introduction

Optimal territory size models (reviewed in Schoener 1983, 1987) have primarily been concerned with predicting how territory size changes in relation to two fundamental factors: food abundance and intruder pressure. Consistent with the predictions of these models, territory size typically increases with decreasing food density (e.g., Stimson 1973; Dill et al. 1981; Hixon 1981) and intruder pressure (e.g., Slaney and Northcote 1974; Myers et al. 1979; Tricas 1989) in a wide variety of taxa.

In addition to food abundance and competitor density, Eason and Stamps (1992) hypothesized that the visibility of the environment will affect the territory size of visually oriented animals via three mechanisms. First, low visibility may physically constrain an animal to defend a smaller area simply because it cannot see intruders at a distance. Second, the distance at which a central-place forager can detect prey may be reduced so that there is no benefit to defending a large feeding territory in a low-visibility habitat. Third, in a low-visibility environment, territory holders may have to increase their patrol rates to detect and drive out intruders (Eason and Stamps 1992). Any delay in detecting intruders will lead to a greater loss of resources to the intruder and an increase in the cost required to expel the intruder, who quickly begins to feel "at home" on the territory (e.g., Krebs 1982). Such increases in the cost of defense will decrease the optimal territory size (see Schoener 1983, 1987).

Although several previous studies have suggested that habitat visibility affects territory size (reviewed in Eason and Stamps 1992), the experimental evidence to test this hypothesis is scarce. Perhaps the best evidence is that juvenile lizards (*Anolis aeneus*) defend smaller territories in a low- as compared with a high-visibility environment (Eason and Stamps 1992). In addition, Kalleberg (1958) noted that addition of large stones to a section of a stream aquarium resulted in a decrease in the size of territories and an increase in the density of juvenile Atlantic salmon (*Salmo salar*). The results of this unreplicated study were interpreted as being

Received 30 July 2001. Accepted 25 January 2002. Published on the NRC Research Press Web site at http://cjfas.nrc.ca on 5 March 2002.
J16469

I. Imre[1] **and J.W.A. Grant.** Department of Biology, Concordia University, 1455 de Maisonneuve Boulevard West, Montreal, QC H3G 1M8, Canada.
E.R. Keeley. Department of Biological Sciences, Idaho State University, Pocatello, ID 83209, U.S.A.

[1]Corresponding author (e-mail: i_imre@alcor.concordia.ca).

 DOI: 10.1139/F02-010 © 2002 NRC Canada

caused by visual isolation between neighbouring fish. Alternatively, the salmon may have been using the stones as a velocity refuge (Bachman 1984), allowing them to minimize their cost of swimming while having access to a high rate of drifting aquatic invertebrates (e.g., Jenkins 1969; Fausch 1984; Fausch 1993). Kalleberg's (1958) findings are particularly important for salmonid ecologists because, if true, they represent a novel way to increase population density (see Grant et al. 1998).

We examined the relationship between visibility, territory size, and population density using young-of-the-year rainbow trout (*Oncorhynchus mykiss*) as our test species. Specifically, we tested the prediction that decreasing visibility will result in smaller territories and a higher population density. We attempted to distinguish between the potential effects of visibility and a velocity refuge by adding either large stones, like Kalleberg (1958), or plywood dividers, which provided only visual isolation.

Materials and methods

Experimental subjects

On 15 May 2000, 70 pairs of mature rainbow trout were collected from the Blackwater River and stripped of sperm and eggs. The gametes were transported in chilled containers to the Fraser Valley Trout Hatchery (49°0.9′N, 122°16.4′W) near Abbottsford, B.C., where they were held overnight in a 4°C holding room. On 16 May 2000, the eggs from 4–5 females (10 000 – 15 000 eggs) were intermixed with the sperm from 4–5 males. This process was repeated 14 more times, to create a total of 15 groups of embryos. Embryos were held in 7°C water until they reached the eyed stage of development. Then they were held at 9.5°C until they had absorbed their yolk sac.

On 27 June 2000, approximately 2600 fish were haphazardly sampled from the 15 groups of juvenile rainbow trout at the Fraser Valley Trout Hatchery. The experimental subjects were moved to the Cultus Lake Laboratory (49°3.3′N, 122°1.4′W) and held in a fiberglass trough at 13°C until they were distributed into the experimental stream channels on 28 June 2000. Fish were fed with dry pelleted fish food (grade 1 Nutra Plus®, Moore Clark, Surrey, B.C.) before and during the experiment.

Experimental set-up

We used 12 experimental stream channels constructed on the outdoor compound of the Cultus Lake Laboratory. Each channel was 5 m long, 0.92 m wide, and 0.40 m deep. Channels were organized into four columns of three in a blocked staircase design (see Keeley 2000). The channels were interconnected with plastic troughs; the outflow of each channel was screened to prevent the escape of fish.

To simulate the shade provided by riparian cover characteristic of headwater streams and to prevent mortality from aerial predators, channels were individually covered with sheets of burlap supported by a wooden frame 1.32 m above the top edge of each channel. The experimental set-up and water supply are described in more detail by Keeley (2000).

To provide natural water flow conditions for the fish, the bottom of the stream channels was covered with one layer of small (64–128 mm) and large (128–256 mm) cobbles (table 5.6 in Gordon et al. 1992). Gaps between cobbles were filled with coarse gravel (32–64 mm) to provide a relatively smooth, natural substrate with minimal visual isolation for fish. The water depth and velocity were measured (at 50% of the water depth, using a Flo-Mate velocity meter, model 2000, Marsh–McBirney Inc., Frederick, Md.) at three locations along three transects perpendicular to the water flow (Fig. 1). The mean water velocity and mean water depth in each channel was used as a replicate for statistical analyses. Water temperature was measured twice daily (at 07:30 and 16:00) and was maintained at mean ± standard deviation 12.4 ± 0.9°C. End screens were checked and cleaned of debris three times a day. The flow rate in the channels was checked several times daily, and adjusted if necessary.

Each of the 12 channels was subjected to one of three treatments (i.e., 4 replicates per treatment): two treatments with low visibility (cobble and divider, see below) and a control treatment with high visibility. In the cobble treatment, we placed 22 stones (100–165 mm in diameter, 60–100 mm in height) on top of the substrate, but fully submerged, in a grid arrangement (Fig. 1). This treatment, which was similar to one used by Kalleberg (1958), provided both visual isolation and velocity refuges. In the divider treatment we inserted 22 vertical plywood rectangles (100 mm long, 200 mm high, and 3 mm thick) into the substrate parallel to the water flow to provide visual isolation but no velocity refuge (Fig. 1). The control treatment had the basic substrate that provided little or no velocity refuge or visual isolation. The treatments were assigned to the channels to remove any potential effects of the channel position. Each treatment appeared once in the upper, middle, and lower position in the first three columns of channels. The upstream–downstream treatment order in the fourth column was the same as in the first column. After placing the cobbles and the plywood structures into the stream channels, water velocity was measured again across the same transects.

Stream channels were stocked with 213 fish (mean ± standard deviation fork length 2.59 ± 0.09 cm), corresponding to a percent habitat saturation of 82.4% (Grant and Kramer 1990). This stocking density (46.3 individuals·m^{-2}) approximated the conspecific density that juvenile salmonids would experience shortly after emergence (see review by Grant and Kramer 1990). Fish were assigned randomly to stream channels in groups of 25 individuals.

Since stream-dwelling salmonids feed primarily on drifting aquatic invertebrates (e.g., McNicol et al. 1985; Keeley and Grant 1995), food was presented to fish in a manner similar to stream drift. The daily ration of food was spread evenly on the belt (20 cm wide, 50 cm long) of an automatic belt feeder (Zeigler Bros. Inc., Gardners, Pa.), that delivered the food 0.5 m from the upstream end of the stream channel at a constant rate over a period of 12 h (07:00–19:00) to simulate the invertebrate drift during daytime hours. Fish received a daily ration of 1.44 g of food per stream channel, approximating the maximum abundance of drifting aquatic invertebrates encountered by juvenile salmonids in natural streams (Keeley 2000). Food particles naturally occurring in the lake water were filtered out at the inflow with a 250-μm nylon mesh.

At the end of the 10-day experiment (8 July 2000), fish were removed from the stream channels and killed with an

© 2002 NRC Canada

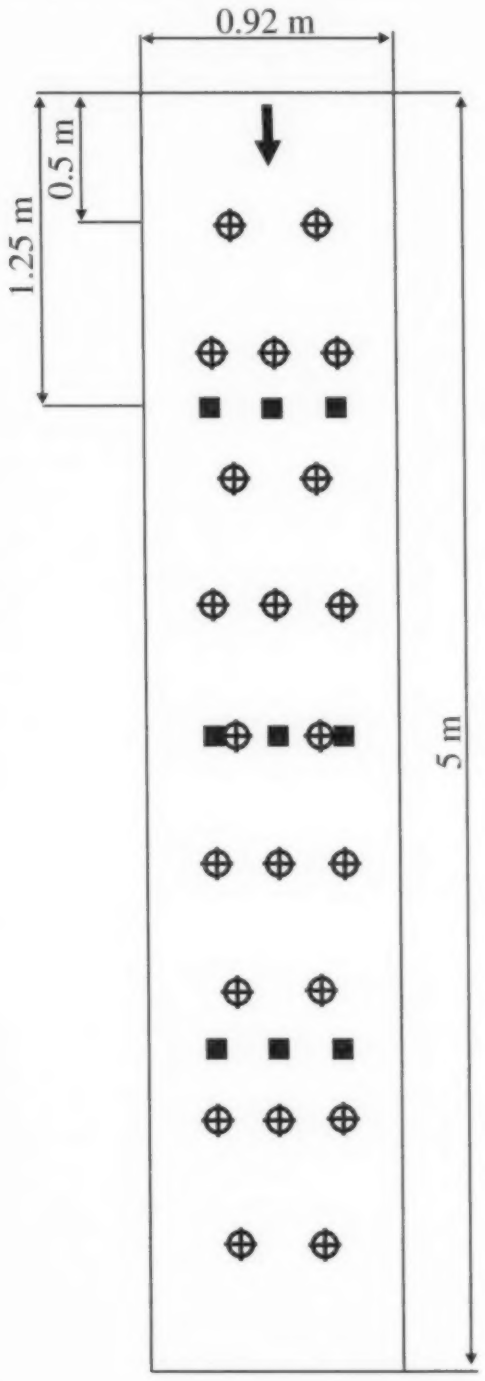

Fig. 1. General outline of an experimental stream channel. Crosses within circles indicate the position of the cobbles or dividers added to provide velocity refuge and (or) visual isolation in the experimental treatments; solid squares show the location of the water velocity and depth measurements in all treatments. Arrow at top of channel indicates direction of water flow.

overdose of anaesthetic (Eno, SmithKline Beecham, Oakville, Ont.), as required by the rearing permit issued by the British Columbia Ministry of Fisheries. The final population density in each channel was recorded. To obtain mean fork length and mean weight for each channel, 50 individuals per channel were haphazardly subsampled and measured.

Data collection

We checked each channel three times daily. Any individuals resting against the downstream end screens were considered to be emigrants and were removed, anesthetized, and their number, fork length (to the nearest mm), and weight (to the nearest 0.01 g) were recorded. Every second day, 10 fish from each channel were videotaped to compare the body size of residents and emigrants. The actual body length values were extracted from video images as described in Keeley (2000).

To estimate the local population density in the area where the behavioural data were collected, an observer (I. Imre) counted the number of fish in a 1-m^2 quadrat (1.09 × 0.92 m) positioned 0.8 m from the upstream end of the channel. Prior to counting, the observer waited for 5 min to allow the fish to return to their initial swimming station and resume their foraging activity (see Grant and Noakes 1987). Fish were counted in each channel on either day 8 or 9 of the experiment.

Behavioural data necessary to calculate territory sizes were collected by videotaping a 0.5 × 0.5 m area in the upper half of each stream channel for 30 min with an S-VHS video camera (on a tripod) inserted through the opening between two consecutive sheets of burlap. The area used for videotaping was within the 1-m^2 quadrat used for fish counts and was located in the same position in all channels. The first 5 min of each taping session were not used for the reason mentioned above. Only focal individuals (Martin and Bateson 1993) participating in at least five aggressive interactions over the observation period (25 min) were used for territory size calculations. Territorial fish initiated aggressive interactions and foraging attempts from a single, central, focal point. Aggressive distance was defined as the distance between the focal point of the fish and the position of an intruder when it elicited a chase. Foraging distance was the distance between the focal point of the fish and the position where a food item was captured. We measured 5–10 aggressive distances and 20 foraging distances per focal individual. The actual distances were calculated in relation to grid lines drawn 10 cm apart on the walls of the channels and a rope (marked at 10-cm intervals) located in the centre of each channel. Territory size based on aggressive data was calculated as the area of a circle, using the mean aggressive distance as the radius (Keeley and Grant 1995; Keeley and McPhail 1998; Keeley 2000). The minimum convex polygon method (Schoener 1981) was used to calculate the size of 95% foraging areas to confirm the patterns of territory size based on aggressive interactions, as some focal individuals were observed defending their territories only five times. The videotaping sessions were completed during the eighth and ninth day of the experiment.

From the videotapes, we computed the rates of foraging and aggression. To test whether fish with larger territories were able to keep competitors farther away, and hence de-

© 2002 NRC Canada

fend a larger foraging zone, we measured (to the nearest mm) the distance to the nearest neighbour in each of three directions: upstream, left, and right. We did not use data for neighbours downstream of the focal fish, because they rarely chased in that direction (also see Keeley and McPhail 1998; Keeley 2000). From these data the mean distance to the nearest neighbour was calculated for each focal individual.

A mean value for each channel (based on 3–5 focal individuals) was used as a datum when comparing the territory size, aggression rate, foraging rate, and distance to the nearest neighbour among treatments.

Statistical analyses

One-way analysis of covariance (ANCOVA; with local population density obtained from quadrat counts as a covariate) was used to test for differences in territory size and foraging area among treatments. Foraging and aggression rates, final fork length, final weight, fork length of territorial fish, distance to nearest neighbour, local population density (obtained from quadrat counts) during the experiment, and final population density in the different treatments were compared using a one-way analysis of variance (ANOVA). A paired t test was used to compare the fork length of residents and emigrants (data paired by channel and sampling date), the fork length of territorial fish and other residents in the same channel (data paired by channel), and the length of chases directed towards obstacles vs. open areas (data paired by individual). The assumption of normality was assessed using the Kolmogorov–Smirnov test (with Lilliefors probabilities). Levene's test was used to test the assumption of homogeneity of variances. All statistical tests were performed with Statistica 5.0 (StatSoft Inc. 1995). The critical level of significance was set at 0.05.

Results

The average water depth ($F_{[2,9]} = 0.36$, $P = 0.71$) and current velocity ($F_{[2,9]} = 2.53$, $P = 0.13$) did not differ significantly among the three treatments (Table 1A). The water velocity was, however, lower immediately downstream of the cobbles, resulting in a tendency for the overall water velocity to be lower in the cobble treatment.

In all three treatments, the fish had a similar distribution pattern. Few fish were within 0.5 m of the upstream end because of the absence of food and the turbulence of the water. The density of animals was highest just downstream of the food-dispensing location, and then gradually decreased towards the downstream end of each channel.

The number of fish trying to emigrate (Fig. 2) was high during the second and third day of the experiment, but declined thereafter. Floaters, defined as fish that do not feed from a fixed focal point (Puckett and Dill 1985), were present at the beginning of the experiment, but were rarely observed at the end. Most fish had a single, centrally placed focal point from which foraging attempts and aggressive interactions were initiated. However, not all individuals were equally aggressive; the observed frequency of aggression ranged from zero, where individuals held a station but avoided interactions with adjacent fish, to high (maximum aggression rate 2.3 interactions·min^{-1}), where focal fish vigorously excluded all intruders from their territory. In high-density situations, fish stations were often layered one over another in the water column.

Territory size based on aggressive behaviour decreased with increasing local population density (Fig. 3*a*, ANCOVA $F_{[1,8]} = 13.28$, $P = 0.007$). After statistically controlling for the effect of population density, territory size (Table 1B) differed significantly among treatments (Fig. 3*a*, ANCOVA $F_{[2,8]} = 18.31$, $P = 0.001$). As predicted by the visual isolation hypothesis, territory size was significantly larger in the control treatment than in the low-visibility treatments (contrast analysis between adjusted means $F_{[1,8]} = 36.55$, $P < 0.001$), but territory size did not differ significantly between the divider and cobble treatments (contrast analysis between adjusted means $F_{[1,8]} = 0.004$, $P = 0.95$). The interaction between territory size and local population density was also not significant (ANCOVA: $F_{[2,6]} = 0.49$, $P = 0.63$). In total, the ANCOVA model accounted for 85.5% of the variation in territory size: territory size (m^2) = intercept – 0.000203 × local density (no·m^{-2}), where the intercept equals 0.0256, 0.0183, and 0.0182 for the control, divider, and cobble treatments, respectively.

Foraging area based on a 95% minimum convex polygon also decreased with increasing local population density (Fig. 3*b*, ANCOVA $F_{[1,8]} = 6.81$, $P = 0.031$) and differed among treatments (Fig. 3*b*, ANCOVA $F_{[2,8]} = 6.06$, $P = 0.025$). Foraging area (Table 1B) was larger in the control treatment than in the other two treatments (contrast analysis between adjusted means: $F_{[1,8]} = 10.12$, $P = 0.013$), and did not differ between the cobble and divider treatments (contrast analysis between adjusted means $F_{[1,8]} = 2.50$, $P = 0.15$), supporting the patterns in territory size. As earlier, the interaction between foraging area and local population density was not significant (ANCOVA $F_{[2,6]} = 2.63$, $P = 0.15$). The ANCOVA model accounted for 65.7% of the variation in foraging area: foraging area (m^2) = intercept – 0.0000554 × local density (no·m^{-2}), where the intercept is 0.00936, 0.00834, and 0.00741 for the control, divider, and cobble treatments, respectively. Neither measure of territory size (aggressive data $r = 0.04$, $P = 0.81$, $n = 40$; foraging data $r = 0.16$, $P = 0.32$, $n = 40$) was related to the size of territorial fish, perhaps because of a narrow range in body length (2.4–3.7 cm). Rates of aggression (Table 1B, $F_{[2,9]} = 0.97$, $P = 0.42$) and foraging (Table 1B, $F_{[2,9]} = 0.33$, $P = 0.73$) did not differ significantly among treatments.

Most focal fish in the low-visibility treatments, and some in the control treatment, had obstructions (i.e., divider, cobble, or side of the channel) in one or two of the three directions (upstream, right, and left), in which aggression occurred frequently. To determine how these obstructions influenced territory size, we compared the chase distances in directions towards obstructions vs. directions with no obstructions. Chases in directions with obstructions (mean ± standard error = 5.7 ± 0.51 cm) were significantly shorter (paired $t_{14} = 3.68$, $p = 0.002$, $N = 15$) than chases in directions with no obstructions (mean ± standard error 6.9 ± 0.56 cm).

The distance to the nearest neighbour did not differ significantly among treatments ($F_{[2,9]} = 3.40$, $P = 0.08$) but tended to be smaller in the low-visibility treatments (Table 1B). At the level of the individual, however, fish with larger territo-

© 2002 NRC Canada

Table 1. Descriptive statistics (mean ± standard error, $n = 4$) for abiotic and biotic variables in the control, divider, and cobble treatments used to test the effect of visual isolation on territory size and population density in juvenile rainbow trout (*Oncorhychus mykiss*).

(A) Abiotic variables.	Control	Divider	Cobble
Water depth (cm)	11.6 ± 0.44	11.9 ± 0.33	11.5 ± 0.29
Water velocity ($cm \cdot s^{-1}$)	5.3 ± 0.43	5.1 ± 0.22	4.4 ± 0.14
(B) Biotic variables.			
Territory size (aggressive data) (cm^2)	162.0 ± 16.2	83.2 ± 11.0	104.9 ± 17.7
Territory size (foraging data) (cm^2)	67.8 ± 4.78	56.0 ± 2.20	53.0 ± 6.52
Aggression rate (interactions·min^{-1})	0.43 ± 0.06	0.63 ± 0.13	0.58 ± 0.11
Foraging rate (attempts·min^{-1})	6.2 ± 0.46	6.8 ± 0.57	6.3 ± 0.46
Local population density (quadrat counts, no·m^{-2})	46.6 ± 5.1	49.3 ± 6.8	38.1 ± 5.8
Final population density (no·m^{-2})	25.9 ± 2.1	27.1 ± 1.5	23.3 ± 2.2
Final fork length (cm)	3.2 ± 0.03	3.2 ± 0.03	3.2 ± 0.02
Final body weight (g)	0.28 ± 0.004	0.29 ± 0.013	0.28 ± 0.007
Fork length of territorial fish (cm)	2.9 ± 0.11	3.0 ± 0.05	2.9 ± 0.06
Distance to nearest neighbour (cm)	10.8 ± 1.1	7.9 ± 0.25	9.8 ± 0.83

Fig. 2. Mean number (± standard deviation) of fish caught on end screens over the duration of the experiment in the control (○), divider (■), and cobble (▲) treatments.

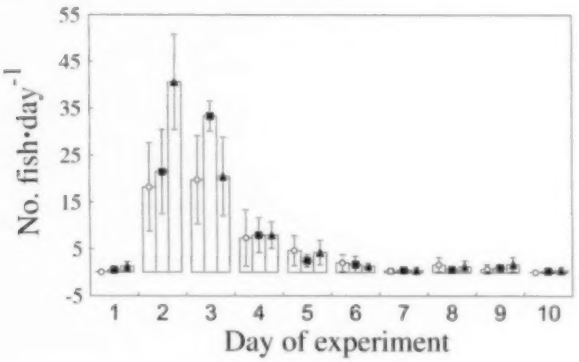

Fig. 3. Relationship between local population density obtained from quadrat counts and territory size based on (*a*) aggressive data and (*b*) foraging data for the control (○, solid line), divider (■, long-dashed line), and cobble (◆, short-dashed line) treatments. The regression lines are from the analysis of covariance (ANCOVA). The lines for the divider and cobble treatments are virtually identical in (*a*).

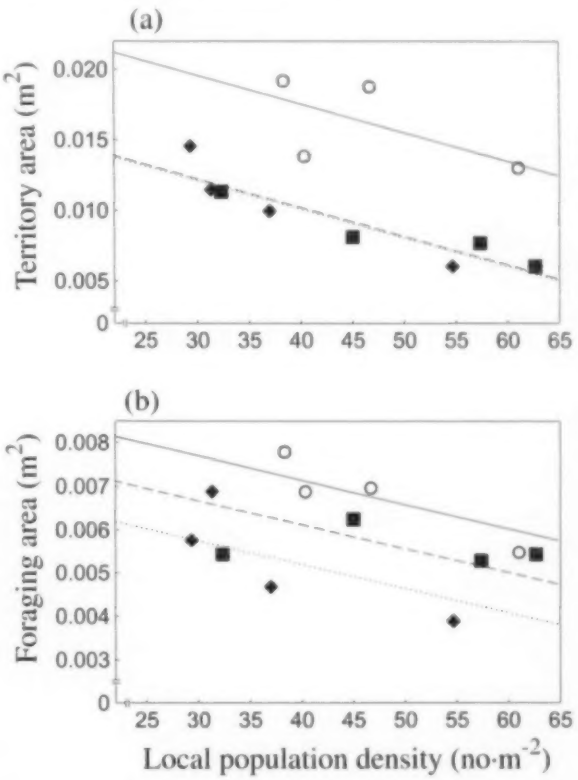

ries were able to keep neighbours farther away ($r = 0.54$, $P = 0.0004$, $n = 39$). Despite differences in territory size, there were no significant differences among treatments in final population density (Table 1B, $F_{[2,9]} = 1.01$, $P = 0.40$) or local fish density obtained from quadrat counts (Table 1B, $F_{[2,9]} = 0.98$, $P = 0.41$).

Overall, fish increased in fork length by ~0.6 cm (23.2% of their initial fork length) over the duration of the experiment. Resident fish did not differ significantly in their final fork length (Table 1B, $F_{[2,9]} = 0.004$, $P = 0.99$) or final body weight (Table 1B, $F_{[2,9]} = 0.21$, $P = 0.82$) among treatments. Resident fish were significantly longer than fish collected from end screens (paired $t_{36} = -3.60$, $P < 0.001$). Focal fish used for territory size calculations did not differ in fork length among treatments (Table 1B, $F_{[2,9]} = 0.96$, $P = 0.42$), but surprisingly, focal fish were smaller than the average resident in each channel (paired $t_{11} = 4.10$, $P = 0.002$).

Discussion

This study contributes to a small but growing body of literature (reviewed by Eason and Stamps 1992) indicating that visibility influences space use. In a seminatural environment with low visibility, juvenile rainbow trout defended territories that were 0.5 to 0.6 the size of those in the high-visibility control. The similarity in territory size between the

© 2002 NRC Canada

divider and the cobble treatment suggests that visual isolation rather than a velocity refuge accounts for the reduction in territory size of focal fish. Interestingly, the average territory size of juvenile Atlantic salmon (*Salmo salar*) (Kalleberg 1958) and *Anolis aeneus* lizards (Eason and Stamps 1992) in low-visibility environments also decreased to approximately half the size observed in high-visibility environments. To produce an equivalent decrease in territory size as observed in our study (i.e., 37.5–50% decrease) would require a 3.1- to 5.2-fold increase in food abundance (Grant et al. 1998). Hence, habitat visibility appears to be a powerful way of manipulating territory size.

Rainbow trout in the high-visibility environment defended territories that were on average 67% of the size predicted by an interspecific relationship for stream-dwelling salmonids (Grant and Kramer 1990) and approximately 20% of the size defended by wild juvenile steelhead of comparable size (Keeley and McPhail 1998). The relatively small territories observed in our study were likely the result of the high initial stocking density and the high daily food ration (Keeley 2000). As in previous studies (e.g., Slaney and Northcote 1974; Dill et al. 1981; Keeley 2000), territory size decreased with increasing local population density. Surprisingly, we found no relationship between territory size and body size, perhaps because of a narrow range in body size.

Like juvenile lizards (Eason and Stamps 1992), juvenile rainbow trout seemed to avoid visual barriers, so that the barriers were typically near the perimeter of their territories. Nevertheless, these barriers still constrained the size of their territories because their chase distances were shorter in directions toward an obstruction. Similarly, brown trout (*Salmo trutta*) swimming near or between woody debris had shorter chase distances than conspecifics interacting in a control treatment without woody debris (Sundbaum and Näslund 1998).

In our study, focal fish with larger territories were able to keep neighbours farther away, but this effect did not translate into significant differences in local or final population density. This is in contrast to other studies that have shown a link between territory size and population density of juvenile salmonids (Grant and Kramer 1990; Grant et al. 1998; Keeley 2000). In this study, population density did not differ among treatments, perhaps because fewer than half of the 8–24 individuals on the videotapes were aggressive at all during the 25-min observation periods and only 3–5 individuals were sufficiently aggressive to warrant the calculation of their territory size. Not all individuals of salmonid populations defend territories (e.g., Puckett and Dill 1985; Grant and Noakes 1988), so the importance of territoriality as a mechanism of population regulation may depend on the proportion of individuals defending territories. Alternatively, it is possible that the proportion of individuals defending territories was sufficient to affect population density, but the experiment was too short to reach the equilibrium density.

The presence of physical structures in the water column often causes local fish abundance to increase (e.g., Saunders and Smith 1962; Fausch and Northcote 1992; Gowan and Fausch 1996), presumably because fish are attracted to the structures for the cover they provide. In contrast, in our study, rainbow trout tended to avoid the cobbles and dividers.

In summary, our study supports the idea that territory size decreases with decreasing visibility. Territorial juvenile rainbow trout in the low-visibility environments held territories that were ~37.5–50% smaller in size than territories held in the high-visibility control environment, but population density did not differ among treatments.

Acknowledgments

We are grateful to S.Ó. Steingrímsson, C.A. Johnson, I.L. Girard, L. Weir, and C. Breau for their comments on this study. J.S. Scroggie and M. Phillpotts helped with preparation of the experiment. We thank D. Larson and K. Scheer at the Fraser Valley Trout Hatchery for supplying our experimental subjects and B. Stanton at the Chilliwack River Hatchery for the loan of equipment. Further thanks are due to E. Parkinson (B.C. Ministry of Fisheries) and to Cultus Lake Laboratory (Department of Fisheries and Oceans) for their generous logistical support. The manuscript benefited tremendously from the constructive criticism offered by C. Gowan and an anonymous reviewer. The research was financially supported by an operating grant from the Natural Sciences and Engineering Research Council of Canada (NSERC) to J.W.A. Grant, and a grant from Forest Renewal B.C. to E.R. Keeley. I. Imre was supported by a Natural Sciences and Engineering Research Council postgraduate fellowship and the David J. Azrieli graduate fellowship (from Concordia University) during this study.

References

Bachman, R.A. 1984. Foraging behaviour of free-ranging wild and hatchery brown trout in a stream. Trans. Am. Fish Soc. **113**: 1–32.

Dill, L.M., Ydenberg, R.C., and Fraser, A.H.G. 1981. Food abundance and territory size in juvenile coho salmon (*Oncorhynchus kisutch*). Can. J. Zool. **59**: 1801–1809.

Eason, P.K., and Stamps, J.A. 1992. The effect of visibility on territory size and shape. Behav. Ecol. **3**: 166–172.

Fausch, K.D. 1984. Profitable stream positions for salmonids: relating specific growth rate to net energy gain. Can. J. Zool. **62**: 441–451.

Fausch, K.D. 1993. Experimental analysis of microhabitat selection by juvenile steelhead (*Oncorhynchus mykiss*) and coho salmon (*O. kisutch*) in a British Columbia stream. Can. J. Fish. Aquat. Sci. **50**: 1198–1207.

Fausch, K.D., and Northcote, T.G. 1992. Large woody debris and salmonid habitat in a small coastal British Columbia stream. Can. J. Fish. Aquat. Sci. **49**: 682–693.

Gordon, N.D., McMahon, T.A., and Finlayson, B.L. 1992. Stream hydrology: an introduction for ecologists. John Wiley & Sons Ltd., Chichester.

Gowan, C., and Fausch, K.D. 1996. Long-term demographic responses of trout populations to habitat manipulation in six Colorado streams. Ecol. Appl. **6**: 931–946.

Grant, J.W.A., and Kramer, D.L. 1990. Territory size as a predictor of the upper limit to population density of juvenile salmonids in streams. Can. J. Fish. Aquat. Sci. **47**: 1724–1737.

Grant, J.W.A., and Noakes, D.L.G. 1987. Escape behaviour and use of cover by young-of-the-year brook trout, *Salvelinus fontinalis*. Can. J. Fish. Aquat. Sci. **44**: 1390–1396.

Grant, J.W.A., and Noakes, D.L.G. 1988. Aggressiveness and foraging mode of young-of-the-year brook charr, *Salvelinus fontinalis* (Pisces, Salmonidae). Behav. Ecol. Sociobiol. **22**: 435–445.

© 2002 NRC Canada

Grant, J.W.A., Steingrímsson, S.Ó., Keeley, E.R., and Cunjak, R.A. 1998. Implications of territory size for the measurement and prediction of salmonid abundance in streams. Can. J. Fish. Aquat. Sci. **55**(Suppl. 1): 181–190.

Hixon, M.A. 1981. An experimental analysis of territoriality in the California reef fish *Embiotoca jacksoni* (Embiotocidae). Copeia, 1981: 653–665.

Jenkins, T.M., Jr. 1969. Social structure, position choice and microdistribution of two trout species (*Salmo trutta* and *Salmo gairdneri*) resident in mountain streams. Anim. Behav. Monogr. **2**: 56–123.

Kalleberg, H. 1958. Observations in a stream tank of territoriality and competition in juvenile salmon and trout (*Salmo salar* L., and *S. trutta* L.). Inst. Freshw. Res. Drottningholm Rep. **39**: 55–98.

Keeley, E.R. 2000. An experimental analysis of territory size in juvenile steelhead trout. Anim. Behav. **59**: 477–490.

Keeley, E.R., and Grant, J.W.A. 1995. Allometric and environmental correlates of territory size in juvenile Atlantic salmon (*Salmo salar*). Can. J. Fish. Aquat. Sci. **52**: 186–196.

Keeley, E.R., and McPhail, J.D. 1998. Food abundance, intruder pressure, and body size as determinants of territory size in juvenile steelhead trout (*Oncorhynchus mykiss*). Behaviour, **135**: 65–82.

Krebs, J.R. 1982. Territorial defense in the great tit (*Parus major*): do residents always win? Behav. Ecol. Sociobiol. **11**: 185–194.

Martin, P., and Bateson, P. 1993. Measuring behaviour: an introductory guide. 2nd ed. Cambridge University Press, Cambridge.

McNicol, R.E., Scherer, E., and Murkin, E.J. 1985. Quantitative field investigations of feeding and territorial behaviour of young-of-the-year brook charr, *Salvelinus fontinalis*. Environ. Biol. Fishes, **12**: 219–229.

Myers, J.P., Conners, P.G., and Pitelka, F.A. 1979. Territory size in wintering sanderlings: the effects of prey abundance and intruder density. Auk, **96**: 551–561.

Puckett, K.J., and Dill, L.M. 1985. The energetics of feeding territoriality in juvenile coho salmon (*Oncorhynchus kisutch*). Behaviour, **92**: 97–111.

Saunders, J.W., and Smith, M.W. 1962. Physical alteration of stream habitat to improve brook trout production. Trans. Am. Fish. Soc. **91**: 185–188.

Schoener, T.W. 1981. An empirically based estimate of home range. Theor. Popul. Biol. **20**: 281–325.

Schoener, T.W. 1983. Simple models of optimal-feeding territory size: a reconciliation. Am. Nat. **121**: 608–629.

Schoener, T.W. 1987. Time budgets and territory size: some simultaneous optimization models for energy maximizers. Am. Zool. **27**: 259–291.

Slaney, P.A., and Northcote, T.G. 1974. Effects of prey abundance on density and territorial behaviour of young rainbow trout (*Salmo gairdneri*) in laboratory stream channels. J. Fish. Res. Board Can. **31**: 1201–1209.

StatSoft Inc. 1995. Statistica for Windows. Vol. 1–5. 2nd ed. StatSoft, Tulsa, Okla.

Stimson, J. 1973. The role of the territory in the ecology of the intertidal limpet *Lottia gigantea* (Gray). Ecology, **54**: 1020–1030.

Sundbaum, K., and Näslund, I. 1998. Effects of woody debris on the growth and behaviour of brown trout in experimental stream channels. Can. J. Zool. **76**: 56–61.

Titus, R.G. 1990. Territorial behavior and its role in population regulation of young brown trout (*Salmo trutta*): new perspectives. Ann. Zool. Fenn. **27**: 119–130.

Tricas, T.C. 1989. Determinants of feeding territory size in the corallivorous butterflyfish, *Chaetodon multicinctus*. Anim. Behav. **37**: 830–841.

© 2002 NRC Canada

Freshwater mussel abundance and species richness: GIS relationships with watershed land use and geology

Kelly E. Arbuckle[1] and John A. Downing

Abstract: We tested the hypotheses that mussel species richness and density are related to landscape features of watersheds. Measures of species richness and mussel density were estimated at 118 sites in 36 watersheds in the state of Iowa, U.S.A., a landscape characterized by >90% agricultural development. Geographical Information Systems (GIS) and regression analyses examined seven land use categories and nine geological descriptors, determining that both mean density and species richness were best correlated with mean watershed slope and the prevalence of alluvial deposits. Our analyses imply that agricultural watersheds with high slopes impact mussel abundance and richness through siltation and destabilization of stream substrate. Because alluvial deposits improve groundwater flux to streams, results suggest that relatively stable stream flows in alluvial watersheds improve mussel persistence. A second set of 82 observations on 38 independent watersheds corroborates the analyses, although historical and local impacts cause correlations between new observations and predictions to be weak.

Résumé : Pour éprouver l'hypothèse selon laquelle la richesse en espèces et la densité des moules sont reliées aux caractéristiques du paysage du bassin versant, nous avons estimé la richesse en espèces et la densité des moules de 118 sites appartenant à 36 bassins versants en Iowa, un paysage utilisé à plus de 90 % pour l'agriculture. À l'aide de systèmes d'information géographique et d'analyses de régression, nous avons étudié sept catégories d'utilisation du territoire et neuf descripteurs géologiques et trouvé que la densité moyenne et la richesse en espèces sont en corrélation principalement avec la pente moyenne du bassin versant et l'importance des dépôts alluviaux. Nos analyses permettent de croire que les bassins versants agricoles à forte pente ont d'importantes répercussions sur l'abondance et la richesse des moules à cause de l'envasement et de la déstabilisation des cours d'eau. Parce que les dépôts alluviaux améliorent le flux des eaux souterraines vers les cours d'eau, nos résultats suggèrent que les débits relativement stables dans les bassins versants alluviaux favorisent la persistance des moules. Une seconde série de 82 observations provenant de 38 autres bassins versants corroborent les résultats des analyses, mais à cause de facteurs historiques et des conditions locales, les corrélations entre ces nouvelles observations et nos prédictions sont faibles.

[Traduit par la Rédaction]

Introduction

Freshwater mussels are among the most imperiled animals worldwide (Master 1990). A variety of anthropogenic stressors, including habitat destruction and degradation, commercial exploitation, and water pollution, have been implicated in the disappearance of these animals (Pennak 1989; Bogan 1993; Williams and Neves 1995). Effective conservation and restoration of mussel populations depends upon an understanding of how they are impacted by landscape-driven alterations in water quality.

Received 23 March 2001. Accepted 27 November 2001. Published on the NRC Research Press Web site at http://cjfas.nrc.ca on 5 March 2002.
J16278

K.E. Arbuckle. Office of Environmental Services, Iowa Department of Transportation, 800 Lincoln Way, Ames, IA 50010, U.S.A.
J.A. Downing.[2] Department of Animal Ecology, Iowa State University, 124 Science II, Ames, IA 50011-3221, U.S.A.

[1]Name changed to K.E. Poole during publication.
[2]Corresponding author (e-mail: downing@iastate.edu).

The land–water interface can have important effects on the persistence of aquatic organisms (Karr and Schlosser 1978; Richards and Host 1994; Roth et al. 1996). Watershed characteristics are often closely related to biotic and abiotic characteristics of streams (Schlosser 1991; Rabeni and Jacobson 1993; Wang et al. 1997). For example, surficial geological features determine hydrologic patterns and channel morphology at the watershed scale and influence macroinvertebrate assemblages (Richards et al. 1996). In addition, landscape changes such as urbanization, logging, and the conversion of native land cover to agricultural crop production often lead to degraded habitat conditions.

Land use, topographic relief, and geologic history influence stream water quality. Land use activities that remove vegetative cover decrease infiltration rates and the moisture-holding capacity of soils (Brooks et al. 1997). Topographic relief of the landscape surrounding streams also influences water quality (Elliot and Ward 1995). For example, disturbed, high-relief watersheds have greatest overland flow, produce relatively large amounts of sediment in runoff water, and have high-gradient streams, all of which can destabilize substrates, rendering stream conditions unsuitable for freshwater mussels. Although low-relief watersheds have less runoff

 DOI: 10.1139/F02-006 © 2002 NRC Canada

impact, low-gradient streams are prone to siltation. This is especially true in agricultural areas where sediment is often the major stream pollutant. Further, geologic features like surficial alluvial aquifers influence water recharge, and thus groundwater and surface water quality (Anderson 1998). The stable discharge of groundwater from alluvial aquifers in present-day stream valleys can prevent loss of the biota via desiccation of permanent rivers.

In spite of the potential importance of watershed characteristics, much of the study of mussel–habitat relationships has been performed on the scale of the local stream-reach (e.g., Strayer and Ralley 1993; Di Maio and Corkum 1995; Layzer and Madison 1995). Some studies have related mussel abundance and distribution to local stream attributes such as hydrologic variability (Di Maio and Corkum 1995) and substrate composition (Strayer and Ralley 1993), but local characteristics like sediment quality (e.g., granulometry) have explained little variation in stream mussel distributions (e.g., Strayer and Ralley 1993). Because larger-scale landscape features influence water quality, and thus, the development of aquatic communities (Richards and Host 1994; Richards et al. 1996; Roth et al. 1996), population persistence can be influenced by landscape features such as surface geology, soil, and riparian land use (Strayer 1983; Morris and Corkum 1996; Brim Box and Mossa 1999). Understanding relationships between watershed-scale landscape characteristics and mussel populations may therefore contribute to the protection of these threatened animals.

The objective of this study was to determine the relationship of watershed land use and geomorphic features to mussel species richness and population density in an intensely agricultural region that has been a historical center for mussel biodiversity. We sought to develop statistical models to characterize watershed characteristics conducive to high mussel species richness or density and to test these models on independent samples from different watersheds.

Materials and methods

Study design

The overall study plan was to use descriptive Geographic Information Systems (GIS) modeling to derive watershed attributes (e.g., land use, geology, and topographic relief) followed by regression analysis to determine relationships between landscape features and mussel density and mussel species richness. Specifically, we (*i*) used GIS descriptive modeling techniques to quantify selected landscape characteristics of watersheds surveyed in 1998 and 1999, (*ii*) used regression and correlation analysis to determine the significance of relationships between watershed characteristics and mussel species richness and population density data derived in a 1998 survey, (*iii*) used these models to identify potentially mussel-friendly watersheds to be sampled in the 1999 survey, and (*iv*) tested the strength of original predictive models using mussel density and species richness data collected in the independent 1999 field survey.

Study area

Our study sites were located in the Mississippi River basin, distributed over the state of Iowa (U.S.A.) (Fig. 1), which has been considered a historical center of mussel diversity in North America (Pennak 1989). The landscape features of this region are the result of recent and historical glacial and erosional processes. Geological landscape evolution left nine distinct geologic regions and widespread regional pockets of alluvial deposition (Prior 1991). Elevation ranges from a low (146 m above sea level) in the southeast corner to a high of 509 m in the northwest corner of the study area. Nearly 90% of the landscape is currently in agricultural production (Thompson 1992), so watersheds receive considerable agricultural impact.

Field survey

We surveyed mussel populations in 36 watersheds in 1998 and 38 watersheds in 1999 (see Fig. 1). Data on the occurrence of mussel species used in this analysis were collected in initial field surveys made during July–September 1998 at 118 sites and follow-up samples taken at 82 sites in July–September 1999. Sites sampled in 1998 were the inland stream sites that were previously sampled in 1984–1985 in an assessment of Iowa's "best" mussel habitat and thus represented much of the finest lotic habitat in the state at that time. Data collected in 1984–1985 and 1998 show substantial declines in species richness over this period (K.E. Arbuckle and J.A. Downing, unpublished data).

The criteria used to select sites sampled in 1998 included (*i*) streams (excluding Mississippi River sites) that had been previously surveyed as representative of the State's "best" mussel habitat (Frest 1987); but (*ii*) we only sampled streams where depth was suitable for use of visual and tactile survey methods while wading (i.e., <1.5 m depth). The criteria used in selecting streams for the 1999 survey included (*i*) interior stream reaches recommended (but not previously sampled) as representative of very good mussel habitat by Frest (1987); or (*ii*) areas identified by the 1998 predictive study (see below) as having the potential to support mussels. In 1999, only sites where stream depth was suitable for use of visual and tactile survey methods while wading were sampled.

At each of these sites, the survey segment was located at least 100 m from a road or bridge access area to minimize disturbance of these structures. All sites were systematically surveyed by three people searching while moving upstream along the stream segment. The length of stream surveyed varied by stream size. We surveyed 200 m in small streams (mean stream width (MSW) <10 m), 500 m in medium streams (MSW 10–25 m), and 1 km of stream in large systems (MSW >25 m). Medium and large streams were only surveyed during periods of low flow.

Mussel survey

Density was quantified using visual and tactile searches of 60 1-m^2 quadrats at each site. We used a restricted random sampling design (Hayek and Buzas 1997) to collect quadrat samples along the entire segment length and from a variety of water depths and habitat types. The stream area was divided into thirds across the channel and into 10 equally spaced segments along the length, and a random number table was used to assign the sample points to be covered by the quadrats sampled in each area. Twenty 1-m^2 quadrats

© 2002 NRC Canada

Fig. 1. Outlines of the 38 watersheds surveyed for freshwater mussels in 1998 (shaded) and 36 watersheds surveyed in 1999 (open), in the state of Iowa, U.S.A.

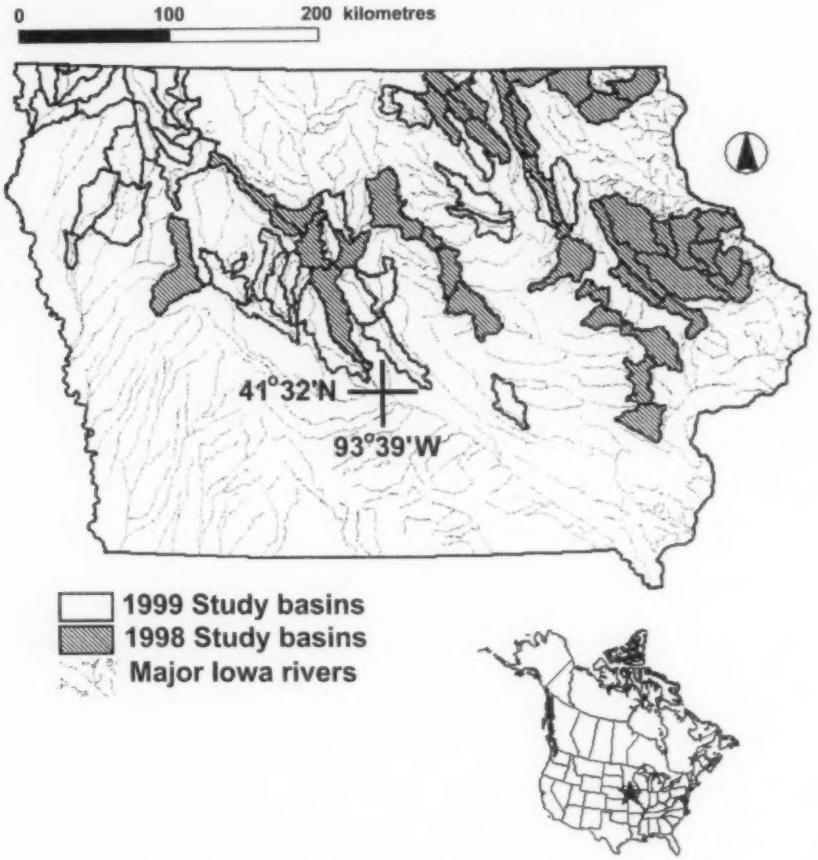

were inspected along the right bank, 20 along the left bank, and 20 in the mid-channel for a total of 60 quadrats at each site. Substrate within the quadrat was excavated to a depth of 20 cm and searched tactilely to locate mussels.

An extensive visual survey of the substrate in shallow water (<0.05 m) was performed simultaneously with the quadrat survey. In addition to the quadrat survey and visual inspections of the substrate outside the quadrats, we searched the stream banks and areas adjacent to the stream for shells. Shells were collected and returned to the laboratory for identification. Living mussels were identified, photographed, and returned to the stream.

A list of species and number of individuals observed inside and outside the quadrats was compiled for each site. Between 1 and 15 (average ca. 3) sampling sites were analyzed within each of 74 watersheds. Species identifications were confirmed in the laboratory using digital images of living animals and shell material obtained at each site. Mean mussel density ($\overline{D}_{98}$, $\overline{D}_{99}$) and mean species richness ($\overline{R}_{98}$, $\overline{R}_{99}$) estimates for each watershed were calculated as the arithmetic average of all densities or richness estimates from all sites within each of the watersheds. Although these data would be sufficient to calculate most indices of biotic diversity, we have chosen to analyze richness and density separately for clarity of interpretation and to avoid choosing among the aggregate indices of diversity.

GIS watershed analysis

Watershed characteristics were assessed to relate population density and species richness to land use and geology. GIS analysis was used to prepare 17 watershed descriptions for each basin surveyed in 1998 and 1999. GIS data used in these analyses were obtained from the Iowa Department of Natural Resources (IDNR) Natural Resource GIS (NRGIS) library. Calculated variables derived from the GIS data included the fraction of land area composed of alluvial deposits, the average topographic relief (estimated as average percent slope), the incidence of eight important geologic formations (Cambrian, Cretaceous, Devonian, Jurassic, Mississippian, Ordovician, Pennsylvanian, Silurian; estimated as fractions of land area), and the incidence of seven land use types (urban, agricultural, range, forest, water, wetland, and barren land, estimated as fractions of land area). These landscape features were selected for this analysis because they each have the potential to influence water quality in ways that are relevant to mussel persistence. GIS software used to

© 2002 NRC Canada

Table 1. Results of the bivariate regression analyses of percent watershed alluvium and mussel density and species richness in watersheds analyzed in 1998 for 38 watersheds in the state of Iowa, U.S.A.

Dependent variable	Independent variable	r^2	T	P
Density ($\overline{D}_{98}$)	Slope	0.36	–4.41	0.000
Species richness ($\overline{R}_{98}$)	Slope	0.27	–3.43	0.002
Density ($\overline{D}_{98}$)	Alluvium	0.20	2.92	0.006
Species richness ($\overline{R}_{98}$)	Alluvium	0.12	2.10	0.043

Note: The T values and probabilities shown are for regression coefficients in eqs. 1–4. P indicates the probability that a T value of equal or greater magnitude would be obtained through chance alone.

Fig. 2. Bivariate relationships between mussels and watershed characteristics. Relationship between (*a*) average mussel density in watersheds and mean watershed slope, (*b*) average mussel density in watersheds and watershed alluvial deposits, (*c*) average mussel species richness in watersheds and mean watershed slope, and (*d*) average mussel species richness in watersheds and watershed alluvial deposits. Solid lines represent regression relationships (eqs. 1–4).

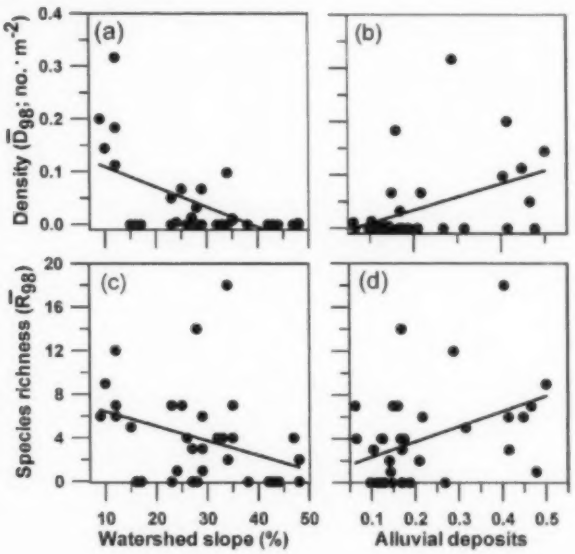

prepare the watershed descriptions were ArcView® extensions, X-Tools®, Spatial Analyst®, and Spatial Tools® (ESRI, Redlands, Calif.; http://www.esri.com).

Analytical methods

The statistical influences of watershed characteristics on watershed average mussel species richness ($\overline{R}_{98}$) and density ($\overline{D}_{98}$) were determined using regression analyses of the survey results from the 118 sites in 36 watersheds surveyed in 1998. We sought to determine statistically significant ($p < 0.05$) bivariate relationships between $\overline{R}_{98}$ and $\overline{D}_{98}$ and a total of 17 candidate variables describing watershed landscapes (e.g., geology and land use characteristics, topography, and alluvium) using regression and correlation analysis. We then investigated potential multivariate relationships between $\overline{R}_{98}$ and $\overline{D}_{98}$ and those candidate variables found to be statistically significant in the bivariate analyses. This was accomplished using backward elimination multiple regression methods where independent variables were eliminated based on a retention criterion of $p < 0.05$ for partial significance of regression coefficients.

Independent model test

To test the efficacy of these regression models to predict mussel densities and species richness in independent data, the bivariate regression models were applied to an independent set of watershed $\overline{R}$ and $\overline{D}$ values collected at 82 sites in 38 watersheds during 1999. Models of $\overline{R}_{98}$ and $\overline{D}_{98}$ were used to predict mussel density ($\hat{D}_{99}$) and mussel species richness ($\hat{R}_{99}$) using 1999 watershed descriptors (e.g., landscape features and geology). To evaluate the effectiveness of individual models, correlation and graphical analyses were used to relate predicted values ($\hat{R}_{99}$, $\hat{D}_{99}$) to field measurements ($\overline{R}_{99}$, $\overline{D}_{99}$).

Results

Watershed-wide averages of mussel density within a stream reach were low (cf. Downing and Downing 1992), averaging only 0.04 (standard deviation, $s = 0.07$; $n = 36$) and 0.06 ($s = 0.21$; $n = 38$) animals·m^{-2} within the basins surveyed in 1998 and 1999, respectively. Watershed species richness averaged 2.05 for sites sampled in 1998 and 1.47 for those sampled in 1999. Thirty percent of the watersheds surveyed in 1998 and 37% of the watersheds surveyed in 1999 had no living mussels, even though these sites represent the best mussel habitat in this formerly mussel-rich region.

Bivariate regression analysis showed that topographic relief, as measured by mean percent slope, was significantly correlated with mussel density and mussel species richness (Table 1). The regression equations

$$(1) \quad \overline{D}_{98} = 0.148 - 0.0038 S_{98}$$

$$(2) \quad \overline{R}_{98} = 5.63 - 0.123 S_{98}$$

indicate that mussel density ($\overline{D}_{98}$) and species richness ($\overline{R}_{98}$) were negatively correlated with the average slope (S_{98}) of the watersheds. Both density and species richness decreased with increased watershed slope. Variation in mussel species richness and density with watershed slope was substantial; for example, mussel densities averaged about 0.18·m^{-2} in sites within watersheds with low slopes (<15%), but averaged <30% of this density at slopes >20% (Fig. 2*a*). Watershed species richness averaged around 8 species when slopes were <15% but less than 50% of this richness at slopes >20% (Fig. 2*c*).

© 2002 NRC Canada

Fig. 3. Correlations between predicted and observed (*a*) mussel species richness and (*b*) mussel density. Observations were based on an independent data set (data collected in 1999) using the slope models derived from data collected in 1998 (eqs. 1 and 2). Solid lines represent 1:1 correspondence of observations and predictions. Please note extremely high values that occurred off-scale of this graph (see arrows in panel *b*). Also shown on the upper abscissa are the watershed slopes corresponding to the predictions of mussel densities (eqs. 1–2).

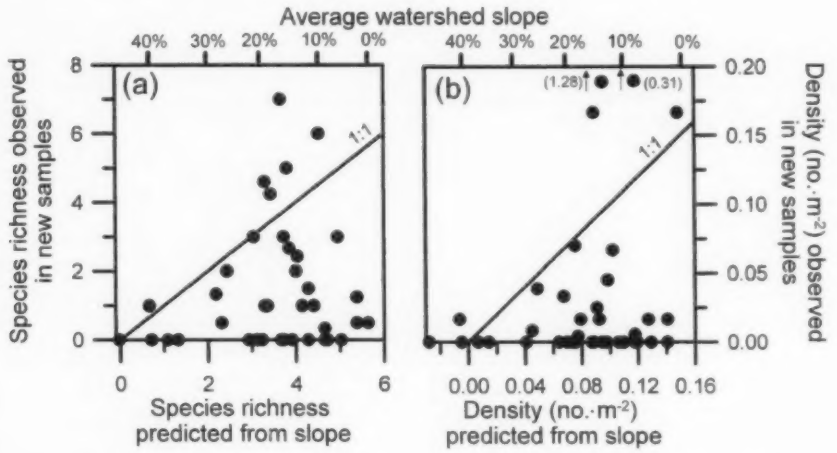

Bivariate regression analysis also showed that alluvial deposits were significantly correlated with mussel density and mussel species richness (Table 1). The regression equations

$$(3) \quad \overline{D}_{98} = -0.016 + 0.0025A_{98}$$

$$(4) \quad \overline{R}_{98} = 0.553 + 0.0716A_{98}$$

indicate mussel density ($\overline{D}_{98}$) and species richness ($\overline{R}_{98}$) were positively correlated with average percent alluvial deposits (A_{98}) in the watershed. Variation in mussel density and species richness with alluvial deposits was substantial. For example, mean watershed mussel densities averaged around $0.1 \cdot m^{-2}$ in watersheds with >35% alluvium, whereas densities were generally <25% of this level in watersheds with <15% alluvium (Fig. 2*b*). Likewise, watersheds with >35% alluvium average around six species, whereas watersheds with <15% alluvium had about one third of this average richness (Fig. 2*d*).

Despite the large amount of data collected, we could find no multivariate relationships between $\overline{R}_{98}$ and $\overline{D}_{98}$ and the variables alluvial deposits and slope. Backward elimination multiple regression methods where independent variables were eliminated based on a retention criterion of $p < 0.05$ for partial significance of regression coefficients resulted in the removal of all candidate variables except mean watershed slope. There was only a very weak collinearity between these two watershed descriptors ($r = -0.5$), so both appear to have an effect.

Because regression models may be influenced by the specific structure of the data set used to construct them, or particular characteristics of the study sites, the general utility of the models can be checked by using them to predict independent sets of data. In this case, we used models based on observations made in 1998 to predict observations made on other sites sampled in 1999. Predictions of mussel density ($\hat{D}_{99}$) and mussel species richness ($\hat{R}_{99}$) were made by substituting the slope (S_{99}) and alluvial (A_{99}) descriptors prepared for the watersheds surveyed in 1999 into eqs. 1–4. To determine the strength of model(s) for predicting mussel density and mussel species richness in this independent set of data, comparisons were made between the predicted and actual values using the alluvial and slope models. Correlations between actual ($\overline{D}_{99}$) and predicted mussel density ($\hat{D}_{99}$), and actual ($\overline{R}_{99}$) and predicted species richness ($\hat{R}_{99}$) when using the slope (eqs. 1 and 2) and alluvial (eqs. 3 and 4) models, were quite weak (Spearman's $\rho = 0.11$–0.19; $p < 0.05$), but were characterized by positive triangular relationships rather than linear trends (e.g., Figs. 3*a*, 3*b*). Despite the absence of strong, linear, statistical relationships, the models yielded directionally correct predictions. For example, neither model predicted low species richness or low mussel density (Fig. 3) where field measurements were high. Rather, the models predicted high mussel species richness and mussel density in areas where actual observations of richness and density were often found to be low.

Discussion

The negative correlations of slope with mussel density and mussel species richness suggest a strong impact of erosional–depositional properties of watersheds. Topographic relief influences hydrologic regimes, and when used as a surrogate for stream gradient and erosional potential of agriculturally disturbed soils, is likely to relate to the biological and ecological limitations of mussel populations. Water is quickly removed from the landscape in areas of high relief, which can result in greatly increased soil erosion, flashy streams (Brooks et al. 1997), and high rates of substrate transport (Newbury 1984). Further, flashy streams and substrate transport can both interfere with mussels' ability to maintain a stable position on the stream bottom. Dislodged mussels, unable to preserve a suitable position for the removal of oxygen and food from the water, are unlikely to survive. Substrate stability generally has an important influence on freshwater mussel distributions (Stern 1983; Strayer and Ralley 1993; Di Maio and Corkum

© 2002 NRC Canada

1995). In disturbed landscapes such as Iowa, areas of high mean topographic relief are likely to present unfavorable mussel habitats and therefore have probably developed low mussel density and lower species richness over the course of impact.

Alluvial deposits may act to improve and (or) maintain conditions for mussels because they alter the quantity of groundwater in a watershed by increasing rates of freshwater transmission and storage (Anderson 1998). Agricultural development in Iowa and elsewhere has resulted in large-scale watershed alterations by draining wetlands and channelizing streams, both of which lead to increased inter- and intra-annual hydrologic variability. Stream flow during dry periods is typically maintained in this region by groundwater discharge from alluvial aquifers to streambeds (Prior 1991). Mussel populations in rivers with abundant alluvial deposits are probably less impacted by periods of extreme low flow than those in areas without this groundwater source. Aquatic species throughout Midwestern North America are adversely affected by extreme water fluctuations (Page et al. 1997), which are ameliorated by groundwater flux through alluvial deposits. Watersheds with the greatest deposits of alluvium are, therefore, relatively hydrologically stable, buffering the impacts of extreme environmental conditions on aquatic communities.

Few studies have used broad-scale field surveys to relate landscape features to mussel species richness or density. Although some have related landscape features such as surface geology (Strayer 1983) and land cover (Morris and Corkum 1996) to mussel species distribution, most have examined local effects (i.e., stream reach conditions), ignoring the broader aspects of watersheds that may influence mussels. Our analysis demonstrates the importance of incorporating terrestrial conditions at a watershed scale into studies investigating factors influencing mussel distribution and abundance.

It is rare that multiple data sets are collected from different broad-scale field surveys to develop and test predictive models of population abundance and biodiversity. Our analysis of watershed geomorphic features and mussel species richness and density indicate that slope and alluvium, reflecting patterns of siltation and habitat stability, are correlated with mussel persistence in this agricultural region. Although correlations between model predictions and new observations of species richness and density were weak, positive relationships and graphical patterns in the data indicate agreement in trends. Some of the variability and unpredictability hampering mussel conservation efforts may therefore result from failure to focus on the broader landscape factors influencing mussel distributions.

Our analyses suggest that watershed-scale GIS may be an important tool for evaluating aquatic resources. The predictive power of the independent variables was between 0.12 and 0.36, the lowest r^2 values in this study being consistent with those seen in other studies seeking relationships between mussel distributions and habitat characteristics (0.06–0.22; Strayer 1993; Strayer and Ralley 1993). Localized and historical effects of watershed impacts likely explain large residual variation in watershed-scale analyses. For example, the transitory and patchy nature of agricultural impacts (e.g., chemical spills, flooding, storm-driven erosion events) is impossible to account for and would contribute to low predictive power. This is especially clear if one considers that many of the zero values for current densities and species richness may have resulted from short-term mortality events unrelated to watershed characteristics. Watershed-mediated impacts on fish could also influence the viability of mussel species. This may be important for all but one of the species we studied, since most have obligate parasitic larval stages. Unfortunately, consistently collected fish abundance and richness data were too rare to be accounted for in this analysis.

Our analyses show that, on a large scale, mussel abundance and biodiversity in this agriculturally impacted region of the U.S. were related to landscape features linked to erosional and groundwater processes. On one hand, high slope, which might normally have a positive impact on mussels in unperturbed landscapes with stable land cover and intact riparian zones, can lead to great erosion and substrate instability in the altered geography of anthropogenic impacts. On the other hand, survival of mussels may be greatest where geological formations like alluvial deposits stabilize the variations associated with land clearing and altered drainage. Our analysis indicates that mussel conservation efforts are most critical in highly sloping landscapes with less permeable soils, where low groundwater flows might lead to unfavorable conditions. It also suggests that high rates of mussel disappearance in this region may be in part linked to large-scale watershed alterations. The persistence of mussel populations and the maintenance of aquatic biodiversity at specific sites are, therefore, dependent upon good management throughout the watershed.

References

Anderson, W.I. 1998. Geology of Iowa: over 2 billion years of change. Iowa State University Press, Ames.

Bogan, A.E. 1993. Freshwater bivalve extinctions (Mollusca: Unionoida): a search for causes. Am. Zool. **33**: 599–609.

Brim Box, J., and Mossa, J. 1999. Sediment, land use, and freshwater mussels: prospects and problems. J. North Am. Benthol. Soc. **18**: 99–117.

Brooks, K.N., Ffolliott, P.F., Gregersen, H.M., and DeBano, L.F. 1997. Hydrology and the management of watersheds. Iowa State University Press, Ames.

Di Maio, J., and Corkum, L.D. 1995. Relationship between the spatial distribution of freshwater mussels (Bivalvia: Unionidae) and the hydrological variability of rivers. Can. J. Zool. **73**: 663–671.

Downing, J.A., and Downing, W.L. 1992. Spatial aggregation, precision, and power in surveys of freshwater mussel populations. Can. J. Fish. Aquat. Sci. **49**: 985–991.

Elliot, W.J., and Ward, A.D. 1995. (*Editors.*) Soil erosion and control practices. *In* Environmental hydrology. Lewis Publishers, Boca Raton, Fla. pp. 177–203.

Frest, T.J. 1987. Mussel survey of selected interior Iowa streams. University of Northern Iowa. Final Report to Iowa Department of Natural Resources and the U.S. Fish and Wildlife Service. Des Moines, Iowa.

Hayek, L.C., and Buzas, M.A. 1997. Surveying natural populations. Columbia University Press, New York.

Karr, J.R., and Schlosser, I.J. 1978. Water resources and the land water interface. Science, **201**: 229–234.

Layzer, J.B., and Madison, L.M. 1995. Microhabitat use by freshwater mussels and recommendations for determining their instream flow needs. Regul. Rivers Res. Manag. **10**: 329–345.

© 2002 NRC Canada

Master, L. 1990. The imperiled status of North American aquatic animals. Biodivers. News, **3**: 5–8.

Morris, T.J., and Corkum, L.D. 1996. Assemblage structure of freshwater mussels (Bivalvia: Unionidae) in rivers with grassy and forested riparian zones. J. North Am. Benthol. Soc. **15**: 576–586.

Newbury, R.W. 1984. Hydrologic determinants of aquatic insect habitats. *In* The ecology of aquatic insects. *Edited by* V.H. Resh and D.M. Rosenberg. Praeger, New York. pp. 323–357.

Page, L.M., Pyron, M., and Cummings, K.S. 1997. Impacts of fragmentation on midwestern aquatic organisms. *In* Conservation in highly fragmented landscapes. *Edited by* M.W. Schwartz. Chapman & Hall, New York. pp. 189–212.

Pennak, R.W. 1989. Fresh-water invertebrates of the United States. 3rd ed. Wiley & Sons, Inc., New York.

Prior, J.C. 1991. Landforms of Iowa. University of Iowa Press, Iowa City, Iowa.

Rabeni, C.F., and Jacobson, R.B. 1993. The importance of fluvial hydraulics to fish-habitat restoration in low-gradient streams. Freshwater Biol. **29**: 211–220.

Richards, C., and Host, G.E. 1994. Examining land use influences on stream habitats and macroinvertebrates: a GIS approach. Water Resour. Bull. **30**: 729–738.

Richards, C., Johnson, L.B., and Host, G.E. 1996. Landscape-scale influences on stream habitats and biota. Can. J. Fish. Aquat. Sci. **53**: 295–311.

Roth, N.E., Allan, J.D., and Erickson, D.L. 1996. Landscape influences on stream biotic integrity assessed at multiple spatial scales. Landsc. Ecol. **11**: 141–156.

Schlosser, I.J. 1991. Stream fish ecology: a landscape perspective. Bioscience, **41**: 704–712.

Stern, E.M. 1983. Depth distribution and density of freshwater mussels (Unionidae) collected with SCUBA from the lower Wisconsin and St. Croix Rivers. Nautilus, **97**: 36–42.

Strayer, D. 1983. The effects of surface geology and stream size on freshwater mussel (Bivalvia: Unionidae) distribution in southeastern Michigan, U.S.A. Freshw. Biol. **13**: 253–264.

Strayer, D.L. 1993. Macrohabitats of freshwater mussels (Bivalvia: Unionacea) in streams of the northern Atlantic Slope. J. North Am. Benthol. Soc. **12**: 236–246.

Strayer, D.L., and Ralley, J. 1993. Microhabitat use by an assemblage of stream-dwelling unionaceans (Bivalvia), including two rare species of *Alasmidonta*. J. North Am. Benthol. Soc. **12**: 247–258.

Thompson, J.R. 1992. Prairies, forests, and wetlands: the restoration of natural landscape communities in Iowa. University of Iowa Press, Iowa City, Iowa.

Wang, L., Lyons, J., Kanehl, P., and Gatti, R. 1997. Influences of watershed landuse on habitat quality and biotic integrity in Wisconsin streams. Fisheries, **22**: 6–12.

Williams, J.D., and Neves, R.J. 1995. Freshwater mussels: a neglected and declining aquatic resource. *In* Our living resources: a report to the nation on the distribution, abundance, and health of U.S. plants, animals, and ecosystems. *Edited by* E.T. LaRoe, G.S. Farris, C.E. Puckett, P.D. Doran, and M.J. Mac. U.S. Department of the Interior National Biological Service, pp. 177–179.

© 2002 NRC Canada

Effects of ultraviolet radiation on rates and size distribution of primary production by Lake Erie phytoplankton

Véronique P. Hiriart, Bruce M. Greenberg, Stephanie J. Guildford, and Ralph E.H. Smith

Abstract: The impact of natural solar ultraviolet radiation (UVR), particularly UVB (297–320 nm), on phytoplankton primary production in Lake Erie was investigated during the spring and summer of 1997. Radiocarbon incorporation and size-selective filtration was used to trace total production and its distribution among particulate and dissolved pools. On average, 1-h exposures produced half the UVB-dependent inhibition of total production realized in 8-h exposures, indicating rapid kinetics of photoinhibition. Cumulative UVB-dependent photoinhibition averaged 36% in 8-h simulated surface exposures. The efficiency of photoinhibition was greater for N-deficient than N-replete communities, but was not related to phytoplankton light history, P limitation, or the dominant genera. The proportion of recently fixed carbon occurring in the dissolved pool after 8-h exposures was significantly greater in higher-UVB treatments, whereas the share in picoplankton (<2 μm) was significantly lower. Significant UVB-dependent inhibition of total production was limited on average to relatively severe exposures, but the rapid kinetics of inhibition and the apparent effects on the allocation of carbon suggest it may be important to the lake's food web. Differences in optical properties and thermal stratification patterns suggested that the relatively turbid west basin was potentially more susceptible to UVR photoinhibition than the more transparent east or central basins.

Résumé : Nous avons étudié l'impact de la radiation solaire ultraviolette (UVR) naturelle, particulièrement de l'UVB (297–320 nm), sur la production primaire du phytoplancton au lac Érié durant le printemps et l'été 1997. L'incorporation de radiocarbone et la filtration d'après la taille nous ont permis de suivre la production totale et sa répartition dans les compartiments particulaire et dissous. En moyenne, des expositions de 1 h produisaient la moitié de l'inhibition de la production totale due à l'UVB qui se faisait dans des expositions de 8 h, ce qui indique l'existence d'une cinétique rapide de la photoinhibition. La photoinhibition due à l'UVB cumulative correspondait en moyenne à 36 % lors d'expositions de 36 h qui simulaient les conditions de surface. L'efficacité de la photoinhibition était plus grande chez les communautés privées de N que chez celles qui en étaient saturées; par ailleurs, l'efficacité n'était reliée ni aux conditions antérieures d'exposition du phytoplancton à la lumière, ni à la carence de P, ni à la dominance générique dans la communauté. La proportion de carbone fraîchement fixé dans le compartiment dissous après des expositions de 8 h était significativement plus grande lorsque les quantités d'UVB étaient fortes, alors que la part dans le phytoplancton (<2 μm) était significativement réduite. Les inhibitions significatives de la production totale dues à l'UVB ne se produisaient généralement que lors d'expositions importantes; cependant, la cinétique rapide de l'inhibition et les effets apparents sur l'allocation du carbone laissent croire que l'inhibition a des conséquences importantes sur le réseau trophique du lac. Des différences dans les propriétés optiques et les patterns de stratification thermique indiquent que le bassin occidental relativement turbide est potentiellement plus vulnérable à la photoinhibition due à l'UVB que les bassins central et oriental qui ont une eau plus transparente.

Traduit par la rédaction

Introduction

In the past two decades, the depletion of the stratospheric ozone layer has stimulated research on the biological consequences of increased exposure to solar ultraviolet B (UVB, nominally 280–320 nm) radiation, with particular emphasis on marine phytoplankton (e.g., Schofield et al. 1995; Neale et al. 1998*a*). Ultraviolet radiation (UVR) at the Earth's surface includes both UVB and UVA (320–400 nm), and is a significant influence on primary production by phytoplankton (e.g., Neale et al. 1998*a*, 1998*b*). Sensitivity to UVR varies among phytoplankton species and assemblages, because of differing phenotypic (e.g., external morphology and cellular organelle arrangement) and genotypic (e.g.,

Received 2 November 2001. Accepted 4 October 2001. Published on the NRC Research Press Web site at http://cjfas.nrc.ca on 5 March 2002.
J16045

V.P. Hiriart,[1] B.M. Greenberg, S.J. Guildford, and R.E.H. Smith. Department of Biology, University of Waterloo, Waterloo, ON N2L 3G1, Canada.

[1]Corresponding author (e-mail: vphiriar@sciborg.uwaterloo.ca).

 DOI: 10.1139/F01-212 © 2002 NRC Canada

DNA base content and sequence; antioxidant synthesis and repair capabilities) characteristics (Karentz et al. 1991; Bothwell et al. 1993). The relationship of UVR exposure to the taxonomic composition of algal communities (e.g., Bothwell et al. 1993; Halac et al. 1997) and to the cell size of the target algae (e.g., Karentz et al. 1991; Laurion and Vincent 1998) is variable, but potentially as important as UVR effects on total production (e.g., Williamson 1995). In addition to the link between phytoplankton size and (or) taxonomy and suitability as food for grazers, the production and quality of algae are also linked to the activity of bacteria and the microbial food web. Even healthy phytoplankton release organic carbon in dissolved form, contributing importantly to the pool of labile dissolved organic carbon (DOC), which helps support bacterioplankton and the microbial food web (Bjørsen 1988; Lignell 1990). The production and availability of this algal-derived DOC can be changed by UVR exposure of the algae (Pausz and Herndl 1999) and by photomodification after release (e.g., Tranvik and Kokalj 1998).

The Laurentian Great Lakes are the most important freshwater resources in North America. Lake Erie in particular has historically sustained a high fish diversity and biomass (Bolsenga and Herdendorf 1993). Once a famous example of anthropogenic eutrophication, Lake Erie has been restored to an oligotrophic–mesotrophic condition because of internationally organized restrictions on phosphorus loading (e.g., Dahl et al. 1995; Charlton et al. 1999). Decreased nutrient loads and the invasion of the filter-feeding zebra and quagga mussels (*Dreissena* sp.) have been associated with increased water clarity in many parts of Lake Erie since 1988 (e.g., Charlton et al. 1999). Today, there is concern that primary production in Lake Erie may be insufficient to meet the demands of the dreissenid mussels and to maintain the fish community. Increased UVR exposure consequent to water clarification, as well as stratospheric ozone depletion, may be a critical additional stress. Research on the consequences of UVR exposure in Lake Erie and the other Laurentian Great Lakes nonetheless remains sparse (Smith et al. 1999; Marwood et al. 2000; Wilhelm and Smith 2000).

In this study, photoinhibition in Lake Erie phytoplankton communities exposed to UVR was measured during spring and summer, the seasons of greatest UVR exposure. The rate and extent of UVB-dependent photoinhibition was assessed and compared against several factors that may modify the susceptibility to UVR damage (e.g., nutrient status, light history, and phytoplankton community composition; e.g., Gala and Giesy 1991; Lesser et al. 1994; Villafañe et al. 1995). The effects of UVR on the distribution of recently produced organic carbon among size classes of particles (<2 µm and >2 µm size fractions) and the DOC pool were investigated. The current study concentrated specifically on the effects of UVB, the only waveband significantly affected by stratospheric ozone depletion.

Materials and methods

Study site

Sampling and field experiments were conducted at stations throughout Lake Erie (42°N, 81°W). Lake Erie (Fig. 1) has an area of 25 500 km^2 and is separated into three distinct basins distinguished by their bathymetry and differing trophic status and water clarity (Burns 1985; Dahl et al. 1995). The smaller west basin (mean depth (Z_m) = 7.6 m; 3680 km^2) is mesotrophic and turbid, owing to high nutrient and sediment inputs. The larger central basin (Z_m = 17.8 m; 15 390 km^2) receives less nutrient and sediment loading (largely from the west basin) and is oligotrophic. The east basin (Z_m = 27.0 m; 6150 km^2) is the deepest, clearest, and most oligotrophic of the three basins. The deeper east and central basins normally stratify during the summer months, while the relatively shallow west basin typically remains unstratified.

Experimental design and sampling protocol

Experiments were conducted on the CCGS *Limnos* at various stations during five cruises from early May to late August 1997 (Table 1) under relatively clear sky conditions. The physical structure of each lake station was measured by conductivity, temperature, and depth sensors (SBE-25 models, EBTT and Water Quality Profiler, Sea-Bird Electronics Inc., Bellevue, Wash.). In addition, casts of a Sea-Bird SBE-19 equipped with a Sea-Tech fluorometer (Sea-Bird Electronics Inc., Bellevue, Wash.) were conducted to characterize the in vivo chlorophyll *a* fluorescence profile of the water column. Incident solar radiation spectra were measured with a diode-array spectroradiometer (InstaSpec, Oriel Corp., Stratford, Conn.) equipped with a collecting sphere, at 0.5-nm intervals from 295 to 700 nm every 30 min (Smith et al. 1999). In practice, little radiation could be accurately quantified at the lower end of the measured spectrum (<297 nm), so UVB in this study was quantified as the amount of radiation between 297 and 320 nm. The radiometer was calibrated with a lamp traceable to the National Bureau of Standards specifications and wavelength calibration was done with reference to known absorption lines in the incident solar spectrum. The same radiometer was used to measure the spectral transmission of the optical filters and incubation vessels used in the time series experiments.

Wherever possible, underwater penetration of photosynthetically active radiation (PAR) was measured using a LI-COR LI-1000 (Lincoln, Nebr.) with an underwater cosine quantum sensor. The light attenuation coefficient was then determined and used to calculate the percent mean PAR within the mixed layer. Mean PAR was calculated as

$$(1) \qquad I_a = \frac{I_o}{-k_{dPAR}Z_e}(e^{-k_{dPAR}Z_e} - 1)$$

where I_a is irradiance at depth a, I_o is the percent incident irradiance (100%), k_{dPAR} is the vertical light attenuation coefficient, and Z_e is the depth of the epilimnion.

Whole-water samples for on-board experiments were taken early in the morning at 5-m depth (except 3 m on 1 July) with Niskin bottles so the incubations could begin by 10:00 (EDT). In these time-series experiments, all reported photosynthetic rates are means of three replicate samples from independent incubation vessels. Lake water samples were inoculated with ^{14}C sodium bicarbonate (ICN Biomedicals, Irvine, Calif.; 2 µCi µL^{-1}) and dispensed into acid-washed quartz tubes (55-mL capacity) or polystyrene flasks (65-mL capacity). The incubation vessels were then placed in ultraviolet-transmitting Plexi-

© 2002 NRC Canada

Fig. 1. Lake Erie and the stations sampled in 1997 for time-series experiments.

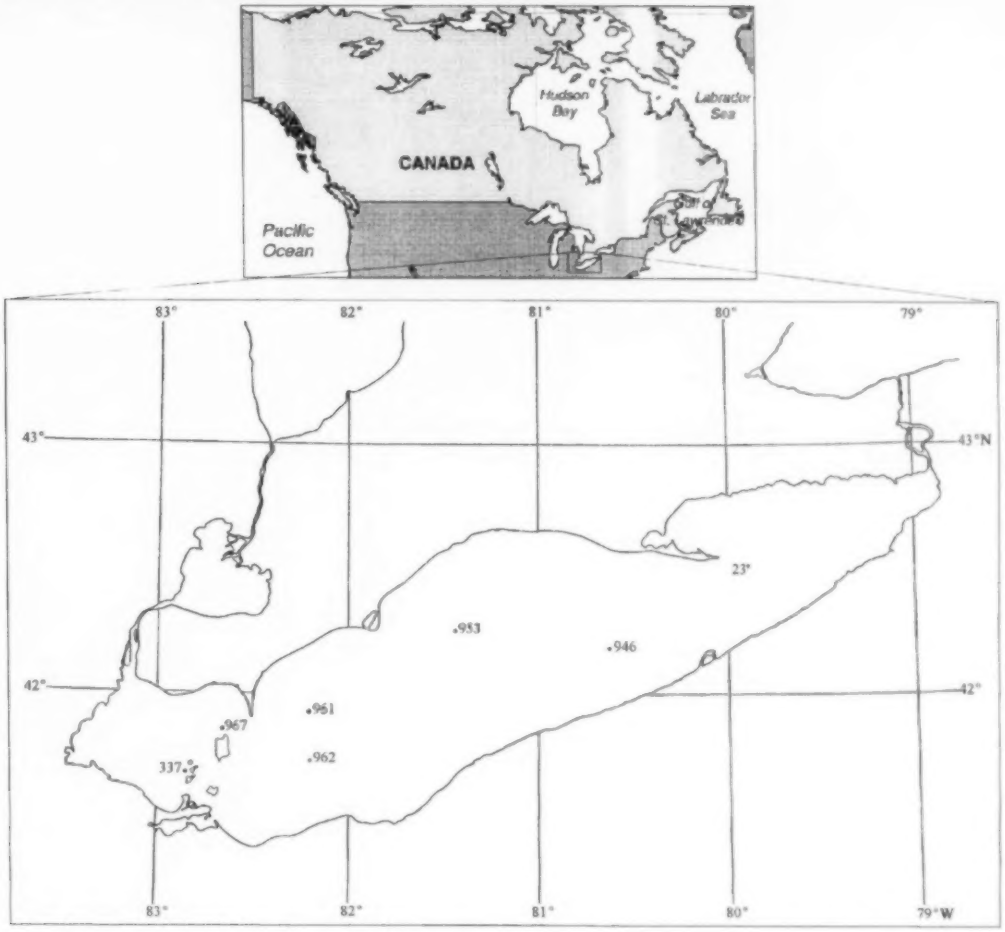

glas deck-boxes (23 cm × 23 cm × 3.5 cm) fitted with different optical filters and sampled at pre-established time intervals. Any attenuation of PAR and (or) UVR radiation attributed to the Plexiglas was accounted for. Temperature was maintained by continuously circulating surface lake water with <1 cm submersion of both the quartz tubes and the polystyrene flasks. Quartz tubes were sampled following 0.5 h, 1 h, 2 h, 4 h, 6 h, and 8 h of exposure, whereas polystyrene flasks were sampled after 1 h, 3 h, and 8 h.

At each sampling time and at time zero, a 5-mL subsample from each experimental vessel was acidified with 100 µL of 6 M HCl, allowed to de-gas for 24 h, and fixed with 15 mL of EcoLume™ scintillation cocktail (ICN Pharmaceuticals, Costa Mesa, Calif.). Total activity (200 µL) samples were also taken to verify the isotope additions. At the end of the incubation period, an additional 5-mL sample from each treatment was taken and size fractioned, filtering through overlapping filters of different pore sizes, into >2 µm (2-µm membrane filter, Nucleopore, AMD, Mississauga, Ont.), 0.7–2 µm (glass fibre, GF/F, AMD, Mississauga, Ont.), and DOC (collected filtrate) fractions to assess the relative distribution of the carbon tracer. The 2-µm fraction, operationally defined by a GF/F filter, will contain bacteria. The filtrate sample was acidified and fixed as above, while each filter was also acidified with 100 µL of 6 M HCl and after 24 h, fixed with 5 mL of EcoLume™ scintillation cocktail. Photosynthetic carbon assimilation was calculated using dissolved inorganic carbon concentrations measured on filtered (glass fibre, GF/F) lake water from each station. Initial total chlorophyll *a* concentration was measured by fluorometry (e.g., Smith et al. 1999) and phytoplankton community composition by microscopic examination of samples preserved with Lugol's iodine.

The optical filters were window screen (ca. 50% transmission at all wavelengths) and Mylar-D, which selectively removes UVB. Different combinations of these filters with the two different types of experimental vessels yielded a total of eight treatments with two levels of irradiance (100% and 50% PAR) and four different spectral qualities (100%, 50%, 30%, and 15% UVB exposure levels) (Fig. 2). All of the experimental treatments conducted in this study included at least a portion of the UVA waveband, but the main emphasis

© 2002 NRC Canada

Table 1. Summary of limnological variables of the stations sampled for time-series experiments conducted on Lake Erie between the months of May and August 1997.

Date	Station	Basin	Epilimnion thickness (m)	Epilimnion temperature (°C)	Chlorophyll *a* at 5 m (μg·L^{-1})	k_{dPAR} (m^{-1})	Mean % PAR of incident
7 May	946	C	22 (iso.)	6	1.5	0.43	10.6
3 June	946	C	22 (iso.)	8.8	2.5	0.29	15.1
4 June	337	W	9 (iso.)	13.2	9.8	1.61	6.9
5 June	961	C	19 (iso.)	13.4	1.2	0.83[a]	6.3
1 July	23	E	5	20.3	0.7	0.36	46.4
2 July	967	W	8	23.5	2.1	0.36	32.8
29 July	23	E	15	22	3.5*	0.24	27
30 July	953	C	12	22.2	1.4	0.32	25.5
31 July	962	C	11	23.7	2	0.36[a]	24.8
27 August	337	W	9 (iso.)	21.1	15.5	1.16	9.6

Note: PAR, photosynthetically active radiation; k_{dPAR}, vertical attenuation coefficient; iso., isothermal.

[a]Values of k_{dPAR} derived from the following relationship: k_{dPAR} = –0.026·transmission + 2.258, a relationship derived from measured k_{dPAR} and transmission values from conductivity, temperature, and depth meter casts.

*Note that on this date in vivo chlorophyll *a* fluorescence was not uniformly distributed within the mixed layer (see Fig. 4c).

is on comparisons between UVB-exposed and UVB-excluded (Mylar-D) treatments (Table 2).

Measures of response to UVB and PAR

The sensitivity of the different algal assemblages to UVB was assessed using a UVB inhibition efficiency index ((J·m^{-2})$^{-1}$)

$$(2) \qquad UVB_{inh.\ eff.} = \frac{1 - PS_{exposed} / PS_{screened}}{UVB_{dose}}$$

where $PS_{exposed}$ and $PS_{screened}$ are cumulative photosynthesis in treatments exposed to UVB or screened from it by Mylar-D. UVB_{dose} is the unweighted cumulative UVB exposure (J·m^{-2}). The unweighted UVB exposure was used because the spectral quality within these treatments did not vary appreciably between sampling dates and the unweighted UVB exposure showed a good linear relationship with the weighted (*Phaeodactylum tricornutum* BWF; Cullen et al. 1992) exposure. There were four pairs of exposed versus screened treatments (Table 2) and the $UVB_{inh.\ eff.}$ values did not differ significantly among the treatment pairs. However, only the 50% incident exposure quartz treatments (Q50, Table 2) were used for statistical and graphical analysis of relationships between UVB sensitivity and potential modifying factors (e.g., nutrient status). Q50 offered a relatively high ratio of UVB to PAR and UVA in the exposed treatment (Table 2) but a relatively low (50%) total irradiance of PAR and UVA, which should maximize discrimination of UVB effects versus those from PAR and UVA.

A light gradient incubator was additionally used at each station to assess light adaptation and the contribution of PAR to photoinhibition (Smith and Maly 1993). Nine to 18 subsamples of 5 mL each were incubated for 1 h, with photosynthetic carbon assimilation estimated by the acidification method as described above. Light was from a quartz halogen lamp (PAR only), ranging from 0.4 to ~2000 μE·m^{-2}·s^{-1}. The photosynthetic light response was fitted to the model of Platt et al. (1980)

$$(3) \qquad P^B = P_s^B \cdot (1 - e^{-\alpha^B I / P_s^B}) \cdot e^{-\beta^B I / P_s^B}$$

where P_s^B is the maximum rate of photosynthesis attainable in the absence of photoinhibition, α^B is the initial slope of the response (a measure of light utilization efficiency), and β^B is the photoinhibition parameter. There was in fact no photoinhibition in any of the experiments (β^B = 0), so the model was refitted without the photoinhibition term to estimate the actual light saturated rate (maximum) of photosynthesis, P_m^B, and P_m^B:α^B, the photoadaptation parameter, or I_k.

Fig. 2. Percent transmission of ultraviolet radiation (UVR) wavelengths for the different spectral treatments. Solid line, quartz tube, Q100+ treatment; dotted line, quartz tube with Mylar-D, Q100–treatment; short broken line, polystyrene flask, P30+ treatment; long broken line, polystyrene flask with Mylar-D, P30 treatment. The same spectral treatments were repeated with 50% neutral density attenuation (Q50+, etc.) to achieve half the total irradiance at all wavelengths.

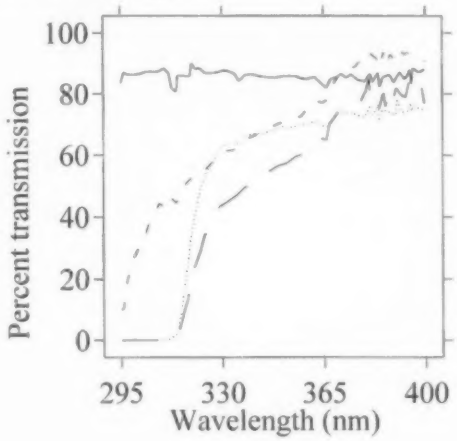

Nutrient status

Phosphorus (P) deficiency was evaluated by three indices, alkaline phosphatase activity (APA), P debt assays, and phosphorus turnover times (measured by ^{33}P-PO_4 uptake) and nitrogen (N) deficiency by one index, the N debt assay (Guildford et al. 1994). Results were interpreted to indicate no deficiency, mild, moderate, or severe deficiency by com-

© 2002 NRC Canada

Table 2. Approximate percentage of incident photosynthetically active radiation (PAR), ultraviolet A (UVA), and ultraviolet B (UVB) in the different spectral treatments of the time-series experiments.

Treatment	% PAR	% UVA	% UVB
Q100+ (100% full spectrum)	100	100	100
Q100– (100% minus UVB)	100	100	0
Q50+ (50% full spectrum)	50	50	50
Q50– (50% minus UVB)	50	50	0
P30+ (100% polystyrene)	100	50	30
P30– (100% polystyrene minus UVB)	100	50	0
P15+ (50% polystyrene)	50	25	15
P15– (50% polystyrene minus UVB)	50	25	0

Note: Q, quartz tubes; P, polystyrene flasks.

parison with values suggested by Healey and Hendzel (1979), based on culture work with freshwater phytoplankton.

Statistical analysis

Analysis of variance (ANOVA) was used to investigate the dependence of UVB sensitivity on environmental parameters. ANOVA was also used to test for effects of light and nutrient status as well as effects of UVB on DOC production. The size-specific particulate organic carbon production rates violated the normality assumption for ANOVAs and could not be appropriately transformed. These data were analysed by nonparametric ranking analysis to test for effects of UVB or other environmental variables on the size distribution of production. Owing to the large spatial variability in biological and physicochemical characteristics in Lake Erie, both the parametric and nonparametric analyses treated each station as a block, thereby removing the variability caused by location. Planned, pairwise, a posteriori comparisons were made using the post-hoc Tukey test to compare UVB exposure level effects, overall UVB effect, and nutrient status effects.

Results

Limnological conditions

A total of 134 temperature profiles revealed the variability in establishment and depth of seasonal thermoclines over the sampling period and among basins. Seasonal thermoclines were not observed at any station in May, and increased in frequency and mean depth from June to August (mean epilimnion depth ca. 15 m). Water clarity was spatially heterogenous, with a distinct east–west gradient in PAR attenuation. Median values of the diffuse vertical attenuation coefficient for PAR showed highest penetration in the east basin, with a median seasonal euphotic (1% incident) depth of 18.1 m. By comparison, the central and west basins had median seasonal euphotic depths of 14.4 m and 7.3 m, respectively.

The average seasonal thermocline depth was also basin specific with maximum values occurring in the deeper east basin (median 15.0 ± 5.3 m). Although the east and central basin stations typically stratified in the warm summer months (97.5% and 88.1% of the surveyed stations, respectively), the west basin stations did not develop thermoclines as frequently (48.1% of the surveyed stations). Additionally, shallow, "temporary" thermoclines, defined as a slight change in temperature (ca. 0.5–1°C·m^{-1}) with depth, typically occurring in the top two metres of the water column, were also recorded in about 30% of all stations for which both temperature and in vivo fluorescence profiles (a total of 37 stations) were available. These so-defined temporary thermoclines were differentiated from seasonal thermoclines, which were typically deeper (10–20 m) and exhibited sharper changes in temperature with depth (ca. 2–3°C·m^{-1}). In 1997, temporary thermoclines were noted more frequently in early June compared with July and August, and predominantly occurred in the west basin. Vertical profiles usually showed lower in vivo chlorophyll *a* fluorescence above these temporary thermal boundaries than below (e.g., Fig. 3*a*).

The limnological conditions for each station at which experiments were done are listed in Table 1. Seasonal thermoclines were not established at any of the experimental stations in May, June, and August, whereas in July all showed signs of thermal stratification. With one exception, the water samples collected for each experiment were representative of the mixed layer, as evidenced by the vertically uniform in vivo chlorophyll *a* fluorescence and temperature distributions. The epilimnion of the east basin station 23, sampled in late July at 10:45, was not uniformly mixed (Fig. 3*c*). This station was also sampled on 1 July and on both these occasions, subsurface chlorophyll *a* fluorescence maxima were observed near the seasonal thermocline. Although uniform mixing was evident within the epilimnion on 1 July, the calmer waters on 29 July were associated with a depth-dependent in vivo chlorophyll *a* fluorescence distribution within the epilimnion (Figs. 3*b*, 3*c*). Subsurface chlorophyll *a* fluorescence maxima were also noted at stations 953 and 962 sampled in July, at 11 and 14 m (top of seasonal thermocline) depths, respectively. Light availability, as indicated by mean PAR (Table 1), attained its maximum in the shallow surface mixed layer on 1 July and minimal values under unstratified conditions at deep stations (e.g., 5 June) and in the relatively turbid west basin (e.g., 27 August).

Phytoplankton characteristics

Nutrient status of the whole-water samples was assessed with various indicators (see Materials and methods; S.J. Guildford, unpublished data). Reported here is the overall assignment of nitrogen and phosphorus deficiency based on all the nutrient status indicators (Table 3). Moderate nitrogen and (or) phosphorus deficiency occurred at all stations except the west basin station 337 sampled on 4 June and 27 August and the east basin station 23 sampled on 1 and 29 July. When N and P deficiency occurred, the degree of defi-

© 2002 NRC Canada

Fig. 3. Temperature and in vivo chlorophyll *a* fluorescence profiles. (*a*) Shallow (1-m) temporary thermocline with corresponding depression in in vivo chlorophyll *a* fluorescence, station 357 sampled 4 June 1997. (*b*) Subsurface chlorophyll *a* fluorescence maximum with uniform chlorophyll *a* distribution within the surface mixed layer (5 m), station 23 sampled 29 July 1997. (*c*) Subsurface chlorophyll *a* fluorescence maximum with incomplete mixing of the epilimnion (15 m) evidenced by the depth dependent change in fluorescence, station 23 sampled 1 July 1997. Solid line, relative fluorescence units; dashed line, temperature (°C); RFU, relative fluorescence units.

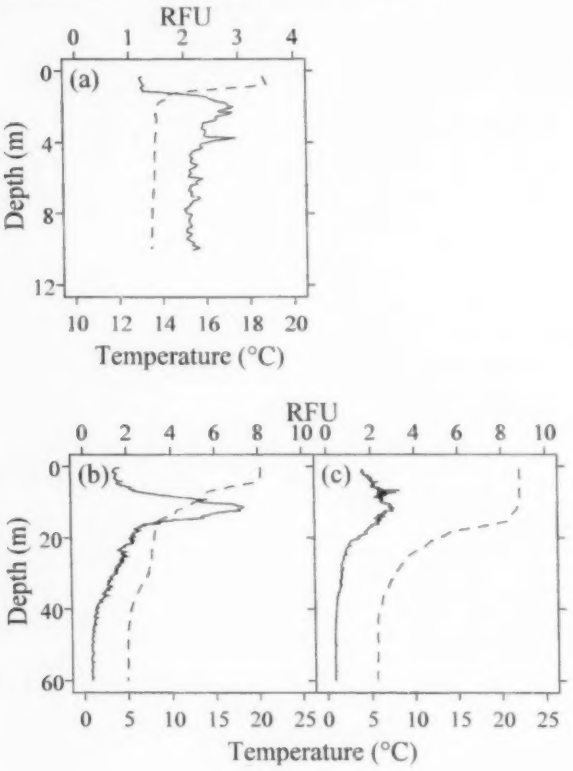

ciency was in the moderate range according to the criteria of Healey and Hendzel (1979).

The photosynthesis–irradiance curves from the light gradient incubator allowed estimates of the maximum photosynthetic rates (P_m^B), the initial slope (α^B), and the light saturation parameter (I_k) (Table 3), and thus an assessment of the photoadaptive state of the phytoplankton. Low I_k (<100 $\mu E \cdot m^{-2} \cdot s^{-1}$) values were observed on three experimental dates (3 June, 4 June, and 29 July), suggesting that the phytoplankton were adapted to relatively low light conditions. One station (27 August) suggested a more high-light adapted state, whereas other stations were intermediate (Table 2).

The dominant genera of nano- and micro-phytoplankton varied between experimental dates but diatoms were important throughout, frequently dominating or codominating the mixed assemblages. Small flagellates of the *Ochromonas* (Chyrsophyceae) and *Cryptomonas* (Cryptophyta) genera were also commonly important. Picoplankton were not enu-

Table 3. Dominant nano- and micro-phytoplankton genera, photosynthetic parameters, nutrient status, and $UVB_{inh.\ eff.}$ for the different stations sampled in Lake Erie.

Date	Station	Dominant genera of nano- and micro-phytoplankton	P_m^B	α_B	I_k	Nutrient deficiency status		$UVB_{inh.\ eff.}$	
						P	N	1 h	8 h
7 May	946	*Aulacoseira*	4.62 ± 0.20	7.22 ± 0.83	177.7	N	Y	12.83	1.18
3 June	946	*Stephanodiscus*	2.86 ± 0.13	13.06 ± 1.94	60.9	Y	N	3.96	0.32
4 June	337	*Diatoma*/*Aulacoseira*	5.68 ± 0.26	18.06 ± 2.78	87.4	N	N	1.35	1.07
5 June	961	*Dinobryon*/*Aulacoseira*	n.a.	n.a.	n.a.	N	Y	4.01	0.6
1 July	23	*Dinobryon*	3.93 ± 0.18	8.89 ± 1.11	122.8	N	N	2.47	0.59
2 July	967	*Ochromonas*/*Aulacoseira*	3.66 ± 0.25	8.06 ± 1.67	126.2	Y	N	2.04	2.59
29 July	23	*Anabaena*/*Cryptomonas*	4.65 ± 0.30	14.72 ± 2.22	87.7	N	N	6.88	1.22
30 July	953	*Dinobryon*/*Fragilaria*	4.92 ± 0.33	10.56 ± 2.22	129.5	Y	Y	7.36	1.85
31 July	962	*Fragilaria*/*Ochromonas*	8.39 ± 0.46	21.11 ± 3.61	110.4	Y	N	3.96	0.2
27 August	337	*Aulacoseira*/*Cryptomonas*	5.13 ± 0.17	5.27 ± 0.28	270	N	N	–0.98	0.13

Note: Values for the maximum photosynthetic rates (P_m^B; $\mu g\ C \cdot \mu g\ chlorophyll\ a^{-1} \cdot h^{-1}$) and the initial slope (α^B; $\mu g\ C \cdot m^2 \cdot \mu g\ chlorophyll\ a^{-1} \cdot E^{-1}$) represent the fitted values ± the asymptotic standard error of the estimate. The light saturation parameter (I_k; $\mu E \cdot m^{-2} \cdot s^{-1}$) values were calculated as P_m^B/α^B and are reported here as indicators of light adaptation status. Nitrogen and phosphorus nutrition status, assessed using all nutrient status indicators (see Materials and methods), are reported for whole-water samples (Y, nutrient deficient; N, nutrient sufficient). $UVB_{inh.\ eff.}$ reported in this table was calculated using th 50% photosynthetically active radiation (PAR) quartz tube treatments.

© 2002 NRC Canada

merated, but the size-fractionated primary production rates (below) indicated a substantial presence of photosynthetically active picoplankton.

Time course and extent of UVB inhibition

Rates of photosynthesis at the outset of the incubations varied among experiments and frequently decreased to relatively low levels within the first 2 h of exposure in both UVB-exposed and -shielded treatments (e.g., Figs. 4*a*, 4*d*). Cumulative photosynthetic rates normalized to uninhibited, light saturated rates showed that the rate of decrease of relative photosynthesis was notably reduced in all treatments after the first 2–3 h of exposure (Figs. 4*c*, 4*f*). The harshest treatments (100% PAR, UVA, and UVB) consistently resulted in the greatest suppression of photosynthesis. At comparable PAR exposure levels, the 30% and 15% UVB exposure level treatments usually demonstrated less photoinhibition than the corresponding 100% and 50% UVB treatments (Fig. 4), reflective of the milder UVR exposure encountered in the polystyrene flasks (30% and 15% UVB) (Fig. 2).

When phytoplankton were shielded from UVB radiation with Mylar-D, higher rates of photosynthesis were generally achieved, although at times differences were small (e.g., Figs. 4*a*, 4*b*, 4*d*, 4*e*). On average (Table 4), the most severe exposures to UVB (100%) diminished cumulative photosynthesis by 16.4% in short-term incubations (1 h), but the inhibition could be as high as 33.0% (e.g., 29 July; station 23 east basin). After 8 h of incubation, such exposures to UVB resulted in 36.3% less cumulative photosynthesis on average, and as much as 57.7% less (e.g., 29 July). Rapid kinetics of photoinhibition were evident in all treatments (Figs. 4*c*, 4*f*), particularly in 100% UVB exposure treatments, where ca. 50% of the UVB-dependent inhibition of cumulative photosynthesis was attained within the first hour of exposure (Table 3). The harshest UVB treatment yielded the greatest inhibition in both short and long incubations, and below 50% exposure, the effects of UVB were on average not significant.

The contribution of PAR to photoinhibition in the short term was assessed by reference to the photosynthesis–irradiance response of phytoplankton in the light gradient incubator (PAR only). There was no statistically significant evidence for PAR-dependent inhibition. The maximum levels of PAR in the incubator were comparable to the maximum solar PAR levels observed. Although the spectral quality differed between the incubator lamp and the natural solar radiation, it appeared unlikely that PAR would cause appreciable inhibition on the 1-h time scale. The potential inhibition by PAR in longer-term (8-h) exposures could not be investigated with this experimental design.

Inhibition efficiency of UVB

Efficiency of inhibition by UVB ($UVB_{inh.\ eff.}$) was variable between lake stations and sample dates but spatial and temporal patterns were difficult to discern with our opportunistic sampling scheme. ANOVA showed that the $UVB_{inh.\ eff.}$ index did not vary significantly with UVB exposure level, but it did vary significantly with time ($p < 0.00001$, $r^2 = 0.243$). Higher $UVB_{inh.\ eff.}$ values for the short versus long exposures were found, suggesting rapid kinetics of UVB-dependent inhibition as well as a nonlinear response to UVB. This nonlinearity was further emphasized when attempts were made to describe the inhibition of cumulative photosynthesis as a linear function of the cumulative weighted UVB and short UVA (297–347 nm) exposure. A linear regression through the combined data yielded a highly significant relationship ($p < 0.00001$), but the amount of variance explained was low ($r^2 = 0.126$). Analysis of individual dates revealed nonsignificant relationships in three experiments (range of p values <0.000001–0.565) and considerable variation in the slope (i.e., sensitivity). Thus, there did not appear to be a consistent linear response among the communities encountered here.

Because of the rapid nature of the kinetics of UVB-dependent photoinhibition and the possible masking effects of UVA and PAR, it was assumed that any difference in sensitivity to UVB would more likely be reflected in the 1-h versus the 8-h $UVB_{inh.\ eff.}$ index. Attempts were therefore made to identify any relationships between the 1-h index of UVB sensitivity and species composition, nutrient status, and (or) light history. With this relatively small data set, only simple and strong effects would be identifiable and little success was achieved in finding them. Community composition was not an obviously decisive factor, since the same genera (e.g., *Dinobryon*) or higher groups (e.g., diatoms) could be dominant in both relatively sensitive and relatively tolerant assemblages (Table 2). Visual inspection of scatter plots of APA, P debt, and N debt (not shown) failed to indicate any simple or statistically significant relationships between these nitrogen or phosphorus deficiency indicators and the UVB sensitivity of the phytoplankton. Algal assemblages assessed as nitrogen deficient had higher 1-h $UVB_{inh.\ eff.}$ indices than those deemed nitrogen sufficient (ANOVA $p < 0.05$, $r^2 = 0.432$). This relationship was not present with the 8-h $UVB_{inh.\ eff.}$ values. Further inspection of scatter plots failed to indicate any relationships between sensitivity and either photoadaptive state (I_k) or light history (mean PAR). The environmental influences examined and the phytoplankton species composition may well have contributed to the observed variation in sensitivity, but with the possible exception of nitrogen limitation, an overriding control by any one factor could not be demonstrated.

UVB effects on particulate and DOC production

The proportion of labelled carbon present as dissolved organic carbon ($DO^{14}C$) after 8 h of incubation was usually higher in UVB-exposed than -shielded treatments, but on average the effects were significant ($p < 0.0001$, $r^2 = 0.940$) only at the highest (100% PAR and UVB) and lowest exposures (50% PAR and 15% UVB) (Table 5). Among UVB exposed treatments, the 100% UVB exposures demonstrated significantly ($p < 0.00001$) higher percent $DO^{14}C$ than all other exposure levels. Among UVB shielded treatments, those receiving 100% PAR displayed significantly higher ($p < 0.00001$) percent $DO^{14}C$ than all others.

Nonparametric ranking analysis of the particle size fractions revealed that the proportion of labelled carbon in the picoplankton was significantly ($p < 0.00001$, $r^2 = 0.957$) lower in UVB-exposed than UVB-shielded treatments. The effect was significant on average only at the highest (100% PAR and UVB) and lowest (50% PAR and 15% UVB) expo-

© 2002 NRC Canada

Fig. 4. (*a*, *d*) Interval total primary production rates, (*b*, *e*) cumulative total production, and (*c*, *f*) relative cumulative production measured in all spectral treatments versus elapsed time at station 337, 4 June 1997 (*a*, *b*, *c*) and at station 953, 30 July 1997 (*d*, *e*, *f*). Interval production rates are approximate instantaneous rates at indicated times, whereas cumulative production is the total incorporated carbon up to the indicated time. Relative cumulative production is normalized to cumulative production under noninhibiting conditions. Error bars represent 2 standard errors. ●, 100% PAR, UVA, and UVB; ○, 100% PAR and UVA without UVB; ■, 100% PAR, 50% UVA, and 30% UVB; □, 100% PAR, 50% UVA without UVB; ▲, 50% PAR, UVA, and UVB; △ = 50% PAR, UVB without UVB; ★, 50% PAR, 25% UVA, and 15% UVB; ☆, 50% PAR, 25% UVA without UVB. Chl *a*, chlorophyll *a*.

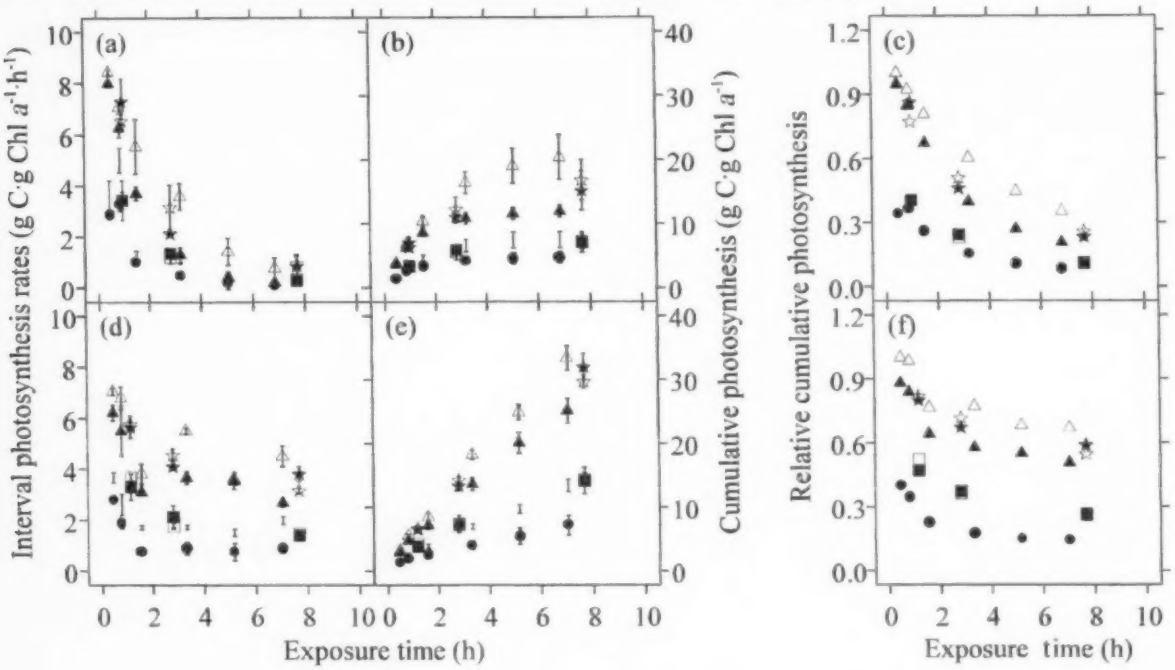

Table 4. Average percent UVB-dependent inhibition of cumulative photosynthesis (PS) following 1 h and 8 h of exposure to different spectral treatments, and the 1-h and 8-h $UVB_{inh.\ eff.}$ values for the different UVB exposure levels.

		1 h		8 h	
UVB exposure	PAR exposure	% UVB inhibition	$UVB_{inh.\ eff.}$	% UVB inhibition	$UVB_{inh.\ eff.}$
100	100	**16.4 ± 4.3**$_{10}$	5.1 ± 1.9$_{10}$	**36.3 ± 6.1**$_{10}$	1.6 ± 0.4$_{10}$
50	50	**8.7 ± 2.1**$_{10}$	4.4 ± 1.2$_{10}$	**15.5 ± 3.8**$_{10}$	1.0 ± 0.3$_{10}$
30	100	–4.5 ± 4.6$_{9}$	–2.7 ± 2.7$_{9}$	–0.5 ± 7.4$_{8}$	–1.3 ± 1.1$_{8}$
15	50	5.1 ± 2.8$_{9}$	4.3 ± 4.4$_{9}$	14.2 ± 7.8$_{8}$	2.1 ± 1.3$_{8}$

Note: % UVB inhibition was calculated as $100\cdot(PS_{UVB\ shielded} - PS_{UVB\ exposed})/PS_{UVB\ shielded}$ within the different treatments. Averages are ±1 standard error; subscripts are the number of samples used in the average computation. Bold values are significantly ($\alpha = 0.05$) different from zero. PAR, photosynthetically active radiation.

sures (Table 5). The effects of UVB on the proportion of total production occurring in the larger phytoplankton size fraction were smaller. On average, the harshest treatments (100% PAR and UVB) showed a borderline significant increase in the proportion of labelled carbon in the large-size fractions with UVB exposure ($p = 0.051$), and a significant increase in the 100% PAR, 30% UVB treatment (Table 5).

Comparing among UVB exposed treatments only, the exposure level had a pronounced effect on the share of total production in picoplankton, with the picoplankton share significantly ($p < 0.00001$) depressed in the harshest exposure compared with others. The share in larger plankton was, by contrast, higher ($p < 0.01$) in the harshest exposure. These effects of exposure level will reflect the variation of PAR and UVA, as well as UVB, among treatments. They indicate significant, but moderate-sized, average effects of total photoinhibitory stress on the disposition of recently fixed carbon among size classes and dissolved versus particulate phases. Nonparametric ranking analysis did not reveal any significant effects of nutrient status on the relative proportion of dissolved versus particulate production.

Discussion

The effects of UVB on planktonic primary production have to date been most extensively and rigorously studied in

© 2002 NRC Canada

Table 5. Average percentage of total labelled carbon in three different carbon pools after 8 h incubation in each radiation treatment (Table 2).

	PAR/UVB treatment label			
	100/100	50/50	100/30	50/15
Dissolved				
With UVB	$14.9 \pm 0.9_{21}$	$8.2 \pm 0.4_{21}$	$9.6 \pm 0.8_{21}$	$10.2 \pm 1.2_{20}$
Without UVB	$10.9 \pm 0.5_{21}$	$7.6 \pm 0.5_{21}$	$10.1 \pm 0.7_{20}$	$7.4 \pm 0.6_{21}$
Particulate				
>2 μm				
With UVB	$60.0 \pm 3.6_{19}$	$54.7 \pm 4.5_{19}$	$57.8 \pm 3.3_{21}$	$55.6 \pm 3.5_{20}$
Without UVB	$56.3 \pm 3.7_{21}$	$55.4 \pm 4.0_{20}$	$54.0 \pm 3.6_{20}$	$52.3 \pm 4.0_{21}$
<2 μm				
With UVB	$25.2 \pm 3.0_{20}$	$37.4 \pm 4.6_{18}$	$32.7 \pm 3.3_{21}$	$34.2 \pm 3.1_{20}$
Without UVB	$32.8 \pm 3.5_{21}$	$37.1 \pm 3.7_{20}$	$35.9 \pm 3.7_{20}$	$40.4 \pm 3.9_{21}$

Note: Each value is the mean of all replicates over eight experiments (7 May and 1 July excluded, data not available) ±1 standard error; subscripts denote the number of samples.

relatively clear oceanic waters, particularly those of the Southern Ocean (e.g., Cullen et al. 1992; Neale et al. 1998*a*, 1998*b*) where the Antarctic ozone hole is such a prominent feature. Lake Erie, by contrast, is a moderately turbid system even by freshwater standards. Its phytoplankton might, therefore, be expected to display acclimation to relatively low exposures, and to be correspondingly vulnerable to UVB damage (e.g., Neale et al. 1998*a*). Evidence for inhibition of short-term primary production by UVB was indeed found. The effects were rapid and often extensive, consistent with fluorescence-based assays of photosynthetic competence in Lake Erie phytoplankton (Marwood et al. 2000). Although variable, the degree of UVB-dependent inhibition under simulated near-surface conditions was within the range found in other studies of both marine and freshwater phytoplankton (e.g., Villafañe et al. 1995; Furgal and Smith 1997) and did not suggest exceptional sensitivity of Lake Erie phytoplankton. The effects of UVB can easily be masked by coincident inhibition by PAR and (or) UVA in relatively long incubations like those used here (Cullen et al. 1992). The estimates of UVB effect presented here, like those from other studies employing relatively lengthy incubations (e.g., Gala and Geisy 1991), should therefore be regarded as minimal.

The sensitivity of algae to UVR is moderated by mechanisms that help the organisms to avoid effective exposure (e.g., screening compounds) as well as mechanisms that promote repair (e.g., DNA photolyase activity). Both aspects (avoidance and repair) are influenced by the interactive effects of radiation of differing wavelengths. Only with an appropriate model for the spectral and kinetic responses of the processes of interest (e.g., photosynthesis) can the sensitivity of different algal communities to any particular waveband (e.g., UVB) be accurately compared or integrated over meaningful depth and time scales (e.g., Smith and Cullen 1995). Such models have been validated for only a few types of phytoplankton communities, however (Neale et al. 1998*a*, 1998*b*; Smith et al. 1998). As an initial descriptive approach, variations in sensitivity were analysed with a simple index ($UVB_{inh.\ eff.}$) that entertains a linear exposure–response relationship, regardless of the time scale of observation. Such an approach has been used, implicitly or explicitly, by other researchers (e.g., Gala and Giesy 1991; Boucher and Prézelin 1996) and gives an intuitively obvious, if flawed, index. Concentrating on relatively short-term (1-h) $UVB_{inh.\ eff.}$ values should minimize the confounding effects of photoinhibition and (or) remediation of UVB damage by longer wavelengths (Prézelin et al. 1994).

Although over a 10-fold range in the 1-h $UVB_{inh.\ eff.}$ was observed among experiments, the variation in sensitivity could not be related to the species composition. Taxonomic composition should be important because the repair of UVB-induced DNA photoproducts and photosystem reaction center damage is taxon specific (Karentz et al. 1991; Xiong et al. 1997), as is the induction and effectiveness of screening compounds (e.g., Hannach and Sigleo 1998). Using a $UV_{inh.\ eff.}$ index similar to the one used in this study, Gala and Giesy (1991) reported apparently characteristic differences between diatom–chrysophycean and cyanobacterial assemblages in Lake Michigan and suggested that pigment composition might be responsible. During this Lake Erie study, communities were rather consistently dominated (among the nano- and micro-phytoplankton) by diatoms and chrysophyceans, which may have limited the scope for detecting broad taxonomic influences. Unquantified variations among the picoplankton may have further impeded detection of taxonomic influences.

In addition to intrinsic, taxonomically related characteristics, algal sensitivity to UVR can also depend on environmental modifying factors such as water clarity, mixing depth, and mixing rates (e.g., Neale et al. 1998*a*), light history (e.g., Villafañe et al. 1995), and (or) nutrient availability (e.g., Lesser et al. 1994). The measures of light climate and photoadaptive state in this study failed to reveal any relationships with the $UVB_{inh.\ eff.}$ for Lake Erie phytoplankton, however. Evidence for the importance of light history and (or) photoadaptive state in natural plankton communities has been derived mainly from comparisons of samples from very different ocean regions or depths (e.g., Villafañe et al. 1995) or among different samples of polar phytoplankton, all at very low temperature (e.g., Neale et al. 1998*a*). The present study, involving only surface mixed-layer samples from one

© 2002 NRC Canada

temperate lake, may not have encountered sufficient variation in photoadaptive state to reveal the effects against the background of other influences.

It was observed that the 1-h $UVB_{inh.\ eff.}$ sensitivity index was higher under conditions of N deficiency. The evidence for frequent symptoms of N deficiency in Lake Erie phytoplankton was surprising, since Lake Erie is generally regarded and managed as a P-limited system (Charlton et al. 1999), yet a relationship between N status and UVR effects is quite understandable. Nitrogen is an essential nutrient used in the synthesis of amino acids and proteins. Proteins are sensitive to UVB radiation because their aromatic amino acids (e.g., tyrosine) absorb in the UV range of the spectrum (Häder and Tevini 1987; Karentz et al. 1991). Consequently, structural and functional changes can occur when the disulfide groups of proteins are split by UV radiation (short and longer UV wavelengths) (Häder and Tevini 1987). The D1 herbicide binding protein of the PSII complex (Greenberg et al. 1989) and the carbon-fixing enzyme, ribulose-1,5-bisphosphate carboxylase–oxygenase (Rubisco) (Lesser 1996), are examples of proteins photomodified by UVB radiation. A limited supply of nitrogen for the repair and (or) resynthesis of these key proteins may enhance the sensitivity of Lake Erie phytoplankton to UVB radiation. Sensitivity of phytoplankton to excess visible radiation is known to occur under nutrient-limiting conditions, and under nitrogen-limited conditions, the turnover rate of critical proteins and protein-pigment complexes is reduced (Lesser et al. 1994). On the other hand, from an ecological point of view, N limitation could pose a greater threat as this would drive the algal community towards N-fixing, buoyancy-regulating, surface-living species that would be subjected to maximum impacts from the natural UVR levels. These current results are, to our knowledge, the first evidence of interactions between nutrients and UVR effects in nature.

The relationship between N status and UVB inhibition efficiency disappeared in longer incubations. A likely explanation for this, and for the large decrease of UVB inhibition efficiency with increasing incubation time, is that progressive inhibition by PAR and (or) UVA masked the effects of UVB (Cullen et al. 1992; Neale et al. 1998*a*). The continuous-labelling protocol used in this study is also a potential source of confounding effects, owing to diel variations of photosynthetic capacity (Boucher and Prézelin 1996) and intracellular tracer equilibration processes (Smith and Platt 1984). The protocol is nonetheless similar to methods employed successfully by others (e.g., Smith et al. 1998) and is probably not the principal source of the large apparent temporal variation in sensitivity. The apparent rapidity of UVB photoinhibition, which our relatively coarse sampling intervals probably caused us to underestimate, means that relatively brief exposures to UVB in surface waters, as would occur under strong mixing conditions, can be damaging to primary production (e.g., Arts and Rai 1997; Neale et al. 1998*b*; Marwood et al. 2000).

The impacts UVR can have on phytoplankton are not limited to those on total primary production. Shifts in phytoplankton species composition have been reported following UVR exposures (e.g., Mostajir et al. 1999), as have changes in the chemical composition of algae (e.g., Wang and Chai 1994) and in the extent of extracellular release of DOC (Pausz and Herndl 1999). In Lake Erie, the percent of total primary production appearing as DOC was greatest in treatments receiving the most radiation, and especially if UVB was present. This may reflect alterations to the mechanisms of release from phytoplankton, which may be passive (Bjørsen 1988) or active (Lignell 1990). Passive release will reflect membrane permeability, which can be altered by UVR-mediated photooxidation of membrane lipids and lead to increased "leakage" (cf. Chamberlain and Moss 1987). Whether UVR can also directly or indirectly stimulate the active external transport of algal DOC is unknown. High light encountered in surface waters has been linked to increased production of extracellular release products (Mague et al. 1980), a possible consequence of increased photorespiration (Williams 1990). Although other studies have reported no effects of UVR on the relative proportion of organic carbon in the particulate versus the dissolved pools (e.g., Pausz and Herndl 1999), the results of this study are in agreement with data from Lake Erie in 1995 (R.E.H. Smith, unpublished data), which indicated even larger UVB-dependent stimulation of dissolved production than found here.

The observed accumulation of labelled carbon in the DOC, especially in long incubations, will also reflect a balance between release from phytoplankton and utilization by heterotrophic microorganisms. UVR does inhibit bacterial production, including Lake Erie bacterioplankton specifically (Wilhelm and Smith 2000). Without further data, we cannot discriminate the relative importance of utilization versus production to the observed effects. Whatever the mechanism, however, the results do indicate a change in the immediate fate, as well as magnitude, of primary production according to radiation exposure.

The share of picoplankton in total production was diminished by radiation, and specifically UVB, exposure, whereas larger phytoplankton were less affected at the stations we visited in Lake Erie. This additional aspect of radiation effects on the quality of primary production may reflect size-specific variations in mechanisms for coping with radiation stress. Mycosporine-like amino acids (MAAs), which may confer protection from UVR (Roy 2000), are synthesized selectively among phytoplankton taxa (Xiong et al. 1997). The photoprotective efficiency of MAAs and other "sunscreens" is related to the size of the organisms using them, and theory suggests that only cells >1 μm can benefit (Garcia-Pichel 1994). The <2-μm Lake Erie phytoplankton may not make effective use of UVR-absorbing pigments, a possible explanation for their higher sensitivity to the UVB portion of the solar spectrum. Even if larger cells do not benefit from sunscreens like MAAs, their size and surface–volume ratios may afford a degree of protection to sensitive targets, notably the nucleus (Karentz et al. 1991). The apparently greater sensitivity of the picoplankton size fraction may additionally reflect UVB effects on bacterioplankton, some of which would have been present in our small particle size fraction. If UVB diminished the incorporation of radiolabelled phytoplankton exudate by bacteria, as may be expected (Wilhelm and Smith 2000), then we would observe an apparent decrease of primary production in the picoplankton fraction. We cannot separate these possible mechanisms with the current data, but they are important subjects for further research. Picoplankton biomass, on average, approximates that

© 2002 NRC Canada

of the combined nano- and micro-phytoplankton in the Laurentian Great Lakes (Fahnenstiel et al. 1998) and altered distributions of production could have significant implications for the food web.

In Lake Erie, UVR is rapidly attenuated in the water column, with lake-wide median 1% depths of integrated UVB and UVA of 1.5 m and 2.5 m for spring and summer of 1997 (Smith et al. 1999). The present results indicated that, on average, significant UVB effects on total primary production were limited to exposures ≥50% of surface incident, for which the corresponding depths would be only 0.3 m in east and central basins and 0.2 m in west basin. As a percentage of the photic zone (1% PAR depth), the 50% UVB zone is only 1.5, 1.9, and 3.1% for east, central, and west basins respectively. It is tempting to conclude that UVB can be only a trivial influence, given such minimal depths of effective penetration, but a better resolution of the kinetics and wavelength dependence of UVR effects is needed before accepting such a conclusion. We have probably underestimated the true rate and extent of UVB impact, because of the simultaneous effects of PAR and (or) UVA in our experimental design, and the natural mixing regime will often subject the phytoplankton to brief, but severe UVB exposures (cf. Neale et al. 1998*a*, 1998*b*). Likewise, the true significance of UVB effects on the immediate fate of primary production (allocation among particle sizes and dissolved pools) was probably minimized by our coarse temporal sampling design. A study with better spectral and kinetic resolution may reveal stronger UVB effects, although the few studies with adequate resolution published to date do suggest that UVB usually accounts for a small portion of the total photoinhibition of marine phytoplankton primary production (e.g., Neale et al. 1998*b*).

Intuitively, it might be expected that the west basin, as the most turbid, would be less vulnerable to UVR effects than the other basins. In fact, the 1% UVB photic depth represents a greater part of the photic zone (ca. 20%) in the west than in the other basins, as does the 50% UVB depth. The present study has also revealed that shallow temporary thermoclines form more frequently in the west than in the other basins. In other lakes, such shallow thermoclines are associated with more severe UVR effects (Milot-Roy and Vincent 1994). Whether UVR, and UVB specifically, are of major importance to the ecology of Lake Erie remains to be seen, but it would appear that the more turbid portion of the lake is likely to experience the greatest influence. By extension, we should not assume that other systems with high levels of turbidity (e.g., Lake Champlain) are immune to the effects of UVR.

Acknowledgments

This work was supported by the Natural Sciences and Engineering Research Council (R.S.) and Environment Canada (R.S.). We gratefully acknowledge Murray Charlton of Environment Canada and the captain and crew of the CCGS *Limnos* for making this work possible. We thank Jenni Kerteston for providing invaluable technical assistance in the field and the laboratory and we thank John Furgal for his diligence in collecting and collating the invaluable radiometry data. We also thank the three anonymous reviewers whose suggestions and comments greatly improved the quality of this manuscript.

References

Arts, M.T., and Rai, H. 1997. Effects of enhanced ultraviolet-B radiation on the production of lipid, polysaccharide and protein in three freshwater algal species. Freshwater Biol. **38**: 597–610.

Bjørsen, P.K. 1988. Phytoplankton exudation of organic matter: why do healthy cells do it? Limnol. Oceanogr. **33**: 151–154.

Bolsenga, S.J., and Herdendorf, C.E. (*Editors.*) 1993. Lake Erie and Lake St.-Clair Handbook. Wayne State University Press, Detroit.

Bothwell, M.L., Sherbot, D., Roberge, A.C., and Daley, R.J. 1993. Influence of natural ultraviolet radiation on lotic periphyton diatom community growth, biomass accrual, and species composition: Short-term versus long-term effects. J. Phycol. **29**: 24–35.

Boucher, N.P., and Prézelin, B.B. 1996. Spectral modeling of UV inhibition of in situ Antarctic primary production using a field-derived biological weighting function. Photochem. Photobiol. **64**: 407–418.

Burns, N.M. 1985. Erie: the lake that survived. Rowan & Allanheld, Totowa, N.J.

Chamberlain, J., and Moss, S.H. 1987. Lipid peroxidation and other membrane damage produced in *Escherichia coli* K1060 by near-UV radiation and deuterium oxide. Photochem. Photobiol. **45**: 625–630.

Charlton, M.N., LeSage, R., and Milne, J.E. 1999. Lake Erie in transition: the 1990's. *In* The state of Lake Erie (SOLE)- past, present and future. *Edited by* M. Munawar, T.A. Edsall, and I.F. Munawar. Backhuys Publishers, Leiden. pp. 97–124.

Cullen, J.J., Neale, P.J., and Lesser, M.P. 1992. Biological weighting function for the inhibition of phytoplankton photosynthesis by ultraviolet radiation. Science (Washington, D.C.), **258**: 646–650.

Dahl, J.A., Graham, D.M., Dermott, R., Johannsson, O.E., Millard, E.S., and Myles, D.D. 1995. Lake Erie 1993, western, west central and eastern basins: change in trophic status, and assessment of the abundance, biomass and production of the lower trophic levels. Can. Tech. Rep. Fish. Aquat. Sci. No. 2070.

Fahnenstiel, G.L., Krause, A.E., McCormick, M.J., Carrick, H.J., and Schelske, C.L. 1998. The structure of the planktonic food-web in the St. Lawrence Great Lakes. J. Gt. Lakes Res. **24**: 531–554.

Furgal, J.A., and Smith, R.E.H. 1997. Ultraviolet radiation and photosynthesis by Georgian Bay phytoplankton of varying nutrient and photoadaptive status. Can. J. Fish. Aquat. Sci. **54**: 1659–1667.

Gala, W.R., and Giesy, J.P. 1991. Effects of ultraviolet radiation on the primary production of natural phytoplankton assemblages in Lake Michigan. Ecotoxicol. Environ. Saf. **22**: 345–361.

Garcia-Pichel, F. 1994. A model for internal self-shading in planktonic organisms and its implications for the usefulness of ultraviolet sunscreens. Limnol. Oceanogr. **39**: 1704–1717.

Greenberg, B.M., Gaba, V., Canaani, O., Malkin, S., Mattoo, A.K., and Edelman, M. 1989. Separate photosensitizers mediate degradation of the 32-kDa photosystem II reaction center protein in the visible and UV spectral regions. Proc. Natl. Acad. Sci. U.S.A. **86**: 6617–6620.

Guildford, S.J., Hendzel, L.L., Kling, H.J., Fee, E.J., Robinson, G.G.C., Hecky, R.E., and Kasian, S.E.M. 1994. Effects of lake size on phytoplankton nutrient status. Can. J. Fish. Aquat. Sci. **51**: 2769–2783.

Häder, D.-P., and Tevini, M. 1987. General photobiology. Pergamon Press, Great Britain. pp. 293–309.

Halac, S., Felip, M., Camarero, L., Sommaruga-Wögrath, S., Psenner, R., Catalan, J., and Sommaruga, R. 1997. An in situ enclosure ex-

© 2002 NRC Canada

periment to test the solar UVB impact on plankton in a high-altitude mountain lake. I. Lack of effect on phytoplankton species composition and growth. J. Plankton Res. **19**: 1671–1686.

Hannach, G., and Sigleo, A.C. 1998. Photoinduction of UV-absorbing compounds in six species of marine phytoplankton. Mar. Ecol. Prog. Ser. **174**: 207–222.

Healey, F.P., and Hendzel, L.L. 1979. Indicators of phosphorus and nitrogen deficiency in five algae in culture. J. Fish. Res. Board Can. **36**: 1364–1369.

Karentz, D., Cleaver, J.E., and Mitchell, D.L. 1991. Cell survival characteristics and molecular responses of Antarctic phytoplankton to ultraviolet-B radiation. J. Phycol. **27**: 326–341.

Laurion, I., and Vincent, W.F. 1998. Cell size versus taxonomic composition as determinants of UV-sensitivity in natural phytoplankton communities. Limnol. Oceanogr. **43**: 1774–1779.

Lesser, M.P. 1996. Acclimation of phytoplankton to UV-B radiation: oxidative stress and photoinhibition of photosynthesis are not prevented by UV-absorbing compounds in the dinoflagellate *Prorocentrumn micans*. Mar. Ecol. Prog. Ser. **132**: 287–297.

Lesser, M.P., Cullen, J.J., and Neale, P.J. 1994. Carbon uptake in a marine diatom during acute exposure to ultraviolet B radiation: relative importance of damage and repair. J. Phycol. **30**: 183–192.

Lignell, R. 1990. Excretion of organic carbon by phytoplankton: its relation to algal biomass, primary productivity and bacterial secondary productivity in the Baltic Sea. Mar. Ecol. Prog. Ser. **68**: 85–99.

Mague, T.H., Friberg, E., Hughes, D.J., and Morris, I. 1980. Extracellular release of carbon by marine phytoplankton; a physiological approach. Limnol. Oceanogr. **25**: 262–279.

Marwood, C.A., Smith, R.E.H., Furgal, J.A., Charlton, M.N., Solomon, K.R., and Greenberg, B.M. 2000. Photoinhibition of natural phytoplankton populations in Lake Erie exposed to solar ultraviolet radiation. Can. J. Fish. Aquat. Sci. **57**: 371–379.

Milot-Roy, V., and Vincent, W.F. 1994. UV radiation effects on photosynthesis: the importance of thermoclines in a subarctic lake. Arch. Hydrobiol. Beih. **43**: 171–184.

Mostajir, B., Demers, S., de Mora, S., Belzile, C., Chanut, J.-P., Gosselin, M., Roy, S., Zulema Villegas, P., Fauchot, J., Bouchard, J., Bird, D., Monfort, P., and Levasseur, M. 1999. Experimental test of the effect of ultraviolet-B radiation in a planktonic community. Limnol. Oceanogr. **44**: 586–596.

Neale, P.J., Cullen, J.J., and Davis, R.F. 1998*a*. Inhibition of marine photosynthesis by ultraviolet radiation: variable sensitivity of phytoplankton in the Weddell-Scotia Confluence during the austral spring. Limnol. Oceanogr. **43**: 433–448.

Neale, P.J., Davis, R.F., and Cullen, J.J. 1998*b*. Interactive effects of ozone depletion and vertical mixing on photosynthesis of Antarctic phytoplankton. Nature (London), **392**: 585–589.

Pausz, C., and Herndl, G.J. 1999. Role of ultraviolet radiation on phytoplankton extracellular release and its subsequent utilization by marine bacterioplankton. Aquat. Microb. Ecol. **18**: 85–93.

Platt, T., Gallegos, C.L., and Harrison, W.G. 1980. Photoinhibition of photosynthesis in natural assemblages of marine phytoplankton. J. Mar. Res. **38**: 687–701.

Prézelin, B.B., Boucher, N.P., and Schofield, O. 1994. Evaluation of field studies of UVB radiation effects on Antarctic marine primary productivity. *In* Stratospheric ozone depletion/UV-B radiation in the biosphere. *Edited by* R.H. Biggs and M.E.B. Joyner. Springer-Verlag, Berlin. pp. 181–194.

Roy, S. 2000. Strategies for the minimisation of UV-induced damage. *In* The effects of UV radiation in the marine environment. *Edited by* S.J. De Mora, S. Demers, and M. Vernet. Cambridge University Press, Cambridge. pp. 177–205.

Schofield, O., Kroon, B.M.A., and Prézelin, B.B. 1995. Impact of ultraviolet-B radiation on photosystem II activity and its relationship to the inhibition of carbon fixation rates for antarctic ice algae communities. J. Phycol. **31**: 703–715.

Smith, R.C., and Cullen, J.J. 1995. Effects of UV radiation on phytoplankton. Rev. Geophys. **33**: 1211–1223.

Smith, R.E.H., and Maly, J.A. 1993. Photosynthetic carbon assimilation and allocation by surface and deep phytoplankton in Colpoys Bay (western Georgian Bay). Can. J. Fish. Aquat. Sci. **50**: 2235–2244.

Smith, R.E.H., and Platt, T. 1984. Carbon exchange and ^{14}C tracer methods in a nitrogen-limited diatom, *Thalassiosira pseudonana*. Mar. Ecol. Prog. Ser. **16**: 75–87.

Smith, R.E.H., Furgal, J.A., and Lean, D.R.S. 1998. The short-term effects of solar ultraviolet radiation on phytoplankton photosynthesis and photosynthate allocation under contrasting mixing regimes in Lake Ontario. J. Gt. Lakes Res. **24**: 427–441.

Smith, R.E.H., Furgal, J.A., Charlton, M.N., Greenberg, B.M., Hiriart, V., and Marwood, C. 1999. The attenuation of ultraviolet radiation in a large lake with low dissolved organic matter concentrations. Can. J. Fish. Aquat. Sci. **56**: 1351–1361.

Tranvik, L., and Kokalj, S. 1998. Decreased biodegradability of algal DOC due to interactive effects of UV radiation and humic matter. Aquat. Microb. Ecol. **14**: 301–307.

Villafañe, V.E., Helbling, E.W., Holm-Hansen, O., and Chalker, B.E. 1995. Acclimatization of Antarctic natural phytoplankton assemblages when exposed to solar ultraviolet radiation. J. Plankton Res. **17**: 2295–2306.

Wang, K.S., and Chai, T. 1994. Reduction of omega-3 fatty acids by UV-B irradiation in microalgae. J. Appl. Phycol. **6**: 415–421.

Wilhelm, S.W., and Smith, R.E.H. 2000. Bacterial carbon production in Lake Erie is influenced by viruses and solar radiation. Can. J. Fish. Aquat. Sci. **57**: 317–26.

Williams, P.J.L.B. 1990. The importance of losses during microbial growth: commentary on the physiology, measurement and ecology of the release of dissolved organic material. Mar. Microb. Food Webs, **4**: 175–206.

Williamson, C.E. 1995. What role does UV-B radiation play in freshwater ecosystems? Limnol. Oceanogr. **40**: 386–392.

Xiong, F., Komenda, J., Kopecky, J., and Nedbal, L. 1997. Strategies of ultraviolet-B protection in microscopic algae. Physiol. Plant. **100**: 378–388.

© 2002 NRC Canada

Distribution of freshwater diatoms in 64 Labrador (Canada) lakes: species–environment relationships along latitudinal gradients and reconstruction models for water colour and alkalinity

Marie-Andrée Fallu, Nancie Allaire, and Reinhard Pienitz

Abstract: The distribution of modern diatom assemblages in surficial sediments of 64 Labrador (Canada) lakes across broad vegetational biomes was studied in order to explore species–environment relationships and to develop transfer functions for paleoenvironmental reconstruction. The study sites were situated along a latitudinal gradient (51°27′ to 57°37′N) and classified according to six catchment vegetation types: wetland (peatland) forest, spruce/fir forest, lichen woodland, forest–tundra, coastal tundra, and tundra. Canonical correspondence analysis revealed that among 28 environmental variables determined for each site, water colour and alkalinity accounted for most of the variance in the diatom data. Using weighted-averaging partial least squares techniques, we developed transfer functions for inference of water colour (CLR) (r^2_{jack} = 0.85, root mean square error of prediction (RMSEP) = 0.18log(CLR + 1) or 1.51 Pt units) and alkalinity (ALK) (r^2_{jack} = 0.63, RMSEP = 0.25log(ALK + 1) or 1.78 μeq·L^{-1}) from the percent abundance of the 132 most abundant diatom taxa. By determining diatom distribution in relation to more detailed vegetation types within the boreal forest zone (wetland forest, spruce/fir forest, and lichen woodland), this calibration data set demonstrated the potential of these assemblages for revealing more subtle changes in lake catchment vegetation over time.

Résumé : La répartition des assemblages fossiles de diatomées dans les sédiments de surface de 64 lacs du Labrador (Canada) situés dans différentes régions géographiques a été étudié afin de déterminer les relations existantes entre les espèces et leur environnement et de développer des fonctions de transfert pour effectuer des reconstitutions environnementales. Les lacs sont situés le long d'un transect latitudinal (51°27′ à 57°37′N) et se classent selon six zones de végétation; forêt des milieux humides (tourbières), pessière/sapinière, pessière à lichen, toundra forestière, toundra côtière et toundra. Des analyses canoniques de correspondances ont été utilisées pour les 28 variables environnementales et ont révélé que la couleur de l'eau et l'alcalinité expliquaient le mieux la répartition des espèces de diatomées. En utilisant l'analyse des moyennes pondérées des moindres carrés partiels, des fonctions de transfert ont été développées pour inférer la couleur de l'eau (CLR) (r^2_{jack} = 0.85, erreur des moindres carrés partiel de prédiction (RMSEP) = 0.18log(CLR + 1) ou 1.51 unités Pt) et l'alcalinité (ALK) (r^2_{jack} = 0.63, RMSEP = 0.25log(ALK + 1) ou 1.78 μeq·L^{-1}) à partir des 132 taxa de diatomées les plus abondants. En déterminant la répartition des diatomées selon des zones de végétation plus détaillées à l'intérieur de la forêt boréale (forêt des milieux humides (tourbières), pessière/sapinière, pessière à lichen), ces données permettent aussi de démontrer le potentiel des assemblages de diatomées pour déceler des changements plus subtiles du couvert végétal du bassin versant des lacs.

Introduction

Global warming scenarios predict that the greatest changes in climate will occur within the boreal and north polar regions (e.g., Kattenberg et al. 1996). The consequences of such climatic changes could translate into major shifts in vegetation in these high latitude areas, which in turn could further modify climate via albedo and other feedback mechanisms (Bonan et al. 1995). In northern and alpine regions, a close relationship between climate and vegetation has been observed (Payette et al. 1989; Pielke and Vidale 1995). This interdependence is also reflected in the limnological conditions of northern and high altitude lakes, which change abruptly across vegetational boundaries within the tree-line ecotone (e.g., Duff et al. 1999). Paleolimnological studies within this ecotone and in recently deglaciated landscapes have similarly revealed that there have been large-scale modifications of the aquatic environment in response to past catchment vegetation changes brought about by climate-related shifts in tree line (e.g., Pienitz et al. 1999; Pienitz

Received 02 May 2001. Accepted 12 December 2001. Published on the NRC Research Press Web site at http://cjfas.nrc.ca on 5 March 2002.
J16332

M.-A. Fallu,[1] N. Allaire, and R. Pienitz.[1] Paleolimnology–Paleoecology Laboratory, Centre d'études nordiques (CEN) and Département de géographie, Université Laval, Québec, QC G1K 7P4, Canada.

[1]Corresponding authors (e-mail: mafallu@hotmail.com; reinhard.pienitz@cen.ulaval.ca).

 DOI: 10.1139/F01-211 © 2002 NRC Canada

and Vincent 2000) and by successional changes following deglaciation (Engstrom et al. 2000).

The striking physical and chemical changes in lakes across arctic and alpine tree lines are also reflected in the zonal distributional patterns of freshwater diatoms (class Bacillariophyceae). Studies of modern diatom assemblages in high latitude and high altitude regions have contributed to a better understanding of diatom species–environment relationships and the development of transfer functions to predict past environmental changes (reviewed in Lotter et al. 1999). In the circumpolar region of the northern hemisphere, inference models have been developed for the reconstruction of dissolved organic carbon (DOC), which is derived from terrestrial vegetation and soils (e.g., Pienitz and Smol 1993; Fallu and Pienitz 1999). Other diatom-based inference models have been developed for the reconstruction of water colour (e.g., Korsman and Birks 1996; Seppä and Weckström 1999), alkalinity (e.g., Korsman and Birks 1996; Rühland 1996), dissolved inorganic carbon (DIC) (Pienitz and Smol 1993), total organic carbon (TOC) (e.g., Seppä and Weckström 1999; Rosén et al. 2000), pH (e.g., Rosén et al. 2000; Bigler and Hall 2002), water depth, lake surface water temperature (e.g., Pienitz et al. 1995; Weckström et al. 1997), and air temperature (e.g., Rosén et al. 2000; Bigler and Hall 2002). These models provide the starting point for more detailed, quantitative paleolimnological reconstructions in high latitude regions and, in the case of the DOC/TOC and water colour models, a means for the study of the links between terrestrial (vegetation) and aquatic environments. However, studies of relationships between diatoms and catchment vegetation to date have focused only on distinguishing coarse lake catchment vegetation zones (i.e., boreal forest, forest–tundra, or tundra lakes). The present study encompasses six different catchment vegetation types (wetland forest, spruce/fir forest, lichen woodland, forest–tundra, coastal tundra, tundra) and therefore provides an opportunity to evaluate how vegetation within the boreal forest and the degree of paludification affect diatom community structure.

Only a few studies focusing on the postglacial stratigraphies of diatom assemblages have been completed to date in northeastern Québec – Labrador (e.g., Clark et al. 1989; Allaire 1997), and no extensive studies examining diatom distributions have yet been carried out in this vast territory. The present paper aims to provide the first detailed inventory of these important bioindicators through a survey of diatom distributions in the surface sediments of 64 lakes located across steep ecoclimatic gradients and ecotonal boundaries. We used a multivariate statistical approach to determine which environmental variables best explained the observed distributional patterns. The variation in diatom assemblages across the latitudinal gradient from boreal forest to arctic tundra conditions in Labrador were analyzed, and the autecological preferences of the identified diatom taxa were determined. The second part of the paper assesses the applicability and predictive ability of two weighted-averaging partial least squares (WA-PLS) inference models for alkalinity and water colour developed using the diatom and environmental data for future use with diatom-based paleolimnological studies in Labrador. Finally, we evaluated the usefulness of diatoms as proxies of catchment vegetation changes in the northern region.

Materials and methods

Description of study region and sites

The 64 lake sites in Labrador and adjacent Québec are situated between 51°27′ to 57°37′N and 56°11′ to 64°32′W (Fig. 1). The lakes were specifically chosen to span a broad climatic gradient so that the study area included different ecoclimatic zones. Most of the lakes were unnamed and therefore were given sampling numbers. Of the 64 lakes studied, sites 4, 10–15, 19, and 20 are situated within catchments dominated by wetland (peatland) forests; sites 5–9, 16–18, and 21–27 are within spruce/fir forests; sites 28–34 are within lichen woodland; sites 57–63, 65, 66, and 69 are within forest–tundra; sites 1–3 are within coastal tundra; and sites 35–41, 43–52, and 54–56 are within tundra catchments.

The study region has been described in detail in earlier studies on the Holocene history of vegetation and soils in Labrador (Lamb 1980; Engstrom and Hansen 1985) and the present-day influence of vegetation and hydrology on the humus budgets of lakes (Engstrom 1987), as well as within the context of modern training sets for pollen (Lamb 1984) and chironomids (Walker et al. 1991). These studies also review the geology, deglaciation history, climatology, and limnology of the area.

In summary, the bedrock geology is dominated by granites and granodiorites of Precambrian age that belong to the Canadian Shield. The sites are located on bedrock belonging to three different geological provinces (Grenville, Churchill, and Nain). Till of differing thickness sporadically occurs throughout the area. Sites 30–33 are located on postglacial marine sediments deposited during high sea level stands and are composed of gravel, sand, silt, and clay (Water Resources Division 1992). The climate of Labrador comprises three major ecoclimatic regions (Oceanic High Boreal through the Low Arctic) (Ecoregions Working Group 1989). From south to north, annual precipitation ranges from 900 to 750 mm, and annual temperature ranges from 1.5 to –2°C (Water Resources Division 1992).

Three major physiognomic zones can be distinguished along a latitudinal gradient in Labrador (Hare 1959): boreal forest, forest–tundra, and tundra (Fig. 1). Within the boreal forest zone, three different vegetation types can be found in the catchments of lakes: wetland forest, spruce/fir forest, and lichen woodland (Hare 1959). In maritime southeastern Labrador, the denser spruce/fir forests are restricted to sheltered areas in river valleys (*Abies balsamea*, *Picea mariana*, and *P. glauca*), whereas the open wetland forests are characterized by sparsely forested (*Picea mariana*) mires and muskegs (Lamb 1984). The lichen woodland zone is characterized by an open forest of *Picea mariana* with a lichen-dominated ground flora, a vegetation type that can also be found in the forest–tundra zone and on xeric sites in the closed forest region (Lamb 1984). The lichen woodland zone with its open *Picea mariana* forests and extensive lichen ground cover represents the transition towards the forest–tundra zone (Lamb 1984). The latter consists of patches of open *Picea* and *Larix* woodlands in lowlands and tundra-covered uplands. The vegetation of the tundra zone is composed of small dwarf shrubs (*Betula glandulosa*, *Alnus crispa*, and a few species of *Salix*), graminoids, herbs, mosses, and lichens (Lamb 1984).

© 2002 NRC Canada

Fig. 1. Map illustrating the location of the 64 Labrador lakes, Eastern Canada.

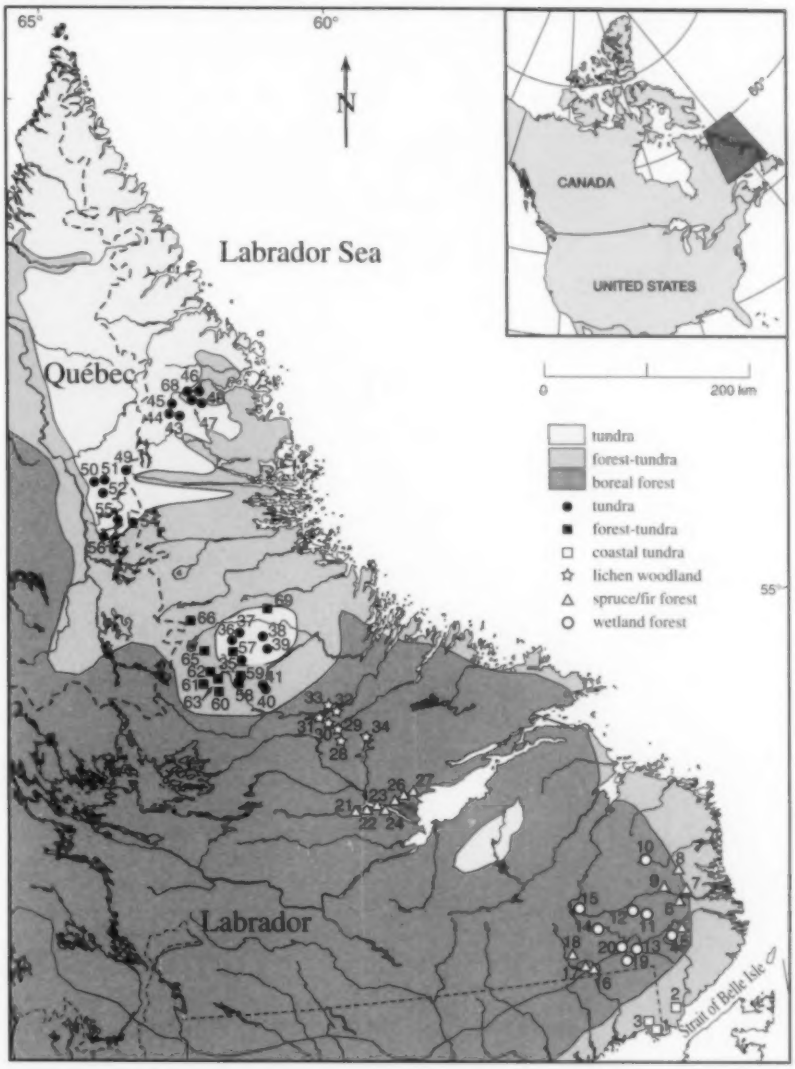

Sampling and measurement procedures

The surficial sediments of the 64 study sites were sampled by the Limnological Research Centre (LRC) of the University of Minnesota during July–August of 1979. The top 3 cm of sediments was collected at the deepest point of each lake basin (Lamb 1984), none of which was connected to upstream lakes or fed by large affluents (Engstrom 1987). Sediments were collected with a free-fall modified Hongve sampler (Wright 1990). Field sampling techniques (sediment and water samples) and laboratory analysis (water chemistry) procedures have been described in detail by Lamb (1984), Engstrom and Hansen (1985), and Engstrom (1987). Specific conductance, pH, apparent water colour (measured by a comparator method with calibrated platinum–cobalt (Pt–Co) standards), water transparency (Secchi depth), and alkalinity were measured in the field, whereas all other water chemistry analyses were performed in the laboratory. Topographic maps (1 : 50 000) and aerial photographs (1 : 17 000) were used to determine catchment and lake area as well as to determine predominant vegetation, along with field observations (Engstrom 1987). The physical and chemical characteristics for the 64 lakes where diatoms were studied are summarized in Table 1.

The preparation and analysis of diatom samples followed standard techniques. Diatoms were extracted from sediments using acid digestion techniques (HNO_3 and H_2SO_4, 50:50) before being mounted on microscope slides using Naphrax®. Some of the surficial sediments were previously counted by Keith Camburn (4435 Huntington Drive, Gastonia, NC 28056, U.S.A.). The taxonomy was standardized by recounting several levels and assuring similar results. For each sample, approximately 500 diatom valves were counted. Identifications were made to the lowest taxonomic level possible (e.g., variety) at 1000× magnification. Diatom taxon-

© 2002 NRC Canada

Table 1. Summary of selected limnological data for the 64 study lakes in Labrador, arranged according to catchment vegetation type.

	Coastal tundra (3 lakes)			Spruce/fir forest (15 lakes)			Wetland forest (9 lakes)			Lichen woodland (7 lakes)			Forest–tundra (10 lakes)			Tundra (20 lakes)			Total (all 64 lakes)		
Variable	Min.	Max.	Mean	Min.	Max.	Mean	Min.	Max.	Mean	Min.	Max.	Mean	Min.	Max.	Mean	Min.	Max.	Mean	Min.	Max.	Mean
ALK ($\mu eq \cdot L^{-1}$)	66	2154	763	7	106	35	3	68	33	28	463	217	34	138	84	10	94	36	3	2154	97
CLR (Pt units)	5	40	18	10	70	50	50	130	89	5	10	8	5	20	14	5	20	6	5	130	30
Depth (m)	5	23	14	3	50	14	1	2	2	3	29	19	3	15	8	3	50	15	1	50	12
ORG (g)	12	20	16	20	44	33	3	33	20	10	44	22	17	42	29	2	36	18	2	44	24
pH	5.9	7.9	6.8	5.2	6.7	5.7	5.0	6.4	6.0	6.4	7.6	7.0	5.9	7.0	6.5	6.0	7.1	6.5	5.0	7.9	6.3
Specific cond. ($\mu S \cdot cm^{-1}$)	25	203	85	8	74	19	5	16	11	6	50	28	5	17	10	1	11	4	1	203	16
Trans. (m)	2.5	7.0	4.5	2.0	6.0	3.4	1.0	2.0	1.3	3.0	12.5	9.8	3.0	10.0	6.0	3.0	15.0	10.6	1.0	15.0	6.5
AREA (ha)	4	105	56	40	135	78	38	235	128	62	195	119	73	105	86	27	173	83	4	235	91
Alt. (m)	43	195	94	57	385	203	221	406	340	126	306	267	352	589	507	260	623	513	43	623	369
Catch. (ha)	61	341	204	84	2086	627	200	1570	744	168	635	410	421	3944	1125	159	3829	991	61	3944	791
Temp. (°C)	12.4	14.0	13.5	11.5	16.0	14.0	13.8	18.0	16.7	12.8	15.2	13.5	10.9	12.0	11.5	7.6	12.0	10.4	7.6	18.0	12.8
Ca ($mg \cdot L^{-1}$)	1.5	36.7	13.3	0.7	2.2	1.2	0.9	2.1	1.2	0.8	8.0	4.2	0.6	2.1	1.4	0.4	2.0	0.9	0.4	36.7	2.0
Mg ($mg \cdot L^{-1}$)	0.6	7.4	2.9	0.2	0.4	0.3	0.2	0.5	0.3	0.1	0.8	0.5	0.2	0.4	0.3	0.1	0.4	0.2	0.1	7.4	0.4
Na ($mg \cdot L^{-1}$)	2.0	3.7	2.6	0.6	1.7	1.0	0.6	1.2	0.8	0.3	1.3	0.7	0.4	1.1	0.6	0.2	0.6	0.4	0.2	3.7	0.8
K ($mg \cdot L^{-1}$)	0.3	0.6	0.5	0.1	17.7	1.7	0.2	4.5	0.7	0.1	0.3	0.2	0.1	0.2	0.1	0.0	0.3	0.1	0.0	17.7	0.6
Cl ($mg \cdot L^{-1}$)	3.3	4.9	3.9	0.3	18.4	2.3	0.5	4.5	1.1	0.3	0.5	0.4	0.1	0.4	0.2	0.0	0.5	0.2	0.0	18.4	1.0
SO_4 ($mg \cdot L^{-1}$)	1.8	2.8	2.3	1.0	5.6	1.6	0.6	1.7	0.9	0.7	4.1	1.7	0.6	1.0	0.8	0.4	1.0	0.7	0.4	5.6	1.1
Fe ($mg \cdot L^{-1}$)	0.1	0.1	0.1	0.1	0.4	0.2	0.3	3.0	1.0	0.1	0.1	0.1	0.1	0.1	0.1	0.1	0.1	0.1	0.1	3.0	0.3
PO_4 ($\mu g \cdot L^{-1}$)	6	14	11	6	28	14	10	74	38	1	7	5	4	13	7	2	65	8	1	74	13
Si ($mg \cdot L^{-1}$)	0.1	0.7	0.4	0.3	2.7	1.2	0.4	2.9	0.9	0.1	1.6	1.0	0.6	2.8	1.3	0.1	2.4	0.8	0.1	2.9	1.0

Note: Min., minimum; Max., maximum; ALK, alkalinity; CLR, colour; Depth, maximum depth; ORG, organic content (LOI); Specific cond., specific conductivity; Trans., Secchi disk transparency; AREA, lake area; Alt., lake elevation; Catch., catchment area; Temp., surface water temperature.

© 2002 NRC Canada

omy followed that outlined and illustrated in Fallu et al. (2000).

Numerical analysis

The diatoms preserved in the surface lake sediments and the measured physical, chemical, and biological data were used to develop a calibration set to estimate the environmental optima and tolerances of the diatom taxa. The diatom species data are based on the relative abundance (percent of total diatoms) of taxa identified in surficial sediment samples. The available environmental data consist of 28 physical (9), chemical (13), and biological (6) variables measured for each lake including six vegetation zones (Table 1). The six main vegetation zones (wetland forest, spruce/fir forest, lichen woodland, coastal tundra, forest–tundra, and tundra) included in the calibration set of lakes were entered as binary codes (value 0 or 1). All variables and their abbreviations are presented in Table 1 except longitude (long.) and latitude (lat.). The distribution of the environmental data was verified using the computer program CALIBRATE version 0.3 (Juggins and ter Braak 1992). The positively skewed nature of most of the environmental variables was eliminated by a log(x), log(x + 1), or square root transformation, whereas normally distributed environmental variables were not transformed.

The data screening process followed Fallu and Pienitz (1999). Diatom taxa attaining a relative abundance of ≥1% in at least one of the 64 lakes were included in the numerical analyses and in the development of the inference models. Samples were deleted if they had environmental variables with extreme (>10×) influence, as detected by leverage diagnostics in a preliminary canonical correspondence analysis (CCA) (Birks et al. 1990*a*). Species and sample ordinations were performed using the computer program CANOCO for Windows, version 4.0 (ter Braak and Šmilauer 1998).

A principal components analysis (PCA) was performed to summarize the major patterns of variation within the environmental data and to examine relationships among environmental variables and sampling sites. Environmental variables were centered and standardized to allow them to be directly comparable. Detrended correspondence analysis (DCA; Hill and Gauch 1980), with detrending by linear segments and nonlinear rescaling of axes, was used to explore the principal patterns of floristic variation within the set of sampling sites. DCA also determined the compositional gradient lengths along DCA axes 1 (3.84 standard deviation (SD) units) and 2 (2.87 SD units), which justified the subsequent use of unimodal ordination methods (ter Braak and Prentice 1988). The results of DCA analyses are presented in Allaire (1997). A canonical variate analysis (CVA) was used to determine which environmental variables accounted for significant variance between the groups. The latter (site clusters) are based on catchment vegetation type. In the CVA, site clusters are used as binary variables instead of species data. Sites with extreme environmental values (>20×) were removed, as detected by the leverage diagnostic. Because the number of vegetation zones used in the CVA is far fewer than the number of species used in the CCA, a different cutoff criterion for leverage diagnostic was applied. CCA was also used to identify which environmental variables were the most important in explaining diatom assemblage distributions.

To remove the effects of collinearity (= amount of redundancy within the environmental information) in the CVA and CCA, only those variables were selected that explained a significantly additional proportion of the variance independent of the other variable. In the CVA and CCA, environmental variables with a variance inflation factor (VIF) exceeding 15 were eliminated (ter Braak 1988). Next, a series of CVAs and CCAs constrained to one variable were run to test the significance of each environmental variable on the first axis using Monte Carlo permutation tests with 199 unrestricted permutations ($P \leq 0.05$). The variables that did not have a significant influence on the data distribution were excluded from further analysis. Finally, in the CCA, the remaining variables were used to find pairs of highly correlated ($r > 0.6$) environmental variables identified from a Pearson correlation matrix. For each pair, partial CCAs were performed with one variable as the sole variable and the other as a covariable. The variable was then tested for its significance on the first canonical axis (Monte Carlo permutation test with 999 unrestricted permutations, $P \leq 0.05$). When the test was not significant (variables explaining the same part of the variance), the variable explaining the highest amount of variance in the diatom distributions was kept from the pair. This data screening process resulted in a group of variables with statistically independent and significant correlations with distributions of diatom assemblages.

The forward selection option of the CVA and CCA was then used to identify the smallest subset of variables explaining the most variation in the diatom data. Each variable was tested through Monte Carlo permutation tests (with 999 unrestricted permutations), with variables added to the model until the significant level of $P \leq 0.05$ was exceeded. Rare species were downweighted in the CCA ordinations. The selected variables in the CCA are those that can be used to develop environmental reconstruction models.

The quantitative transfer functions were developed using the computer program CALIBRATE, version 0.3 (Juggins and ter Braak 1992). Both linear-based partial least squares regression and calibration (PLS) and unimodal weighted-averaging (WA) regression and calibration models were tested and their predictive capacities were compared (Table 2). A $WA_{(tol)}$ option (with tolerance downweighting) was also used (with both inverse and classical deshrinking) in order to downweight the taxa with high tolerances (Birks et al. 1990*b*). The recently developed WA-PLS, which uses the weighted residual correlations in the species data to improve estimates of taxon optima in the final WA predictor (ter Braak and Juggins 1993), was also applied. The program CALIBRATE enabled the creation of Gaussian logit regression graphs for all of the species. These graphs show the distribution (unimodal vs. linear vs. sigmoidal) of the species in the data set. Only the data for the potential indicator taxa are presented in Appendix A.

All models were tested twice, once with the original relative abundance (%) values and a second time following square root transformation of the percentage species data. The r^2, root mean square error of prediction (RMSEP), and maximum bias of the models were calculated by "leave-one-out" (or jackknifing) cross-validation procedures (e.g., ter

© 2002 NRC Canada

Table 2. Performance statistics for different water colour (log(CLR + 1)) and alkalinity (log(ALK + 1)) inference models.

		Untransformed species data		Square root transformed species data	
Models		Classical	Inverse	Classical	Inverse
Water colour					
WA	r^2	0.74	0.73	0.71	0.71
	RMSEP	0.24	0.24	0.26	0.25
$WA_{(tol)}$	r^2	0.60	0.60	0.45	0.44
	RMSEP	0.33	0.30	0.40	0.35
PLS 3 components	r^2		0.72		
	RMSEP		0.26		
PLS 4 components	r^2				0.83
	RMSEP				0.19
WA-PLS 2 components	r^2		0.77		
	RMSEP		0.22		
WA-PLS 4 components	r^2				0.85
	RMSEP				0.18
Alkalinity					
WA	r^2	0.61	0.60	0.62	0.61
	RMSEP	0.28	0.26	0.28	0.25
$WA_{(tol)}$	r^2	0.60	0.59	0.57	0.57
	RMSEP	0.28	0.26	0.31	0.27
PLS 1 component	r^2		0.30		
	RMSEP		0.53		
PLS 2 components	r^2				0.60
	RMSEP				0.26
WA-PLS 1 component	r^2		0.60		
	RMSEP		0.26		
WA-PLS 2 components	r^2				0.63
	RMSEP				0.25

Note: RMSEP, root mean square error of prediction; WA, weighted-averaging; PLS, partial least squares.

Braak and Juggins 1993). The transfer functions considered to be the best ("minimum adequate model", sensu Crawley 1993 in Birks 1998) were those with the highest coefficient of determination (r^2_{jack}), lowest RMSEP, and low mean and maximum bias.

Results

Principal components analysis

The PCA indicates good separation of calibration lakes along major environmental and vegetational gradients (Fig. 2). Two sites had to be removed from the data set as they showed extreme values for some of the environmental variables as detected by the leverage diagnostics in a preliminary CCA. Site 2 had extreme values for magnesium (7.4 $mg \cdot L^{-1}$), calcium (36.7 $mg \cdot L^{-1}$), conductivity (203 $\mu S \cdot cm^{-1}$), and alkalinity (2154 $\mu eq \cdot L^{-1}$), whereas site 9 had high values of potassium (17.7 $mg \cdot L^{-1}$), chloride (18.4 $mg \cdot L^{-1}$), and sulphate (5.6 $mg \cdot L^{-1}$). The variables longitude and altitude were eliminated; however, latitude and the vegetation zones were retained as passive variables (e.g., with no direct influence on the ordination axes) in order to gain a better understanding of how the limnological variables are distributed geographically in the data set.

The PCA was performed on a data set of 62 lakes and 19 environmental variables (plus 7 passive variables). The cumulative percentage of variance within the environmental data explained by the first two PCA axes is 51.4%, with eigenvalues of $\lambda_1 = 0.31$ and $\lambda_2 = 0.21$, respectively. The lakes located in the wetland forest form a distinct group in the lower right quadrant, reflecting dark water colour (CLR) associated with high water temperature, high PO_4 concentrations, high iron (Fe) concentration, high organic matter content (ORG) of the sediments, and low pH and water depth. The spruce/fir forest lakes are grouped in the right half of the ordination, well separated from wetland forest sites. Tundra sites are mostly positioned on the left. They are characterized by high water transparency (Trans.) and low summer water temperature (Temp.), also by low conductivity and ion concentrations. The lakes situated in the coastal tundra are characterized by high conductivity and ion concentration. The forest–tundra and some of the lichen woodland lakes occupy a median position in the ordination, indicating similar chemical and limnological conditions among sites. Four lichen woodland sites are positioned separately in the top right quadrant, reflecting marked differences in water chemistry related to high alkalinity values as a result of marine deposit in the area. Overall, the relative positioning of the sample sites reflects environmental and limnological gradi-

© 2002 NRC Canada

Fig. 2. Principal components analysis (PCA) ordination of 19 environmental variables (*a*) in the 62 lake data set (*b*). Dashed arrows in (*a*) indicate passive environmental variables.

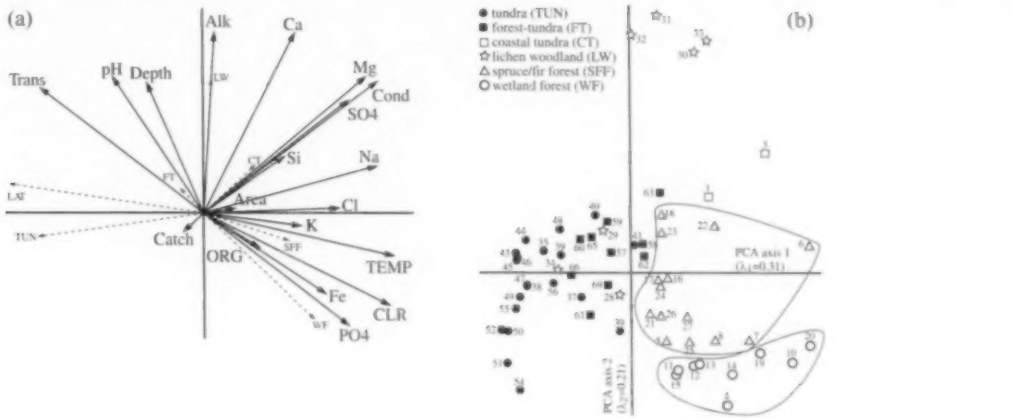

ents that are closely associated with changing vegetation zones along the latitudinal transect from tundra conditions in the north to spruce/fir and wetland-dominated forests in the south.

Canonical variates analysis

The original data set was composed of 64 lakes and 28 environmental variables including six vegetation zones. Because there were only three sites in the coastal tundra zone and one of them (site 2) had variables of extreme influence (see above), the latter vegetation zone was removed. Sites 6, 9, 10, 19, and 20 had to be removed because of environmental variables with extreme influence. Longitude, latitude, and altitude were removed for reasons mentioned above. The conductivity variable was deleted because of a high VIF. In a series of CVAs, Catch., Area, K, and Si were removed because they did not explain a significant amount of the variance in the vegetation types.

The CVA analysis included 56 lakes, 14 environmental variables, and five groups representing vegetation zones. After forward selections, only five environmental variables remained: water colour, calcium, iron, alkalinity, and water temperature (Fig. 3). The cumulative percentage variance of cluster grouping–environment relationship explained by axes 1 and 2 is 65.9%. Axis 1 clearly separates the vegetation zones along a colour gradient that is closely related to changes in temperature and iron. The wetland forest sites are concentrated in the lower right quadrant, representing high colour and iron content. Along the same axis, they are followed by spruce/fir forest sites, also influenced by water colour but to a lesser degree. The three other lake types are characterized by low water colour. Division between forest–tundra and tundra sites is less striking than between wetland forest and spruce/fir forest, but it is still perceptible. It also appears that the tundra sites are characterized by low water temperature. Lichen woodland sites are split into two groups, as seen in the PCA (Fig. 2). The first group occupies the central part of the ordination, between the forest–tundra and the spruce/fir forest sites, and represents the transition between these two catchment types. The other group is positioned in the upper part of the ordination, well separated from all other sites. These four sites are influenced by high water alkalinity resulting from local marine sediment, which is represented by axis 2. The CVA ordination confirms the environmental similarities of sites within vegetation zones and the limnological differences among sites from different vegetation zones.

Canonical correspondence analysis

After the data screening, several species, sites, and environmental variables were removed from the original data set of 303 diatoms, 64 lakes, and 28 environmental variables. Of the 303 diatom taxa (in 21 genera) identified in the surface sediment samples of the study lakes, a total of 132 taxa met the selection criteria (≥1% in at least one lake). Most of these were periphytic species belonging to the genera *Achnanthes*, *Cymbella*, *Eunotia*, *Fragilaria*, and *Navicula*. Lakes 2, 3, 9, and 20 were deleted as they had environmental data having an extreme influence, as assessed by the leverage diagnostics. Vegetation zones and latitude were run as passive variables, whereas longitude was removed. The variables of conductivity and chloride (Cl) were deleted for their high VIF values. In the CCAs constrained to one variable, catchment (Catch.) and potassium (K) did not have a significant influence on diatom distributions and therefore were excluded from further analysis. From all pairs tested for their correlations, only temperature and phosphate (PO_4) did not show independent influences on diatom distributions. Temperature was retained, representing an association with the eliminated variable of PO_4.

A CCA analysis was performed with 60 lakes, 15 environmental variables, and 132 species. Axes 1 and 2 of the final CCA, with eigenvalues of $\lambda_1 = 0.40$ and $\lambda_2 = 0.32$, accounted for 18.6% of the cumulative variance of the diatom data. CCA axes 1 and 2 explained a large proportion of the variance in the diatom–environment relationship (42.7%). The diatom–environment correlations for axes 1 and 2 were also high, with values of 0.91 and 0.95, respectively, indicating a strong relationship between the diatom species and the 15 environmental variables. Forward selection and unrestricted Monte Carlo permutation tests showed that eight environmental variables explained a significant proportion ($P \leq 0.05$) of the variance in the species data. In decreasing order of importance, these are water colour, alkalinity, lake

© 2002 NRC Canada

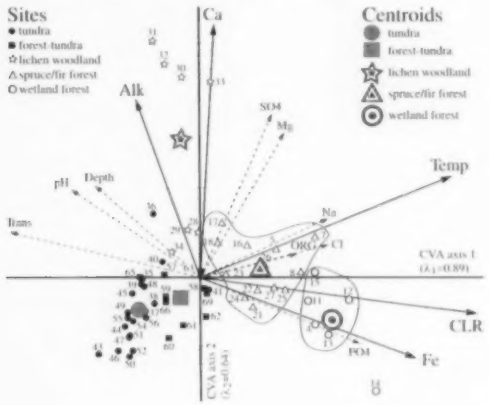

Fig. 3. Canonical variate analysis (CVA) ordination of five vegetation groups (one centroid representing each group) and 14 environmental variables for the 56 lake data set. Dashed arrows indicate passive environmental variables.

depth (Depth), iron, water transparency, sediment organic content, calcium (Ca), and summer surface-water temperature. These eight forward-selected variables accounted for 76.7% of the variance explained by the initial 15 variables. A final CCA performed with these eight variables yielded eigenvalues of $\lambda_1 = 0.38$ and $\lambda_2 = 0.31$, and together they capture 17.8% of the variance in the diatom data. The diatom–environment correlations for CCA axes 1 (0.89) and 2 (0.94) were high, and the cumulative variance proportion explained in the diatom–environment relationship was 53.8%.

The results of this CCA are illustrated by a simultaneous ordination representing the taxa and the samples, which are directly related to the environmental variables (Fig. 4). The CCA biplot of the environmental-site scores (Figs. 4*a*, 4*b*) shows a clear separation between the lakes belonging to different catchment vegetation zones based on the underlying patterns in diatom assemblage composition. In particular, the strongly coloured, iron-rich, warmer wetland forest (peatland) lakes occupy distinct positions in the lower right quadrant, reflecting dystrophic conditions that seem to favour a distinct subset of diatoms (Fig. 4*c*; see Appendix B for complete names). Diatom assemblages from the spruce/fir forest zone are quite different from those in tundra lakes, although some overlap is present, presumably because the zonal boundaries are not as sharp as with the wetland forest zone. The distinction between the diatom assemblages found in the tundra zones and in the lichen woodland zone was less evident from the CCA (Figs. 4*a*, 4*c*). This can be explained by the greater limnological and floristic similarity between these lake types and their catchments. However, among this group, some lichen woodland lakes (30–33) showed the strongest affinity with high water alkalinity values, likely resulting from the influence of carbonate-rich deposits of postglacial marine origin.

Overall, water colour and alkalinity were the two most important variables determining diatom community structure. The floristic composition of the tundra lakes was characterized by the dominance of small species typical of dilute oligotrophic lakes, such as *Achnanthes marginulata* (14), *Navicula* sp. [cf. *begerii*] (95), *N. digitulus* (106), *N. krasskei* (103), *N. parasubtilissima* (116), *Aulacoseira distans* var. *nivalis* (27), and *A. distans* var. *nivaloides* (28). These taxa occur in the left quadrants of the biplot corresponding to most of the tundra lakes (Fig. 4*c*). In the upper right quadrant, lichen woodland lakes are dominated by alkaliphilous species, such as *Cocconeis neothumensis* (38), *Cymbella descripta* (41), *Cyclotella kuetzingiana* (51), *C. michiganiana* (52), *Fragilaria construens* (74), *F. lapponica* (77), *F. pseudoconstruens* (84), *Navicula absoluta* (92), and *N.* sp. [cf. *submuralis*] (115). Other alkaliphilous species can also be found in that quadrant, but they could also be related to forest tundra lakes. These taxa include *Achnanthes laterostrata* (11), *A. pusilla* (16), *Fragilaria capucina* (69), *Navicula pseudoscutiformis* (108), and *N. seminuloides* (112). The floristic composition of diatom communities in the spruce/fir forest lakes showed higher species richness, the most common taxa being *Achnanthes subatomoides* (5), *Aulacoseira ambigua* (25), *Cymbella* sp. [cf. *schubartii*] (48), *Eunotia paludosa* var. *trinacria* (68), *Fragilaria lata* (78), *Navicula cocconeiformis* (98), *N. disjuncta* (99), *N. soehrensis* var. *hassiaca* (114), and *N. ventralis* (118). These taxa are located in the two lower quadrants of the biplot. The diatom taxa typically found in wetland forest lakes (lower right quadrant, Figs. 4*b*, 4*c*) include *Fragilaria construens* var. *binodis* (72), *F. construens* sp. [cf. var. *pumila*] (73), *F. construens* var. *venter* (75), *F. pinnata* var. *acuminata* (80), *F. pinnata* var. *lancettula* (81), and *Navicula* spp. (e.g., *N. arvensis* (94)), which seem to be associated with strongly coloured warm lakes with high Fe concentration and low alkalinity conditions (Figs. 4*b*, 4*c*).

Weighted-averaging models

CCA showed that water colour and alkalinity are the two environmental variables with the statistically greatest significance ($P \leq 0.05$) influencing diatom distribution in the Labrador data set. In constrained CCAs with water colour and alkalinity as the only variables, the eigenvalues for the first and the second axes produced ratios of 0.58 and 0.61, respectively. Thus, water colour and alkalinity promised to be appropriate variables for the development of reliable inference models.

Among all models tested, the four-component WA-PLS model with square root transformation of percent species data best represented the diatom – water colour relationship (Table 2). The model predicts water colour values that are closely related to the actual observed values (Fig. 5), with a jackknifed r^2_{jack} of 0.85 between observed and predicted colour values, a RMSEP of 0.18log(CLR + 1) (backtransformed value = 1.51 Pt units), and a maximum bias of 0.12. A two-component WA-PLS provided the best model for alkalinity, with a slightly lower r^2_{jack} (0.63), a RMSEP of 0.25 log(ALK + 1) (backtransformed value = 1.78 $\mu eq \cdot L^{-1}$), and a maximum bias of 0.26 (Table 2, Fig. 5).

Optima and tolerances of diatom taxa

The WA model allowed the calculation of alkalinity and water colour optima and tolerances for the 132 diatom species, as well as their effective number of occurrences (Appendix B). The WA optima for water colour range from 5 Pt units (*Cocconeis neothumensis*, *Navicula absoluta*, *N. agrestis*, *N. submolesta*, and *Nitzschia hantzschiana*) to 83 Pt units (*Fragilaria polygonata*). Alkalinity optima range

© 2002 NRC Canada

Fig. 4. Biplot of 60 sites (*a*), eight environmental variables (*b*), and 132 species (*c*) scores in the final canonical correspondence analysis (CCA) of the lake data set. Taxon names are presented in Appendix B. Dashed arrows in (*b*) indicate passive environmental variables.

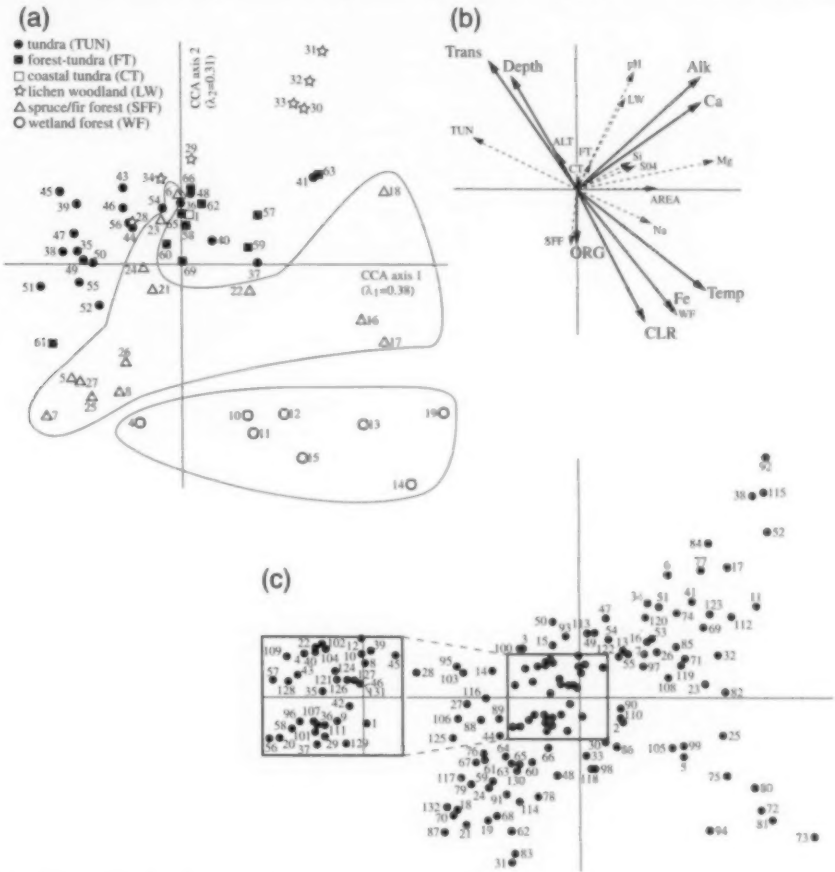

from 8 $\mu eq \cdot L^{-1}$ (*Eunotia paludosa* var. *trinacria*) to 467 $\mu eq \cdot L^{-1}$ (*Navicula absoluta*). The optima calculated here are in close agreement with those reported from northern Sweden for alkalinity and water colour (Korsman and Birks 1996; see Table 3) and from Canada's Northwest Territories for alkalinity (Rühland 1996; see Table 3).

Potential indicator taxa

For the selection of potential indicator taxa, the criteria outlined in Stevenson et al. (1991), Pienitz et al. (1995), and Fallu and Pienitz (1999) were followed: (*i*) more than 10% of the variance of a particular species had to be explained by the variable of interest in the constrained CCA; (*ii*) the tolerance of the species had to be less than the mean tolerance for all the taxa; and (*iii*) the species had to be present in 10 or more of the study lakes. Nine taxa fulfilled these criteria for water colour and 19 for alkalinity (Table 4), and their distribution is shown in Appendix A. These taxa give only a first approximation of lake water colour and alkalinity and should be used only for preliminary interpretations. For example, *Cyclotella michiganiana*, which has a very high WA alkalinity optimum of 306.5 $\mu eq \cdot L^{-1}$, was not accepted as a potential indicator taxon because its WA tolerance is broader than the mean tolerance of all taxa and because it occurred in only five lakes. However, this species was found only in high alkalinity lakes. Further research should aim at expanding the calibration set to increase the overall gradient length of alkalinity.

Gaussian logit regressions

With respect to alkalinity, many taxa (80) follow a Gaussian unimodal response model, whereas several (36) follow a linear-logit (sigmoidal) model, increasing (20 taxa) or decreasing with alkalinity (16). Some taxa (16) show no relation with alkalinity. As for colour, 78 taxa follow a Gaussian unimodal response model, whereas 20 taxa follow an increasing sigmoidal model and 18 taxa follow a decreasing one. Only 16 taxa show no relationship with colour. The Gaussian logit regression curves are presented for the potential indicator taxa in Appendix A. All potential alkalinity indicator taxa follow a unimodal response, whereas six out of nine taxa show this response among the potential colour indicator taxa.

Discussion

The ordination analyses of the Labrador data set showed a clear separation between lakes from forested and unforested

© 2002 NRC Canada

Fig. 5. (*a*) Plot of observed versus diatom-predicted colour and (*b*) observed versus residual values, based on WA-PLS with four components. (*c*) Plot of observed versus diatom-predicted alkalinity and (*d*) observed versus residual values, based on WA-PLS with two components.

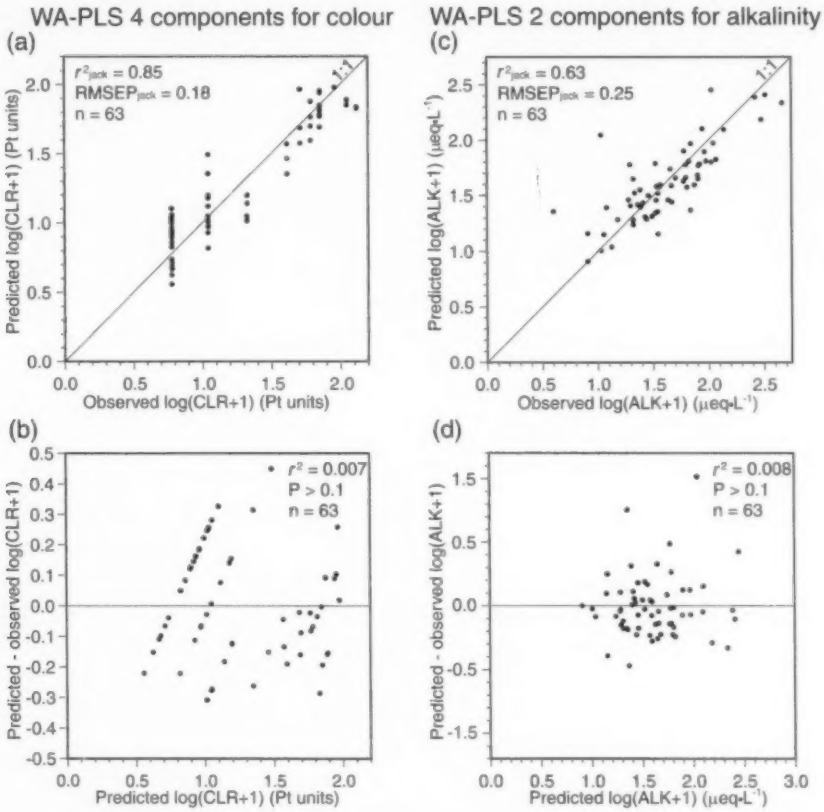

regions. The PCA enabled the differentiation of sites by their chemical and physical characteristics, whereas the CVA showed distinct divisions between groups of sites classified by vegetation zones. The CCA indicated that a relatively large proportion of the variance in the diatom data was accounted for by the environmental variables included in the calibration set. Most striking are the well-defined differences between the wetland forest and the spruce/fir forest lakes when comparing the results of PCA, CVA, and CCA. Wetland forest sites are characterized by darkest water colour, highest iron concentrations, and highest temperature (correlated with high PO_4 values). These two vegetation types have been grouped under the term boreal forest in many previous studies (e.g., Rühland 1996; Fallu and Pienitz 1999; Laing and Smol 2000). Our study shows that by distinguishing these two types, a finer understanding of diatom distribution in these lakes will allow more detailed reconstructions of lake catchment environments. This kind of information will be beneficial to paleohydrological and paleoclimatological studies.

The floristic composition of the diatom assemblages in the surface sediment samples showed several distinct changes along the sampling transect. The most apparent trend observed is a shift from communities dominated by centric taxa considered to be benthic-tychoplanktonics (e.g., *Aulacoseira* spp.) in the more acidic and coloured wetland lakes to those dominated by small periphytic pennate taxa (e.g., *Achnanthes* spp.) in the transparent and cold arctic tundra lakes. The overall declining relative abundance of large-celled centric and pennate diatoms with increasing latitude has previously been observed in lakes distributed along latitudinal transects crossing the tree line in North America (Pienitz et al. 1995; Fallu and Pienitz 1999; Lotter et al. 1999). Fallu and Pienitz (1999) and Laing et al. (1999) compared the floristic patterns between their study sites and those reported from other circumpolar regions and found strong floristic similarities. Despite the geographic distance and differences in the degree of anthropogenic disturbances, these species seem to have similar environmental preferences.

The strong alkalinity signal found in the Labrador data set confirms numerous previous regional studies that found this variable and its related factors to be influential in explaining diatom distributions. Alkalinity-related variables (e.g., DIC, pH) are often found to be the most important variables influencing the distribution and the abundance of diatom taxa (e.g., Dixit et al. 1993; Lotter et al. 1997; Weckström et al. 1997), including the assemblages from subarctic and arctic regions (Pienitz and Smol 1993; Pienitz et al. 1995). In Labrador, higher alkalinity values were observed in the lichen woodland region because of local bedrock dominated by a

© 2002 NRC Canada

Table 3. Comparison of diatom alkalinity optima inferred from calibration data sets in Québec–Labrador (present study), northern Sweden (Korsman and Birks 1996), and Canada's Northwest Territories (Rühland 1996) and comparison of water colour optima inferred from Québec–Labrador (present study) and northern Sweden (Korsman and Birks 1996).

	ALK optimum ($\mu eq \cdot L^{-1}$)*			CLR optimum (Pt units)	
Taxa	Korsman and Birks	This study	Rühland	Korsman and Birks	This study
Achnanthes altaica		37	~48		
A. didyma	85	71	~70		
A. kuelbsii	42	42			
A. laterostrata				20	17
A. levanderi		54	~62		
A. marginulata		34	~36		
Asterionella ralfsii var. *americana*	16	17			
Aulacoseira distans var. *humilis*				17	14
A. distans var. *nivalis*	33	24	~18		
A. lirata	40	30	~24		
A. perglabra	36	30	~30		
A. perglabra var. *floriniae*	35	28			
Cymbella gaeumannii		35	~36		
C. gracilis		35	~40		
C. hebridica		25	~34		
C. microcephala				20	10
C. silesiaca		41	~40		
Eunotia exigua	22	29			
E. faba		24	~28		
E. incisa				54	53
Fragilaria brevistriata				22	15
F. construens var. *venter*				31	30
F. lapponica				13	8
F. lata	28	18			
F. pseudoconstruens				13	8
F. virescens var. *exigua*		34	~34		
Frustulia rhomboides		22	~26		
F. rhomboides var. *saxonica*		27	~22		
Gomphonema parvulum		48	~48		
Navicula digitulus				16	19
N. laevissima				25	26
N. leptostriata	30	34			
N. pseudoscutiformis		61	~74		
N. vitiosa				25	18
Nitzschia perminuta		37	~44	21	14
Pinnularia microstauron		39	~40		
Stauroneis anceps		33	~34	26	19

Note: ALK, alkalinity; CLR, water colour.

*Because Rühland (1996) reported alkalinity values measured in mg $CaCO_3 \cdot L^{-1}$, her data were transformed into $\mu eq \cdot L^{-1}$, see Wetzel and Likens (2000) for formula used in transformations ($20 \times$ mg $CaCO_3 \cdot L^{-1} = 1$ $\mu eq \cdot L^{-1}$).

drift-covered belt composed of carbonate-rich sedimentary rocks (Colman-Sadd and Scott 1994). Most of the alkaliphilous diatoms were found in this region, indicating that the particular geological substrate in this part of the study region may strongly influence the lake water chemistry and the composition of diatom communities. For example, Laing and Smol (2000) demonstrated the importance of geological conditions in northern Russia where substrate-related changes in water chemistry overrode climatic gradients in explaining diatom distributions among different regions.

Water colour is the other environmental variable that appears to explain much of the variability in the distribution of diatoms in Labrador. Water colour was measured in the field to avoid error resulting from humus losses during lengthy field storage of samples (Engstrom 1987). It provides a measure of humic content, or a degree of lake dystrophy, and represents a proxy for DOC. The strong colour signal in this data set was not surprising, as changes in lake water DOC and related processes (e.g., changes in water colour, transparency, and spectral composition of transmitted light; chemical interactions affecting the bioavailability of nutrients and trace metals) are known to strongly influence diatom distributions (e.g., Pienitz and Smol 1993; Korsman and Birks 1996; Fallu and Pienitz 1999). Diatom-based inference models for DOC have been developed for freshwater lakes in temperate North America (Kingston and Birks 1990; Dixit et al. 1993), Europe (Stevenson et al. 1991; Korsman and Birks 1996), and subarctic regions of the Northwest Ter-

© 2002 NRC Canada

Table 4. Potential indicator diatom taxa for water colour (CLR) and alkalinity (ALK).

N	Code	Species	Optima	Tolerance	% Variance explained	Number of occurrences
Colour (Pt units)						
40	CYMLAPP	*Cymbella lapponica* Grunow in Cleve & Möller	8	2.0	11.1	13
47	CYMMINU	*Cymbella minuta* Hilse ex Rabenhorst	8	1.8	12.7	15
122	NITFONT	*Nitzschia* sp. [cf. *fonticola* Grunow in Van Heurck]	9	1.8	20.9	29
4	ACHCURT	*Achnanthes* sp. [cf. *curtissima* Carter]	9	2.2	26.0	36
29	AULDITE	*Aulacoseira distans* var. *tenella* (Nygaard) Florin	43	2.3	21.2	18
24	ASTRAAM	*Asterionella ralfsii* var. *americana* Körner	53	2.1	27.6	16
60	EUNINCI	*Eunotia incisa* Gregory	53	1.9	40.9	20
81	FRAPILA	*Fragilaria pinnata* var. *lancettula* (Schumann) Hustedt in Schmidt et al.	62	2.2	21.3	11
94	NAVARVE	*Navicula arvensis* Hustedt	68	1.7	36.5	19
Alkalinity ($\mu eq \cdot L^{-1}$)						
24	ASTRAAM	*Asterionella ralfsii* var. *americana* Körner	17	1.8	19.6	16
117	NAVTENU	*Navicula tenuicephala* Hustedt	17	1.7	11.4	12
67	EUNSUBA	*Eunotia subarcuatoides* Alles, Nörpel & Lange-Bertalot	18	1.9	19.0	15
76	FRACONA	*Fragilaria constricta* Ehrenberg	18	2.1	20.1	18
79	FRAOLDE	*Fragilaria oldenburgiana* Hustedt	18	1.8	16.1	15
78	FRALATA	*Fragilaria lata* (Cleve-Euler) Renberg	18	2.0	18.3	17
59	EUNHEMI	*Eunotia hemicyclus* (Ehrenberg) Ralfs in Pritchard	19	1.9	15.8	14
48	CYMSCHU	*Cymbella* sp. [cf. *schubartii* Hustedt]	19	2.1	18.2	16
96	NAVBREM	*Navicula bremensis* Hustedt	21	2.0	11.5	16
88	FRURHOM	*Frustulia rhomboides* (Ehrenberg) De Toni	22	2.0	26.5	35
27	AULDINI	*Aulacoseira distans* var. *nivalis* (W. Smith) Haworth	24	1.9	20.3	36
58	EUNFABA	*Eunotia faba* Ehrenberg	24	2.1	10.4	21
44	CYMHEBR	*Cymbella hebridica* (Grunow) Cleve	25	2.2	22.4	37
116	NAVPARA	*Navicula parasubtilissima* Kobayasi and Nagumo	27	2.0	11.6	35
89	FRURHSA	*Frustulia rhomboides* var. *saxonica* (Rabenhorst) De Toni	27	2.1	20.7	49
37	AULPEFL	*Aulacoseira perglabra* var. *floriniae* (Camburn) Haworth	28	2.1	16.0	46
103	NAVKRAS	*Navicula krasskei* Hustedt	31	1.7	10.3	13
7	ACHDIDY	*Achnanthes didyma* Hustedt	71	2.2	22.5	23
23	ASTFORM	*Asterionella formosa* Hassal	82	2.0	11.7	14

Note: The taxa are presented with their optimum and tolerance, the percent of their variance explained by the variable of interest in a constrained CCA, and their number of occurrences. Numbers (*N*) for taxa refer to those used in Fig. 4. Codes for names are used in Appendix A with illustrations of WA optimum and tolerance ranges.

ritories (Pienitz and Smol 1993) and northwestern Québec (Fallu and Pienitz 1999). Basin hydrology and the nature of the catchment vegetation and soils are important factors controlling the concentration of humic compounds in surface waters (Curtis and Schindler 1997; D'Arcy and Carignan 1997; Gibson et al. 2001). In Labrador, the water colour (DOC) gradient showed an inverse correlation with latitude. The influence of water colour seems to be attenuated in lichen woodland, forest–tundra, and tundra sites, as a dramatic change in the mean water colour could be observed, from 89 Pt units in wetland forest lakes and 50 Pt units in spruce/fir forest lakes to 14 Pt units in forest–tundra, 8 Pt units in lichen woodland, and 6 Pt units in tundra lakes. In the forested zone of the Subarctic in Québec and Labrador, the soils are often composed of peat because litter production is much higher than decomposition. The water run-off occurs mainly as surface flow and enters these lakes with rich-coloured humic acid contents because the acids have not been filtered by mineral soils (Engstrom 1987). As the vegetation becomes more patchy, the humic acid obtained

© 2002 NRC Canada

by decomposition percolates through mineral soils and is mineralized, leading to surface water carrying less coloured humic compounds. In the tundra, the sparse vegetation cover results in clear-water lakes with extremely low humic acid inputs (Engstrom 1987). In this study, other environmental variables were also associated with the water colour (DOC) gradient, such as water transparency and surface water temperature, as well as the concentrations of total phosphorus and iron.

The WA-PLS calibration models may be used to infer past lake water alkalinity and water colour from fossil diatom assemblages preserved in the sediments of Labrador lakes within the alkalinity range of 3–463 $\mu eq \cdot L^{-1}$ and the water colour range of 5–130 Pt units. Because they tend to slightly overestimate the values at the lower end of the gradient and underestimate them at the higher end, these models would perform best on a site from the central part of the gradient. The water colour and alkalinity inferences are based on the optima and tolerances of 132 diatom species common in Labrador. As discussed above, colour is a suitable variable to reconstruct past optical conditions in lakes that are related to shifts in catchment vegetation and DOC concentrations. Studies using similar models commonly showed progressive loss of alkalinity over time, abrupt increases in water colour that coincides with the arrival of trees (Saulnier-Talbot and Pienitz 2002), and subsequent shifts that are closely correlated with vegetation and soil changes in the catchment (Engstrom et al. 2000; Pienitz and Vincent 2000).

The ecological preferences estimated by the WA calibration models show good correspondence with those of other studies. When compared with Fallu and Pienitz (1999), the water colour model shows several similarities. For example, *Actinella punctata*, *Eunotia incisa*, *Fragilaria lata*, and *Melosira arentii* tended to have higher water colour and DOC optima in both northern Québec and Labrador. Optima that are below average were inferred in both regions for *Achnanthes curtissima*, *A. levanderi*, *A. suchlandtii*, *Cyclotella ocellata*, *Cymbella gaeumannii*, *C. lapponica*, *Fragilaria pseudoconstruens*, *Navicula jaernefeltii*, *N. krasskei*, and *Nitzschia* sp. [cf. *fonticola*]. The water colour optima for selected indicator species in this study are comparable with the potential DOC indicator species identified by Fallu and Pienitz (1999). One taxon seems to be a particularly good indicator of low DOC concentrations (or low Pt units): *Nitzschia* sp. [cf. *fonticola*] with a DOC optimum of 5.13 $mg \cdot L^{-1}$ (Fallu and Pienitz 1999) and a water colour optimum of 9 Pt units. Good correspondence to other studies also exists with respect to alkalinity preferences. The taxon *Cyclotella michiganiana* is known to prefer highly alkaline conditions (Stevenson et al. 1991; Rühland 1996). The optima of many taxa in Labrador show values close to the optima reported from Sweden and the Northwest Territories (N.W.T.) (Korsman and Birks 1996; Rühland 1996; this study). However, though the ecological optima inferred for taxa in the N.W.T. and Labrador follow similar trends, a few differences could also be observed. The alkalinity optima inferred for N.W.T. taxa seem to be generally higher than those inferred for Labrador species. Also, the taxa representing the lower alkalinity range in Labrador are not listed among the 116 most common diatom taxa in the N.W.T. (e.g., *Eunotia paludosa* var. *trinacria*, *Fragilaria acidobiontica*). This is likely due to the generally higher alkalinity of lakes in the Slave and Bear provinces of the N.W.T. (alkalinity values ~4 $\mu eq \cdot L^{-1}$ to ~1998 $\mu eq \cdot L^{-1}$ vs. 8.9 $\mu eq \cdot L^{-1}$ to 306.5 $\mu eq \cdot L^{-1}$ in Labrador). Major differences can be found in the optima of the two small taxa *Navicula minuscula* and *Navicula seminuloides*, which may be due to taxonomic uncertainties.

In conclusion, the final CCA of the Labrador lake set demonstrated that water colour and alkalinity were significantly correlated with diatom community composition ($P \leq 0.005$). Based on this observation, it was assumed that the relationship between water colour and diatoms, and between alkalinity and diatoms, was sufficiently robust to produce reliable inference models for the reconstruction of these environmental variables from fossil diatom assemblages. However, even though water colour and alkalinity fulfilled the requirements for developing inference models, it should be kept in mind that other unmeasured variables not included in the Labrador data set may also exert a strong influence, such as physical mixing, day-length effects, grazing, parasitism, and availability of microhabitats. Information about these environmental variables could improve the ordination, but they were not available for the Labrador calibration set.

The species–environment relationships revealed by the Labrador data confirm observations that alkalinity–pH–DIC and water colour – DOC gradients strongly impact diatom distributions across broad geographic regions in the Subarctic (reviewed in Lotter et al. 1999). They also suggest that lake water colour and alkalinity are variables of particular ecological importance, especially in electrolyte-poor, oligotrophic freshwater ecosystems. Changes in wetland patterns and vegetation cover in the catchment associated with climate warming will modify water colour (transparency) and DOC concentrations in the recipient lakes (Forsberg 1992; Vincent and Pienitz 1996), which will likely result in marked shifts in diatom assemblage composition and aquatic community structure (Seppä and Weckström 1999; Weckström and Korhola 2001). Although these kinds of shifts have been observed in other studies, our results may help detect more subtle changes within the boreal forest zone (spruce/fir forest and wetland forest). Quantitative estimates of past lake water colour and alkalinity will therefore provide important information concerning the changes in physical (e.g., underwater light regime) and chemical conditions of northern lakes driven by climatic change and (or) successional changes in catchment vegetation and soils. Future studies should aim to achieve a finer resolution of catchment properties, such as the degree of paludification, forest density, and the species composition of forest cover, and thereby further enhance the value of diatoms as proxies for change in the terrestrial environment surrounding study lakes.

Acknowledgements

We thank D.R. Engstrom (Limnological Research Center) for providing the Labrador surface sediments and limnological data and K. Camburn for part of the initial diatom counts. The analyses of the environmental and diatom data were supported by Natural Sciences and Engineering Research Council

© 2002 NRC Canada

of Canada and Fonds pour la Formation de Chercheurs et l'Aide à la Recherche (Québec) research grants to R.P. and by logistical support from the Centre d'études nordiques. We would also like to thank S. Juggins and C.J.F. ter Braak for providing prerelease copies of their CALIBRATE program. S.C. Fritz, M.B. Hay, T. Laing, W.F. Vincent, I.R. Walker, and two anonymous reviewers are thanked for providing helpful comments to earlier versions of the manuscript.

References

Allaire, N. 1997. Relation entre les assemblages de diatomées et les variables environnementales de 70 lacs du Labrador et résultats préliminaires d'une étude paléolimnologique du lac Hope Simpson. M.A. thesis, Université Laval, Québec, QC.

Bigler, C., and Hall, R.I. 2002. Diatoms as indicators of climatic and limnological change in Swedish Lapland: a 100-lake calibration set and its validation for paleoecological reconstructions. J. Paleolimnol. **27**: 97–115.

Birks, H.J.B. 1998. Numerical tools in palaeolimnology—progress, potentialities, and problems. J. Paleolimnol. **20**: 307–322.

Birks, H.J.B., Juggins, S., and Line, J.M. 1990*a*. Lake surface–water chemistry reconstructions from palaeoecological data. *In* The surface waters acidification programme. *Edited by* B.J. Mason. Cambridge University Press, Cambridge. pp. 301–311.

Birks, H.J.B., Line, J.M., Juggins, S., Stevenson, A.C., and ter Braak, C.J.F. 1990*b*. Diatoms and pH reconstructions. Philos. Trans. R. Soc. Lond. B. Biol. Sci. **327**: 263–278.

Bonan, G.B., Chapin, F.S., III, and Thompson, S.L. 1995. Boreal forest and tundra ecosystems as components of the climate system. Clim. Change, **29**: 145–167.

Clark, P.U., Short, S.K., Williams, K.M., and Andrews, J.T. 1989. Late Quaternary chronology and environments of Square Lake, Torngat Mountains, Labrador. Can. J. Earth Sci. **26**: 2130–2144.

Colman-Sadd, S., and Scott, S.A. 1994. Newfoundland and Labrador: traveller's guide to the geology and the guidebook to stops of interest. Government of Newfoundland and Labrador, St. John's, Nfld.

Crawley, M.J. 1993. GLIM for ecologists. Blackwell Scientific Publications, Oxford.

Curtis, P.J., and Schindler, D.W. 1997. Hydrologic control of dissolved organic matter in low-order Precambrian Shield lakes. Biogeochemistry, **36**: 125–138.

D'Arcy, P., and Carignan, R. 1997. Influence of catchment topography on water chemistry in southeastern Québec Shield lakes. Can. J. Fish. Aquat. Sci. **54**: 2215–2227.

Dixit, S.S., Cumming, B.F., Kingston, J.C., Smol, J.P., Birks, H.J.B., Uutala, A.J., Charles, D.F., and Camburn, K.E. 1993. Diatom assemblages from Adirondack lakes (New York, U.S.A.) and the development of inference models for retrospective environmental assessment. J. Paleolimnol. **8**: 27–47.

Duff, K.E., Laing, T.E., Smol, J.P., and Lean, D.R.S. 1999. Limnological characteristics of lakes located across arctic treeline in northern Russia. Hydrobiologia, **391**: 205–222.

Ecoregions Working Group. 1989. Ecoclimatic regions of Canada, first approximation. Ecological Land Classification Series No. 23, Environment Canada, Ottawa.

Engstrom, D.R. 1987. Influence of vegetation and hydrology on the humus budgets of Labrador lakes. Can. J. Fish. Aquat. Sci. **44**: 1306–1314.

Engstrom, D.R., and Hansen, B.C.S. 1985. Postglacial vegetational change and soil development in southeastern Labrador as inferred from pollen and chemical stratigraphy. Can. J. Bot. **63**: 543–561.

Engstrom, D.R., Fritz, S.C., Almendinger, J.E., and Juggins, S. 2000. Chemical and biological trends during lake evolution in recently deglaciated terrain. Nature (London), **408**: 161–166.

Fallu, M.-A., and Pienitz, R. 1999. Diatomées lacustres de Jamésie–Hudsonie (Québec) et modèle de reconstitution des concentrations de carbone organique dissous. Ecoscience, **4**: 603–620.

Fallu, M.-A., Allaire, N., and Pienitz, R. 2000. Freshwater diatoms from northern Québec and Labrador (Canada): species–environment relationships in lakes of boreal forest, forest–tundra and tundra regions. Bibliotheca Diatomologica. Vol. 45. J. Cramer, Berlin, Stuttgart.

Forsberg, C. 1992. Will an increased greenhouse impact in Fennoscandia give rise to more humic and colored lakes? Hydrobiologia, **229**: 51–58.

Gibson, J.A.E., Vincent, W.F., and Pienitz, R. 2001. Hydrologic control and diurnal photobleaching of CDOM in a subarctic lake. Arch. Hydrobiol. **152**:143–159.

Hare, F.K. 1959. A photo-reconnaissance survey of Labrador–Ungava. The Queen's Printer, Ottawa.

Hill, M.O. 1973. Diversity and evenness: a unifying notation and its consequences. Ecology, **54**: 427–432.

Hill, M.O., and Gauch, H.G. 1980. Detrended correspondence analysis: an improved ordination technique. Vegetatio, **42**: 47–58.

Juggins, S., and ter Braak, C.J.F. 1992. CALIBRATE—a program for species–environmental calibration by [weighted-averaging] partial least squares regression. Environmental Change Research Centre, University College London, London.

Kattenberg, A., Giorgi, F., Grassl, H., Meehl, G.A., Mitchell, J.F.B., Stouffer, R.J., Tokioka, T., Weaver, A.J., and Wigley, T.M. 1996. Climate models—projections for future climate. *In* The science of climate change. *Edited by* Houghton, J.T., et al. Cambridge University Press, Cambridge. pp. 283–357.

Kingston, J.C., and Birks, H.J.B. 1990. Dissolved organic carbon reconstructions from diatom assemblages in PIRLA project lakes, North America. Philos. Trans. R. Soc. Lond. B, Biol. Sci. **327**: 279–288.

Korhola, A., Weckström, J., Holmström, L., and Erästö, P. 2000. A quantitative Holocene climatic record from diatoms in northern Fennoscandia. Quat. Res. **54**: 284–294.

Korsman, T., and Birks, H.J.B. 1996. Diatom-based water chemistry reconstructions from northern Sweden: a comparison of reconstruction techniques. J. Paleolimnol. **15**: 65–77.

Laing, T.E., and Smol, J.P. 2000. Factors influencing diatom distributions in circumpolar treeline lakes of northern Russia. J. Phycol. **36**: 1035–1048.

Laing, T.E., Pienitz, R., and Smol, J.P. 1999.Freshwater diatom assemblages from 23 lakes located near Norilsk, Siberia: a comparison with assemblages from other circumpolar treeline regions. Diatom Res. **14**: 285–305.

Lamb, H.F. 1980. Late Quaternary vegetational history of southeastern Labrador. Arct. Alp. Res. **12**: 117–135.

Lamb, H.F. 1984. Modern pollen spectra from Labrador and their use in reconstructing Holocene vegetational history. J. Ecol. **72**: 37–59.

Lotter, A.F., Birks, H.J.B., Hofmann, W., and Marchetto, A. 1997. Modern diatom, cladocera, chironomid, and chrysophyte cyst assemblages as quantitative indicatiors for the reconstruction of past environmental conditions in the Alps. I. Climate. J. Paleolimnol. **18**: 395–420.

Lotter, A.F., Pienitz, R., and Schmidt, R. 1999. Diatoms as indicators of environmental change near arctic and alpine treeline. *In* The diatoms: applications to the environmental and earth sciences. *Edited by* E.F. Stoermer and J.P. Smol. Cambridge University Press, Cambridge. pp. 205–226.

© 2002 NRC Canada

Payette, S., Filion, L., Delwaide, A., and Bégin, C. 1989. Reconstruction of tree-line vegetation response to long-term climate change. Nature (London), **341**: 429–432.

Pielke, R.A., and Vidale, P.L. 1995. The boreal forest and the polar front. J. Geophys. Res. **100**: 25 755–25 758.

Pienitz, R., and Smol, J.P. 1993. Diatom assemblages and their relationship to environmental variables in lakes from the boreal forest–tundra ecotone near Yellowknife, Northwest Territories, Canada. Hydrobiologia, **269/270**: 391–404.

Pienitz, R., and Vincent, W.F. 2000. Effects of climate change relative to ozone depletion on UV exposure in subarctic lakes. Nature (London), **404**: 484–487.

Pienitz, R., Smol, J.P., and Birks, H.J.B. 1995. Assessment of freshwater diatoms as quantitative indicators of past climatic change in the Yukon and Northwest Territories, Canada. J. Paleolimnol. **13**: 21–49.

Pienitz, R., Smol, J.P., and MacDonald, G.M. 1999. Paleolimnological reconstruction of Holocene climatic trends from two boreal treeline lakes, Northwest Territories, Canada. Arct. Antarct. Alp. Res. **31**: 82–93.

Rosén, P., Hall, R.I., Korsman, T., and Renberg, I. 2000. Diatom transfer-functions for quantifying past air temperature, pH and total organic carbon concentration from lakes in northern Sweden. J. Paleolimnol. **24**: 109–123.

Rühland, K. 1996. Assessing the use of diatom assemblages as paleoenvironmental proxies in the Slave and Bear geological provinces, NWT, Canada. M.Sc. thesis, Queen's University, Kingston, Ont.

Saulnier-Talbot, É., and Pienitz, R. 2002. Isolement postglaciaire d'un bassin côtier près de Kuujjuaraapik–Whapmagoostui : une analyse biostratigraphique diatomifère. Geogr. Phys. Quat. **55**. In press.

Seppä, H., and Weckström, J. 1999. Holocene vegetational and limnological changes in the Fennoscandian tree-line area as documented by pollen and diatom records from Lake Tsuolbmajavri, Finland. Ecoscience, **6**: 621–635.

Stevenson, A.C., Juggins, S., Birks, H.J.B., Anderson, D.S., Anderson, N.J., Battarbee, R.W., Berge, F., Davis, R.B., Flower, R.J., Haworth, E.Y., Jones, V.J., Kingston, J.C., Kreiser, A.M., Line, J.M., Munro, M.A.R., and Renberg, I. 1991. The surface water acidification project palaeolimnology programme: modern diatom/lake-water chemistry data. ENSIS Publishing, London.

ter Braak, C.J.F. 1988. CANOCO—a FORTRAN program for canonical community ordination by [partial] [detrended] [canonical] correspondence analysis, principal components analysis and redundancy analysis (version 2.1). TNO Institute of Applied Computer Science, Statistics Department, Wageningen, The Netherlands, Technical Report LWA-88-02.

ter Braak, C.J.F., and Juggins, S. 1993. Weighted averaging partial least squares regression (WA-PLS): an improved method for reconstructing environmental variables from species assemblages. Hydrobiologia, **269/270**: 485–502.

ter Braak, C.J.F., and Prentice, I.C. 1988. A theory of gradient analysis. Adv. Ecol. Res. **18**: 271–317.

ter Braak, C.J.F., and Šmilauer, P. 1998. CANACO reference manual and user's guide to CANOCO for Windows: software for canonical community ordination (version 4). Microcomputer Power, Ithaca, N.Y.

Vincent W.F., and Pienitz, R. 1996. Sensitivity of high-latitude freshwater ecosystems to global change: temperature and solar ultraviolet radiation. Geosci. Can. **23**: 231–236.

Walker, I.R., Smol, J.P., Engstrom, D.R., and Birks, H.J.B. 1991. An assessment of Chironomidae as quantitative indicators of past climatic change. Can. J. Fish. Aquat. Sci. **48**: 975–987.

Water Resources Division. 1992. Water resources atlas of Newfoundland. Department of Environment and Lands, Government of Newfoundland and Labrador, St. John's, Nfld.

Weckström, J., and Korhola, A. 2001. Patterns in the distribution, composition and diversity of diatom assemblages in relation to ecoclimatic factors in Arctic Lapland. J. Biogeogr. **28**: 31–45.

Weckström, J., Korhola, A., and Blom, T. 1997. The relationship between diatoms and water temperature in thirty subarctic Fennoscandian lakes. Arct. Alp. Res. **29**: 75–92.

Wetzel, R.G., and Likens, G.E. 2000. Limnological analysis. 3rd ed. Springer, New York.

Wright, H.E., Jr. 1990. An improved Hongve sampler for surface sediments. J. Paleolimnol. **4**: 91–92.

(Appendices A and B follow.)

© 2002 NRC Canada

Appendix A

Graphic illustration of weighted-averaging (WA) optimum and tolerance range of diatom indicator taxa for colour (CLR, Fig. A1) and alkalinity (ALK, Fig. A2). The estimated WA optimum of each taxon is shown as a vertical line at the top of each plot, as well as the fitted Gaussian logit curves. Taxon names are presented in Table 4.

Fig. A1. Weighted-averaging optimum and tolerance range of diatom indicator taxa for water colour.

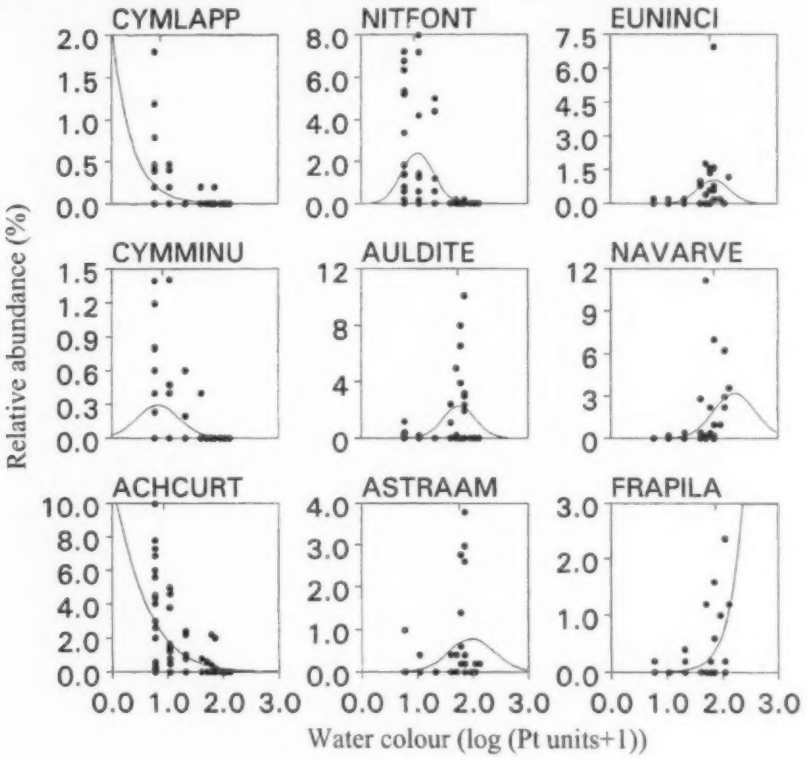

© 2002 NRC Canada

Fig. A2. Weighted-averaging optimum and tolerance range of diatom indicator taxa for water alkalinity.

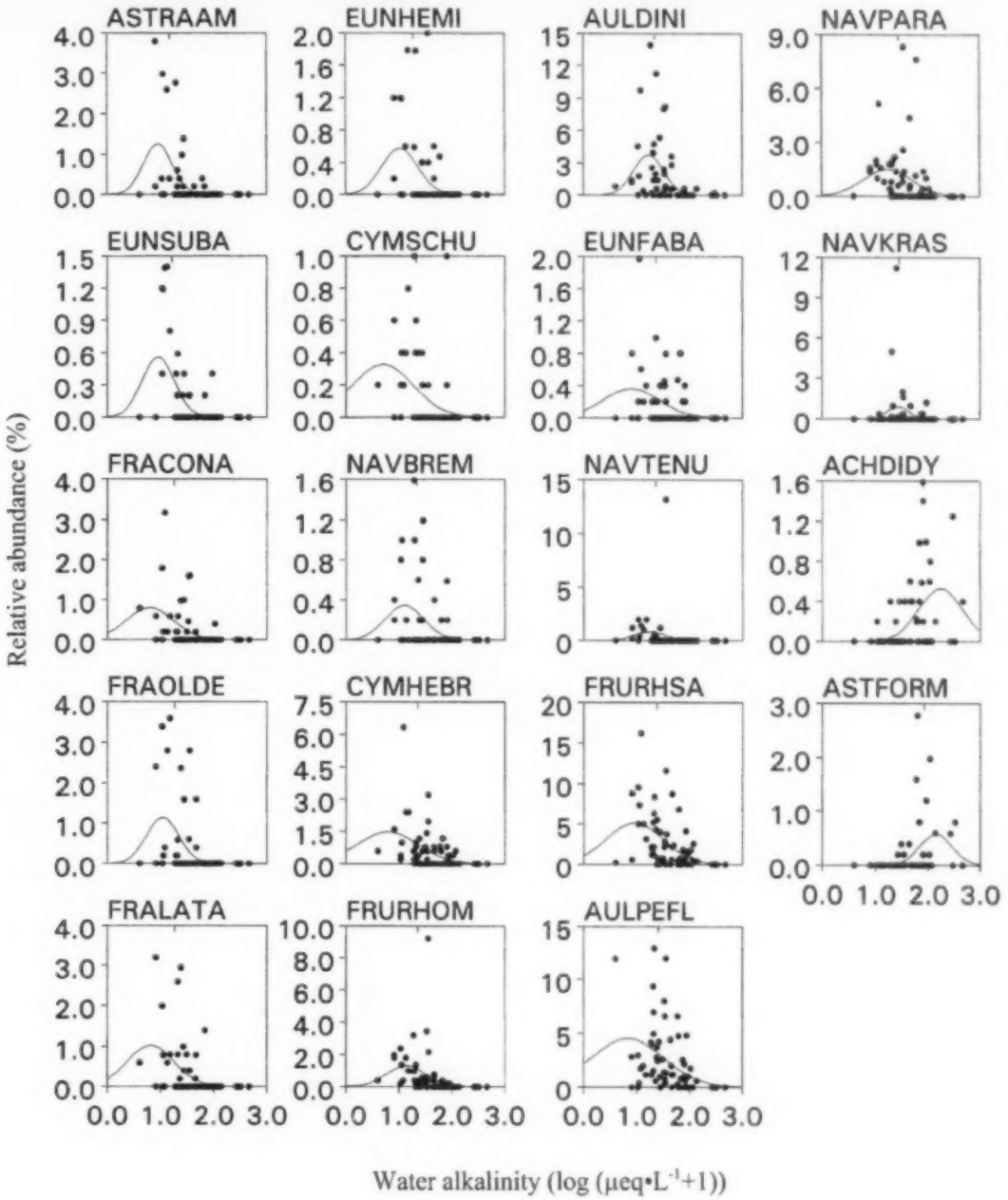

© 2002 NRC Canada

Appendix B

Table B1. Weighted-averaging optima and tolerances for water colour (CLR, Pt units) and alkalinity (ALK, $\mu eq \cdot L^{-1}$), number of occurrences, and effective number of occurrences (*N2*, Hill 1973) of the 132 screened taxa.

	Taxon name	CLR optimum	CLR tolerance	ALK optimum	ALK tolerance	Occurrences	Hill's *N2*
1	*Achnanthes altaica* (Poretzky) Cleve-Euler	22	3.0	37	2.3	38	33.0
2	*Achnanthes bicapitata* Hustedt	46	2.7	53	1.5	8	6.7
3	*Achnanthes carissima* Lange-Bertalot in Lange-Bertalot & Krammer	7	1.6	37	3.0	6	4.7
4	*Achnanthes* sp. [cf. *curtissima* Carter]	9	2.2	43	2.2	36	29.0
5	*Achnanthes subatomoides* (Hustedt) Lange-Bertalot & Archibald in K. & L.-B.	30	2.9	41	2.3	34	26.0
6	*Achnanthes* sp. 1	8	2.2	77	2.9	9	7.7
7	*Achnanthes didyma* Hustedt	14	2.4	71	2.2	23	20.5
8	*Achnanthes flexella* (Kützing) Brun	13	2.7	45	2.8	12	10.6
9	*Achnanthes chlidanos* Hohn & Hellerman	18	3.0	38	2.6	29	26.4
10	*Achnanthes kuelbsii* Lange-Bertalot in Lange-Bertalot & Krammer	8	2.2	42	2.5	12	9.5
11	*Achnanthes laterostrata* Hustedt	17	2.3	150	2.7	3	2.4
12	*Achnanthes levanderi* Hustedt	11	2.4	54	2.4	39	29.9
13	*Achnanthes petersenii* Hustedt	12	2.3	67	2.3	19	16.4
14	*Achnanthes marginulata* Grunow in Cleve & Grunow	9	2.3	34	2.1	55	37.7
15	*Achnanthes minutissima* Kützing	9	2.0	59	2.5	40	28.8
16	*Achnanthes pusilla* Grunow in Cleve & Grunow	15	2.5	68	2.6	29	23.7
17	*Achnanthes suchlandtii* Hustedt	13	2.4	134	2.6	17	13.0
18	*Actinella punctata* Lewis	46	2.5	12	1.8	8	6.3
19	*Nupela paludigena* (Scherer) Lange-Bertalot	70	1.3	12	1.2	1	1.0
20	*Anomoeoneis brachysira* (Brébisson in Rabenhorst) Grunow in Cleve	17	2.9	30	2.3	50	40.2
21	*Brachysira styriaca* (Grunow in Van Heurck) Ross in Hartley	64	1.3	12	1.5	8	7.1
22	*Brachysira neoexilis* Lange-Bertalot in Lange-Bertalot & Moser	10	2.5	37	2.3	36	25.9
23	*Asterionella formosa* Hassal	20	2.7	82	2.0	14	11.7
24	*Asterionella ralfsii* var. *americana* Körner	53	2.1	17	1.8	16	12.1
25	*Aulacoseira ambigua* (Grunow) Simonsen	32	2.8	55	2.2	20	17.1
26	*Aulacoseira distans* var. *humilis* Cleve-Euler	14	1.5	119	2.4	3	2.6
27	*Aulacoseira distans* var. *nivalis* (W. Smith) Haworth	14	3.0	24	1.9	36	26.3
28	*Aulacoseira distans* var. *nivaloides* (Camburn in Camburn & Kingston) Haworth	11	2.7	27	1.9	25	7.3
29	*Aulacoseira distans* var. *tenella* (Nygaard) Florin	43	2.3	26	2.1	18	13.4
30	*Aulacoseira distans* (Ehrenberg) Simonsen	23	3.2	36	2.2	48	35
31	*Melosira* sp.[cf. *goetzeana* O. Müller]	78	1.4	12	1.7	5	3.7
32	*Aulacoseira subarctica* (O. Müller) Haworth	16	2.3	82	2.2	13	7.0
33	*Aulacoseira lirata* (Ehrenberg) Kützing	29	3.0	30	2.6	39	30.0
34	*Aulacoseira lirata* f. *biseriata* (Grunow) Camburn	9	2.9	50	5.9	5	4.3
35	*Aulacoseira* sp. [cf. *nygaardii* (Camburn) Camburn in Camburn & Charles 1986]	17	3.3	31	1.8	17	15.4
36	*Aulacoseira perglabra* (Østrup) Haworth	18	3.2	30	2.1	45	34.4
37	*Aulacoseira perglabra* var. *floriniae* (Camburn) Haworth	18	3.0	28	2.1	46	37.1
38	*Cocconeis neothumensis* Krammer	5	1.3	228	4.0	2	1.9
39	*Cymbella* sp. [cf. *aequalis* W. Smith in Greville]	7	1.7	53	3.3	6	5.1

© 2002 NRC Canada

Table B1 (*continued*).

	Taxon name	CLR optimum	CLR tolerance	ALK optimum	ALK tolerance	Occurrences	Hill's *N*2
40	*Cymbella lapponica* Grunow in Cleve & Möller	8	2.0	36	2.0	13	11.3
41	*Cymbella descripta* (Hustedt) Krammer & Lange-Bertalot	10	1.7	144	2.5	12	11.0
42	*Cymbella gracilis* (Ehrenberg) Kützing	18	2.8	35	2.5	43	35.7
43	*Cymbella gaeumannii* Meister	10	2.4	35	2.1	50	39.3
44	*Cymbella hebridica* (Grunow) Cleve	17	3.1	25	2.2	37	30.7
45	*Cymbella microcephala* Grunow in Van Heurck	10	1.9	61	2.2	17	15.1
46	*Cymbella silesiaca* Bleisch in Rabenhorst	12	2.4	41	2.5	14	12.7
47	*Cymbella minuta* Hilse ex Rabenhorst	8	1.8	59	2.8	15	13.8
48	*Cymbella* sp. [cf. *schubartii* Hustedt]	44	2.5	19	2.1	16	14.7
49	*Cyclotella rossii* Håkansson	9	2.1	59	2.3	23	14.2
50	*Cyclotella tripartita* Håkansson	8	1.9	50	2.9	7	5.9
51	*Cyclotella kuetzingiana* Thwaites	11	2.1	78	2.8	16	14.0
52	*Cyclotella michiganiana* Skvortzow	7	1.4	287	1.6	5	4.1
53	*Cyclotella ocellata* Pantocsek	15	2.2	73	2.5	5	4.1
54	*Cyclotella stelligera* (Cleve & Grunow) Van Heurck	14	2.6	53	2.5	50	33.4
55	*Cyclotella bodanica* var. *lemanica* (O. Müller ex Schröter) Bachman	11	2.1	59	2.1	26	20.1
56	*Eunotia bilunaris* (Ehrenberg) Mills	26	3.0	28	2.2	29	24.6
57	*Eunotia exigua* (Brébisson ex Kützing) Rabenhorst	12	2.6	29	2.0	21	18.7
58	*Eunotia faba* Ehrenberg	21	3.2	24	2.1	21	18.4
59	*Eunotia hemicyclus* (Ehrenberg) Ralfs in Pritchard	34	2.6	19	1.9	14	12.4
60	*Eunotia incisa* Gregory	53	1.9	21	2.4	20	15.4
61	*Eunotia intermedia* (Krasske ex Hustedt) Nörpel & Lange-Bertalot	29	3.1	18	2.0	10	8.0
62	*Eunotia* sp. 16	39	2.1	22	1.6	4	3.3
63	*Eunotia major* (W. Smith) Rabenhorst	53	2.1	15	2.3	9	7.1
64	*Eunotia pectinalis* (Dillwyn) Rabenhorst	47	2.3	19	2.5	9	5.6
65	*Eunotia rhynchocephala* Hustedt	29	2.8	24	2.5	25	22.1
66	*Eunotia satelles* (Nörpel & Lange-Bertalot) Nörpel & Lange-Bertalot	27	2.9	22	2.7	18	15.3
67	*Eunotia subarcuatoides* Alles, Nörpel & Lange-Bertalot	28	3.0	18	1.9	15	13.1
68	*Eunotia paludosa* var. *trinacria* (Krasske) Nörpel in Lange-Bertalot & Nörpel	64	1.5	8	1.7	5	4.4
69	*Fragilaria capucina* Desmazières	12	2.1	88	2.3	7	6.2
70	*Fragilaria acidobiontica* Charles	58	1.6	11	1.5	8	5.8
71	*Fragilaria brevistriata* Grunow in Van Heurck	15	2.4	88	2.5	25	16.9
72	*Fragilaria construens* var. *binodis* (Ehrenberg) Grunow	58	2.4	36	2.8	10	8.4
73	*Fragilaria* sp. [cf. *construens* var. *pumila* Grunow in Van Heurck]	39	3.0	47	2.2	16	11.3
74	*Fragilaria construens* (Ehrenberg) Grunow	11	1.9	92	2.7	23	15.7
75	*Fragilaria construens* var. *venter* (Ehrenberg) Grunow in Van Heurck	30	2.9	48	2.4	24	16.6
76	*Fragilaria constricta* Ehrenberg	24	3.0	18	2.1	18	14.9
77	*Fragilaria lapponica* Grunow (in Van Heurck)	8	1.8	134	3.2	7	6.4
78	*Fragilaria lata* (Cleve-Euler) Renberg	47	2.5	18	2.0	17	14.6
79	*Fragilaria oldenburgiana* Hustedt	28	2.8	18	1.8	15	12.3
80	*Fragilaria pinnata* var. *acuminata* A. Mayer	37	2.7	48	2.5	18	14.7
81	*Fragilaria pinnata* var. *lancettula* (Schumann) Hustedt in Schmidt et al.	62	2.2	40	2.4	11	9.2

© 2002 NRC Canada

Table B1 (*continued*).

	Taxon name	CLR optimum	CLR tolerance	ALK optimum	ALK tolerance	Occurrences	Hill's *N*2
82	*Fragilaria pinnata* Ehrenberg	18	2.9	68	2.7	39	29.2
83	*Fragilaria polygonata* Cleve-Euler	83	1.3	8	1.8	4	3.3
84	*Fragilaria pseudoconstruens* Marciniak	8	1.7	125	3.7	7	4.9
85	*Fragilaria vaucheriae* (Kützing) Petersen	16	1.6	97	2.2	2	1.7
86	*Fragilaria virescens* var. *exigua* Grunow in Van Heurck	23	3.1	34	2.3	52	42.9
87	*Frustulia* sp. [cf. *magaliesmontana* Cholnoky]	64	1.3	9	1.3	3	2.7
88	*Frustulia rhomboides* (Ehrenberg) De Toni	18	3.3	22	2.0	35	25.5
89	*Frustulia rhomboides* var. *saxonica* (Rabenhorst) De Toni	15	2.9	27	2.1	49	38.1
90	*Gomphonema parvulum* (Kützing) Kützing	20	2.7	48	2.2	10	8.7
91	*Melosira arentii* (Kolbe) Nagumo & Kobayasi	55	1.7	17	1.9	9	7.8
92	*Navicula absoluta* Hustedt	5	1.3	467	1.2	1	1.0
93	*Navicula agrestis* Hustedt	5	1.3	41	4.3	3	2.3
94	*Navicula arvensis* Hustedt	68	1.7	28	2.0	19	12.8
95	*Navicula* sp. [cf. *begerii* (Krasske) Krasske]	17	3.3	18	1.8	4	3.5
96	*Navicula bremensis* Hustedt	29	3.2	21	2.0	16	14.1
97	*Navicula bryophila* Petersen	11	2.0	64	1.9	15	12.7
98	*Navicula cocconeiformis* Gregory ex Greville	28	3.0	29	3.2	28	22.4
99	*Navicula disjuncta* Hustedt	34	2.5	34	2.8	9	8.1
100	*Navicula submolesta* Hustedt	5	1.3	39	1.7	4	3.4
101	*Navicula leptostriata* Jørgensen	18	3.0	34	2.5	48	43.0
102	*Navicula jaernefeltii* Hustedt	10	1.3	45	1.2	1	1.0
103	*Navicula krasskei* Hustedt	8	2.3	31	1.7	13	8.7
104	*Navicula kuelbsii* Lange-Bertalot in Lange-Bertalot & Krammer	8	1.5	42	1.2	2	1.7
105	*Navicula laevissima* Kützing	26	3.1	46	2.6	14	13.1
106	*Navicula digitulus* Hustedt	19	3.1	19	1.6	9	7.5
107	*Navicula mediocris* Krasske	17	2.9	30	2.2	41	35.8
108	*Navicula pseudoscutiformis* Hustedt	19	2.7	61	2.7	28	25.5
109	*Navicula pseudoventralis* Hustedt	46	8.9	45	2.5	2	1.8
110	*Navicula pupula* Kützing	19	3.1	38	3.0	24	21.1
111	*Navicula schmassmannii* Hustedt	22	3.2	31	2.4	28	23.7
112	*Navicula seminuloides* Hustedt	16	3.1	122	1.9	7	6.2
113	*Navicula seminulum* Grunow	7	1.6	51	2.8	9	8.1
114	*Navicula soehrensis* var. *hassiaca* (Krasske) Lange-Bertalot	41	2.7	16	2.4	15	12.6
115	*Navicula* sp. [cf. *submuralis* Hustedt]	8	1.9	294	2.3	3	2.5
116	*Navicula parasubtilissima* Kobayasi & Nagumo	11	2.8	27	2.0	35	28.2
117	*Navicula tenuicephala* Hustedt	31	2.7	17	1.7	12	8.0
118	*Navicula ventralis* Krasske	23	4.3	16	2.5	5	4.7
119	*Navicula vitiosa* Schimanski	18	2.9	75	2.3	32	25.7
120	*Nitzschia liebetruthii* Rabenhorst	9	1.9	84	2.7	7	6.7
121	*Nitzschia amphibia* Grunow	10	1.8	42	2.9	5	4.6
122	*Nitzschia* sp. [cf. *fonticola* Grunow in Van Heurck]	9	1.8	62	2.3	29	22.0
123	*Nitzschia hantzschiana* Rabenhorst	5	1.3	65	1.2	1	1.0
124	*Nitzschia perminuta* (Grunow) M. Peragallo	14	3.0	37	2.3	27	24.8
125	*Pinnularia* sp. [cf. *braunii* var. *amphicephala* (Grunow) Cleve]	14	3.1	18	1.9	8	7.1
126	*Pinnularia mesolepta* (Ehrenberg) W. Smith Morphotyp 3 sensu Krammer	11	2.5	40	2.2	44	34.4
127	*Pinnularia microstauron* (Ehrenberg) Cleve	10	2.4	39	2.4	23	19.7
128	*Pinnularia rupestris* Hantzsch in Rabenhorst	7	2.4	33	1.9	5	3.8
129	*Stauroneis anceps* Ehrenberg	19	2.9	33	2.3	34	31.0

© 2002 NRC Canada

Table B1 (*concluded*).

	Taxon name	CLR optimum	CLR tolerance	ALK optimum	ALK tolerance	Occurrences	Hill's *N*2
130	*Stenopterobia delicatissima* (Lewis) Brébisson ex Van Heurck	25	2.9	25	2.5	16	13.6
131	*Tabellaria flocculosa* (Roth) Kützing	18	2.8	37	2.5	55	41.6
132	*Tabellaria quadriseptata* Knudson	62	1.3	9	1.2	3	2.8

© 2002 NRC Canada

Effects of feeding on waterborne silver uptake and depuration in rainbow trout (*Oncorhynchus mykiss*)

Barbara O.B. Bertram and Richard C. Playle

Abstract: Rainbow trout (*Oncorhynchus mykiss*, ~50 g) were exposed to 0.1 μM $AgNO_3$ in ion-poor water (Ca ~300 μM, pH ~7, 13°C) with or without being fed 2% of their body weight daily. Gills, plasma, livers, and bile were sampled after 4 h, 24 h, and 1 week. Feeding did not alter Ag uptake by trout, and did not prevent decreases in plasma Na and Cl caused by Ag. To study Ag depuration, trout were exposed to 0.1 μM $AgNO_3$ for one week and then were placed in Ag-free, ion-poor water with or without being fed 1% of their body weight daily. Plasma Ag decreased over the 15-day depuration period (elimination rate, k_e = 0.085 day^{-1}), but there were no effects of feeding on Ag depuration. There were no physiological differences between fed and unfed fish except for slightly higher plasma glucose concentrations and higher condition factors in fed fish by the end of the Ag depuration period. Thus, once Ag has entered a fish, subsequent elimination (e.g., from the plasma) is not affected by food-related processes such as biliary excretion or increased metabolic rate, or by external factors like food debris in the water.

Résumé : Nous avons exposé des truites arc-en-ciel (*Oncorhynchus mykiss*, ~50 g) à jeun ou nourries d'une ration quotidienne équivalant à 2 % de leur masse à du $AgNO_3$ 0,1 μM dans de l'eau faiblement ionisée (Ca ~300 μM, pH ~7, 13°C). Nous avons fait des prélèvements de branchies, de plasma, de foie et de bile 4 h, 24 h et une semaine après l'exposition. L'alimentation n'affectait pas l'incorporation de l'Ag chez la truite et n'enrayait pas les chutes de Na et de Cl plasmatiques causées par l'Ag. Pour étudier la dépuration de l'Ag, nous avons exposé des truites à jeun ou nourries d'une ration quotidienne équivalant à 1 % de leur masse à du $AgNO_3$ 0,1 μM pendant une semaine, puis les avons placé dans de l'eau peu ionisée en l'absence d'Ag. L'Ag plasmatique a décru pendant les 15 h de la période de dépuration (k_e = 0,085 $jour^{-1}$) et l'alimentation est restée sans effet sur le processus. Il n'y avait pas de différences physiologiques entre les poissons nourris et les poissons à jeun, à l'exception de concentrations plasmatiques de glucose légèrement plus élevées et des coefficients d'embonpoint supérieurs chez les poissons nourris à la fin de la période de dépuration de l'Ag. Ainsi, une fois l'Ag incorporé dans le poisson, l'élimination subséquente (i.e. du plasma) n'était pas affectée par les processus alimentaires, tels que l'excrétion biliaire ou le taux accru de métabolisme, ni par les facteurs externes tels que la présence de débris de nourriture dans l'eau.

[Traduit par la Rédaction]

Introduction

Silver (Ag) is released into the aquatic environment through mining, industrial discharges, and in sewage (see review by Purcell and Peters 1998). Although usually at low concentrations in the aquatic environment, dissolved Ag interacts first with the gills of fish (Hogstrand and Wood 1998; Wood et al. 1999; Rose-Janes and Playle 2000). The acute toxic effects of dissolved Ag in freshwater fish are exhibited at the gills rather than internally, and result in a disruption of Na^+ and Cl^- transport. It is probably ionic Ag^+ that interacts at freshwater fish gills, where it enters a proton-coupled Na^+ channel at the apical surface (Bury and Wood 1999), then is transported actively across the basolateral membrane of the gills in an adenosine triphosphate (ATP)-dependent process (Bury et al. 1999*a*). Complexing agents in the water such as organic matter and chloride, and competing agents such as Ca^{2+}, Na^+, and Mg^{2+} decrease acute $AgNO_3$ toxicity to fish (e.g., Bury et al. 1999*b*; Karen et al. 1999; McGeer et al. 2000).

Metals like Ag are available to aquatic organisms through direct uptake across the gill epithelium, and also from food, which is taken up across the gut. It has been suggested that the pattern of metal distribution within the tissues of the fish reflects the route of metal uptake, where waterborne exposure results in gill metal accumulation and dietary exposure results in metal accumulation by the intestine (Köck et al. 1998). Freshwater fish continually lose plasma ions by diffusion to their hypotonic environment and gain water passively by osmosis; therefore, freshwater fish drink very little water (e.g., Wood et al. 1999, and references therein), resulting in little or no Ag reaching the intestine unless it is bound by or contained in food ingested by the fish. That is, the act of feeding may pose an additional route of metal uptake in freshwater fish. In addition, when a fish is feeding, bile is secreted into the intestine for the digestion of neutral lipids, and the act of digesting food may result in an additional

Received 11 April 2001. Accepted 12 December 2001. Published on the NRC Research Press Web site at http://cjfas.nrc.ca on 5 March 2002.
J16310

B.O.B. Bertram and R.C. Playle.[1] Department of Biology, Wilfrid Laurier University, Waterloo, ON N2L 3C5, Canada.

[1]Corresponding author (e-mail: rplayle@wlu.ca).

 DOI: 10.1139/F02-004 © 2002 NRC Canada

route of metal elimination through the biliary fecal route, aside from elimination through the urine and integument routes. Food may therefore act as either a sink or a source for a contaminant, which has practical implications as to whether organisms are fed during toxicity testing.

Although uptake and depuration studies have been undertaken with freshwater fish that have accumulated Ag from the water (Garnier et al. 1990) and from the diet (Garnier and Baudin 1990), the effect of feeding on uptake and depuration of waterborne Ag has not been studied. Feeding could conceivably have multiple effects on the uptake of a nonessential metal like Ag. For example, food in the water could complex Ag^+ so that less Ag^+ is available to be taken up at fish gills, reducing its uptake. Food in the water could also result in an additional intestinal route of uptake for waterborne Ag, increasing its uptake. Increased metabolic rate due to from digestive processes (specific dynamic action) could increase uptake of Ag at the gills as the fish passes more water over the gills to extract more oxygen, or increase uptake of Ag^+ by the gills as a consequence of a general increase in metabolic processes. Peak elevations of metabolic rate in fish after feeding are commonly two- to four-fold compared to prefeeding metabolic rates (Peck 1998). With regards to depuration, feeding would be expected to increase the elimination of a metal like Ag. For example, food and feces could act as complexing agents in the water to increase Ag elimination, specific dynamic action could increase Ag elimination through an increased volume of water passing over the gills and through increased metabolic processes, and the biliary fecal route could provide an additional route of Ag elimination.

Our first objective was to determine the effects of feeding on the accumulation of a nonessential metal from water. Rainbow trout (*Oncorhynchus mykiss*) were exposed to ~0.1 μM $AgNO_3$ for one week in ion-poor water, with or without being fed 2% of their body weight daily. Ion-poor (soft) water was used in these exposures, to maximize Ag uptake by the fish (e.g., Rose-Janes and Playle 2000). $AgNO_3$ at 0.1 μM is close to the 96-h LC50 value of trout in fresh water, and is much higher than Ag concentrations found even in sewage outfall and is in a more available form than, for example, silver sulphides and silver thiosulphates (Purcell and Peters 1998; Shafer et al. 1998; Bell and Kramer 1999); this concentration of Ag was necessary to ensure measurable Ag accumulation by the fish. Gills, plasma, liver, and bile were analyzed for Ag content, and plasma Na, Cl, and glucose (a stress indicator in fish) were analyzed to determine the extent of physiological impairment from the $AgNO_3$ exposure. Our second objective was to determine the influence of feeding on depuration of previously accumulated Ag, with the hypothesis that fed fish would lose Ag more quickly than unfed fish, for reasons given in the previous paragraph. Trout tissues have low background Ag concentrations and Ag analysis is sensitive, so Ag is an ideal metal to use to assess the effects of feeding on the uptake and depuration of nonessential metals accumulated from the water column.

Methods and materials

Fish holding and acclimation

Rainbow trout from 50 to 70 g in weight were obtained from Rainbow Springs Hatchery (Thamesford, Ont.) at least two weeks before the start of an experiment. Fish were housed according to guidelines set by the Canadian Council of Animal Care. Fish were held for at least one week in aerated well water (920 μM Na, 1402 μM Ca, pH 7.6, 14°C) and were fed ~5% of their body weight every other day with 3.0 pt Corey Aquaculture Trout and Charr grower (Corey Feed Mills Ltd., Fredericton, N.B.). This feed contained a minimum of 50% crude protein and 20% crude fat, a maximum of 2.5% crude fibre, 0.8% sodium, and 1.5% calcium. One week before an experiment, the trout were acclimated to ion-poor (soft) water supplied by a reverse osmosis system (Series E Reverse Osmosis System, Culligan, Oakville, Ont.). Water chemistry was 198 μM Cl, 195 μM Na, 312 μM Ca, pH 7.5, and 13.5°C. One week of acclimation to ion-poor water is sufficient in our laboratory, as indicated by stable physiology in control fish (see Results). Fish were not fed during soft water acclimation.

Uptake experiment

After the acclimation period, 35 fish were randomly assigned to each of four 60-L polyethylene Ag treatment containers. Control fish were exposed in a separate container to Ag-free soft water. All four containers for exposure to Ag were supplied from one head tank (3.5 mM stock $AgNO_3$ solution (Sigma) delivered by peristaltic pump and diluted with soft water to obtain 0.1 μM Ag, ~10.8 $\mu g \cdot L^{-1}$ Ag). Each container had a flow rate of 150 $mL \cdot min^{-1}$ of reverse osmosis water and all containers were aerated. Fish in two of these containers plus the control container were fed 2% of their total body weight per day (with Corey Aquaculture Trout and Charr grower); fish in the other two containers were not fed while being exposed to Ag. The fed fish were given food approximately 0.5 h after the Ag exposure began. Subsequently, the fish were fed at the same time each morning. Five fish per bucket were sampled after 4 h, 24 h, and 1 week of exposure. Note that the two Ag exposures (fed and unfed) were replicated but the fed control fish were not, because of water and space limitations.

Depuration experiment

For the Ag depuration experiment all fish except control fish were exposed for one week to Ag only (nominal 0.1 μM Ag) after one week of soft water acclimation as given above for the uptake experiment. Fish were not fed over the week-long Ag-loading period; because feeding had no effect on Ag uptake (see Results), fish fed or not fed during Ag loading would likely have similar Ag depuration (see Discussion). Note that by the first day of depuration, none of the fish had been fed for two weeks (1 week acclimation, 1 week Ag loading). At the end of one week, the Ag-loaded fish were randomized and transferred to four new 60-L containers supplied with Ag-free, ion-poor water at 150 $mL \cdot min^{-1}$ each. Fish in two of these depuration containers were fed 1% of their total body weight each afternoon of the depuration period; the other Ag-loaded fish were not fed. Control fish were fed 1% of their body weight per day; we did not have enough water and space to include starved controls. For this depuration study the feeding regimen was reduced to 1% feeding to decrease fouling of the water (see Results). Four control fish and two fish from each Ag

© 2002 NRC Canada

depuration container were sampled at the beginning of the depuration period (3–4 h after transfer) for reference. Thereafter, five fish from each of the four Ag depuration containers (two fed and two unfed), and five fish from the control container (fed) were sampled at 1, 2, 4, 6, and 8 days of Ag depuration; on day 15 all remaining fish were sampled.

Sampling procedures

For both the uptake and depuration experiments, fish were randomly sampled and placed individually into MS 222 anaesthetic for 5 min. Fish were weighed to the nearest 0.1 g and fork length was measured to the nearest mm. Condition factors were calculated according to Horn (1998):

$$\text{Condition factor} = \frac{\text{body weight (g)}}{[\text{fork length (cm)}]^3} \times 100$$

Blood (500–1000 μL) from anesthetised fish was drawn by caudal puncture using an ice cold, 1-mL Luerlock Hamilton syringe rinsed with heparinized saline (0.008 g heparin sodium salt (Sigma) to 25 mL Cortland saline). Twenty microlitres of blood was placed in 5 mL of Drabkin's reagent (Sigma) for later hemoglobin (Hb) analysis. For lactate analysis, 100 μL of blood was dispensed into a microcentrifuge tube with 200 μL of 8% perchloric acid (Baker analyzed Reagent, Phillipsburg, N.J.), refrigerated, and centrifuged. A portion of the blood was dispensed into two heparinized hematocrit tubes and spun for 5 min in a Readacrit centrifuge (Clay Adams, N.J.). Hematocrit (Ht) was calculated by dividing the packed cell length by the total sample length in the tube and is expressed as a percentage of total blood volume. Mean cell hemoglobin concentration (MCHC, in $g \cdot dL^{-1}$) was calculated by dividing Hb concentration by Ht. Remaining blood was dispensed into a microcentrifuge tube and spun with an IEC MicroMB Microcentrifuge (Needham Heights, Mass.) at 12 700 × *g* for 2 min. Plasma was removed and temporarily stored in a freezer at –20°C.

A portion of gill tissue was extracted from the second gill arch from the right side of each fish with stainless steel forceps and scissors. Gill samples were agitated for 15 s in 100 mL of reverse osmosis water to remove loosely bound Ag (e.g., Rose-Janes and Playle 2000; Schwartz and Playle 2001) and then placed into separate microcentrifuge tubes, labelled, and stored in the freezer. The liver of each fish was also removed with stainless steel forceps and scissors and rinsed in 100 mL of reverse osmosis water to remove any bile transferred from the gall bladder during sampling. The liver was placed into a 7-mL scintillation vial and stored temporarily in a freezer. The gall bladder was removed (whole if possible) and the bile was analyzed for Ag content. At the conclusion of the sampling period, whole blood, plasma, gill, and liver samples were removed from the –20°C freezer and placed in a –40°C freezer until later analysis.

Sample analysis

Gill samples were thawed, weighed, then heated in 1 M Ultrapure HNO_3 (5 times the tissue weight; Ultrex II Ultrapure HNO_3 Baker Analyzed reagent) for 3 h at 80°C in an oven. A 100-μL portion of each of the gill digest supernatant was placed into new microcentrifuge tubes and further diluted with 900 μL of ultrapure water, resulting in ~0.1 M HNO_3 solution. Portions of liver samples (60–100 mg) were prepared for analysis in the same manner as the gills. Plasma samples were thawed and diluted in the ratio of 50 μL plasma to 450 μL 0.1 M Ultrapure HNO_3. Bile was diluted in the ratio of 10 μL bile to 990 μL 0.1 N Ultrapure HNO_3. Gill, plasma, liver, bile, and water samples were analyzed for Ag content using a graphite furnace atomic absorption spectrophotometer (AAS, argon gas; Varian AA-1275 with GTA-95 atomizer, Mulgrave, Vic., Australia) using an Aldrich standard solution. Ten microlitres of each sample was injected, and the operating protocol for the samples as given by Varian was 5 s at 85°C, 30 s at 95°C, 10 s at 120°C, 8 s at 400°C, and 4.9 s at 2000°C, during the first 2.9 s of which the absorbance at 328.1 nm was measured.

Water pH was measured using a PHM82 pH meter (Bach-Simpson Ltd., London, Ontario) with GK2401C combination electrode. Water samples were taken in combusted borosilicate vials (4 h at 450°C) for total organic carbon (TOC) content analysis on a Shimadzu Total Carbon Analyzer (TOC-5050A; Mandel Scientific Co. Ltd., Guelph, Ont.). Water samples were also taken in two 7-mL scintillation vials for Na, Ca, Cl, and Ag analysis, were acidified using two drops of 16 M Ultrapure HNO_3, and were stored at 4°C until analysis. Water and plasma samples were analyzed for Ca and Na content by flame AAS using a Perkin-Elmer model 3100 (Norwalk, Conn.). Samples analyzed for Ca (1 mL) had 20 μL of $LaCl_3$ added to reduce phosphate interference.

Blood lactate was measured enzymatically (lactate dehydrogenase – NADH, Sigma kit #826-B). Plasma glucose was also measured enzymatically (hexokinase glucose-6-phosphate dehydrogenase; Sigma kit #16-20). Hemoglobin was measured colourimetrically by a cyanmethemoglobin method with 20-μL aliquots of whole blood (Sigma kit #525-A). Water and plasma Cl were measured using a mercuric-thiocyanate method (Sigma-Aldrich kit #461-M).

Data presentation and statistical analyses

Statistical analysis of the data was done using the SigmaStat statistical program (DOS version 1.03, Jandel Scientific, San Rafael, Calif.). Chi-square analysis with Yates correction was used to compare fish mortalities. Comparisons of treatments at one sampling time consisted of one-way analysis of variance (ANOVA) followed by the Student–Newman–Keuls method of pairwise comparison or by the nonparametric Kruskal–Wallis one-way ANOVA on ranks when the normality test failed in the ANOVA analysis. For all figures, the mean plus one standard deviation are given. Asterisks indicate significant differences between fed or unfed Ag treatment groups compared with the control group at that sampling time. Crosses indicate a difference between fed or unfed Ag treatment groups at that time. Significant differences are indicated by one, two, and three symbols for $P < 0.05$, $P < 0.01$, and $P < 0.001$, respectively.

Results

Uptake experiment

In the Ag uptake experiment, both fed and unfed fish were exposed to an average of 0.11 μM Ag added as $AgNO_3$ (Table 1). The silver exposures resulted in 0% mortality in fish exposed to Ag with feeding (0 of 58 fish) and significantly

© 2002 NRC Canada

Table 1. Chemical characteristics of ion-poor water alone (fed control fish), ion-poor water containing $AgNO_3$ (unfed fish), and ion-poor water containing $AgNO_3$ (fish fed 2% of their body weight per day) during the Ag uptake experiment.

	Control (Fed)	Ag Only	Ag plus feeding
Ag	0.008 ± 0.001 (8)	0.118 ± 0.151 (14)	0.095 ± 0.120 (14)
TOC	7.4 ± 4.7 (4)	2.8 ± 0.9 (8)	5.5 ± 2.6 (8)
Cl	306 ± 134 (8)	91 ± 90 (16)	138 ± 88 (15)
Na	220 ± 83 (10)	199 ± 39 (19)	209 ± 30 (19)
Ca	384 ± 163 (11)	218 ± 182 (19)	200 ± 124 (17)
pH	6.9 ± 0.2 (3)	7.2 ± 0.2 (6)	7.2 ± 0.3 (5)
Temperature	13.0 ± 1.4 (3)	13.0 ± 1.2 (6)	13.0 ± 1.2 (6)

Note: Silver, Cl, Na, and Ca concentrations are in μM, and total organic carbon (TOC) concentrations are in mg $C \cdot L^{-1}$. Temperature is in°C, and all values are means ±1 standard deviation (*n*).

higher mortality (10%) in fish exposed to Ag without feeding (6 of 61 fish; $P = 0.042$). There was no mortality in control fish until day 6 when a blocked airline caused 6 of 29 fish (21%) to die. The fed control and fed Ag-exposed groups had higher water TOC concentrations than the unfed treatment (Table 1) because of the added food. Our measured water Ag concentrations fluctuated even in our flow-through system, a common problem with Ag because of its propensity to adsorb to container walls and other surfaces (e.g., Garnier et al. 1990).

Fish exposed to Ag with or without daily feedings of 2% of their body weight accumulated Ag in the gills, plasma, liver, and bile. Fish exposed to Ag had significantly more Ag on or in their gills than control fish at each sampling time (Fig. 1*a*). Plasma and liver Ag concentrations were also usually significantly greater in both fed and unfed fish exposed to Ag when compared with control fish (Figs. 1*b*, 1*c*). There was no significant accumulation of Ag in the bile in either fed or unfed fish exposed to Ag until the 1-week sampling time (Fig. 1*d*). We observed that fed fish generally had smaller gall bladders than unfed fish. There were no significant differences in gill, plasma, liver, or bile Ag concentrations between the fed and unfed Ag-exposed fish at any sampling time.

Plasma Na and Cl concentrations were significantly lower at one week in both fed and unfed Ag exposed fish compared with control fish (Figs. 2*a*, 2*b*). There were no significant changes in plasma Ca concentrations between control fish and fish from either Ag exposure treatment; these values ranged from 1.2 to 1.8 mM (data not presented; see Bertram 2000 for details). There were no significant differences in plasma Cl, Na, or Ca concentrations between fed or unfed fish exposed to Ag. A significant difference in plasma glucose concentration occurred at 24 h between fed fish exposed to Ag and control fish (Fig. 2*c*). Fish in both Ag exposures had higher but variable plasma glucose concentrations at 1 week when compared with control fish. There were no significant differences in blood Hb, Ht, and MCHC between control fish and fish from either Ag exposure or between fed and unfed Ag-exposed fish at any of the sampling times (data not presented; see Bertram 2000 for details). The only significant difference in blood lactate was due to the blocked airline in the control tank on day 6 (details in Bertram 2000).

The average condition factor at the end of one week for fed control fish was 1.03 ± 0.07 (±1 standard deviation, $n = 5$), for fed Ag-exposed fish it was 1.00 ± 0.11 (10), and for unfed Ag-exposed fish the average condition factor was 1.08 ± 0.29 (10), with no significant differences between them.

Depuration experiment

Fish were exposed to 0.06-μM waterborne $AgNO_3$ for one week (Table 2) before being randomized and placed into the fed and unfed depuration treatments. Water TOC concentrations in this experiment were lower than those in the uptake experiment, because we reduced the daily feeding regimen to 1% of their body weight to reduce fouling of the water tanks. There was 0% mortality observed during the one-week Ag loading period. During the 15-day depuration period, 3% mortality occurred in control fish (1 of 35 fish), 7% mortality was seen in the unfed Ag depuration fish (5 of 73 fish), and 0% mortality was seen in the fed Ag depuration fish (0 of 64 fish). These mortalities were not significantly different ($P = 0.091$).

Trout exposed to Ag for one week usually had higher concentrations of Ag in the gills, plasma, liver, and bile during the depuration period compared with control fish, with only infrequent differences between the fed and unfed fish depurating Ag. Gill Ag concentrations remained elevated in the Ag-exposed fish, with no decrease in Ag concentrations over 15 days (Fig. 3*a*). Fish depurating Ag with or without feeding usually had higher plasma Ag concentrations compared with control fish until day 8 of the depuration period (Fig. 3*b*). Plasma Ag concentrations in the fed and unfed fish depurating Ag were significantly different from one another only on day 6 of depuration (cross, Fig. 3*b*).

There was some indication of an increase in liver Ag concentrations during the first day of the depuration period in Ag-exposed fish. Otherwise, liver Ag concentrations were consistently higher than control values with no evidence of Ag depuration over 15 days (Fig. 3*c*). There were no significant differences between fed and unfed fish liver Ag concentrations at any of the sampling times. Bile Ag concentrations of trout previously exposed to Ag were generally higher than control values, although not always statistically greater (Fig. 3*d*). There was little evidence of Ag depuration from the bile of the Ag-exposed fish. On days 2 and 6 there were no bile samples from the fed control fish because their gall bladders were too empty to retrieve the 10-μL bile sample needed for the assay. Usually, unfed Ag-exposed fish had full gall bladders, and the fed Ag-exposed fish had gall blad-

© 2002 NRC Canada

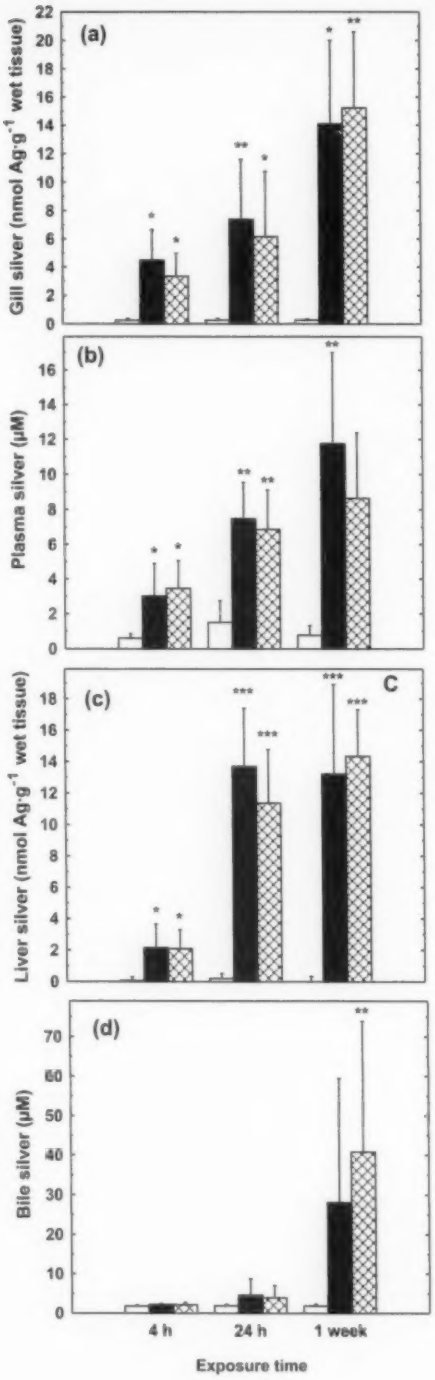

Fig. 1. (*a*) Gill, (*b*) plasma, (*c*) liver, and (*d*) bile Ag concentrations of trout exposed to 0.11 μM waterborne Ag with or without feeding (2% body weight per day). Grouped from left to right, bars represent the mean ±1 standard deviation of fish sampled after an exposure of 4 h, 24 h, and one week to the fed control (open bars), silver only (solid bars), or silver plus feeding treatments (hatched bars). Asterisks represent significant differences between the exposure treatment and control at that sampling time (*$P < 0.05$; **$P < 0.01$; ***$P < 0.001$). Control bars represent five fed fish sampled from one container; Ag only bars and Ag with feeding bars each represent 10 fish, five sampled from each replicate container.

ders that ranged from mostly full to almost empty. The only significant difference between fed and unfed fish depurating Ag was on day 6, when the unfed fish had higher bile Ag concentrations than fish being fed (Fig. 3*d*).

At the start of the Ag depuration phase, both groups of fish exposed to Ag for seven days had lower plasma Cl concentrations than control fish. However, following one day in Ag-free water, plasma Cl concentrations returned to control levels (Fig. 4*a*). There were no significant differences between treatments for plasma Na, and only one significant difference for plasma Ca (data not presented; see Bertram 2000 for details). Generally, during the first six days of depuration both groups of fish previously exposed to Ag had elevated plasma glucose concentrations compared with control fish, but there were not always statistical differences (Fig. 4*b*). There were no significant differences in plasma glucose between fed and unfed fish depurating Ag except on day 15, when the unfed fish had lower plasma glucose than either group of fed fish. There were no differences in blood Hb, Ht, MCHC, or lactate between control fish and fish from either Ag depuration treatment at any of the sampling times. The only exception occurred on day 1 when fish fed during depuration had significantly higher blood Ht than unfed fish (47 ± 7% (10) versus 39 ± 6% (10); for details see Bertram 2000). We have no explanation for this higher average; usual Ht values in this experiment were ~40%.

Fish not fed during the depuration period had a significantly lower average condition factor than control fish on day 6 and day 15, and had a significantly lower condition factor than fish being fed while depurating Ag on day 15 (Fig. 4*c*). Fish previously exposed to Ag and fed during depuration also had lower condition factors than control fish on day 6 and day 15. On day 15 the control fish weighed 76.9 ± 7.3 g and averaged 18.9 ± 0.5 cm (5) in length, the fed fish depurating Ag were 72.3 ± 28.6 g and 18.7 ± 2.2 cm (13) long, and the unfed fish depurating Ag weighed 45.7 ± 14.5 g and were 16.8 ± 1.8 cm (10) long. These unfed fish lost weight and weighed significantly less on day 15 than the fed fish that gained weight, but the unfed fish were not significantly shorter.

Depuration kinetics for plasma

The gills, plasma, liver, and bile all accumulated Ag during the one-week loading period (Fig. 3), but only the plasma lost Ag during the 15-day depuration period (Fig. 3*b*) and is therefore amenable to elimination rate analysis. To mathematically model the concentration of a contaminant in a first-order one-compartment model (assumed here for plasma), the elimination rate (k_e) of the contaminant is determined first from depuration data (Wicklund et al. 1990; Hickie et al. 1995; Newman 1998). The linear regression of the natural log values of the concentration in a compartment

© 2002 NRC Canada

Fig. 2. Plasma (*a*) Na, (*b*) Cl, and (*c*) glucose concentrations from trout exposed to 0.11 μM Ag with or without daily 2% body weight feeding. Open bars represent fed control fish, solid bars represent fish exposed to Ag but not fed, and hatched bars represent fish exposed to Ag while being fed. Refer to Fig. 1 caption and Results section for further details.

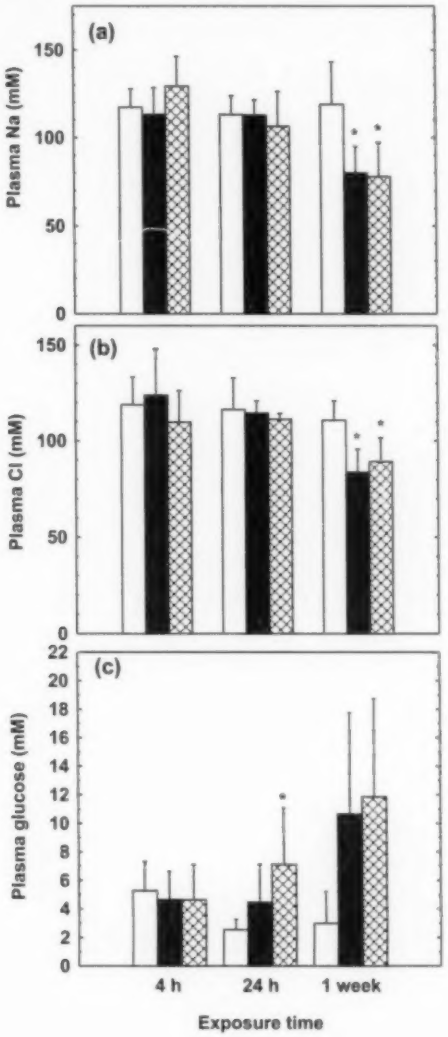

over time yields a slope that is $-k_e$. The elimination rate for Ag in the plasma compartment (all data considered) is 0.085 day^{-1} (Fig. 5*a*), a biological half-life of 8.2 days (e.g., $t_{1/2} = 0.693/k_e$).

The k_e value of 0.085 day^{-1} was used to fit an elimination curve to the plasma Ag depuration data. The elimination of a contaminant from a compartment can be calculated by the formula

$$C_t = C_0 e^{-k_e t}$$

where C_t is the contaminant concentration in the compartment of interest at any time (t) during depuration, C_0 is the initial concentration of the contaminant in the compartment at the beginning of the depuration period, and k_e is the rate constant describing the elimination of the contaminant. For C_0, we used the mean plasma Ag concentration at the beginning of the depuration period (3.1 μM) because there was no significant difference between the two sets of Ag-exposed fish that had been randomly assigned to the two treatments (Fig. 3*b*). The calculated elimination curve for the combined depuration plasma Ag data is given in Fig. 5*b*.

Discussion

We used silver to determine the effects of feeding on the uptake of a nonessential metal from the water column by fish, and to study the effects of feeding on the depuration of a nonessential metal previously accumulated from the water column. Feeding could have multiple effects on metal uptake, but the uptake of Ag by trout was not affected by feeding. We hypothesized that feeding fish would increase the elimination of previously accumulated metal through complementary processes, but feeding had no effect on Ag depuration by trout. The Ag uptake and elimination experiments are discussed separately below.

Effects of feeding on waterborne Ag uptake

Feeding rainbow trout 2% of their body weight per day did not affect the accumulation of waterborne Ag by the gills, plasma, livers, and bile of fish exposed to 0.1 μM $AgNO_3$ in ion-poor water for one week. There are a number of explanations for these results. First, Ag speciation in the water may not have been substantially affected by the increased organic material in the water from food and feces, so that similar amounts of Ag^+ were available to interact at the gills. Second, complexation of some Ag^+ in the water by organic matter could have been countered by an increased flow of water (and therefore Ag^+) past the gills to satisfy the increased metabolic rate caused by specific dynamic action, so that net Ag^+ uptake at the gills was unchanged; a general increase in metabolic processes would produce the same result. Third, organic matter in the water could have bound some cationic Ag^+, but the ingestion of food with its Ag burden could have resulted in Ag uptake at the intestine to replace Ag that would otherwise have been taken up at the gills. Fourth, Ag could have been excreted in the bile in fed fish but was subsequently reabsorbed by the intestine instead of being eliminated in the feces (e.g., enterohepatic circuit; St. Pierre et al. 2001). We favour the first explanation because the physiological effects of the $AgNO_3$ exposures were not reduced by feeding, indicating similar amounts of Ag^+ interacting at the gills.

In our exposures, the significant decreases in plasma Na and Cl at the end of the one-week Ag exposure were not prevented by feeding. This suggests that the presence of more organic matter in the water had little effect on Ag speciation in the exposure water and subsequent Ag uptake at the gills. Alternatively, if complexation of some Ag^+ did occur, it could have been countered by the increased metabolic rate of specific dynamic action (the second explanation in the previous paragraph). Waterborne Ag^+ acts on the gills to cause disruptions of ionoregulation (Wood et al. 1996*a*, 1999), whereas Ag accumulated by fish through the diet ap-

© 2002 NRC Canada

Table 2. Chemical characteristics of control conditions and exposures of trout to Ag in ion-poor water for one week (Ag loading), plus water characteristics during depuration of Ag from fish held in ion-poor water only and from fish held in ion poor water and fed 1% of their body weight daily.

	Ag loading		Ag depuration		
	Control	Ag exposure	Control	Not fed	Fed
Ag	0.002 ± 0.001 (7)	0.060 ± 0.069 (18)	0.000 ± 0.001 (13)	0.000 ± 0.001 (26)	0.000 ± 0.001 (25)
TOC	4.0 ± 1.4 (2)	3.0 ± 1.8 (7)	1.9 ± 0.3 (5)	1.4 ± 0.3 (10)	3.0 ± 0.8 (10)
Cl	220 ± 60 (5)	42 ± 30 (13)	102 ± 56 (11)	77 ± 85 (17)	87 ± 82 (17)
Na	166 ± 20 (5)	167 ± 14 (18)	179 ± 8 (10)	176 ± 34 (20)	205 ± 182 (20)
Ca	232 ± 18 (5)	128 ± 57 (20)	232 ± 92 (7)	146 ± 78 (18)	147 ± 62 (17)
pH	7.1 ± 0.1 (2)	7.1 ± 0.4 (8)	7.2 ± 0.1 (2)	7.2 ± 0.3 (6)	7.1 ± 0.2 (6)
Temperature	15.3 ± 1.4 (3)	15.4 ± 1.2 (12)	14.0 ± 0.2 (6)	14.1 ± 0.2 (13)	14.2 ± 0.3 (14)

Note: Silver, Cl, Na, and Ca concentrations are in μM, and total organic carbon (TOC) concentrations are in mg $C \cdot L^{-1}$. Temperature is in °C, and all values are means ±1 standard deviation (*n*).

pears to be physiologically benign (Galvez and Wood 1999; Galvez et al. 2001). Decreases in plasma ions in response to $AgNO_3$ exposures have been seen by us and by others, and these effects are eliminated if the concentration of Ag^+ complexing agents in the water are high enough (e.g., thiosulphate, organic matter; Wood et al. 1996*a*, 1996*b*). Previously, we needed 24–35 mg $C \cdot L^{-1}$ TOC (added as Aldrich humic acid) to keep ~0.1 μM $AgNO_3$ off of trout gills over four days (Rose-Janes and Playle 2000) because although Ag binds strongly to organic matter, it also binds strongly to the gills and therefore can saturate Ag uptake sites at the gills (McGeer et al. 2000).

In previous feeding studies, the protective effect of feeding against Ag toxicity to fathead minnows (*Pimephales promelas*) was attributed to the complexing ability of the food to tie up Ag from the water column (Erickson et al. 1998). A similar effect was found for static versus flow-through tests; in both these cases where Ag toxicity was decreased there was an increase in TOC of the water of about 1 mg $C \cdot L^{-1}$ (Erickson et al. 1998). These workers also saw greatly reduced Ag toxicity in fish and *Daphnia magna* exposed to $AgNO_3$ in St. Louis River water, with TOC of 18.5 mg $C \cdot L^{-1}$, versus 1.5 mg $C \cdot L^{-1}$ in their lab water. In our study, trout exposed to 0.1 μM $AgNO_3$ without feeding had 10% mortality but 0% mortality when fed, although Ag uptake at the gills and in other compartments was not affected by feeding. Pelgrom et al. (1994) found that fed tilapia (*Oreochromis mossambicus*) took up less waterborne Cu than did unfed fish, but there was no difference in uptake for waterborne Cd. Complexation of waterborne Cu but not Cd by organic matter in the water may be the explanation for their results, because organic matter binds Cu better than Cd (e.g., Richards et al. 1999).

There was fast accumulation of Ag by the gills and plasma, slower accumulation of Ag by the liver, and even slower Ag accumulation in the bile, with no significant accumulation of Ag in the bile until the 1 week sampling time. Fed fish generally had smaller gall bladders than unfed fish, indicating that bile was being secreted by these fish into the gut to aid digestion. Secretion of Ag-laden bile, however, had no effect on Ag accumulation by the liver or the Ag concentrations in the plasma or gills of the fish. Silver released in the bile could have been taken up again in the intestine instead of being excreted in the feces, but the existence of this type of "short circuit" cannot be determined from our data. It is also possible that the fish exposed to Ag had suppressed appetites (e.g., Wood et al. 1999). Although we did not quantify the amount of food eaten by the fish, condition factors of the fish did not differ, which suggests that differences in feeding rate were not important.

Effects of feeding on Ag depuration

As with Ag uptake, feeding fish 1% of their body weight per day had no effect on Ag elimination from the gills, plasma, liver, or bile over the 15-day depuration period. We hypothesized that fed fish would eliminate Ag faster than unfed fish because of food and feces in water complexing Ag, increased Ag elimination from specific dynamic action, and elimination of Ag in the bile. If fish eliminated Ag through bile, an increased Ag depuration rate from the liver would be expected, but this was not the case: even though fed fish generally had less bile in their gall bladders, there was no change in liver Ag concentrations. There remains the possibility that Ag released in the bile was taken up again in the intestine instead of being excreted in feces, but we cannot tell from our data.

Plasma Ag had a biological half-life of 8.2 days, and the continuous decrease in plasma Ag in fed and unfed fish depurating Ag was most likely attributed to the transport of Ag from the plasma to other tissues, such as the liver (Wood et al. 1996*a*). Gill, liver, and bile Ag in both groups of Ag-exposed fish showed no decrease in Ag concentrations over the 15-day depuration period; longer depuration studies are necessary to study elimination from these compartments that bind Ag relatively tightly. Silver induces the production of metallothionein in fish liver and gills (Hogstrand et al. 1996); therefore, it is not surprising that we did not detect elimination of Ag from these tissues in two weeks (see also Garnier et al. 1990, below). However, our sampling protocol would have missed very fast elimination of Ag from the plasma and gills, if it was ongoing, owing to the 3-h delay between transfer of fish to Ag-free water and the first sampling time. The transient nature of gill Ag burdens is illustrated well in fig. 4 of the review by Wood et al. (1999), where gill Ag concentrations could decrease by half in 2 h. Carbonell and Tarazona (1994) found an extremely fast elimination half-life (7.2 min) from the plasma for an intravenous injection of $CuSO_4$ into rainbow trout, followed by a slower but still rapid elimination half life of 195.5 min (3.3 h). Presumably this plasma Cu was going to nonex-

© 2002 NRC Canada

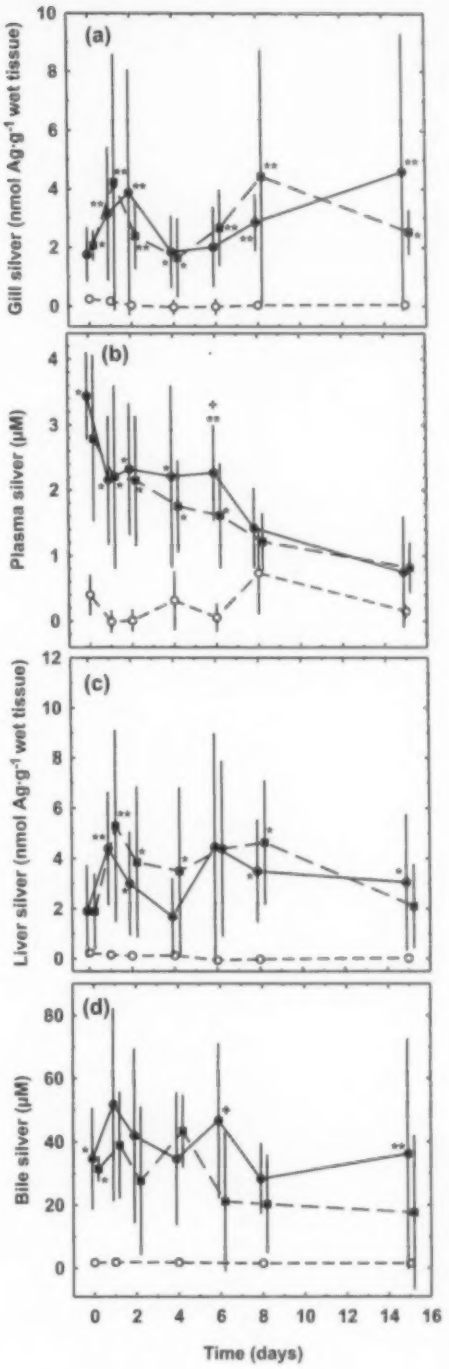

Fig. 3. (*a*) Gill, (*b*) plasma, (*c*) liver, and (*d*) bile Ag concentrations of trout exposed for one week to 0.06 μM waterborne Ag then placed in Ag-free water with or without feeding (1% body weight per day). Symbols have been offset horizontally where necessary for clarity. Asterisks represent significant differences between the depuration treatments and fed control fish at that sampling time and crosses represent significant differences between the two depuration treatments. At the start of depuration (day 0), control symbols (○) represent four fed fish sampled from one container (±1 standard deviation), and the depuration only (●) and depuration with feeding (■) symbols each represent four fish, two sampled from each replicate container. After day 0, control symbols represent five fish at each sampling time, and the Ag depuration symbols represent 10 fish each (five from each replicate container), except on day 15 when 13 fed fish depurating Ag were sampled.

changeable pools within the fish, such as the liver and kidneys, which have been shown to accumulate metals from more exchangeable pools during depuration of metals, as was found for Ag (Garnier and Baudin 1990; Garnier et al. 1990 (below); some indication in our study) and for Cd (Harrison and Klaverkamp 1989; Wicklund et al. 1990; Thomann et al. 1997).

Garnier et al. (1990) exposed fingerling brown trout (*Salmo trutta* L.) to waterborne ^{110m}Ag for 57 days and followed its depuration for 28 days; the fish were fed ~1% of their body mass per day throughout. At the end of the uptake period, approximately 70% of the ^{110m}Ag was in the liver, although the liver was ~1.5% of brown trout body mass (Garnier et al. 1990). The gills contained about 2% of the ^{110m}Ag and represented about 4% of fish mass. These workers could not calculate a ^{110m}Ag elimination rate for their fish, because the total amount of ^{110m}Ag was not significantly different at the end of the 28-day depuration phase compared to the beginning. Garnier et al. (1990) concluded that strong binding of Ag to sulphur ligands in proteins like metallothionein in the gill, digestive tract, and especially the liver prevented Ag elimination, although biological (growth) dilution did occur. Similarly, Garnier and Baudin (1990) demonstrated that ^{110m}Ag accumulated from food given to brown trout over 34 days remained in the trout even after a 27-day depuration period, which agrees with our results for the gills, liver, and bile. These workers showed that the fish retained ~90% of the initial Ag accumulation by the end of the depuration period; 63% of the ^{110m}Ag was stored within the liver, increasing to 79% of the ^{110m}Ag load after the 27-day depuration period (not a significant increase). Gill Ag accounted for ~1% of the total body content of fish fed ^{110m}Ag-loaded food, and the gills represented ~4% of fish mass; there was no change in gill ^{110m}Ag after 27 days of depuration aside from growth dilution (Garnier and Baudin 1990).

Garnier and Baudin (1990) used a simplified model of simultaneous ^{110m}Ag transfer from water and food to trout, and calculated that the uptake of ^{110m}Ag from water would predominate during the first 13 days, after which the food route would predominate. In another study, the half-life of ingested ^{110m}Ag in viscera of five female American plaice (*Hippoglossoides platessoides*) ranged from 13 to 102 days, with a mean of 48 days (Rouleau et al. 2000); these workers concluded that the hepatobiliary pathway was the main route for Ag excretion, since ^{110m}Ag obtained in the diet was relocated to the liver and bile from other tissues during depuration. From our results, a recent model of the effects of silver/hydrogen peroxide (Ag^+/H_2O_2) residual disinfectant in drinking water does not need to consider whether fish were

© 2002 NRC Canada

Fig. 4. Plasma (*a*) Cl, (*b*) glucose concentrations, and (*c*) condition factors from trout exposed for one week to 0.06-μM Ag then placed in Ag-free water with or without daily 1% body weight feeding. ○, fed control fish; ●, fish depurating Ag but not fed; ■, fish depurating Ag while being fed. Refer to Fig. 3 caption and Results section for more details.

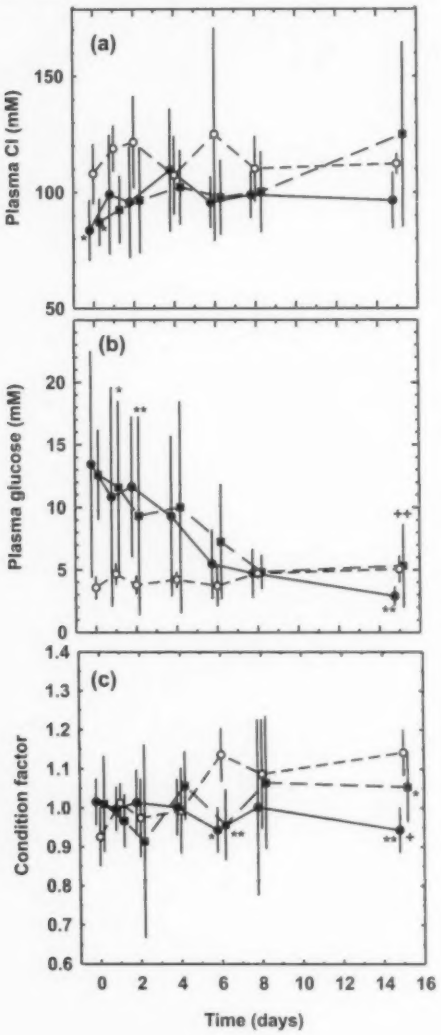

fed during the development of the elimination rates used in the model (Warila et al. 2001).

By the end of the 15-day depuration period, our unfed fish depurating Ag had a lower condition factor than fed fish depurating Ag and fed control fish. These fish had not been fed for a total of one month by the end of the depuration period. The relatively long period of food deprivation could have affected the biochemical composition of the tissues, changed the size of internal organs, and influenced the turnover rate of different tissues (O'Connor et al. 2000), but even so, did not influence the elimination of accumulated Ag or significantly affect fish mortality. By the end of the 15-day depuration period, fed control fish had higher condition factors compared to fed fish depurating Ag. That is, fed control fish were able to convert more energy towards growth because they did not have to deal with stress caused by the Ag exposure (e.g., low plasma Cl and high glucose concentrations). Alternatively, the appetites of the fish previously exposed to Ag were reduced compared with the fed control fish; we did not quantify the amount of food eaten by the fish.

Fig. 5. (*a*) Linear regression of the natural log values of the combined plasma Ag concentrations of fed (■) and unfed (●) fish depurating Ag from day 0 to 15 of the depuration period. The slope of the line is –0.085 with a correlation coefficient (r) of 0.974 ($P < 0.001$); 95% confidence intervals are shown. (*b*) Calculated plasma Ag elimination (thick solid line) for the depuration period, determined using the elimination rate of –0.085 day^{-1} from the linear regression of the combined plasma Ag data. ○, control values. See Results for details.

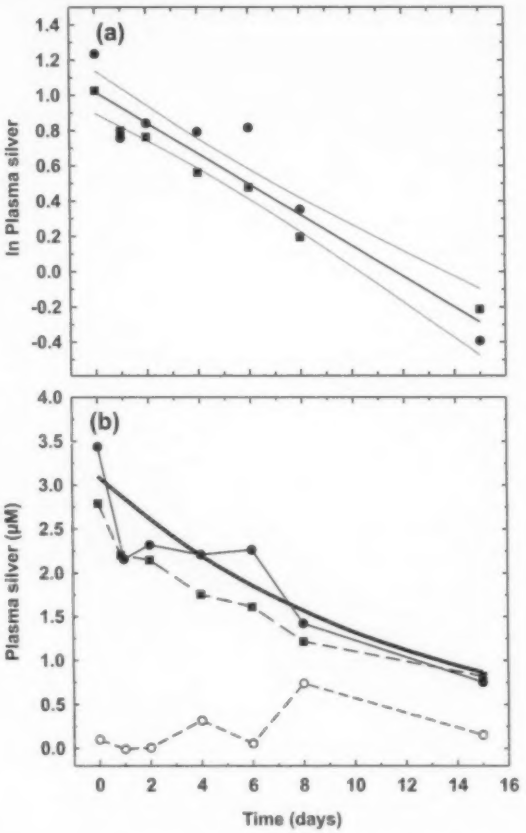

In summary, feeding rainbow trout 2% of their body weight daily had no effect on the amount of Ag accumulating over one week in the gills, plasma, liver, or bile. Feeding also had no effect on the physiological disturbances caused by the Ag exposure (e.g., decreased plasma Na and Cl concentrations), although fish survival was better. Feeding trout 1% of their body weight daily during a 15-day Ag depuration period had no effect on the elimination of previously accumulated Ag from the gills, plasma, livers, or bile, but fed fish had higher

© 2002 NRC Canada

condition factors. Plasma Ag concentrations decreased once the Ag exposure ended, with a biological half-life of 8.2 days, whereas the gills, liver, and bile showed no decrease in Ag over two weeks. The biliary fecal route of elimination, organic matter in water, specific dynamic action, or other physiological or physical factors related to feeding did not increase Ag elimination from the fish.

Acknowledgements

Nancy Rose-Janes and Stephanie Farwell are thanked for their laboratory assistance. This work was funded by Kodak Canada Inc., by matching funding from the Natural Science and Engineering Research Council of Canada (NSERC) Industrially Oriented Research Program, and by Wilfrid Laurier University.

References

Bell, R.A., and Kramer, J.R. 1999. Structural chemistry and geochemistry of silver–sulfur compounds: a critical review. Environ. Toxicol. Chem. **18**: 9–22.

Bertram, B. 2000. Modifying effects of dissolved organic matter, thiosulphate, chloride, and feeding on silver uptake and depuration in rainbow trout (*Oncorhynchus mykiss*). M.Sc. thesis, University of Waterloo, Waterloo, Ont., Canada.

Bury, N.R., and Wood, C.M. 1999. Mechanism of branchial apical silver uptake by rainbow trout is via the proton-coupled Na^+ channel. Am. J. Physiol. **277**: (Regulatory Integrative Comp. Physiol. **46**): R1385–R1391.

Bury, N.R., Grosell, M., Grover, A.K., and Wood, C.M. 1999*a*. ATP-dependent silver transport across the basolateral membrane of rainbow trout gills. Toxicol. Appl. Pharmacol. **159**: 1–8.

Bury, N.R., Galvez, F., and Wood, C.M. 1999*b*. Effects of chloride, calcium, and dissolved organic carbon on silver toxicity: comparison between rainbow trout and fathead minnows. Environ. Toxicol. Chem. **18**: 56–62.

Carbonell, G., and Tarazona, J.V. 1994. Toxicokinetics of copper in rainbow trout (*Oncorhynchus mykiss*). Aquat. Toxicol. **29**: 213–221.

Erickson, R., Brooke, L., Kahl, M., Vende Vender, F., Harting, S., Markee, T., and Spehar, R. 1998. Effects of laboratory test conditions on the toxicity of silver to aquatic organisms. Environ. Toxicol. Chem. **17**: 572–578.

Galvez, F., and Wood, C.M. 1999. Physiological effects of dietary silver sulfide exposure in rainbow trout. Environ. Toxicol. Chem. **18**: 84–88.

Galvez, F., Hogstrand, C., McGeer, J.C., and Wood, C.M. 2001. The physiological effects of a biologically incorporated silver diet in rianbow trout (*Oncorhynchus mykiss*). Aquat. Toxicol. **55**: 95–112.

Garnier, J., and Baudin, J. 1990. Retention of ingested ^{110m}Ag by a freshwater fish, *Salmo trutta* L. Water Air Soil Pollut. **50**: 409–421.

Garnier, J., Baudin, J.P., and Foulquier, L. 1990. Accumulation from water and depuration of ^{110m}Ag by a freshwater fish, *Salmo trutta* L. Water Res. **24**: 1407–1414.

Harrison, S.E., and Klaverkamp, J.F. 1989. Uptake, elimination and tissue distribution of dietary and aqueous cadmium by rainbow trout (*Salmo gairdneri* Richardson) and lake whitefish (*Coregonus clupeaformis* Mitchell). Environ. Toxicol. Chem. **8**: 87–97.

Hickie, B.E., McCarty, L.S., and Dixon, D.G. 1995. A residue-based toxicokinetic model for pulse-exposure toxicity in aquatic systems. Environ. Toxicol. Chem. **14**: 2187–2197.

Hogstrand, C., and Wood, C.M. 1998. Toward a better understanding of the bioavailability, physiology and toxicity of silver in fish: implications for water quality criteria. Environ. Toxicol. Chem. **17**: 567–561.

Hogstrand, C., Galvez, F., and Wood, C.M. 1996. Toxicity, silver accumulation and metallothionein induction in freshwater rainbow trout during exposure to different silver salts. Environ. Toxicol. Chem. **15**: 1102–1108.

Horn, M.H. 1998. Feeding and digestion. *In* The Physiology of fishes. 2nd ed. *Edited by* D.H. Evans. CRC Press, New York. pp. 43–63.

Karen, D.J., Ownby, D.R., Forsythe, B.L., Bills, T.P., La Point, T.W., Cobb, G.B., and Klaine, S.J. 1999. Influence of water quality on silver toxicity to rainbow trout (*Oncorhynchus mykiss*), fathead minnows (*Pimephales promelas*), and water fleas (*Daphnia magna*). Environ. Toxicol. Chem. **18**: 63–70.

Köck, G., Triendl, M., and Hofer, R. 1998. Lead (Pb) in artic char (*Salvelinus alpinus*) from oligotrophic apline lakes: gills versus digestive tract. Water Air Soil Pollut. **102**: 303–312.

McGeer, J.C., Playle, R.C., Wood, C.M., and Galvez, F. 2000. A physiologically based biotic ligand model for predicting the acute toxicity of waterborne silver to rainbow trout in freshwaters. Environ. Sci. Technol. **34**: 4199–4207.

Newman, M.C. 1998. Fundamentals of Ecotoxicology. Sleeping Bear Press Inc., Chelsea, Mich. pp. 25–49.

O'Connor, K.I., Taylor, A.C., and Metcalfe, N.B. 2000. The stability of standard metabolic rate during a period of food deprivation in juvenile Atlantic salmon. J. Fish. Biol. **57**: 41–51.

Peck, L.S. 1998. Feeding metabolism and metabolic scope in Antarctic marine ectotherms. *In* Cold ocean physiology. *Edited by* H.O. Pörtner and R.C. Playle. Cambridge University Press, Cambridge, U.K. pp. 356–390.

Pelgrom, S.M.G.J., Lamers, L.P.M., Garritsen, J.A.M., Pels, B.M., Lock, R.A.C., Balm, P.H.M., and Wendelaar Bonga, S.E. 1994. Interactions between copper and cadmium during single and combined exposure in juvenile tilapia *Oreochromis mossambicus*: influence of feeding condition on whole body metal accumulation and the effect of the metals on tissue water and ion content. Aquat. Toxicol. **30**: 117–135.

Purcell, T.W., and Peters, J.J. 1998. Sources of silver in the environment. Environ. Toxicol. Chem. **17**: 539–546.

Richards, J.G., Burnison, B.K., and Playle, R.C. 1999. Natural and commercial dissolved organic matter protects against the physiological effects of a combined cadmium and copper exposure on rainbow trout (*Oncorhynchus mykiss*). Can. J. Fish. Aquat. Sci. **56**: 407–418.

Rose-Janes, N.G., and Playle, R.C. 2000. Protection by two complexing agents, thiosulphate and dissolved organic matter, against the physiological effects of silver nitrate to rainbow trout (*Oncorhynchus mykiss*) in ion poor water. Aquat. Toxicol. **51**: 1–18.

Rouleau, C., Gobiel, C., and Tjälve, H. 2000. Accumulation of silver from the diet in two marine benthic predators: the snow crab (*Chionoeceted opilio*) and American plaice (*Hippoglossoides platessoides*). Environ. Toxicol. Chem. **19**: 631–637.

Schwartz, M.L., and Playle, R.C. 2001. Adding magnesium to the silver–gill binding model for rainbow trout (*Oncorhynchus mykiss*). Environ. Toxicol. Chem. **20**: 467–472.

Shafer, M.M., Overdier, J.T., and Armstrong, D.E. 1998. Removal, partitioning, and fate of silver and other metals in wastewater treatment plants and effluent-receiving streams. Environ. Toxicol. Chem. **17**: 630–641.

St. Pierre, M.V., Kullak-Ublick, G.A., Hagenbuch, B., and Meier,

© 2002 NRC Canada

P.J. 2001. Transport of bile acids in hepatic and non-hepatic tissues. J. Exp. Biol. **204**: 1673–1686.

Thomann, R.V., Shkreli, F., and Harrison, S. 1997. A pharmacokinetic model of cadmium in rainbow trout. Environ. Toxicol. Chem. **16**: 2268–2274.

Warila, J., Batterman, S., and Passino-Reader, D.R. 2001. A probabilistic model for silver bioaccumulation in aquatic systems and assessment of human health risks. Environ. Toxicol. Chem. **20**: 432–441.

Wicklund, A., Norrgren, L., and Runn, P. 1990. The influence of cadmium and zinc on cadmium turnover in the zebrafish, *Brachydanio rerio*. Arch. Environ. Contam. Toxicol. **19**: 348–353.

Wood, C., Hogstrand, C., Galvez, F., and Munger, R. 1996*a*. The physiology of waterborne silver toxicity in freshwater rainbow trout (*Oncorhynchus mykiss*) 1. The effects of ionic Ag^+. Aquat. Toxicol. **35**: 93–109.

Wood, C., Hogstrand, C., Galvez, F., and Munger, R. 1996*b*. The physiology of waterborne silver toxicity in freshwater rainbow trout (*Oncorhynchus mykiss*) 2. The effects of silver thiosulphate. Aquat. Toxicol. **35**: 111–125.

Wood, C., Playle, R.C., and Hogstrand, C. 1999. Physiology and modeling of mechanisms of silver uptake and toxicity in fish. Environ. Toxicol. Chem. **18**: 71–83.

© 2002 NRC Canada

Measuring changes in the direction and magnitude of size-selective mortality in a commercial fish population

A.F. Sinclair, D.P. Swain, and J.M. Hanson

Abstract: A 28-year time series (1971–1998) of backcalculated length-at-age was used to investigate changes in the direction and magnitude of size-selective mortality of prerecruit and adult Atlantic cod (*Gadus morhua*) in the southern Gulf of St. Lawrence, Canada. Size selection changed from favouring fast growth in the 1970s to favouring slow growth in the late 1980s and 1990s. There was an intervening period of disruptive selection where fast and slow growth was favoured while intermediate growth rates were selected against. The intensity of size selection declined at the end of the study period following the closure of the commercial fishery. These different forms of selection (positive directional, negative directional, and disruptive selection) can all be accounted for by the sharply dome-shaped curve of fishing mortality against length observed in the fishery.

Résumé : Une série chronologique de longueurs à un âge donné obtenues par rétrocalcul sur une période de 28 ans (1971–1998) a servi à étudier les changements de direction et d'intensité de la mortalité reliée à la taille chez les prérecrues et les adultes de la morue franche (*Gadus morhua*) du sud du Golfe du Saint-Laurent, Canada. La sélection de la taille qui favorisait une croissance rapide dans les années 1970 a changé pour favoriser une croissance lente à la fin des années 1980 et dans les années 1990. Il y a eu une période intermédiaire de sélection diversifiante, pendant laquelle les croissances rapides et lentes ont été avantagées et les taux de croissance intermédiaires défavorisés. L'importance de la sélection de la taille a diminué vers la fin de la période d'étude après l'interdiction de la pêche commerciale. Ces différentes formes de sélection (dirigée positive, dirigée négative et diversifiante) s'expliquent toutes par la courbe accentuée en dôme qui décrit la relation entre la mortalité due à la pêche et la longueur au sein de cette population d'importance commerciale.

[Traduit par la Rédaction]

Introduction

It is reasonable to expect that fisheries exert strong phenotypic selection for size-at-age (Hanson and Chouinard 1992; Machiels and Wijsman 1996; Kristiansen and Svåand 1998). There is considerable individual variation in size-at-age and growth in fish populations providing a gradient for size selection. Most fishing gears are designed to be size selective. Minimum mesh-size regulations are commonly used for trawls, seines, and gillnets to allow smaller fish to escape. Hook and bait sizes on longline gear will also affect the size of captured fish. Fish populations are often partially segregated by size, thus allowing fishing effort to be directed towards fish of specific sizes (Sinclair 1992; Swain and Wade 1993). Fisheries have major impacts on stock abundance with many of the world's fish populations being depleted by overfishing. It follows that these same fisheries should affect population mean size-at-age through size-selective mortality. If some of the phenotypic variation in size-at-age is genetic, then fishing may cause evolutionary change in growth and maturation (Law 2000; Stokes and Law 2000).

Failure to account for size-selective mortality may cause biased estimation of growth rates, mortality rates, and biological reference points for management (Ricker 1969; Favro et al. 1979; Parma and Deriso 1990). When investigating causes for changes in population mean size-at-age, it seems reasonable to consider possible effects of size-selective mortality along with other environmental factors such as temperature and population density. Nevertheless, it is rare to find its inclusion in this type of investigation.

Size-selective mortality can be studied by reconstructing the growth histories of individual fish using backcalculations based on bony structures such as otoliths, scales, and fin rays. For fish caught at age i in year t it is possible to backcalculate their lengths at age $i - x$ in year $t - x$. When representative samples of individual cohorts at successive ages are available, size-selective mortality can be estimated by comparing backcalculated lengths at age $i - x$ between fish caught in year t and those caught in year $t - x$.

We have developed methods for detecting changes in the magnitude and direction of size-selective mortality on a commercial fish population. The methods were applied to Atlantic cod (*Gadus morhua*) in the southern Gulf of St. Lawrence, Canada, over the period 1972–1998. There were important changes in the commercial fishery that affected the pattern of fishery-induced size-selective mortality. The

Received 24 May 2001. Accepted 30 January 2002. Published on the NRC Research Press Web site at http://cjfas.nrc.ca on 5 March 2002.
J16372

A.F. Sinclair.[1] Fisheries and Oceans Canada, Pacific Biological Station, Nanaimo, BC V9R 5K6, Canada.
D.P. Swain and J.M. Hanson. Fisheries and Oceans Canada, Gulf Fisheries Centre, Moncton, NB E1C 9B6, Canada.

[1]Corresponding author (e-mail: sinclairal@pac.dfo-mpo.gc.ca).

 DOI: 10.1139/F02-015 © 2002 NRC Canada

regulated mesh sizes for the dominant fishing gears (otter trawl and seine) increased during this period. The first minimum mesh-size regulations were introduced in 1967. The minima were increased in 1974 and 1981 (Halliday et al. 1989). There were also significant changes in exploitation rate in this fishery. The population was moderately exploited throughout the 1970s to mid-1980s. There was a rapid increase in exploitation that culminated in a stock collapse and fishery closure in September 1993. Since then, the stock has been lightly exploited as bycatch in other groundfish fisheries in the area and in sentinel surveys (Chouinard et al. 1999). We relate estimated changes in size-selective mortality to these changes in the commercial fishery.

Methods

Data collection

The basic data were obtained from stratified random bottom trawl surveys conducted annually during September from 1971 to 1998. These surveys provided synoptic estimates of the relative abundance and biological characteristics (including mean length-at-age) of Atlantic cod and other groundfish species in the area (Hurlbut and Clay 1990). Otoliths (saggitae) were collected on a length-stratified basis from each research tow for age determination and archived for future reference. The original otolith collection was subsampled for backcalculations in the following manner. The analyses used fish aged 3–11 because few fish age 12 and older were sampled in many years. For the period 1971–1997, random samples of otoliths were selected from the lower (0–25%), upper (75–100%), and middle (37.5–62.5%) quartiles of the estimated population length frequencies at age and year-class. A maximum of 25 otoliths per year-class, age, and quartile were selected. In 1998, random samples of up to 75 otoliths were taken from each age. A total of 13 008 otoliths were successfully read as part of the study.

Given the stratified sampling scheme, the weight of all observations from fish of length l in year t at age i ($w_{l,t,i}$) was

$$(1) \qquad w_{l,t,i} = \frac{N_{l,t,i}}{O_{l,t,i}\sum_{l} N_{l,t,i}}$$

where $N_{l,t,i}$ represents the survey estimate of the number of fish in the population at length l in year t at age i, and $O_{l,t,i}$ represents the number of fish in the backcalculation sample at length l in year t and age i.

Backcalculations

The otoliths were either manually broken (1971–1982) or resin embedded and sectioned (1983–1998) through the nucleus. Ages were determined by counting the number of hyaline zones on the otolith cross section. The distance from the nucleus of the otolith to the outside edge of each hyaline zone along the longest axis of the cross section was recorded for backcalculations. This edge was assumed to correspond with the end of the winter slow-growth period, which occurs in April. Otoliths were read with a dissecting microscope and measurements were made either using an ocular micrometer (1971–1993) or with an image analysis system (NIH Image, 1994–1998, http://rsb.info.nih.gov/nih-image/). All age determinations and measurements were made by experienced technicians and their consistency was monitored by regular blind checks against a reference collection.

Individual fish lengths-at-age were backcalculated using the biological intercept procedure described by Campana (1990). The biological intercept is the position on the otolith radius/fish length plane at which the relationship between the two variables becomes linear. We estimated the biological intercept from a nonparametric density plot of the scattergram of otolith radius/fish length for the cohorts sampled at all ages used in the study (the 1968–1987 year-classes) (SAS Institute Inc. 1994). Contour lines showing the density of data points in the scattergram were determined using a bivariate normal kernel smoother. The outermost contour enclosed approximately 90% of the observations. The density plot (Fig. 1) shows a characteristic V-shape because faster-growing fish have proportionately smaller otoliths (Campana 1990; Casselman 1990). The biological intercept for backcalculations was estimated by determining the intersection of two lines drawn along the upper and lower limits of the outermost contour of the density plot. The arc thus described would include all backcalculated lengths-at-age from otolith radius/fish length pairs contained therein. In so doing, the backcalculated lengths-at-age would tend to fall within the range of observations. We chose a biological intercept of $O_0 = 0.44$ mm otolith radius, $L_0 = 2.44$ cm fish length, and estimated length at age i (L_i) as

$$(2) \qquad L_i = L_c + (O_i - O_c)(L_c - L_0)(O_c - O_0)^{-1}$$

where L_c is fish length at capture and O_c is otolith radius at capture. Additional otolith measurements were made for age-0, -1, and -2 fish from the 1987 year-class to verify this choice of biological intercept. These additional points are shown in Fig. 1. Ninety percent of these measurements fall within the biological intercept arc, thus supporting the estimated value.

Difference in means test for size selection

One test for size-selective mortality is to compare, within year-classes, the mean backcalculated lengths at a given age among successive ages of capture. We used pairs of ages that were three years apart. The backcalculated length at the annulus corresponding to the younger of the two ages in the pair was the basis for the tests. For example, the backcalculated length at the third annulus was used for the age-3 and age-6 groups, whereas the backcalculated length at the fourth annulus was used for the age-4 and age-7 groups. Separate analysis of variance (ANOVA) of the following form was used for each age group.

$$(3) \qquad L'_{i,t,y} = \beta_0 + \beta_1 Y + \beta_2 I(Y) + \varepsilon$$

where $L'_{i,t,y}$ is the mean backcalculated length at age i of a fish caught in year t of year-class y, Y is a nominal variable for year-class, and I is a nominal variable for age of capture. The age of capture was i for the younger age in the pair and $i + 3$ for the older age. The year of capture was $i + y$ for the younger age in the pair and $i + y + 3$ for the older age.

The parameter vector β_2 and the associated standard-error vector were used to test the null hypothesis of no difference in backcalculated length-at-age between different ages of

© 2002 NRC Canada

Fig. 1. Summary of the approach used to calculate the biological intercept used in backcalculations. The contour lines are a nonparametric density plot of otolith radius vs. fish length measurements. The biological intercept was defined by the intersection of lines drawn parallel to the upper and lower portions of the outermost contour. The individual data points are for ages 0, 1, and 2 fish of the 1987 year-class, and these were not used to draw the density plot.

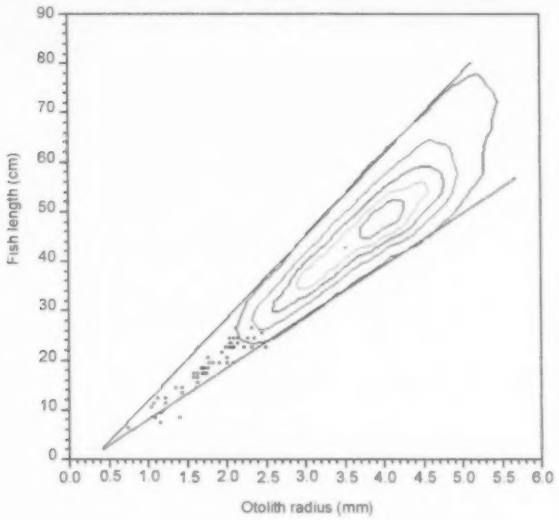

capture. A decline in the mean backcalculated length as the age of capture increases suggests that smaller individuals had a higher survival rate than larger individuals, i.e., evolutionary selection for small size. An increase in mean backcalculated length with age of capture indicates selection for large size. The β_2 parameter vectors and their 95% confidence intervals were plotted against the year when the younger age group in the pair was caught to examine time trends in size-selective mortality.

Fitness function test for size selection

Size selection may have different forms. Selection may be directional, favouring either large or small individuals. Directional selection may produce either depressed or increased mean size-at-age in the population along with unimodal distributions of size-at-age. Selection may also be disruptive by favouring both small and large individuals while selecting against intermediate-sized individuals. Disruptive selection will affect the variance in size-at-age but may not affect the population mean size-at-age (and thus may not be detected by the difference-in-means test). In extreme cases, it may produce bimodal distributions of size-at-age. Finally, selection may be stabilizing, favouring intermediate sizes while selecting against extremes. Again, stabilizing selection will affect the variance but may not affect the mean.

To examine relationships between size and survival more closely, we estimated relative fitness or survival as a function of backcalculated length-at-age using generalized additive models (MathSoft Inc. 1999). For each year-class from 1967 to 1987, we compared backcalculated length at age 4 between fish captured as 4-year-olds and those captured as 9- to 11-year-olds. (Ages 9 to 11 were grouped together because of small sample sizes at these older ages in many year-classes.) Following Anderson (1995), we first estimated $h(l)$, the conditional probability that a fish of backcalculated length l at age 4 was caught in the sample of survivors (i.e., ages 9 to 11) given that it was caught in one of the two samples. To do this, we coded fish caught at age 4 as 0 and those caught at ages 9 to 11 as 1, and estimated $h(l)$ using a weighted generalized additive model assuming a binomial error distribution and a logit link

$$(4) \qquad h(l) = e^{u}/(1 - e^{u})$$

where u is a cubic B-spline smooth function of l, with the smoothing parameter λ chosen by generalized cross validation. Observations were weighted according to eq. 1. Anderson (1995) showed that the relative survival function $f(l)$ is given by

$$(5) \qquad f(l) = (n_1/n_2)(h(l)/(1 - h(l)))$$

where n_1 and n_2 are the sample sizes at age 4 and ages 9 to 11, respectively. Fish in the tails of the length distributions were grouped together when fitting these models. This was done because the samples at ages 9 to 11 contained backcalculated lengths that were more extreme than any observed in the samples at age 4. Fish in each tail were assigned the weighted average length of all the fish in that tail in the two samples.

Because of small sample sizes, we investigated selection functions further using blocks of year-classes. We chose blocks within which the form of selection appeared to be uniform, based on the analyses described above and scatterplots of length-at-age. We assumed the same fitness function for all year-classes within a block but fit the function separately within each year-class (because sample sizes differed between year-classes). Because of this complication, we modified our approach, according to Manly (1985). It can be shown that this approach is equivalent to that described by Anderson (1995). Given that a fish q is in one of the two samples of year-class y, the probability that it is in sample k is

$$(6) \qquad P_{kqy} = f_{kl}n_{ky}/(n_{1y} + f_{2l}n_{2y})$$

where sample 1 is the sample of 4-year-old fish, sample 2 is the sample of fish aged 9 to 11, l is the backcalculated length at age 4 for fish q, n_{1y} and n_{2y} are sample sizes at age 4 and 9 to 11, respectively, for year-class y, f_{1l} is 1 for all l (since sample 1 is taken before the selection episode), and f_{2l} describes survival between age 4 and ages 9 to 11 as a function of l. Following Manly (1985), we assumed the following model for fitness from age 4 to ages 9 to 11 as a function of l:

$$(7) \qquad f_{2l} = e^{u(l)}$$

where u is a polynomial function of l, including linear and, if justified, quadratic terms. The analyses using splines within individual year-classes suggested that quadratic polynomials were sufficient to capture the main features of the selection curves. The exponential form of eq. 7 ensures that values predicted for fitness are not negative.

© 2002 NRC Canada

The likelihood function for the data is

$$(8) \qquad L = \prod_{q=1}^{m} P_{kqy}$$

where m is the total number of individuals in the samples at ages 4 and 9 to 11 from the block of year-classes, and the q^{th} individual is in year-class y and sample k. We estimated the relative survival function f_{2l} by choosing values for the parameters in eq. 7 that minimized the weighted negative log likelihood

$$(9) \qquad \sum -v_q \ln(P_{kqy})$$

where v_q is the weight for fish q. The weights given by eq. 1 were scaled to sum to the sample size within each age-class. Significance of each term was assessed using likelihood ratio χ^2 tests between hierarchical models. Confidence bands about the selection curves were estimated by bootstrapping, with 1000 replicates. Bias in the parameter estimates was negligible (1% or less).

We also examined variation in the form of selection with age (or size) using the same blocks of year-classes. We compared backcalculated length at age 4 between fish caught at age 4 versus those caught at age 7, and backcalculated length at age 6 between fish caught at age 6 and those caught at ages 9 to 11.

Simulations of size-selective mortality

An individual-based simulation was used to demonstrate possible effects of size-selective mortality on the population mean length-at-age and to provide data to test our methods of detection. A subsample of backcalculated growth trajectories for individual fish was selected from the database to represent the potential spread of growth characteristics of a cohort. A subsample of four age-10 or -11 fish per year-class was drawn at random from the database, for a total of 112 fish. Separate von Bertalanffy growth curves were fitted to the backcalculated lengths-at-age of each fish, and the predicted lengths-at-age were used in the simulations.

Three length-dependent fishing mortality functions were used to simulate periods of different size selection in the fishery. A base function was estimated as the ratio of annual catch at length in the fishery divided by population at length estimates from the annual surveys for the period 1982–1993 (Sinclair 1998). The function was strongly dome-shaped with peak fishing mortality at 70 cm (Fig. 2). The other two functions had the same shape but were shifted to the left, peaking at 57 cm and 50 cm, respectively.

The interaction between the variation in size-at-age of individual fish and selectivity of the fishery was modelled as follows. Length at age i of an individual fish q was a von Bertalanffy function. Fishing mortality was modelled as a function of length (Fig. 2). The relative abundance (relative to 1 at age 0) of fish q at age i (years) was

$$(10) \qquad N_{iq} = e^{-(iM + \sum_{g=0}^{i-1} F_{gq})}$$

assuming $M = 0.2$ for all ages. The cohort mean length-at-age was

Fig. 2. Lengths-at-age of fish in the simulated cohort (●) and the fishing mortality (F)-at-length curves used in the size-selective mortality simulations. The curve with short dashes was estimated using data from the 1982–1993 period, and this curve peaked at 70 cm total length. The other two curves were shifted to the left to peak at 50 cm (long- and short-dashed line) and 57 cm (dotted line), respectively.

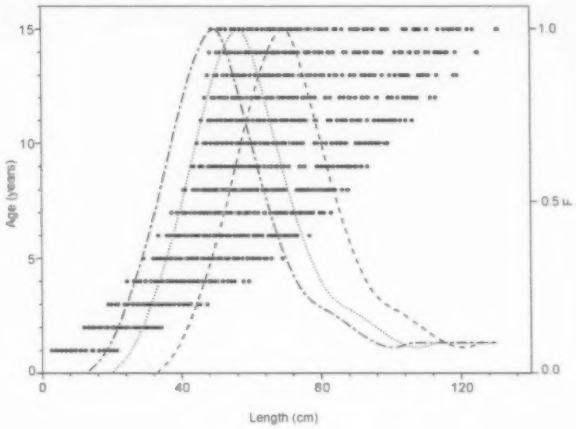

$$(11) \qquad \bar{L}_i = \frac{\sum_{q=1}^{m} L_{iq} N_{iq}}{\sum_{q=1}^{m} N_{iq}}$$

where there are m fish in the population.

Results

There have been remarkable changes in length distributions at age in the southern Gulf of St. Lawrence cod population over the study period (Fig. 3). Length distributions at age 4 were similar among early (1968–1971), middle (1975–1978), and late (1980–1983) year-classes. The distributions were unimodal, peaking at about 40 cm. Distributions remained unimodal at age 8. However, the early year-classes showed a broader distribution and higher modal length (70 cm), whereas the distributions for the middle and late year-classes were skewed and had lower modal lengths (49 cm). There were relatively few age-12 individuals of the early year-classes caught in the surveys and the distribution of length-at-age was fairly uniform. For the middle and late year-classes, the distributions were highly skewed with a dominant mode in the mid-50-cm range and a long tail toward longer lengths. At ages 13+, the length distribution of the early year-classes was unimodal, while that of the middle year-classes was distinctly bimodal. There was little change in the position of the dominant mode in the length distributions for the middle and late year-classes from age 8 and older. In contrast, there was a steady increase in the modes and ranges of distributions of length-at-age for the early year-classes.

© 2002 NRC Canada

Fig. 3. Length–frequency distributions of selected year-classes and ages of southern Gulf of St. Lawrence cod (*Gadus morhua*) sampled in annual research vessel surveys. Distributions are the percent frequency within year-classes, averaged over the four year-classes in each period.

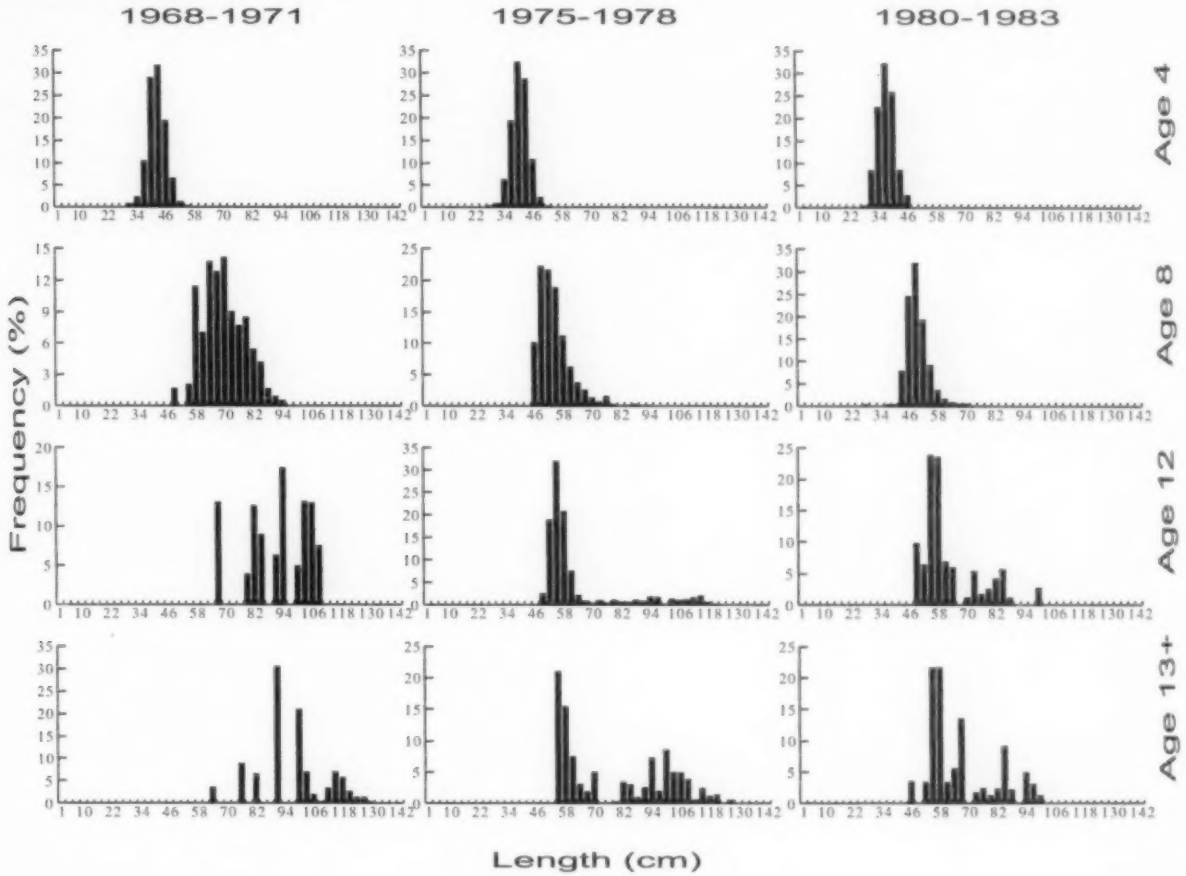

Difference in means

The main effects in the ANOVAs for size-selective mortality were all highly significant (Table 1). The estimated differences in backcalculated lengths at a common age for different pairs of ages indicate that there have been significant changes in both the direction and magnitude of size selection (Fig. 4). During the early to mid-1970s, the backcalculated lengths-at-age from the older fish were greater than those obtained from younger fish, suggesting that there was selection for large size-at-age during this time. This trend was evident for all ages, but was strongest between ages 7 and 10. The pattern was reversed during the 1980s and early 1990s. For the age pairs 3 and 6, 4 and 7, 5 and 8, and 6 and 9, there was a tendency for the backcalculated lengths-at-age obtained from older fish to be less than those obtained from younger fish, suggesting selection for small size-at-age. The differences in backcalculated size-at-age were reduced at the end of the time series, suggesting that directional size-selective mortality had ceased.

Fitness test

Dramatic changes in the form of size selection have occurred between the 1967 and 1987 year-classes (Fig. 5). In the earliest cohorts in this time series, survival was greatest for fish with large lengths at age 4. In later cohorts, the pattern was reversed, with greatest survival for fish with small lengths at age 4. In many cohorts, there were indications of disruptive selection with greater survival for fish with either large or small lengths at age 4, though usually survival was substantially greater at one tail of the length distribution than at the other. Disruptive selection was most consistently evident in the intermediate cohorts in the time series (1975–1978), and was strongest in the 1977 cohort.

These patterns were confirmed by the more detailed analyses within blocks of year-classes (Fig. 6). The linear term in the selection function was highly significant in all three cases ($P < 0.005$). The quadratic term was most significant in the 1975–1978 year-classes ($P < 0.0001$) and less significant ($0.01 < P < 0.05$) in the 1968–1971 and 1980–1984 year-classes. Size selection between age 4 and ages 9 to 11 appeared to be purely directional in the earlier (1968–1971) and later (1980–1984) year-classes, but disruptive in the intervening (1975–1978) year-classes. The direction of selection reversed between the early and late year-classes. Sur-

© 2002 NRC Canada

Table 1. Summary statistics from ANOVA of backcalculated lengths-at-age.

Ages	Year-classes	N	R^2	Y (df = 24)	$I(Y)$ (df = 25)
3 and 6	1968–1992	3249	0.32	43.48	19.39
4 and 7	1967–1991	3087	0.36	62.35	9.48
5 and 8	1966–1990	2887	0.54	123.59	13.30
6 and 9	1965–1989	2685	0.56	135.16	6.80
7 and 10	1964–1988	2240	0.57	115.02	6.01
8 and 11	1963–1987	1755	0.58	85.58	8.67

Note: The last two columns give the F values for the main effects. Y and I represent the main effects of year-class and age, respectively. All are highly significant ($P < 0.0001$). df, degrees of freedom.

Fig. 4. Within-year-class differences in mean backcalculated lengths at a common age but from fish caught three years apart. Separate plots are given for ages (*a*) 3 to 6, (*b*) 4 to 7, (*c*) 5 to 8, (*d*) 6 to 9, (*e*) 7 to 10, and (*f*) 8 to 11. The differences are calculated as the mean of the older fish less the mean of the younger fish. Vertical lines are 95% confidence intervals.

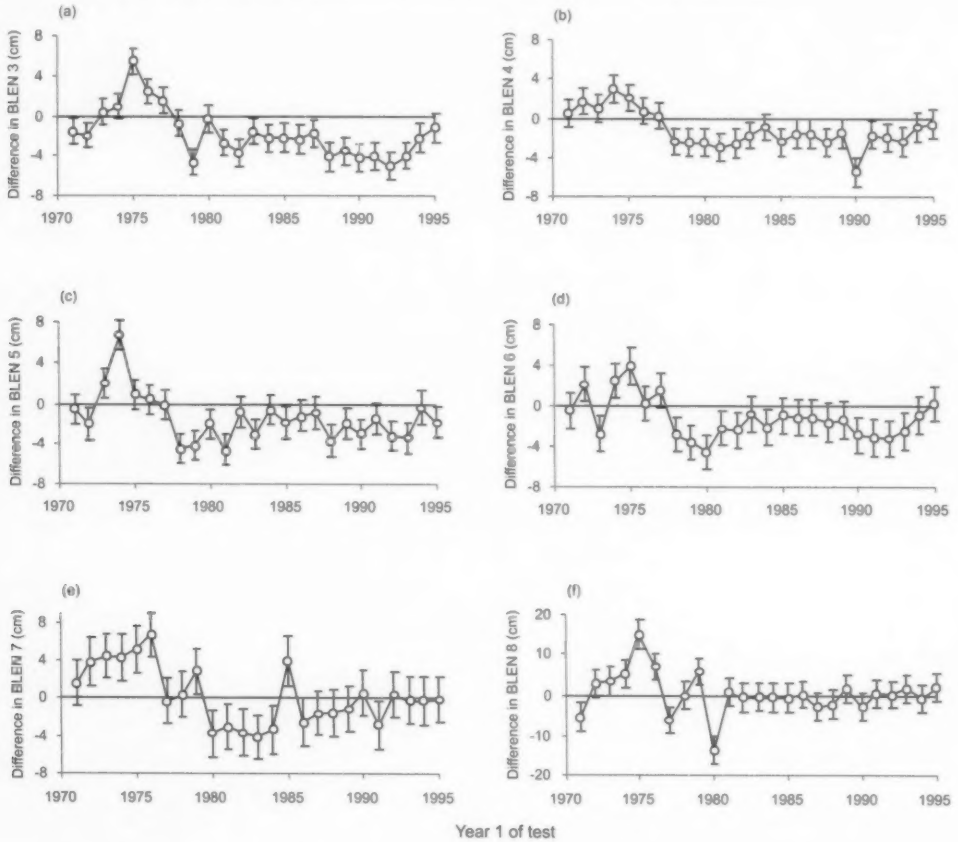

vival was greatest for fish with large lengths at age 4 in the 1968–1971 year-classes but for those with small lengths at age 4 in the 1980–1984 year-classes. In the 1975–1978 year-classes, survival was significantly greater for fish with either small or large lengths at age 4 than for fish with intermediate lengths. However, though selection was significantly disruptive for these intermediate year-classes, survival was substantially greater for the smallest lengths than for the largest lengths in these year-classes.

The form of size selection also changed with age or size within cohorts (Fig. 7). In the 1968–1971 cohorts, both linear and quadratic terms were significant in the function describing size selection between ages 4 and 7, but only the linear term was significant in the selection function between ages 6 and 9 to 11. In both cases, size selection was primarily directional, with greater survival for larger fish. However, the survival advantage between ages 4 and 7 was restricted to the largest fish, whereas survival between ages 6 and 9 to 11 increased steadily with size over its entire range. In the 1975–1978 cohorts, only the linear term was significant in the size-selection function between ages 4 and 7, whereas both linear and quadratic terms were significant

© 2002 NRC Canada

Fig. 5. Relative survival from age 4 to ages 9+ as a function of backcalculated length at age 4 for each year-class from 1967 to 1987. For each year-class, the surface is set to zero at lengths beyond those in the fitted samples for that year-class.

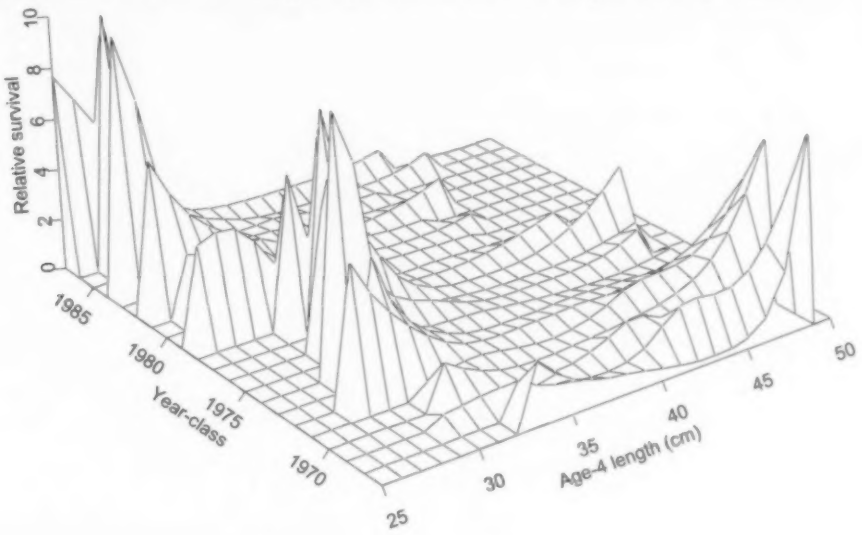

in the function between ages 6 and 9 to 11. Selection was directional between ages 4 and 7, with greater survival for smaller fish, but was disruptive between ages 6 and 9 to 11, with greatest survival for the largest fish. In the 1980–1984 cohorts, again only the linear term was significant in the selection function between ages 4 and 7, whereas both terms were significant in selection between ages 6 and 9 to 11. Again, selection was purely directional between ages 4 and 7, with greater survival for smaller fish. Selection was disruptive between ages 6 and 9 to 11, although in this case, the survival advantage was considerably greater for the smallest fish than for the largest fish.

Simulations

Mean lengths-at-age of the simulated cohort were strongly influenced by the location of the fishery selection window (Fig. 8). When compared with the mean lengths-at-age for the unfished cohort, mean lengths of the fished cohorts were depressed over the younger ages for each selection window and there was an upward inflection in mean lengths at older ages for each window. This form of population mean length-at-age is inconsistent with the von Bertalanffy growth model, even though each fish in the simulation followed a von Bertalanffy growth curve. The "fished" mean lengths-at-age exceeded the "unfished" values at older ages for the selection windows centred at 50 cm and 57 cm.

The "difference in means" index of size-selective mortality successfully captured differences in size selection for the three test selection windows in the simulations (Fig. 9). For the selection pattern centred at 50 cm, the index was negative for the ages 1 to 4, 2 to 5, and 3 to 6. It was neutral for ages 4 to 7, then became positive for older age groups. The pattern was similar for the selection window centred at 57 cm, except that the shift in direction of selection occurred at an older age. The index remained negative across all ages in the case where the selection window was centred at 70 cm.

Changes in the index are reflected in the cohort mean lengths-at-age. The index was initially negative for all three selection windows and the mean lengths-at-age were all depressed relative to the unfished cohort. The upward inflection in cohort mean length-at-age and the index occurred first for the selection window centred at 50 cm, second for the window centred at 57 cm, and last for the window centred at 70 cm.

The "fitness test" successfully indicated differences in the direction of size selection in the simulations. This is demonstrated by the relative survival at length between ages 6 and 9 for the three selection windows (Fig. 10). Size selection was directional for the window centred at 50 cm with higher relative survival at longer lengths. Selection was disruptive for the window centred at 57 cm with higher relative survival for smaller and larger fish. Selection was directional but favoured smaller fish for the selection window centred at 70 cm.

These results are consistent with the "difference in means" index. Where selection favoured larger fish (50-cm window), the difference in means index was positive. Where selection was disruptive (57-cm window), the difference in means index was neutral. Where selection favoured smaller fish (70-cm window), the difference in means index was negative.

Discussion

We have described tests for size-selective mortality based on cohort-specific changes in backcalculated lengths-at-age of fish surviving to successively older ages. Two tests were used. The first was based on changes in mean backcalculated length-at-age. We reasoned that if the backcalculated length-at-age declined as the cohort got older, then there was evolutionary selection for smaller individuals. Conversely, if the backcalculated length got larger, there was selection for larger individuals. The second test involved calculating the relative survival of individuals over the entire length range.

© 2002 NRC Canada

Fig. 6. Size-dependent relative survival from age 4 to ages 9+ in three periods: (*a*) 1968–1971, (*b*) 1975–1978, and (*c*) 1980–1984 year-classes. Dashed lines are 95% confidence bands.

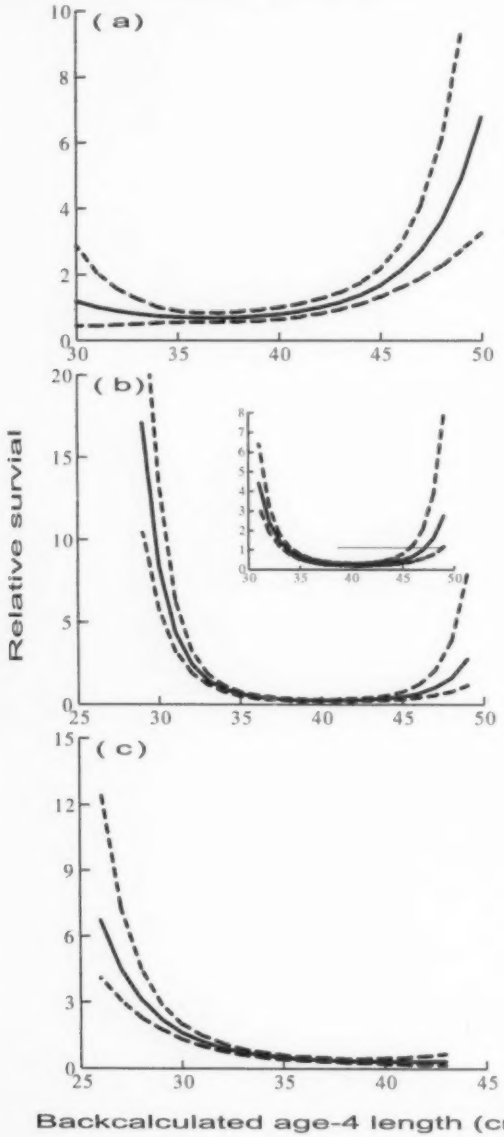

This allowed the detection of both directional (favouring large or small individuals) and disruptive selection. The latter was indicated by high relative survival of both large and small individuals and reduced survival at intermediate sizes.

The backcalculation method we used makes two main assumptions. The first is that for all fish there was a common origin of otolith radius and fish length. We used the biological intercept approach of Campana (1990), who suggested that this intercept was where the relationship between these two variables became linear. The choice of a common origin was not, however, critical to our results. We repeated the backcalculations using a biological intercept of 0, 0. The result was an increase in the backcalculated lengths-at-age, the magnitude of which increased with age. As a result, the differences in backcalculated lengths-at-age were higher for all year-classes. However, the pattern of change in the direction of size-selective mortality remained the same.

A second assumption was that of a linear relationship within individuals between otolith radius and fish length originating at the biological intercept. It is well known that faster-growing fish have smaller otoliths at a given length than slower-growing fish (Campana 1990). To avoid the bias that this relationship can cause in backcalculations, we used the biological intercept procedure rather than regression-based estimators. However, we know of no information on relationships between the rates of fish and otolith growth within individuals. Additional insight into this question may be available from laboratory and aquaculture studies where fish growth rates are manipulated by changes in feeding regimes or temperature. If these same fish were measured at regular intervals and their otoliths marked appropriately, then individual fish length and otolith radius trajectories could be followed.

Sampling of the population by the trawl survey was probably size selective for the younger ages, with smaller fish underrepresented in the survey catches. In this case, selection favouring large fish will be underestimated, whereas that favouring small fish will be overestimated in analyses including young ages. Analyses using preliminary estimates of size selectivity of the trawl survey indicate that this effect was negligible for all ages greater than 4 years and slight even between ages 3 to 6 and 4 to 7. Trends in size-selective mortality over time were the same with and without corrections based on the preliminary estimates of selection by the survey trawl. Nonetheless, we excluded fish caught at age 3 from the fitness tests and from analyses testing effects on length-at-age (Sinclair et al. 2002) to minimize effects of size selection by the survey.

Our results indicate that the form of selection has changed in a regular way, from directional selection favouring large size in the early cohorts, through disruptive selection favouring small and large size in intermediate cohorts, to directional selection favouring small size in late cohorts. Closure of the commercial fishery resulted in a cessation of size-selective mortality. This pattern is also consistent with the observed changes in distribution of length-at-age in the population. Year-classes fished during the 1970s reached greater lengths-at-age than those fished in the 1980s and 1990s. Modal length-at-age differed little between the middle and late year-classes and the distribution of length-at-age became highly skewed and then bimodal at older ages for these year-classes. These changes in length distribution are consistent with an early period of positive directional selection, followed by a period of disruptive selection and then a period of negative directional selection.

These contrasting forms of selection can be partially accounted for by the selectivity of the fishery. Fishing mortality is dome shaped with respect to length (Sinclair 1998). This is likely a result of the use of size-selective fishing gear, segregation of fish on the fishing grounds by size and age (Swain 1993), and a concentration of fishing effort in ar-

© 2002 NRC Canada

Fig. 7. Changes in size-dependent survival between age groups for three groups of year-classes. Dashed lines are 95% confidence bands.

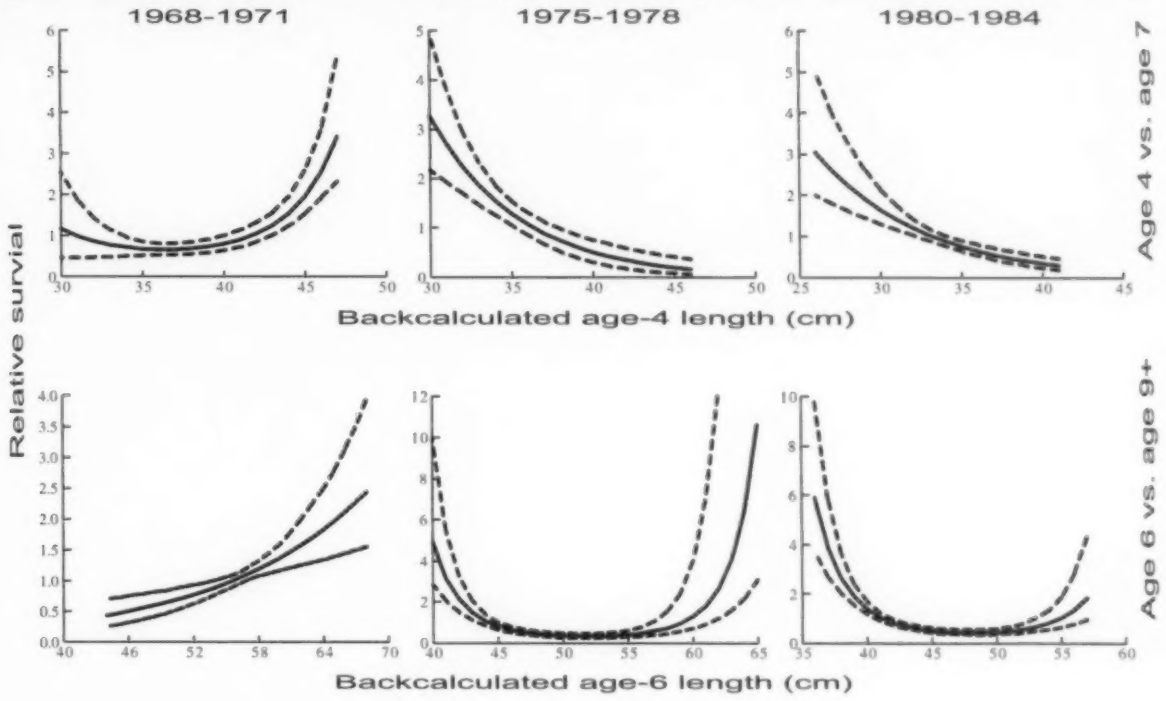

Fig. 8. Simulated mean lengths-at-age of a cohort fished with fishing mortality (F)-at-length curves peaking at 50 cm (long- and short-dashed line), 57 cm (dotted line), and 70 cm (short-dashed line). These are compared with the mean lengths-at-age of an unfished cohort (solid line).

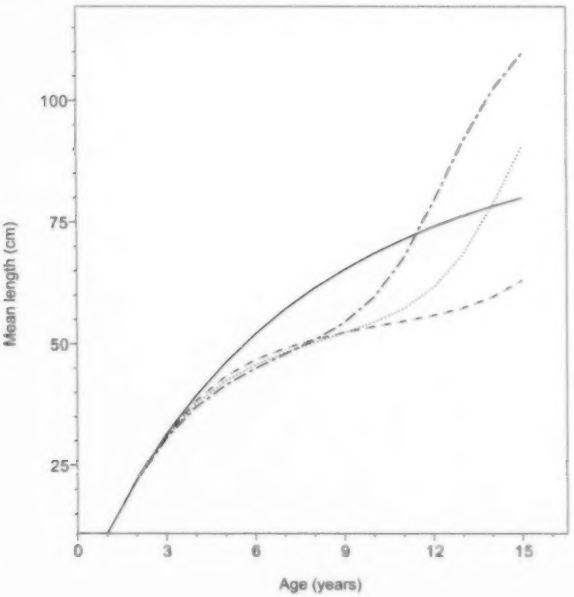

eas of high fish concentration. As a result, fishing mortality is highest at intermediate sizes. This creates the trade-off between fast and slow growth that is necessary to generate disruptive selection. On one hand, fast-growing fish have the disadvantage that they become vulnerable to the fishery at an earlier age than slow-growing fish. On the other hand, fast-growing fish have the advantage that they will grow through the vulnerable window more quickly than slow-growing fish.

The balance of selection will depend on average growth rates in the population relative to the position of the window of vulnerability to the fishery along the length axis. Changes in this balance will result in changes in the form of size selection by the fishery. When growth rates are sufficiently high or when the partial recruitment dome is shifted towards sufficiently small lengths (i.e., small mesh size), then fast-growing fish that grow quickly through the window of vulnerability will be at a selective advantage. When growth rates are sufficiently low or when the partial recruitment dome is shifted towards sufficiently large lengths (i.e., large mesh size), then slow-growing fish with delayed vulnerability to the fishery will be at a selective advantage. When growth rates are at some intermediate level or when the partial recruitment dome is shifted to intermediate lengths, then both the slowest-growing and fastest-growing fish will have a selective advantage over fish with intermediate growth rates. Changes in regulated mesh size can shift the widow of vulnerability to the fishery. Changes in environmental conditions (e.g., temperature and food) can change growth rate. We explore the relative importance of size-selective mortal-

© 2002 NRC Canada

Fig. 9. Simulated differences in mean backcalculated lengths at a common age in fish from the same cohort caught three years apart. The panels are for fishing mortality (F)-at-length curves centred at (*a*) 50 cm, (*b*) 57 cm, and (*c*) 70 cm. The differences are calculated as the mean of the older fish less the mean of the younger fish.

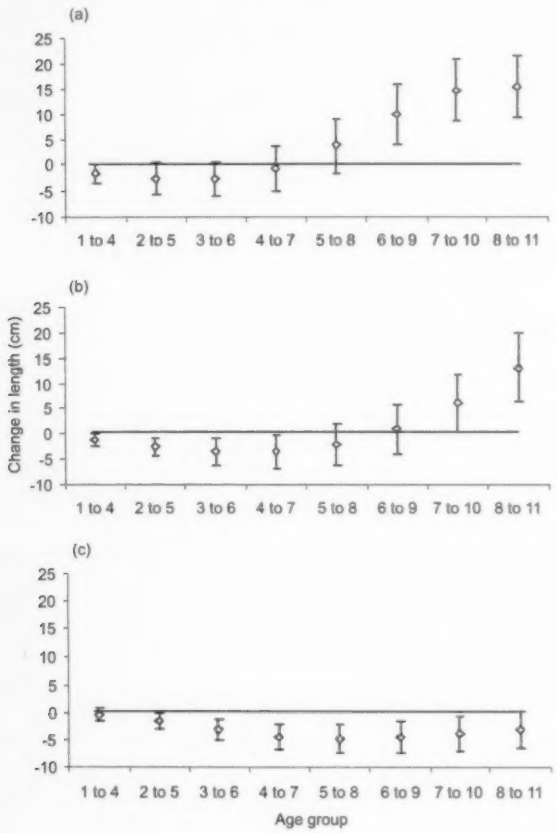

Fig. 10. Simulated size-dependent relative survival between ages 6 and 9 of a cohort fished with fishing mortality (F)-at-length curves centred at 50 cm (long- and short-dashed line), 57 cm (dotted line), and 70 cm (dashed line) total length.

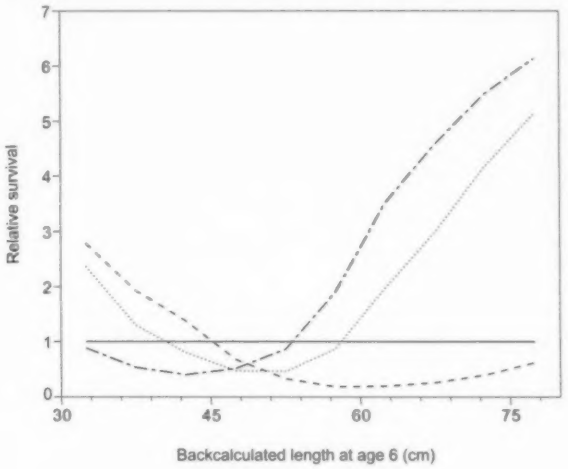

ity and environmental effects (population density and temperature) on size-at-age of this cod population in a subsequent analysis (Sinclair et al. 2002).

The mechanism outlined above for the changes in the form of size selection between cohorts is also consistent with the observed changes in the form of selection with age within cohorts. The selective advantage to small size tended to be greater at earlier ages, whereas the advantage to large size tended to be greater at older ages.

Although we have not investigated the potential genetic effects of this size-selective mortality, an evolutionary response to this selection is a troubling possibility. While the heritability of growth is unknown for Atlantic cod, available evidence from other fish species in the wild suggests that it may be in the range of 0.2 to 0.3 (Stokes and Law 2000). In the southern Gulf, selection favoured small size-at-age from the late 1970s until the closure of the cod fishery in 1993, roughly 3–4 cod generations. Fishing mortality rose to very high levels in the late 1980s and early 1990s to a point where the annual exploitation rate was nearly 70% for ages 7 and older (Chouinard et al. 1999). Given the strong size selectivity of the fishery, the high mortality rates that it has imposed, and the evidence for rapid evolutionary responses in production-related traits (e.g., size at maturity) (Reznick et al. 1997), an evolutionary decline in body size would be expected (Stokes and Law 2000). Indeed, length-at-age of southern Gulf cod has recovered little since the closure of the cod fishery in 1993 even though size-selective mortality has apparently ceased. Density-dependent effects should promote rapid growth at the current low abundance of this population. Environmental conditions were harsh in the southern Gulf in the early to mid-1990s, but have now moderated. The continued small size-at-age of southern Gulf cod is consistent with a genetic response to the size-selective mortality imposed by the fishery in the 1980s and early 1990s. If this is the case, improvement in the growth rate can be expected to be slow.

Acknowledgements

We would like to thank S. Campana for kind suggestions regarding otolith backcalculations. G. Chouinard provided helpful comments on earlier versions of the manuscript. L. Currie and J. Murphy spent many hours doing otolith measurements and we appreciate their attention to detail.

References

Anderson, C.S. 1995. Calculating size-dependent relative survival from samples taken before and after selection. *In* Recent developments in fish otolith research. *Edited by* D.H. Secor, J.M. Dean and S.E. Campana. The Belle W. Baruch Library in Marine Science. 19. University of S. Carolina Press, Columbia, S.C. pp. 455–466.

Campana, S.E. 1990. How reliable are growth back-calculations based on otoliths? Can. J. Fish. Aquat. Sci. **47**: 2219–2227.

Casselman, J.M. 1990. Growth and relative size of calcified structures of fish. Trans. Am. Fish. Soc. **119**: 673–688.

© 2002 NRC Canada

Chouinard, G.A., Sinclair, A., Currie, L., Poirier, G., and Swain, D. 1999. Assessment of cod in the southern Gulf of St. Lawrence, March 1999. DFO Canadian Stock Assessment Secretariat Research Document 99/023.

Favro, L.D., Kuo, P.K., and McDonald, J.F. 1979. Population-genetic study of the effects of selective fishing on the growth rate of trout. J. Fish. Res. Board Can. **36**: 552–561.

Halliday, R.G., Hay, D.E., and Metuzals, K.I. 1989. Wastage at sea of American plaice (*Hippoglossoides platessoides* (Fabricius)) in the southern Gulf of St. Lawrence fishery in the 1970s. Can. Tech. Rep. Fish. Aquat. Sci. No. 1663.

Hanson, J.M., and Chouinard, G.A. 1992. Evidence that size-selective mortality affects growth of Atlantic cod (*Gadus morhua* L.) in the southern Gulf of St. Lawrence. J. Fish Biol. **41**: 31–41.

Hurlbut, T., and Clay, D. 1990. Protocols for research vessel cruises within the Gulf Region (demersal fish) (1970–1987). Can. Manuscr. Rep. Fish. Aquat. Sci. No. 2082.

Kristiansen, T.S., and Svåand, T. 1998. Effect of size-selective mortality on growth of coastal cod illustrated by tagging data and an individual-based growth and mortality model. J. Fish Biol. **52**: 688–705.

Law, R. 2000. Fishing, selection, and phenotypic evolution. ICES J. Mar. Sci. **57**: 659–668.

Machiels, M.A.M., and Wijsman, J. 1996. Size-selective mortality in an exploited perch population and the reconstruction of potential growth. Ann. Zool. Fenn. **33**: 397–401.

Manly, S.F.J. 1985. The statistics of natural selection on animal populations. Chapman and Hall, New York.

MathSoft Inc. 1999. S-Plus 2000: Guide to Statstics. MathSoft Inc., Seattle, Wash.

Parma, A.M., and Deriso, R.B. 1990. Dynamics of age and size composition in a population subject to size -selective mortality: effects of phenotypic variability in growth. Can. J. Fish. Aquat. Sci. **47**: 274–289.

Reznick, D.H., Shaw, F.H., Rodd, F.H., and Shaw, R.G. 1997. Evaluation of the rate of evolution in natural populations of guppies (Poecilia reticulata). Science, **275**: 1934–1937.

Ricker, W.E. 1969. Effect of size selective mortality and sampling bias on estimates of growth, mortality, production, and yield. J. Fish. Res. Board Can. **26**: 479–541.

SAS Institute Inc. 1994. JMP® statistics and graphics guide: statistical software for the Macintosh from SAS Institute Inc. SAS Institute Inc., Cary, N.C.

Sinclair, A. 1992. Fish distribution and partial recruitment: the case of eastern Scotian Shelf cod. J. Northwest Atl. Fish. Sci. **13**: 15–24.

Sinclair, A.F. 1998. Estimating trends in fishing mortality at age and length directly from research survey and commercial catch data. Can. J. Fish. Aquat. Sci. **55**: 1248–1263.

Sinclair, A.F., Swain, D.P., and Hanson, J.M. 2002. Disentangling the effects of size-selective mortality, density, and temperature on length-at-age. Can. J. Fish. Aquat. Sci. **59**: 372–382.

Stokes, K., and Law, R. 2000. Fishing as an evolutionary force. Mar. Ecol. Prog. Ser. **208**: 307–309.

Swain, D.P. 1993. Age- and density-dependent bathymetric pattern of Atlantic cod (*Gadus morhua*) in the southern Gulf of St. Lawrence. Can. J. Fish. Aquat. Sci. **50**: 1255–1264.

Swain, D.P., and Wade, E.J. 1993. Density-dependent geographic distribution of Atlantic cod (*Gadus morhua*) in the southern Gulf of St. Lawrence. Can. J. Fish. Aquat. Sci. **50**: 725–733.

© 2002 NRC Canada

Disentangling the effects of size-selective mortality, density, and temperature on length-at-age

A.F. Sinclair, D.P. Swain, and J.M. Hanson

Abstract: The relative importance of size-selective mortality, density-dependent growth, and temperature on growth of a commercial fish population was investigated using an integrated statistical analysis. Two indices of size-selective mortality were determined using otolith backcalculations. One index measured the direct effect on population mean growth increments in the year of the growth increment. The second index measured the cumulative effect on the growth potential of a cohort. Indices of population density, occupied temperature, and bottom temperature were developed from annual synoptic research vessel surveys of the population. We simultaneously tested effects of these factors using a modified von Bertalanffy growth model. The strongest effect was variation in size-selective mortality, followed by a negative effect of population density and a weak positive effect of occupied temperature. Effects of bottom temperature conditions were not significant. Failure to simultaneously consider alternative mechanisms, especially size-selective mortality, can lead to incorrect conclusions about the role of environmental factors in determining growth of fishes.

Résumé : Une analyse statistique intégrée nous a permis d'étudier les effets relatifs de la mortalité spécifique à la taille, de la croissance reliée à la densité et de la température sur la croissance d'une population commerciale de poissons. Deux indices de mortalité spécifique à la taille ont été conçus d'après des rétrocalculs basés sur les otolithes. Le premier mesure l'effet direct sur les accroissements moyens durant l'année de l'accroissement. Le second mesure l'effet cumulatif sur le potentiel de croissance d'une cohorte. Des indices de densité de population, de température expérimentée et de température du fond ont pu être développés à partir de données synoptiques annuelles d'inventaire de la population accumulées par les navires de recherche. Nous avons évalué simultanément les effets de ces facteurs à l'aide d'un modèle de croissance de von Bertalanffy. L'effet le plus marqué est celui de la mortalité spécifique à la taille, suivi de l'effet négatif de la densité de population et enfin d'un effet légèrement positif dû à la température expérimentée. Les conditions de température du fond n'ont pas d'effets significatifs. Négliger de tenir compte simultanément des tous les mécanismes de rechange, particulièrement de la mortalité spécifique à la taille, peut donner lieu à des conclusions erronées sur le rôle que jouent les facteurs de l'environnement sur la croissance des poissons.

[Traduit par la Rédaction]

Introduction

Many factors affect mean length-at-age in fish populations. Three commonly proposed explanations for interannual variability include the effects of changes in environment on growth, most notably temperature, density-dependent effects on growth, and size-selective mortality. These factors can operate singly or in combination. The effects of temperature on fish growth have been studied extensively under laboratory conditions. The relationship between temperature and growth is usually nonlinear with maximum growth at intermediate values. Whereas most studies have reported or suggested a positive relationship between temperature and growth, the expected direction of the effect of temperature depends on an interaction with food ration. The optimum temperature for growth declines as food ration declines (e.g., Elliot 1975; Woiwode and Adleman 1991). Thus, growth could decline with increasing temperature when food is limiting. Brander (1995) suggests that most of the variations in size-at-age among north Atlantic cod (*Gadus morhua*) populations can be accounted for by temperature. Density-dependent growth, where growth is inhibited by intraspecific competition for food at large stock sizes, has been reported for many marine species (e.g., Overholtz 1989; Helser and Almeida 1997). Most fishing gears are size selective and there is considerable variation in growth rate among individual fish of a given age. This provides both the means and opportunity for the selective removal of fast-growing fish and depression of the population mean length-at-age (e.g., Hanson and Chouinard 1992; Kristiansen and Svåand 1998; Sinclair et al. 2002).

Whereas all three mechanisms provide possible explanations for changes in length-at-age of fish populations, the research and management implications of each are very different. If environmental conditions are responsible, then

Received 24 May 2001. Accepted 8 January 2002. Published on the NRC Research Press Web site at http://cjfas.nrc.ca on 5 March 2002.
J16373

A.F. Sinclair.[1] Fisheries and Oceans Canada, Pacific Biological Station, Nanaimo, BC V9R 5K6, Canada.
D.P. Swain and J.M. Hanson. Fisheries and Oceans Canada, Gulf Fisheries Centre, Moncton, NB E1C 9B6, Canada.

[1]Corresponding author (e-mail: sinclairal@pac.dfo-mpo.gc.ca).

 DOI: 10.1139/F02-014 © 2002 NRC Canada

increased knowledge of the effect could be useful in forecasting future yields from the stock. Additional emphasis could be placed on collecting appropriate environmental data for forecasts. If growth is density dependent, then models used to determine biological reference points for management (e.g., yield per recruit and spawning stock biomass per recruit) will need to take this into account (Helser and Brodziak 1998). In some cases, large population sizes may be undesirable because of growth inhibition. If population mean size-at-age is affected by fishery-induced size selection, one needs to consider both the effects on reference points for management and the possibility of genetic selection with its impacts on future population characteristics (Favro et al. 1979; Parma and Deriso 1990). Research into optimal gear selectivity and harvest rates would be warranted. Clearly, it is important to properly identify the causal mechanism before modifying management policy. Indeed, misidentification of the causal mechanism could lead to undesirable results.

In this paper, we consider all three mechanisms described above and have ranked their importance in explaining variation in population mean length-at-age of Atlantic cod in the southern Gulf of St. Lawrence, Canada. Size-at-age in this population has varied considerably since 1971 (Fig. 1, data from Chouinard et al. 1999). Although no trend is evident at age 3, for older ages the mean length-at-age was high in the 1970s, declined from the late 1970s to the mid-1980s, and has been low since then. Indices of size selection were developed from a database of backcalculated length-at-age (Sinclair et al. 2002). Indices of population density, and of occupied (where cod were caught) and bottom (habitat-wide) temperatures during the growing season were also developed. We used both nonlinear and linear models to simultaneously test the effects of size selection, population density, and temperature on mean length-at-age and growth. The importance of simultaneously testing alternative hypotheses is discussed.

Methods

All symbols and subscripts used in the growth analysis are described in Table 1. All backcalculated variables are denoted by a prime symbol and represent population means. The backcalculated lengths and growth increments have three subscripts. The first position denotes the annulus (or age) (i) of backcalculation. The second position gives the year (t) in which the fish were caught. The third position is the year-class (y). The backcalculated lengths represent the fish length at the beginning of the growing season, which is April for this stock.

All data and samples used in this study were obtained from stratified random bottom trawl surveys conducted annually in September 1971–1998. Otoliths (saggitae) were collected on a length-stratified basis from each research tow for age determination. The otoliths were archived for future reference. These were used to backcalculate length-at-age of ages 3 to 11 (year) fish in each year. Additional details of the data collections and backcalculation method are given in Sinclair et al. (2002).

An index of population density ($N_{i,y}$) was developed to reflect levels of intraspecific competition. Because competition is expected to be strongest between individuals of similar sizes (and thus with similar diets), the index was calculated as the sum of survey estimates of mean numbers per tow ($A_{i,y}$) at three adjacent ages in the same year

(1) $$N_{i,y} = A_{i-1,y+1} + A_{i,y} + A_{i+1,y-1}$$

The research survey estimates were obtained from Chouinard et al. (1999). The density variables were z-score standardized for each age to equalize the scale of measurement. The bottom temperature index (V_t) was calculated as the stratified mean of the tow-by-tow bottom temperature measurements taken during the September surveys. The occupied temperature index ($T_{i,y}$) was calculated as the catch-weighted stratified mean temperature by age and year-class. The surveys were conducted during the growing season and thus the temperature and density indices were assumed to reflect conditions that would most affect growth.

Fig. 1. Mean length at ages 3 to 11 for southern Gulf of St. Lawrence cod (*Gadus morhua*; 1971–1998) estimated from annual bottom-trawl surveys. The age lines are labelled alternatively with circles, squares and crosses beginning with age 3.

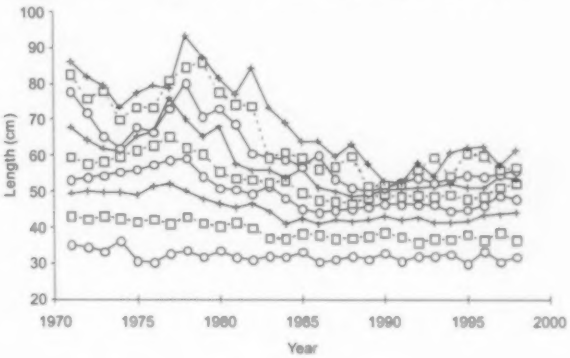

Indices of size-selective mortality

We reasoned that size-selective mortality would have two main effects on population mean length-at-age and growth. One would be a direct effect on the annual mean length increment of a cohort. The second would be a cumulative effect on the growth potential of surviving animals.

Growth rates are often calculated from differences in population mean lengths at successive ages within cohorts. Size-selective mortality would affect this increment. For example, if smaller individuals had higher survival than larger individuals, the population mean length-at-age following the period of size-selective mortality would be lower than if mortality had been size-neutral. The estimated growth increment would be biased downward. However, the actual growth increment of the surviving fish, in this case the smaller fish, would be larger than that estimated by the difference in annual population means.

To account for this effect, a direct size-selection index ($S'_{i,y}$) was determined as the difference between the population mean backcalculated length (L) at age $i - 1$ calculated from fish caught in year $i + y$ and those caught in year $i + y - 1$

(2) $$S'_{i,y} = L'_{i-1,i+y,y} - L'_{i-1,i+y-1,y}$$

© 2002 NRC Canada

Table 1. Summary of notation used for the growth equations.

$\bar{L}_{i,y}$	Population mean length at age i and year-class y
$L'_{i,t,y}$	Backcalculated length at age i from fish caught in year t of year-class y
$D'_{i,t,y}$	Backcalculated growth increment from age $i-1$ to age i for fish caught in year t of year-class y
$C'_{i,y}$	Index of cumulative size selection for fish caught at age i of year-class y $C'_{i,y} = L'_{4,i+y,y} - L'_{4,4+y,y}$
$S'_{i,y}$	Index of direct size selection for fish caught at age i of year-class y $S'_{i,y} = L'_{i-1,i+y,y} - L'_{i-1,i+y-1,y}$
$\hat{L}_{i,y}$	Predicted mean length of fish age i of year-class y
$N_{i,y}$	Index of population density at age i of year-class y
$T_{i,y}$	Catch-weighted mean temperature at age i and year-class y
V_t	Mean bottom temperature in year t
$A_{i,y}$	The mean numbers per tow in the research vessel survey for age i and year-class y

Note: All backcalculated variables are denoted by a prime symbol. The backcalculated lengths and growth increments have three subscripts. The first position denotes the annulus (or age) of backcalculation. The second position gives the year in which the fish were caught. The third position is the year-class. The backcalculated lengths represent the fish length at the beginning of the growing season, which is April for this stock.

Negative values indicate that the fish surviving to year $i + y$ were smaller at age $i - 1$ than were fish surviving to year $i + y - 1$. We reasoned that, in such cases, the annual growth increment measured by the difference in population mean length at age i and $i - 1$ for year-class y would be less than if the index was ≥0, all other things remaining equal. We expected the growth parameter associated with this index to have a positive sign.

The second effect of size-selective mortality would be on the growth potential of the survivors. The selective removal of large (or small) individuals would result in the surviving population having a lower (or higher) growth potential. The backcalculated length at age 4 was taken as a growth potential marker for individual fish. This choice was based on the relationship between backcalculated length at young ages and subsequent length-at-age. From the backcalculation database, age-10 and -11 fish were classified into fast- and slow-growing components based on a cluster analysis of their backcalculated lengths at ages 1 to 10 using k-means ($k = 2$) and Ward's method. The ability to discriminate fast- (group 1) and slow-growing (group 2) fish using only backcalculated length at ages 1, 2, 3, or 4 was investigated. The highest discrimination was found with length at age 4, where the percent correct classification was 86% for group 1 and 95% for group 2 (Table 2). The discriminatory power of length at ages 1 and 2 was quite low for the fast-growing group (group 1) at 37% and 57%, respectively. The correlation between the length at age 10 and that at ages 1 and 2 was also relatively weak ($r = 0.24$ and 0.49, respectively), whereas that at age 4 was comparatively strong ($r = 0.77$).

The second size-selection index will be referred to as the cumulative index ($C'_{i,y}$) and it is defined as the year-class-specific difference in the population mean backcalculated length at age 4 between fish caught in year $y + i$ and those caught in year $y + 4$.

$$(3) \qquad C'_{i,y} = L'_{4,i+y,y} - L'_{4,4+y,y}$$

A negative value indicates that smaller, and thus slower-growing, age-4 fish had a higher survival rate than larger fish from that cohort. We expected the growth parameter associated with this index to have a positive sign.

Growth analysis

The von Bertalanffy growth equation has been commonly used to model growth of fish. Although it is possible to linearize the equations (as shown below), there are inherent problems when analyzing annual means because the observations are used as both dependent and independent variables. This problem is avoided if a nonlinear formulation is used to predict annual mean length-at-age (Millar and Myers 1990). It is also possible to use a linear formulation if growth increment data are taken from individual fish. Thus, we have applied a nonlinear analysis to annual mean lengths-at-age and a linear analysis to backcalculated mean growth increment data.

We followed a hierarchical model selection process. The residual sums of squares (RSS) were recorded from models including all possible combinations of effects. For each effect in each model, the sum of squared residuals explained by adding that effect to a model including the other effects was calculated (type III sums of squares). The intent was to find the most parsimonious model that had the lowest RSS and in which each parameter was statistically significant ($P < 0.05$) based on type III sums of squares.

Millar and Myers (1990) investigated three nonlinear formulations of the von Bertalanffy equation that incorporated environmental effects. (*i*) A reversible effect on the growth constant (k), (*ii*) a reversible effect on the terminal length (L_∞), and (*iii*) an irreversible effect on L_∞. We found that formulation (*ii*) provided the best treatment of our data in terms of stability of solutions and overall percent variance explained.

The procedure for the nonlinear estimation was as follows. We began the analyses at age 4, the age of full recruitment to the research survey. It is possible that the size composition of younger fish was not sampled representatively. For each cohort in the analysis, we first estimated the mean length (predicted mean length, $\hat{L}$) at age 4 as

Step 1: age 4

© 2002 NRC Canada

Table 2. Discriminatory power of knowing the length at a relatively young age in predicting the growth potential of individual fish.

	Percent correct classification		
Age	Fast growth	Slow growth	Correlation of length at ages 1 to 4 vs. length at age 10
1	37%	96%	0.24
2	57%	97%	0.49
3	71%	94%	0.62
4	86%	95%	0.77

Note: Cluster analysis was used to classify age-10 and -11 fish into fast- and slow-growth groups based on their backcalculated lengths at ages 1 to 10. The second and third columns give the results of a discriminant analysis of growth type based on observed backcalculated lengths at ages 1 to 4. The final column gives the correlations between backcalculated length at ages 1 to 4 and age 10.

$$(4)\quad \hat{L}_{4,y} = L_{\infty 4,y}(1 - e^{-k(4-t_0)})$$

$$(5)\quad L_{\infty 4,y} = \beta_0 + \beta_4 L'_{4,4+y,y}$$

where t_0 and k are standard von Bertalanffy coefficients, $L'_{4,4+y,y}$ was used as an indicator of variability in growth in the initial years (ages 0 to 3) of the cohort's existence. For ages 5 to 11, the mean lengths-at-age are estimated by summing the estimated mean length at the previous age and the predicted length increment.

Step 2: ages 5 to 11

$$(6)\quad \hat{L}_{i,y} = \hat{L}_{i-1,y} + (L_{\infty i,y} - \hat{L}_{i-1,y})(1 - e^{-k})$$

$$(7)\quad L_{\infty i,y} = \beta_0 + \beta_4 L'_{4,i+y-1,y} + \beta_5 S'_{i,y} + \beta_6 N_{i,y} + \beta_7 T_{i,y} + \beta_8 V_{i+y}$$

The model parameters β_0, β_4, β_5, β_6, β_7, and β_8 were estimated to represent the effects of environmental variables on L_∞. The equation shows all the explanatory variables ($L'_{4,i+y-1,y}$, $S'_{i,y}$, $N_{i,y}$, $T_{i,y}$, V_{i+y}). However, to test the significance of each parameter, all possible combinations were used and the RSS recorded. The significance of the "1-parameter" models (i.e., models with one parameter in addition to the four parameters in the base model) was judged by comparison with a base model that included $L'_{4,4+y,y}$ in step 1 but no explanatory variables in step 2. Note that for ages 5 to 11, the cumulative size-selection factor reduces to the backcalculated length at age 4 for fish caught at age $i - 1$ of year-class y. The cumulative index was used to describe the growth potential of the cohort at the beginning of the growth increment. The direct index was used to describe how the growth increment was modified by size-selective mortality in the year that the growth increment occurred. The eight model parameters (k, t_0, β_0, β_4, β_5, β_6, β_7, β_8) were estimated by minimizing the squared differences between observed and predicted mean lengths-at-age using Proc NLIN of SAS (SAS Institute Inc. 1985). There were 195 observations in the analysis.

A linear analysis of backcalculated growth increments was also used to test for the effects of size-selective mortality, temperature, and density on length-at-age. The growth increments of individual fish were backcalculated between the last and second last annuli and averaged at age and year-class. The von Bertalanffy growth equation may be rearranged (Gulland 1983, p. 91) to represent this increment as

$$(8)\quad D'_{i,i+y,y} = L'_{i,i+y,y} - L'_{i-1,i+y,y} = (L_\infty - L'_{i-1,i+y,y})(1 - e^{-k})$$

Additional explanatory variables (E) were added in a manner that affects L_∞ similar to the nonlinear analysis.

Let $L_\infty = \beta_\infty + \beta_1 E$

$$\beta_3 = 1 - e^{-k}$$

then

$$(9)\quad D'_{i,i+y,y} = \beta_3\beta_\infty + \beta_3\beta_1 E - \beta_3 L'_{i-1,i+y,y}$$

The linear regression, including all explanatory variables, becomes

$$(10)\quad D'_{i,i+y,y} = \beta_0 + \beta_2 L'_{4,4+y,y} + \beta_4 C'_{i,y} + \beta_6 N_{i-1,y} + \beta_7 T_{i-1,y} + \beta_8 V_{i+y-1} - \beta_3 L'_{i-1,i+y,y}$$

Note the subscripts for the environmental effects N, T, and V are for one year before the fish were captured. This is because the growth increment being measured occurred between April in the year previous to capture and March in the year of capture. Most of the growth occurred in the months of April to October in the year previous to capture. The base model for the linear analysis included $L'_{4,4+y,y}$ to account for variability in growth in the early years of the cohort's life (i.e., prior to age 4). Note also that the annual size-selection index was not included in the linear analysis. This is because growth increment data were obtained solely from fish that survived to the year of capture, not from differences in annual population means, as was the case in the nonlinear analysis. There were 192 observations in the analysis.

Results

Nonlinear growth analysis

The most parsimonious nonlinear model included direct size selection, cumulative size selection, population density, and occupied temperature (Table 3). The lowest RSS for the one-parameter models was obtained with a model that included the direct size-selection index. Models with only cumulative size selection, population density, or occupied temperature also had relatively low RSS. The poorest fit was obtained with bottom temperature. For the two-parameter models, the lowest RSS was for a model with direct size selection and population density, followed closely by the

© 2002 NRC Canada

Table 3. Residual sums of squares (RSS) and sums of squares explained by the addition of specific variables for all 1-, 2-, 3-, 4-, and 5-parameter nonlinear growth models.

		Sum of squares explained by this variable				
Model	RSS	*C*	*S*	*N*	*T*	*V*
Base	4356					
1 Parameter						
C	2552	**1804**				
*S**	1408		**2948**			
N	2575			**1781**		
T	2940				**1416**	
V	4311					45
2 Parameters						
CS	942	**466**	**1610**			
CN	1714	**861**		**838**		
CT	2255	**561**			**297**	
CV	2179	**2132**				**373**
*SN**	924		**1651**	**484**		
ST	1000		**1816**		**408**	
SV	1396		**2915**			12
NT	2294			**522**	**281**	
NV	2377			**1934**		**198**
TV	2675				**1636**	**141**
3 Parameters						
CTV	1735	**940**			**444**	**520**
CNV	1678	**699**		**501**		**36**
CNT	1702	**592**		**553**	12	
*CSN**	619	**305**	**1095**	**323**		
CST	789	**211**	**1466**		**153**	
CSV	889	**507**	**1290**			**53**
SNT	815		**1479**	**185**	**109**	
SNV	849		**1528**	**547**		**75**
STV	986		**1689**		**410**	14
NTV	2281			**394**	**96**	13
4 Parameters						
*CSNT**	606	**209**	**1096**	**183**	**13**	
CSNV	619	**230**	**1059**	**270**		0
CNTV	1614	**667**		**121**	**64**	**88**
CSTV	685	**301**	**1050**		**204**	**104**
SNTV	799		**1482**	**187**	**50**	**16**
5 Parameters						
CSNTV	601	**198**	**1013**	**18**	**18**	5

Note: The variables are cumulative size selection (*C*), direct size selection (*S*), population density (*N*), occupied temperature (*T*), and mean bottom temperature (*V*). Bold type indicates variables that were statistically significant at the $\alpha = 0.05$ level. *Lowest sum of squares for the respective number of parameters when the model is significant at $\alpha = 0.05$.

model with cumulative size selection and direct size selection. In all four cases where direct size selection was included in a two-parameter model, its addition accounted for a greater reduction in RSS than did the addition of the other variable to a model including direct size selection. In three of the two-parameter models that included cumulative size selection, the addition of this variable accounted for a greater reduction in RSS than if the other variables were added to a model that included cumulative size selection. The lowest RSS for a three-parameter model was obtained with direct size selection, cumulative size selection, and population density. The second lowest RSS was for a model with cumulative size selection, direct size selection, and occupied temperature. In all six cases where direct size selection was included in a three-parameter model, its addition accounted for a greater reduction in RSS than if the other variables were added to a model including direct size selection. The lowest RSS in a four-parameter model was obtained with cumulative size selection, direct size selection, population density, and occupied temperature. The addition of bottom temperature to a model with cumulative size selection, direct size selection, and population density had little effect on the RSS and an *F*-test was not significant for the additional parameter. Similarly, an *F*-test did not justify using the most complex five-parameter model. The parameter estimates for the preferred model are given below.

$$(11)\quad \hat{L}_{4,y} = (-5.0105 + 2.8131 L'_{4,4+y,y})(1 - e^{-0.0819(4+2.4894)})$$

© 2002 NRC Canada

$$(12)\quad \hat{L}_{i,y} = \hat{L}_{i-1,y} + (-5.0105 + 2.8131 L'_{4,i+y,y} + 11.485 S'_{i,y} - 5.0803 N_{i,y} + 2.8955 T_{i+y} - \hat{L}_{i-1,y})(1 - e^{-0.0819}) \quad \text{for } 5 \le i \le 11$$

The relative influence of the four variables on predicted size-at-age in the nonlinear analysis was determined by multiplying the variable standard deviation by the parameter estimate. The influence, in relative order, was direct size selection (28.8), cumulative size selection (6.6), population density (5.1), and occupied temperature (2.7).

It would have been possible to model cod growth without the size-selection indices and it is instructive to ask what conclusions might have been drawn from such an analysis. If one followed a similar hierarchical model forming process, one would accept a model including population density and occupied temperature. The lowest RSS for a one-parameter model was obtained with population density. For a two-parameter model, the lowest RSS was for a model including population density and occupied temperature. However, the RSS for this model (2294) was considerably higher than that obtained from the two-parameter model including direct size selection and population density (924) and the three-parameter model that included direct size selection, cumulative size selection, and population density (619). The bottom temperature parameter was not statistically significant in the three-parameter model.

The model residuals from the best analysis without size-selective mortality terms showed a substantial temporal trend (Fig. 2). There were large positive residuals in the late 1970s, indicating the model predictions were considerably lower than the observations. There were large negative residuals in the early 1970s and mid-1990s as well. The residual pattern indicated a much better model fit in the preferred analysis that included size-selective mortality (Fig. 2). This suggests that size-selective mortality was a major contributor to the relatively high lengths-at-age observed in the late 1970s and the relatively small lengths in the 1990s.

The effects of size selection, population density, and occupied temperature on the annual mean estimates of L_∞ were summarized as the annual means, across ages, of the parameter estimates times the respective independent variables. For example, for direct size selection, the annual effect for year $i + y$ was calculated as

$$\frac{\sum_{i=4}^{11} \beta_5 S'_{i,y}}{8}$$

The annual variation in L_∞ was affected most by variation in the direct size-selection index (Fig. 3). Direct size selection was the dominant variable in the 1970s producing high estimates of L_∞. The direction reversed but was still dominant during most of the 1980s, but the effect was close to neutral in the latter years of the analysis. Cumulative size selection was the next most important effect, followed closely by population density. Cumulative size selection had a positive effect on L_∞ during the late 1970s. This switched to a negative effect throughout the 1980s and 1990s. During the 1990s, cumulative size selection had the dominant effect on L_∞.

Fig. 2. Model residuals (cm) of mean length-at-age from the best nonlinear growth analyses that (*a*) excluded and (*b*) included size-selective mortality terms.

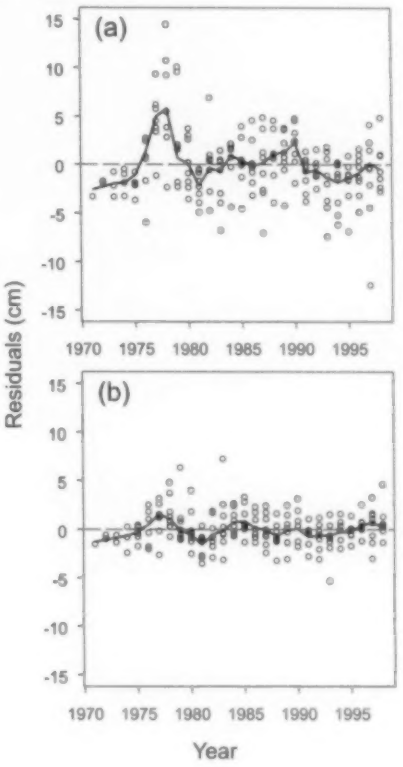

Population density had a positive effect on L_∞ in the 1970s; this changed to a moderate negative effect in the mid-1980s when population size was relatively high, and this effect reversed to a positive effect during the 1990s when population size declined. Occupied temperature had a moderate positive effect on L_∞ in the mid-1970s and early 1980s, a slight negative effect in the mid-1980s to late 1980s, and little effect through the 1990s.

Linear growth analysis

The most parsimonious linear model was obtained using the cumulative size selection and population density variables (Table 4). The one-parameter models including cumulative size selection, population density, or occupied temperature were all statistically significant at the $p < 0.05$ level. The model with only bottom temperature was not. The lowest RSS was obtained with a model including cumulative size selection and the remaining variables produced successively higher RSS in the order of population density, temperature occupied, and bottom temperature. For the two-parameter models, five produced statistically significant parameter estimates for both parameters. The lowest RSS was obtained for the model with cumulative size selection and population density. The bottom temperature parameter was not statistically significant in the model containing cumulative size se-

© 2002 NRC Canada

Fig. 3. The effect of (*a*) direct size selection, (*b*) cumulative size selection, (*c*) population density, and (*d*) occupied temperature on the annual mean predicted L_∞ (cm) from the nonlinear growth analysis.

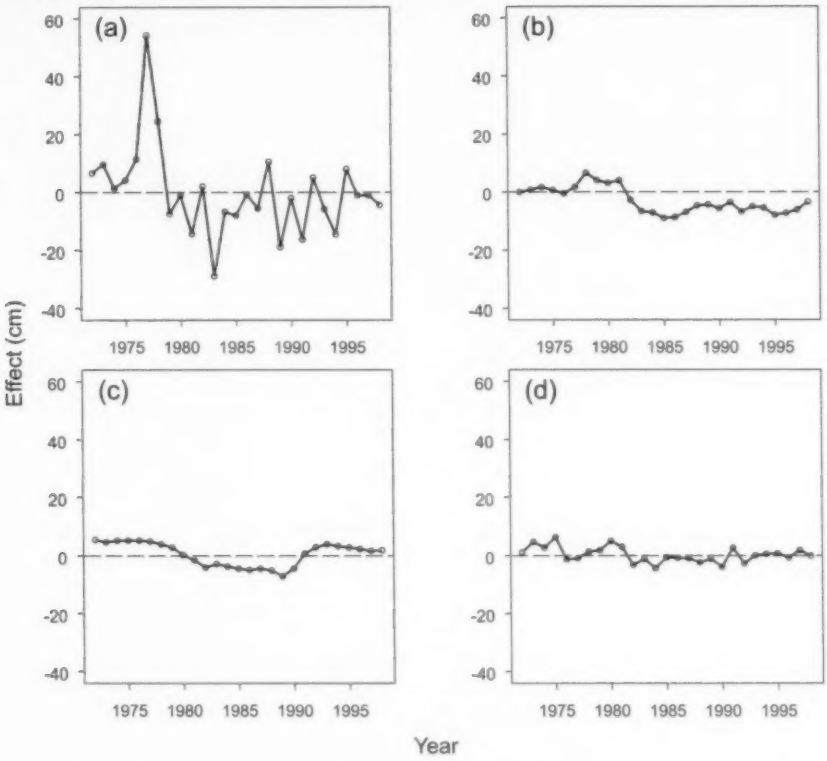

lection. The lowest RSS for a three-parameter model was obtained with the cumulative size selection, population density, and occupied temperature variables. However, the occupied temperature parameter was not statistically significant. In the four-parameter model, neither temperature parameter was significant. The parameter estimates for the preferred model are given below.

$$(13)\quad D'_{i,i+y,y} = 0.805 - 0.129L'_{i-1,i+y,y} + 0.280L'_{4,4+y,y} + 0.295C'_{i,y} - 0.420N_{i-1,y}$$

If one followed a similar hierarchical model-forming process, but ignored the cumulative size-selection variable, one would accept a model including population density and occupied temperature. However, the RSS for this model (199) was considerably higher than that obtained from the two-parameter model including cumulative size selection and population density (119).

The temporal pattern in model residuals from the linear analyses with and without size-selective mortality terms was similar to that from the nonlinear analysis (Fig. 4). When size-selective mortality was not included in the analysis, there were large positive residuals in the late 1970s and many negative residuals in the 1990s. When the size-selective mortality term was included in the analysis, the temporal pattern was greatly improved.

The effects of cumulative size selection and population density on the predicted annual length increments are presented in Fig. 5. These are summarized as the annual means, across ages, of the parameter estimate times the respective independent variables. Population density was low in the early to mid-1970s and the predicted effect on length increment was close to +0.4 cm·year^{-1}. This declined as the population size increased in the late 1970s, and reached approximately –0.5 cm·year^{-1} throughout much of the 1980s. The population declined in the late 1980s and reached a minimum in the early 1990s, at which time the predicted effect on annual mean length increments increased to around +0.3 cm·year^{-1}. The predicted effect of cumulative size selection on the predicted length increment was variable but positive in the 1970s, then it became negative in the early 1980s and reached values as low as –1.0 cm·year^{-1} in 1985. The effect varied between –1.0 and –0.5 cm·year^{-1} throughout the remainder of the study period, although there was a slight increase in the final three years.

Discussion

Our main objective was to determine the relative importance of size-selective mortality, population density, and temperature on size-at-age of a commercial fish stock. Laboratory and field studies have demonstrated that all three factors can affect size-at-age. However, we are not aware of any other study that has attempted to rank their relative importance on

© 2002 NRC Canada

Table 4. Residual sums of squares (RSS) and sums of squares explained by the addition of specific variables for all 1-, 2-, 3-, and 4-parameter linear growth models.

		SS explained by this variable			
Model	RSS	*C*	*N*	*T*	*V*
Base	291				
1 Parameter					
*C**	147	**144**			
N	207		**84**		
T	259			**32**	
V	290				1
2 Parameters					
*CN**	119	**88**	**28**		
CT	142	**117**		**5**	
CV	145	**145**			2
NT	199		**60**	**8**	
NV	201		**89**		**6**
TV	254			**36**	**5**
3 Parameters					
CTV	134	**119**		**11**	**8**
CNV	119	**82**	**26**		0
CNT	118	**81**	**24**	1	
NTV	198		**56**	3	1
4 Parameters					
CNTV	117	**81**	**17**	2	1

Note: The variables are cumulative size selection (*C*), population density (*N*), occupied temperature (*T*), and mean bottom temperature (*V*).*Lowest sum of squares for the respective number of parameters. Bold type indicates variables that were statistically significant at the $\alpha = 0.05$ level.

Fig. 4. Model residuals (cm) of length increments from the best linear growth analyses that (*a*) excluded and (*b*) included size-selective mortality terms.

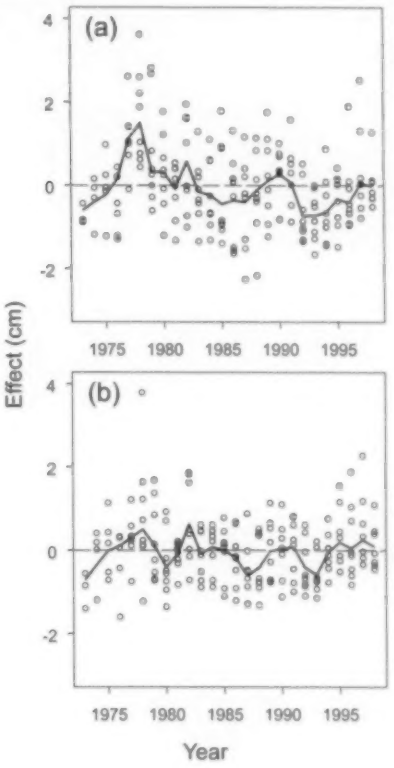

a wild population of any fish species. A number of authors have attempted to model growth of North Sea flatfishes (backcalculated increments from otoliths of commercially caught fishes) as a function of water temperature, eutrophication, population density, and habitat disruption (e.g., Millner and Whiting 1996; Rijnsdorp and van Leeuwen 1996). While they were not strictly comparable to our system, the results were informative. In both studies of flatfish growth, population density (negative), eutrophication (positive), and beam trawl effort (positive) had significant effects on mean length-at-age, whereas temperature measures had no significant effect. Because of the small numbers of otoliths examined in each year (usually <20 otoliths per 5-cm length class), it would have been impossible for the authors to have tested a size-selective mortality index as done in our study. Eutrophication is not a concern in the southern Gulf of St. Lawrence, and possible biases introduced by use of commercially caught fishes (changes in selectivity due to changes in gear or mesh size) were explicitly accounted for by use of fish caught in research trawls.

All of the data used in our analyses were obtained from annual synoptic research vessel surveys, which provided a representative view of the population's characteristics and its environment during the feeding season. All factors were tested in a nonlinear analysis of annual population mean length-at-age and a linear analysis of length increments estimated from backcalculations. The results indicate that size-selective mortality was the dominant factor, followed by population density, and a relatively weak occupied temperature effect. Bottom temperature, measured here as mean bottom temperature during the research vessel surveys, did not produce a significant effect on growth. If we included only one factor at a time, we would find a statistically significant effect for each factor except bottom temperature, but fail to identify the dominant factor in two of three significant cases.

Size-selective mortality was the dominant effect in the growth analyses as indicated by the order in which terms were added to both the nonlinear and linear analyses, the RSS explained by each variable in the preferred models, and the relative magnitude of the predicted effects indicated that size-selective mortality was the dominant effect. There was strong selection for larger fish throughout most of the 1970s and this explained a large part of the above-average lengths-at-age and growth increments during this period. The direction of size selection reversed in the 1980s leading to a large reduction in size-at-age. The direct size-selection index was the stronger of the two size-selection indices in the nonlinear analysis. Its effect on length-at-age has been neutral since the closure of the commercial cod fishery in this area in 1993. The cumulative index was a significant factor in the analysis of population means and the most important factor in the analysis of backcalculated length increments. It was still having a negative effect on growth in the most recent years despite the fishery closure. This suggests that size-selective mortality has important impacts on the growth potential of the population and its effects remain long after the

© 2002 NRC Canada

Fig. 5. The effect of (*a*) cumulative size selection and (*b*) population density on the predicted mean annual backcalculated length increments (cm) from the linear growth analysis.

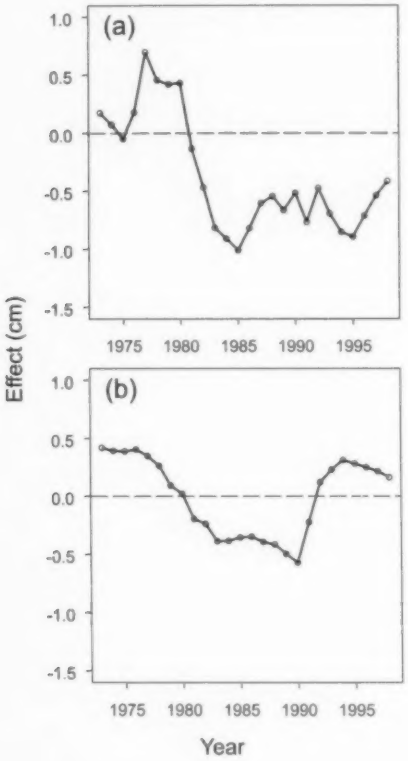

main cause of the selection, fishing in this case, was greatly reduced.

Population density was the next most important effect in the growth analyses. Given that intraspecific competition for food is well established for many fish populations, this was not an unexpected result. Population density was the second main effect to enter both the nonlinear and linear models, explained a large fraction of the model RSS, and the predicted effects exceeded those of temperature. The predicted population density effect on growth was positive in the 1970s and negative in the 1980s, thus being in the same direction as size-selective mortality. However, the density-dependent effect became positive in the 1990s when population size declined and partially compensated for direct and cumulative size-selective mortality in the early 1990s when fishing mortality was high.

Occupied temperature was the third main effect to enter the nonlinear analysis, but was not statistically significant in the linear analysis. Bottom temperature was not a significant factor in either the nonlinear or linear growth analysis. This suggests that variation in temperature had a relatively weak effect on growth. It should also be noted that occupied temperature may interact with population density given evidence for density-dependent habitat selection for this stock (Swain and Kramer 1995). Cod tend to occupy relatively cold temperatures during the feeding season when population density is high. Thus, the population density term in growth models may partly account for effects of occupied temperature (and vice versa).

Although we selected what we considered to be the best environmental indices, it is quite possible that these do not capture the truly important signals. For example, declines in the duration of the feeding season due to delayed migration in cold winters may be an important environmental effect that is not well captured by our September bottom temperature index. Similarly, we have used population abundance as an index for density-dependent effects, though these effects will also depend on variation in prey abundance, availability, and quality. At this time, we do not possess suitable indices for any of these other factors.

That mean lengths-at-age have remained low even after the closure of the commercial fishery suggests that there may have been longer-term changes in population growth characteristics. The cumulative size-selective mortality effect, where existing year-classes have a reduced growth potential, has been a contributing factor and will remain so until the affected cohorts expire. However, it appears that slow-growing individuals may now dominate the population at the youngest ages. Although we have not investigated the potential genetic effects, it is possible that sustained size-selective mortality could cause changes in the gene pool from which recovery to average growth patterns could be even slower (Law 2000).

Our analyses have been focused on changes in population mean length-at-age and mean growth increments. We have not considered the effect that size selection may have on the variance of size-at-age and growth. In our analysis of changes in the direction and magnitude of size-selective mortality (Sinclair et al. 2002), we noted that the population was exposed to disruptive selection where both fast- and slow-growing individuals were favoured. This would presumably increase the variance in size-at-age while having little effect on the mean. It is possible to investigate this phenomenon using individual-based growth models. However, this type of work was beyond the scope of our analysis.

Other recent studies have attributed much of the variation in size-at-age and growth of Atlantic cod to an effect of temperature (e.g., Campana et al. 1995; Dutil et al. 1999; Shelton et al. 1999). However, other potential explanatory factors (e.g., population density, size-selective fishing mortality) were not simultaneously tested along with the effect of temperature in these studies. Thus, effects attributed to temperature may have been spurious, resulting from confounding interactions between temperature and other possible causal factors. For example, Campana et al. (1995) described a large-scale spatial gradient in size-at-age of cod along the eastern coast of Canada and attributed this to a corresponding gradient in bottom water temperature. However, Sinclair and Swain (1996) noted that the gradient in size-at-age also corresponded with a gradient in cod density, with the highest densities in the area with the smallest size-at-age. Our study suggests that both of these factors occurred but were weaker than the effect of size-selective fishing mortality on the southern Gulf cod population. Whether size-selective fishing mortality has had a similar effect on

© 2002 NRC Canada

other northwest Atlantic cod populations is not well understood.

Dutil et al. (1999) suggested that declines in size-at-age of northern Gulf of St. Lawrence cod were related to a cooling of the Gulf from above-average conditions in the early 1980s to below-average conditions in the early 1990s. They noted that correlations between indices of size-at-age and temperature conditions (averaged over the life span of a cohort up to its age of capture) were positive, suggesting faster growth when conditions were warmer. However, these correlations were nonsignificant after adjusting for autocorrelation, although the power of these tests was low (effective degrees of freedom ranged from 3 to 6). Moreover, Castonguay et al. (1999) found that there was no change in the temperatures occupied by cod, leading to the suggestion that the effect of temperature was indirect, perhaps resulting from an earlier migration to the overwintering grounds and shorter feeding season when conditions were cold. Dutil et al. (1999) discounted the possibility of density-dependent effects on growth of northern Gulf cod, noting that correlations between size-at-age and stock biomass were positive (i.e., opposite to the negative correlation expected under density dependence) and that size-at-age remained small in the 1990s when stock biomass had declined to low levels. However, simultaneous tests of the effects of temperature and abundance were not conducted, leaving open the possibility that effects of abundance were obscured by confounding with temperature conditions (and vice versa). Furthermore, in our view, tests for density dependence should relate size-at-age to indices that integrate effects of abundance over the life span of the cohort up to the age at capture (e.g., as Dutil et al. 1999 did in their temperature tests), or should relate annual abundance indices to annual growth increments (e.g., as in this study), rather than relating size-at-capture to stock biomass in the year of capture.

Dutil et al. (1999) also discounted size-selective fishing mortality as a cause of the changes in size-at-age of northern Gulf cod. They noted that cumulative fishing mortality did not increase throughout the 1980s while size-at-age declined, and argued that there would be no consequent increase in size-selective mortality. However, they do report increases in regulated mesh size during this same period. In our view, an increase in mesh size would reduce the vulnerability of small fish to fishing. If fishing mortality remains the same, i.e., if the same proportion of the year-class is removed by fishing, this would mean fishing mortality on larger individuals would have to increase, while that on smaller fish would decrease. The limited backcalculation data presented by Dutil et al. (1999) suggest that mortality was size-selective on recruiting age-classes of northern Gulf cod, with greater mortality for faster-growing cod. The possibility that changes in the intensity of this size selection contributed to the changes observed in size-at-age of northern Gulf cod has not been excluded, and warrants further investigation.

Failure to simultaneously consider alternative mechanisms, especially size-selective mortality, can lead to incorrect conclusions about the role of environmental factors in determining growth. Population density appeared to be the dominant environmental effect on growth of southern Gulf cod in models that did not include indices of size-selective mortality. If we had done this analysis considering only temperature, we would have found a statistically significant result supporting our presumption. Given the apparent importance of size-selective mortality in determining size-at-age of this cod stock, the similarities in trends in length-at-age and fishing regulations in other northwest Atlantic cod stocks (Chouinard and Fréchet 1994; Frank et al. 1994; Taggart et al. 1994), and the relative ease with which indices of size selection can be created from archived otolith collections, it would be prudent to investigate its importance for other stocks before drawing firm conclusions about the relative importance of environmental effects on growth.

Acknowledgements

G. Chouinard provided helpful comments on earlier versions of the manuscript. L. Currie and J. Murphy spent many hours doing otolith measurements and we appreciate their attention to detail. Two anonymous reviewers provided useful comments on an earlier version of the manuscript. R. Kronlund helped with several of the figures.

References

Brander, K.M. 1995. The effect of temperature on the growth of Atlantic cod (*Gadus morhua*). ICES J. Mar. Sci. **52**: 1–10.

Campana, S.E., Mohn, R.K., Smith, S.J., and Chouinard, G.A. 1995. Spatial implications of a temperature-based growth model for Atlantic cod (*Gadus morhua*) off the eastern coast of Canada. Can. J. Fish. Aquat. Sci. **52**: 2445–2456.

Castonguay, M., Rollet, C., Fréchet, A., Gagnon, P., Gilbert, D., and Brêthes, J.-C. 1999. Distribution changes of Atlantic cod (*Gadus morhua*) in the northern Gulf of St. Lawrence in relation to an oceanic cooling. ICES J. Mar. Sci. **56**: 333–344.

Chouinard, G.A., and Fréchet, A. 1994. Fluctuations in the cod stocks of the Gulf of St. Lawrence. ICES Mar. Sci. Symp. **198**: 121–139.

Chouinard, G.A., Sinclair, A., Currie, L., Poirier, G., and Swain, D. 1999. Assessment of cod in the southern Gulf of St. Lawrence, March 1999. DFO Canadian Stock Assessment Secretariat Research Document No. 99/023.

Dutil, J.-D., Castonguay, M., Gilbert, D., and Gascon, D. 1999. Growth, condition, and environmental relationships in Atlantic cod (*Gadus morhua*) in the northern Gulf of St. Lawrence and implications for management strategies in the Northwest Atlantic. Can. J. Fish. Aquat. Sci. **56**: 1818–1831.

Elliot, J.M. 1975. The growth rate of brook trout (*Salmo trutta* L.) fed on reduced rations. J. Anim. Ecol. **44**: 823–842.

Favro, L.D., Kuo, P.K., and McDonald, J.F. 1979. Population-genetic study of the effects of selective fishing on the growth rate of trout. J. Fish. Res. Board Can. **36**: 552–561.

Frank, K.T., Drinkwater, K.F., and Page, F.H. 1994. Possible causes of recent trends and fluctuations in Scotian Shelf / Gulf of Maine cod stocks. ICES Mar. Sci. Symp. **198**: 110–120.

Gulland, J.A. 1983. Fish stock assessment. A manual of basic methods. John Wiley & Sons, Chichester.

Hanson, J.M., and Chouinard, G.A. 1992. Evidence that size-selective mortality affects growth of Atlantic cod (*Gadus morhua* L.) in the southern Gulf of St. Lawrence. J. Fish Biol. **41**: 31–41.

© 2002 NRC Canada

Helser, T.E., and Almeida, F.P. 1997. Density-dependent growth and sexual maturity of silver hake in the north-west Atlantic. J. Fish Biol. **51**: 607–623.

Helser, T.E., and Brodziak, J.K.T. 1998. Impacts of density-dependent growth and maturation on assessment advice to rebuild depleted U.S. silver hake (*Merluccius bilinearis*) stocks. Can. J. Fish. Aquat. Sci. **55**: 882–892.

Kristiansen, T.S., and Svåand, T. 1998. Effect of size-selective mortality on growth of coastal cod illustrated by tagging data and an individual-based growth and mortality model. J. Fish Biol. **52**: 688–705.

Law, R. 2000. Fishing, selection, and phenotypic evolution. ICES J. Mar. Sci. **57**: 659–668.

Millar, R.B., and Myers, R.A. 1990. Modelling environmentally induced change in growth for Atlantic Canada cod stocks. ICES CM 1990/G:24.

Millner, R.S., and Whiting, C.L. 1996. Long-term changes in growth and population abundance of sole in the North Sea from 1940 to the present. ICES J. Mar. Sci. **53**: 1185–1195.

Overholtz, W.J. 1989. Density-dependent growth in the Northwest Atlantic stock of Atlantic mackerel (*Scomber scombrus*). J. Northw. Atl. Fish. Sci. **9**: 115–121.

Parma, A.M., and Deriso, R.B. 1990. Dynamics of age and size composition in a population subject to size-selective mortality: effects of phenotypic variability in growth. Can. J. Fish. Aquat. Sci. **47**: 274–289.

Rijnsdorp, A.D., and van Leeuwen, P.I. 1996. Changes in growth of North Sea plaice since 1950 in relation to density, eutrophication, beam-trawl effort, and temperature. ICES J. Mar. Sci. **53**: 1199–1213.

SAS Institute Inc. 1985. SAS/STAT user's guide, release 5 ed. SAS Institute Inc., Cary, N.C.

Shelton, P.A., Lilly, G.R., and Colbourne, E. 1999. Patterns in the annual weight increment for Div. 2J+3KL cod and possible prediction for stock projection. J. Northw. Atl. Fish. Sci. **25**: 151–159.

Sinclair, A.F., and Swain, D.P. 1996. Comment: spatial implications of a temperature-based growth model for Atlantic cod (*Gadus morhua*) off the eastern coast of Canada. Can. J. Fish. Aquat. Sci. **53**: 2909–2911.

Sinclair, A.F., Swain, D.P., and Hanson, J.M. 2002. Measuring changes in the direction and magnitude of size-selective mortality in a commercial fish population. Can. J. Fish. Aquat. Sci. **59**: 361–371.

Swain, D.P., and Kramer, D.L. 1995. Annual variation in temperature selection by Atlantic cod *Gadus morhua* in the southern Gulf of St. Lawrence, Canada, and its relation to population size. Mar. Ecol. Prog. Ser. **116**: 11–23.

Taggart, C.T., Anderson, J., Bishop, C., Colbourne, E., Hutchings, J., Lilly, G., Morgan, J., Murphy, E., Myers, R., Rose, G., and Shelton, P. 1994. Overview of cod stocks, biology, and environment in the northwest Atlantic region of Newfoundland, with emphasis on northern cod. ICES Mar. Sci. Symp. **198**: 140–157.

Woiwode, J.G., and Adleman, I.R. 1991. Effects of temperature, photoperiod, and ration size on growth of hybrid striped bass × white bass. Trans. Am. Fish. Soc. **120**: 217–229.

© 2002 NRC Canada

Age-structured meta-analysis of U.S. West Coast rockfish (Scorpaenidae) populations and hierarchical modeling of trawl survey catchabilities

Russell B. Millar and Richard D. Methot

Abstract: The swept-area estimates of biomass from the triennial groundfish trawl surveys on the shelf of the U.S. West Coast are believed to seriously underestimate rockfish (Scorpaenidae) stock biomasses. The bulk catchability (Q), defined to be the ratio between swept-area biomass and actual biomass, is herein modeled using a Bayesian age-structured meta-analysis of suitable West Coast rockfish stocks. Six shelf stocks of rockfish were used. The posterior distribution of Q was insensitive to choice of prior and gives a probability of about 0.05 that the bulk catchability of a randomly selected shelf rockfish species will be unity or higher. Between survey variability in bulk catchabilities was modeled as a multiplicative main effect. With individual posterior probabilities in excess of 0.99, bulk catchabilities were lower than normal in 1977 and 1980 and higher than normal in 1989 and 1998. The low catchabilities in 1977 and 1980 are consistent with previously identified problems with lack of bottom contact in the earlier years of the survey. Future work will extend the model to incorporate dynamic modeling of unassessed rockfish stocks, and suggestions for this are given.

Résumé : Les estimations de biomasse basées sur la surface balayée obtenues lors de l'inventaire triennal au chalut des poissons de fond sur la plate-forme continentale de la côte ouest des États-Unis sous-estiment considérablement, croit-on, les biomasses des stocks de sébastes. Nous avons modélisé la capturabilité globale, Q, définie comme le rapport entre la biomasse basée sur la surface balayée et la biomasse réelle, à l'aide d'une méta-analyse bayésienne qui tient compte de la structure en âge chez des stocks appropriés de sébastes de la côte ouest. Six stocks de sébastes de la plate-forme continentale ont été étudiés. La distribution a posteriori de Q n'est pas sensible au choix des valeurs a priori et donne une probabilité d'environ 0,05 que la capturabilité globale d'une espèce de sébaste choisie au hasard soit égale ou supérieure à 1. La variabilité d'un inventaire à un autre a été modélisée comme un effet principal multiplicateur. Avec des probabilités individuelles a posteriori supérieures à 0,99, la capturabilité globale était inférieure à la normale en 1977 et en 1980 et supérieure à la normale en 1989 et en 1998. La faible capturabilité en 1977 et en 1980 s'explique sans doute par le manque de contact avec le fond lors des premières années de l'inventaire, un problème identifié antérieurement. On devra dans le futur étendre le modèle pour y incorporer la modélisation dynamique de stocks pas encore étudiés et on trouvera ici des suggestions pour le faire.

[Traduit par la Rédaction]

Introduction

There are 68 known species of rockfish (Scorpaenidae) between the Gulf of California and the Aleutian Islands (Eschmeyer et al. 1983). At present, up to 20 West Coast rockfish stocks are assessed and individually managed by the Pacific Fisheries Management Council. Commercial catches of the remaining rockfish stocks are subject to a combined allowable catch based on the historical landings within each management area (Rogers et al. 1996).

Bottom trawl surveys for the Washington to California shelf have been conducted by The Resource Assessment and Conservation Engineering Division of the Alaska Fisheries Science Center (National Marine Fisheries Service, Seattle, Wash.) every 3 years since 1977. The species composition of the catch can be extremely varied; for example, the 1998 survey caught 168 different fish species from 55 families (Shaw et al. 2000). Rockfish was the most species-rich family in the 1998 survey, with 37 species represented.

Swept-area estimates of biomass are calculated from each

Received 24 January 2001. Accepted 24 January 2002. Published on the NRC Research Press Web site at http://cjfas.nrc.ca on 5 March 2002.
J16187

R.B. Millar.[1,2] Department of Statistics, Private Bag 92019, University of Auckland, Auckland, New Zealand.
R.D. Methot. Fisheries Resource Analysis and Monitoring Division, National Marine Fisheries Service, 2725 Montlake Boulevard East, Seattle WA 98112-2097, U.S.A.

[1]Corresponding author (e-mail: greebie@scitec.auckland.ac.nz).

[2]This work was done while the first author was a visiting research scientist at the FRAM Division of the National Marine Fisheries Service, 2725 Montlake Blvd East, Seattle WA 98112-2097, U.S.A.

 DOI: 10.1139/F02-009 © 2002 NRC Canada

of the triennial trawl surveys for every rockfish stock encountered. However, these estimates are treated as relative biomass estimates (rather than absolute) if used in a rockfish stock assessment because the catchability of the survey trawl is believed to be different from unity and to vary from stock to stock. Bulk catchability (Q, the ratio of swept-area biomass to true biomass) will be unity if there is no trawl avoidance or herding and the surveyed ground is representative of the stock's habitat. Neither of these requirements holds for the West Coast groundfish survey. There is video evidence of rockfish escaping under the footrope (Rogers et al. 1996), which will lead to swept-area biomass being an underestimate of true biomass, corresponding to Q less than unity. In addition, there are large areas of rough bottom habitat that are untrawlable. If this untrawlable rough bottom is a preferred habitat and has higher rockfish density then trawled areas, then Q will be further reduced. Conversely, if the untrawlable ground is unfavourable habitat then swept-area biomass could be greater than true biomass. For the fully assessed stocks examined by Rogers et al. (1996), the estimates of Q ranged from 0.2 to 0.9.

The purpose of this study is to perform a meta-analysis on the survey trawl bulk catchabilities of selected assessed rockfish stocks. It will not be assumed that Q is common to each stock in the assemblage, but rather, that the values of Q across the stocks can reasonably be described by some underlying probability distribution. If this assumed model structure is reasonable, then it allows the bulk catchability of each stock to be more precisely estimated. Moreover, it can be used to provide prior information on the catchability of similar unassessed stocks and ultimately may permit inference about their biomass from the survey swept-area estimates.

The simplest type of meta-analysis would combine information about Q obtained from the individual stock assessments of suitable rockfish stocks. For example, this information about Q could be in the form of a point estimate and standard error. Variance components analysis (Searle et al. 1992) could then be used to apportion the variability between estimated Qs into an estimation component and a component measuring the between stock variability of the true unknown Qs.

A meta-analysis using the individually estimated Qs and their standard errors was not possible here because the use of the triennial survey data in rockfish assessments varies from stock to stock. Typically, the triennial survey data are just one data component in a complex age-structured model using other data such as recruitment surveys and catch-per-unit effort and catch-at-age data from multiple gear types. It is standard practice for likelihoods corresponding to each of these data components to be given different weightings that are individually adjusted during the stock review process. The estimated Q, and to an even greater extent its variability, depends on the relative weighting given to the triennial survey data.

Moreover, a meta-analysis of individually estimated Qs would not permit simultaneous (over stocks) modeling of year effects. In particular, one of the main reasons that the stock assessors frequently ignore or downweight the triennial survey data is the feeling that the surveys suffer from year effects. It has been shown that year effects of nonneglible size may occur in standardized research surveys (e.g., Myers and Cadigan 1995), and the West Coast triennial surveys would be particularly susceptible to this because they use chartered commercial vessels and are unable to use the same vessels and skippers each time. In addition, it is ultimately desired that information about the multitude of unassessed rockfish stocks could be obtained from the meta-analysis. This phase of the analysis is currently under development and will require modeling of the commercial catch and triennial survey estimates of the unassessed stocks in parallel with the assessed stocks (e.g., Gaichas and Ianelli 1999).

The objective herein was to implement a meta-analysis using a dynamic model for each stock used, thereby permitting the modeling of year effects and providing the flexibility for future extension to unassessed stocks. Because of the impracticality of working with simultaneous full assessments, the approach pursued was to perform simultaneous mini-assessments based on age-structured models of the biomass of each stock.

Materials and methods

Selection of species

The species assemblage work of Rogers and Pikitch (1992) identified an Oregon–Washington shelf assemblage of bottom rockfish including bocaccio (*Sebastes paucispinis*), canary (*Sebastes pinniger*), sharpchin, yelloweye, and yellowtail (*Sebastes flavidus*), a deepwater assemblage including darkblotched, splitnose, and yellowmouth, and an assemblage for widow (*Sebastes entomelas*) rockfish alone. The work of Weinberg (1994) largely corroborated these results, though Weinberg placed widow rockfish in the shelf assemblage.

The available rockfish stock assessments yielded four species included in Weinberg's (1994) shelf assemblage: bocaccio, canary (northern stock), widow, and yellowtail. To these four we added canary (southern stock) and chilipepper (*Sebastes goodei*), a southern species known to be present with canary.

Model justification

Each of the individual assessments uses maximum likelihood implemented using either Stock Synthesis (Methot 1990) or the Automatic Differentiation Model Builder software (ADMB, Fournier 2000). It would be desirable to use the full information about Q from these assessments as input into the meta-analysis. This would formally require specification of the full likelihood function from each assessment. Unfortunately, these likelihoods are extremely complex formulae involving an assortment of constants, data, and parameters. For example, the constants used could include natural mortality, coefficients of variation, magnitude of ageing errors, age-at-recruitment, maximum age, lengths-at-age, weights-at-length, selectivity-at-age, catches, and many others. Data may come from surveys, catch-per-unit-effort, catch-at-age, and more. Included among the parameters could be catchabilities, recruitments, and numbers-at-age. The lists of constants, data, and parameters given above are simply by way of example, and such lists are often in flux during the stock review process. For example, a quantity

© 2002 NRC Canada

such as natural mortality might be treated as a constant in one model and estimated as a parameter in a different version of the model.

For this present investigation, it would be impracticable to use the full likelihood functions because this would be equivalent to performing a simultaneous full assessment for each of the assessed stocks. Instead, the objective was to use a meta-analysis approach that could be implemented using the information provided in the written stock assessment reports for each of the stocks concerned. This necessitated use of a grossly simplified age-structured model for each stock, the validity of which is left to the Discussion.

The essence of an age-structured model is the specification of the age structure at some initial time and specification of the removals-by-age and recruitment in subsequent years. The reasonableness of any time series of numbers-at-age so derived is quantified by the likelihood for the given data. These essential features are preserved by the biomass model used herein. However, the model used herein for each stock is greatly simplified by taking the estimated recruitment series from the full assessment as fixed to within a multiplicative constant. The data to which the model is fitted are the estimated biomass (from the assessment report) immediately before the start of the recruitment series and the swept-area estimates from the triennial surveys.

Data

If y_0^R denotes the year in which the estimated recruitment series reported in the stock assessment document begins, then the estimated (in the stock assessment) recruited biomass in the previous year, $b_{y_0^R-1}$, is regarded as a datum and is modeled as

$$(1) \qquad b_{y_0^R-1} = B^*_{y_0^R-1} e^u$$

where $B^*_{y_0^R-1}$ is the true recruited biomass and u is Normal with mean zero and variance chosen to give the estimated coefficient of variation (CV) of $b_{y_0^R-1}$ as specified in the stock assessment report.

The triennial survey swept-area biomass estimates (Fig. 1) and their CVs for the surveys from 1977 to 1995 were obtained from Wilkins (1996), and the 1998 values were obtained from Shaw et al. (2000). The range of depth and latitudes did vary slightly between some surveys, and these swept-area estimates are based on a standardized range. However, the 1980, 1983, and 1986 surveys did not cover the extreme southern portion of this standardized range. Survey catches in this southern portion from other survey years show that bocaccio and chilipepper are present in this southern portion, and these data were used to estimate the missing swept-area estimates by calculating the proportion found in the southern portion and applying this to the 1980, 1983, and 1986 surveys. To reflect the crudeness of this procedure, a CV of 100% was assumed for these imputed swept-area estimates in the southern portion.

The triennial survey estimates of swept-area biomass, I, are modeled as

$$(2) \qquad I_y = QB_y e^{v_y}, \quad y = 1977,1980,...,1998$$

or equivalently

$$(3) \qquad \log(I_y) = q + \log(B_y) + v_y, \quad y = 1977,1980,...,1998$$

where B_y is the biomass available to the survey, $q = \log(Q)$, and the v_y are iid Normal errors with mean zero. The variance of v_y was chosen to give the estimated CV of I_y provided from the analysis of the triennial survey catch data.

Parameters

The age-structured biomass model has three parameters (Table 1) for each stock. These are historical recruitment (R_0), recruitment series multiplier (d), and bulk catchability of the triennial survey (Q).

The necessary biological quantities (e.g., natural mortality, weight-at-age, selectivity-at-age, maximum age), catch data, and (relative) recruitment series were taken to be fixed and known. The values for these were taken directly from the most recent stock assessment of each stock. These were bocaccio (1999), both canary stocks (1999), chilipepper (1998), widow (2000), and yellowtail (2000). Where necessary, the primary author of the assessment document was contacted for further elaboration and to fill in any gaps in the required input.

With the above quantities assumed known and fixed, for any values of parameters R_0 and d, the numbers-at-age in each year can then be computed. Multiplying these by weight-at-age and summing over ages produces the recruited biomass, B^* (Table 2). The biomass available to the triennial survey (B) is obtained by further multiplying by the selectivity-at-age of the survey gear, before summing over ages.

When the age-structured biomass models are fitted simultaneously in the meta-analysis, then R_{0j}, d_j, and $Q_j = e^{q_j}$ will denote the parameters of the model for stock j. Between-survey deviations in bulk catchability were modeled as a multiplicative main effect. That is, on the log scale,

$$q_{yj} = q_j + \Delta q_y$$

where q_{yj} is the log(catchability) of stock j in year y.

Hierarchical meta-analysis model

The rockfish assessments assume lognormal variability on the survey estimates (eq. 2), and therefore it is more natural to work on the log scale (eq. 3) and to specify the hierarchical model in terms of the log(catchability) parameter, $q = \log(Q)$, instead of Q. The hierarchical meta-analysis places structure on the log(catchability) of each stock in the assemblage by assuming that they are from a common distribution $f(q|\mu_q, \sigma_q^2)$. The structure assumed here is

$$(4) \qquad q|\mu_q, \sigma_q^2 \sim N(\mu_q, \sigma_q^2)$$

Two commonly used methodologies for implementing such a hierarchical model are empirical Bayes and hierarchical Bayes. The details of empirical and hierarchical Bayes analysis can be found in a number of sources (e.g., Casella 1985; Gelman et al. 1995; Efron 1996), and a brief description only is given below.

Empirical Bayes obtains maximum likelihood estimates and, in fact, is not a Bayesian technique at all. In this application, empirical Bayes analysis would find maximum likelihood estimates of R_{0j} and d_j for each of the six stocks and

© 2002 NRC Canada

Fig. 1. Natural log of swept-area biomass estimates from the triennial groundfish survey on the U.S. West Coast shelf: (*a*) bocaccio; (*b*) canary (south); (*c*) canary (north); (*d*) chilipepper; (*e*) widow; and (*f*) yellowtail.

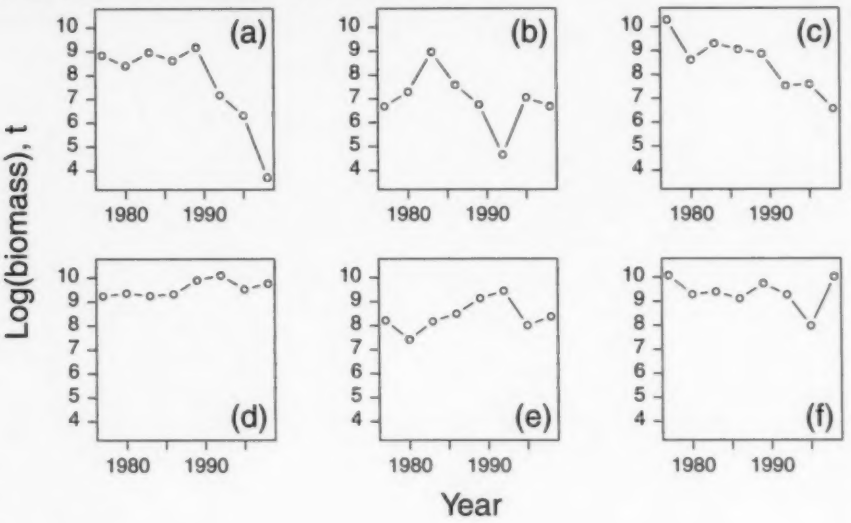

Table 1. Notation.

Constants	
Natural mortality	m
Age of recruitment	a_0
Plus group age	a^+
Start of recruitment index	y_0^R
Start of catch data	y_0^C
Selectivity of commercial gear	s_a^c, $a_0 \le a \le a^+$
Selectivity of triennial survey	s_a^t, $a_0 \le a \le a^+$
Weight-at-age	W_a, $a_0 \le a \le a^+$
Catch data	C_y, $y_0^C \le y$
Recruitment index	R_y, $y_0^R < y$
Indices	
Age	a, $a_0 \le a \le a^+$
Year	y, $y_0^C \le y$
Data	
Triennial survey estimates	I_y, y = 1977,1980,...,1998
Reported recruited biomass in year $y_0^R - 1$	$b_{y_0^R-1}$
Parameters	
Historical recruitment	R_0
Recruitment index multiplier	d
Bulk catchability	Q (= e^q)
Catchability deviations	Δq_y, y = 1977,1980,...,1998
Calculated quantities	
Numbers at age and year	$N_{a,y}$, $a_0 \le a \le a^+$, $y_0^C \le y$
Biomass available to survey	B_y, y = 1977,1980,...,1998
Recruited biomass in year $y_0^R - 1$	$B^*_{y_0^R-1}$
Harvest proportion	h_y, $y_0^C \le y$

estimates of μ_q, σ_q^2 and the eight triennial survey deviations in log(catchability) (Δq_y).

The hierachical Bayes approach specifies prior distributions on the unobserved quantities and implements a Bayesian analysis to obtain their posterior distributions. In particular, the prior distribution on μ_q and σ_q^2, $\pi(\mu_q, \sigma_q^2)$, is called a hyperprior, and integration of $f(q|\mu_q, \sigma_q^2)$ with respect to this hyperprior yields the marginal prior on q. That is,

$$\pi(q) = \int\int f(q|\mu_q,\sigma_q^2)\,\pi(\mu_q,\sigma_q^2)\,d\mu_q\,d\sigma_q^2 \quad (5)$$

© 2002 NRC Canada

Table 2. The formulae given here describe the age-structured biomass model that was applied to each stock.

$W_a = \alpha[L_\infty(1 - e^{-k(a-t_o)})]^\beta$
$h_y = \dfrac{C_y}{\sum_a s_a^C N_{a,y} W_a}$
$N_{a,y_0^C} = e^{R_0} e^{-(a-a_0)m}, \quad a_0 \le a < a^+$
$N_{a^+,y_0^C} = N_{a^+-1,y_0^C}(1 - e^{-m})^{-1}$
$N_{a_0,y} = e^{R_0}, \quad y_0^C \le y < y_0^R$
$N_{a_0,y} = dR_y, \quad y_0^R \le y$
$N_{a,y} = N_{a-1,y-1}(1 - s_a^C h_{y-1})e^{-m}, \quad a_0 < a < a^+, \; y_0^C < y$
$N_{a^+,y} = (N_{a^+-1,y-1}[1 - s_{a^+-1}^C h_{y-1}] + N_{a^+,y-1}[1 - s_{a^+}^C h_{y-1}])e^{-m}, \quad y_0^C < y$
$B_y = \sum_a s_a^I N_{a,y} W_a$
$B_{y_0^R-1}^{\Phi} = \sum_a N_{a,y_0^R-1} W_a$

Note: The initial year, y_0^C, is the first year of available catch data. A constant historical recruitment is used up to the start of the recruitment index in year y_0^R. In all assessments, the recruitment index began in the same year or later than the catch series (i.e., $y_0^C \le y_0^R$).

The division among statisticians regarding which is the better methodology to use exists at both the practical and philosophical levels. Here, the decision to use hierarchical Bayes was driven by the awareness that the results would be applied in the Bayesian sense. For example, the hyperposterior distribution on μ_q and σ_q^2, $\pi(\mu_q, \sigma_q^2|\mathbf{D})$, can be used to obtain the marginal posterior for log(catchability),

$$(6) \qquad \pi(q|\mathbf{D}) = \int\int f(q|\mu_q,\sigma_q^2)\,\pi(\mu_q,\sigma_q^2|\mathbf{D})\mathrm{d}\mu_q\mathrm{d}\sigma_q^2$$

where **D** denotes the data used in the meta-analysis. This posterior distribution represents knowledge about q subsequent to the Bayesian analysis herein and, hence, could be considered a prior distribution on q in future Bayesian analyses of other suitable stocks in the shelf assemblage.

Equation 6 differs from eq. 5 only by the replacement of the hyperprior on (μ_q, σ_q^2) by its hyperposterior, thereby using the knowledge about μ_q and σ_q^2 obtained from the meta-analysis. Equation 6 does not apply to the catchability of stocks used in the meta-analysis because these catchabilities appear in the likelihood function for **D**. That is, knowledge about these catchabilities is provided directly from the data, rather than through the hyperposterior. To make this distinction, the posteriors for the log(catchability) of stocks used in the meta-analysis will will be denoted by $p_j(q|\mathbf{D})$, where the j subscript (j = 1, ...,6) is used to denote the log(catchability) of bocaccio, canary (southern stock), canary (northern stock), chilipepper, widow, and yellowtail, respectively. The posteriors for catchability will be denoted $p_j(Q|\mathbf{D})$.

A normal hyperprior distribution was placed on μ_q, and an inverse gamma distribution was placed on σ_q^2. To check sensitivity to prior specification, two sets of hyperpriors on μ_q and σ_q^2 were used. The parameters of the hyperpriors were selected by inspecting the resulting marginal prior (from eq. 5) on $Q = e^q$ (Fig. 2).

Hyperprior 1

$$\mu_q \sim N(0, 1)$$

$$\sigma_q^2 \sim \Gamma^{-1}(1, 2)$$

Hyperprior 2

$$\mu_q \sim N(-1, 1)$$

$$\sigma_q^2 \sim \Gamma^{-1}(1, 1)$$

where $\Gamma^{-1}(\alpha, \beta)$ denotes an inverse gamma distribution with the associated gamma distribution having mean $\alpha\beta$ and variance $\alpha\beta^2$. The first induces a vague prior for Q with median slightly in excess of unity and an extremely long and slowly decaying right tail (Table 3, Fig. 2). The second prior is mildly informative and reflects a higher prior belief that catchability is below unity (Table 3, Fig. 2).

The historical recruitments (R_{0j}) and recruitment index constants (d_j) were given flat priors on the log scale (the usual noninformative prior for scale parameters). Between-survey deviations in log(catchability) (Δq_y) were given a vaguely informative normal prior with mean 0 and standard deviation 0.5.

The hierarchical Bayesian model was implemented using the ADMB software (Fournier 2000), which uses the Metropolis–Hastings form of Markov Chain Monte Carlo to sample from the joint posterior distribution (Gelman et al. 1995).

DAG representation of model

Directed acyclic graphs (DAGs) are explained in Meyer and Millar (1999) and a very brief description only is given here. The DAG representation (Fig. 3) of the above model represents fixed quantities using rectangular nodes. Eliptical nodes represent stochastic quantities, which may be model parameters or functions of model parameters. Double-width arrows indicate that the target is a deterministic function of the quantities in the source nodes. Single-width arrows indicate that the target is a stochastic value with distribution depending on the values of the quantities in the source nodes, which herein applies to quantities $b_{y_0^R-1}$ (eq. 1), I_y (eq. 2), and q (eq. 4). Repetitive parts of the model are shown within the large stacked "plates".

Results

The joint posterior of 28 quantities was monitored: the R_{0j}, d_j, and q_j parameters from the age-structured biomass model for each of the six stocks, the eight triennial survey deviations in log(catchability), and μ_q and σ_q^2. Samples from the joint posterior were generated at a rate of 125 000 per hour on a 500 MHz computer. However, preliminary inspection of the samples showed high autocorrelation, and because of this and the need to moderate the quantity of information saved to disk, a 1 in 500 thinning of the chain was used. For both the vague and informative hyperpriors on μ_q and σ_q^2, this thinning was applied to a run of 1 000 000 samples, resulting in 2000 samples from the joint posterior being saved to disk. Convergence and stationarity were verified using the BOA diagnostic package (freely available from http://www.public-health.uiowa.edu/boa/).

© 2002 NRC Canada

Fig. 2. Marginal prior and posterior densities for (*a*) μ_q, (*b*) σ_q^2, (*c*) log(catchability), q, and (*d*) bulk catchability (Q): vague prior (– · – ·); resulting posterior (– – – –); informative prior (– – · ·); resulting posterior (····).

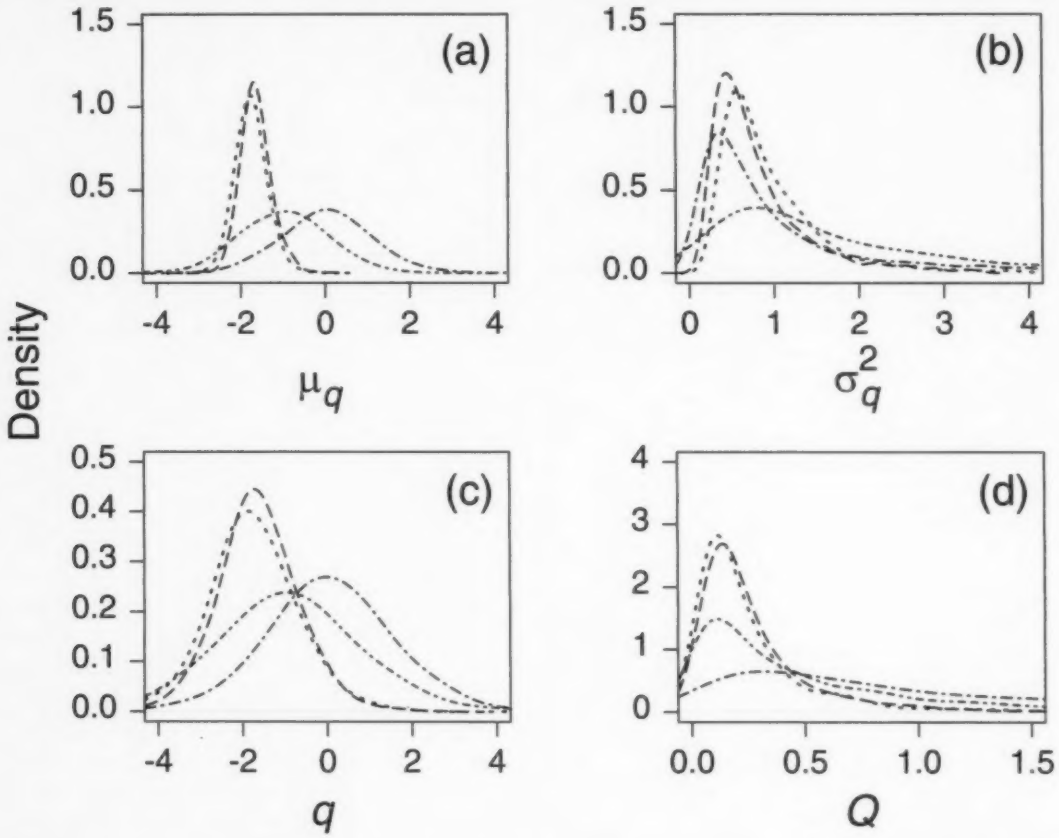

Table 3. Summary statistics for the prior and posterior distributions of bulk catchability, Q, arising from the vague and informative hyperpriors on μ_q and σ_q^2.

	10% quantile	Lower quantile	Median	Upper quantile	90% quantile	Prob($Q > 1$)
Vague hyperprior						
$\pi(Q)$	0.16	0.41	1.04	2.61	6.23	0.51
$\pi(Q\|\mathbf{D})$	0.06	0.11	0.19	0.35	0.67	0.06
LN(–1.63,0.92)	0.06	0.10	0.20	0.37	0.67	0.05
Informative hyperprior						
$\pi(Q)$	0.05	0.15	0.39	1.16	3.32	0.27
$\pi(Q\|\mathbf{D})$	0.05	0.09	0.17	0.33	0.63	0.05
LN(–1.75,1.07)	0.05	0.09	0.17	0.35	0.65	0.05

Note: Also shown are the summary statistics for a lognormal (LN) distribution having the same mean and variance (on the log scale) as the posterior distribution of $q = \log(Q)$.

The marginal posterior densities of μ_q, σ_q^2, q (eq. 6), and Q are similar under both hyperpriors (Fig. 2), despite the fact that the modes of the priors are quite different. This suggests that the hierarchical model is informative about catchability. The three quartiles of the posterior density for Q, $\pi(Q|\mathbf{D})$, differ by at most 0.02 under the two hyperpriors, and the posterior probability that Q will exceed unity is 0.06 under the vague hyperprior and 0.05 under the informative hyperpior (Table 3).

For both hyperpriors, $\pi(q|\mathbf{D})$ is close to normal (Fig. 2), suggesting that $\pi(Q|\mathbf{D})$ should be well approximated by a lognormal distribution. The quantiles from the lognormal distribution with parameters (on the log scale) corresponding to the mean and variance of $\pi(q|\mathbf{D})$ are close to the observed quantiles of $\pi(Q|\mathbf{D})$ (Table 3) and these lognormal distributions would provide accurate and convenient induced priors for Q in future inference.

The posterior densities, $p_j(Q|\mathbf{D})$, for the bulk catchabilities of the six stocks used in the meta-analysis are virtually identical under both hyperpriors (Fig. 4). The posterior for widow

© 2002 NRC Canada

Fig. 3. Model representation in the form of directed acyclic graphs. (Nonitalicized quantities are used to denote vectors with respect to age, for example, $\mathbf{s}^C_j$ denotes the vector of selectivity-at-age for stock j by the commercial gear.) (*a*) Component of the model fitted to the recruited biomass in the year before the start of the recruitment index (eq. 1); (*b*) component of the model fitted to the triennial survey estimates of swept-area biomass (eq. 2). The nodes labeled $I_{y,j}$ and $\mathrm{Var}(I_{y,j})$ are only applicable for the 8 years (between 1977 and 1998 inclusive) in which the survey was conducted.

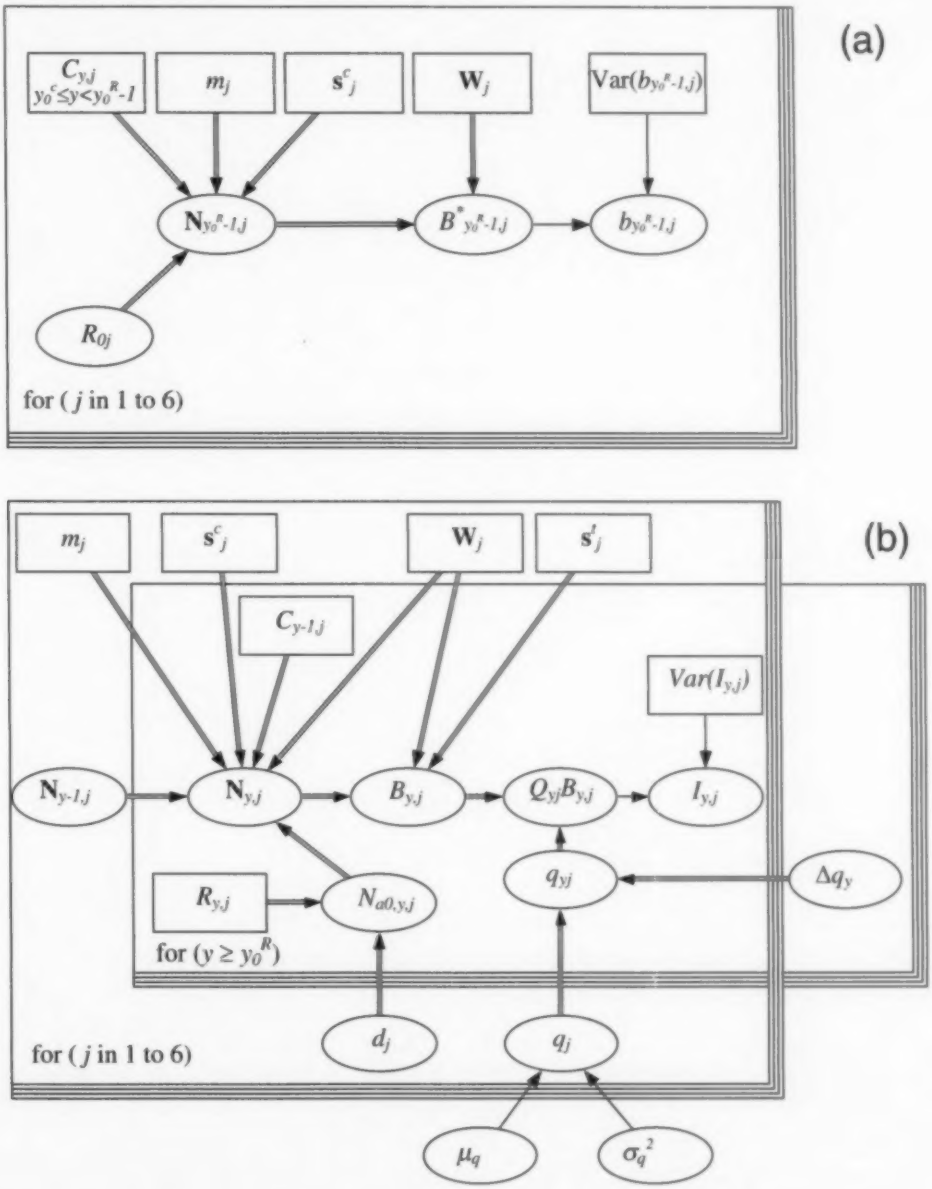

rockfish is noticeably different from that of the other five stocks, putting almost all mass on values of Q_{widow} below 0.1.

The posterior densities for between survey deviations in q (Fig. 5) show that some surveys have high posterior probability of having catchability differing from average. In particular, with individual probabilities in excess of 0.99, the 1977 and 1980 surveys had below average catchability, and the 1989 and 1998 surveys had above average catchability. These deviations are on the scale of $q = \log(Q)$, and hence a deviation of –0.25 (say) corresponds to catchability dropping to $e^{-0.25} = 0.78$ of average.

Discussion

Rockfish catchability

The vague and informative hyperpriors on μ_q and σ_q^2 produce (via eq. 5) prior probabilities of 0.51 and 0.27, respectively, of Q being in excess of unity. The posterior

© 2002 NRC Canada

Fig. 4. Marginal posterior densities for log(catchability), $p_j(q|\mathbf{D})$, from using the vague hyperprior: (*a*) bocaccio; (*b*) canary (south); (*c*) canary (north); (*d*) chilipepper; (*e*) widow; and (*f*) yellowtail. The posteriors obtained from using the informative hyperprior are essentiaily identical and are not shown.

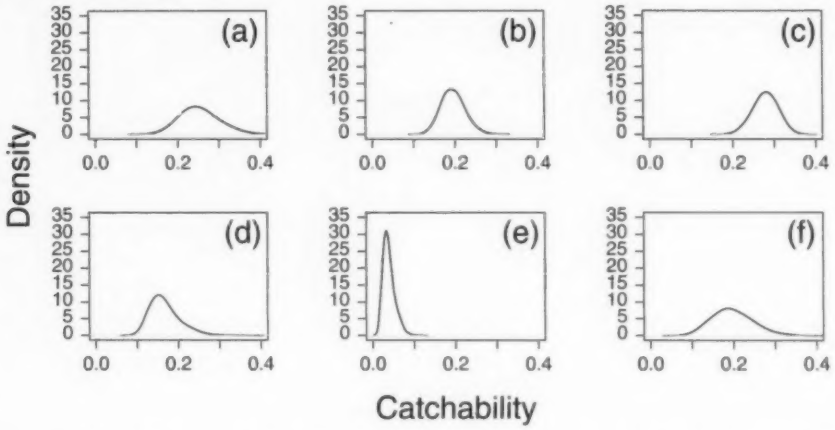

Fig. 5. Marginal posterior densities on between survey deviations in log(catchability), Δq_v, from using the vague hyperprior: (*a*) 1977; (*b*) 1980; (*c*) 1983; (*d*) 1986; (*e*) 1989; (*f*) 1992; (*g*) 1995; and (*h*) 1998. The posteriors obtained from using the informative hyperprior are essentially identical and are not shown.

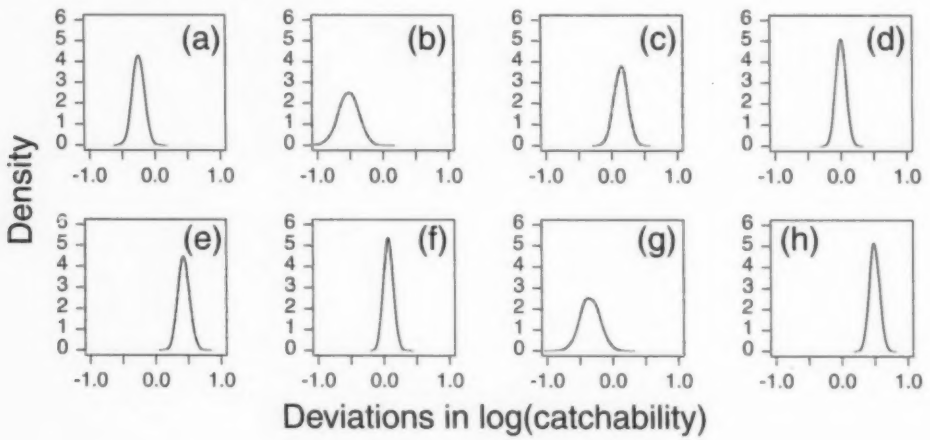

distribution $\pi(Q|\mathbf{D})$ (from eq. 6) can be interpretted as an "induced prior" for Q in the sense that it would serve as a prior distribution for the catchability of that stock if a similar new stock was to be added to the shelf assemblage. This "induced prior" puts a much lower probability on the catchability of the new stock being in excess of unity because it is utilizing the knowledge obtained from this meta-analysis of six other stocks in the assemblage.

There is strong evidence that widow rockfish have a considerably lower catchability than the other five stocks. This was not unexpected because it is known that widow rockfish exhibit diurnal schooling behaviour that is atypical for rockfish and spend time off the bottom and, in fact, have been targeted by a midwater trawl fishery (Gunderson 1984). Arguably, widow rockfish could have been omitted for these reasons.

The inclusion or exclusion of stocks from the meta-analysis is a difficult decision and is intimately related to what other stocks one might which to apply the induced prior to. Here, all available assessed shelf-assemblage rockfish stocks were used, and therefore, there are less caveats regarding the applicability of these results to other (presently unassessed) shelf stocks. Had widow been excluded, then $\pi(Q|\mathbf{D})$ would be tighter because of reduced variability in catchability between stocks. This would be reflecting use of an assemblage with stocks believed to have reasonably similar catchabilities, and in consequence, applicability of the posterior to a new stock becomes more dependent on that new stock being like the others in the assemblage. In Bayesian terminology, the stocks must be considered "exchangeable". Here, this means that they must all adhere to eq. 4. A modification of this would be to include biological information on the stock, perhaps by making μ_q a function of a relevant biological variable.

A recent re-inspection of the individual-haul catches in

© 2002 NRC Canada

the triennial trawl surveys (Zimmerman et al. 2001) has indicated a problem with the gear maintaining bottom contact, and it is particularly severe in 1977 and 1980. These years correspond to two strong negative deviations in survey catchability.

Model criticism

The biggest weakness of the age-structured biomass model used herein may be the use of the estimated recruitment series from the full assessments. The model uses these recruitment sequences as fixed and known indices of relative recruitment, so in effect the recruitment values used in the model can only vary in overall magnitude. Within the highly parameterized full assessment models, the recruitment sequence can vary in magnitude and in yearly deviations (subject to possible penalties on lack of smoothness). Thus, the age-structured biomass model is not able to model some of the uncertainty in the inputted values of the estimated recruitment sequence. However, this may not be too severe because most of the full assessments use extensive catch-at-age data, and therefore, there may not be a great amount of variability in the estimated (relative) recruitment deviations.

Referees of this manuscript pointed out that the results may be sensitive to the model specification and the assumed inputs, especially the assumption of known natural mortality. Such concerns apply to fisheries models in general. In Bayesian models, it is often a simple matter (Millar and Meyer 2000*a*) to incorporate many of these model variants (by putting a prior distribution on natural mortality, say). The more difficult matter is model assessment and comparison, which is currently an area of active research in the theoretical Bayesian literature.

A further relevant consideration in Bayesian modeling is the reliability of the Markov Chain Monte Carlo implementation used to obtain the samples from the joint posterior distribution. Here, these samples were very highly autocorrelated and only 1 in every 500 was saved to disk. This rate of thinning is very extreme, but it did result in a sample that satisfied the convergence diagnostics. Reparameterizing the model can be very effective at reducing the autocorrelation (Millar and Meyer 2000*b*) and is an approach that could be explored here. Another possibility would be to take the reference biomass datum (eq. 1) in an intermediate year rather than the year prior to the start of the recruitment series.

Future work will investigate the potential to obtain inference about unassessed rockfish species. An approach similar to that of Gaichas and Ianelli (1999) could be used. They used dynamic state–space models to smooth the biomass estimates of "other species" from the Gulf of Alaska triennial bottom trawl surveys. Their biomass dynamics equation was

$$(7) \qquad B^*_y = B^*_{y-1} e^{w_y} - C_{y-1}$$

where w_y are iid Normal random variables that describe the natural variability in biomass and C_{y-1} is the catch in year $y - 1$. Equation 7 provides a smoothed biomass trajectory that can be fitted to the observed triennial survey data. Within a Bayesian analysis, the posterior density $\pi(Q|\mathbf{D})$ could be used as an induced prior on Q. In addition, further information may be incorporated by modeling some commonality between the harvest proportions across species (Gaichas and Ianelli 1999).

References

Casella, G. 1985. An introduction to empirical Bayes data analysis. Am. Stat. **39**: 83–87.

Efron, B. 1996. Empirical Bayes methods for combining likelihoods. J. Am. Stat. Assoc. **91**: 538–565.

Eschmeyer, W.N., Herald, E.S., and Hammann, H. 1983. A field guide to Pacific coast fishes of North America. Houghton Mifflin Co., Boston, Mass.

Fournier, D.A. 2000. An introduction to AD Model Builder Version 4 for use in nonlinear modeling and statistics. Otter Research Ltd., Sidney, B.C., Canada.

Gaichas, S., and Ianelli, J.N. 1999. An approach to analyzing multispecies complexes in data limiting situations. Appendix E. *In* Stock assessment and fishery evaluation for groundfish resources in the Gulf of Alaska region as projected for 2000. North Pacific Fishery Management Council, P.O. Box 103136, Anchorage, AK 99510.

Gelman, A., Carlin, J.B., Stern, H.S., and Rubin, D.B. 1995. Bayesian data analysis. Chapman and Hall, London.

Gunderson, D.R. 1984. The great widow rockfish hunt of 1980–1982. N. Am. J. Fish. Manag. **4**: 465–468.

Methot, R.D. 1990. Synthesis model: an adaptable framework for analysis of diverse stock assessment data. INPFC Bull. **50**: 259–277.

Meyer, R., and Millar, R.B. 1999. BUGS in Bayesian stock assessment. Can. J. Fish. Aquat. Sci. **56**: 1078–1087.

Millar, R.B., and Meyer, R. 2000*a*. Bayesian state–space modeling of age-structured data: fitting a model is just the beginning. Can. J. Fish. Aquat. Sci. **57**: 43–50.

Millar, R.B., and Meyer, R. 2000*b*. Non-linear state space modelling of fisheries biomass dynamics by using Metropolis–Hastings within-Gibbs sampling. Appl. Stat. **49**: 327–342.

Myers, R.A., and Cadigan, N.G. 1995. Statistical analysis of catch-at-age data with correlated errors. Can. J. Fish. Aquat. Sci. **52**: 1265–1273.

Rogers, J.B., and Pikitch, E.K. 1992. Numerical definition of groundfish assemblages caught off the coasts of Oregon and Washington using commercial fishing strategies. Can. J. Fish. Aquat. Sci. **49**: 2648–2656.

Rogers, J.B., Wilkins, M.E., Kamikawa, D., Wallace, F., Builder, T., Zimmerman, M., Kander, M., and Culver, B. 1996. Appendix E: status of the remaining rockfish in the Sebastes complex in 1996 and recommendations for management in 1997. *In* Appendix Volume II to the Status of the Pacific Coast groundfish fishery through 1996 and recommended acceptable biological catches for 1997. Pac. Fish. Manag. Council, Portland, OR 97201.

Searle, S.R., Casella, G., and McCulloch, C.E. 1992. Variance components. Wiley, New York.

Shaw, F.R., Wilkins, M.E., Weinberg, K.L., Zimmermann, M., and Lauth, R.R. 2000. The 1998 Pacific West Coast bottom trawl survey of groundfish resources: estimates of distribution, abundance, and length and age composition. U.S. Department of Commerce, NOAA Tech. Memo. NMFS-AFSC-114.

Weinberg, K.L. 1994. Rockfish assemblages of the middle shelf and upper slope off Oregon and Washington. Fish. Bull. **92**: 620–632.

Wilkins, M.E. 1996. Appendix F: long term trends in abundance: results of triennial bottom trawl surveys of west coast groundfish resources between 1977 and 1995. *In* Appendix Volume II to the Status of the Pacific Coast groundfish fishery through

© 2002 NRC Canada

1996 and recommended acceptable biological catches for 1997. Pac. Fish. Manag. Council, Portland, OR 97201.

Zimmerman, M., Wilkins, M.E., Weinberg, K.L., Lauth, R.R., and Shaw, F.R. 2001. Retrospective analysis of suspiciously small catches in the National Marine Fisheries Service West Coast triennial bottom trawl survey. U.S. Department of Commerce, NOAA, NMFS-AFSC Processed Rep. 2001-03.

© 2002 NRC Canada

Accounting for local physiological adaptation in bioenergetic models: testing hypotheses for growth rate evolution by virtual transplant experiments

Stephan B. Munch and D.O. Conover

Abstract: We constructed bioenergetic models for locally adapted populations of Atlantic silversides, *Menidia menidia*, from different latitudes (Nova Scotia and South Carolina) to determine how genetic variation in growth physiology affects model parameters and predicted growth and to test two hypotheses on the evolution of countergradient variation in growth rate. Model parameters were estimated simultaneously for each population through a penalized likelihood approach incorporating laboratory measurements of metabolism, specific dynamic action, consumption, and growth. The resulting population-specific parameters differed by an average of 28%. The models were validated by successful ($R^2 > 0.9$) prediction of growth in independent experiments under natural light and temperature conditions and by predicting growth in the field ($R^2 > 0.95$). We then performed virtual reciprocal transplant simulations to test the alternative hypotheses that growth rate along a latitudinal gradient evolves in response to temperature or resource availability. Predictions for each transplanted population deviated significantly from observed growth for each native population, demonstrating the importance of accounting for interpopulation variation in model parameters. Our results indicate that the latitudinal cline in growth rate cannot be explained solely by thermal adaptation but may have arisen owing to the combined effects of temperature and food availability.

Résumé : Nous avons élaboré un modèle bioénergétique pour étudier comment la variation génétique de la physiologie de la croissance affecte les paramètres du modèle et la croissance prédite ainsi que pour vérifier deux hypothèses sur l'évolution de variation à contre-gradient dans le taux de croissance chez des populations adaptées localement de capucettes, *Menidia menidia*, de latitudes différentes (Nouvelle-Écosse et Caroline du Sud). Une méthodologie de vraisemblance pénalisée qui incorpore les données de laboratoire sur le métabolisme, l'action dynamique spécifique, la consommation et la croissance nous a permis d'estimer simultanément pour chaque population les paramètres du modèle. Les paramètres spécifiques des populations différaient en moyenne de 28 %. Le modèle a été validé par la réalisation de prédictions de croissance dans des expériences indépendantes en laboratoire sous des conditions naturelles de lumière et de température ($R^2 > 0{,}9$) et en nature ($R^2 > 0{,}95$). Nous avons ensuite procédé à des simulations de transplantations réciproques virtuelles pour éprouver l'hypothèse alternative voulant que le taux de croissance varie le long d'un gradient latitudinal en fonction de la température et de la disponibilité des ressources. La croissance prédite pour chaque population transplantée différait significativement de celle qui prévalait chez la population indigène, ce qui démontre l'importance de tenir compte de la variation entre les populations quant aux paramètres du modèle. Nos résultats montrent que le gradient latitudinal des taux de croissance ne peut s'expliquer simplement par l'adaptation thermique, mais qu'il doit provenir des effets combinés de la température et de la disponibilité des ressources.

[Traduit par la Rédaction]

Introduction

Bioenergetic models (Kerr 1971; Kitchell et al. 1977) are commonly used to estimate growth or consumption of fish in several environments. These models are typically constructed at the species level and are based on parameters estimated through a set of lab experiments or borrowed from other species. Even when used over broad geographic ranges (Chambers et al. 1995), all prior bioenergetic models have ignored local adaptation in growth physiology and thereby implicitly assumed that variation in growth within a species is entirely environmental. Recent findings, however, challenge the notion that local adaptation in growth physiology may be ignored. Geographic variation in the genetic capacity for growth has been demonstrated for numerous fishes, e.g., the Atlantic silverside (*Menidia menidia*; Conover and Present 1990), Atlantic salmon (*Salmo salar*; Nicieza et al. 1994), striped bass (*Morone saxatilis*; Conover et al. 1997), and pumpkinseed (*Lepomis gibbosus*; Arendt and Wilson 1999). These fishes and others exhibit a common pattern of

Received 14 November 2000. Accepted 16 January 2002. Published on the NRC Research Press Web site at http://cjfas.nrc.ca on 5 March 2002.
J16065

S.B. Munch[1] and D.O. Conover. Marine Sciences Research Center, State University of New York at Stony Brook, Stony Brook, NY 11794-5000, U.S.A.

[1]Corresponding author (e-mail: munch@pro.msrc.sunysb.edu).

 DOI: 10.1139/F02-013 © 2002 NRC Canada

local adaptation known as countergradient variation (CnGV; Conover 1990; Conover and Shultz 1995), which exists when the distribution of genetic effects on a trait counters environmental effects such that phenotypic variation along an environmental gradient is minimized (Levins 1968).

Because of the seemingly obvious fitness benefits of rapid growth and large size in the early life history of fishes (Houde 1987; Sogard 1997; Blanckenhorn 2000), the existence of CnGV is paradoxical. Why would southern populations evolve rates of growth that are submaximal? Several alternate hypotheses attempting to explain locally adapted growth rates exist in the literature. The most common is that populations are adapted to the local thermal regime (Lonsdale and Levinton 1985) such that the ability to grow at high temperatures is achieved at the expense of growth at low temperatures. An alternative explanation not frequently applied to growth in fishes is that populations are adapted to local food availability (Niewiarowski and Roosenburg 1993), i.e., adaptation of growth to resource-limited environments is achieved at the expense of capacity for growth when resources are abundant. Which of these hypotheses may explain CnGV remains unclear.

In this study, we focus on CnGV over a latitudinal gradient, i.e., northern populations have a greater intrinsic capacity for growth than southern conspecifics. Our objectives are twofold. First, we evaluate the importance of local adaptation in growth physiology to bioenergetic modeling by constructing and comparing models for populations of the Atlantic silverside from two different latitudes, Nova Scotia and South Carolina. Second, we use these population-specific models to conduct virtual transplant experiments to test two possible explanations for the evolution of CnGV.

Methods

The Atlantic silverside is an annual species common to estuaries along the eastern coast of the North America from northern Florida to Nova Scotia. Spawning occurs from spring through early summer, and juveniles reach adult size by late autumn. Despite their much shorter growing season (Conover and Present 1990), the northern populations reach slightly greater size at age 1 compared with southern counterparts. Common garden experiments, in which fish from different populations are reared under identical conditions, have demonstrated that genetic effects account for the two-fold difference in maximum growth rate among silverside populations (Conover and Present 1990). Rapid growth in the north is favored by selection because winter survival is highly size dependent (Conover 1990). The selective forces that result in slow growth of southern silversides are less obvious. The following paragraphs describe the physiological data used to construct the models, the maximum likelihood procedure by which all model parameters were obtained, model validation, and the virtual transplant trials.

Physiological data

First- or second-generation lab-reared silversides were used in all experiments to control for environmental and maternal effects. Because *M. menidia* is an obligate schooling species and individuals behave abnormally in isolation, all physiological data were measured on groups of size-matched fish. Standard metabolism, specific dynamic action (SDA), and maximum consumption were measured over the range of temperatures and body sizes occurring during a growing season using cultured silversides originating from Nova Scotia (NS) and South Carolina (SC). The details of the rearing procedures and experimental protocols have been published elsewhere (Present and Conover 1992; Billerbeck et al. 2000) and are only outlined here. Some of the physiological data were reported in Billerbeck et al. (2000). Additional experiments using protocols and equipment identical to those used by Billerbeck are noted below.

Standard metabolism and SDA

NS and SC silversides ranging in size from 0.25 to 5.0 g (wet weight) were acclimated to test temperatures (12, 17, 23, and 28°C) for at least a week prior to the trials. Standard metabolism was measured in a multichannel, flow-through respirometer. The fish were allowed to acclimate to the 1-L test chambers overnight. The number of fish in each chamber was varied to ensure that a measurable decrease in O_2 could be achieved. Flow through the chambers was regulated to maintain O_2 between 70 and 80% saturation. The chambers were sufficiently small that movement was restricted such that measured O_2 consumption reflects "routine" rather than active rates of metabolism. To correct for the effects of bacterial consumption and drift in the probe readings, O_2 uptake was calculated as the difference between concentrations measured in a fish-free control chamber and the concentration measured in the chamber with fish. Uptake rate is the product of this difference and the rate of flow through the chamber. Data for 17, 23, and 28°C were obtained from Billerbeck et al. (2000). SDA data for fish between 0.23 and 2.96 g (wet weight) at 17 and 28°C fed both restricted and unlimited meals were obtained from Billerbeck et al. (2000).

Consumption

Consumption was measured for groups of 3 or 4 size-matched NS and SC silversides ranging from 0.25 to 2.5 g. Consumption data for 17 and 28°C were obtained from Billerbeck et al. (2000). Additional experiments were conducted at 23°C. Fish were acclimated to the feeding regime and 23°C in the test chambers for at least a week prior to the start of the trials. Test chambers were of sufficient size (60 cm diameter) to permit normal levels of activity. The fish were reweighed at the start of the trial and initial dry weights were estimated from a wet–dry regression (R^2 = 0.99, n = 315). Trials lasted between 10 and 21 days depending on initial size and temperature such that measurable growth occurred. Measured amounts of live adult *Artemia* were given daily to ensure ad libitum feeding. Dead *Artemia* were removed and weighed every 1–2 days. At the end of the experiment, total consumption was determined as the difference between the total weight of *Artemia* fed and that removed divided by the number of fish in the trial.

Model formulation and parameterization

Respiration (mg O_2·day^{-1}), SDA (mg O_2·g dry *Artemia*$^{-1}$), and consumption (g dry *Artemia*·day^{-1}) were modeled as functions of temperature (°C), dry fish weight (g), and meal size (g dry *Artemia*). The functions used to fit the data were

© 2002 NRC Canada

chosen in keeping with previous bioenergetic studies (Hewett and Johnson 1987):

$$(1a) \quad R = a_r W^{b_r} e^{\theta_r T}$$

$$(1b) \quad S = a_s C^{b_s} e^{\theta_s T}$$

$$(1c) \quad C = a_c W^{b_c} f_c(T)$$

where W is fish dry weight (g), T is temperature, R is respiration, S is SDA, and C is consumption. Fitted parameters are represented by a_r, b_r, θ_r, etc. Although there was an effect of weight on SDA, partial correlation analysis showed that this could be explained by the relationship between body weight and meal size; therefore, SDA was modeled as a function of meal size and temperature. All model functions were the same for both populations except for the temperature dependence of consumption ($f_c(T)$). To account for known differences in the temperature dependence of consumption (Present and Conover 1992; Billerbeck et al. 2000), the following population-specific temperature functions were necessary:

$$(2) \quad f_c(T) = \begin{cases} (1 + e^{-\theta_c(T - i_c)})^{-1} & \text{NS} \\ e^{\theta_c T} & \text{SC} \end{cases}$$

resulting in a sigmoid temperature response for NS with inflection specified by i_c and an exponential response for SC. No credible pair of models could be generated with a single temperature function. Previous bioenergetic models have used sigmoid temperature responses for fish nearing their temperature for maximum consumption ($T_{C_{max}}$), whereas exponential curves are more appropriate for situations in which temperatures are well below $T_{C_{max}}$ (Hewett and Johnson 1987). The temperature-response functions used imply that 28°C is much closer to $T_{C_{max}}$ for NS fish than for SC silversides. This is consistent with the fact that NS silversides are from much colder water than SC silversides.

The daily growth increment was modeled as

$$(3) \quad dW = [J_a(1 - u)C - J_o(\text{Act}\cdot R + S)]/J_f$$

where J_a and J_f are energy density estimates for *Artemia* and silversides, respectively, J_o is the oxycalorific conversion, u is the fraction of ingested energy lost to excretion and egestion, and Act is the activity multiplier. Energy density estimates for both populations and for live Artemia were obtained by proximate analysis. Energy equivalents ($J \cdot mg^{-1}$) were assumed to be 39.56 for fat, 23.65 for protein, and 17.16 for carbohydrate (Winberg 1971). The standard value for oxycalorific conversion was used (0.0136 J·mg O_2^{-1}, Elliott and Davison 1975). Apart from the energy density estimates and oxycalorific conversion, all model parameters were estimated from the experiments outlined above.

Our consumption experiments occurred over periods from 7 to 21 days and the fish grew as much as 89%. This growth represents additional information that can be extracted from the data set, assuming that it can be predicted by a bioenergetic model. We used this additional information to obtain estimates of activity and egestion through a penalized likelihood approach (Hilborn and Mangel 1997). A likelihood model with four components representing respiration (L_R), SDA (L_S), total consumption (L_{CT}), and growth (L_G) was constructed. Likelihood models L_R, L_S, and L_{CT} were chosen based on preliminary analyses (Shapiro–Wilks test for normality) of residuals from separate regressions. Respiration residuals were normally distributed, whereas SDA and total consumption residuals were normalized after log transformation. Therefore, the likelihood functions for respiration and SDA were

$$(4) \quad L_R = (2\pi\sigma_R^2)^{-\frac{N_R}{2}} \times \exp\left(-(2\sigma_R^2)^{-1}\sum_{i=1}^{N_R}\{R_i - a_r W_i^{b_r} e^{\theta_r T_i}\}^2\right)$$

$$(5) \quad L_S = (2\pi\sigma_S^2)^{-\frac{N_S}{2}} \times \exp\left(-(2\sigma_S^2)^{-1}\sum_{i=1}^{N_S}\{\ln(S_i) - \ln(a_s W_i^{b_s} e^{\theta_s T_i})\}^2\right)$$

where N is the number of observations in each data set and σ^2 is the error variance. In previous growth experiments (D. Conover, unpublished data), weight distributions were normal with standard deviation increasing approximately linearly with time, which is consistent with previous theoretical treatments of growth processes (DeAngelis et al. 1993). The error model for final size therefore depends on time, in a manner analogous to weighted linear regression (Draper and Smith 1966). The likelihood functions for total consumption and growth in the consumption trials were

$$(6) \quad L_{CT} = (2\pi\sigma_{CT}^2)^{-\frac{N_C}{2}} \times \exp\left(-(2\sigma_{CT}^2)^{-1}\sum_{i=1}^{N_C}\{\ln(\text{CT}_i) - \ln(\text{CM}(W_i, d_i, T_i))\}^2\right)$$

$$(7) \quad L_G = \left(\prod_{i=1}^{N_C} 2\pi\sigma_G^2 d_i^2\right)^{-\frac{1}{2}} \times \exp\left(-\sum_{i=1}^{N_C}\{W_{f_i} - \text{WM}(W_i, d_i, T_i)\}^2(2\sigma_G^2 d_i^2)^{-1}\right)$$

where CT_i is the total food consumed per fish and W_{f_i} is the mean final weight of the fish in the ith consumption trial. $\text{CM}(W_i, d_i, T_i)$ and $\text{WM}(W_i, d_i, T_i)$ are the values of total consumption and final weight predicted by starting the model from the average initial weight (W_i) and running for d_i days at temperature of T_i°C corresponding to the conditions of the ith consumption trial.

Bioenergetic models typically contain 12 or more parameters. Direct estimation of more than one or two model parameters from growth data is difficult because many parameter sets, most of which are biologically implausible, will describe the data equally well. The likelihood approach that we have adopted uses three types of constraints to restrict the range of possible solutions to those that are biologically sensible. The respiration and SDA components are based directly on the experimental data and provide empiri-

© 2002 NRC Canada

cal constraint for the fit of the parameters apart from the performance of the bioenergetic model. Two additional constraints were added. The fitting routine was prevented from arriving at negative parameters (biologically impossible given the model formulation) by the addition of a step penalty (L_{NEG}) with value ~0 if any parameter was negative, 1 otherwise. A common problem with bioenergetics models parameterized through a series of separate regression analyses is the appearance of the "premature asymptote", i.e., predicted growth slows or stops at sizes well below those in nature. Therefore, a shape constraint was added such that decelerating growth at small body sizes and optimal temperatures incurred a quadratically increasing cost. The inclusion of this penalty is justified by the observation that growth in juvenile silversides is linear to exponential over the range of constant temperatures measured. The specific form of this penalty was

$$(8)\quad L_{SHAPE} = \begin{cases} \exp\left(-\left(100\left.\dfrac{d^2W}{dt^2}\right|_{\substack{W=0.5\\T=23}}\right)^2\right), & \left.\dfrac{d^2W}{dt^2}\right|_{\substack{W=0.5\\T=23}} < 0 \\ 1, & \left.\dfrac{d^2W}{dt^2}\right|_{\substack{W=0.5\\T=23}} \geq 0 \end{cases}$$

The parameters were found by maximizing the log likelihood

$$(9)\quad L_T = L_R \times L_S \times L_{CT} \times L_G \times L_{NEG} \times L_{SHAPE}$$

using a steepest descent algorithm (Pierre 1969). Initial guesses at the parameter sets for each population were obtained by nonlinear regressions for respiration, SDA, and consumption. Twice the difference between the combined log likelihood of the population specific models and the log likelihood of a single model based on the pooled data sets should be approximately distributed as χ^2_{15} (Hilborn and Mangel 1997) and was used to test for significant differences among the population specific models. To evaluate the performance of the models, approximate R^2 values for the model fits were calculated as $1 - SS_{res}/SS_{total}$. This measure is identical to the "model efficiency" statistic of Loague and Green (1991). The fit to the lab data was tested for bias using a simultaneous F test of unit slope and zero intercept for regressions of observed vs. predicted values (Dent and Blackie 1979).

Model uncertainty

Comparing predictions of the population-specific models requires that we account for the uncertainty in the data sets from which the models were built. To do so, we generated Monte Carlo confidence intervals by sampling from the error distributions obtained in model fitting. Specifically, we numerically integrated the stochastic model

$$(10)\quad dW(t) = \left[J_a(1-u)Ce^{E_C-\frac{\sigma_C}{2}} - J_o\left\{Act(R+E_R) + Se^{E_S-\frac{\sigma_S}{2}}\right\}\right]J_f^{-1}$$

where E_R, E_C, and E_S are normally distributed random variables independently sampled at each time step. Because E_C and E_S are back transformed from log–log fits, half of their standard deviation is subtracted to remove bias in the simulated data (Hilborn and Mangel 1997). Confidence intervals for the model were obtained from the 2.5 and 97.5 percentiles of 5000 replicate integrations for each simulation. This approach assumes that the error variance in our lab experiments is predominantly measurement error and (or) daily variation in physiological variables all occurring independently of one another. Although physiological variables may be correlated, the data were measured in separate experiments on different individuals. Therefore, no information was available to determine the true degree of correlation. To address the magnitude of the uncertainty caused by the assumption of independence, we conducted two sets of simulations in which the errors were perfectly correlated such that variance in growth was either maximized or minimized (e.g., variance in growth is maximized by a positive correlation among errors in R and S, both of which are negatively correlated with C). The degree of correlation relevant to this study should reproduce the observed variance in size at each point in time.

Model validation

We conducted a pair of 60-day growth experiments under ambient summer water temperatures and photoperiods in the greenhouse at the Flax Pond Marine Lab, Old Field, New York. Fifty size-matched NS and SC silversides were stocked in two 1800-L round tanks at an average initial weight of 0.27 ± 0.004 g (standard error, SE). Tanks received a continuous flow of seawater from Flax Pond, a natural salt marsh bordering the lab. Fish were allowed 1 week of acclimation before the start of the experiment. Fish were fed to satiation with measured amounts of frozen adult *Artemia* four or more times per day, and temperature was recorded (nearest 0.1°C) every 15 min. Approximately every 10 days, all fish were weighed to the nearest milligram and returned to the tank. Observed growth was compared with growth predicted by the population-specific models using the mean initial size and daily average temperatures. Energy density for frozen *Artemia* (12.11 J·mg dry weight^{-1}) was obtained from the manufacturer's nutritional information using the conversions for protein, lipid, and carbohydrate described above (Winberg 1971). No other alterations were made to the models. Approximate R^2 were calculated for each model as described in Model formulation and parameterization. Statistical validation consisted of regression tests of zero intercept and unit slope for predicted vs. observed growth (Dent and Blackie 1979).

Model corroboration and virtual transplant

We considered two alternate explanations for slow growth: thermal adaptation and low food availability. In the first case, we hypothesized that populations at different latitudes

© 2002 NRC Canada

are adapted to the local thermal regime at the expense of performance in other environments (Lonsdale and Levinton 1985). In the second, we hypothesized that slow growth is an adaptation to low resource levels (Niewiarowski and Roosenburg 1993; Arendt 1997). A classic approach to identifying these kinds of trade-offs is to conduct reciprocal transplant experiments in which the performance of each genotype may be evaluated in the opposite environment. Reciprocal transplants are, however, impractical in Atlantic silversides and other highly mobile marine fishes where confinement in the wild is not feasible. As an alternative, we used bioenergetic models to conduct a set of "virtual transplant" experiments.

To do this, the population-specific models were run under annual temperature cycles from NS and SC, starting from the observed initial sizes of fish in the field. Daily temperatures and biweekly measurements of age-0 silversides in the Annapolis River, N.S., were obtained from Jessop (1983). Because of a 10-day gap in the time series in July, the temperature data were supplemented with data from the Miramichi River, New Brunswick, 1991–1993 (Lafleur et al. 1995), corrected to the same mean July temperature. Interpolation using only the Annapolis River time series made little difference in the model outcome. Approximately weekly measurements of age-0 silversides in the North Inlet, S.C., were obtained from Sosebee (1991). Biweekly temperature measurements from this location from 1981 to 1984 (Ogburn et al. 1988) and two sites near Folly Beach, S.C., 1969–1971 (Anderson et al. 1977), were used. Daily temperatures were interpolated using a cubic spline.

Model corroboration consisted of comparing size trajectories for wild fish with predicted growth of each native population via regression of predicted vs. observed values. Approximate R^2 were calculated for each model as described in Model formulation and parameterization. No adjustment of model parameters was made to improve the fit to the field data. Obviously, consumption or activity rates could have been "tuned" to improve the fit to the field data for each native population. Having no basis for doing so with the transplanted populations, we assumed that the unadjusted model predictions would be adequate estimates of relative growth for NS and SC fish in each locale.

Two sets of virtual transplant trials were conducted to test for adaptation to either the local thermal regime or local food availability. Because body size at the end of the growing season is a strong determinant of winter survival and subsequent fecundity (Conover 1990), we used size at the end of a growing season as our proxy for fitness and considered superior growth of each population in its native environment to be an indication of local adaptation (but see Discussion for alternative interpretation). In the first case, we allowed the transplanted fish unlimited rations under NS and SC temperature cycles to test the hypothesis that silversides are adapted to their local thermal regime. If this hypothesis is correct, growth of NS silversides should exceed that of SC in a NS thermal environment and vice versa. In the second case, we tested the hypothesis that silversides are adapted to local food availability (as well as thermal regime) by allowing the transplanted population to eat only as much as the native population. We assumed that it is not possible for the SC fish to eat more than their maximum ration and because NS silversides eat more than SC silversides, this trial was restricted to comparing growth for both populations on a SC ration in a SC thermal environment. If the hypothesis of adaptation to local food availability is true, we expect that SC silversides will exhibit superior growth to NS silversides when both populations were limited to a SC ration in an SC environment.

Results

Model fitting

The fits to the respiration and SDA data (Figs. 1*a*, 1*b*) were quite good with approximate R^2 values for NS and SC of 0.93 and 0.94 for respiration and 0.81 and 0.78 for SDA. The fit to the total consumption data (Fig. 1*c*) was good for NS ($R^2 = 0.78$) but poor for SC ($R^2 = 0.35$). Although there is a strong correlation between the observed growth in the consumption trials and the model prediction (Fig. 1*d*), the best-fit model consistently overestimates growth, leading to low approximate R^2 values (NS, 0.56; SC, 0.63). The regression test of unit slope and zero intercept showed no significant bias except for the growth data.

A complete list of model parameters is given in Table 1. Because the difference between the total log likelihood of the population specific models and a pooled model was 38.86, the NS and SC models were significantly different ($\chi^2_{15} = 77.73$, $p < 0.001$).

The allometric exponents for respiration (b_r), SDA (b_s), and consumption (b_c) were similar in the population-specific models, differing by no more than 14%. For both populations, the fitted allometries were similar to previously published values for other species (Hewett and Johnson 1987). The activity multipliers (Act) that resulted from the model fitting were 1.95 and 1.92, whereas the fraction of energy lost to excretion and egestion (u) was 0.09 and 0.02 for NS and SC, respectively. These values for u are lower than the generally accepted 0.2 (Hewett and Johnson 1987) and likely represent an underestimate of live *Artemia* energy density, rather than exceptional digestive efficiency. NS and SC silversides differ in each comparable parameter by an average of 28%. The greatest differences between the populations were in the weight dependence of consumption (a_c, 167%) and in the fraction of ingested energy lost to excretion and egestion (u, 127%). These parameters together indicate that under common conditions, a 1-g NS silverside consumes 37% more energy than a 1-g SC silverside at 24°C.

Model validation

In our independent validation trials, NS silversides grew at an average rate of 30 mg·day^{-1}, whereas SC silversides grew at 10 mg·day^{-1} (Fig. 2), and the mean sizes of the two populations were significantly different after 10 days of growth (t test, $p > 0.001$). The daily temperatures ranged from 17 to 27°C, generally increasing over the course of the trial. Using these temperature data and the initial mean size, population-specific model predictions were produced. The models predict growth in the validation trials well (Fig. 2); the approximate R^2 values for NS and SC were 0.91 and 0.99, respectively. Neither the NS nor SC models was significantly biased.

© 2002 NRC Canada

Fig. 1. Fit of model to laboratory data. Solid circles, data for Nova Scotia (NS) silversides; open circles, South Carolina (SC) silversides. Approximate R^2 are calculated as described in the text. (*a*) Standard metabolism: NS, $R^2 = 0.93$; SC, $R^2 = 0.94$. (*b*) Specific dynamic action, SDA: NS, $R^2 = 0.81$; SC, $R^2 = 0.78$. (*c*) Total consumption: NS, $R^2 = 0.78$; SC, $R^2 = 0.35$. (*d*) Final weight: NS, $R^2 = 0.56$; SC, $R^2 = 0.63$.

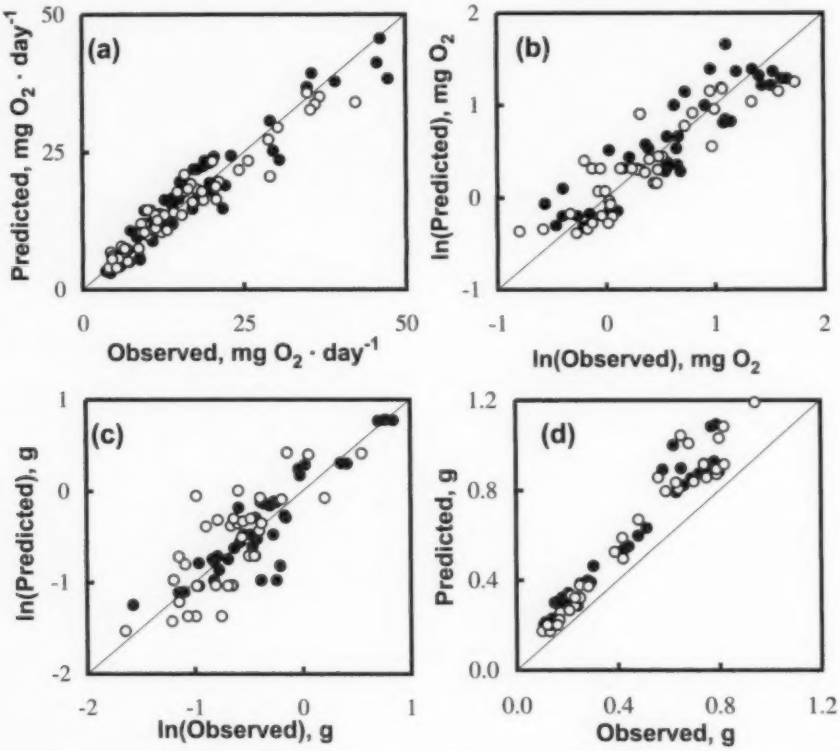

The Monte Carlo confidence intervals for the NS and SC models are shown in Fig. 2. The confidence bounds for the NS and SC model predictions do not overlap beyond the 18th day. This indicates that the differences in model predictions are significantly greater than can be accounted for by uncertainty in the laboratory data. The observed standard deviations in weight of NS and SC silversides increased at rates of 3.3 and 2.3 mg·day^{-1}, respectively, whereas their predicted standard deviations increased at rates of 3.1 and 2.5 mg·day^{-1}, respectively. Model standard deviations were based on the assumption that errors in the respiration, SDA, and consumption models are uncorrelated. The impact of this assumption was assessed by introducing perfect correlations ($r = 1$ or -1) among errors such that variance in growth was maximized or minimized. This correlation produced an increase (decrease) in the model standard deviation of 40% (60%). Even assuming maximum variance, the model predictions were significantly different beyond day 36.

Model corroboration and virtual transplants

The predicted growth for each population in its native thermal environment was very close to that in the wild (Fig. 3): the approximate R^2 values were 0.99 and 0.93 for NS and SC, respectively. These predictions were determined entirely by the recorded temperature and initial size; no parameters from the original model were adjusted to improve the fit. Growth predicted by the SC model transplanted to a NS thermal environment was significantly lower than observed growth. However, growth of the modeled NS silversides transplanted to a SC thermal environment was significantly greater than the observed growth. Because NS is superior at both latitudes, this contrast indicates that the slow growth of southern silversides does not represent purely temperature adaptation.

Our second hypothesis was that slow growth at low latitudes represents adaptation to low food availability in a southern thermal environment. To examine this hypothesis, we estimated the growth of NS silversides in a SC thermal environment when limited to a SC ration (Fig. 4). Predicted growth was significantly lower than observed, indicating decreased NS growth efficiency on reduced rations.

Discussion

Although other authors (Chambers et al. 1995) have hinted at the potential importance of local adaptation to bioenergetic modeling, ours is the first study to address this issue directly by comparing parameter values and model predictions for two distinct populations. The NS and SC models differ in all parameters by more than 10%, and model pre-

© 2002 NRC Canada

Table 1. Bioenergetic model parameters for Nova Scotia (NS) and South Carolina (SC) silversides.

Model function	Parameter	NS	SC
Respiration:	a_r	6.0479	7.2874
$R = a_r W^{b_r} e^{\theta_r T}$	b_r	0.8067	0.7030
	θ_r	0.0797	0.0640
Sample size	N_R	71	68
Error variance	σ^2_R	7.5282	5.4993
	R^2	0.93	0.94
Specific dynamic action:	a_s	52.9997	33.1153
$S = a_s C^{b_s} e^{\theta_s T}$	b_s	0.9724	0.8531
	θ_s	0.0203	0.0215
Sample size	N_S	42	38
Error variance	σ^2_s	0.0791	0.0752
	R^2	0.81	0.78
Consumption:	a_c	0.2103	0.0188
$C = a_c W^{b_c} f_c(T)$	b_c	0.5266	0.5700
NS: $f_c(T) = (1 + e^{-\theta_c (T - i_c)})^{-1}$	θ_c	0.1637	0.0634
SC: $f_c(T) = e^{\theta_c T}$	i_c	21.4568	NA
Sample size	N_C	38	37
Error variance	σ^2_{CT}	0.0649	0.1271
	R^2	0.78	0.35
Growth:	Act	1.9554	1.9220
$dW(T) = [J_a(1 - u)C - J_o(\text{Act}\cdot R + S)]/J_f$	u	0.0886	0.0199
Sample size	N_G	38	37
Error variance (× days^2)	σ^2_G	0.2445	0.5895
	R^2	0.56	0.63
Constants	J_f	23.29	22.52
	J_o	0.0136	
	J_a	Live 16.74	Frozen 12.11

Note: Parameter estimates, sample sizes, and error variances for each data set are given. R^2 values given are calculated as described in the text. NA, not applicable.

Fig. 2. Results of the validation trial. Solid and open circles represent mean sizes of Nova Scotia (NS) and South Carolina (SC) silversides, respectively. Error bars are 95% confidence limits for the means. Solid lines represent the sizes predicted by the population-specific models. Broken lines are 95% Monte Carlo confidence intervals for model prediction. Approximate R^2 are 0.91 and 0.99 for NS and SC, respectively. The inset shows the temperature recorded during the trial.

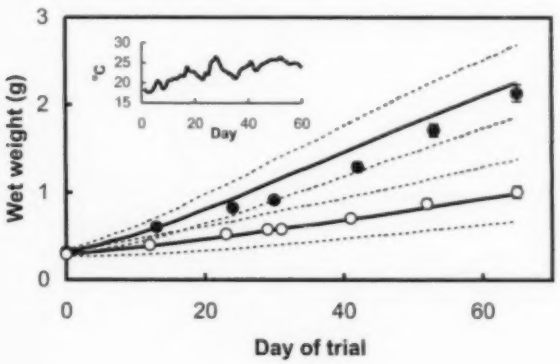

dictions are significantly different. The population-specific models predicted growth in our independent validation trials quite well, and the predicted growth of fish in the field was exceptionally accurate. Given the success of the model in predicting sizes in the independent validation and field data, it seems likely that poor growth in the consumption experiments is a confinement effect.

Sensitivity analyses involving 10% changes in individual parameters are frequently used to bolster conclusions drawn from model predictions (Bartell et al. 1986). Because the model sensitivity is nonlinear for most of the parameters, the interpretation of such analyses would be hampered if parameters could differ from their estimated values by more than 10% or if multiple parameters varied simultaneously. Because all NS and SC parameters differ by more than 10%, our results indicate that using sensitivity analyses to justify the application of a single bioenergetic model to predicting growth for multiple populations may be inappropriate. Although useful for identifying important areas for further study, single-parameter perturbations may instill undue confidence in models when all parameters for local populations differ simultaneously. Alternatively, confidence intervals for model predictions may be constructed from uncertainty in the data used to estimate parameters. To do so, an estimate of the correlation among physiological variables is neces-

© 2002 NRC Canada

Fig. 3. Model corroboration and virtual transplant trials with unlimited rations for Nova Scotia (NS) and South Carolina (SC) silversides. Insets show temperature data used in simulations. (*a*) Growth in NS. Solid circles represent observed sizes of NS silversides (Jessop 1983), and the bold lines represent predicted growth for NS (R^2 = 0.99) and SC silversides in a NS thermal environment. (*b*) Growth in SC. Open circles represent observed sizes of SC silversides (Sosebee 1991), and the bold lines represent predicted growth for NS and SC silversides (R^2 = 0.93) in a SC thermal environment. In both panels, broken lines are 95% confidence intervals from Monte Carlo simulations.

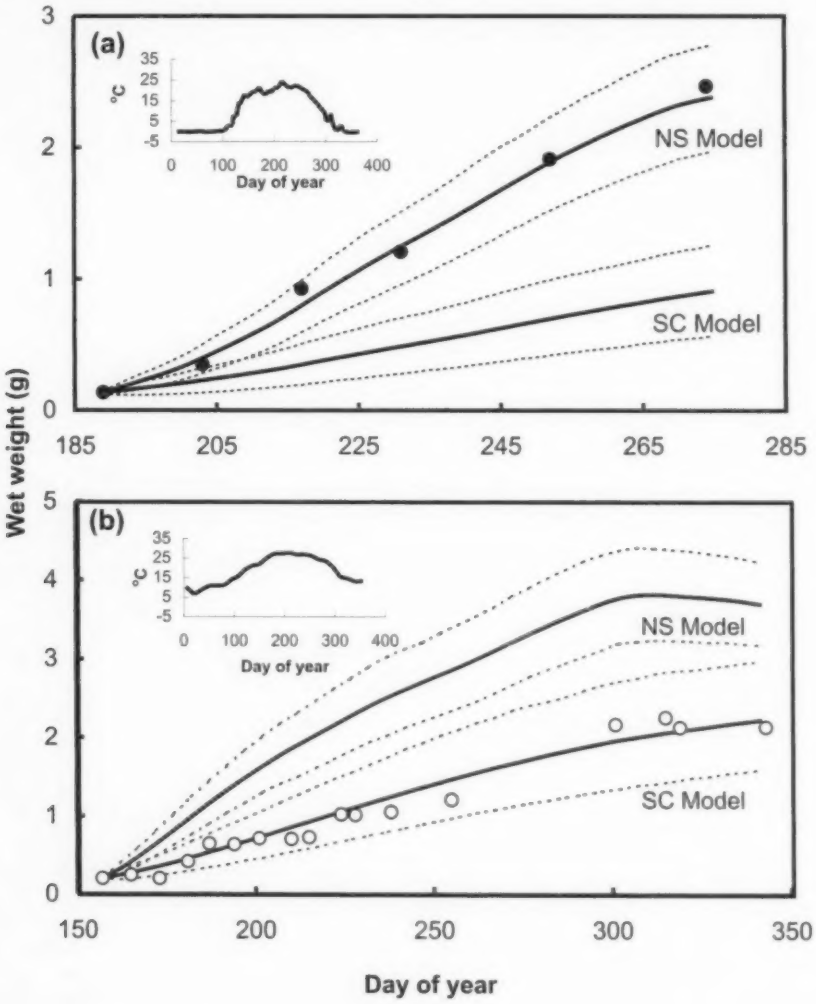

sary. Although the confidence intervals that we used proved to be adequate descriptors of the variability in fish size, estimating the degree of correlation between physiological variables remains an important area for bioenergetic- and individual-based modeling.

It is regarded as impractical to measure all model parameters for each species, let alone local populations, and many bioenergetic models have been constructed by borrowing parameters from the literature. Although we are not alone in criticizing species borrowing (Ney 1993), our results clearly demonstrate that accounting for local adaptation in growth physiology may dramatically improve the performance of bioenergetic models. Of course, to do so, model parameters must be measured on a geographic scale commensurate with local adaptation, which represents a substantial increase in the amount of labor required. The likelihood-based method of model fitting that we adopted allows complete parameter sets to be estimated from a subset of the experiments that would be required to measure all parameters directly. In addition to the reduction in experimental work, the models thus obtained are independent, thereby allowing straightforward statistical comparisons.

In most applications of bioenergetic models, the proportion of maximum consumption (P) is adjusted a posteriori such that the model predicts growth in the field, typically resulting in values of P less than 0.8. One potential criticism of our work is that our predictions of growth have assumed that the consumption and activity rates measured in the lab

© 2002 NRC Canada

Fig. 4. Virtual transplant trial with limited rations. Open circles represent observed sizes of South Carolina (SC) silversides (Sosebee 1991), and the bold lines represent predicted growth of a Nova Scotia (NS) silverside in a SC thermal environment when limited to a SC ration. Broken lines are 95% confidence intervals from Monte Carlo simulations. Temperature data are the same as in Fig. 3.

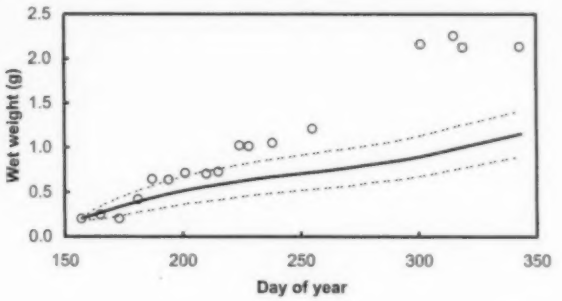

were the same as those in the field, that is, we set $P = 1$ and used the values of Act estimated from the lab data. Because our approach differs from most prior uses of bioenergetic models, we estimated the range of P and Act values that could have been used to predict growth of NS and SC silversides. To do this, we calculated the envelope of P and Act values for which the approximate R^2 was greater than or equal to that based on the values of Act estimated in our lab experiments and assuming $P = 1$ (Fig. 5). The resulting regions have a positive slope because a decrease in consumption must be balanced by a decrease in activity for equivalent growth to occur. The slopes of these regions differ because the ratio of maximum consumption to resting metabolism is greater for NS silversides than for SC silversides. Consequently, the change in Act needed to balance a change in P is greater for NS than for SC. For SC silversides, this envelope extends below Act = 1 and has been truncated (because active metabolism must be greater than resting, Act·1). Based on this calculation, it is clear that, as in all bioenergetic models, a fairly broad range of P and Act will describe the data equally well. Therefore, the fit to the field data alone cannot be used to justify our assumption of a maximum ration, and additional information is needed.

Two lines of evidence support the assertion that the fish obtain their maximum ration in the field. First, to predict growth using a reduced consumption rate, we must simultaneously assume that activity rates are commensurately decreased. The activity multipliers obtained from our lab experiments proved adequate for explaining growth in the independent validation trials (1800-L, 2-m-diameter tanks) in which the fish were exposed to a mild current and fed ad libitum (i.e., $P = 1$). Further, free-swimming neritic silversides live in energetically demanding tidal environments and must swim to avoid predators, and it is unlikely that they would have lower active metabolic rates than fish in our 60-cm-diameter test chambers. Second, previous studies have shown that growth of silversides fed unlimited rations in the lab was no faster than the observed growth of fish in the field (Present and Conover 1992; Billerbeck et al. 2000). Eliminating P and Act as free parameters contradicts the conventional wisdom among bioenergetics modelers. However, the accuracy with which our population-specific models predict growth in the field, the degree to which these same models predict growth in the validation trials where P is known to be 1, and the observation that fish in the field grow at their maximum rate, all suggest that the maximum ration assumption is reasonable.

Fig. 5. Equivalent growth for different consumption and activity rates. The solid and open circles represent the proportion of maximum consumption (P) and activity multiplier (Act) used in this study for Nova Scotia (NS) and South Carolina (SC) silversides, respectively. Because post-hoc fitting of P and Act ought to increase predictive power, the approximate R^2 for these points serves as a lower bound for acceptable parameters. The solid (NS) and open (SC) ellipses indicate the regions of P and Act values for which the approximate R^2 for growth in the field equals or exceeds the lower bound.

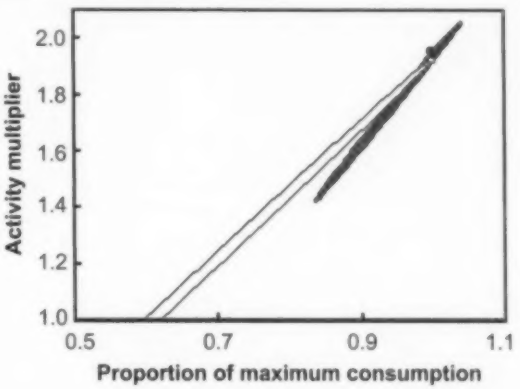

The proportion of maximum consumption is generally the parameter to which bioenergetic models are most sensitive (Bartell et al. 1986). Given the existence of local adaptation in growth physiology, the proper interpretation of this parameter when fit a posteriori is unclear. For instance, if only the NS model was used, we could predict SC growth by varying P (albeit less accurately). Based on these results, we would infer that silversides achieved a decreased proportion of their maximum ration as latitude decreased. This approach has been used to quantify habitat suitability for such species as rainbow trout (*Oncorhynchus mykiss*)and rainbow smelt (*Osmerus mordax*; Lantry and Stewart 1993; Railsback and Rose 1999).

However, if only the SC model was used, we would have to conclude that the model was wrong; to predict rapid NS growth, P would have to be substantially greater than one. Others have correctly pointed to variation in activity levels as a source of interpopulation variability in growth (Boisclair and Leggett 1989). This caveat should be made more general; our results indicate that it may be inappropriate to assume that differences in growth among local populations are due solely to variation in any single parameter. In cases where substantial local physiological adaptation exists, predictions of a model based on one population's physiology in a new location should be interpreted as a virtual transplant experiment, rather than a prediction of growth for fish native to the new locale. Moreover, if local adaptation in growth physiology is common, then models constructed by borrow-

© 2002 NRC Canada

ing parameters from other species are chimeras, assemblages of parts that represent no natural population.

We used the population-specific models to examine two selective agents in growth rate evolution: temperature and low food availability. It is widely held that fast growth and large size lead to increased fitness in the early life history of fish (Houde 1987; Sogard 1997). For age-0 Atlantic silversides, body size at the end of the growing season is a strong determinant of winter survival and subsequent fecundity (Conover 1990). Significantly superior growth of each native population in its own environment was taken to indicate local adaptation in that a genotype superior in both locations should spread throughout the range of the species.

In the first transplant, growth was predicted assuming unlimited rations. The predicted growth of the transplanted fish (e.g., SC in NS) was significantly different from the observed field growth for both populations. On unlimited rations, NS outgrew SC in both thermal environments. If faster growth and larger body size are beneficial, then the NS thermal physiology would have higher fitness in SC. Because there are no apparent barriers to gene flow (Conover 1998), nothing should prevent NS genotypes from spreading southward if they are truly superior.

When restricted to a SC ration, predicted growth of NS silversides was significantly less than that of SC silversides in a southern thermal environment. Our lab experiments indicated that NS silversides pay elevated costs in respiration and SDA. If NS silversides were limited to the consumption rates exhibited by SC silversides, then the elevated metabolic costs of the NS genotype would prevent them from achieving growth equivalent to the SC genotype in a southern thermal environment. Although corroborating field evidence of food availability at each latitude is lacking, our argument is not without precedent.

Resource limitation has been used to explain canalized slow growth in other species (Arendt 1997). Fence lizards from low food habitats exhibit faster growth on limited rations than lizards from high food habitats (Niewiarowski and Roosenburg 1993). Slow growth as an adaptation to low resources has been demonstrated in several species of plants as well (Arendt 1997). Implicit in this hypothesis is the assumption that the capacity for rapid growth can only be maintained at some cost to fitness. The growth of NS silversides on SC rations in the southern thermal environment indicates that rapid growth occurs at the expense of energetic efficiency.

Our argument thus far has relied heavily on the hypothesis that fast growth and large body size lead to higher fitness (Houde 1987; Sogard 1997). There may, however, be fitness costs to rapid growth. Recent work on several species has suggested that rapid growth results in decreased swimming performance (Gregory and Wood 1999; Kolok 1999). Decreased swimming performance (Billerbeck et al. 2001) for fast-growing fish has also been demonstrated for Atlantic silversides. Moreover, fast-growing silversides have decreased survival probability in laboratory predation trials (Lankford et al. 2001) when compared with slow growers of the same size. If this is true in general, then CnGV may be explained as a balance between competing costs and benefits of growth. Rapid northern growth may be selected for by size-dependent winter mortality, but as the severity of winter decreases with latitude, the relative importance of growth rate dependent predation risk increases, resulting in slower southern growth. A test of this hypothesis is presently underway.

There is no a priori reason to suspect that the latitudinal differences that we have demonstrated for silverside physiology are exceptional. On the contrary, CnGV in growth rate is a common phenomenon among ectotherms. Evidence for CnGV has been found in many fish species, including Atlantic halibut (*Hippoglospus hippoglospus*; Jonassen et al. 2000), Atlantic salmon (Nicieza et al. 1994), and striped bass (Conover et al. 1997), as well as several reptiles, amphibians, and invertebrates (Conover and Shultz 1995). If local adaptation in growth physiology of the sort found in silversides is commensurately common, it would seem that the relevance of locally adapted physiology to bioenergetic modeling has been greatly underestimated.

Acknowledgments

We thank Jean Billerbeck, Tom Hurst, and T. Lankford for data, laboratory assistance, and useful discussion. We also thank Bob Cerrato, Marc Mangel, and three anonymous reviewers for comments on previous drafts of this manuscript. This publication was supported by the National Sea Grant College Program of the U.S. Department of Commerce's National Oceanic and Atmospheric Administration under award No. NA86RG0056 to the Research Foundation of the State University of New York for New York Sea Grant. This work received additional support from the Ocean Sciences Division of the National Science Foundation, grant number OCE-953029. The views expressed herein do not necessarily reflect the views of any of these organizations.

References

Anderson, W., Dias, J., and Dias, K. 1977. The macrofauna of the surf zone off Folly Beach, SC. NOAA Tech. Rep. NMFS SSRF-704. Grice Marine Biological Laboratory, Charleston, S.C.

Arendt, J. 1997. Adaptive intrinsic growth rates: an integration across taxa. Q. Rev. Biol. **72**: 149–177.

Arendt, J., and Wilson, D.S. 1999. Countergradient selection for rapid growth in pumpkinseed sunfish: disentangling ecological and evolutionary effects. Ecology, **80**: 2793–2798.

Bartell, S., Breck, J., and Gardner, R. 1986. Individual parameter perturbation and error analysis of fish bioenergetics models. Can. J. Fish. Aquat. Sci. **43**: 160–168.

Billerbeck, J.M., Schultz, E.T., and Conover, D.O. 2000. Adaptive variation in energy acquisition and allocation among latitudinal populations of the Atlantic silverside. Oecologia, **122**: 210–219.

Billerbeck, J.M., Lankford, T.E., and Conover, D.O. 2001. Evolution of intrinsic growth and energy acquisition rates. I. Trade-offs with swimming performance in *Menidia menidia*. Evolution, **55**: 1863–1872.

Blanckenhorn, W.U. 2000. The evolution of body size: what keeps organisms small? Q. Rev. Biol. **75**: 385–407.

Boisclair, D., and Leggett, W. 1989. The importance of activity in bioenergetics models applied to actively foraging fishes. Can. J. Fish. Aquat. Sci. **46**: 1859–1867.

Chambers, R.C., Rose, K.A., and Tyler, J.A. 1995. Recruitment and recruitment processes of winter flounder, *Pleuronectes americanus*, at different latitudes: implications of an individual-based simulation model. Neth. J. Sea. Res. **34**: 19–43.

© 2002 NRC Canada

Conover, D.O. 1990. The relationship between capacity for growth and length of growing season: evidence for and implications of countergradient variation. Trans. Am. Fish. Soc. **119**: 416–430.

Conover, D.O. 1998. Local adaptation in marine fishes: evidence and implications for stock enhancement. Bull. Mar. Sci. **62**: 477–493.

Conover, D.O., and Present, T. 1990. Countergradient variation in growth rate: compensation for length of the growing-season among Atlantic silversides from different latitudes. Oecologia, **83**(3): 316–324.

Conover, D.O., and Schultz, E.T. 1995. Phenotypic similarity and the evolutionary significance of countergradient variation. Trends Ecol. Evol. **10**: 248–252.

Conover, D.O., Brown, J.J., and Etisham, A. 1997. Countergradient variation in growth of young striped bass (*Morone saxatilis*) from different latitudes. Can. J. Fish. Aquat. Sci. **54**: 2401–2409.

DeAngelis, D.L., Rose, K.A., Crowder, L.B., Marschall, E.A., and Lika, D. 1993. Fish cohort dynamics: application of complementary modeling approaches. Am. Nat. **142**: 604–622.

Dent, J.B., and Blackie, M.J. 1979. Systems simulation in agriculture. Applied Science Publishers Ltd., London.

Draper, N.R., and Smith, H. 1966. Applied regression analysis. Wiley, New York.

Elliott, J.M., and Davison, W. 1975. Energy equivalents of oxygen consumption in animal energetics. Oecologia, **19**: 195–201.

Gregory, T.R., and Wood, C. 1999. Interactions between individual feeding behaviour, growth, and swimming performance in juvenile rainbow trout (*Oncorhynchus mykiss*) fed different rations. Can. J. Fish. Aquat. Sci. **56**: 479–486.

Hewett, S.D., and Johnson, B.J. 1987. Fish bioenergetics. University of Wisconsin Sea Grant Tech. Rep. WIS-SG(2-250), Madison, Wis.

Hilborn, R., and Mangel, M. 1997. The ecological detective: confronting models with data. Princeton University Press, Princeton, N.J.

Houde, E.D. 1987. Early life dynamics and recruitment variability. Am. Fish. Soc. Symp. **2**: 17–29.

Jessop, B.M. 1983. Aspects of the life history of the Atlantic silverside (*Menidia menidia*) of the Annapolis River, Nova Scotia. Can. Manuscr. Rep. Fish. Aquat. Sci. 1694.

Jonassen, T.M., Imsland, A.K., and Fitzgerald, R. 2000. Geographic variation in growth and food conversion efficiency of juvenile Atlantic halibut related to latitude. J. Fish Biol. **56**: 279–294.

Kerr, S.R. 1971. Analysis of laboratory experiments on growth efficiency of fishes. J. Fish. Res. Board Can. **28**: 801–808.

Kitchell, J.F., Stewart, D.J., and Weininger, D. 1977. Applications of a bioenergetics model to yellow perch (*Perca flavescens*) and walleye (*Stizostedion vitreum vitreum*). J. Fish. Res. Board Can. **34**(Spec. Issue 10): 1922–1935..

Kolok, A.S. 1999. Interindividual variation in the prolonged locomotor performance of ectothermic vertebrates: a comparison of fish and herpetofaunal methodologies and a brief review of the recent fish literature. Can. J. Fish. Aquat. Sci. **56**: 700–710.

Lafleur, C., Pettigrew, B., and St-Hilaire, A. 1995. Seasonal and short-term variations in the estuarine structure of the Miramichi. *In* Water, science, and the public: the Miramichi ecosystem. *Edited by* E.M.P. Chadwick. Can. Spec. Publ. Fish. Aquat. Sci. 123. pp. 45–71.

Lankford, T.E., Billerbeck, J.M., and Conover, D.O. 2001. Evolution of intrinsic growth and energy acquisition rates. II. Trade-offs with vulnerability to predation in *Menidia menidia*. Evolution, **55**: 1873–1881.

Lantry, B.F., and Stewart, D.J. 1993. Ecological energetics of rainbow smelt in the Laurentian Great Lakes—an interlake comparison. Trans. Am. Fish. Soc. **122**: 951–976.

Levins, R. 1968. Evolution in changing environments. Princeton University Press, Princeton, N.J.

Loague, K., and Green, R.E. 1991. Statistical and graphical methods for evaluating solute transport models: overview and application. J. Contam. Hydrol. **7**: 51–73.

Lonsdale, D.J., and Levinton, J.S. 1985. Latitudinal differentiation in copepod growth—an adaptation to temperature. Ecology, **66**: 1397–1407.

Ney, J.J. 1993. Bioenergetics modeling today—growing pains on the cutting edge. Trans. Am. Fish. Soc. **122**: 736–748.

Nicieza, A.G., Reiriz, L., and Brana, F. 1994. Variation in digestive performance between geographically disjunct populations of Atlantic salmon—countergradient in passage time and digestion rate. Oecologia, **99**: 243–251.

Niewiarowski, P.H., and Roosenburg, W. 1993. Reciprocal transplant reveals sources of variation in growth rates of the lizard *Sceloporus undulatus*. Ecology, **74**: 1992–2002.

Ogburn, M.V., Allen, D.M., and Michener, W.K. 1988. Fishes, shrimps and crabs of the North Inlet Estuary, SC: a four-year seine and trawl survey. Baruch Institute Tech. Rep. No. 88-1. University of South Carolina, Columbia.

Pierre, D.A. 1969. Optimization theory with applications. Wiley, New York.

Present, T., and Conover, D.O. 1992. Physiological basis of latitudinal growth differences in *Menidia menidia*: variation in consumption or efficiency? Funct. Ecol. **6**: 23–31.

Railsback, S.F., and Rose, K.A. 1999. Bioenergetics modeling of stream trout growth: temperature and food consumption effects. Trans. Am. Fish. Soc. **128**: 241–256.

Sogard, S.M. 1997. Size-selective mortality in the juvenile stage of teleost fishes: a review. Bull. Mar. Sci. **60**: 1129–1157.

Sosebee, K. 1991. Life history of a southern population of the Atlantic silverside, *Menidia menidia*, and comparisons with other latitudes. M.S. thesis, State University of New York at Stony Brook, Stony Brook, N.Y.

Winberg, G.G. 1971. Methods for the estimation of production of aquatic animals. Academic Press, New York.

© 2002 NRC Canada

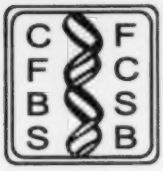

CANADIAN FEDERATION OF BIOLOGICAL SOCIETIES

MONTRÉAL 2002

45TH ANNUAL MEETING • 45E CONGRÈS ANNUEL

June/juin 12-15, 2002

Palais des Congrès de Montréal • Montréal, Québec, Canada

THEME I: NEUROLOGICAL DEVELOPMENT

Theme Chair: Remi Quirion, Director, CIHR Institute of Neurosciences, Mental Health and Addiction, McGill University and Douglas Hospital Research Center, Verdun, Quebec.

SYMPOSIA:

- Neurodevelopmental mechanisms in neurological and psychiatric disorders
- Gene therapy for diseases of the nervous system
- Neurogenesis in adult brain. Are therapeutic application just around the corner?
- Axon regeneration and repair in the injured spinal cord

THEME II: PHYSICAL ACTIVITY, NUTRITION AND CHRONIC DISEASE

Theme Chairs: Mary-Ellen Harper, Department of Biochemistry, Microbiology & Immunology, University of Ottawa; Ottawa, ON
Terry Graham, Department of Human Biology and Nutritional Sciences, University of Guelph, Guelph, ON

SYMPOSIA:

- Bioenergetics and Obesity
- Roles of Nutrition and Exercise in Type 2 diabetes
- Nutrition and Exercise in the Prevention and Management of Cardiovascular Disease and Associated Risk Factors
- Nutrition, Physical Activity and Aging

THEME I & II PLENARY LECTURES
See CFBS website for details. / Voir le site web de FCSB pour plus de détails.

HEALTH CANADA SYMPOSIUM: NEUROTOXICOLOGY
Chair: Dr. Santokh Gill, Health Canada, Ottawa, ON

DANONE INSTITUTE OF CANADA SYMPOSIUM
Behavioural Determinants of Childhood Obesity
Chair: Dr. Peter Jones, McGill University, Montreal, QC

CFBS: BIOTERRORISM SCIENCE POLICY FORUM
Chair: Dr. Bruce Sells, CFBS Executive Director, Ottawa, ON

EMPLOYMENT FAIR • FOIRE D'EMPLOI
Fri., June 14 / Ven. 14 Juin, 2002
Register at www.cfbs.org / S'inscrire à www.cfbs.org

SCIENTIFIC EXHIBITS AND POSTER SESSIONS
EXPOSITIONS SCIENTIFIQUES ET SESSIONS DES AFFICHES
Thur. & Fri., June 13-14 / Jeu. 13 et Ven. 14 Juin

AWARD LECTURES
CONFÉRENCES DES PRIX ATTRIBUÉS
Gordin Kaplan Award Lecture (CFBS)
Murray L. Barr Junior Scientist Award Lecture (CAANCB)
J.C.B. Award Lecture (CAANCB)
Centrum Foundation New Scientist Award Lecture (CSNS)
AstraZeneca Award Lecture (AstraZeneca Canada Inc.)

CFBS TRAVEL AWARDS • FCSB PRIX DE VOYAGES
See CFBS website for details. / Voir le site web de FCSB pour plus de détails.

McGill CME Credits Approved • EMC crédits apprové par McGill

CANADIAN FEDERATION OF BIOLOGICAL SOCIETIES
305 - 1750 Courtwood Crescent, Ottawa, Ontario K2C 2B5
Tel.: (613) 225-8889 • Fax.: (613) 225-9621 • E-Mail: wantonious@cfbs.org

For further information / Pour plus d'information: WWW.CFBS.ORG

Salmonine Introductions to the Laurentian Great Lakes: An Historical Review and Evaluation of Ecological Effects

By/par Stephen S. Crawford

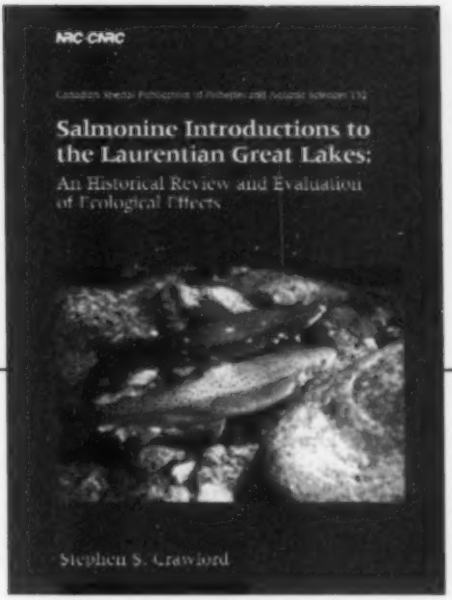
NRC CNRC
Salmonine Introductions to the Laurentian Great Lakes:
An Historical Review and Evaluation of Ecological Effects
Stephen S. Crawford

$42.95/42,95 $

Other countries $42.95 US
À l'étranger 42,95 $US

Softcover / Edition brochée
205 pages
ISBN 0-660-17639-4 ISSN 0706-6481
(Can. Spec. Publ. Fish. Aquat. Sci. 132)
NRC No. / N° du CNRC 42734

Orders may be submitted by mail or fax to: Les commandes peuvent être soumises par courrier ou par télécopieur à :

Order Office/Bureau des commandes
NRC Research Press/Presses scientifique du CNRC
National Research Council/Conseil national de recherches
Ottawa, ON K1A 0R6, Canada
Telephone/Téléphone : (613) 990-2254
Fax/Télécopieur : (613) 952-7656
E-mail/Courriel : research.journals@nrc.ca
Website: http://researchjournals.nrc.ca
Site web : http://pressesscientifiques.cnrc.ca

PLEASE PRINT/LETTRES MOULÉES

☐ Payment enclosed / Paiement inclus Charge to/ Imputer à ☐ Visa ☐ MasterCard ☐ AMEX

Account no./N° de compte Expiry date/Date d'expiration

Name/Nom

Signature

Address/Adresse

City/Ville Province

Postal code/Code postal Country/Pays

Telephone/Téléphone Fax/Télécopieur

E-mail/courriel

Prepayment required unless order is accompanied by a purchase order number. Cheques or money orders should be made payable to : "Receiver General for Canada, Credit NRC". For all orders outside Canada, rates are in U.S. Dollars. All sales are final.
Les commandes doivent être payées d'avance à moins qu'elles ne soient accompagnées d'un numéro de bon de commande. Les chèques ou mandats doivent être libellés au « Receveur général du Canada, crédit du CNRC ». Toutes les ventes sont finales.

Marine Protected Areas and Fisheries Closures in British Columbia

By/par Glen S. Jamieson and/et Joanne Lessard

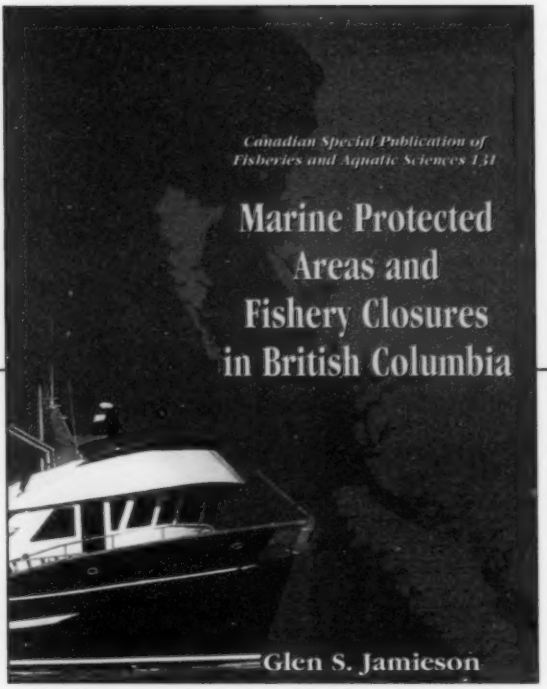
Canadian Special Publication of Fisheries and Aquatic Sciences 131
Marine Protected Areas and Fishery Closures in British Columbia
Glen S. Jamieson

$69.95/69,95 $

Other countries $69.95 US
À l'étranger 69,95 $US

Softcover / Edition brochée
414 pages
ISBN 0-660-17788-9 ISSN 0706-6481
NRC No./N° du CNRC 42846
(Can. Spec. Publ. Fish. Aquat. Sci. No. 131)

Orders may be submitted by mail or fax to: Les commandes peuvent être soumises par courrier ou par télécopieur à :

Order Office/Bureau des commandes
NRC Research Press/Presses scientifique du CNRC
National Research Council/Conseil national de recherches
Ottawa, ON K1A 0R6, Canada
Telephone/Téléphone : (613) 990-2254
Fax/Télécopieur : (613) 952-7656
E-mail/Courriel : research.journals@nrc.ca
Website: http://researchjournals.nrc.ca
Site web : http://pressesscientifiques.cnrc.ca

PLEASE PRINT/LETTRES MOULÉES

☐ Payment enclosed / Paiement inclus ☐ Charge to/ Imputer à ☐ Visa ☐ MasterCard ☐ AMEX

Account no./N° de compte | Expiry date/Date d'expiration

Name/Nom

Signature

Address/Adresse

City/Ville | Province

Postal code/Code postal | Country/Pays

Telephone/Téléphone | Fax/Télécopieur

E-mail/courriel

Prepayment required unless order is accompanied by a purchase order number. Cheques or money orders should be made payable to : "Receiver General for Canada, Credit NRC". For all orders outside Canada, rates are in U.S. Dollars. All sales are final.
Les commandes doivent être payées d'avance à moins qu'elles ne soient accompagnées d'un numéro de bon de commande. Les chèques ou mandats doivent être libellés au « Receveur général du Canada, crédit du CNRC ». Toutes les ventes sont finales.

Marie-Andrée Fallu, Nancie Allaire, and Reinhard Pienitz	**329–349**	Distribution of freshwater diatoms in 64 Labrador (Canada) lakes: species–environment relationships along latitudinal gradients and reconstruction models for water colour and alkalinity
Barbara O.B. Bertram and Richard C. Playle	**350–360**	Effects of feeding on waterborne silver uptake and depuration in rainbow trout (*Oncorhynchus mykiss*)
A.F. Sinclair, D.P. Swain, and J.M. Hanson	**361–371**	Measuring changes in the direction and magnitude of size-selective mortality in a commercial fish population
A.F. Sinclair, D.P. Swain, and J.M. Hanson	**372–382**	Disentangling the effects of size-selective mortality, density, and temperature on length-at-age
Russell B. Millar and Richard D. Methot	**383–392**	Age-structured meta-analysis of U.S. West Coast rockfish (Scorpaenidae) populations and hierarchical modeling of trawl survey catchabilities
Stephan B. Munch and D.O. Conover	**393–403**	Accounting for local physiological adaptation in bioenergetic models: testing hypotheses for growth rate evolution by virtual transplant experiments
		PERSPECTIVE
Ji X. He and Donald J. Stewart	**250–261**	A stage-explicit expression of the von Bertalanffy growth model for understanding age at first reproduction of Great Lakes fishes

National Research Council Canada
Ottawa, Canada K1A 0R6

Conseil national de recherches Canada
Ottawa, Canada K1A 0R6

Postage paid at Ottawa
Publications mail
Registration No. 1240579

Port payé à Ottawa
Poste-publication
Enregistrement n° 1240579

Canadian Journal of Fisheries and Aquatic Sciences

Volume 59, Number 2, February 2002

Journal canadien des sciences halieutiques et aquatiques

Volume 59, numéro 2, février 2002

ARTICLES

Yvan Simard, Diane Lavoie, and François J. Saucier	**197–210**	Channel head dynamics: capelin (*Mallotus villosus*) aggregation in the tidally driven upwelling system of the Saguenay – St. Lawrence Marine Park's whale feeding ground
Øyvind Fiksen and Aril Slotte	**211–217**	Stock–environment recruitment models for Norwegian spring spawning herring (*Clupea harengus*)
Aki Mäki-Petäys, Ari Huusko, Jaakko Erkinaro, and Timo Muotka	**218–228**	Transferability of habitat suitability criteria of juvenile Atlantic salmon (*Salmo salar*)
Graham D. Sherwood, Ivano Pazzia, Andrew Moeser, Alice Hontela, and Joseph B. Rasmussen	**229–241**	Shifting gears: enzymatic evidence for the energetic advantage of switching diet in wild-living fish
D.G. Chen, J.R. Irvine, and A.J. Cass	**242–249**	Incorporating Allee effects in fish stock–recruitment models and applications for determining reference points
Craig D. Snyder, John A. Young, David P. Lemarié, and David R. Smith	**262–275**	Influence of eastern hemlock (*Tsuga canadensis*) forests on aquatic invertebrate assemblages in headwater streams
David C. Stewart, Gordon W. Smith, and Alan F. Youngson	**276–281**	Tributary-specific variation in timing of return of adult Atlantic salmon (*Salmo salar*) to fresh water has a genetic component
William H. Eldridge, Marc D. Bacigalupi, Ira R. Adelman, Loren M. Miller, and Anne R. Kapuscinski	**282–290**	Determination of relative survival of two stocked walleye populations and resident natural-origin fish by microsatellite DNA parentage assignment
Paul D. Spencer, Thomas K. Wilderbuer, and Chang Ik Zhang	**291–302**	A mixed-species yield model for eastern Bering Sea shelf flatfish fisheries
I. Imre, J.W.A. Grant, and E.R. Keeley	**303–309**	The effect of visual isolation on territory size and population density of juvenile rainbow trout (*Oncorhynchus mykiss*)
Kelly E. Arbuckle and John A. Downing	**310–316**	Freshwater mussel abundance and species richness: GIS relationships with watershed land use and geology
Véronique P. Hiriart, Bruce M. Greenberg, Stephanie J. Guildford, and Ralph E.H. Smith	**317–328**	Effects of ultraviolet radiation on rates and size distribution of primary production by Lake Erie phytoplankton

Continued on inside back cover / Suite au verso

Canada

Printed in Canada by / Imprimé au Canada par
University of Toronto Press Inc.
Typesetting by / Typographie par
NRC Research Press / Presses scientifiques du CNRC

0706-652X(200202)59:2;1-K